EXPLORATION OF NATURAL PRODUCT LEADS FOR MULTITARGET-BASED TREATMENT OF CANCER - COMPUTATIONAL TO EXPERIMENTAL JOURNEY

EDITED BY: Rajeev K. Singla, Marcus Scotti and Supratik Kar
PUBLISHED IN: Frontiers in Pharmacology

frontiers Research Topics

ISSN 1664-8714
ISBN 978-2-88974-686-6
DOI 10.3389/978-2-88974-686-6

About Frontiers

Frontiers is more than just an open-access publisher of scholarly articles: it is a pioneering approach to the world of academia, radically improving the way scholarly research is managed. The grand vision of Frontiers is a world where all people have an equal opportunity to seek, share and generate knowledge. Frontiers provides immediate and permanent online open access to all its publications, but this alone is not enough to realize our grand goals.

Frontiers Journal Series

The Frontiers Journal Series is a multi-tier and interdisciplinary set of open-access, online journals, promising a paradigm shift from the current review, selection and dissemination processes in academic publishing. All Frontiers journals are driven by researchers for researchers; therefore, they constitute a service to the scholarly community. At the same time, the Frontiers Journal Series operates on a revolutionary invention, the tiered publishing system, initially addressing specific communities of scholars, and gradually climbing up to broader public understanding, thus serving the interests of the lay society, too.

Dedication to Quality

Each Frontiers article is a landmark of the highest quality, thanks to genuinely collaborative interactions between authors and review editors, who include some of the world's best academicians. Research must be certified by peers before entering a stream of knowledge that may eventually reach the public - and shape society; therefore, Frontiers only applies the most rigorous and unbiased reviews.
Frontiers revolutionizes research publishing by freely delivering the most outstanding research, evaluated with no bias from both the academic and social point of view. By applying the most advanced information technologies, Frontiers is catapulting scholarly publishing into a new generation.

What are Frontiers Research Topics?

Frontiers Research Topics are very popular trademarks of the Frontiers Journals Series: they are collections of at least ten articles, all centered on a particular subject. With their unique mix of varied contributions from Original Research to Review Articles, Frontiers Research Topics unify the most influential researchers, the latest key findings and historical advances in a hot research area! Find out more on how to host your own Frontiers Research Topic or contribute to one as an author by contacting the Frontiers Editorial Office: frontiersin.org/about/contact

EXPLORATION OF NATURAL PRODUCT LEADS FOR MULTITARGET-BASED TREATMENT OF CANCER - COMPUTATIONAL TO EXPERIMENTAL JOURNEY

Topic Editors:
Rajeev K. Singla, Sichuan University, China
Marcus Scotti, Federal University of Paraíba, Brazil
Supratik Kar, Jackson State University, United States

Citation: Singla, R. K., Scotti, M., Kar, S., eds. (2022). Exploration of Natural Product Leads for Multitarget-Based Treatment of Cancer - Computational to Experimental Journey. Lausanne: Frontiers Media SA. doi: 10.3389/978-2-88974-686-6

Table of Contents

frontiers in Pharmacology

EDITORIAL
published: 22 February 2022
doi: 10.3389/fphar.2022.850151

Editorial: Exploration of Natural Product Leads for Multitarget-Based Treatment of Cancer—Computational to Experimental Journey

Rajeev K. Singla[1,2]*, *Marcus T. Scotti*[3] *and Supratik Kar*[4]

[1]Institutes for Systems Genetics, Frontiers Science Center for Disease-Related Molecular Network, West China Hospital, Sichuan University, Chengdu, China, [2]iGlobal Research and Publishing Foundation, New Delhi, India, [3]Postgraduate Program in Natural and Synthetic Bioactive Products, Federal University of Paraíba, João Pessoa, Brazil, [4]Interdisciplinary Center for Nanotoxicity, Department of Chemistry, Physics and Atmospheric Sciences, Jackson State University, Jackson, MS, United States

Keywords: secondary metabolites, natural anti-cancer agents, herbal medicine, anti-cancer lead, chembioinformatics

Editorial on the Research Topic

Exploration of Natural Product Leads for Multitarget-Based Treatment of Cancer—Computational to Experimental Journey

Natural products are being used for the treatment of various diseases and disorders. A series of studies are undergoing from computational to clinical level to assess the translational potential of natural products (Scotti et al., 2016; Singla and Dubey, 2019; Singla et al., 2019; Kapusta et al., 2020; Singla et al., 2021a; Bansal et al., 2021; Singla et al.; Singla et al., 2021c; Dk and Nj, 2021; Singla et al.; Singla et al., 2021e; Singla et al.; Madaan et al., 2021; Marzocco et al., 2021; Okoh et al.; Talukdar et al., 2021). Cancer is one of the major public health burdens significantly impacting on a global level to both developed as well as the developing countries (Bray et al., 2018; Singla et al., 2021e; Qi et al., 2021; Joon et al., 2022). Specifically for the poor and underdeveloped countries, it is quite important to find cost-effective and sustainable resources for the treatment and management of cancer, as it will reduce the financial strain on them (Suryanarayana Raju et al., 2015; Singla et al.). Further, the high vulnerability to the point mutations leading to the development of resistance to the existing anticancer drugs, it is relevant to explore new multitarget leads to overcome resistance. This research topic was thus devised to collect the studies where natural products have been investigated for their multitarget potential against cancer.

Liu et al., in their article "Targets and Mechanism Used by Cinnamaldehyde, the Main Active Ingredient in Cinnamon, in the Treatment of Breast Cancer", had used both *in silico* and *in vitro* methodologies for the screening of targets for the bioactive constituents against breast cancer. They had utilized information from various databases, including TCMSP, TCMID, OMIM, etc, and various bioinformatic tools like STRING, Cytoscape, Gene ontology, KEGG, etc for the analysis of relationship between cinnamon phytoconstituents and breast cancer's targets. Results from both the computational and experimental studies led them to conclude cinnamaldehyde as a promising multifunctional molecule.

Yuan et al., in their article "Transcriptome Profiling and Cytological Assessments for Identifying Regulatory Pathways Associated With Diorcinol N-Induced Autophagy in A3 Cells" had noticed the potential of a fungal originated secondary metabolite, Diorcinol N for the treatment and management of acute lymphoblastic leukemia. The authors had utilized both the bioinformatic

OPEN ACCESS

Edited and reviewed by:
Javier Echeverria,
University of Santiago, Chile

***Correspondence:**
Rajeev K. Singla
rajeevsingla26@gmail.com

Specialty section:
This article was submitted to Ethnopharmacology, a section of the journal Frontiers in Pharmacology

Received: *07 January 2022*
Accepted: *31 January 2022*
Published: *22 February 2022*

Citation:
Singla RK, Scotti MT and Kar S (2022) Editorial: Exploration of Natural Product Leads for Multitarget-Based Treatment of Cancer—Computational to Experimental Journey. Front. Pharmacol. 13:850151. doi: 10.3389/fphar.2022.850151

tools and *in vitro* methodologies. Diorcinol N was capable of controlling the growth of A3 leukemia cells in a multimodal way.

Wei et al., in their article "Computational and *In Vitro* Analysis of Plumbagin's Molecular Mechanism for the Treatment of Hepatocellular Carcinoma" had studied Plumbagin, naphthoquinone from *Plumbago zeylanica* L., for the treatment and management of hepatocellular carcinoma. Results from the network pharmacology-based analysis were further validated experimentally using the human hepatocellular carcinoma cell lines, SMMC-7721 and BEL-7404. To combat hepatocellular carcinoma, authors had observed that Plumbagin was able to exert anticancer effects *via* multiple targets and signaling pathways, including that related to oxidative stress, autophagy, and apoptosis.

Jiang et al. In their article "Network Pharmacology and Pharmacological Evaluation Reveals the Mechanism of the Sanguisorba Officinalis in Suppressing Hepatocellular Carcinoma" had identified 41 bioactive ingredients from *Sanguisorba Officinalis* by utilizing some databases like TCMSP and BATMAN-TCM, which then reduced to 12 after filtering through ADME parameters. Network pharmacology approaches were used to analyze those 12 compounds against the selected targets of hepatocellular carcinoma. The results were validated experimentally using human hepatocellular carcinoma cell lines, HepG2, MHCC97H, SMCC7721, and BEL-7404. Based on the bioinformatics analysis, they noticed four compounds like quercetin, kaempferol, mairin, and beta-sitosterol. Overall, they had concluded the significance of *Sanguisorba Officinalis* as an anticancer agent against hepatocellular carcinoma.

Rahman et al., in their review article "Phytochemicals as a Complement to Cancer Chemotherapy: Pharmacological Modulation of the Autophagy-Apoptosis Pathway" had critically analyzed and compiled the knowledge about the plant-based natural products which were having potential to modulate autophagy and apoptosis. The authors had represented the pathways well in the form of interactive figures. They illustrated the detailed pathways for the phytomolecules like 18-α-Glycyrrhetinic acid, Oxyresveratrol, and other polyphenolic and alkaloids. They had also indicated the phytochemicals which have currently been investigated in the clinical trials for the treatment and management of various types of cancer.

Ghanbari-Movahed et al., in their systematic review article "A Systematic Review of the Preventive and Therapeutic Effects of Naringin Against Human Malignancies" had covered several studies indicating the potential of naringin, either alone or synergistic with other drugs or as metal complexes for the treatment and management of various types of human malignancies. They had also specified the plant sources for naringin, all of which belong to the Citrus genus and Rutaceae family. They had reported the significance of naringin against various cancers like bladder, leukemia, lymphoma, brain, breast, cervical, colon, colorectal, esophageal, laryngeal, liver, lung, neuroblastoma, ovarian, prostate, osteosarcoma, chondrosarcoma, melanoma, gastric, and thyroid cancer. Thus, naringin is a multitarget and multiple signaling pathways acting bioactive molecule.

Rasool et al., in their article "Evaluation of the Anticancer Properties of Geranyl Isovalerate, an Active Ingredient of Argyreia nervosa Extract in Colorectal Cancer Cells" had evaluated the effect of geranyl isovalerate against HCT116 and HT29 cell lines related to colorectal cancer. The authors adopted various experimental methodologies for cytotoxicity, live and dead cell detection, JC-1 staining, generation of reactive oxygen species (ROS), genes related to apoptosis, and proteins related to apoptosis. Their results indicated the significance of geranyl isovalerate and generated further interest to assess the translational potential of this WHO-approved food additive as a food supplement.

Sampaio et al., in their systematic review article "Antitumor Effects of Carvacrol and Thymol: A Systematic Review" had covered the literature published from 2003 to 2021 and systematically analyzed the significance of carvacrol, and its isomeric analog, thymol, in the treatment and management of various types of cancer. Authors have recorded the scientific evidence claiming anticancer potential of these two molecules against cancers like that of breast, liver, colon, liver, lung, prostate, etc. Accordingly, authors have indicated various chemopreventive and antimetastatic effects of these molecules as per the recorded literature. Further studies on these molecules can provide vital information about their therapeutic and translational potential to reach the bedside.

Chavda et al., in their review article "Advanced Computational Methodologies Used in the Discovery of New Natural Anticancer Compounds" had discussed the utility aid of computational techniques in the advancement of natural products-based research with a focus on anticancer compounds. In Table 1, they had also discussed 25 natural compounds with details about their anticancer potential, while Table 2 briefly indicated the computational methodologies and tools used during natural anticancer research. Further, the illustrations made by authors represented the global cancer statistics, stepwise structure elucidation, and protocol for fragment-based screening. This article highlighted the crucial role of reliable computational methodologies in the translational process of natural anticancer agents.

Allegra et al., in their article "Evaluation of the IKKβ Binding of Indicaxanthin by Induced-Fit Docking, Binding Pose Metadynamics, and Molecular Dynamics" had assessed the molecular level mechanistic information related to the inhibition of hIKKβ by Indicaxanthin (a betaxanthin from betalain class), using computational tools and techniques like induced-fit docking, binding pose metadynamics, MD simulations, as well as MM-GBSA binding free energy calculation. Previous reports indicated that Indicaxanthin exhibited activity against human melanoma cells by modulating NF-κB and ceasing IκBα degradation. This had generated interest in the team of Mario to explore the mechanisms further on the molecular level, and their results have indeed provided insights and significant knowledge for readers and researchers.

Nuclear factor-κB signalling pathway is a significant and well-known factor influencing immunity, inflammation, cancer, and functioning of the nervous system (Liu et al., 2017; Albensi, 2019).

Uddin et al., in their review article "Natural Small Molecules Targeting NF-κB Signaling in Glioblastoma" had discussed the structural and functional properties of NF-κB, role of NF-κB in glioblastoma, as well as the information about small natural products like resveratrol, quercetin, apigenin, isothiocyanates, sulforaphane, etc which were able to target NF-κB in glioblastoma. This article will be interesting for the readers, researchers, and clinicians to explore the translational potential of these natural products for the treatment and management of the most aggressive brain cancer, glioblastoma multiforme.

Crotoxin, a major constituent from the venom of *Crotalus durissus* terrificus, is a known for its pharmacological actions like anticancer activity against breast cancer (Almeida et al., 2021), pain alleviation (Teixeira et al., 2020), antithrombotic (de Andrade et al., 2019), etc, along with its venomous effects. Kato et al., in their research article "Crotoxin Inhibits Endothelial Cell Functions in Two- and Three-dimensional Tumor Microenvironment" studied the antiangiogenic role of the crotoxin in detail and mentioned as to how it will be supportive in the inhibition of tumor progression.

Feng et al. in their research article "Downregulation of ATP1A1 Expression by Panax notoginseng (Burk.) F.H. Chen Saponins: A Potential Mechanism of Antitumor Effects in HepG2 Cells and *In Vivo*", had evaluated the saponin enriched formulation (commercial source containing notoginsenoside R1, ginsenoside Rg1, ginsenoside Re, ginsenoside Rb1, and ginsenoside Rd) of *Panax notoginseng* (Burk.) F.H. Chen against ATP1A1, an important target for the treatment and management of hepatic carcinoma. They had noticed that the saponin enriched formulation was able to downregulate ATP1A1 and its associated signaling pathway when observed in HepG2 cells. These observations will increase the interest of clinicians' and researchers' interest in assessing the translational potential of this saponin enriched formulation of *Panax notoginseng* (Burk.) F.H. Chen.

Singla et al., in their review article "Natural Product-Based Studies for the Management of Castration-Resistant Prostate Cancer: Computational to Clinical Studies", had covered the literature from last 36 years, and analysed the information about natural products which were effective against castration-resistant prostate cancer (CRPC). They had covered the epidemiology, tumor microenvironment, signaling pathways, genomic targets related information of CRPC. They had covered the computational studies, preclinical studies, and clinical studies that had proved the therapeutic potential of the natural products against CRPC. Clinical studies are undergoing for the phytomolecules like curcumin, EGCG, gossypol, quercetin, lycopene, soy isoflavones, and resveratrol. These observations will increase the interest of clinicians and researchers to assess the translational potential of natural products for the treatment and management of CRPC.

This research topic "Exploration of Natural Product Leads for Multitarget-Based Treatment of Cancer - Computational to Experimental Journey" has been successful in collecting 14 articles: 4 review articles, 2 systematic reviews, and 8 research articles, covering scientific literature pertaining to acute lymphoblastic leukemia, breast cancer, hepatocellular carcinoma, colorectal cancer, melanoma, glioblastoma, and castration-resistant prostate cancer. This research topic has its significance because it has further the knowledge about various natural products like carvacrol, thymol, naringin, diorcinol-N, cinnamaldehyde, plumbagin, crotoxin, geranyl isovalerate, indicaxanthin, *Sanguisorba Officinalis* L., and *Panax notoginseng* (Burk.) F.H. Chen Saponins.

We express our thanks to all the authors for contributing wonderful works in our research topic. To disseminate the knowledge to a wider audience, social media tools are of immense significance. The utilization of hashtags like #INPST, #NPMND and #DHPSP on Twitter or other social media resulted in the greater circulation of the articles and is being considered as digital health promotion (Kletecka-Pulker et al., 2021; Singla, 2021). We strongly encourage the authors and readers to use these hashtags to further promote their scientific literature. Moreover, twitter users can quote @FrontPharmacol to promote their articles published in Frontiers in Pharmacology.

AUTHOR CONTRIBUTIONS

RS, MS, and SK have collectively conceived and written the text. All authors contributed to the article and approved the submitted version.

REFERENCES

Albensi, B. C. (2019). What Is Nuclear Factor Kappa B (NF-Kb) Doing in and to the Mitochondrion. *Front Cel Dev Biol* 7, 154. doi:10.3389/fcell.2019.00154

Almeida, C. F., Amaral, C., Augusto, T. V., Correia-da-Silva, G., Marques de Andrade, C., Torqueti, M. R., et al. (2021). The Anti-cancer Potential of Crotoxin in Estrogen Receptor-Positive Breast Cancer: Its Effects and Mechanism of Action. *Toxicon* 200, 69–77. doi:10.1016/j.toxicon.2021.07.003

Bansal, H., Singla, R. K., Behzad, S., Chopra, H., Grewal, A. S., and Shen, B. (2021). Unleashing the Potential of Microbial Natural Products in Drug Discovery: Focusing on Streptomyces as Antimicrobials Goldmine. *Curr. Top. Med. Chem.* 21 (26), 2374–2396. doi:10.2174/1568026621666210916170110

Bray, F., Ferlay, J., Soerjomataram, I., Siegel, R. L., Torre, L. A., and Jemal, A. (2018). Global Cancer Statistics 2018: GLOBOCAN Estimates of Incidence and Mortality Worldwide for 36 Cancers in 185 Countries. *CA Cancer J. Clin.* 68 (6), 394–424. doi:10.3322/caac.21492

D, S. R., Kumar, T. N. V. G., Mathew, J., JeyaprakashKandale, A., Kandale, A., and Singla, R. K. (2015). Synthesis & Biological Evaluation of 1, 3, 4- Oxadiazoles as Anticancer Agents. *Igjps* 05 (01), 01–05. doi:10.35652/igjps.2015.17

de Andrade, C. M., Rey, F. M., Bianchini, F. J., Sampaio, S. V., and Torqueti, M. R. (2019). Crotoxin, a Neurotoxin from *Crotalus durissus* Terrificus Snake Venom, as a Potential Tool against Thrombosis Development. *Int. J. Biol. Macromol* 134, 653–659. doi:10.1016/j.ijbiomac.2019.05.018

Dk, D., and Nj, P. (2021). Anti-Inflammatory Effect of Neuracanthus Sphaerostachyus Dalz. Leaves on Experimental Colitis in Rats. *Igjps* 11 (01), 07–14. doi:10.35652/igjps.2021.111002

Joon, S., Singla, R. K., Shen, B., and Kamal, M. A. (2022). QSCR Analysis of Cytotoxicity of 6-Fluoro-3-(4h-1,2,4-Triazol-3- Yl)quinolin-4(1h)-Ones on Chinese Hamster Ovary Cell Line: Design of REPUBLIC1986. *Curr. Med. Chem.* 29 (2), 369–379. doi:10.2174/0929867328666210623150552

Kapusta, K., Kar, S., Collins, J. T., Franklin, L. M., Kolodziejczyk, W., Leszczynski, J., et al. (2020). Protein Reliability Analysis and Virtual Screening of Natural Inhibitors for SARS-CoV-2 Main Protease (Mpro) through Docking, Molecular

Mechanic & Dynamic, and ADMET Profiling. *J. Biomol. Struct. Dyn.* 39 (17), 1–18. doi:10.1080/07391102.2020.1806930

Kletecka-Pulker, M., Mondal, H., Wang, D., Parra, R. G., Maigoro, A. Y., Lee, S., et al. (2021). Impacts of Biomedical Hashtag-Based Twitter Campaign: #DHPSP Utilization for Promotion of Open Innovation in Digital Health, Patient Safety, and Personalized Medicine. *Curr. Res. Biotechnol.* 3, 146–153. doi:10.1016/j.crbiot.2021.04.004

Liu, T., Zhang, L., Joo, D., and Sun, S. C. (2017). NF-κB Signaling in Inflammation. *Signal. Transduct Target. Ther.* 2 (1). doi:10.1038/sigtrans.2017.23

Madaan, R., Singla, R. K., Kumar, S., Dubey, A. K., Kumar, D., Sharma, P., et al. (2021). Bergenin - A Biologically Active Scaffold: Nanotechnological Perspectives. *Ctmc* 21. doi:10.2174/1568026621666211015092654

Marzocco, S., Singla, R. K., and Capasso, A. (2021). Multifaceted Effects of Lycopene: A Boulevard to the Multitarget-Based Treatment for Cancer. *Molecules* 26 (17). doi:10.3390/molecules26175333

Qi, X., Wang, R., Lin, Y., Yan, D., Zuo, J., Chen, J., et al. (2021). A Ferroptosis-Related Gene Signature Identified as a Novel Prognostic Biomarker for Colon Cancer. *Front. Genet.* 12. doi:10.3389/fgene.2021.692426

Scotti, L., Singla, R. K., Ishiki, H. M., MendoncaMendonca, F. J. F., da Silva, M. S., Barbosa Filho, J. M., et al. (2016). Recent Advancement in Natural Hyaluronidase Inhibitors. *Curr. Top. Med. Chem.* 16 (23), 2525–2531. doi:10.2174/1568026616666160414123857

Singla, R. K., and Dubey, A. K. (2019). Molecules and Metabolites from Natural Products as Inhibitors of Biofilm in Candida Spp. Pathogens. *Curr. Top. Med. Chem.* 19 (28), 2567–2578. doi:10.2174/1568026619666191025154834

Singla, R. K., Gupta, R., Joon, S., Gupta, A. K., and Shen, B. (2021c). Isolation, Docking and In Silico ADME-T Studies of Acacianol: Novel Antibacterial Isoflavone Analogue Isolated from Acacia Leucophloea Bark. *Curr. Drug Metab.* 22 (11), 893–904. doi:10.2174/1389200222666211005091417

Singla, R. K., Kumar, R., Khan, S., MohitKumari, K., Kumari, K., and Garg, A. (2019). Natural Products: Potential Source of DPP-IV Inhibitors. *Curr. Protein Pept. Sci.* 20 (12), 1218–1225. doi:10.2174/1389203720666190502154129

Singla, R. K., Sai, C. S., Chopra, H., Behzad, S., Bansal, H., Goyal, R., et al. (2021e). Natural Products for the Management of Castration-Resistant Prostate Cancer: Special Focus on Nanoparticles Based Studies. *Front. Cel Dev Biol* 9, 745177. doi:10.3389/fcell.2021.745177

Singla, R. K. (2021). Secondary Metabolites as Treatment of Choice for Metabolic Disorders and Infectious Diseases and Their Metabolic Profiling - Part 3. *Curr. Drug Metab.* 22 (6), 412–414. doi:10.2174/1389200222062107081030l9

Singla, R. K., Agarwal, T., He, X., and Shen, B. (2021a). Herbal Resources to Combat a Progressive & Degenerative Nervous System Disorder- Parkinson's Disease. *Cdt* 22 (6), 609–630. doi:10.2174/1389450121999201013155202

Talukdar, N., Devi, R., and Barman, I. (2021). A Comparative Study between Aqueous and Ethanolic Extracts of Allium Odorum Linn with Reference to its Antioxidant and AlphaAmylase Inhibition Activities. *Igjps* 11 (01), 56–61. doi:10.35652/igjps.2021.111008

Teixeira, N. B., Sant'Anna, M. B., Giardini, A. C., Araujo, L. P., Fonseca, L. A., Basso, A. S., et al. (2020). Crotoxin Down-Modulates Pro-inflammatory Cells and Alleviates Pain on the MOG35-55-Induced Experimental Autoimmune Encephalomyelitis, an Animal Model of Multiple Sclerosis. *Brain Behav. Immun.* 84, 253–268. doi:10.1016/j.bbi.2019.12.009

Conflict of Interest: The authors declare that the research was conducted in the absence of any commercial or financial relationships that could be construed as a potential conflict of interest.

Publisher's Note: All claims expressed in this article are solely those of the authors and do not necessarily represent those of their affiliated organizations, or those of the publisher, the editors and the reviewers. Any product that may be evaluated in this article, or claim that may be made by its manufacturer, is not guaranteed or endorsed by the publisher.

frontiers in Pharmacology

ORIGINAL RESEARCH
published: 15 October 2020
doi: 10.3389/fphar.2020.570450

Transcriptome Profiling and Cytological Assessments for Identifying Regulatory Pathways Associated With Diorcinol N-Induced Autophagy in A3 Cells

Xiao-Long Yuan[1], Xiu-Qi Li[1,2], Kuo Xu[1], Xiao-Dong Hou[1], Zhong-Feng Zhang[1], Lin Xue[3], Xin-Min Liu[1] and Peng Zhang[1]**

[1] Tobacco Research Institute, Chinese Academy of Agricultural Sciences, Qingdao, China, [2] Graduate School of Chinese Academy of Agricultural Sciences, Beijing, China, [3] Wannan Tobacco Group Company Limited, Xuancheng, China

OPEN ACCESS

Edited by:
Rajeev K. Singla,
Sichuan University, China

Reviewed by:
Qian Sun,
Institute of Systems Genetics, China
Manos Christos Vlasiou,
University of Nicosia, Cyprus

***Correspondence:**
Xin-Min Liu
liuxinmin@caas.cn
Peng Zhang
zhangpeng@caas.cn

Specialty section:
This article was submitted to Ethnopharmacology, a section of the journal Frontiers in Pharmacology

Received: 15 July 2020
Accepted: 09 September 2020
Published: 15 October 2020

Citation:
Yuan X-L, Li X-Q, Xu K, Hou X-D, Zhang Z-F, Xue L, Liu X-M and Zhang P (2020) Transcriptome Profiling and Cytological Assessments for Identifying Regulatory Pathways Associated With Diorcinol N-Induced Autophagy in A3 Cells. Front. Pharmacol. 11:570450. doi: 10.3389/fphar.2020.570450

Fungal secondary metabolites serve as a rich resource for exploring lead compounds with medicinal importance. Diorcinol N (DN), a fungal secondary metabolite isolated from an endophytic fungus, *Arthrinium arundinis*, exhibits robust anticancer activity. However, the anticancer mechanism of DN remains unclear. In this study, we examined the growth-inhibitory effect of DN on different human cancer cell lines. We found that DN decreased the viability of A3 T-cell leukemia cells in a time- and concentration-dependent manner. Transcriptome analysis indicated that DN modulated the transcriptome of A3 cells. In total, 9,340 differentially expressed genes were found, among which 4,378 downregulated genes and 4,962 upregulated genes were mainly involved in autophagy, cell cycle, and DNA replication. Furthermore, we demonstrated that DN induced autophagy, cell cycle arrest in the G1/S phase, and downregulated the expression of autophagy- and cell cycle-related genes in A3 cells. By labeling A3 cells with acridine orange/ethidium bromide, Hoechst 33,258, and monodansylcadaverine and *via* transmission electron microscopy, we found that DN increased plasma membrane permeability, structural disorganization, vacuolation, and autophagosome formation. Our study provides evidence for the mechanism of anticancer activity of DN in T-cell leukemia (A3) cells and demonstrates the promise of DN as a lead or even candidate molecule for the treatment of acute lymphoblastic leukemia.

Keywords: acute lymphocytic leukemia, autophagy, diorcinol N, G1/S phase arrest, transcriptome profiling

INTRODUCTION

Acute lymphoblastic leukemia (ALL) is a hematological malignancy associated with uncontrolled proliferation and transformation of lymphoid progenitor cells within the bone marrow (Soulier and Cortes, 2015). Over the past few decades, the revolution in tumor cell biology and chemotherapeutic strategies coupled with high-throughput sequencing has led to significant improvement in outcomes for pediatric patients (Hunger and Mullighan, 2015). The survival rate of leukemia patients can reach 90% in children under 14 years of age, while it can decrease to 40% in adults between 25 and 64 years of age and to almost 15% in adults aged over 65 (Curran and Stock, 2015; Hunger and Mullighan, 2015; Kansagra et al., 2018). The poor prognosis for the elderly is because of the ease of metastasis to different organs and frequent relapse (Aldoss and Stein, 2018). The most difficult problem is in the treatment of hematologic malignancies is that few treatments show the desired therapeutic efficacy or achieve complete responses (Phelan and Advani, 2018). Further, the use of localized surgery and radiation approaches may not always be possible to prevent the dissemination of tumor cells (Malard and Mohty, 2020). To date, chemotherapy is the most preferred treatment of choice for these patients (Paul et al., 2017). Therefore, there is an urgent need to develop novel therapies that overcome resistance to the currently administered anticancer drugs for ALL cells.

Secondary metabolites, especially those produced by endophytic fungi, have been demonstrated to be rich sources of not only anticancer lead compounds with high potential against ALL cells, but have also contributed significantly to the discovery of novel drugs (Deshmukh et al., 2019). For example, Ophiobolins A, B, C, and K, obtained from three fungal strains in the Aspergillus section Usti, could reduce leukemia cell viability and induce cell apoptosis at nanomolar concentrations. Secalonic acid D, isolated as a secondary metabolite of the mangrove endophytic fungus No ZSU44, exhibited potent cytotoxicity to ALL cells. Further studies have indicated that secalonic acid D led to cell cycle arrest of G1 phase related to the downregulation of c-Myc *via* activation of GSK-3β, followed by degradation of β-catenin. Consequently, it is necessary to explore more secondary metabolites in endophytic fungi and to investigate their potential anticancer activity.

Diorcinols are prenylated diphenyl ether derivatives that are isolated from numerous endophytic fungi and possess various biological activities. For example, diorcinol D, which was isolated from an endolichenic fungus, showed fungicidal activity against *Candida albicans* by destroying the cytoplasmic membrane and generating reactive oxygen species (ROS) (Li et al., 2015). Diorcinol J, which was produced by co-cultivation of marine fungi, *Aspergillus sulphureus* and *Isaria feline*, can induce the expression of heat shock protein (Hsp70) in Ehrlich ascites carcinoma cells (Zhuravleva et al., 2016). Recently, in our ongoing search for structurally diverse metabolites with novel cytotoxic mechanisms, a new prenylated diphenyl ether, diorcinol N (DN), was isolated and identified from an endophytic fungus *Arthrinium arundini*, which was collected from fresh leaves of *Nicotiana tabacum* L. (Zhang et al., 2018). DN displayed promising cytotoxicity against the human THP-1 monocytic cell line in a cytotoxic assay (Li et al., 2018).

Thus, DN appears to be a potential candidate for blood cancer treatment and can be used as a lead for the development of novel, targeted anti-leukemia drugs. In this study, we performed cell-based assays and transcriptome profiling to investigate the anticancer mechanism of DN. First, we studied the effects of DN on the viability of selected human cancer cell lines. Transcriptome analysis was used to analyze DN-regulated genes and related signaling pathways that are responsible for growth and autophagy in A3 cells. In addition, the molecular mechanism of growth inhibition and autophagy induction by DN in this cell line was investigated *via* ultrastructural observation, flow cytometry, and quantitative reverse-transcription polymerase chain reaction (qRT-PCR).

Abbreviations: ALL, Acute Lymphoblastic Leukemia; AO/EB, Acridine Orange/Ethidium Bromide; AMPK, Adenosine 5'-monophosphate (AMP)-Activated Protein Kinase; ATG, Autophagy-Related Gene; CCK-8, Cell Counting Kit-8; CDK, Cyclin-Dependent Kinase; CycD, Cyclin D; CycE, Cyclin E; DMSO, Dimethyl Sulfoxide; DN, Diorcinol N; EtOAc, Ethyl Acetate; FBS, Fetal Bovine Serum; FC, Fold Change; FCS, Fetal Calf Serum; FoxO, Forkhead Box; FPKM, Fragments Per Kilobase Of Transcript Of Exon Model Per Million Reads Mapped; GAPDH, Glyceraldehyde-3-Phosphate Dehydrogenase; GO, Gene Ontology; HPLC, High Performance Liquid Chromatography; HRESIMS, High Resolution Electrospray Ionization Mass Spectrometry; IC_{50}, The Half Maximal Inhibitory Concentration; KEGG, Kyoto Encyclopedia of Genes and Genomes; MCM2, Minichromosome Maintenance Complex Component 2; MDC, Monodansylcadaverine; MEM, Minimum Essential Medium; MeOH, Methanol; mTOR, Mammalian Target of Rapamycin; NMR, Nuclear Magnetic Resonance; p21, Cyclin-Dependent Kinase Inhibitor 1α; p27, Cyclin-Dependent Kinase Inhibitor 1β; PBMCs, Peripheral Blood Mononuclear Cells; PBS, Phosphate-Buffered Saline; PE, Petroleum Ether; PI3K, Phosphoinositide 3-Kinase; qRT-PCR, Quantitative Reverse-Transcription Polymerase Chain Reaction; RNase H, Reverse Transcriptase H; ROS, Reactive Oxygen Species; RP, Reverse Phase; RPMI, Roswell Park Memorial Institute; RT, Reverse Transcription; SE, Standard Error; TBST, Tris-buffered saline containing 0.1% Tween 20; TEM, Transmission Electron Microscopy; TGFβ, Transforming Growth Factor Beta; TNF, Tumor Necrosis Factor.

MATERIALS AND METHODS

Chemicals and Fungal Material

High-performance liquid chromatography (HPLC) was performed using a Waters ultra-performance liquid chromatography-class system equipped with a C_{18} column (1.6 μm, 2.1 × 50 mm) and a photodiode array detector. The chromatographic conditions were as follows: mobile phase: 10% methanol (MeOH), 0–5 min; 10%–100% MeOH, 5–35 min; 100% MeOH, 35–45 min; 100%–10% MeOH, 45–50 min; 10% MeOH, 50–60 min; flow rate: 1 ml/min; ultraviolet detection: 235 nm. High-resolution electrospray ionization mass spectrometry (HRESIMS) data were obtained with a Thermo Scientific LTQ Orbitrap XL spectrometer (Thermo Scientific, Waltham, MA, USA). The ^{1}H, ^{13}C, and two-dimensional nuclear magnetic resonance (NMR) spectra were measured using an Agilent DD2 spectrometer (500 and 125 MHz, respectively) (Agilent, Santa Clara, CA, USA). Open column chromatography was performed using silica gel (200

−300 mesh, Qingdao Haiyang Chemical Factory, Qingdao, China), Lobar LiChroprep RP-18 (Merck, Darmstadt, Germany), and Sephadex LH-20 (Merck). All solvents used for HPLC, HRESIMS, and NMR analyses were of analytical grade (purchased from Merck, Darmstadt, Germany). The fungal strain, *A. arundinis*, was previously isolated from fresh leaves of *Nicotiana tabacum* L., with the GenBank number MK182939 and CGMCC number 14792 (Zhang et al., 2018).

Cell Cultures

All cell lines used in this study were purchased from the Chinese Academy of Sciences Committee on Type Culture Collection Cell Bank (Shanghai, China) and then conserved in the Tobacco Research Institute of Chinese Academy of Agricultural Sciences. The human lymphoblastic leukemia Jurkat and A3 cell lines and human lung cancer HCC827 cell lines were cultured using Roswell Park Memorial Institute (RPMI) 1640 medium (RPMI-1640; #A1049101, Invitrogen, Carlsbad, CA, USA) containing 10% fetal bovine serum (FBS; #16140071, Gibco, Carlsbad, CA, USA). The human breast cancer cell lines, MCF-7 and MDA-MB-231, human cervical cancer cell line, HeLa, and human prostate cancer cell lines DU-145 and PC-3, were cultured in Minimum Essential Medium (MEM; #10370021, Invitrogen, Carlsbad, CA, USA) supplemented with 10% FBS. The human lung cancer cell line, A549, was maintained in Ham's F-12K (Kaighn's) Medium (#21127022, Invitrogen, Carlsbad, CA, USA) supplemented with 10% FBS. We isolated peripheral blood mononuclear cells (PBMCs) *via* density-gradient centrifugation using a Lymphocyte Separation Solution (NakalaiTesque, Kyoto, Japan). Subsequently, we harvested the PBMCs by centrifugation at 1,500 rpm for 10 min at 22°C and then resuspended them in RPMI 1640 with 10% FBS (Gibco). All cells were cultured in a humidified atmosphere containing 5% CO_2 at 37°C.

Purification of DN From *A. arundinis*

The general isolation procedure for DN is shown in **Figure 1**. Details of fermentation, extraction, and isolation procedures have been reported previously (Zhang et al., 2018). Briefly, to obtain sufficient amounts of DN, large-scale fermentation was performed with the productive strain, *A. arundinis*, in liquid Potato Dextrose Broth medium. The broth (approximately 200 L) was extracted exhaustively with 100 L of ethyl acetate (EtOAc), which was evaporated to yield 86 g of residue. The residue was subjected to silica gel column chromatography with a mobile phase consisting of mixed petroleum ether (PE)-EtOAc (from 10:1 to 1:1, v/v) to yield four fractions (Frs. 1–4). Fr. 4 (8.0 g), eluting with PE-EtOAc 1:1, was applied to Lobar LiChroprep reverse phase (RP)-18 with a MeOH-H_2O gradient (from 1:9 to 1:0) to give three subfractions (Frs. 4.1–4.3). Fr. 4.3 was separated using silica gel (dichloromethane-MeOH 20:1), followed by Sephadex LH-20 (MeOH) to yield DN (120 mg). Finally, DN with a purity of more than 98% was obtained and dissolved in dimethyl sulfoxide (DMSO) to prepare a 100-mM stock solution. Since a large number of experiments have shown that 0.1% DMSO is not cytotoxic to different tumor cells (Chou et al., 2018; Chiang et al., 2019; Song et al., 2020), DN was diluted further in cell culture media for use in the treatment of cells, so that the final concentration of DMSO in wells was 0.1% at the highest concentration of DN used in the study. Viability assays showed that 0.1% DMSO was non-toxic to cells (data not shown). All solvents (EtOAc, PE, dichloromethane, MeOH, and DMSO) used for column chromatography were of chemical grade (purchased from Sinopharm Chemical Reagent Co., Ltd, Shanghai, China).

Cell Viability Analysis

The effects of DN on cell viability were investigated by using the Cell Counting Kit-8 (CCK-8) assay. Briefly, 3.0×10^4 cells/well

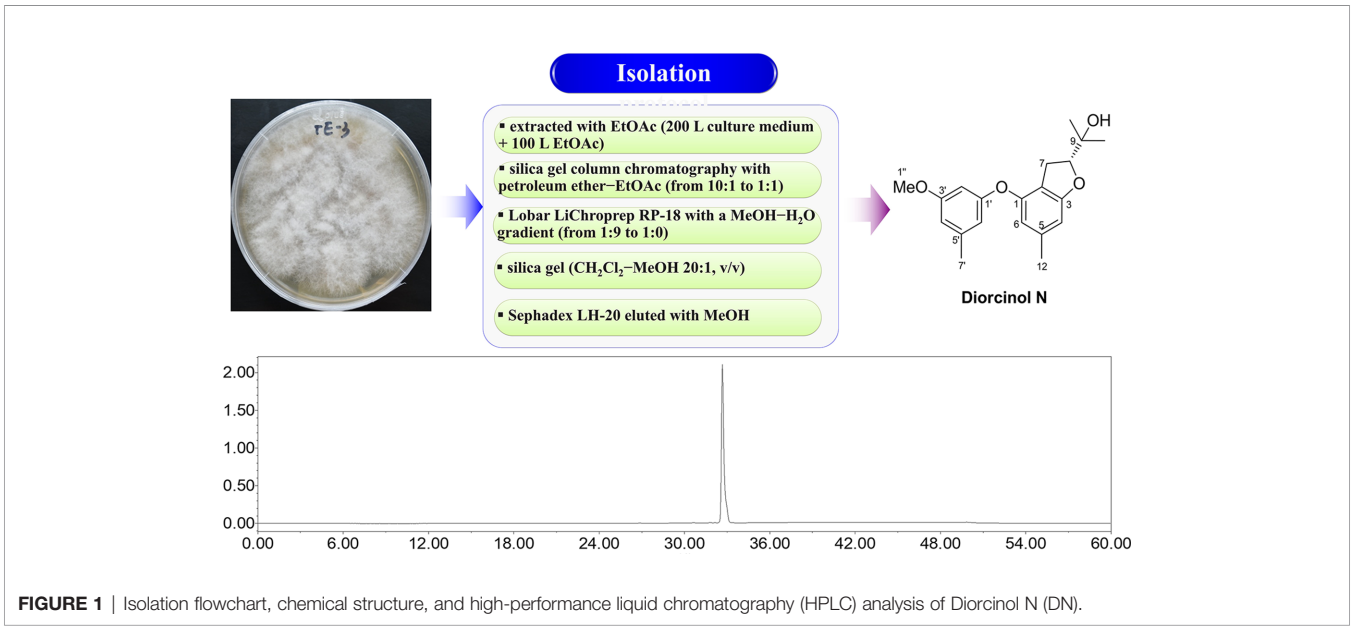

FIGURE 1 | Isolation flowchart, chemical structure, and high-performance liquid chromatography (HPLC) analysis of Diorcinol N (DN).

were seeded in 96-well plates for 24 h of incubation. Then, the cells were co-cultured for 24, 48, and 72 h with various concentrations of DN (0, 3.125, 6.25, 12.5, 25, 50, and 100 μM), after which cell viability was assessed using the CCK-8 Cell Proliferation and Cytotoxicity Assay Kit (#CA1210, Solarbio, Beijing, China). Absorbance was measured using a microplate spectrophotometer (Multiskan GO, Thermo Scientific, Waltham, MA, USA) at 490 nm.

Cell Cycle Analysis

After treatment with 6.25, 12.5, and 25 μM DN for 48 h, 1×10^6 A3 cells/ml were collected, washed three times with phosphate-buffered saline (PBS), and fixed overnight by incubation with 70% ethanol. The fixed cells were stained using a DNA Content Quantitation Assay Kit (#CA1510, Solarbio, Beijing, China) for cell cycle analysis. The test data were analyzed using Multicycle (Phoenix Flow Systems, San Diego, CA).

Fluorescence Microscopy

The morphology of A3 cells was observed by staining with acridine orange/ethidium bromide (AO/EB; Sigma-Aldrich Corp., St. Louis, MO, USA) and monodansylcadaverine (MDC; ab139484; Abcam), as described previously, and then with Hoechst 33258 (Wu et al., 2018; Laha et al., 2019; Zhang et al., 2020). Briefly, A3 cells were subjected to 6.25, 12.5, and 25 μM DN for 48 h for fluorescence microscopy. For AO/EB staining, cells were harvested and washed three times with PBS. Subsequently, the cells were stained with 0.1 ml of 4 μg/ml AO/EB solution (Sigma-Aldrich Corp., St. Louis, MO, USA) at 37°C in the dark for 15 min. For MDC labeling, resuspended cells were incubated with fluorescent dye at 37°C in the dark for 45 min. The cells were centrifuged and resuspended with 100 μl of assay buffer according to the manufacturer's protocol for the Autophagy Detection Kit (ab139484; Abcam). The remaining A3 cells were fixed with 70% ethanol and incubated with 1 μg/ml Hoechst 33258 solution (Sigma-Aldrich Corp., St. Louis, MO, USA) at room temperature for 10 min. A confocal laser scanning microscope was used to observe the morphology of each group of cells (Leica Microsystems, Hessen Wetzlar, Germany).

Cellular Ultrastructure Examination

Cellular ultrastructure was examined using conventional transmission electron microscopy (TEM), as described previously (Yuan et al., 2017). Briefly, A3 cells treated with different concentrations of DN (6.25, 12.5, and 25 μM) for 48 h were collected as mentioned in *Cell Cycle Analysis*. The cells were subsequently fixed with 2.5% glutaraldehyde (Analytical grade reagent; Sinopharm Chemical Reagent Co., Ltd, Beijing, China) containing 0.1 M sucrose (Analytical grade reagent; Sinopharm Chemical Reagent Co., Ltd) and 0.2 M sodium cacodylate (Analytical grade reagent; Sinopharm Chemical Reagent Co., Ltd) for 24 h at 4°C, followed by the addition of 10 g/L OsO_4 (Analytical grade reagent; Sinopharm Chemical Reagent Co., Ltd). The cells were then dehydrated, embedded in epoxy resin, cut into sections, and observed with an H700 transmission electron microscope (Hitachi, Tokyo, Japan).

RNA Extraction

A3 cells were treated with 12.5 and 25 μM DN for 48 h, while untreated A3 cells served as the control. Total RNA was isolated from each sample using the Cell RNA Kit (Omega Bio-Tek, Inc., Norcross, GA, USA) according to manufacturer's instructions. The quality and concentration of the RNA were estimated using a NanoPhotometer spectrophotometer (IMPLEN, Westlake Village, CA, USA), and the integrity of the RNA was detected on 1% agarose gels. High-quality RNAs were used for library construction and quantitative analysis.

Library Construction for Digital Gene Expression Sequencing

For RNA library construction, a total of 5 μg of RNA per sample was used as input to produce sequencing libraries using an NEBNext Ultra RNA Library Prep Kit for Illumina (NEB, Ipswich, MA, USA) according to the manufacturer's recommendations. During the process of library construction, a unique barcode was added to each sample to distinguish between the different samples. Briefly, we isolated and purified mRNA from total RNA using poly-T oligo-attached magnetic beads. The first strand of cDNA was synthesized using random hexamer primer and M-MuLV Reverse Transcriptase H (RNase H) from the fragmented RNAs. Then, the second strand of cDNA was synthesized using DNA polymerase I and RNase H. After repairing the cohesive ends with exonuclease/polymerase and adenylation of 3′ ends, a specific adapter was added in each sample through amplification. Finally, PCR products of length ranging from 150 bp to 200 bp were purified using AMPure beads (Beckman Coulter, Beverly, MA, USA). The quality and quantity of the final libraries were assessed by using an Agilent Bioanalyzer 2100 (Agilent Technologies, Palo Alto, CA, USA) before sequencing.

Analysis of Differentially Expressed Genes

After filtering reads containing adapter, reads containing ploy-N, and low-quality reads from raw data, clean data were mapped to the human genome. Then, the number of reads mapped to each gene were calculated using HTSeq v0.6.0 (Illumina Inc, Santa Clara, CA, USA). The differential expression between the DN-treated and control groups was calculated by using the DESeq R package (1.18.0). Their expression levels were measured using fragments per kilobase of transcript of exon model per million reads mapped (FPKM) values. Genes with an adjusted p-value <0.05 found using DESeq2 were considered to be differentially expressed.

Functional Annotation and Gene Ontology (GO)/Kyoto Encyclopedia of Genes and Genomes (KEGG) Enrichment Analysis

For functional annotation of differentially expressed genes, GOseq R package and KOBAS software were used to analyze GO enrichment and KEGG pathways, respectively (Kanehisa and Goto, 2000; Young et al., 2010; Kanehisa et al., 2016).

Real-Time Quantitative PCR Validation

Total RNA was extracted from the DN treated and control groups, as previously described in 2.8, and reverse-transcribed into cDNA using a PrimeScript™ reverse transcription (RT) reagent Kit

(Takara, Otsu, Japan) according to the manufacturer's instructions. Two other pairs of primers for glyceraldehyde-3-phosphate dehydrogenase (GAPDH) and β-actin were used as internal controls for normalization of gene expression, as shown in **Supplementary File S5**. Primers of 16 differentially expressed genes used for quantitative reverse-transcription polymerase chain reaction (qRT-PCR) analysis were designed using PrimerQuest (https://sg.idtdna.com/PrimerQuest/Home). The qRT-PCR was performed using LightCycler 480 (Roche, Basel, Switzerland). The reaction volume was 20 μl; it contained 10 μl of SYBR mix (#A25741, Thermo Fisher, Waltham, MA, USA), 0.6 μl of each primer, 2 μl of cDNA template, and 6.8 μl of RNase-free water. The thermocycling program was as follows: 95°C for 5 min, followed by 45 cycles of 95°C for 10 s, 57°C for 10 s, and 72°C for 20 s. Relative gene expression levels were calculated by using the $2^{-\Delta\Delta Ct}$ method (Zhang et al., 2020).

Western Blotting

A3 cells were treated with 6.25, 12.5, and 25 μM DN for 48 h, and harvested and washed with cold PBS. Total protein was extracted from RIPA Lysis Buffer (#P0013B, Beyotime, Shanghai, China) with 1% phenylmethyl sulfonylfluoride. The protein concentrations of different samples were determined using the BCA assay, as described previously (Heshmati et al., 2020). Proteins were electrophoresed using 8–15% SDS-PAGE and electrically transferred onto poly (vinylidene fluoride) membranes (ISEQ00010 0.22 μm, Millipore, MA, USA) successively. After blocking with 5% non-fat milk, the membranes were incubated with rabbit anti-AMPK, p-AMPK (Thr172), mTOR, p-mTOR (Ser2448), ATG1, p-ATG1 (Ser555), Beclin-1, p-Beclin-1 (Ser93), and GAPDH antibodies (Cell Signaling Technology, MA, USA) at 4°C overnight. After incubation, membranes were washed with Tris-buffered saline containing 0.1% Tween 20 (TBST) and incubated with horseradish peroxidase-conjugated secondary antibodies or anti-rabbit IgG antibodies for 1.5 h at room temperature. The proteins were visualized using Millipore's enhanced chemiluminescence (ECL) and detection system (ChemiDoc Touch, BioRad, Germany).

Statistical Analysis

In our study, three replicates were used for each treatment. Data are shown as means ± standard error (SE) of three replicates. The SPSS 21.0 software package (SPSS, Chicago, IL, USA) was used to detect statistically significant differences among different groups. Differences were considered statistically significant when $p < 0.05$.

RESULTS

Isolation of DN From *A. arundinis*

Repeated column chromatography using silica gel, a reversed-phase C_{18} column, and Sephadex LH-20 were used for compound isolation from *A. arundinis* cultures. The chemical structure of DN was determined using mass spectrometry and NMR. DN was isolated as a yellowish oil. Its molecular formula was established as $C_{20}H_{24}O_4$, as evidenced from the quasimolecular ion peak at *m/z* 327.1597 $[M - H]^-$ (calcd. for $C_{20}H_{23}O_4$, 327.1602) in its (–)-HRESIMS spectrum. The structure of DN was finally elucidated as a prenylated diphenyl ether by comparison of its NMR data with those reported previously in the literature (Zhang et al., 2020). HPLC analysis indicated that the purity of DN was > 98% (**Figure 1**).

In Vitro Growth Inhibitory Effect of DN

Growth inhibition effects induced by DN on different tumor cell lines were investigated using the CCK-8 assay. Six cancer cell lines were treated with different concentrations (0.39–50 μM) of DN for 48 h. DN showed concentration-dependent inhibitory effects on the growth of these different cancer cell lines (**Figure 2A**). However, the cell lines showed different levels of sensitivity to DN. The most remarkable effect was observed for A3 cells (IC_{50} = 16.31 μM) (**Figure 2A**). Since A3 cells are T cell leukemia cells, we examined the sensitivity of different leukemia cell lines to DN. Concentration- and time-dependent growth inhibition was observed for three leukemia cell lines, A3, Jurkat, and PBMCs (**Figures 2B–D**). As A3 cells were the most sensitive to DN compared to PBMCs and Jurkat cells, they were used in subsequent experiments.

DN Modulated the Transcription of Different Genes in A3 Cells

To investigate the anticancer mechanism of DN, transcriptional profiling analysis was performed for untreated A3 cells and A3 cells treated with different concentrations of DN. RNA-Seq was used to generate 65,926,953 reads in the 12.5 μM-DN-treated group, 45,756,714 reads in the 25-μM-DN-treated group, and 66,200,048 reads in the control group (**Table S1**). These reads were mapped to the human genome and the unique mapping rates were found to be over 80%, which represented 8400, 9340, and 9832 expressed genes, respectively (**Table S1**). Then, the expression levels of these genes were quantified based on FPKM values (**Figure 3A** and **Table S1**). These results indicated that compared to the control group, 2,964 and 3,011 genes were uniquely expressed in the 12.5-μM-DN- and 25-μM-DN-treated groups, respectively (**Figure 3B**). Using $P < 0.05$ and a 2-fold change (FC) as the conditions for discrimination, 8400 differentially expressed genes were found in the 12.5-μM-DN-treated group, among which 47.85% (4859) were downregulated and 42.15% (3541) were upregulated (**Figure 3C**, **Tables S2**, **S3**). Moreover, the number of differentially expressed genes rose as the concentration of DN increased (**Figure 3D**, **Tables S4**, **S5**). To assess the expression patterns of mRNAs at different concentrations of DN, heatmaps were used to determine overall transcriptomic differences. The heatmaps showed accurate repeatability and high reliability (**Figures 3E, F**).

GO and KEGG Enrichment Analyses of Differentially Expressed Genes in DN-Treated A3 Cells

Based on the *p*-value thresholds described above, the differentially expressed genes were divided into four clusters. Among four

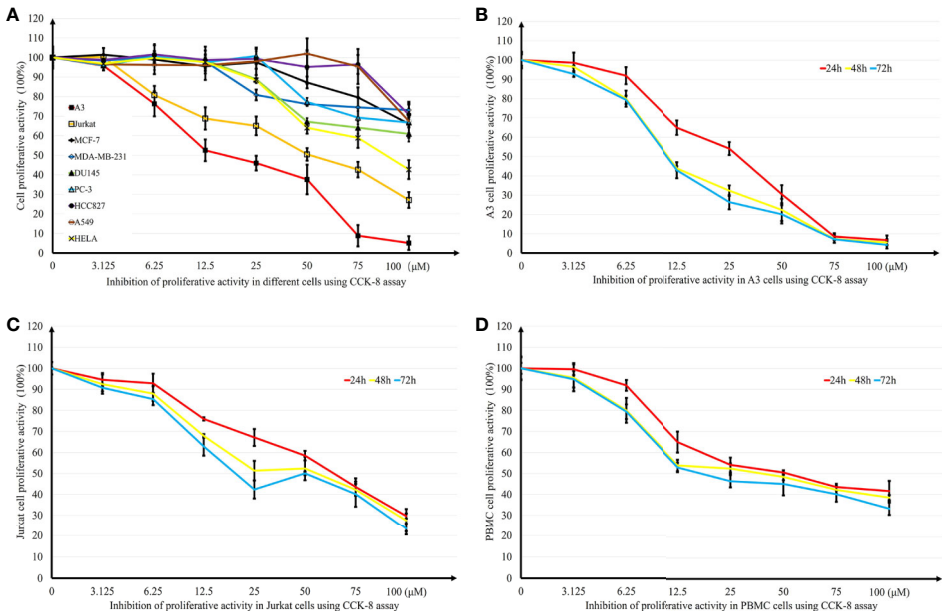

FIGURE 2 | Effects of Diorcinol N (DN) on cancer cell lines. **(A)** Inhibitory effects of DN on nine cancer cell lines (lymphoblastic leukemia cell lines A3 and Jurkat; breast cancer cell lines MCF-7 and MDA-MB-231; prostate cancer cell line DU-145 and PC-3; lung cancer cell line A549 and HCC827); cervical cancer cell line HeLa. **(B–D)** Inhibitory effects of DN on three leukemia cell lines: lymphoblastic leukemia cell lines, A3 and Jurkat, and human peripheral blood mononuclear cells (PBMCs). (n = 5).

clusters, clusters 3 was significantly enriched with 3,413 differentially expressed genes (**Figure S1**). In addition, cluster 2 containing 155 differentially expressed genes was significantly enriched as the upregulated cluster. To estimate the functions of genes that were differentially expressed between the treated and control groups, GO category and KEGG pathway analyses were performed for the differentially expressed genes. The enrichment of GO categories for these genes showed that the upregulated genes were mainly involved in the cellular response to endoplasmic reticulum stress, autophagy, mitochondrion disassembly, protein polyubiquitination, and vacuole organization (**Figure 4A**, **Tables S6**, **S7**), whereas the downregulated genes were mainly related to DNA replication, mitotic cell cycle phase transition, chromosome segregation, G1/S transition of mitotic cell cycle, and cell cycle G1/S phase transition (**Figure 4B**, **Tables S6**, **S7**). Analysis of the metabolic pathways in which these differentially expressed genes participated showed that the most enriched upregulated pathways were involved in adenosine 5'-monophosphate-activated protein kinase (AMPK) signaling, autophagy, epidermal growth factor receptor signaling, phagosome formation, Notch signaling, forkhead box O (FoxO) signaling, and tumor necrosis factor (TNF) signaling (**Figure 4C**, **Tables S8**, **S9**), whereas the most enriched downregulated gene pathways included cell cycle, DNA replication, oxidative phosphorylation, nucleotide excision repair, and mismatch repair (**Figure 4D**, **Tables S8**, **S9**). The effects of DN were most closely associated with the pathways of autophagy (**Figure S2**), cell cycle (**Figure S3**), and DNA replication (**Figure S4**), all of which can decrease cell viability. These findings indicate that DN may modulate A3 cell biological processes by inhibiting the cell cycle and inducing autophagy.

DN Induced G1/S-Phase Arrest in A3 Cells

To explore the effects of DN on the cell cycle of A3 cells, cells were treated with 6.25, 12.5, and 25 μM DN for 48 h and analyzed using flow cytometry. As shown in **Figures 5A, B**, treatment with DN significantly increased the cell population in the G1 phase from 54.55% for untreated cells to 79.31% for 25-μM-DN-treated A3 cells. Additionally, DN-treated cells showed a reduction in the population in S phase (18.15% (6.25 μM), 11.41% (12.5 μM), and 10.12% (25 μM DN)) from 24.3% for untreated cells, and a reduction in the population in the G2 phase (18.82% (6.25 μM), 14.95% (12.5 μM), and 10.81% (25 μM)) from 21.25% for untreated cells. These findings indicate that DN induced A3 cell cycle arrest in the G1/S phase.

DN Induced Autophagy in A3 Cells

To further examine the mechanism of anticancer activity in DN-treated A3 cells, cytological changes were observed using fluorescence microscopy and TEM. The results indicated that A3 cells showed dose-dependent autophagy-like cytological changes (**Figure 6**) after exposure to DN at doses ranging from 6.25 to 25 μM. The observed morphological features included elevated permeability (**Figure 6A**), atypical chromatin (**Figure 6B**), ultrastructural disorganization (**Figure 6C**), and autophagic vacuoles (**Figure 6C**). Furthermore, autophagic vacuoles were assessed using imaging studies with the use of MDC staining.

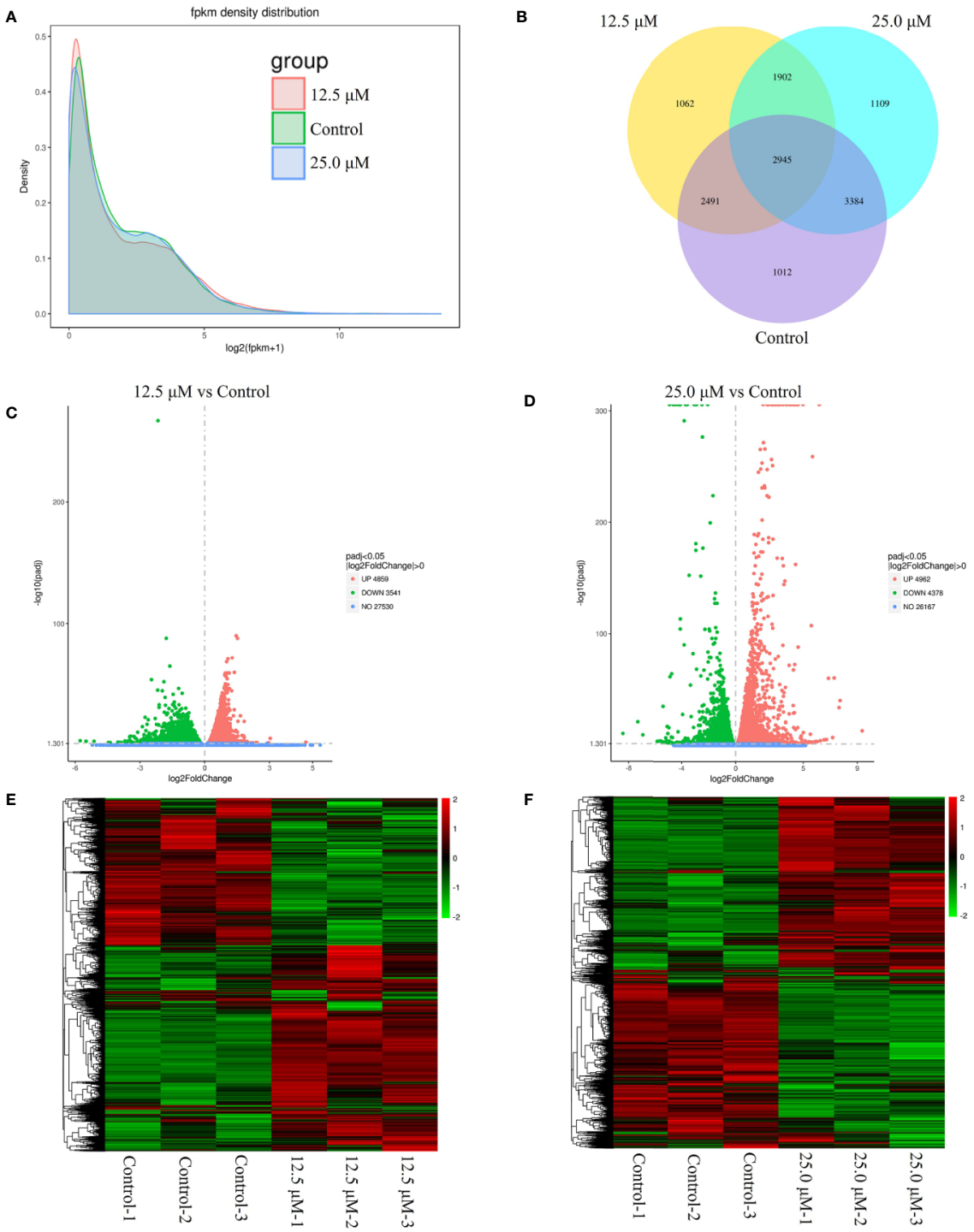

FIGURE 3 | Overview of genes that were differentially expressed between untreated cells and diorcinol N (DN)-treated (12.5 and 25 μM) A3 cells. **(A)** FPKM density distribution. **(B)** Venn diagram of the differentially expressed genes between DN-treated A3 cells and control cells. **(C)** Volcano diagram of the differentially expressed genes between 12.5-μM-DN-treated A3 cells and control cells. **(D)** Volcano diagram of the differentially expressed genes between 25.0-μM-DN-treated A3 cells and control cells. **(E)** Heatmaps of upregulated and downregulated genes in 12.5-μM-DN-treated A3 cells and control cells. **(F)** Heatmaps of upregulated and downregulated genes in 25-μM-DN-treated A3 cells and control cells. FPKM, fragments per kilobase of transcript of exon model per million reads mapped.

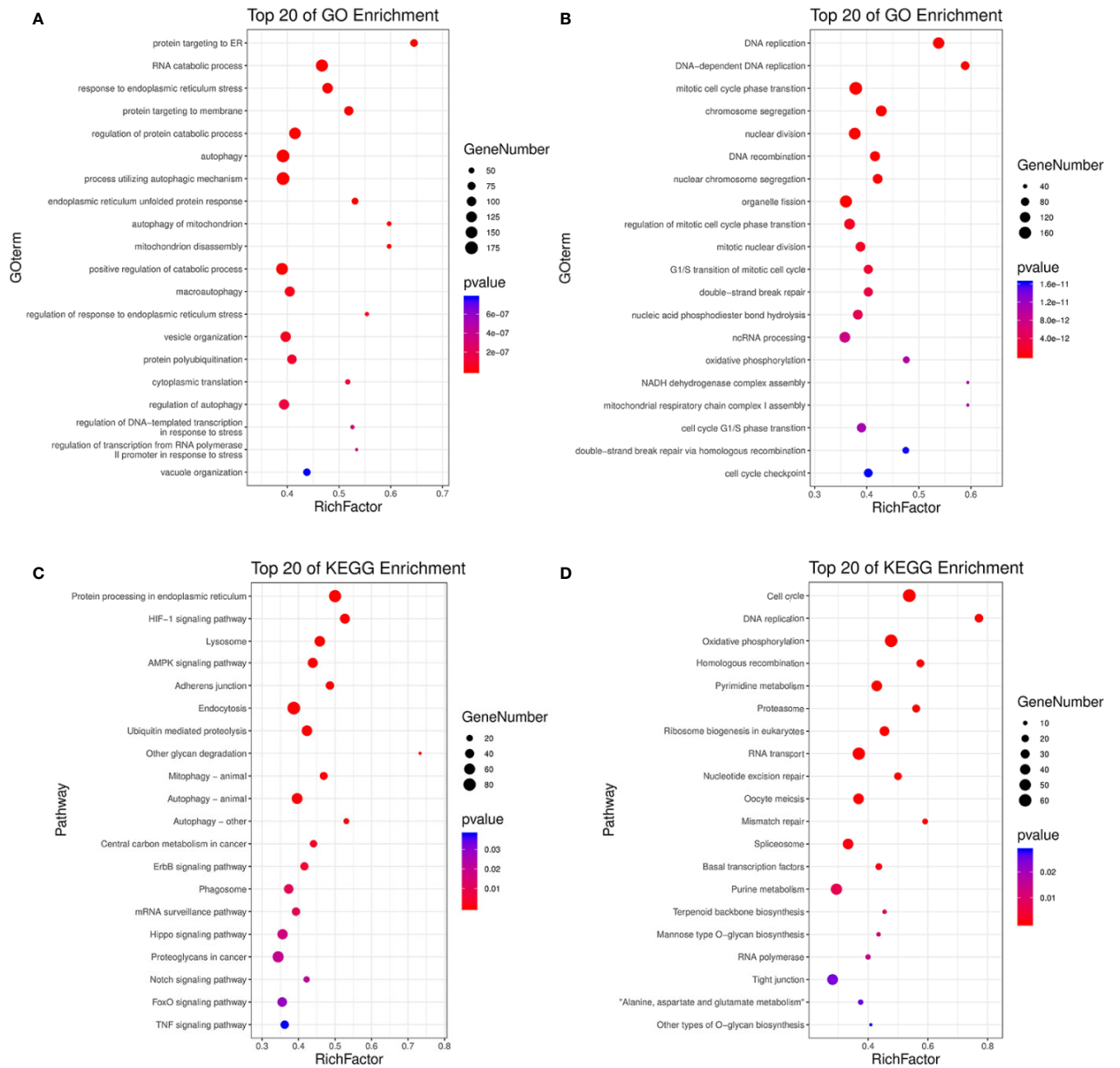

FIGURE 4 | GO and KEGG analyses of differentially expressed genes. **(A, B)** Upregulated and downregulated genes linked with GO enrichment terms. **(C, D)** Upregulated and downregulated genes that were enriched in KEGG pathways. GO, gene ontology; KEGG, Kyoto Encyclopedia of Genes and Genomes; bubble size, the number of genes belonging to this pathway at the target gene concentration; bubble color, significance value of enrichment; RichFactor, the ratio of the number of genes in the pathway entry of the differentially expressed genes to the total number of genes in the pathway entry of all genes.

Cells with activated autophagy had a green fluorescent signal in the cytoplasm (**Figure 6D**). Increasing MDC fluorescence in A3 cells was observed after DN treatment (**Figure 6E**).

Validation of the Expression of Autophagy- and Cell Cycle-Associated Genes and Proteins

To validate the results of the RNA-Seq analysis, qRT-PCR was performed to validate the expression patterns of 16 differentially expressed genes, which are closely related to autophagy and the cell cycle (**Table S10**). We measured the levels of expression of genes that are involved in autophagy—adenosine 5'-monophosphate (AMP)-activated protein kinase (*AMPK*), autophagy-related gene 1 (*ATG1*), *beclin-1*, vacuolar protein sorting 34 (*VPS34*), autophagy-related gene 7 (*ATG7*), autophagy-related gene 12 (*ATG12*), phosphoinositide 3-kinase (*PI3K*), and mammalian target of rapamycin (*mTOR*)—and in the cell cycle—cyclin D (*CycD*), cyclin E (*CycE*), cyclin-dependent kinase 2 (*CDK2*), cyclin-dependent kinase 4 (*CDK4*), minichromosome maintenance complex component 2

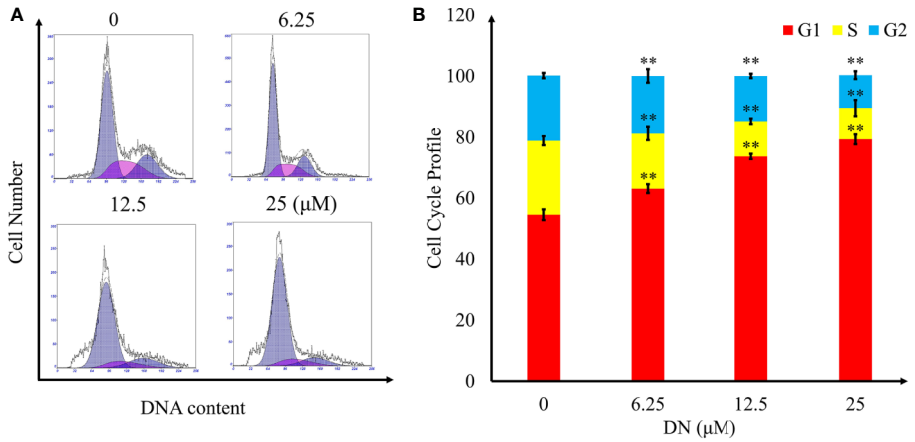

FIGURE 5 | Cell cycle profiling of A3 cells exposed to diorcinol N (DN). **(A)** Cell cycle distribution of DN-treated A3 cells. **(B)** Cell cycle profile of DN-treated A3 cells. **p < 0.01 indicates a significant difference versus the untreated group.

(*MCM2*), transforming growth factor beta (*TGFβ*), cyclin-dependent kinase inhibitor 1α (*p21*), and cyclin-dependent kinase inhibitor 1β (*p27*). The results indicate a significant increase in the expression of genes involved in the promotion of autophagy (*AMPK, beclin-1, ATG1, VPS34*, and *ATG7*) and a reduction in the expression of genes involved in the inhibition of autophagy (*PI3K* and *mTOR*) (**Figure 7A**). Additionally, we detected a significant decrease in *CycD, CycE, CDK2, CDK4*, and *MCM2* transcript levels; these genes play positive roles in the cell cycle, whereas cell cycle inhibitory genes, such as transforming growth factor beta (*TGFβ*), *p21* and *p27*, were upregulated (**Figure 7B**). In addition, AMPK levels of expression and the concentrations of its substrates, beclin-1 protein levels, increased following treatment with DN in a dose-dependent manner (**Figure 7C**). Activated AMPK negatively regulates mTOR and, in turn, enhances autophagy flux. In our experiments, we observed that DN dephosphorylated mTOR in a dose-dependent manner (**Figure 7C**). Finally, DN also induced a dose-dependent increase in the levels of phosphorylated ATG1, which is a downstream target of mTOR (**Figure 7C**).

DISCUSSION

While tremendous progress has been made in the treatment of pediatric ALL, the success rate of current treatments is much more modest in adults (Aldoss and Stein, 2018). Hence, new therapeutic agents are urgently needed for ALL therapy (Thu Huynh and Bergeron, 2017; Dyczynski et al., 2018a). The antifungal, anticancer, and antinociceptive effects of diorcinol have been investigated in previous studies (Gao et al., 2013; Li et al., 2015; Zhuravleva et al., 2016; Li et al., 2018; Zhang et al., 2018). However, the mechanism by which DN exerts anticancer effects on ALL cells requires further elucidation. In this study, we provide evidence that DN inhibited growth and induced autophagy in leukemia cells by modulating multiple cell signaling molecules. To characterize the anticancer mechanism of DN in human cell lines, we first explored the effects of DN on the viability of human cancer cell lines and PBMCs. DN decreased the viability of numerous cancer cell lines in our present study; however, the most obvious anticancer effect of DN was observed on A3 cells in the CCK-8 assay. Digital expressed gene profiling was performed to identify genes that were differentially expressed in untreated and DN-treated A3 cells. GO and KEGG analyses were performed for the 9,340 differentially expressed genes observed in treated and untreated A3 cells. We found that DN could inhibit the growth of A3 cells by affecting biological processes, such as autophagy, cell cycle, DNA replication, vacuole organization, and mitotic nuclear division. However, we detected that the genes associated with the apoptotic pathway were not in the top 20 enrichment list. Thus, DN probably modulated the expression of genes related to autophagy and the cell cycle to a greater degree. The effects of DN on A3 cells were similar to those observed for Ghrelin on Jurkat and Molt-4 human lymphoblastic cell lines (Heshmati et al., 2020).

Studies have reported changes in the expression of genes related to the cell cycle that are relevant to abnormal karyomorphism. Hoechst 33258 labeling revealed DN-induced pyknotic karyomorphism over time. Pyknotic karyomorphism has been found during autophagy in other leukemia cells and is induced by treatment with different kinds of anticancer drugs (i.e., 786-O cells and L-02 cells) (Yuan et al., 2017; Chen et al., 2018). The fidelity of replication is affected by abnormal karyomorphism, and low fidelity of replication could lead to cell cycle arrest (Dyshlovoy et al., 2020; Oh et al., 2020). Our findings indicate that DN arrested the cell cycle of A3 cells at the G1/S phase, which is similar to the effects of previously reported anticancer agents, such as triacanthine and licoricidin (Ji et al., 2017; Shin et al., 2019). In addition, transcriptome profiling and qRT-PCR analyses show that cycle-stimulative genes, such as *CDC, CDE, CDK2*, and *CDK4*, were downregulated in DN-treated A3 cells, whereas cycle-suppressive genes, such as *TGFβ, p21*, and *p27* were upregulated. TGFβ plays a vital role

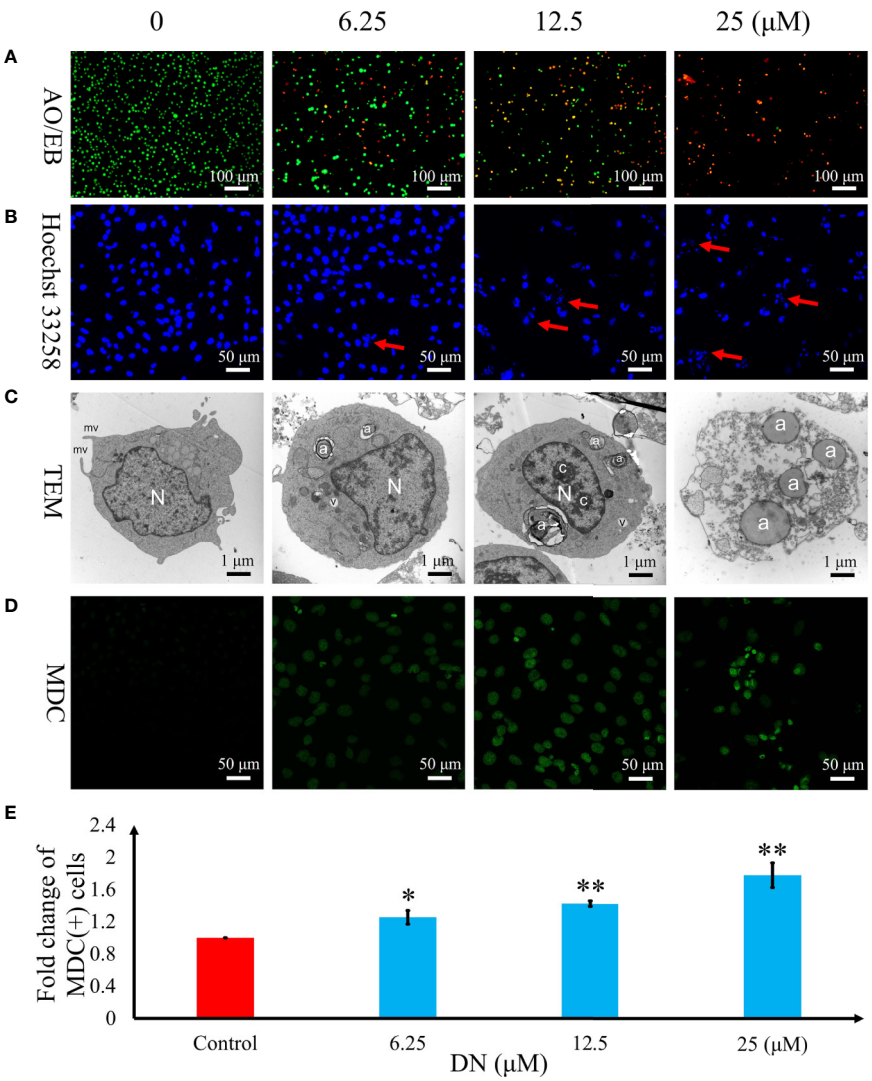

FIGURE 6 | Diorcinol N (DN) induced autophagy in A3 cells. **(A)** Elevated plasma membrane permeability was detected by staining cells in the AO/EB double-staining assay. Original magnification, ×100. **(B)** Autophagy-related nuclear morphological changes were detected by labeling cells with Hoechst 33258. Autophagic cells were defined as those with blue nuclei that exhibited a fragmented/condensed appearance (red arrow). Original magnification, ×200. **(C)** Ultrastructural changes in A3 cells were detected via TEM. a, autophagosome; c, condensed chromatin; mv, microvillus; N, nucleus; v, vacuole. **(D)** The autophagosomes of autophagic cells were labeled using MDC and viewed under a fluorescence microscope. Original magnification, ×200. **(E)** Bar graph showing the quantification of MDC-positive A3 cells. Mean values are shown with standard deviation (SD). AO/EB, acridine orange/ethidium bromide; TEM, transmission electron microscopy; MDC, monodansylcadaverine. *$p < 0.05$, **$p < 0.01$ indicates a significant difference versus the untreated group.

in promoting G1/S phase arrest *via* a complex of mothers against decapentaplegic homolog 2/3/4 and specificity protein 1 (Sun et al., 2019). Phosphorylated tyrosine-containing p27 inhibits CDK4 and CDK2 to cause cell cycle G1/S arrest (Kang et al., 2002; Blain, 2018). As a cyclin-dependent kinase (CDK) inhibitor, p21 binds to cyclin A/CDK2, E/CDK2, D1/CDK4, and D2/CDK4 complex to inhibit the phosphorylation of retinoblastoma protein and thus, inhibit G1/S transition (Kang et al., 2002; Karimian et al., 2016). As a new marker for proliferating cells, MCM2 is one of the six highly conserved proteins that form a double hexameric MCM complex that is essential for the pre-replication apparatus and may be involved in the formation of replication forks for recruiting other DNA replication-related proteins in the G1 phase (Braun and Breeden, 2007). The results show that the downregulated genes are closely related to the cell cycle and thus influence the viability of A3 cells, which is also supported by the results of the Hoechst 33258 staining and cell cycle analysis. The cellular results, together with gene expression, indicate that DN-treated leukemia cells cannot progress through the G1/S checkpoint, which is consistent with previous findings (Vijayaraghavan et al., 2017). Previous studies have shown that the cell cycle is tightly controlled by precise mechanisms, among which autophagy is an important upstream regulator of the cell cycle (Mathiassen et al., 2017; Zheng et al.,

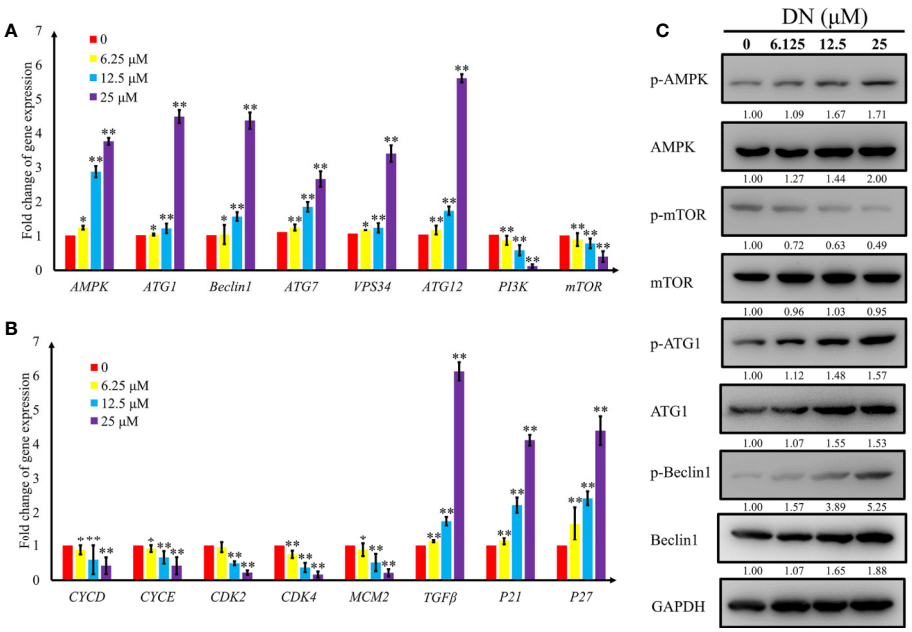

FIGURE 7 | Validation of expression levels of genes related to autophagy and the cell cycle. **(A)** Differentially expressed autophagy-related genes induced by diorcinol N (DN). **(B)** Differentially expressed cell cycle-related genes induced by DN. **(C)** Western blot analysis of AMPK, p-AMPK (Thr172), mTOR, p-mTOR (Ser2448), ATG1, p-ATG1 (Ser555), Beclin1, p-Beclin1 (Ser93) expression A3 cells treated with different concentrations of DN for 48 h. *p <0.05, **p <0.01 indicates a significant difference versus the untreated group.

2019). Therefore, the observed cell cycle arrest, combined with reduced cell viability, caused by DN in A3 cells could explain the autophagy-inducing effect of DN on A3 cells.

Literature evidence identifies autophagy as an important mode of cancer treatment, *via* the promotion of cell cycle arrest (Onorati et al., 2018; Kocaturk et al., 2019). Autophagic cells present characteristics, such as elevated plasma membrane permeability, karyopyknosis, and autophagic body formation (Zhang et al., 2015; Karch et al., 2017; Padman et al., 2017). Therefore, plasma membrane permeability, autophagosomes, karyomorphism, and ultrastructure of DN-treated A3 cells were examined by labeling with AO/EB, Hoechst 33258, and MDC, as well as TEM, respectively, to detect the effects of DN on autophagy. Our results indicate that DN increased the plasma membrane permeability of A3 cells. Previous studies have reported that anticancer agents, such as α-hederin and curcumin, have a similar effect on the permeability of cell membranes (Lorent et al., 2016; Seo et al., 2018). DN has been shown to induce typical autophagic changes in A3 cells, such as cell structure disorder, vacuolation, and autophagosome formation. Moreover, we observed that the increased expression of AMPK at the gene and protein levels, which can directly or indirectly suppress the expression of downstream mTOR (Jia et al., 2019). Downregulated *mTOR* can promote autophagy *via* the formation of the ATG1-ATG13-FIP200 complex, which causes the upregulation of *p21* and *p27*, leading to cell cycle arrest in the G1 phase (Jung et al., 2018; Kazemi et al., 2018). In addition, transcriptional levels of *PI3K*, a negative regulator of autophagy, had decreased, resulting in the downregulation of downstream *mTOR via* the PI3K/ATK/mTOR signaling pathway (Chen et al., 2019). Moreover, beclin-1 is phosphorylated by ATG1 and forms the Beclin-1-VPS34 complex to promote the localization of autophagic proteins in autophagic vesicles (Dyczynski et al., 2018b; Feng et al., 2019). ATG7 acts as an E1-like ubiquitin-activating enzyme to activate ATG12. Subsequently, the activated ATG12 forms a complex with ATG5 and ATG16 to promote the process of autophagy. Our results also show that DN induced autophagy by increasing the expression of autophagy-related genes such *ATG1, ATG7, ATG12, Beclin-1*, and *VPS34* (Dyczynski et al., 2018b; Sun et al., 2018; Wang et al., 2018). Overall, our data support the conclusion that DN regulated gene expression to induce autophagy, which is the main mechanism underlying its anticancer effects in A3 cells.

The fungal metabolite DN exerts its effects against A3 leukemia cells by decreasing their viability, altering plasma membrane permeability, promoting autophagic morphological changes, arresting the cell cycle at the G1/S phase *via* p21, p27, TGF-β, and the PI3K/Akt/mTOR pathways. Although further study is required to investigate the anticancer activity of DN, our study demonstrates the promise of DN as a lead or even a candidate molecule for the treatment of acute lymphoblastic leukemia.

DATA AVAILABILITY STATEMENT

The datasets for this study can be found in the NCBI sequence read archive (https://www.ncbi.nlm.nih.gov/bioproject/637910).

AUTHOR CONTRIBUTIONS

PZ and X-LY designed experiments. X-QL and KX carried out experiments. X-ML analyzed experimental results. LX, X-QL, KX, and X-ML analyzed and interpreted the data. X-LY drafted and revised the manuscript. All authors contributed to the article and approved the submitted version

FUNDING

This work was supported by the Natural Science Foundation of China (grant number 31700295), the Science Foundation for Young Scholars of Institute of Tobacco Research of Chinese Academy of Agricultural Sciences (grant number 2020A01), and the Agricultural Science and Technology Innovation Program (Grant No. ASTIP-TRIC05). The authors declare that this study received funding from the Key Projects of Wannan Tobacco Co., Ltd. (grant no. 20180023). The funder was not involved in the study design, collection, analysis, interpretation of data, the writing of this article or the decision to submit it for publication.

SUPPLEMENTARY MATERIAL

The Supplementary Material for this article can be found online at: https://www.frontiersin.org/articles/10.3389/fphar.2020.570450/full#supplementary-material

REFERENCES

Aldoss, I., and Stein, A. S. (2018). Advances in adult acute lymphoblastic leukemia therapy. *Leuk. Lymphoma* 59, 1033–1050. doi: 10.1080/10428194.2017.1354372

Blain, S. W. (2018). Targeting p27 tyrosine phosphorylation as a modality to inhibit CDK4 and CDK2 and cause cell cycle arrest in breast cancer cells. *Oncoscience* 5, 144–145. doi: 10.18632/oncoscience.427

Braun, K. A., and Breeden, L. L. (2007). Nascent transcription of MCM2-7 is important for nuclear localization of the minichromosome maintenance complex in G1. *Mol. Biol. Cell* 18, 1447–1456. doi: 10.1091/mbc.e06-09-0792

Chen, X., Yang, S., Pan, Y., Li, X., and Ma, S. (2018). Mitochondrial pathway-mediated apoptosis is associated with erlotinib-induced cytotoxicity in hepatic cells. *Oncol. Lett.* 15, 783–788. doi: 10.3892/ol.2017.7359

Chen, Z., Zheng, Y., Cao, W., Zhang, Y., Zhao, Z., Wang, G., et al. (2019). Everolimus-containing therapy vs conventional therapy in the treatment of refractory breast cancer patients with PI3K/AKT/mTOR mutations: A retrospective study. *Cancer Med.* 8, 5544–5553. doi: 10.1002/cam4.2460

Chiang, C., Chung, J., and Hsu, F. (2019). Regorefenib induces extrinsic/intrinsic apoptosis and inhibits MAPK/NF-κB-modulated tumor progression in bladder cancer *in vitro* and *in vivo*. Environ. *Toxicol* 34, 679–688. doi: 10.1002/tox.22734

Chou, Y., Chang, M., Lee, H., Shen, C., Harnod, T., Liang, Y., et al. (2018). Phenethyl isothiocyanate inhibits *in vivo* growth of xenograft tumors of human glioblastoma cells. *Molecules* 23, 2305. doi: 10.3390/molecules23092305

Curran, E., and Stock, W. (2015). How I treat acute lymphoblastic leukemia in older adolescents and young adults. *Blood* 125, 3702–3710. doi: 10.1182/blood-2014-11-551481

Deshmukh, S. K., Gupta, M. K., Prakash, V., and Reddy, M. S. (2019). "Fungal endophytes: a novel source of cytotoxic compounds," in *Endophytes and Secondary Metabolites. Reference Series in Phytochemistry*. Ed. S. Jha (Cham: Springer), 365–426.

Dyczynski, M., Vesterlund, M., Björklund, A. C., Zachariadis, V., Janssen, J., Gallart-Ayala, H., et al. (2018a). Metabolic reprogramming of acute lymphoblastic leukemia cells in response to glucocorticoid treatment. *Cell Death Dis.* 9, 846. doi: 10.1038/s41419-018-0625-7

Dyczynski, M., Yu, Y., Otrocka, M., Parpal, S., Braga, T., Henley, A. B., et al. (2018b). Targeting autophagy by small molecule inhibitors of vacuolar protein sorting 34 (Vps34) improves the sensitivity of breast cancer cells to sunitinib. *Cancer Lett.* 435, 32–43. doi: 10.1016/j.canlet.2018.07.028

Dyshlovoy, S. A., Tarbeeva, D., Fedoreyev, S., Busenbender, T., Kaune, M., Veselova, M., et al. (2020). Polyphenolic compounds from Lespedeza Bicolor root bark inhibit progression of human prostate cancer cells via induction of apoptosis and cell cycle arrest. *Biomolecules* 10, 451. doi: 10.3390/biom10030451

Feng, X., Jia, Y., Zhang, Y., Ma, F., Zhu, Y., Hong, X., et al. (2019). Ubiquitination of UVRAG by SMURF1 promotes autophagosome maturation and inhibits hepatocellular carcinoma growth. *Autophagy*. 15 (7), 1130–1149. doi: 10.1080/15548627.2019.1570063

Gao, H., Zhou, L., Cai, S., Zhang, G., Zhu, T., Gu, Q., et al. (2013). Diorcinols B-E, new prenylated diphenyl ethers from the marine-derived fungus *Aspergillus versicolor* ZLN-60. *J. Antibiot.* 66, 539–542. doi: 10.1038/ja.2013.40

Heshmati, M., Soltani, A., Sanaei, M. J., Nahid-Samiei, M., Shirzad, H., Jami, M. S., et al. (2020). Ghrelin induces autophagy and CXCR4 expression via the SIRT1/AMPK axis in lymphoblastic leukemia cell lines. *Cell. Signal.* 66, 109492. doi: 10.1016/j.cellsig.2019.109492

Hunger, S. P., and Mullighan, C. G. (2015). Acute lymphoblastic leukemia in children. *N. Engl. J. Med.* 373, 1541–1552. doi: 10.1056/NEJMra1400972

Ji, S., Tang, S., Li, K., Li, Z., Liang, W., Qiao, X., et al. (2017). Licoricidin inhibits the growth of SW480 human colorectal adenocarcinoma cells *in vitro* and *in vivo* by inducing cycle arrest, apoptosis and autophagy. *Toxicol. Appl. Pharmacol.* 326, 25–33. doi: 10.1016/j.taap.2017.04.015

Jia, J., Abudu, Y. P., Claude-Taupin, A., Gu, Y., Kumar, S., Choi, S. W., et al. (2019). Galectins control MTOR and AMPK in response to lysosomal damage to induce autophagy. *Autophagy* 15, 169–171. doi: 10.1080/15548627.2018.1505155

Jung, D., Khurana, A., Roy, D., Kalogera, E., Bakkum-Gamez, J., Chien, J., et al. (2018). Quinacrine upregulates p21/p27 independent of p53 through autophagy-mediated downregulation of p62-Skp2 axis in ovarian cancer. *Sci. Rep.* 8, 2487. doi: 10.1038/s41598-018-20531-w

Kanehisa, M., and Goto, S. (2000). KEGG: Kyoto encyclopedia of genes and genomes. *Nucleic Acids Res.* 28, 27–30. doi: 10.1093/nar/28.1.27

Kanehisa, M., Sato, Y., Kawashima, M., Furumichi, M., and Tanabe, M. (2016). KEGG as a reference resource for gene and protein annotation. *Nucleic Acids Res.* 44, D457–D462. doi: 10.1093/nar/gkv1070

Kang, Y. K., Kim, W. H., and Jang, J. J. (2002). Expression of G1-S modulators (p53, p16, p27, cyclin D1, Rb) and Smad4/Dpc4 in intra hepatic cholangiocarcinoma. *Hum. Pathol.* 33, 877–883. doi: 10.1053/hupa.2002.127444

Kansagra, A., Dahiya, S., and Litzow, M. (2018). Continuing challenges and current issues in acute lymphoblastic leukemia. *Leuk. Lymphoma.* 59, 526–541. doi: 10.1080/10428194.2017.1335397

Karch, J., Schips, T. G., Maliken, B. D., Brody, M. J., Sargent, M. A., Kanisicak, O., et al. (2017). Autophagic cell death is dependent on lysosomal membrane permeability through Bax and Bak. *Elife* 17, 30543.

Karimian, A., Ahmadi, Y., and Yousefi, B. (2016). Multiple functions of p21 in cell cycle, apoptosis and transcriptional regulation after DNA damage. *DNA Repair (Amst)* 42, 63–71. doi: 10.1016/j.dnarep.2016.04.008

Kazemi, A., Sadri, M., Houshmand, M., Yazdi, N., Zarif, M. N., Anjam-Najmedini, A., et al. (2018). The anticancer effects of pharmacological inhibition of autophagy in acute erythroid leukemia cells. *Anticancer Drugs* 29, 944–955. doi: 10.1097/CAD.0000000000000668

Kocaturk, N. M., Akkoc, Y., Kig, C., Bayraktar, O., Gozuacik, D., and Kutlu, O. (2019). Autophagy as a molecular target for cancer treatment. *Eur. J. Pharm. Sci.* 134, 116–137. doi: 10.1016/j.ejps.2019.04.011

Laha, D., Deb, M., and Das, H. (2019). KLF2 (kruppel-like factor 2 [lung]) regulates osteoclastogenesis by modulating autophagy. *Autophagy* 15, 2063–2075. doi: 10.1080/15548627.2019.1596491

Li, Y., Chang, W. Q., Zhang, M., Li, X. B., Jiao, Y., and Lou, H. X. (2015). Diorcinol D exerts fungicidal action against *Candida albicans* through cytoplasm membrane destruction and ROS accumulation. *PloS One* 10, e0128693. doi: 10.1371/journal.pone.0128693

Li, Z. X., Wang, X. F., Ren, G. W., Yuan, X. L., Deng, N., Ji, G. X., et al. (2018). Prenylated diphenyl ethers from the marine algal-derived endophytic fungus *Aspergillus tennesseensis*. *Molecules* 23, 2368. doi: 10.3390/molecules23092368

Lorent, J. H., Léonard, C., Abouzi, M., Akabi, F., Quetin-Leclercq, J., and Mingeot-Leclercq, M. P. (2016). α-Hederin induces apoptosis, membrane permeabilization and morphologic changes in two cancer cell lines through a cholesterol-dependent mechanism. *Planta Med.* 82, 1532–1539. doi: 10.1055/s-0042-114780

Malard, F., and Mohty, M. (2020). Acute lymphoblastic leukaemia. *Lancet* 395, 1146–1162. doi: 10.1016/S0140-6736(19)33018-1

Mathiassen, S. G., De Zio, D., and Cecconi, F. (2017). Autophagy and the Cell Cycle: A Complex Landscape. *Front. Oncol.* 7, 51. doi: 10.3389/fonc.2017.00051

Oh, H. N., Lee, M. H., Kim, E., Kwak, A. W., Yoon, G., Cho, S. S., et al. (2020). Licochalcone D induces ROS-dependent apoptosis in gefitinib-sensitive or resistant lung cancer cells by targeting EGFR and MET. *Biomolecules* 10, E297. doi: 10.3390/biom10020297

Onorati, A. V., Dyczynski, M., Ojha, R., and Amaravadi, R. K. (2018). Targeting autophagy in cancer. *Cancer* 124, 3307–3318. doi: 10.1002/cncr.31335

Padman, B. S., Nguyen, T. N., and Lazarou, M. (2017). Autophagosome formation and cargo sequestration in the absence of LC3/GABARAPs. *Autophagy* 13, 772–774. doi: 10.1080/15548627.2017.1281492

Paul, S., Rausch, C. R., Kantarjian, H., and Jabbour, E. J. (2017). Treatment of adult acute lymphoblastic leukemia with inotuzumab ozogamicin. *Future Oncol.* 13, 2233–2242. doi: 10.2217/fon-2017-0233

Phelan, K. W., and Advani, A. S. (2018). Novel therapies in acute lymphoblastic leukemia. *Curr. Hematol. Malig. Rep.* 13, 289–299. doi: 10.1007/s11899-018-0457-7

Seo, S. U., Woo, S. M., Lee, H. S., Kim, S. H., Min, K. J., and Kwon, T. K. (2018). mTORC1/2 inhibitor and curcumin induce apoptosis through lysosomal membrane permeabilization-mediated autophagy. *Oncogene* 37, 5205–5220. doi: 10.1038/s41388-018-0345-6

Shin, S. S., Park, Y. J., Hwang, B., Park, S. L., Han, S. W., Park, S. S., et al. (2019). Triacanthine exerts antitumor effects on bladder cancer *in vitro* and *in vivo*. *Phytomedicine* 64, 153069. doi: 10.1016/j.phymed.2019.153069

Song, Z., Zhang, Y., Zhang, H., Rajendran, R., Wang, R., Hsiao, C.-D., et al. (2020). Isoliquiritigenin triggers developmental toxicity and oxidative stress-mediated apoptosis in zebrafish embryos/larvae via Nrf2-HO1/JNK-ERK/mitochondrion pathway. *Chemosphere* 246, 125727. doi: 10.1016/j.chemosphere.2019.125727

Soulier, J., and Cortes, J. (2015). Introduction to the review series on acute lymphoblastic leukemia. *Blood* 125, 3965–3966. doi: 10.1182/blood-2015-05-635300

Sun, W. L., Wang, L., Luo, J., Zhu, H. W., and Cai, Z. W. (2018). Ambra1 modulates the sensitivity of breast cancer cells to epirubicin by regulating autophagy via ATG12. *Cancer Sci.* 109, 3129–3138. doi: 10.1111/cas.13743

Sun, F., Li, N., Tong, X., Zeng, J., He, S., Gai, T., et al. (2019). Ara-c induces cell cycle G1/S arrest by inducing upregulation of the INK4 family gene or directly inhibiting the formation of the cell cycle-dependent complex CDK4/cyclin D1. *Cell Cycle.* 18, 2293–2306. doi: 10.1080/15384101.2019.1644913

Thu Huynh, V., and Bergeron, S. (2017). Asparaginase toxicities: Identification and management in patients with acute lymphoblastic leukemia. *Clin. J. Oncol. Nurs.* 21, E248–E259. doi: 10.1188/17.CJON.E248-E259

Vijayaraghavan, S., Karakas, C., Doostan, I., Chen, X., Bui, T., Yi, M., et al. (2017). CDK4/6 and autophagy inhibitors synergistically induce senescence in Rb positive cytoplasmic cyclin E negative cancers. *Nat. Commun.* 8, 15916. doi: 10.1038/ncomms15916

Wang, B., Iyengar, R., Li-Harms, X., Joo, J. H., Wright, C., Lavado, A., et al. (2018). The autophagy-inducing kinases, ULK1 and ULK2, regulate axon guidance in the developing mouse forebrain via a noncanonical pathway. *Autophagy* 14, 796–811. doi: 10.1080/15548627.2017.1386820

Wu, X., Xu, Y., Zhu, B., Liu, Q., Yao, Q., and Zhao, G. (2018). Resveratrol induces apoptosis in SGC-7901 gastric cancer cells. *Oncol. Lett.* 16, 2949–2956. doi: 10.3892/ol.2018.9045

Young, M. D., Wakefield, M. J., Smyth, G. K., and Oshlack, A. (2010). Gene ontology analysis for RNA-seq: accounting for selection bias. *Genome Biol.* 11, R14. doi: 10.1186/gb-2010-11-2-r14

Yuan, X. L., Zhang, P., Liu, X. M., Du, Y. M., Hou, X. D., Cheng, S., et al. (2017). Cytological assessments and transcriptome profiling demonstrate that evodiamine inhibits growth and induces apoptosis in a renal carcinoma cell line. *Sci. Rep.* 7, 12572. doi: 10.1038/s41598-017-12918-y

Zhang, G. L., Jiang, L., Yan, Q., Liu, R. H., and Zhang, L. (2015). Anti-tumor effect of matrine combined with cisplatin on rat models of cervical cancer. *Asian Pac. J. Trop. Med.* 8, 1055–1059. doi: 10.1016/j.apjtm.2015.11.005

Zhang, P., Li, X., Yuan, X. L., Du, Y. M., Wang, B. G., and Zhang, Z. F. (2018). Antifungal prenylated diphenyl ethers from *Arthrinium arundinis*, an endophytic fungus isolated from the leaves of tobacco (*Nicotiana tabacum* L.). *Molecules* 23, 3179. doi: 10.3390/molecules23123179

Zhang, S., Xue, R., Geng, Y., Wang, H., and Li, W. (2020). Fisetin prevents HT22 cells from high glucose-induced neurotoxicity via PI3K/Akt/CREB signaling pathway. *Front. Neurosci.* 14, 241. doi: 10.3389/fnins.2020.00241

Zheng, K., He, Z., Kitazato, K., and Wang, Y. (2019). Selective Autophagy Regulates Cell Cycle in Cancer Therapy. *Theranostics* 9 (1), 104–125. doi: 10.7150/thno.30308

Zhuravleva, O.II, Kirichuk, N. N., Denisenko, V. A., Dmitrenok, P. S., Yurchenko, E. A., Min'ko, E. M., et al. (2016). New diorcinol J produced by co-cultivation of marine fungi *Aspergillus sulphureus* and *Isaria felina*. *Chem. Nat. Compd.* 52, 227–230. doi: 10.1007/s10600-016-1601-z

Conflict of Interest: Author LX was employed by the company Wannan Tobacco Group Co., Ltd.

The remaining authors declare that the research was conducted in the absence of any commercial or financial relationships that could be construed as a potential conflict of interest.

frontiers in Pharmacology

ORIGINAL RESEARCH
published: 09 December 2020
doi: 10.3389/fphar.2020.582719

Targets and Mechanism Used by Cinnamaldehyde, the Main Active Ingredient in Cinnamon, in the Treatment of Breast Cancer

Yufei Liu[1†], *Tian An*[2†], *Donggui Wan*[3], *Bowen Yu*[1], *Yingyi Fan*[1], *Xiaohua Pei*[1,4*]

[1]*Beijing University of Chinese Medicine Third Affiliated Hospital, Beijing, China,* [2]*Oncology Department of Integrated Traditional Chinese and Western Medicine, China-Japan Friendship Hospital, Beijing, China,* [3]*School of Traditional Chinese Medicine, Beijing University of Traditional Chinese Medicine, Beijing, China,* [4]*Xiamen Hospital, Beijing University of Chinese Medicine, Xiamen, China*

Background: Breast cancer has become one of the most common malignant tumors in women owing to its increasing incidence each year. Clinical studies have shown that *Cinnamomum cassia* (L.) *J. Presl* (cinnamon) has a positive influence on the prevention and treatment of breast cancer.

Aim: We aimed to screen the potential targets of cinnamon in the treatment of breast cancer through network pharmacology and explore its potential therapeutic mechanism through cell experiments.

Methods: We used the TCMSP, TCM Database @ Taiwan, and TCMID websites and established the active ingredient and target database of cinnamon. Thereafter, we used the GeneCards and OMIM databases to establish a breast cancer-related target database, which matched the cinnamon target database. Based on the matching results, the STRING database was used to analyze the interaction between the targets, and the biological information annotation database was used to analyze the biological process of the target (gene ontology) and the pathway enrichment of Kyoto Encyclopedia of Genes and Genomes (KEGG). After establishing the layout of the analysis, we used Cytoscape 3.6.0 software for network analysis. Finally, the cell experiment was used to verify the anti-breast cancer effect of cinnamaldehyde.

Results: Our research showed that the main components of cinnamon, including cinnamaldehyde, can play a role in the treatment of breast cancer through 59 possible important targets. Subsequently, enrichment analysis by gene ontology and Kyoto Encyclopedia of Genes and Genomes showed that 83 cell biological processes and 37 pathways were associated with breast cancer ($p < 0.05$), including the peroxisome proliferator-activated receptor and PI3K-Akt pathway, which are closely related to tumor cell apoptosis. *In vitro* cell verification experiments showed that cinnamaldehyde can significantly inhibit cell proliferation, change cell morphology, inhibit cell migration and invasion ability, and promote cell apoptosis.

OPEN ACCESS

Edited by:
Rajeev K. Singla,
Sichuan University, China

Reviewed by:
Manoj Kumar Sabnani,
University of Texas at Arlington, United States
Nicolette Jeanette Dorothy Verhoog,
Stellenbosch University, South Africa

****Correspondence:***
Xiaohua Pei
pxh_127@163.com

†These authors have contributed equally to this work

Specialty section:
This article was submitted to Ethnopharmacology, a section of the journal Frontiers in Pharmacology

Received: *13 July 2020*
Accepted: *06 October 2020*
Published: *09 December 2020*

Citation:
Liu Y, An T, Wan D, Yu B, Fan Y and Pei X (2020) Targets and Mechanism Used by Cinnamaldehyde, the Main Active Ingredient in Cinnamon, in the Treatment of Breast Cancer. Front. Pharmacol. 11:582719. doi: 10.3389/fphar.2020.582719

Conclusion: Our results showed that cinnamaldehyde is a potential novel drug for the treatment and prevention of breast cancer.

Keywords: cinnamaldehyde, breast cancer, network pharmacology, active components, MDA-MB-231

INTRODUCTION

Cinnamon, the dried bark of *Cinnamomum cassia* (L.) *J. Presl*, is one of the most commonly used traditional herbs worldwide. Studies have shown that the chemical components of cinnamon exert anti-tumor effects. Cinnamic acid derivatives can inhibit the growth of lung cancer cells (A549), breast cancer cells (MCF-7), and MCF-10A (Reddy et al., 2016). Cinnamon essential oil is cytotoxic *in vitro* and exhibits certain inhibitory effects on PC3, A549, and MCF-7 prostate cancer cells, with PC3 exerting the strongest inhibitory effect (Zu et al., 2010). Trans-cinnamic acid can inhibit melanoma proliferation and tumor growth (Cabello et al., 2009). Eugenol is another important active ingredient in cinnamon. In fact, *in vivo* studies have shown that eugenol can upregulate the expression of p53 and p21WAF1 and promote apoptosis of cancer cells in mice with skin cancer (Kaur et al., 2010). Cinnamaldehyde can also exert a significant anticancer effect on HepG2 hepatoma cells by reducing the expression of the anti-apoptotic protein, Bcl-XL (Ng and Wu, 2011).

Breast cancer is a malignant tumor with a high clinical incidence. Accordingly, approximately 1.39 million new breast cancer patients are identified worldwide each year (Siegel et al., 2018). Its incidence rate is the highest among malignant tumors for women, and its mortality rate ranks second among female malignancies (Bray et al., 2018). In China, the annual growth rate of breast cancer patients has exceeded the world average. According to the 2015 China Breast Cancer Survey, approximately 26,000 new breast cancer patients are diagnosed each year, causing approximately 70,000 deaths each year (Chen et al., 2016). Triple-negative breast cancer (TNBC) is a special type of breast cancer that is characterized by the progesterone receptor (PR), estrogen receptor (ER), and human epidermal growth factor receptor 2 (HER2), all of which are negative (Parise and Caggiano, 2017; Liao et al., 2018). TNBC accounts for 15–20% of all breast cancer pathological types, most of which occur in premenopausal young women, with high malignancy and poor prognosis (Rida et al., 2018). Besides this, 30–40% of TNBC cases can develop metastatic breast cancer, with visceral metastases being more common, especially lung and brain metastases (Foulkes et al., 2010). TNBC is a group of highly heterogeneous mixed breast cancers with seven subtypes, and endocrine and anti-HER2 treatment are ineffective treatment options for this cancer type (Lehmann et al., 2011). Currently, TNBC mainly relies on adjuvant therapy such as chemotherapy. Therefore, there is an urgent need to develop new drugs and targets for the treatment of refractory breast cancer TNBC.

In the current study, we used network pharmacology to predict the main ingredients and potential therapeutic targets that are responsible for the anti-breast cancer effects of cinnamon. Subsequently, based on the results of network analysis, we investigated the gene ontology (GO) terms and pathways of cinnamon and breast cancer, and carried out biological verification using breast cancer cells *in vitro*. Our research findings may provide experimental data for further development and utilization of cinnamon and may serve as a reference for research on traditional herbs for cancer and cancer-related diseases.

METHODS AND MATERIALS

Screening of the Active Ingredients of Cinnamon by Network Pharmacology

We built a network of potential therapeutic targets for cinnamon based on previous research (Lu et al., 2020). Specifically, all ingredients in cinnamon were obtained through three databases: TCM Systems Pharmacology Database and Analysis Platform (TCMSP), TCM Database @ Taiwan (TCM Database @ Taiwan), and the TCM Integrated Database (TCMID). Subsequently, by setting Lipinski rule-based drug-likeness (DL) and oral bioavailability (OB), the active ingredients related to cinnamon were screened (OB ≥ 20%, DL ≥ 0.1).

Correlation Analysis of Cinnamon and the Breast Cancer-Related Targets

The corresponding target of the compound in cinnamon was verified through the TCMSP database. If no target information for the compound was found on the platform, the small-molecule structure information of the component was searched using the PubChem database and saved in the SMILES format. Thereafter, we used Swiss Target Prediction according to its chemistry similarity to find targets. The UniProt database was used to normalize the gene information and eliminate genes without UniProt ID from human samples. The breast cancer-related targets were obtained through the integration of multi-source databases. Specifically, "breast cancer" was used as the search term; the results obtained from the GeneCards database and Online Mendelian Inheritance in Man (https://omim.org/) search were comprehensively analyzed and a breast cancer target library was constructed. Through Venny 2.1.0 (http://bioinfo.cnb.csic.es/tools/venny/index.html), the targets associated with breast cancer and the main compounds in cinnamon were related for a visual demonstration of the targets that intersect between them.

Screening of the Main Components and Targets in Cinnamon for the Treatment of Breast Cancer

The intersection of the corresponding target of the active ingredient in cinnamon and the target of breast cancer disease was used to construct a protein–protein interaction (PPI) map in

the STRING database. The matched targets were analyzed using the Database for Annotation, Visualization, and Integrated Discovery (https://david.ncifcrf.gov/) v6.8. biological information annotation database for target GO (http://geneontology.org/) biological process analysis and Kyoto Encyclopedia of Genes and Genomes (KEGG, https://www.kegg.jp/) pathway enrichment analysis. $p < 0.05$ was considered statistically significant.

Cell Culture and Treatment With Cinnamaldehyde

MDA-MB-231, a human breast cancer cell line, was obtained from the Be Na Culture Collection (Biotechnology Research Institute) and cultured with RPMI 1640 (11875093, INVITROGEN) supplemented with 10% fetal bovine serum (FBS, Corning-Cellgro Bio Inc., New Zealand) and 1% penicillin-streptomycin in an incubator set to 37°C and 5% CO_2. When the confluence of MDA-MB-231 reached 80–90%, it was treated with different concentrations of cinnamaldehyde (CA, 110710-201821; Chemical formula, **Supplementary Figure S1**) for subsequent detection.

Effects of Cinnamaldehyde on the Viability of MDA-MB-231 Cells

The MTT assay was used to analyze the effect of different concentrations of cinnamaldehyde on the viability of MDA-MB-231 cells (Buglak et al., 2018). MDA-MB-231 cells with moderate density were seeded in 96-well plates and cultured with complete medium until adherence occurred. Subsequently, different concentrations of cinnamaldehyde (0, 2.5, 5, 10, 20, 40, 80, and 160 μg/ml) were used to treat breast cancer cells for 24 and 48 h. Thereafter, 20 μl of MTT was added to each well, and the plates were incubated for another 4 h at 37vC. Finally, the medium was aspirated, and DMSO (150 μl/well) was added. A multifunctional microplate reader (FLUO star Omega, BMG Labtech, Germany) was employed to measure the optical density (OD) at 490 nm. GraphPad Prism 8.0 software was used to calculate the IC_{50} at 48 h. The cell proliferation inhibition rate was calculated using the following formula [1 − (OD value of drug group/OD value of the control group)] × 100%.

Effect of Cinnamaldehyde on MDA-MB-231 Cell Morphology

MDA-MB-231 cells (1×10^6 cells/ml) were seeded in 6-well plates, and their morphology was observed under a microscope after treatment with cinnamaldehyde (0, 10, 15, 20 μg/ml) for 48 h. Subsequently, Hoechst 33258 staining was used to observe the effect of different concentrations of cinnamaldehyde on the cytoplasmic morphology of MDA-MB-231 cells (Hagenlocher et al., 2015).

Effects of Cinnamaldehyde on the Apoptosis of MDA-MB-231 Cells

MDA-MB-231 cells (1×10^6 cells/mL) were seeded in 6-well plates and treated with cinnamaldehyde (0, 10, 15, 20 μg/ml) for 24 h. A cell digestion solution (Beijing Solbio Technology Co., Ltd., article number: 20171024) was then used to prepare a cell suspension. Thereafter, 100 μl of the cell suspension was pipetted into a 1.5-ml Eppendorf tube. Subsequently, according to the instructions of the fluorescein thiocyanate (FITC)-conjugated Annexin-V apoptosis detection kit (Becton, Dickinson and Company, Franklin Lake, New Jersey), the cell suspension and 5 μl of Annexin-V-FITC were mixed with 5 μl of propidium iodide (PI, United States, batch number: 7040932) and incubated for 15 min. A 150-μl volume of the binding buffer was then added to each test tube and analyzed by flow cytometry.

Effects of Cinnamaldehyde on the Invasion and Migration of MDA-MB-231 Cells

The cell invasion assay was performed using Corning Transwell Chamber and Matrigel according to a previously described method (Guo et al., 2020). Briefly, a serum-free medium was used to hydrate the Matrigel. Thereafter, cells with different concentrations of cinnamaldehyde intervention and serum-free medium culture were placed in the upper chamber. RPMI 1640 medium supplemented with 10% fetal bovine serum was placed in the lower chamber. After 48 h, the cells were fixed with 4% paraformaldehyde for 30 min and stained with 0.1% crystal violet for 10 min. The invasiveness of the cells was then observed under a microscope.

The migration of cells was investigated using a wound-healing assay. MDA-MB-231 cells (1×10^6) from different administration groups were seeded in triplicate in six-well plates and incubated at 37°C for 48 h. Scratches were generated using a 1-ml micropipette tip when the cells reached 100% confluence. Thereafter, the cells were washed twice with PBS and incubated at 37°C in complete medium. Images were captured after 0 and 48 h, and the wound area was calculated.

Statistical Analysis

Statistical analysis was performed using GraphPad Prism 8 software. All results are presented as mean ± standard deviation (SD). One-way analysis of variance was performed between multiple groups when the homogeneity of variance and normality were met. Otherwise, Dunnett's T3 and nonparametric tests were conducted between multiple groups. $p < 0.05$ was determined as a statistical difference.

RESULTS

Active Compounds of Cinnamon

A total of 147 related components of the whole formula was retrieved from three databases, TCMSP, TCM Database @ Taiwan, and TCMID. Based on the ADME thresholds of OB ≥ 20%, DL ≥ 0.1, and Caco-2 > 0, 12 active ingredients were selected. Thereafter, an herb-compounds network was built as shown in **Figure 1**. Following the construction of the cinnamon-compounds network and an analysis of the 12 active ingredients, the top four ingredients in descending order of edge betweenness were linoleic acid (EIC, MOL000131, OB = 41.9, DL = 0.14, Caco-

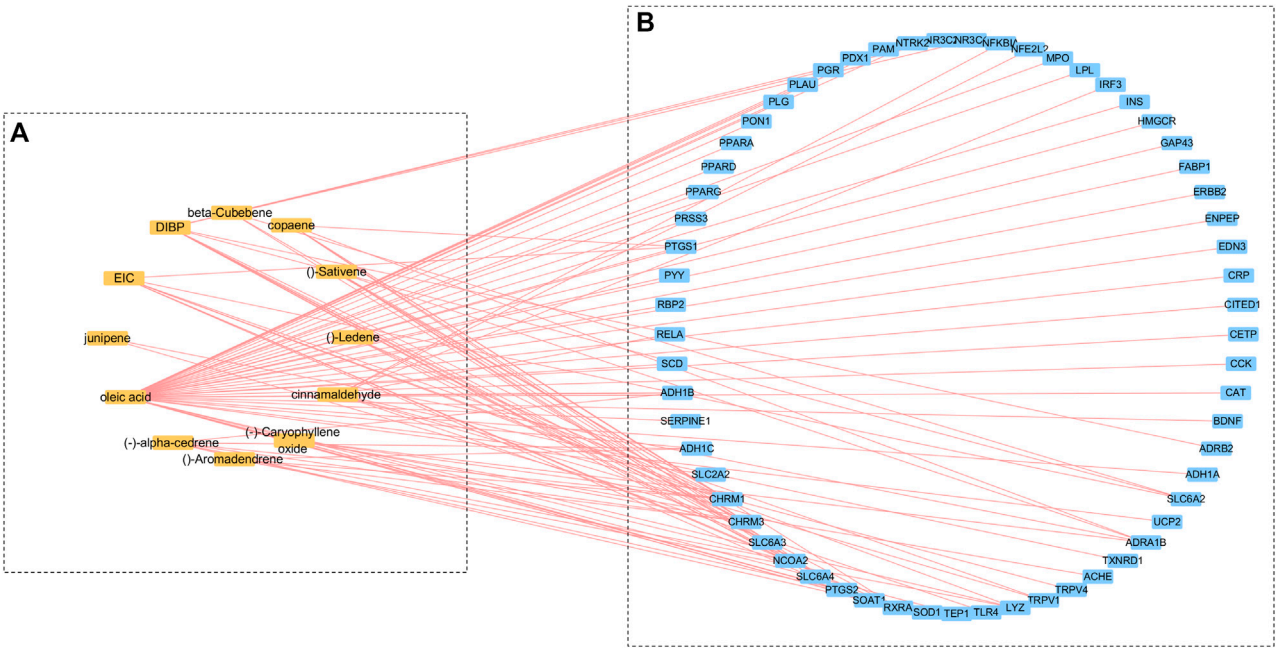

FIGURE 1 | Cinnamon-compounds-breast cancer network. **(A)** Cinnamon-compounds, **(B)** Cinnamon-related compounds-breast cancer. Yellow represents the main compound in cinnamon and blue represents the target associated with breast cancer.

2 = 1.16), oleic acid (MOL000675, OB = 33.13, DL = 0.14, Caco-2 = 1.17), diisobutyl phthalate (DIBP, MOL000057, OB = 49.63, DL = 0.13, Caco-2 = 0.85), and cinnamaldehyde (CA, MOL000449, OB = 31.99, DL = 0.12, Caco-2 = 1.35) (**Figure 1A**).

Prediction and Analysis of the Cinnamon-Related Compounds and Breast Cancer-Related Targets

A target fishing analysis was conducted on the 12 cinnamon-related compounds based on chemical similarity. As a result, 66 related targets were obtained. Through the method of integration of multi-source databases, the target data for breast cancer-related targets from GeneCards (13,933) and OMIM (14,301) were integrated. Thereafter, 61 matching targets of cinnamon and breast cancer-related targets were collected as related targets for the anti-breast cancer effects of cinnamon (**Figure 2.**). Subsequently, we constructed an active ingredient-disease-target network to further screen the effective ingredients responsible for the anti-breast cancer activity of cinnamon (**Figure 1B**). Among the 12 active ingredients, oleic acid, DIBP, and cinnamaldehyde were identified as the more critical ingredients. Therefore, we speculate that cinnamon may play an anti-breast cancer role mainly through this composition.

Target Prediction and Analysis

In the String database, the PPI network of the 61 targets was constructed. After two free nodes were deleted, a total of 59 nodes and 295 edges were found (**Figure 3**). Thereafter, we sorted the targets according to the number of connected nodes (**Figure 4**) to obtain the core targets, including insulin (INS), peroxisome proliferator-activated receptor gamma (PPARG), catalase (CAT), brain-derived neurotrophic factor (BDNF), and prostaglandin-endoperoxide synthase 2 (PTGS2).

GO Biological Process and KEGG Pathway Enrichment Analysis

Through GO function enrichment analysis, we obtained 83 items related to breast cancer, the top 20 of which include the following (**Figure 5A**): amide binding (GO:0033218), steroid hormone receptor activity (GO:0003707), antioxidant activity

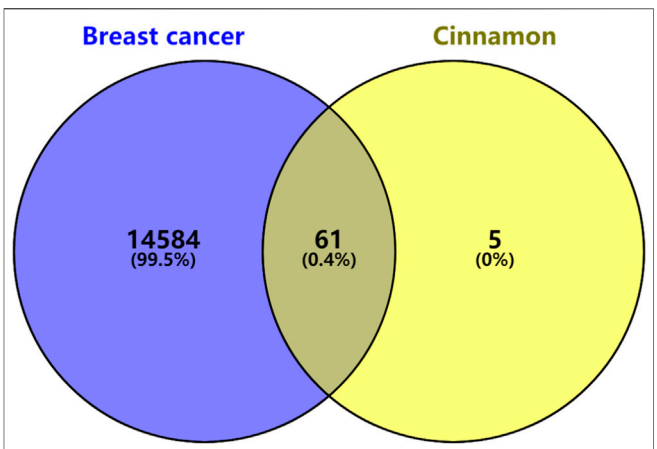

FIGURE 2 | Venn diagram of the targets in breast cancer and cinnamon.

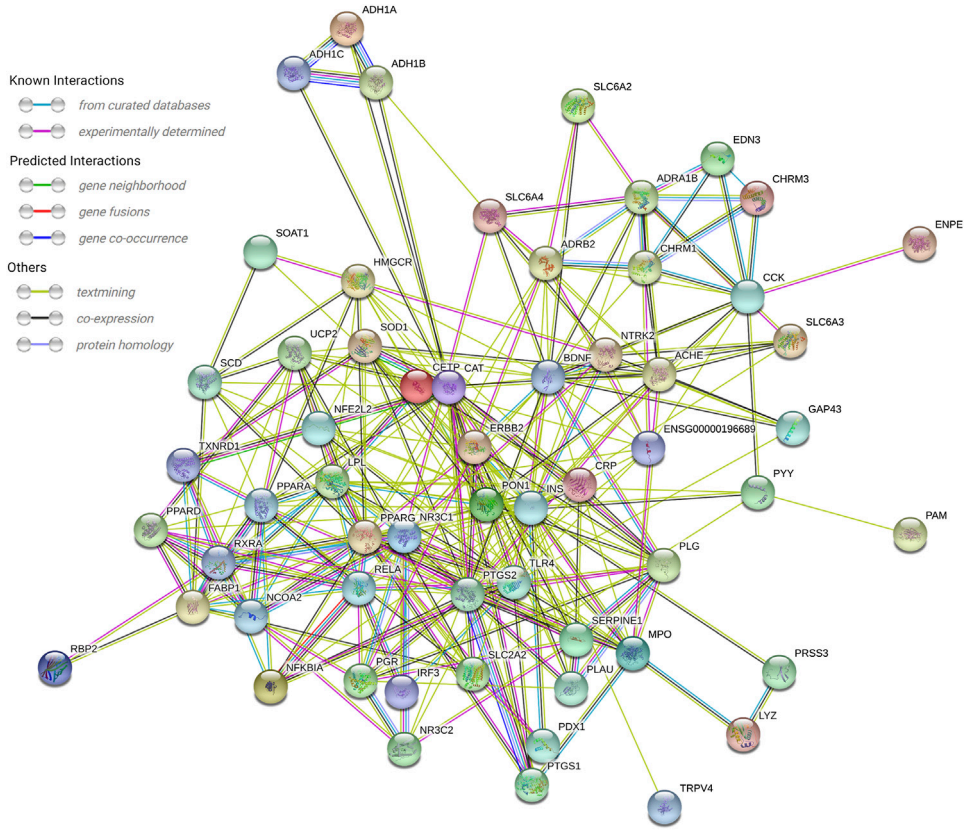

FIGURE 3 | PPI network of 59 nodes. A total of 59 overlapped target genes were used to construct the PPI network.

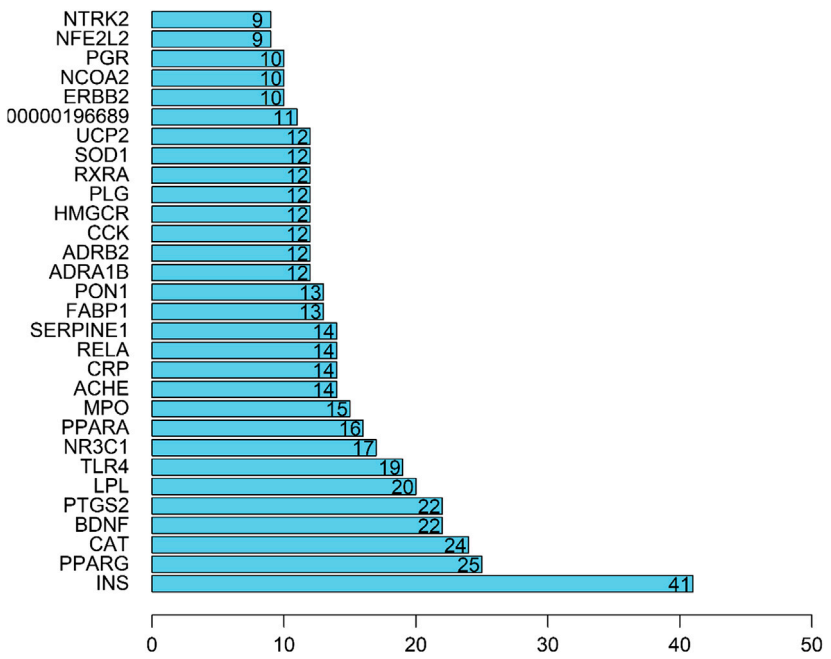

FIGURE 4 | Core target of cinnamon for the treatment of breast cancer.

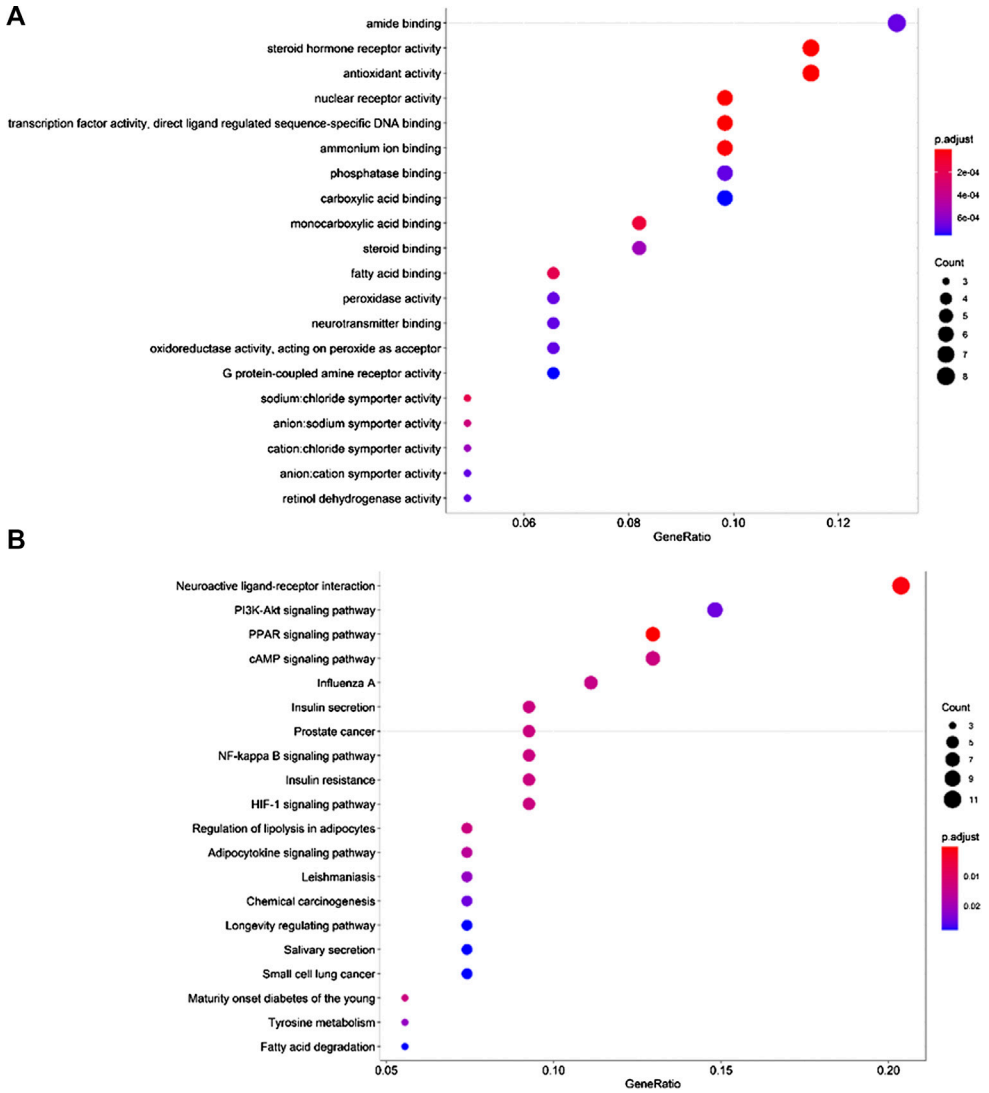

FIGURE 5 | Top 20 GO terms and KEGG pathways. **(A)** GO biological process analysis, **(B)** KEGG pathway analysis.

(GO:0016209), ammonium ion binding (GO:0070405), protease binding (GO:0002020), carboxylic acid binding (GO:0031406), monocarboxylic acid binding (GO:0033293), steroid binding (GO:0005496), fatty acid-binding (GO: 0005504), peroxidase activity (GO:0004601), neurotransmitter binding (GO:0042165), oxidoreductase activity, G protein-coupled amine receptor activity (GO: 0008227), sodium: chloride symporter activity (GO: 0015378), anion: cation symporter activity (GO:0015296), and retinol dehydrogenase activity (GO:0004745). Therefore, it is speculated that cinnamon mainly exerts its anti-breast cancer effects through the above biological processes.

To further reveal the pathways employed by cinnamon against breast cancer, we used $p < 0.05$ as the screening criterion, conducted a KEGG pathway enrichment analysis on 59 targets, and screened out 37 pathways related to breast cancer. Accordingly, we listed the top 20 related items, including neuroactive ligand-receptor interaction (hsa04080), PI3K-Akt pathway (hsa04151), PPAR pathway (hsa03320), cAMP pathway (hsa04024), NF-kappa B pathway (hsa04064), and HIF-1 pathway (hsa04066) (**Figure 5B**). Based on these pathways, the anti-cancer effect of cinnamon on breast cancer may result from a complex multi-pathway synergetic effect.

Inhibitory Effect of Cinnamaldehyde on the Growth of Breast Cancer Cells

MDA-MB-231 cells were treated with cinnamaldehyde. Our results indicated that 2.5, 5, 10, 20, 40 μg/ml cinnamaldehyde inhibited cell proliferation (**Figure 6A**). The IC_{50} of cinnamaldehyde at 24 and 48 h was 16.9 μg/ml and 12.23 μg/ml, respectively, with a 95% confidence interval of 17.81–44.20 (**Figures 6B,C**).

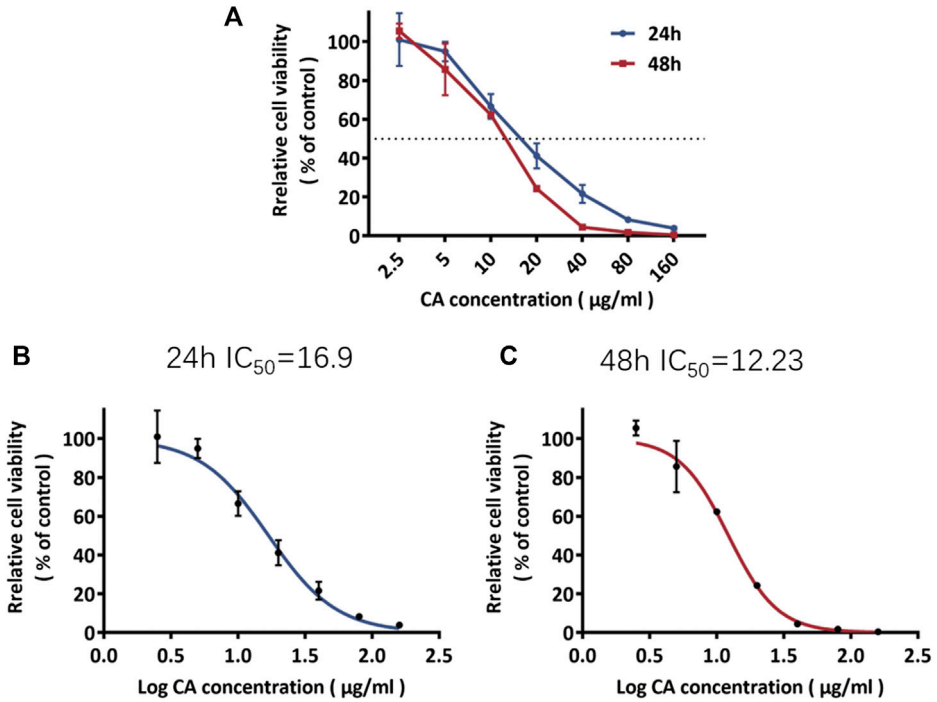

FIGURE 6 | Rate of inhibition of MDA-MB-231 cell proliferation and the IC_{50} of cinnamaldehyde. CA, cinnamaldehyde.

Cinnamaldehyde Affects the Morphological and Cytoplasmic Changes of MDA-MB-231 Cells

In the blank group, the MDA-MB-231 cells were fibrous, uniform in size, smooth, and refractive. Further, the cells exhibited normal growth. However, after 48 h of treatment with different concentrations of cinnamaldehyde (10, 15, 20, and μg/ml), the number of MDA-MB-231 cells significantly decreased, with the 20-μg/ml intervention group demonstrating a more evident decrease. Cinnamaldehyde inhibited the growth and proliferation of MDA-MB-231 cells. In addition, the characteristic morphology of the cells gradually disappeared, the number of cells decreased, the fibers became shorter, and some cells began to cluster (**Figure 7A**). Hoechst 33258 staining showed that with an increase in cinnamaldehyde concentration, the cell spacing of MDA-MB-231 became significantly larger, the cell morphology

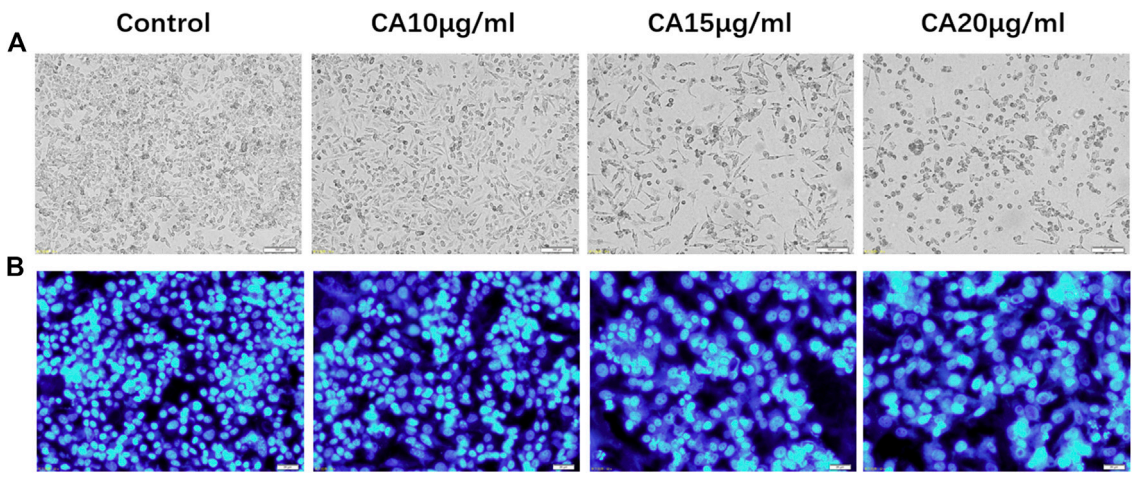

FIGURE 7 | Cell morphological and cytoplasmic changes in MDA-MB-231 cells in the different treatment groups. **(A)** Cell morphological changes of MDA-MB-231 cells in different treatment groups (original magnification, ×100); **(B)** Hoechst 33,258 staining shows changes in the cytoplasm of MDA-MB-231 cells in different cinnamaldehyde treatment groups (original magnification, ×200). CA, cinnamaldehyde.

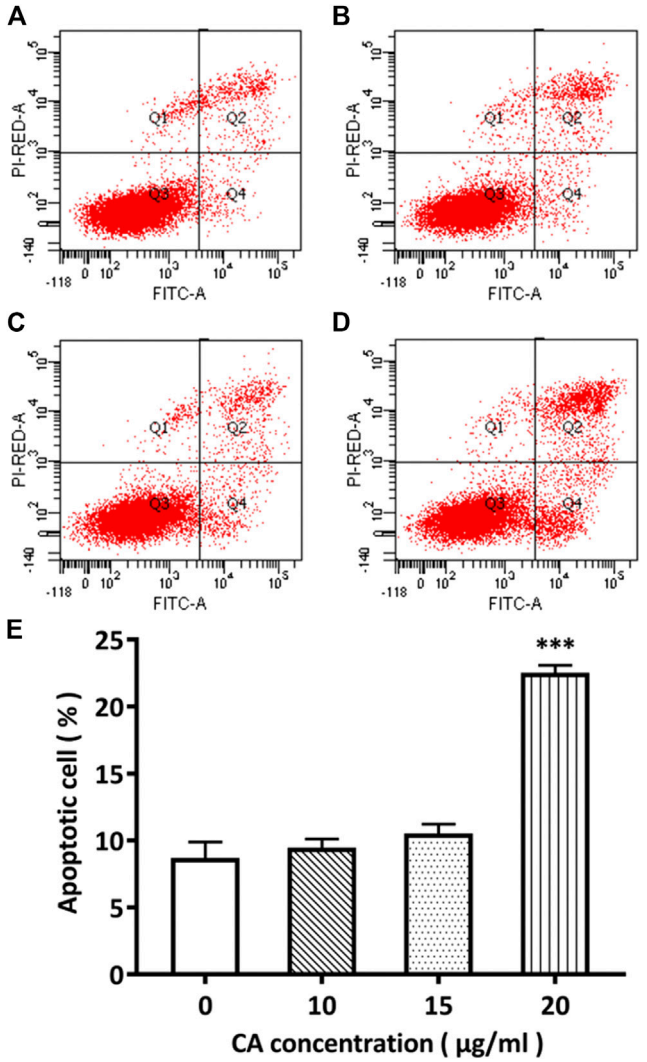

FIGURE 8 | Comparison of the apoptotic rate of MDA-MB-231 cells administered different concentrations of cinnamaldehyde by Annexin V-FITC and PI double staining. **(A)–(E)** shows the cell apoptotic rate in the cinnamaldehyde groups administered different concentrations of cinnamaldehyde (***compared to the control group $p < 0.001$). CA, cinnamaldehyde.

became rounder, the nucleus became larger, chromatin pyknosis was evident, and nuclear fragmentation was aggravated.

Promoting Effect of Cinnamaldehyde on the Apoptosis of Breast Cancer Cells

Flow cytometry was used to detect the effect of different concentrations of cinnamaldehyde on apoptosis. Our results showed that MDA-MB-231 cells exhibited 8.7, 9.5, 10.5, and 22.5% apoptosis when treated with 0, 10, 15, and 20 μg/ml of cinnamaldehyde, respectively. Compared with the control group, the cinnamaldehyde group in the normal quadrant of the 20-μg/ml cinnamaldehyde intervention group was significantly reduced, whereas the early apoptosis quadrant was significantly increased ($p < 0.01$; **Figure 8**).

Inhibitory Effect of Cinnamaldehyde on the Migration and Invasion of Breast Cancer Cells

Transwell experiments revealed that MDA-MB-231 cells had a strong invasive ability. However, after 48 h of cinnamaldehyde intervention, the invasive ability of the cells was reduced in all intervention groups, especially in the 15 and 20 μg/ml groups ($p < 0.01$). In addition, the wound healing test results revealed that 15 and 20 μg/ml cinnamaldehyde intervention significantly reduced the migration ability of MDA-MB-231 cells ($p < 0.05$) (**Figures 9A,B**). Based on the transwell invasion test, the number of transmembrane cells in the control group was 159.3 ± 12.22, whereas that in the cinnamaldehyde group (5, 10, and 15 μg/ml) was 129.3 ± 25.11, 74.67 ± 16.17, and 56 ± 9.54, respectively. Our results showed that there was a statistically significant difference ($p < 0.05$) between the cinnamaldehyde group and the control group as well as a dose-effect relationship (**Figures 9C,D**). Such findings indicate that cinnamaldehyde could significantly inhibit the invasion of breast cancer MDA-MB-231 cells.

DISCUSSION

In recent years, network pharmacology has enabled the integration of functions such as high-throughput omics data analysis, virtual computer calculation, and network database retrieval. Therefore, it has been widely employed in research on a pharmacological basis and as a mechanism of action of Chinese medicine and traditional herbs (Yin et al., 2019; Li et al., 2020). Network pharmacology can combine system biology with multi-directional pharmacology, explore the correlation between the target of each component in traditional Chinese medicine preparations and diseases, and explain its mechanism of action (Zhang et al., 2019). The multi-component and multi-target network research model of network pharmacology breaks the traditional single-component, single-target research model, ultimately providing a new method for comprehensive analysis of compound mechanisms (Yuan et al., 2017). Existing studies have shown that in recent years, network pharmacology has been widely used in the screening of breast cancer and metastatic therapy drugs and targets (Yang et al., 2019; Mao et al., 2020).

In the present study, the effective components of the ancient herb, cinnamon, were analyzed through network pharmacology, and a network of cinnamon-chemical component-breast cancer targets was constructed. Based on our findings, the key chemical constituents in cinnamon were of 12 types, including EIC, oleic acid, DIBP, and cinnamaldehyde, corresponding to 66 active targets, including 61 common targets related to breast cancer. The PPI results showed that its key targets for breast cancer include PPARG, TLR-4, BDNF, and PPAR-α. PPARG is a nuclear receptor that is widely involved in the regulation of lipid metabolism, glucose homeostasis, and tumor progression due to its role as a transcription factor (Shen et al., 2020). Recent studies have shown that PPARG has a tumor suppressor effect and can inhibit the proliferation, migration, and invasion of breast cancer cells (Tan et al., 2013). Corresponding clinical studies have also confirmed that among breast cancer patients, those with high PPARG expression levels have a higher

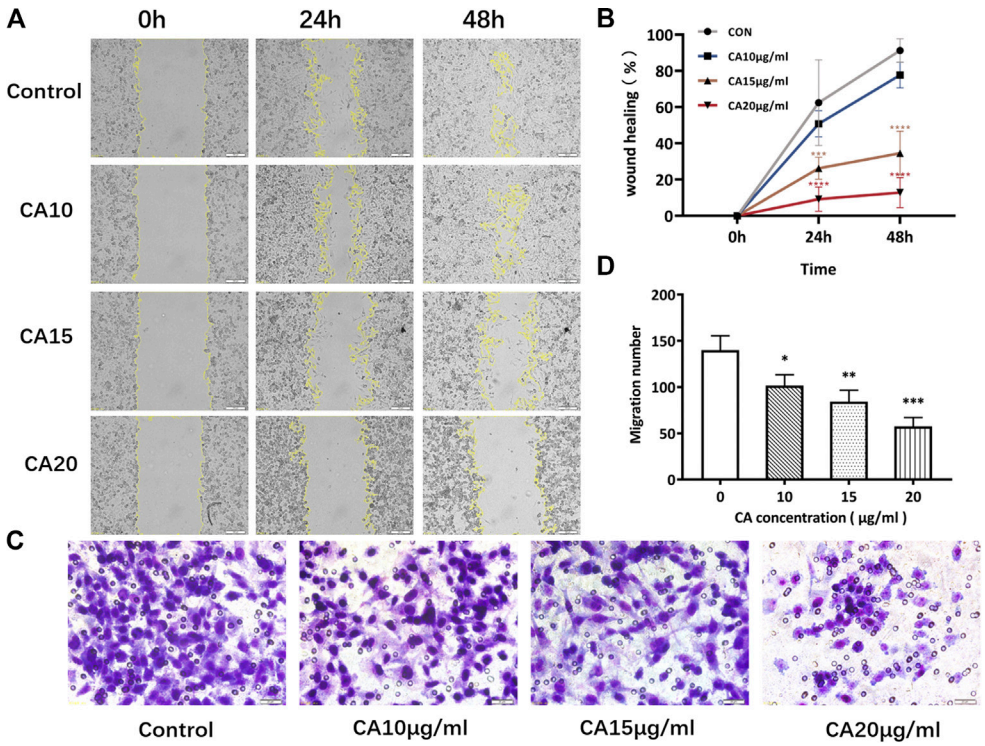

FIGURE 9 | Effects of different concentrations of cinnamaldehyde on the migration and invasion ability of MDA-MB-231 cells after a 48-h intervention. **(A), (B)**, Wound healing assay of MDA-MB-231 cells in different treatment groups (original magnification, ×100). **(C), (D)**, Invasive assay after 48 h of CA intervention (original magnification, ×200) (*, **, ***, **** compared to the control group $p < 0.05$, $p < 0.01$, $p < 0.001$, and $p < 0.0001$, respectively). CA, cinnamaldehyde.

survival rate than patients with low PPARG expression levels (Xu et al., 2019). In this study, we found that the main compounds in cinnamon are most closely related to targets related to breast cancer cell apoptosis, invasion, and metastasis (Wang et al., 2016). For example, the upregulation of TLR-4 and PPAR-α expression is related to breast cancer cell apoptosis (Geng et al., 2018). Further, the upregulation of the adipose transcription factor, PPAR-α, can promote the migration and invasion of breast cancer cells (Blucher et al., 2020). The reduction of NCOA2 expression can induce breast cancer cell apoptosis by regulating the MAPK-ERK signaling pathway (Cai et al., 2019). The upregulation of BDNF can promote breast cancer cell proliferation and invasion (Gao et al., 2017). Therefore, we speculate that cinnamon and its main chemical components may exert an anti-breast cancer effect by regulating the targets and pathways related to breast cancer cell apoptosis, invasion, and metastasis.

GO analysis results showed that the key targets were involved in amide binding, steroid hormone receptor activity, antioxidant activity, transcription factor activity, direct ligand regulated sequence-specific DNA binding, carboxylic acid-binding, steroid binding, fatty acid-binding, peroxidase activity, neurotransmitter binding, oxidoreductase activity (acting on peroxide as an acceptor), G protein-coupled amine receptor activity, and other biological processes. Further pathway analysis revealed that cinnamaldehyde in cinnamon and breast cancer targets are mainly involved in the neuroactive ligand-receptor interaction, PI3K-Akt signaling pathway, PPAR signaling pathway, cAMP signaling pathway, NF-kappa B signaling pathway, and other pathways closely related to cancer. Cinnamaldehyde can also participate in the regulation of cell apoptosis, cell metabolism, inflammation, and other pathways.

The network pharmacological screening results revealed that cinnamaldehyde is one of the main active ingredients in cinnamon. Previous studies have shown that cinnamaldehyde and cinnamaldehyde-derived compounds are drug candidates for the development of anticancer drugs, which has attracted extensive research attention (Hong et al., 2016). Cinnamaldehyde can improve the anti-cancer efficacy of oxaliplatin by promoting the apoptosis of colorectal cancer cells *in vivo* and *in vitro* (Wu et al., 2019). As an antioxidant, cinnamaldehyde can inhibit the spread of cancer by inhibiting the expression of extracellular and intracellular fat factor nicotinamide phosphoribosyltransferase (Chiang et al., 2019). Although compared with other cancers, the role of cinnamaldehyde in breast cancer is not well understood. However, in recent years, related studies have also discovered the anti-proliferation effect of cinnamaldehyde on breast cancer cells *in vitro* and *in vivo* (Lu et al., 2010). In this study, through network pharmacology, we predicted that the targets related to the anti-breast cancer effect of cinnamaldehyde are mainly associated with breast cancer cell apoptosis, invasion, and metastasis. However, the bioinformatics data used for target prediction can only reflect the correlation. Thus, its specific role in regulating breast cancer cell apoptosis, invasion, and metastasis remains unknown. As a result, we verified the effect

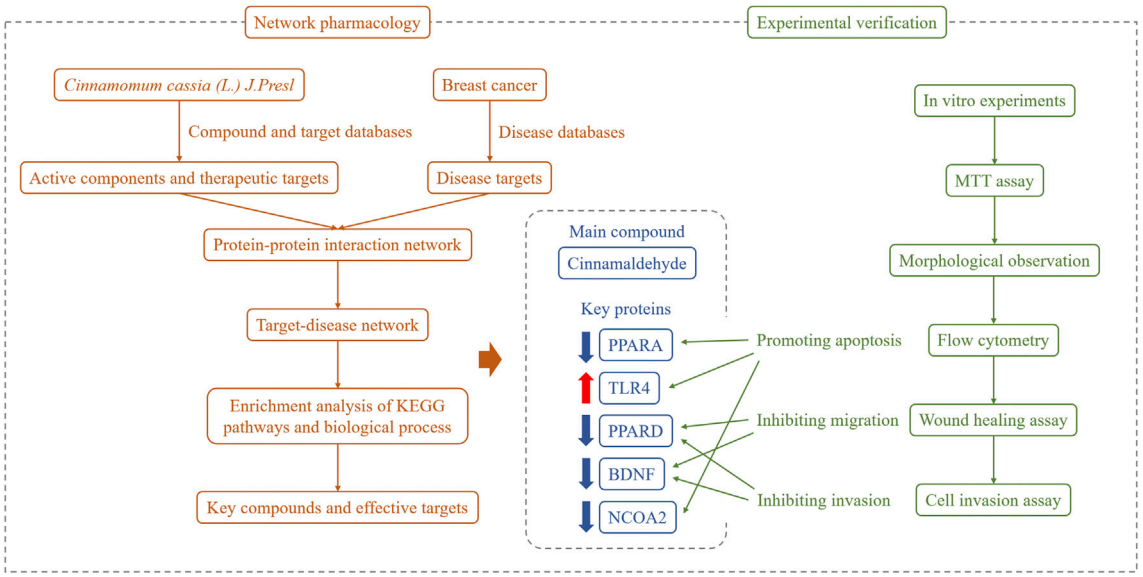

FIGURE 10 | Overall framework of cinnamaldehyde for the treatment of breast cancer. Through the network pharmacological integration strategy, cinnamaldehyde (the main chemical component of cinnamon in breast cancer) was selected. Based on *in vitro* cell experiments, cinnamaldehyde was confirmed to promote the apoptosis of breast cancer tumor cells and inhibit cell migration and invasion.

of cinnamaldehyde on human breast cancer cells through cell experiments and further confirmed the anti-cancer effect and mechanism of the active ingredients of cinnamon. Our research is a supplement to previous research and further reveals the anti-breast cancer effect of cinnamaldehyde.

TNBC is an aggressive breast cancer subtype and one of the most clinically malignant breast cancers; however, there is currently a lack of targeted treatment options (Rigiracciolo et al., 2020). Herein, we selected human TNBC MDA-MB-231 cells for subsequent verification experiments. Impaired apoptosis plays a critical role in the initiation and progression of cancer (Sadeghi et al., 2019). Therefore, we speculated that as a therapeutic agent, cinnamaldehyde may exert an anti-breast cancer effect by affecting the apoptosis-related pathways of cancer cells. Our cell experiments demonstrated that cinnamaldehyde inhibited the proliferation of MDA-MB-231 cells, changed the cytoplasmic morphology, promoted the apoptosis of MDA-MB-231 cells, reduced the invasion and migration ability of MDA-MB-231 cells, and exhibited anti-breast cancer effects. The anti-breast cancer effect of cinnamaldehyde may be related to the eight targets selected for breast cancer. In future experiments, we will conduct further studies on its role and function.

In summary, in the present study, we revealed the main active ingredient in cinnamon and explored its potential targets for the treatment of breast cancer. By establishing a breast cancer disease network and enriching the key nodes and pathways for the regulation of cinnamon active ingredients, we found that antioxidant activity and the PI3K-Akt and NF-κB signaling pathways play important roles in the pharmacological effects of cinnamon. Furthermore, through breast cancer cell experiments, we confirmed that cinnamaldehyde, the main anti-breast cancer component in cinnamon, can inhibit cell proliferation, invasion, and migration; change cytoplasmic morphology; and promote apoptosis. Our research findings provide an experimental and theoretical basis for further applications of cinnamaldehyde in the treatment of breast cancer (**Figure 10**).

DATA AVAILABILITY STATEMENT

The original contributions presented in the study are included in the article/**Supplementary Materials**, further inquiries can be directed to the corresponding author.

AUTHOR CONTRIBUTIONS

XP designed the experiments; YL and TA performed the experiments and wrote the manuscript. BY, DW, and YF analyzed the data. All authors reviewed the manuscript.

FUNDING

This work was financially supported by grants from the National Natural Science Foundation of China (NSFC81774319), Beijing Natural Science Foundation Project (7182098), and the independent subject graduate student projects of Beijing University of Traditional Chinese Medicine (2019-JYB-XS).

SUPPLEMENTARY MATERIAL

The Supplementary Material for this article can be found online at: https://www.frontiersin.org/articles/10.3389/fphar.2020.582719/full#supplementary-material

REFERENCES

Blucher, C., Iberl, S., and Schwagarus, N. (2020). Secreted factors from adipose tissue reprogram tumor lipid metabolism and induce motility by modulating PPARα/ANGPTL4 and FAK [published online ahead of print, 2020 Aug 28]. *Mol. Cancer Res.* 1223, 2019. doi:10.1158/1541-7786.MCR-19-1223

Bray, F., Ferlay, J., and Soerjomataram, I. (2018). Global cancer statistics 2018: GLOBOCAN estimates of incidence and mortality worldwide for 36 cancers in 185 countries. *CA A Cancer J. Clin.* 9(12), 24–28. doi:10.3322/caac.21492

Buglak, N. E., Jiang, W., and Bahnson, E. S. M. (2018). Cinnamic aldehyde inhibits vascular smooth muscle cell proliferation and neointimal hyperplasia in Zucker Diabetic Fatty rats. *Redox Biol.* 19, 166–178. doi:10.1016/j.redox.2018.08.013

Cabello, C. M., Bair, W. B., 3rd, and Lamore, S. D. (2009). The cinnamon-derived Michael acceptor cinnamic aldehyde impairs melanoma cell proliferation, invasiveness, and tumor growth. *Free Radic. Biol. Med.* 46(2), 220–231. doi:10.1016/j.freeradbiomed.2008.10.025

Cai, M., Liang, X., and Sun, X. (2019). Nuclear receptor Coactivator 2 promotes human breast cancer cell growth by positively regulating the MAPK/ERK pathway. *Front Oncol.* 9, 164. doi:10.3389/fonc.2019.00164

Chen, W., Zheng, R., and Baade, P. D., (2016). Cancer statistics in China, 2015. *CA A Cancer J. Clin.* 66(2), 115–132. doi:10.3322/caac.21338

Chiang, Y. F., Chen, H. Y., Huang, K. C., Lin, P. H., and Hsia, S. M. (2019). Dietary antioxidant Trans-cinnamaldehyde reduced Visfatin-induced breast cancer progression: *in vivo* and *in vitro* study. *Antioxidants*. 8(12), 625. doi:10.3390/antiox8120625

Foulkes, W. D., Smith, I. E., and Reis-Filho, J. S. (2010). Triple-negative breast cancer. *N. Engl. J. Med.* 363(20), 1938–1948. doi:10.1056/NEJMra1001389

Gao, B., Hao, S., and Tian, W. (2017). MicroRNA-107 is downregulated and having tumor suppressive effect in breast cancer by negatively regulating brain-derived neurotrophic factor. *J. Gene Med.* 19(12), 33–49. doi:10.1002/jgm.2932

Geng, L., Zhou, W., Liu, B., Wang, X., and Chen, B. (2018). DHA induces apoptosis of human malignant breast cancer tissues by the TLR-4/PPAR-α pathways. *Oncol Lett.* 15(3), 2967–2977. doi:10.3892/ol.2017.7702

Guo, Y., Fan, Y., and Pei, X. (2020). Fangjihuangqi Decoction inhibits MDA-MB-231 cell invasion *in vitro* and decreases tumor growth and metastasis in triple-negative breast cancer xenografts tumor zebrafish model. *Cancer Med.* 9(7), 2564–2578. doi:10.1002/cam4.2894

Hagenlocher, Y., Kiessling, K., Schäffer, M., Bischoff, S. C., and Lorentz, A. (2015). Cinnamaldehyde is the main mediator of cinnamon extract in mast cell inhibition. *Eur. J. Nutr.* 54(8), 1297–1309. doi:10.1007/s00394-014-0810-0

Hong, S. H., Ismail, I. A., Kang, S. M., Han, D. C., and Kwon, B. M. (2016). Cinnamaldehydes in cancer chemotherapy. *Phytother. Res.* 30(5), 754–767. doi:10.1002/ptr.5592

Kaur, G., Athar, M., and Alam, M. S. (2010). Eugenol precludes cutaneous chemical carcinogenesis in mouse by preventing oxidative stress and inflammation and by inducing apoptosis. *Mol. Carcinog.* 49(3), 290–301. doi:10.1002/mc.20601

Lehmann, B. D., Bauer, J. A., Chen, X., et al. (2011). Identification of human triple-negative breast cancer subtypes and preclinical models for selection of targeted therapies. *J. Clin. Invest.*. 121(7), 2750–2767. doi:10.1172/JCI45014

Li, Y., Jiang, X., Song, L., Yang, M., and Pan, J. (2020). Anti-apoptosis mechanism of triptolide based on network pharmacology in focal segmental glomerulosclerosis rats. *Biosci. Rep.* 40(4), BSR20192920. doi:10.1042/BSR20192920

Liao, H. Y., Zhang, W. W., Sun, J. Y., Li, F. Y., He, Z. Y., and Wu, S. G. (2018). The Clinicopathological features and survival outcomes of different histological subtypes in triple-negative breast cancer. *J. Cancer* 9(2), 296–303. doi:10.7150/jca.22280

Lu, H., Zhang, J., Liang, Y., Qiao, Y., Yang, C., He, X., et al. (2020). Network topology and machine learning analyses reveal microstructural white matter changes underlying Chinese medicine Dengzhan Shengmai treatment on patients with vascular cognitive impairment. *Pharmacol. Res.* 24, 156. doi:10.1016/j.phrs.2020.104773

Lu, J., Zhang, K., Nam, S., Anderson, R. A., Jove, R., and Wen, W. (2010). Novel angiogenesis inhibitory activity in cinnamon extract blocks VEGFR2 kinase and downstream signaling. *Carcinogenesis* 31(3), 481–488. doi:10.1093/carcin/bgp292

Mao, Y., Chu, X., Xue, P., Li, L., Su, Y., He, S., et al. (2020). Discussion on the mechanism of "Epimedium epimedii-Cistanche deserticola" for bone metastasis of breast cancer. *J. Hainan Med. Coll.* 26 (04), 262–269. doi:10.1093/carcin/bgp292

Ng, L. T., and Wu, S. J. (2011). Antiproliferative activity of Cinnamomum cassia constituents and effects of Pifithrin-Alpha on their apoptotic signaling pathways in hep G2 cells. *Evid Based Complem. Alternat. Med.* 2011, 492148. doi:10.1093/ecam/nep220

Parise, C. A., and Caggiano, V. (2017). Risk of mortality of node-negative, ER/PR/HER2 breast cancer subtypes in T1, T2, and T3 tumors. *Breast Cancer Res. Treat.* 165(3), 743–750. doi:10.1007/s10549-017-4383-5

Reddy, N. D., Shoja, M. H., Biswas, S., Nayak, P. G., Kumar, N., and Rao, C. M. (2016). An appraisal of cinnamyl sulfonamide hydroxamate derivatives (HDAC inhibitors) for anti-cancer, anti-angiogenic and anti-metastatic activities in human cancer cells. *Chem. Biol. Interact.* 253, 112–124. doi:10.1016/j.cbi.2016.05.008

Rida, P., Ogden, A., and Ellis, I. O. (2018). First international TNBC conference meeting report. *Breast Canc. Res. Treat.* 169(3), 407–412. doi:10.1007/s10549-018-4692-3

Rigiracciolo, D. C., Nohata, N., and Lappano, R. (2020). IGF-1/IGF-1R/FAK/YAP Transduction signaling Prompts growth effects in triple-negative breast cancer (TNBC) cells. *Cells* 9(4), E1010. doi:10.3390/cells9041010

Sadeghi, S., Davoodvandi, A., Pourhanifeh, M. H., et al. (2019). Anti-cancer effects of cinnamon: insights into its apoptosis effects. *Eur. J. Med. Chem.* 178, 131–140. doi:10.1016/j.ejmech.2019.05.067

Shen, S. J., Song, Y., and Ren, X. Y. (2020). MicroRNA-27b-3p promotes tumor progression and metastasis by inhibiting peroxisome proliferator-activated receptor gamma in triple-negative breast cancer. *Front Oncol.* 10, 1371. doi:10.3389/fonc.2020.01371

Siegel, R. L., Miller, K. D., and Jemal, A. (2018). Cancer statistics. *CA A Cancer J. Clin.* 68(1), 7–30. doi:10.3322/caac.21442

Tan, B. S., Kang, O., Mai, C. W., Tiong, K. H., Khoo, A. S., Pichika, M. R., et al. (2013). 6-Shogaol inhibits breast and colon cancer cell proliferation through activation of peroxisomal proliferator activated receptor gamma (PPARgamma). *Canc. Lett.* 336, 127–139. doi:10.1016/j.canlet.2013.04.014

Wang, X., Wang, G., and Shi, Y. (2013). PPAR-delta promotes survival of breast cancer cells in harsh metabolic conditions. *Oncogenesis* 5(6), e232. doi:10.1038/oncsis.2016.41

Wu, C. E., Zhuang, Y. W., Zhou, J. Y., Liu, S. L., Wang, R. P., and Shu, P. (2019). Cinnamaldehyde enhances apoptotic effect of oxaliplatin and reverses epithelial-mesenchymal transition and stemnness in hypoxic colorectal cancer cells. *Exp. Cell Res.* 383(1), 111500. doi:10.1016/j.yexcr.2019.111500

Xu, Y. Y., Liu, H., Su, L., Xu, N., Xu, D. H., Liu, H. Y., et al. (2019). PPARγ inhibits breast cancer progression by upregulating PTPRF expression. *Eur. Rev. Med. Pharmacol. Sci.* 23, 9965–9977.

Yang, B., Wang, N., and Wang, S. (2019). Network-pharmacology-based identification of caveolin-1 as a key target of Oldenlandia diffusa to suppress breast cancer metastasis. *Biomed. Pharmacother.* 112, 108607. doi:10.1016/j.biopha.2019.108607

Yin, S. H., Xu, P., and Wang, B. (2019). Duration of dual antiplatelet therapy after percutaneous coronary intervention with drug-eluting stent: systematic review and network meta-analysis. *BMJ* 365, l2222. doi:10.1136/bmj.l2222

Yuan, H., Ma, Q., and Cui, H. (2017). How can synergism of traditional medicines benefit from network pharmacology?. *Molecules*. 22(7), 1135. doi:10.3390/molecules22071135

Zhang, R., Zhu, X., Bai, H., and Ning, K. (2019). Network pharmacology databases for traditional Chinese medicine: review and Assessment. *Front. Pharmacol.* 10, 123. doi:10.3389/fphar.2019.00123

Zu, Y., Yu, H., and Liang, L. (2010). Activities of ten essential oils towards Propionibacterium acnes and PC-3, A-549 and MCF-7 cancer cells. *Molecules* 15(5), 3200–3210. doi:10.3390/molecules15053200

Conflict of Interest: The authors declare that the research was conducted in the absence of any commercial or financial relationships that could be construed as a potential conflict of interest.

GLOSSARY

cinnamon *Cinnamomum cassia* (L.) J. Presl

TNBC Triple-negative breast cancer

TCMSP Traditional Chinese Medicine Systems Pharmacology Database and Analysis Platform

DL Drug-likeness

TCM Traditional Chinese Medicine

TCMID The Traditional Chinese Medicines Integrated Database

FDR False discovery rate

OB Oral bioavailability

PPI Protein–protein interaction

TS Tanimoto similarity

STP Swiss Target Prediction

OMIM Online Mendelian Inheritance in Man

DAVID The Database for Annotation, Visualization, and Integrated Discovery

GO gene ontology

KEGG Kyoto encyclopedia of genes and genomes

OD optical density

FITC fluorescein isothiocyanate

PI Propidium iodide

SD standard deviation

PPARG Peroxisome Proliferator-Activated Receptor Gamma

INS Insulin

BDNF Brain-derived neurotrophic factor

CAT catalase

CA Cinnamaldehyde

frontiers in Pharmacology

ORIGINAL RESEARCH
published: 04 March 2021
doi: 10.3389/fphar.2021.618522

Network Pharmacology and Pharmacological Evaluation Reveals the Mechanism of the *Sanguisorba Officinalis* in Suppressing Hepatocellular Carcinoma

Nan Jiang[1,2,3†], *Hong Li*[2,4†], *Yueshan Sun*[2,4], *Jing Zeng*[2,4], *Fei Yang*[2,4], *Fahsai Kantawong*[1*] *and Jianming Wu*[1,2,4*]

[1]*Department of Medical Technology, Faculty of Associated Medical Sciences, Chiang Mai University, Chiang Mai, Thailand,* [2]*School of Pharmacy, Southwest Medical University, Luzhou, China,* [3]*International Education School, Southwest Medical University, Luzhou, China,* [4]*Education Ministry Key Laboratory of Medical Electrophysiology, Sichuan Key Medical Laboratory of New Drug Discovery and Drugability Evaluation, Luzhou Key Laboratory of Activity Screening and Drugability Evaluation for Chinese Materia Medica, Southwest Medical University, Luzhou, China*

OPEN ACCESS

Edited by:
Marcus Scotti,
Federal University of Paraíba, Brazil

Reviewed by:
Yashi Mi,
University of Arizona, United States
Qi Wang,
Guangzhou University of Chinese Medicine, China

***Correspondence:**
Jianming Wu
jianmingwu@swmu.edu.cn
Fahsai Kantawong
fahsai.k@cmu.ac.th

[†]*These authors contributed to this work equally*

Specialty section:
This article was submitted to Ethnopharmacology, a section of the journal Frontiers in Pharmacology

Received: *17 October 2020*
Accepted: *20 January 2021*
Published: *04 March 2021*

Citation:
Jiang N, Li H, Sun Y, Zeng J, Yang F, Kantawong F and Wu J (2021) Network Pharmacology and Pharmacological Evaluation Reveals the Mechanism of the Sanguisorba Officinalis *in Suppressing Hepatocellular Carcinoma. Front. Pharmacol. 12:618522. doi: 10.3389/fphar.2021.618522*

Background: *Sanguisorba Officinalis* L. (SO) is a well-known traditional Chinese medicine (TCM), commonly applied to treat complex diseases, such as anticancer, antibacterial, antiviral, anti-inflammatory, anti-oxidant and hemostatic effects. Especially, it has been reported to exert anti-tumor effect in various human cancers. However, its effect and pharmacological mechanism on hepatocellular carcinoma (HCC) remains unclear.

Methods: In this study, network pharmacology approach was applied to characterize the underlying mechanism of SO on HCC. Active compounds and potential targets of SO, as well as related genes of HCC were obtained from the public databases, the potential targets and signaling pathways were determined by protein-protein interaction (PPI), gene ontology (GO) and pathway enrichment analyses. And the compound-target and target-pathway networks were constructed. Subsequently, *in vitro* experiments were also performed to further verify the anticancer effects of SO on HCC.

Results: By using the comprehensive network pharmacology analysis, 41 ingredients in SO were collected from the corresponding databases, 12 active ingredients screened according to their oral bioavailability and drug-likeness index, and 258 potential targets related to HCC were predicted. Through enrichment analysis, SO was found to show its excellent therapeutic effects on HCC through several pathways, mainly related to proliferation and survival via the EGFR, PI3K/AKT, NFκB and MAPK signaling pathways. Additionally, *in vitro*, SO was found to inhibit cell proliferation, induce apoptosis and down-regulate cell migration and invasion in various HCC cells. Moreover, western blot analysis showed that SO treatment down-regulated the expression of p-EGFR, p-PI3K, p-AKT, p-NFκB and p-MAPK proteins in HepG2 cells. These results validated that SO exerted its therapeutic effects on HCC mainly by the regulation of cell proliferation and survival via the EGFR/MAPK and EGFR/PI3K/AKT/NFκB signaling pathways.

Conclusion: Taken together, this study, revealed the anti-HCC effects of SO and its potential underlying therapeutic mechanisms in a multi-target and multi-pathway manner.

Keywords: PI3K/Akt signal pathway, cell proliferation, network pharmacology, hepatocellular carcinoma, *Sanguisorba officinalis* L, EGFR/MAPK signaling

INTRODUCTION

Hepatocellular carcinoma (HCC) is the sixth most commonly diagnosed cancer, ranking the third leading cause of cancer-related death according to GLOBCAN in 2018, with approximately 841,000 new incidences and 782,000 deaths yearly around the world, posing a major health problem (Bray et al., 2018; EASL, 2018). Although survival rates of HCC patients have improved on benefit from modern therapeutic strategies, namely, liver transplantation, radiofrequency ablation, transcatheter arterial chemoembolization, surgical resection, and sorafenib (Liu et al., 2015; EASL, 2019), many HCC patients still face high long-term mortality, recurrence, drug resistance and serious side effects (Cheng et al., 2009; Zhu et al., 2017). Therefore, it is urgent to search for the alternative therapeutic strategies with low toxicity and less drug resistance for HCC.

Traditional Chinese medicine (TCM) with diverse chemical substances has been widely accepted as an effective strategy with less toxicity and higher efficacy for the therapy of cancer (Yuan et al., 2017; Xiang et al., 2019). Researches shown that TCM has the advantages in clinical cancer treatment, especially in suppressing tumor cells, reducing the side effects of radiotherapy and drug resistance, and improving patients' overall survival (Liao et al., 2017; Kuo et al., 2018; Lou et al., 2018). The plant of *Sanguisorba Officinalis* L. (SO), also known as Diyu in Chinese, a widely used herb medicine in east Asia, has been prescribed clinically for more than 2000 years in China (Zhao et al., 2017). According to preliminary reports, SO possessed a variety of pharmacological effects, such as anticancer (Cai et al., 2012), antibacterial (Chen et al., 2015), antiviral (Kim et al., 2010), anti-inflammatory (Seo et al., 2016), anti-oxidant (Zhang et al., 2012) and hemostatic effects (Sun et al., 2012). It was reported that a hot water preparation made of a single herb (SO) has excellent antitumor effect in human oral cancer cells (Shin et al., 2012). Moreover, triterpenoids and tannins isolated from the roots of SO have been shown promising antitumor effects in several cancer researches (Liu et al., 2005; Bai et al., 2019; Li et al., 2019). Notably, it was reported recently that Ziyuglycoside II, a major active compound of SO, markedly impaired HepG2 proliferation, migration and invasion, by blocking EGFR/NF-kB signaling (Liao et al., 2020). However, the effects and mechanism of SO to treat HCC have not been fully elucidated with suitable approaches.

TCM is associated with complex chemical composition and synergistic or antagonistic interactions, making it difficult to systematically study its pharmacological mechanisms with conventional pharmacological approaches (Ma et al., 2015). Fortunately, the concept of network pharmacology, as an integrated approach, derived from systems biology and bioinformatics, was proposed to comprehensively investigate and study the underlying molecular mechanisms of Chinese herb medicine (Ma et al., 2015). Network pharmacology analysis was used to reveal the complex mechanism of TCM, via the construction and visualization of "medicine-target-disease" interaction network, (Li and Zhang, 2013). In recent years, network pharmacology emerged as a powerful tool resonates well with the holistic view of TCM. This approach has been successful applied to investigate the complex mechanism of TCM in many researches (Zhang et al., 2013; He et al., 2019; Wan et al., 2019).

In the present study, we aim to construct the pharmacological network to explore the potential molecular mechanisms and pathways of SO on HCC, using multiple database and computational tools. Additionally, *in vitro* experiments were also performed to verify the underlying molecular mechanism of SO on HCC, as predicted by network pharmacology. The workflow of this study is shown in **Figure 1**.

METHOD

Collection of Chemical Ingredients in *Sanguisorba Officinalis* L. for Network Pharmacology Analysis

As previous reported (Ru et al., 2014), Potential candidate compounds of SO were acquired from the two following databases: 1) Traditional Chinese Medicine Systems Pharmacology Database and Analysis Platform (TCMSP, http://tcmspw.com/tcmsp.php, Version. 2.3) (Ru et al., 2014). A total of 499 registered Chinese herbal medicines and 12,144 ingredients from the Chinese Pharmacopoeia (2010 edition) were collected in the TCMSP database (Ru et al., 2014). 2) Bioinformatics Analysis Tool for Molecular mechanism of Traditional Chinese Medicine (BATMAN-TCM, http://bionet.ncpsb.org/batman-tcm, updated in 2016), including of 46,914 formulas, 8,159 medical herbs, and 25,210 components (Liu et al., 2016).

Active Ingredients Screening Strategy

For oral traditional Chinese medicine, absorption, distribution, metabolism, and excretion (ADME) was employed to screen active components with potential therapeutic effects (Liu et al., 2013). The screening criterion we applied in this research were 1) Oral bioavailability (OB) greater than 30%, 2) Drug-likeness (DL) larger than 0.18. A total of 12 active ingredients and their corresponding 2D and 3D structures were downloaded from the PubChem database (https://pubchem.ncbi.nlm.nih.gov/) (Zhu et al., 2017).

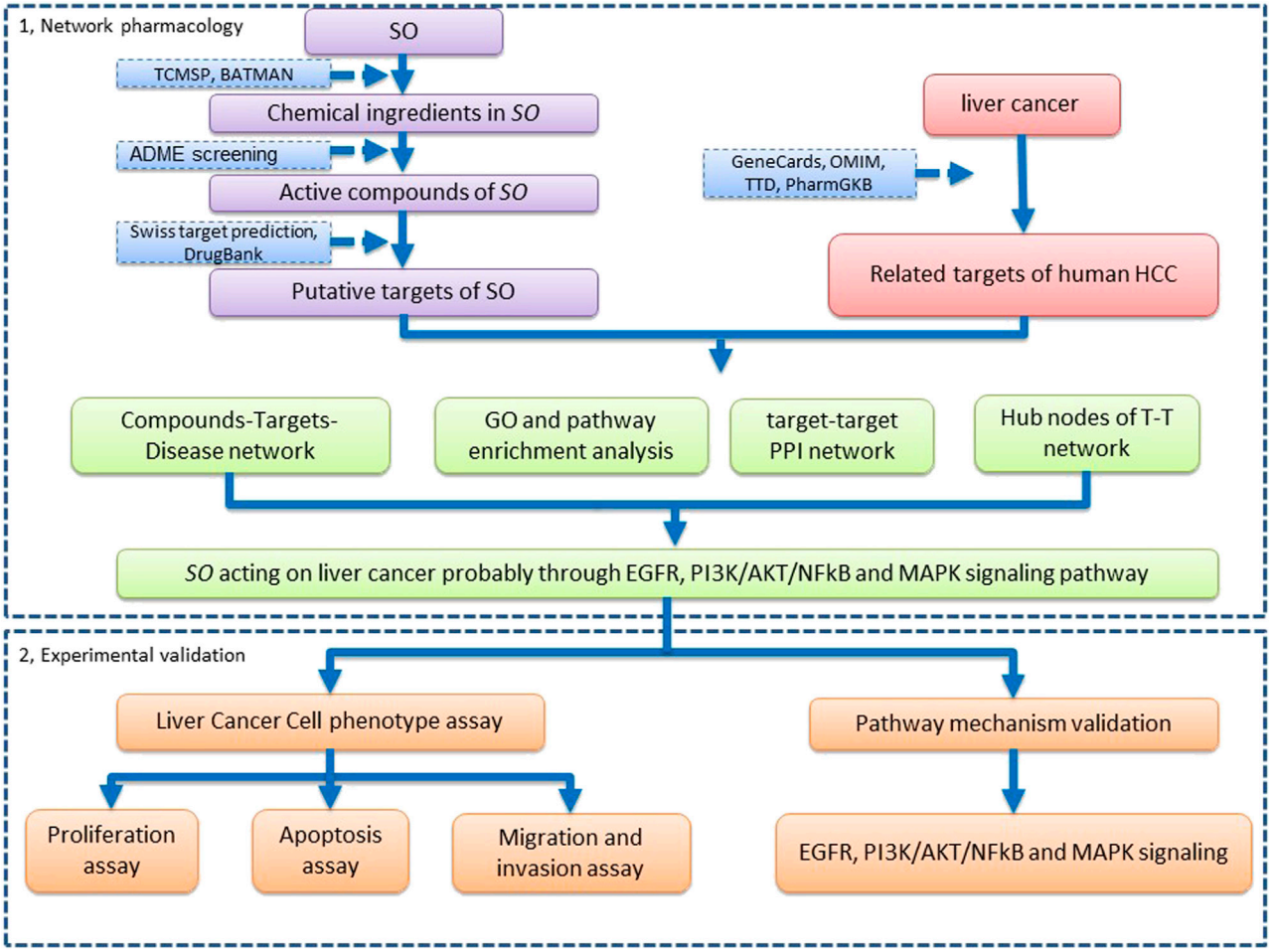

FIGURE 1 | The workflow of network pharmacology analysis and validation of SO on HCC.

Prediction of Targets of the Active Ingredients in *Sanguisorba Officinalis* L.

The related protein targets of bioactive components were retrieved from TCMSP (TCMSP, http://tcmspw.com/tcmsp.php, Version. 2.3) (Ru et al., 2014) and Swiss Target Prediction network database (STP, http://www.swisstargetprediction.ch/, updated in 2019) (Gfeller et al., 2014). The UniProt database (https://www.uniprot.org/) was adopted to change protein names to their corresponding gene symbols (UniProt Consortium, 2018).

Collection of Potential Target Genes for Hepatocellular Carcinoma

The HCC-related gene targets were collected from four databases: GeneCards (https://www.genecards.org/, version. 5.0) database (Stelzer et al., 2016). OMIM (http://www.omim.org/, updated in 2020) database (Amberger and Hamosh, 2017). Therapeutic Target Database (TTD, https://db.idrblab.net/ttd/, updated in 2020) (Li et al., 2018). PharmGKB (https://www.pharmgkb.org/, updated in 2020) (Whirl-Carrillo et al., 2012), using keywords such as "hepatocarcinoma" and "Hepatocellular Carcinoma".

Construction of Protein–Protein Interaction (PPI) Network

Protein–protein interaction network was constructed by the STRING (https://string-db.org/, version. 11.0) database, using the overlap genes between SO active ingredients targets and HCC targets (Szklarczyk et al., 2019), with the species limited to "Homo sapiens", and correlation degree greater than 0.700, as the cut-off confidence score.

Pharmacology Network Construction

Pharmacology networks were generated as follows: 1) Active compound-Target-Disease network of SO (C-T-D network). 2) OS targets—HCC targets PPI network (T-T network). 3) Target - pathway network (T-P network). The pathway annotation of targets was obtained from the KEGG pathway enrichment analysis. All networks were visualized by Cytoscape 3.7.0 (Shannon et al., 2003).

Network Topological Analysis

For network topological analysis, we calculated three parameters to assess topological features of nodes, namely: 1) "Degree" measures links to one node. 2) "Betweenness Centrality" is the number of a node lies on paths between other nodes. 3) "Closeness Centrality" measures the mean distance from a node to other nodes (Tang et al., 2015). The level of the three parameters shows the topological importance of the nodes in the network.

Gene Ontology (GO) and KEGG Pathway Enrichment Analyses

Database for Annotation, Visualization and Integrated Discovery (Huang da et al., 2009) (DAVID, https://david.ncifcrf.gov/, version 6.8) was used for gene ontology (GO) and KEGG pathway enrichment analysis (Kanehisa et al., 2017).

Reagents and Antibodies

Fetal bovine serum (FBS), Dulbecco's modified Eagle's medium (DMEM) were purchased from Gibco (Gibco, Thermo Fisher Scientific, Waltham, MA, United States). Penicillin and streptomycin were obtained from Beyotime (Beyotime, Sichuan, China). Paclitaxel (PTX) purchased from Sigma-Aldrich (St. Louis, MO, United States) Primary antibodies, including anti-EGFR (#4267), anti-p-EGFR (#3777), anti-PI3-kinase (#4249), anti-p-PI3K (#4228), anti-AKT (#4691), anti-p-AKT (#4060), anti-NFκB-P65 (#8242), anti-p-NFκB-P65 (#3033), anti-MAPK (#4695), anti-p-MAPK (#4370), anti-Cleaved Caspase-3 (#9664), anti-PARP (#9542) and β-actin (#4970) were purchased from Cell Signaling Technology Inc. (CST, MA, United States).

Preparation of *Sanguisorba Officinalis* L. Ethanol Extract

Dried roots of SO were obtained from Chengdu Wukuaishi herbal medicine wholesale market (Chengdu, Sichuan, China). The original herb was authenticated by professor Can Tang of the Department of Chinese Materia Medica, Southwest Medical University, China. A voucher specimen (SWMU-YL-DY2019031501) was deposited at the specimen repository of the Department of Traditional Chinese Medicine, Southwest Medical University. Samples (200 g) of dried roots of SO were extracted with 2 L of 75% ethanol and then filtered with a 0.22 μm pore-size filter. The filtrates of ethanol extracts of SO (ESO) were evaporated to dried powder and stored in −20°C for future use.

Phytochemical Analysis of ESO

ESO were qualitatively analyzed by ultra-high-performance liquid chromatography (Exion)—QTOF (X500R) MS system (SCIEX, MA, United States). AB Sciex ExionLC system (AB SCIEX, Foster City, CA, United States), equipped with an ExionLC Solvent Delivery System, an ExionLC AD Auto-sampler, an ExionLC AD Column oven, an ExionLC Degasser, an ExionLC AD Pump, an ExionLC PDA Detector, and an ExionLC Controller, were used for chromatographic analysis. ESO were separated on Phenomenex Kinetex C18 column (100 × 2.1 mm, 2.6 μm, 100 Å) at 40°C. The sample was eluted at a flow rate of 0.2 ml/min in a gradient elution program of A (0.1% formic acid-water (v/v)) and B (0.1% formic acid-acetonitrile(v/v)): 0–2.00 min (5% B); 2.01–18 min (5–50% B); 18.00–20.00 min (50–100% A). The injection volume was 5 μL.

Cell Culture

Human HCC cells (HepG2, MHCC97H, SMCC7721, and BEL-7404) were chosen for the following experiments. HepG2 and SMCC7721 cells were commercially obtained from American Type Culture Collection (ATCC, Manassa, VA, United States); BEL-7404 cells were and MHCC97H cells were kindly gifted by Professor Lv Muhan from department of internal medicine, The affiliated hospital of Southwest Medical University. Cells were cultured in DMEM medium supplemented with 10% FBS, 100 U/ml penicillin-streptomycin and maintained at 37°C in a humidified incubator with 5% CO_2.

Cell Viability Assay

HCC cells were seeded in 96-well plates at density of 4×10^4 cells/ml (100 μL/well) and incubated for 24 h. After pretreatment with different concentrations of ESO (0, 15.625, 31.25, 62.5, 125, 250, 500, and 1,000 μg/ml) for 24, and 48 h. Following the addition of 10 μL CCK8 (Dojindo, Japan) per well, cells were cultured for another 4 h at 37°C. The absorbance was determined at 450 nm using a Microplate Reader (Thermo Fisher Scientific Inc., Waltham, MA, United States).

5-Ethynyl-2′-deoxyuridine (EdU) Assay

The proliferation of HCC cells was determined by EdU assay. After HCC cells (4,000 cells/well) were seeded in 96-well plates and incubated for 24 h, cells were exposed to concentrations of ESO (0, 62.5, 125, and 250 μg/ml) for 24 h and incubated with 10 μM EdU (APExBIO, Houston, United States) for another 2 h. Then the cells were fixed with 3.7% formaldehyde for 15 min and cell nuclei were stained with Hoechst 33,342. Eventually, EdU-positive cells were observed and photographed under a photographed at a magnification of ×100 with an ImageXpress - Micro 4 High-Content Screening system (Molecular Devices, LLC, CA, United States). The EdU-positive cells (%) = The count of red EdU/The count of blue Hoechst 33,342 × 100.

Wound-Healing and Transwell Invasion Assay

For wound-healing assay, HepG2 and SMCC7721 cells were incubated in 6-well plates with 100% confluence. After cells were scratched using a sterile pipette tip on the cell monolayer, medium was removed and the monolayer was washed 3 times with PBS. Then, medium containing indicated concentrations of ESO was added to each well and cell movements into the wound area were obtained after 0 and 24 h incubation with a phase-contrast inverted microscope at a magnification of ×40. The transwell invasion assay was conducted using a Corning transwell chamber system (8.0 μm, #3442, Corning, NY, United States). 1.5×10^5 treated cells were seeded into the upper chamber in the presence of a Matrigel-precoated membrane (#M8370, Solarbio, Beijiang, China) containing 200 μL of serum-free MEM. Then, complete medium

TABLE 1 | Active ingredients and ADME parameters of *SO*.

Mol ID	Molecule name	Structure	OB (%)	DL
MOL000098	Quercetin	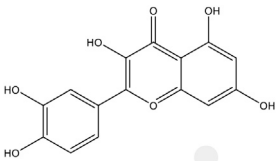	46.43	0.28
MOL000211	Mairin	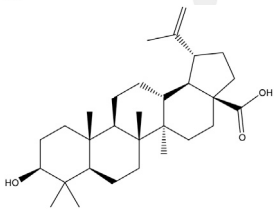	55.38	0.78
MOL000358	Beta-sitosterol	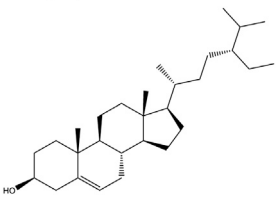	36.91	0.75
MOL000422	Kaempferol	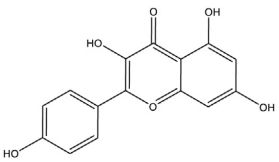	41.88	0.24
MOL005399	Alexandrin_qt	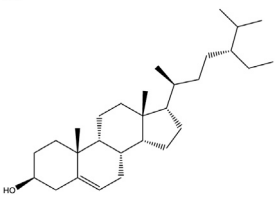	36.91	0.75
MOL005853	Methyl-2,3,6-tri-O-galloyl-β-D-glucopyranoside	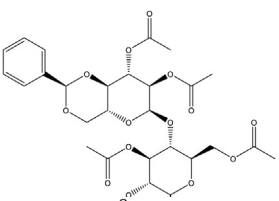	44.95	0.67
MOL005858	3,7,8-Tri-O-methylellagic acid	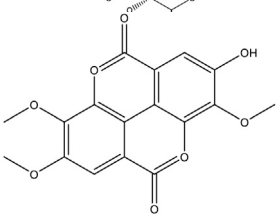	37.54	0.57
MOL005860	3-O-galloylprocyanidin B-3	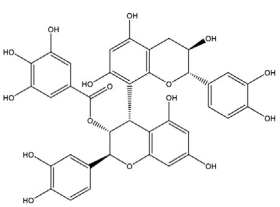	30.06	0.33

(Continued on following page)

TABLE 1 | (*Continued*) Active ingredients and ADME parameters of *SO*.

Mol ID	Molecule name	Structure	OB (%)	DL
MOL005862	Methyl 4,6-di-O-galloyl-beta-D-glucopyranoside	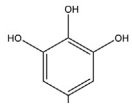	48.07	0.68
MOL005864	Methyl-6-O-galloyl-β-D-glucopyranoside	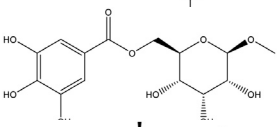	44.85	0.29
MOL005880	Sauvissimoside R1	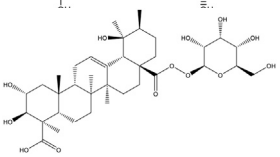	37.39	0.31
MOL005883	Gambiriin B-3	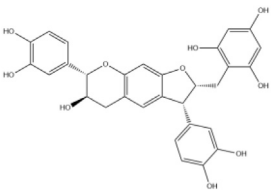	34.99	0.75

(500 μL) containing 10% FBS was added to the bottom chamber. Following incubation for 24 h at 37°C, the chambers were washed twice with phosphate-buffered saline, fixed with 4% paraformaldehyde, and stained with 1% crystal violet solution at room temperature. Cells were counted under a light microscope in five random fields.

Flow Cytometry for Analysis of Cell Apoptosis

Apoptosis was analyzed using an Annexin V-FITC apoptosis detection kit (San Jose, CA, United States). HepG2 and SMCC7721 cells were seeded at a density of 1.5×10^5 cells/well in 6-well plates. After 24 h treatment with ESO at indicated concentrations, the cells were analyzed using an annexin V-FITC/PI Detection Kit from BD Biosciences (San Jose, CA, United States) to detect apoptosis. The apoptotic cells were detected by FACSVerse flow cytometer (BD Biosciences, San Jose, CA, United States). Data acquisition and analysis were performed using the Flowjo software (BD Biosciences, San Jose, CA, United States).

Western Blotting

Cells (1.5×10^5 cells/well) were seeded into 6-well plates. Cell proteins were extracted after treatment of the indicated concentrations of ESO, according to procedures as described previously (Teng et al., 2020). The cells were lyzed in 1 × PIPA buffer, containing 1: 100 protease and phosphatase inhibitor cocktail on ice for 30 min. The protein concentration of the lysate was then determined by the Bradford protein assay reagent (Bio-Rad, CA, United States) according to the manufacturer's instructions. An equal amount of the protein (30 μg per sample) was loaded onto 10% sodium dodecyl sulfate polyacrylamide gel electrophoresis (SDS-PAGE) for separation and transferred onto polyvinylidene difluoride (PVDF) membranes (Bio-Rad, United States). Then, the membranes were blocked with 5% no-fat milk for 1 h at room temperature and incubated with the primary antibodies including anti-EGFR, anti-p-EGFR, anti-PI3-kinase, anti-p-PI3-kinase, anti-AKT, anti-p-AKT, anti-NFκB (p65), anti-p-NFκB (p65), anti-MAPK, anti-p-MAPK and β-actin at 1:1,000 (Cell Signaling Technology, Danvers, MA, United States) overnight at 4°C. Then, the membranes were washed with TBST three times and further incubated with HRP-conjugated secondary antibodies for 1 h at room temperature and the protein bands were developed by an UltraSignal Hypersensitive ECL Chemiluminescent Substrate (4A Biotech Co., Ltd., Beijing, China). and detected by the ChemiDoc MP Imaging System (Bio-Rad, California, United States). The band intensity of proteins was quantified by using ImageJ software (National Institutes of Health, MD, United States), and the relative expression of protein was normalized by expression of β-actin.

Statistical Analysis

All the data were presented as means ± standard deviation (SD). Difference between groups was analyzed by one-way univariate analysis of variance (ANOVA) by Prism 8.0 software (San Diego, CA, United States). if p-value < 0.05, difference was considered to be statistically significant (marked as *). Higher significance levels were established at p-value < 0.01 (marked as **).

RESULT

Identification and Verification of Active Ingredients of *Sanguisorba Officinalis* L.

A total of 41 ingredients of SO were retrieved by searching the TCMSP and BATMAN database (**Supplementary Table S1**), and 12 bioactive ingredients were preliminarily screened out using ADME parameters such as OB and DL, as shown in **Table 1**. And to verify those active ingredients of SO, the 12 compounds of ESO were identified by UHPLC– QTOF, shown in **Supplementary Figure S1**.

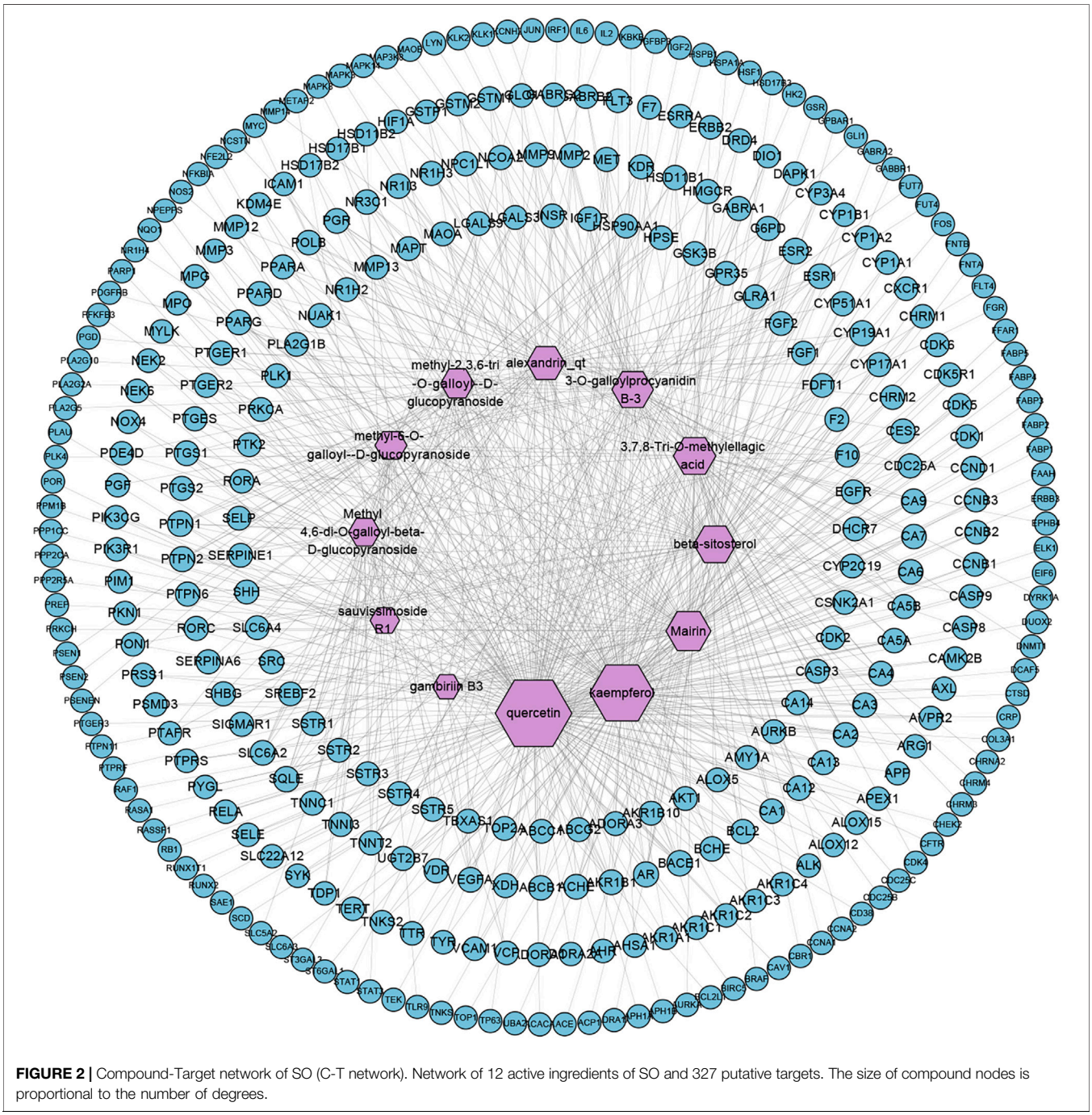

FIGURE 2 | Compound-Target network of SO (C-T network). Network of 12 active ingredients of SO and 327 putative targets. The size of compound nodes is proportional to the number of degrees.

Target Identification of Active Ingredients of *Sanguisorba Officinalis* L.

TCMSP and Swiss Target Prediction database were used to predict the targets of 12 active compounds of *SO*, and a total of 327 targets were obtained after high-possibility screening and overlaps eliminating. And we found that 201 of the 327 putative targets were common to 2 or more of these ingredients, showing that these ingredients act in similar biological processes or pathways, suggesting the synergistic effect of multiple ingredients in *SO*. The compound-target network is shown in **Figure 2**, and according to the number of degrees, the top four ingredients were quercetin, kaempferol, mairin, and beta-sitosterol.

Sanguisorba Officinalis L. Active Compound Target-Hepatocellular Carcinoma Target Interactional Network Analysis

By searching the GeneCards, OMIM, TTD, PharmGKB databases, we obtained 6,569 genes associated with HCC. A total of 258 overlapping genes were obtained by looking for the intersection of the above compound target and the HCC targets (**Figure 3**. and

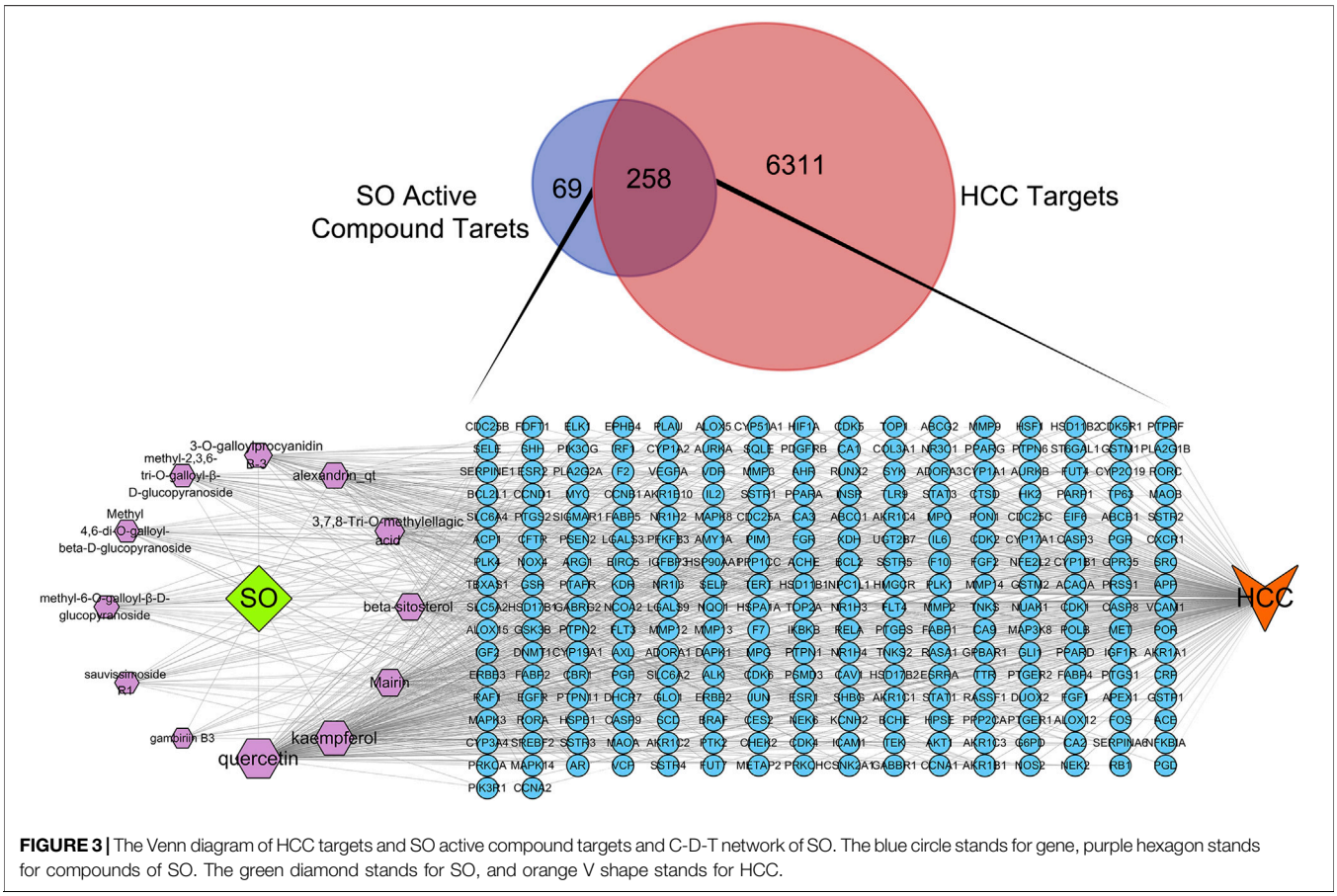

FIGURE 3 | The Venn diagram of HCC targets and SO active compound targets and C-D-T network of SO. The blue circle stands for gene, purple hexagon stands for compounds of SO. The green diamond stands for SO, and orange V shape stands for HCC.

Supplementary Table S2). By inputting compound–disease co-targets data into STRING, we obtained compound target–HCC target PPI network with higher connectivity (interaction score ≥0.700), containing 246 nodes and 1,616 edges (**Figure 4A**). The topological analysis of the PPI network, based on three major network parameters of "degree", "betweenness" and "closeness", was applied to select nodes above two-fold median values as key targets and constructed the hub nodes of the anti-cancer effect of SO on HCC. The threshold values of the first screening were degree ≧ 18, closeness ≧ 0.399 and betweenness ≧ 0.0077, and the results were 30 hub nodes and 215 edges. The 30 key targets were then further screened with the second screening threshold values as degree ≧ 44, closeness ≧ 0.4664, and betweenness ≧ 0.0396. The second screening ended up with 10 hub nodes and 42 edges (**Figure 4B**). In the hub network, the nodes interacted with others numerous edges (66 in AKT1, 59 in MAPK3, 57 in STAT3, 57 in VEGFA, 56 in SRC, 54 in IL6, 54 in EGFR, 53 in MYC, 51 in HSP90AA1 and MAPK8). These results suggested that these high-degree hub targets may account for the essential therapeutic effects of SO in HCC.

GO Biological Process and KEGG Pathway Enrichment Analysis

To explore the therapeutic mechanisms of putative targets of SO on HCC, the GO and KEGG pathway enrichment analyses were performed using DAVID 6.8. There were respectively 474 biological process (BP), 53 cellular component (CC), and 136 molecular function (MF) terms in total, which met the requirements of Gene count ≥2 and p-value ≤ 0.05 (**Supplementary Table S3**). The top 15 significantly enriched GO terms in BP, CC, and MF were plotted in **Figure 5A**, showing that SO may regulate HCC cancer cell proliferation and apoptosis via protein kinase binding, enzyme binding, and transcription factor binding in cytosol, nucleoplasm, extracellular, protein complex and plasma membrane to exert its anti-cancer effect on HCC. To further reveal the underlying mechanism on involved pathways of SO on HCC, KEGG pathway enrichment analysis of involved targets was conducted (**Supplementary Table S4**). The most significantly enriched 15 pathways of SO on HCC were shown in **Figure 5B**. The result also indicated the PI3K/AKT signaling pathways is the top enriched pathway, with 39 involved targets.

Target-Pathway Network Analysis

To further investigate the molecular mechanism of SO alleviated HCC, a target-pathway network was constructed based on top 15 significant signaling pathways and their corresponding genes (**Figure 6**). This network consisted of 109 nodes (94 genes and 15 pathways). In these pathways, PI3K/AKT signaling pathways is the top important one with the highest degree.

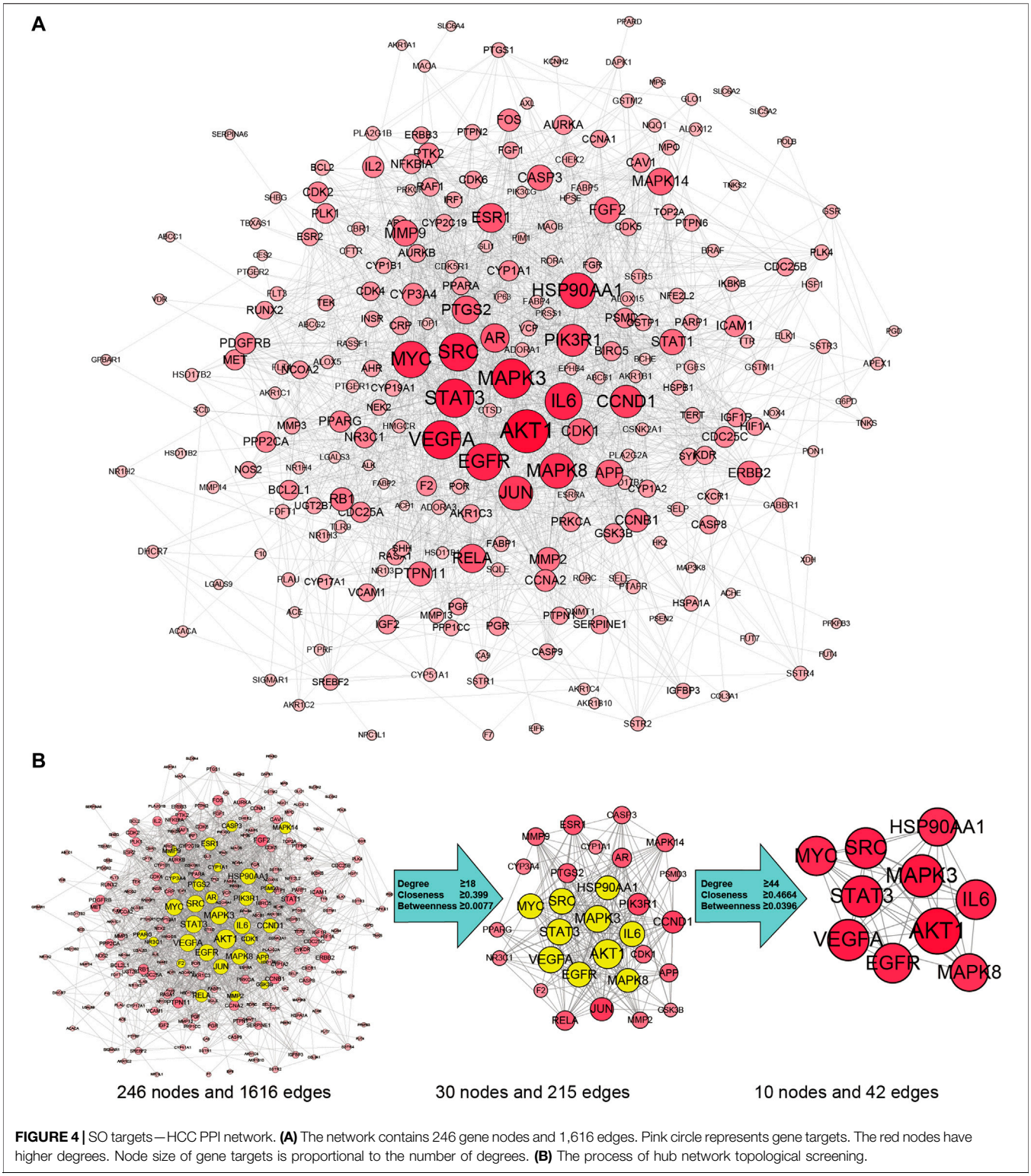

FIGURE 4 | SO targets—HCC PPI network. **(A)** The network contains 246 gene nodes and 1,616 edges. Pink circle represents gene targets. The red nodes have higher degrees. Node size of gene targets is proportional to the number of degrees. **(B)** The process of hub network topological screening.

Among these target genes, AKT1, PIK3R1, EGFR, MAPK3, CCND1, IKBKB, RELA, BRAF, BCL2, BCL2L1, CASP9, MYC and RAF1 were identified as relatively high-degree targets. Therefore, these genes were considered as the key therapeutic genes of SO on HCC. From the drug target prediction, GO and pathway enrichment analysis and pharmacology networks analyses, we suggested that the anti-cancer effects of SO on HCC might be related to regulate cancer cell proliferation and survival via pathways including EGFR, PI3K/AKT, NFκB and MAPK signaling pathways.

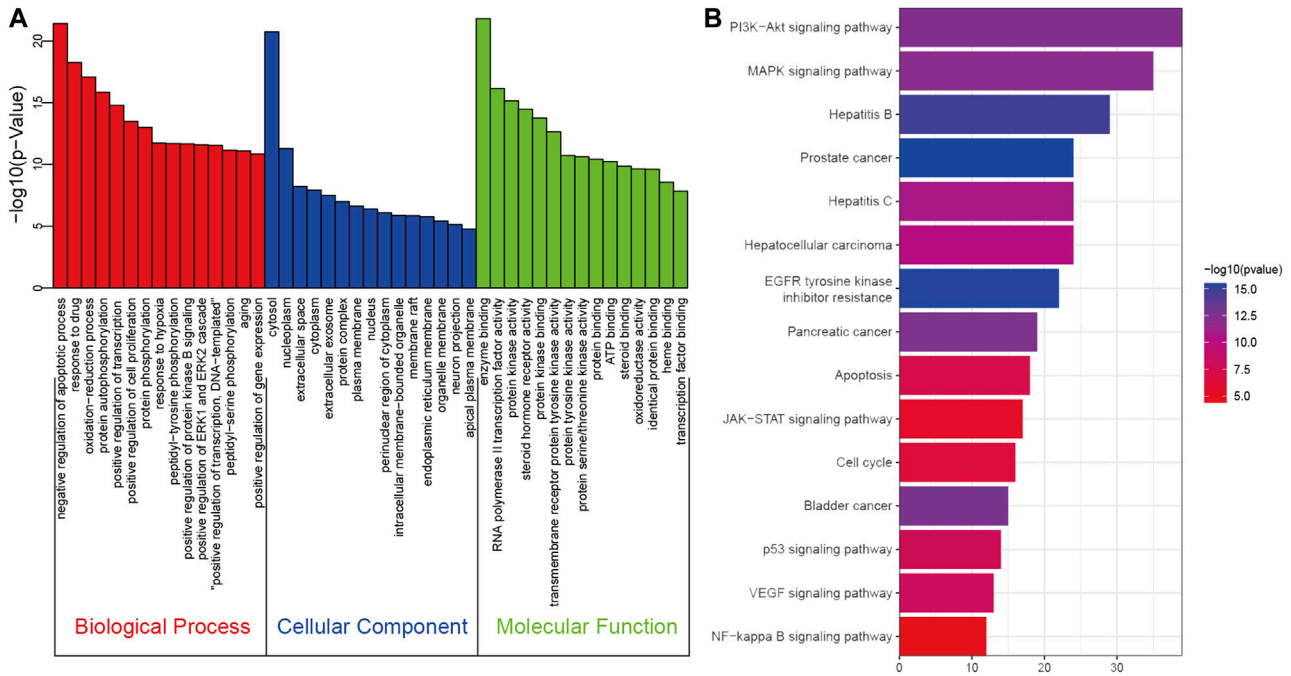

FIGURE 5 | The GO **(A)** and KEGG pathway enrichment **(B)** analysis of 258 therapeutic genes of SO on HCC.

Sanguisorba Officinalis L. Inhibits Hepatocellular Carcinoma Cell Proliferation and Induces Cellular Apoptosis

To assess the anti-proliferative effect of SO on HCC as predicted from network pharmacology analysis, CCK8, Edu, and apoptosis flow cytometry were performed on several HCC cell lines. As shown in **Figure 7A**, ESO remarkably inhibited the viability of HCC cells (HepG2, MHCC97H, SMCC7721, and BEL-7404), in a dose- and time-dependent manner upon treatment for 24 h and 48 h. And according to the IC50 values, BEL-7404 is the least sensitive cell line for ESO, with other HCC cell lines showing almost same level sensitivities. As shown in **Figure 7B**, the EdU assay further confirmed that ESO reduced the percentage of proliferation active cells in a dose-dependent manner, after treatment with increasing ESO for 24 h. **Figure 7C,D** shows that the percentage of apoptotic cells and the apoptosis biomarker (cleaved PARP and cleaved capase 3) were notably increased in a dose-dependent manner, after treatment with ESO for 24 h. In summary, these findings clearly confirmed that ESO inhibit HCC cell proliferation in various aspects.

Sanguisorba Officinalis L. Inhibits Human Hepatocellular Carcinoma Cell Migration and Invasion

To explore SO's effect on migratory and invasive ability in human HCC cells, wound healing and transwell invasion assays were performed. As is shown in **Figure 8A**, compared to the control group, the migration of HepG2 and SMCC7721 cells was markedly inhibited in the ESO treatment group. As is shown in **Figure 8B**, in the transwell invasion assay, the invasion of ESO treated groups were inhibited in a dose-dependent manner. These results confirmed that SO suppressed the migration and invasion of HCC cells.

Sanguisorba Officinalis L. Attenuated Proliferation Pathways in Hepatocellular Carcinoma Cells

Network pharmacology analysis described above suggested that the PI3K/AKT, EGFR, MAPK, and NFκB signaling pathway may be highly related to the anti-cancer mechanism of SO on HCC in regulating HCC cell proliferation and survival. Therefore, we further assessed the expressions level of the EGFR, PI3K, AKT, MAPK and their phosphorylated counterparts by western blot. As shown in **Figure 9**, pretreatment of HepG2 cells with ESO (62.5, 125 and 250 μg/ml) led to apparent repression of phosphorylation level of EGFR, PI3K, AKT, MAPK (p44, p42) and NFκB (p65) in a dose-dependent manner. Taken together, these results suggested that the effect of SO on HCC might be exerted via the EGFR/MAPK and EGFR/PI3K/AKT/NFκB pathways.

DISCUSSION

Development of HCC is a very complicated and multistep biological process, which is associated with diverse molecular and cellular signaling pathways (Forner et al., 2018). Owing to the

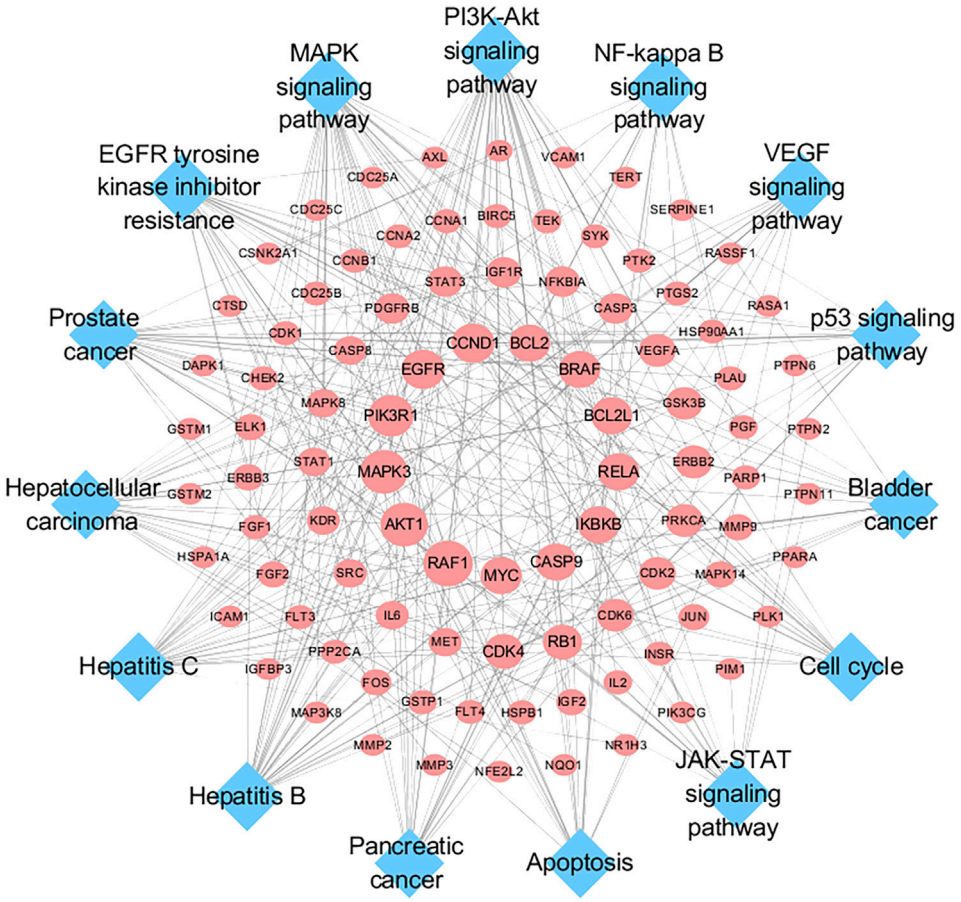

FIGURE 6 | Target-Pathway Network. The red ellipse nodes represent the target nodes. The blue diamond nodes represent the corresponding pathways.

complexity of compounds, TCM may show extensive pharmacological activities with multiple protein targets. However, because of this property, it is difficult to investigate the underlying mechanisms of TCM (Zhang et al., 2019). Network pharmacology, derived from systems biology and bioinformatics, provide a comprehensive and powerful approach for studying the mechanism of complicated TCM (Zhou et al., 2020). In the current study, we applied network pharmacology approach to predict the pharmacological mechanism of SO on HCC, following validation by experimental methods.

Pharmacokinetic properties are very important for drug screening and design. Due to lacking suitable pharmacokinetic properties, drugs could not reach the target organs to exert the therapeutic effect (Tian et al., 2015). In this study, 12 chemical components of SO were identified by the criteria of oral bioavailability ≥30% and drug-likeness index ≥0.18, because of their good absorption and druglike feature. Among these 12 active components, several compounds have been reported to possess anti-cancer effects including HCC. Among of them, quercetin, a natural flavonoid, was reported to exert an anti-carcinogenic effect via increasing p53 and BAX and downregulating ROS, PI3K, COX2 and PKC in HCC cell line (Maurya and Vinayak, 2015). And it was also reported that quercetin exert its anti-cancer effects by promoting apoptosis and autophagy through the modulation of PI3K/Akt/mTOR, Wnt/-catenin, and MAPK/ERK1/2 pathways (Reyes-Farias and Carrasco-Pozo, 2019). Kaempferol, a phytoestrogen, was reported to induce autophagic cell death and inhibit survival and proliferation of human HCC cell lines through targeting AMPK signaling pathway (Han et al., 2017). Moreover, kaempferol treatment was shown to significantly inhibit HIF-1 activity and HCC cell viability under hypoxic conditions (Mylonis et al., 2010). And mairin, also called betulinic acid, a lupane-type pentacyclic triterpene, was shown to induce apoptosis and suppressed metastasis in both HCC cells and NOD/SCID mice model (Wang et al., 2019). All these literatures together with our experimental studies supported the conclusion of network pharmacology prediction and shown a good practice of network pharmacology method in identification of function mechanism of TCM herb.

From the integrated network pharmacology analysis, SO might exert anti-HCC effects by suppressing of cancer cell proliferation and survival, which was reported as the crucial mechanism of HCC development (Llovet et al., 2015). As demonstrated by network pharmacology analysis, SO may

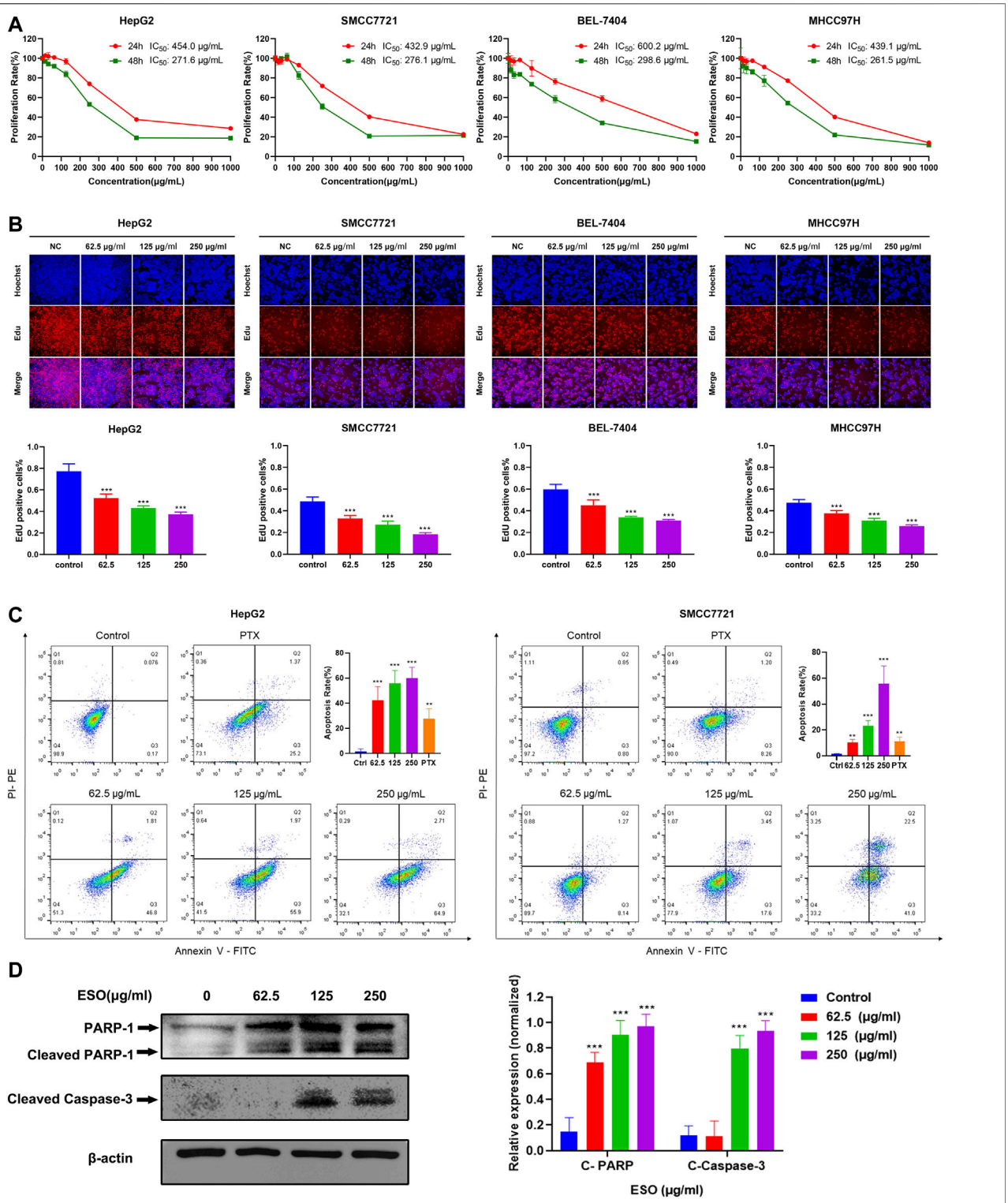

FIGURE 7 | SO inhibits HCC cell proliferation and induces cellular apoptosis. **(A)** the cell viability was tested by CCK8 assay, showing a time- and dose-dependent inhibiting effect of ESO treatment on the viability of HCC cells. $n = 3$. **(B)** EdU assays were performed to verify the effects of ESO treatment on HCC cells proliferation, the rate of EdU-posive cells was calculated. $n = 3$. **(C)** Apoptosis analysis of ESO-treated Hepg2 and SMCC7721 cells was analyzed by flow cytometry after Annexin V-FITC/PI staining. $n = 3$. The concentration of PTX of positive control group was 40 nM, **(D)** The protein levels of PARA and cleaved Capase-3 in HepG2 cell. β-actin was used as an internal control. $^{*}p < 0.05$, $^{**}p < 0.01$, $^{***}p < 0.001$ vs. the nontreated control group.

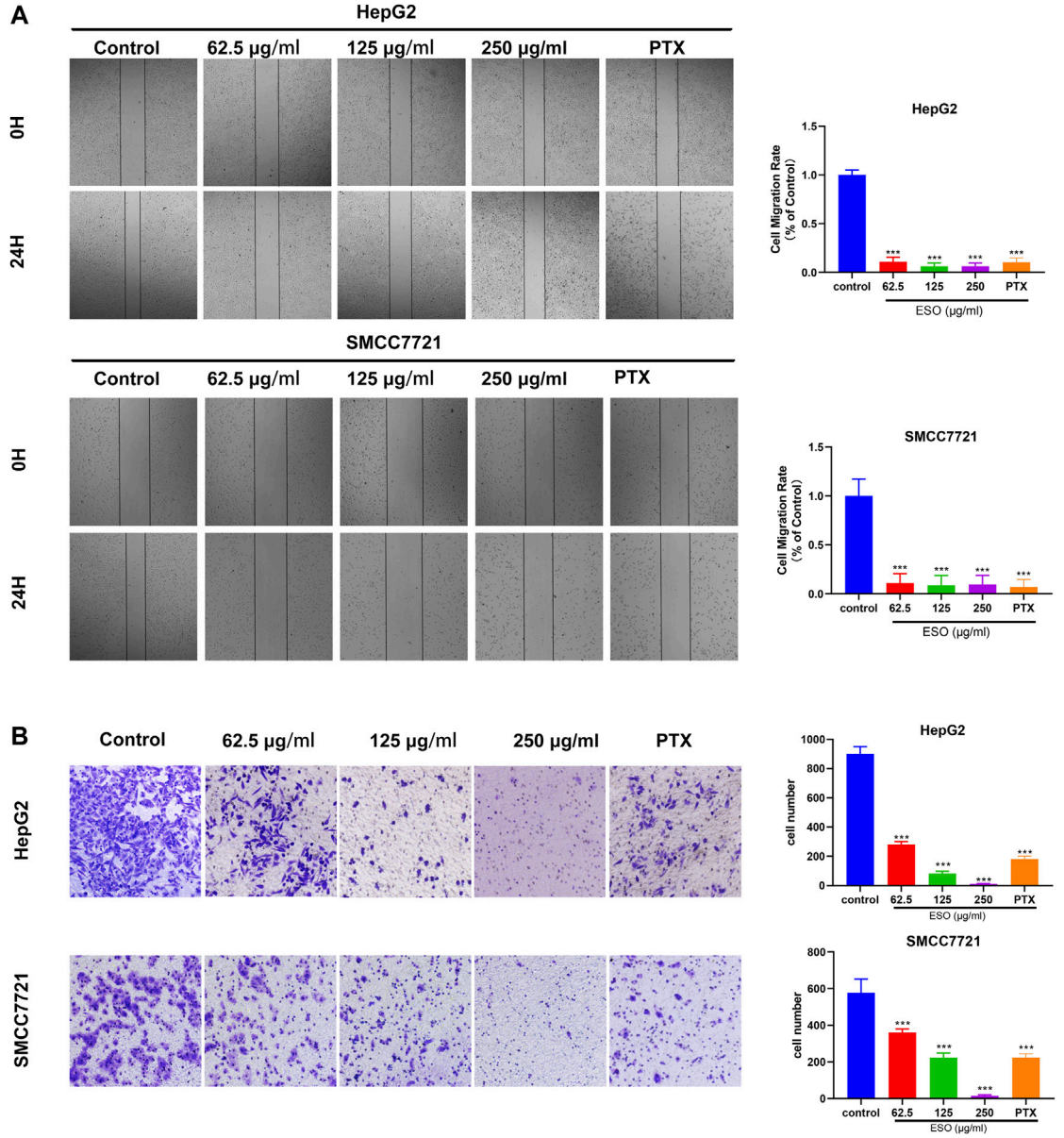

FIGURE 8 | SO inhibits human HCC cell migration and invasion **(A)** Wound healing migration assay of HepG2 and SMCC7721 cells in the presence of ESO. $n = 3$. **(B)** Transwell invasion assay Hepg2 and SMCC7721 cells in the presence of ESO. $n = 3$. The concentration of PTX of positive control group was 40 nM, $^{*}p < 0.05$, $^{**}p < 0.01$, $^{***}p < 0.001$ vs. the nontreated control group.

exert anti-HCC effects mainly by inhibiting proliferation and survival on HCC via EGFR, PI3K/AKT, NFκB, MAPK signaling pathways. To further verify the prediction, various *in vitro* experiments were performed to investigated the therapeutic effects of SO on diverse HCC cells, showing that ESO treatment significantly suppressed HCC cell proliferation, induced cellular apoptosis, and inhibited the cell migration and invasion activities in a dose-dependent manner. Especially, the phosphorylation level of EGFR, PI3K, AKT, MAPK and NFκB (p65) were significantly downregulated in a dose-dependent manner. EGFR, a member of the epidermal growth factor receptor family on cell surface, binds epidermal growth factor to trigger tyrosine kinase phosphorylation, leading to cell proliferation. It was reported that EGFR signaling axis exert a major regulatory effect during liver regeneration, liver cirrhosis and HCC, showing a pivot role of EGFR signaling in the development of liver diseases (Komposch and Sibilia, 2015). Thus, after HCC cells were treated by ESO, the downregulated phosphorylation of EGFR may contribute to its anti-cancer effects. PI3K is a kinase which could phosphorylate the inositol ring of phosphatidylinositol and related second messengers,

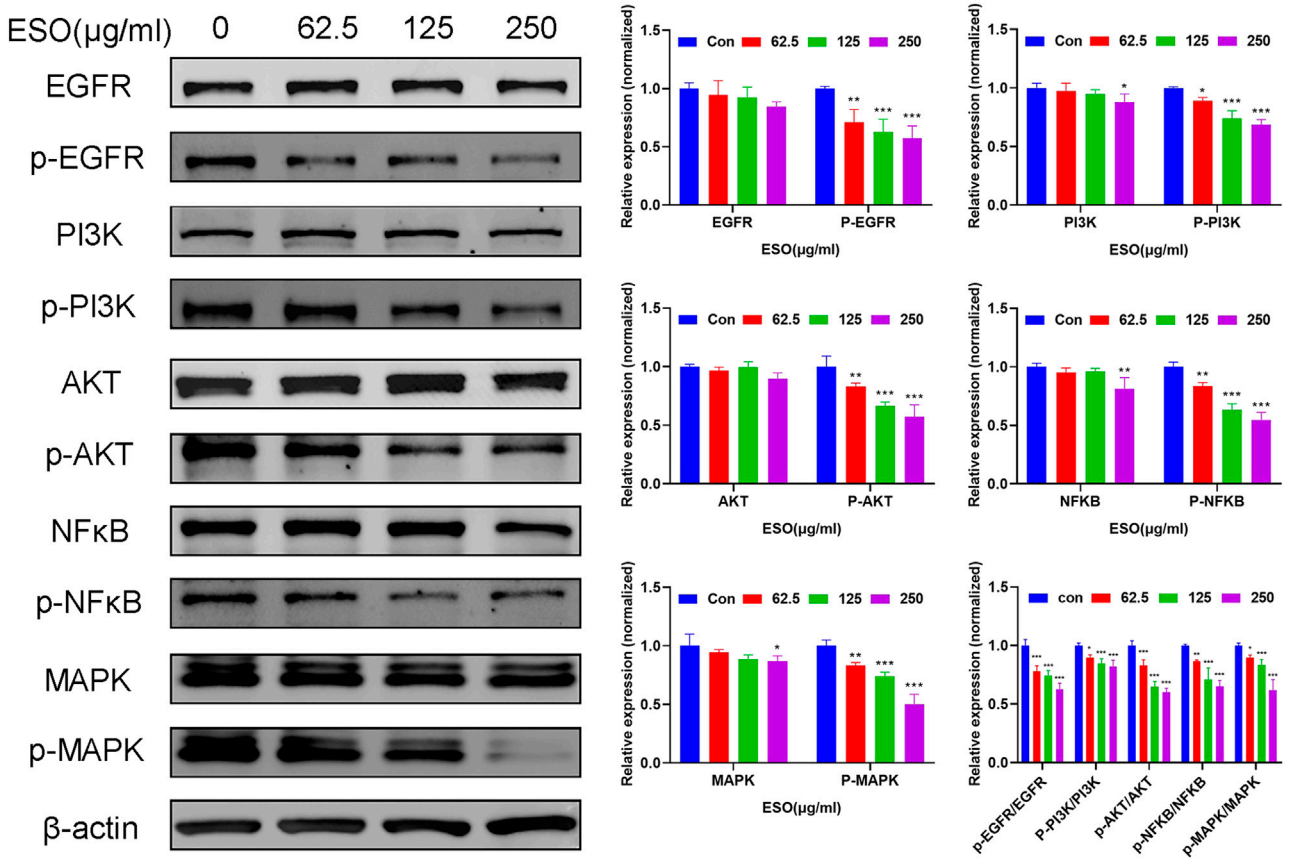

FIGURE 9 | Western blot analysis of related proteins with ESO treatment in HepG2 cells $^{*}p < 0.05$, $^{**}p < 0.01$, $^{***}p < 0.001$ vs. the control group. Statistical results of protein levels ware normalized by control group.

coordinating a variety of cell functions including proliferation and survival. It was reported that the PI3K can be activated by many oncogenes and growth signaling, and upregulated PI3K signaling is regarded as a hallmark of cancer (Fruman et al., 2017). AKT, the major downstream target of PI3K, is a key pivot kinase in signaling communication network and it makes crosstalk between several important pathways, including NF-κB, p53, apoptosis and cell cycle pathways, regulating diverse important cellular processes including cell growth, survival regulation and metabolism in multiple solid tumors (Whittaker et al., 2010). Moreover, it was reported that PI3K/AKT/mTOR signaling pathway is strongly related to HCC development and the inhibition of PI3K signaling axis could be a HCC treatment strategy (Dimri and Satyanarayana, 2020). From our validation in laboratory, after pretreatment with ESO, the apparent decrease of pPI3K and pAKT in HCC cells might contribute to its anti-cancer effects. NFκB, a pleiotropic transcription factor, plays an essential role in inflammation, cell growth, immunity, differentiation, tumorigenesis and apoptosis. The abnormal activation of NFκB are highly associated with cancer development and progression, and the signaling pathways that induce NFκB activation provide promising targets for chemotherapeutic approaches (Karin and Greten, 2005; Karin, 2006). RELA, the 65KD subunit of NFκB, forms the most abundant heterodimeric NFκB complex with NFKB1. It was reported that antisense RELA oligomers exerted antigrowth effects on diverse cancer cells *in vitro* and caused a significant inhibition of tumorigenicity in nude mice tumor models (Sharma and Narayanan, 1996). In this research, target-pathway network shown that RELA, is one of the high-degree targets of SO. And in laboratory experiment, after pretreatment with ESO, a gradually decrease of pNFκB-P65 level in HCC cells was observed in a dose-dependent manner, which might contribute to anti-tumor effects of SO on HCC. Taking EGFR, PI3K, AKT, and NFκB together, Our finding was in accordance with the report that EGFR activation could further trigger the PI3K-AKT-NFκB signaling axis and eventually cause tumor cells proliferation (Engelman et al., 2006; Zhang et al., 2014). MAPK, also known as extracellular signal-regulated kinases (ERKs), act in a signaling cascade that regulates various cellular processes such as proliferation, angiogenesis,differentiation, apoptosis and survival in response to a variety of extracellular signals (Le Gallic et al., 1999). Moreover, it was reported that MAPK phosphorylation level in HCC tissues was 7 times higher than that in adjacent

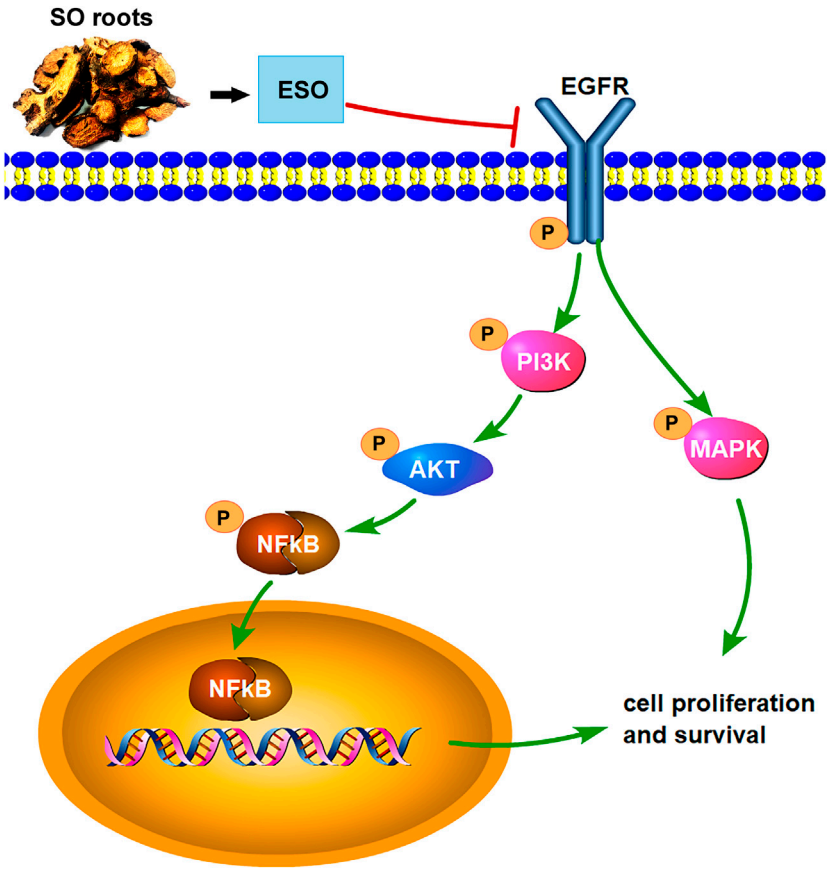

FIGURE 10 | The overview of the regulatory mechanism involved in the anti-cancer effect of SO on HCC.

benign tissues (Huynh et al., 2003). And MAPK signaling activation might be caused by the upstream signals, such as EGFR signaling (Zhang et al., 2017). In our laboratory experiment, after treated with ESO, an apparent downregulation of pEGFR and pMAPK1 in HCC cells was observed, which may might also contribute to its anti-HCC effects.

Taken together, this study for the first time, shows that SO can efficiently suppress cellular proliferation, migration, invasion and induce apoptosis in HCC cells, indicating that SO may inhibit HCC mainly through the EGFR/PI3K/AKT/NFκB and MAPK signaling pathways (**Figure 10**). Owing to budgetary and time constraints, the present study has some limitations. Firstly, the public online databases we used in this research are imperfect and constantly updating, so some of the active ingredients of SO and their target genes might not be included in the analysis. Moreover, there are other signaling pathways (e.g., VEGF, p53 and JAK-STAT signaling pathways) might also play roles in the anti-tumor effect of SO. Further studies are needed to explore the potential function of these pathways. Despite the limitations, this study provides powerful tool and preliminary data for further investigation of SO in HCC. SO might be a potential anti-HCC medicine, which can be developed as a therapeutic option for the treatment of HCC.

CONCLUSION

In conclusion, via the integrating network pharmacology and experimental validation, our study has investigated the underlying mechanism of SO in suppressing HCC. The results suggest that SO might inhibit the proliferation, induce cellular apoptosis and impair the migration and invasion of HCC cells, mainly via regulating of EGFR/PI3K/AKT/NFκB, and MAPK signaling pathways. Moreover, the combined network pharmacology analysis and experimental validation in this study may provide a powerful tool to explore the mechanism of TCM.

DATA AVAILABILITY STATEMENT

The raw data supporting the conclusion of this article will be made available by the authors, without undue reservation, to any qualified researcher.

AUTHOR CONTRIBUTIONS

NJ, HL, and YS conceived and designed the experiments and supervised all the research. HL, NJ, JZ, and FY performed the

experiments. NJ drafted the original manuscript. NJ and HL analyzed the data. JW and FK revised the manuscript. All authors approved the final version of the manuscript.

FUNDING

This research was supported by the National Natural Science Foundation of China (Grant Nos. 81774013, 81804221 and 82074129); the National Science and Technology Major Project of the Ministry of Science and Technology of China (Grant No. 2018ZX09721004-006), Sichuan Science and Technology Program (Grant Nos. 2019JDPT0010, and 2019YJ0473); the Special Research Project of Sichuan Province Administration of Traditional Chinese Medicine (Grant Nos. 2018JC013 and 2018JC038); the Research Project of Sichuan Provincial Education Department (Grant Nos. 18TD0051 and 18ZA0525); the Luzhou Science and Technology Project (Grant No. 2017-S-39(3/5)); the School-level Fund of Southwest Medical University (Grant Nos. 2017-ZRZD-017 and 2017-ZRQN-081), The Science and Technology Strategic Cooperation Programs of Luzhou Municipal People's Government and Southwest Medical University (Grant No. 2019LZXNYDJ11) and the National innovation and entrepreneurship training program for college students (Grant No. 201816032067).

ACKNOWLEDGMENTS

The authors thank Can Tang of the Department of Chinese Materia Medica, School of Pharmacy, Southwest Medical University (Luzhou, Sichuan, China), for authenticating the Sanguisorba Officinalis L. used in this study. We also thank CMU Presidential Scholarship for supporting this research.

SUPPLEMENTARY MATERIAL

The Supplementary Material for this article can be found online at: https://www.frontiersin.org/articles/10.3389/fphar.2021.618522/full#supplementary-material.

REFERENCES

Amberger, J. S., and Hamosh, A. (2017). Searching online Mendelian inheritance in man (OMIM): a knowledgebase of human genes and genetic phenotypes. *Curr. Protoc. Bioinform.* 58, 1–12. doi:10.1002/cpbi.27

Bai, C., Sun, Y., Pan, X., Yang, J., Li, X., Wu, A., et al. (2019). Antitumor effects of Trimethylellagic acid isolated from *Sanguisorba officinalis* L. On colorectal cancer via angiogenesis inhibition and apoptosis induction. *Front. Pharmacol.* 10, 1646. doi:10.3389/fphar.2019.01646

Bray, F., Ferlay, J., Soerjomataram, I., Siegel, R. L., Torre, L. A., and Jemal, A. (2018). Global cancer statistics 2018: GLOBOCAN estimates of incidence and mortality worldwide for 36 cancers in 185 countries. *CA Cancer J. Clin.* 68 (6), 394–424. doi:10.3322/caac.21492

Cai, Z., Li, W., Wang, H., Yan, W., Zhou, Y., Wang, G., et al. (2012). Anti-tumor and immunomodulating activities of a polysaccharide from the root of *Sanguisorba officinalis* L. *Int. J. Biol. Macromol.* 51 (4), 484–488. doi:10.1016/j.ijbiomac.2012.05.029

Chen, X., Shang, F., Meng, Y., Li, L., Cui, Y., Zhang, M., et al. (2015). Ethanol extract of *Sanguisorba officinalis* L. inhibits biofilm formation of methicillin-resistant *Staphylococcus aureus* in an ica-dependent manner. *J. Dairy Sci.* 98 (12), 8486–8491. doi:10.3168/jds.2015-9899

Cheng, A. L., Kang, Y. K., Chen, Z., Tsao, C. J., Qin, S., Kim, J. S., et al. (2009). Efficacy and safety of sorafenib in patients in the Asia–Pacific region with advanced hepatocellular carcinoma: a phase III randomised, double-blind, placebo-controlled trial. *Lancet Oncol.* 10 (1), 25–34. doi:10.1016/S1470-2045(08)70285-7

Dimri, M., and Satyanarayana, A. (2020). Molecular signaling pathways and therapeutic targets in hepatocellular carcinoma. *Cancers* 12 (2), 491. doi:10.3390/cancers12020491

EASL (2019). EASL clinical practice guidelines: drug-induced liver injury. *J. Hepatol.* 70 (6), 1222–1261. doi:10.1016/j.jhep.2019.02.014

EASL (2018). EASL clinical practice guidelines: management of hepatocellular carcinoma. *J. Hepatol.* 69 (1), 182–236. doi:10.1016/j.jhep.2018.03.019

Engelman, J. A., Luo, J., and Cantley, L. C. (2006). The evolution of phosphatidylinositol 3-kinases as regulators of growth and metabolism. *Nat. Rev. Genet.* 7 (8), 606–619. doi:10.1038/nrg1879

Forner, A., Reig, M., and Bruix, J. (2018). Hepatocellular carcinoma. *Lancet* 391 (10127), 1301–1314. doi:10.1016/S0140-6736(18)30010-2

Fruman, D. A., Chiu, H., Hopkins, B. D., Bagrodia, S., Cantley, L. C., and Abraham, R. T. (2017). The PI3K pathway in human disease. *Cell* 170 (4), 605–635. doi:10.1016/j.cell.2017.07.029

Gfeller, D., Grosdidier, A., Wirth, M., Daina, A., Michielin, O., and Zoete, V. (2014). SwissTargetPrediction: a web server for target prediction of bioactive small molecules. *Nucl. Acids Res.* 42, W32–W38. doi:10.1093/nar/gku293

Han, B., Yu, Y. Q., Yang, Q. L., Shen, C. Y., and Wang, X. J. (2017). Kaempferol induces autophagic cell death of hepatocellular carcinoma cells via activating AMPK signaling. *Oncotarget* 8 (49), 86227–86239. doi:10.18632/oncotarget.21043

He, D., Huang, J. H., Zhang, Z. Y., Du, Q., Peng, W. J., Yu, R., et al. (2019). A network pharmacology-based strategy for predicting active ingredients and potential targets of Liu-Wei Di-Huang pill in treating type 2 Diabetes Mellitus. *Drug Des. Dev. Ther.* 13, 3989–4005. doi:10.2147/DDDT.S216644

Huang, W., Sherman, B. T., and Lempicki, R. A. (2009). Systematic and integrative analysis of large gene lists using DAVID bioinformatics resources. *Nat. Protoc.* 4 (1), 44–57. doi:10.1038/nprot.2008.211

Huynh, H., Nguyen, T. T., Chow, K. H., Tan, P. H., Soo, K. C., and Tran, E. (2003). Over-expression of the mitogen-activated protein kinase (MAPK) kinase (MEK)-MAPK in hepatocellular carcinoma: its role in tumor progression and apoptosis. *BMC Gastroenterol.* 3, 19. doi:10.1186/1471-230X-3-19

Kanehisa, M., Furumichi, M., Tanabe, M., Sato, Y., and Morishima, K. (2017). KEGG: new perspectives on genomes, pathways, diseases and drugs. *Nucl. Acids Res.* 45 (D1), D353–D361. doi:10.1093/nar/gkw1092

Karin, M., and Greten, F. R. (2005). NF-κB: linking inflammation and immunity to cancer development and progression. *Nat. Rev. Immunol.* 5 (10), 749–759. doi:10.1038/nri1703

Karin, M. (2006). Nuclear factor-kappaB in cancer development and progression. *Nature* 441 (7092), 431–436. doi:10.1038/nature04870

Kim, H. Y., Eo, E. Y., Park, H., Kim, Y. C., Park, S., Shin, H. J., et al. (2010). Medicinal herbal extracts of Sophorae radix, Acanthopanacis cortex, Sanguisorbae radix and Torilis fructus inhibit coronavirus replication *in vitro*. *Antivir. Ther. (Lond.)* 15 (5), 697–709. doi:10.3851/IMP1615

Komposch, K., and Sibilia, M. (2015). EGFR signaling in liver diseases. *Int. J. Mol. Sci.* 17 (1). doi:10.3390/ijms17010030

Kuo, Y. T., Liao, H. H., Chiang, J. H., Wu, M. Y., Chen, B. C., Chang, C. M., et al. (2018). Complementary Chinese herbal medicine therapy improves survival of patients with pancreatic cancer in Taiwan: a nationwide population-based cohort study. *Integr. Cancer Ther.* 17 (2), 411–422. doi:10.1177/1534735417722224

Le Gallic, L., Sgouras, D., Beal, G., Jr., and Mavrothalassitis, G. (1999). Transcriptional repressor ERF is a Ras/mitogen-activated protein kinase

target that regulates cellular proliferation. *Mol. Cell Biol.* 19 (6), 4121–4133. doi:10.1128/mcb.19.6.4121

Li, S., and Zhang, B. (2013). Traditional Chinese medicine network pharmacology: theory, methodology and application. *Chin. J. Nat. Med.* 11 (2), 110–120. doi:10.1016/S1875-5364(13)60037-0

Li, W., Yang, C. J., Wang, L. Q., Wu, J., Dai, C., Yuan, Y. M., et al. (2019). A tannin compound from Sanguisorba officinalis blocks Wnt/β-catenin signaling pathway and induces apoptosis of colorectal cancer cells. *Chin. Med.* 14, 22. doi:10.1186/s13020-019-0244-y

Li, Y. H., Yu, C. Y., Li, X. X., Zhang, P., Tang, J., Yang, Q., et al. (2018). Therapeutic target database update 2018: enriched resource for facilitating bench-to-clinic research of targeted therapeutics. *Nucl. Acids Res.* 46 (D1), D1121–D1127. doi:10.1093/nar/gkx1076

Liao, W., Fan, L., Zheng, Z., Liu, H., Deng, H., Li, M., et al. (2020). Ziyuglycoside II exerts antiproliferative and antimetastasis effects on hepatocellular carcinoma cells. *Anticancer Drugs* 31 (8), 819–827. doi:10.1097/CAD.0000000000000918

Liao, Y. H., Li, C. I., Lin, C. C., Lin, J. G., Chiang, J. H., and Li, T. C. (2017). Traditional Chinese medicine as adjunctive therapy improves the long-term survival of lung cancer patients. *J. Cancer Res. Clin. Oncol.* 143 (12), 2425–2435. doi:10.1007/s00432-017-2491-6

Liu, C. Y., Chen, K. F., and Chen, P. J. (2015). Treatment of liver cancer. *Cold Spring Harb. Perspect Med.* 5 (9), a021535. doi:10.1101/cshperspect.a021535

Liu, H., Wang, J., Zhou, W., Wang, Y., and Yang, L. (2013). Systems approaches and polypharmacology for drug discovery from herbal medicines: an example using licorice. *J. Ethnopharmacol.* 146 (3), 773–793. doi:10.1016/j.jep.2013.02.004

Liu, X., Cui, Y., Yu, Q., and Yu, B. (2005). Triterpenoids from *Sanguisorba officinalis*. *Phytochemistry* 66 (14), 1671–1679. doi:10.1016/j.phytochem.2005.05.011

Liu, Z., Guo, F., Wang, Y., Li, C., Zhang, X., Li, H., et al. (2016). BATMAN-TCM: a bioinformatics analysis tool for molecular mechANism of traditional Chinese medicine. *Sci. Rep.* 6, 21146. doi:10.1038/srep21146

Llovet, J. M., Villanueva, A., Lachenmayer, A., and Finn, R. S. (2015). Advances in targeted therapies for hepatocellular carcinoma in the genomic era. *Nat. Rev. Clin. Oncol.* 12 (8), 408. doi:10.1038/nrclinonc.2015.12110.1038/nrclinonc.2015.103

Lou, J. S., Yao, P., and Tsim, K. W. K. (2018). Cancer treatment by using traditional Chinese medicine: probing active compounds in anti-multidrug resistance during drug therapy. *Curr. Med. Chem.* 25 (38), 5128–5141. doi:10.2174/0929867324666170920161922

Ma, Y. M., Zhang, X. Z., Su, Z. Z., Li, N., Cao, L., Ding, G., et al. (2015). Insight into the molecular mechanism of a herbal injection by integrating network pharmacology and *in vitro*. *J. Ethnopharmacol.* 173, 91–99. doi:10.1016/j.jep.2015.07.016

Maurya, A. K., and Vinayak, M. (2015). Anticarcinogenic action of quercetin by downregulation of phosphatidylinositol 3-kinase (PI3K) and protein kinase C (PKC) via induction of p53 in hepatocellular carcinoma (HepG2) cell line. *Mol. Biol. Rep.* 42 (9), 1419–1429. doi:10.1007/s11033-015-3921-7

Mylonis, I., Lakka, A., Tsakalof, A., and Simos, G. (2010). The dietary flavonoid kaempferol effectively inhibits HIF-1 activity and hepatoma cancer cell viability under hypoxic conditions. *Biochem. Biophys. Res. Commun.* 398 (1), 74–78. doi:10.1016/j.bbrc.2010.06.038

Reyes-Farias, M., and Carrasco-Pozo, C. (2019). The anti-cancer effect of Quercetin: molecular implications in cancer metabolism. *Int. J. Mol. Sci.* 20 (13), 177. doi:10.3390/ijms20133177

Ru, J., Li, P., Wang, J., Zhou, W., Li, B., Huang, C., et al. (2014). TCMSP: a database of systems pharmacology for drug discovery from herbal medicines. *J. Cheminform.* 6, 13. doi:10.1186/1758-2946-6-13

Seo, C. S., Jeong, S. J., Yoo, S. R., Lee, N. R., and Shin, H. K. (2016). Quantitative analysis and in vitro anti-inflammatory effects of gallic acid, Ellagic acid, and Quercetin from radix Sanguisorbae. *Pharmacogn. Mag.* 12 (46), 104–108. doi:10.4103/0973-1296.177908

Shannon, P., Markiel, A., Ozier, O., Baliga, N. S., Wang, J. T., Ramage, D., et al. (2003). Cytoscape: a software environment for integrated models of biomolecular interaction networks. *Genome Res.* 13 (11), 2498–2504. doi:10.1101/gr.1239303

Sharma, H. W., and Narayanan, R. (1996). The NF-kappaB transcription factor in oncogenesis. *Anticancer Res.* 16 (2), 589–596.

Shin, J. A., Kim, J. S., Kwon, K. H., Nam, J. S., Jung, J. Y., Cho, N. P., et al. (2012). Apoptotic effect of hot water extract of Sanguisorba officinalis L. in human oral cancer cells. *Oncol. Lett.* 4 (3), 489–494. doi:10.3892/ol.2012.748

Stelzer, G., Rosen, N., Plaschkes, I., Zimmerman, S., Twik, M., Fishilevich, S., et al. (2016). The GeneCards suite: from gene data mining to disease genome sequence analyses. *Curr. Protoc. Bioinform.* 54, 30–33. doi:10.1002/cpbi.5

Sun, W., Zhang, Z. L., Liu, X., Zhang, S., He, L., Wang, Z., et al. (2012). Terpene glycosides from the roots of *Sanguisorba officinalis* L. and their hemostatic activities. *Molecules* 17 (7), 7629–7636. doi:10.3390/molecules17077629

Szklarczyk, D., Gable, A. L., Lyon, D., Junge, A., Wyder, S., Huerta-Cepas, J., et al. (2019). STRING v11: protein-protein association networks with increased coverage, supporting functional discovery in genome-wide experimental datasets. *Nucl. Acids Res.* 47 (D1), D607–D613. doi:10.1093/nar/gky1131

Tang, Y., Li, M., Wang, J., Pan, Y., and Wu, F. X. (2015). CytoNCA: a cytoscape plugin for centrality analysis and evaluation of protein interaction networks. *Biosystems* 127, 67–72. doi:10.1016/j.biosystems.2014.11.005

Teng, J. F., Mei, Q. B., Zhou, X. G., Tang, Y., Xiong, R., Qiu, W. Q., et al. (2020). Polyphyllin VI induces caspase-1-mediated pyroptosis via the induction of ROS/NF-κB/NLRP3/GSDMD signal axis in non-small cell lung cancer. *Cancers* 12 (1). doi:10.3390/cancers12010193

Tian, S., Wang, J., Li, Y., Li, D., Xu, L., and Hou, T. (2015). The application of in silico drug-likeness predictions in pharmaceutical research. *Adv. Drug Deliv. Rev.* 86, 2–10. doi:10.1016/j.addr.2015.01.009

UniProt Consortium, T. (2018). UniProt: the universal protein knowledgebase. *Nucl. Acids Res.* 46 (5), 2699. doi:10.1093/nar/gky092

Wan, Y., Xu, L., Liu, Z., Yang, M., Jiang, X., Zhang, Q., et al. (2019). Utilising network pharmacology to explore the underlying mechanism of Wumei Pill in treating pancreatic neoplasms. *BMC Complem. Altern. Med.* 19 (1), 158. doi:10.1186/s12906-019-2580-y

Wang, W., Wang, Y., Liu, M., Zhang, Y., Yang, T., Li, D., et al. (2019). Betulinic acid induces apoptosis and suppresses metastasis in hepatocellular carcinoma cell lines *in vitro* and *in vivo*. *J. Cell Mol. Med.* 23 (1), 586–595. doi:10.1111/jcmm.13964

Whirl-Carrillo, M., McDonagh, E. M., Hebert, J. M., Gong, L., Sangkuhl, K., Thorn, C. F., et al. (2012). Pharmacogenomics knowledge for personalized medicine. *Clin. Pharmacol. Ther.* 92 (4), 414–417. doi:10.1038/clpt.2012.96

Whittaker, S., Marais, R., and Zhu, A. X. (2010). The role of signaling pathways in the development and treatment of hepatocellular carcinoma. *Oncogene* 29 (36), 4989–5005. doi:10.1038/onc.2010.236

Xiang, Y., Guo, Z., Zhu, P., Chen, J., and Huang, Y. (2019). Traditional Chinese medicine as a cancer treatment: modern perspectives of ancient but advanced science. *Cancer Med.* 8 (5), 1958–1975. doi:10.1002/cam4.2108

Yuan, R., Hou, Y., Sun, W., Yu, J., Liu, X., Niu, Y., et al. (2017). Natural products to prevent drug resistance in cancer chemotherapy: a review. *Ann. N. Y. Acad. Sci.* 1401 (1), 19–27. doi:10.1111/nyas.13387

Zhang, B., Wang, X., and Li, S. (2013). An integrative Platform of TCM network pharmacology and its application on a herbal formula, Qing-Luo-Yin. *Evid. Based Complem. Alternat. Med.* 2013, 456747. doi:10.1155/2013/456747

Zhang, G., Ye, X., Ji, D., Zhang, H., Sun, F., Shang, C., et al. (2014). Inhibition of lung tumor growth by targeting EGFR/VEGFR-Akt/NF-κB pathways with novel theanine derivatives. *Oncotarget* 5 (18), 8528–8543. doi:10.18632/oncotarget.2336

Zhang, L., Koyyalamudi, S. R., Jeong, S. C., Reddy, N., Smith, P. T., Ananthan, R., et al. (2012). Antioxidant and immunomodulatory activities of polysaccharides from the roots of *Sanguisorba officinalis*. *Int. J. Biol. Macromol.* 51 (5), 1057–1062. doi:10.1016/j.ijbiomac.2012.08.019

Zhang, W., Huai, Y., Miao, Z., Qian, A., and Wang, Y. (2019). Systems pharmacology for investigation of the mechanisms of action of traditional Chinese medicine in drug discovery. *Front. Pharmacol.* 10, 743. doi:10.3389/fphar.2019.00743

Zhang, X., Liu, K., Zhang, T., Wang, Z., Qin, X., Jing, X., et al. (2017). Cortactin promotes colorectal cancer cell proliferation by activating the EGFR-MAPK pathway. *Oncotarget* 8 (1), 1541–1554. doi:10.18632/oncotarget.13652

Zhao, Z., He, X., Zhang, Q., Wei, X., Huang, L., Fang, J. C., et al. (2017). Traditional uses, chemical constituents and biological activities of plants from the genus Sanguisorba L. *Am. J. Chin. Med.* 45 (2), 199–224. doi:10.1142/S0192415X17500136

Zhou, Z., Chen, B., Chen, S., Lin, M., Chen, Y., Jin, S., et al. (2020). Applications of network pharmacology in traditional Chinese medicine research. *Evid. Based Complem. Alternat. Med.* 2020, 1646905. doi:10.1155/2020/1646905

Zhu, Y. J., Zheng, B., Wang, H. Y., and Chen, L. (2017). New knowledge of the mechanisms of sorafenib resistance in liver cancer. *Acta Pharmacol. Sin.* 38 (5), 614–622. doi:10.1038/aps.2017.5

Conflict of Interest: The authors declare that the research was conducted in the absence of any commercial or financial relationships that could be construed as a potential conflict of interest.

frontiers in Pharmacology

SYSTEMATIC REVIEW
published: 29 March 2021
doi: 10.3389/fphar.2021.639840

A Systematic Review of the Preventive and Therapeutic Effects of Naringin Against Human Malignancies

Maryam Ghanbari-Movahed[1,2], *Gloria Jackson*[3], *Mohammad Hosein Farzaei*[1]* and *Anupam Bishayee*[3]*

[1]Medical Technology Research Center, Health Technology Institute, Kermanshah University of Medical Sciences, Kermanshah, Iran, [2]Department of Biology, Faculty of Science, University of Guilan, Rasht, Iran, [3]Lake Erie College of Osteopathic Medicine, Bradenton, FL, United States

Background: Natural product-based cancer preventive and therapeutic entities, such as flavonoids and their derivatives, are shown to have a noticeable capability to suppress tumor formation and cancer cell growth. Naringin, a natural flavanone glycoside present in various plant species, has been indicated to modulate different signaling pathways and interact with numerous cell signaling molecules, which allows for an extensive variety of pharmacological actions, such as amelioration of inflammation, oxidative stress, metabolic syndromes, bone disorders, and cancer. The purpose of this systematic review is to present a critical and comprehensive assessment of the antitumor ability of naringin and associated molecular targets in various cancers.

Methods: Studies were identified through systematic searches of Science Direct, PubMed, and Scopus as well as eligibility checks according to predefined selection criteria.

Results: Eighty-seven studies were included in this systematic review. There was strong evidence for the association between treatment with naringin alone, or combined with other drugs and antitumor activity. Additionally, studies showed that naringin-metal complexes have greater anticancer effects compared to free naringin. It has been demonstrated that naringin employs multitargeted mechanisms to hamper cancer initiation, promotion, and progression through modulation of several dysregulated signaling cascades implicated in cell proliferation, autophagy, apoptosis, inflammation, angiogenesis, metastasis, and invasion.

Conclusion: The results of our work show that naringin is a promising candidate for cancer prevention and treatment, and might offer substantial support for the clinical application of this phytocompound in the future. Nevertheless, further preclinical and clinical studies as well as drug delivery approaches are needed for designing novel formulations of naringin to realize the full potential of this flavonoid in cancer prevention and intervention.

Keywords: citrus fruits, naringin, cancer, therapy, molecular mechanisms, prevention

OPEN ACCESS

Edited by:
Rajeev K. Singla, West China Hospital, Sichuan University, China

Reviewed by:
Shikha Joon, Jawaharlal Nehru University, India
Manoj Kumar Sabnani, Alloy Therapeutics, Inc., United States

***Correspondence:**
Anupam Bishayee
abishayee@lecom.edu
abishayee@gmail.com
Mohammad Hosein Farzaei
mh.farzaei@gmail.com

Specialty section:
This article was submitted to Ethnopharmacology, a section of the journal Frontiers in Pharmacology

Received: *10 December 2020*
Accepted: *28 January 2021*
Published: *29 March 2021*

Citation:
Ghanbari-Movahed M, Jackson G, Farzaei MH and Bishayee A (2021) A Systematic Review of the Preventive and Therapeutic Effects of Naringin Against Human Malignancies. Front. Pharmacol. 12:639840. doi: 10.3389/fphar.2021.639840

INTRODUCTION

Cancer is a set of complex processes, including unlimited cell proliferation, death of impaired cells, and spatial-temporal changes in cell physiology, that may result in the formation of malignant tumors with the potential for metastasis (Seyfried and Shelton, 2010). There are many different approaches for the treatment of cancer, but some may be ineffective due to increased resistance to classical anticancer drugs as well as adverse side effects (Abotaleb et al., 2019).

Scientific reports and traditional knowledge demonstrate that a high intake of fruits and vegetables is constantly associated with a decreased risk of some type of human cancers, such as lung, colon, prostate, and breast cancer (Neuhouser, 2004). Fruit-based cancer preventive and therapeutic entities, such as flavonoid and their derivatives, have shown a noticeable capability to suppress tumor formation and cancer cell growth (Ramesh and Alshatwi, 2013). Flavonoids are a big class of natural polyphenols, existing in a broad variety of vegetables and fruits commonly consumed by humans. These phytochemicals are divided into different subclasses, including flavonols, flavan-3-ols, isoflavones, flavanones, anthocyanidins, and flavones (Romagnolo and Selmin, 2012). In the context of carcinogenesis, flavonoids intervene with multiple signal transduction cascades and increase apoptosis as well as inhibit metastasis, angiogenesis, and proliferation (Ravishankar et al., 2013).

Naringin, a flavanone glycoside derived from the flavanone naringenin, is present in many plant species, especially citrus fruits (Zhang et al., 2014). It has been indicated to interact with a wide range of signaling molecules and modulate various signaling pathways and thus has multiple pharmacological impacts, such as antioxidant, anti-inflammatory, antiapoptotic, antitumor, and antiviral properties as well as effects on metabolic syndrome, bone regeneration, neurodegenerative disorders, cardiovascular disease, and genetic damage (Bharti et al., 2014; Chen et al., 2016; Joshi et al., 2018; Rivoira et al., 2020). Notably, previous studies have demonstrated that high dietary intake of naringin reduced the risk of certain cancers, such as lung cancer (Le Marchand et al., 2000). Although a few reports exist on the overview of naringin in cancer, these publications are narrative reviews or reviews of the pharmacological activities of naringin without particular emphasis on its antitumor effects and none of them have evaluated naringin individually in the prevention and treatment of cancer (Meiyanto et al., 2012; Rivoira et al., 2020; Memariani et al., 2020). Hence, a critical and comprehensive systematic review on the anticancer ability of naringin and associated molecular targets within different cancers has not been conducted in the past. Accordingly, the objective of this article is to present a critical and up-to-date systematic evaluation of the preventive and therapeutic impacts of naringin and associated cellular and molecular mechanisms of action.

NATURAL PRODUCTS AND MALIGNANCIES

It is known that throughout history, natural products have played an important role in health promotion and disease prevention. Natural products represent a valuable resource in the development and discovery of new drugs, particularly those used for cancer treatment (Newman and Cragg, 2012; Cragg and Pezzuto, 2016; Newman and Cragg, 2020). A large number of the significant advances in cancer treatment are directly associated with the development of natural product-based drugs and the use of these agents to suppress, reverse, or retard the process of carcinogenesis (Cragg and Pezzuto, 2016). Many natural products from herbs, vegetables, plant extracts, and fruits exert chemoprotective properties against carcinogenesis (Amin et al., 2009; Gullett et al., 2010; Lee et al., 2011; Bishayee and Sethi, 2016). Plant secondary metabolites, also known as phytochemicals, belong to four major classes, such as terpenoids, phenolics, alkaloids, and sulfur-containing compounds. A large number of these phytocompounds are strong antioxidants as well as anti-inflammatory agents with reactive groups that confer protective activities. The vast majority of the non-nutrient antioxidants present in various plants are phenolic compounds, including catechins in tea, isoflavones in soybeans, phenolic esters in coffee, quercetin in onions, phenolic acid in red wine, and rosmarinic acid in rosemary (Sheikh et al., 2021). Flavonoids, a subclass of polyphenols, have also been demonstrated to block the cell cycle progression, protect cells from damage due to external factors, suppress mutations, inhibit prostaglandin synthesis, and inhibit carcinogenesis in animal models (Abdulla and Gruber, 2000). Several animal studies have shown a protective effect for isoflavonoids against mammary cancers (Steiner et al., 2008; Basu and Maier, 2018; Ávila-Gálvez et al., 2020). A high isoflavone diet has also been indicated to suppress tumorigenesis in various animal models for prostate cancer (Persky et al., 1994). Multiple lines of experimental evidences suggest that treatment with naringenin or novel naringenin formulations could inhibit various malignancies, such as melanoma, breast, and cervical cancer (Krishnakumar et al., 2011; Rajamani et al., 2018; Choi et al., 2020). Tea is an essential source of flavonols and flavanols. Many experimental studies show an anticancer effect for tea polyphenols (Yang et al., 2001). It has also been indicated that administration of genistein early in life increases the differentiation and early maturation of the rat mammary gland (Persky et al., 1994), conferring protection against breast cancer. Although synthetic cancer drugs cause non-specific cell killing, natural products,

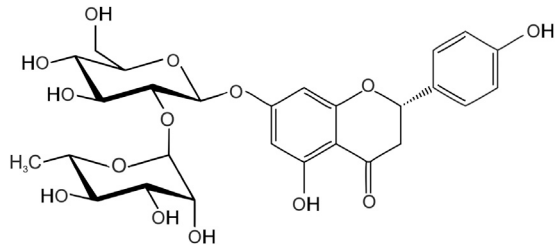

FIGURE 1 | The chemical structure of naringin.

TABLE 1 | Various natural sources of naringin.

Source plant	Naringin content (μg/ml)	References
Citrus × *aurantium* L. [Rutaceae]	19.7	Kawaii et al. (1999)
Citrus × limon (L.) Osbeck [Rutaceae]	22.3	Kawaii et al. (1999)
Citrus deliciosa Ten. [Rutaceae]	8.0	Dhuique-Mayer et al. (2005)
Citrus medica L. [Rutaceae]	18.6	Menichini et al. (2016)
Citrus × aurantium L. [Rutaceae]	230.0	Kawaii et al. (1999)
Citrus × aurantium L. [Rutaceae]	3383.6	de Lourdes Mata Bilbao et al. (2007)
Citrus × aurantium L. [Rutaceae]	21.3	Ooghe et al. (1994)

TABLE 2 | Description of population, intervention, comparator, outcome and study design (PICOS).

Population	• Normal and cancer cell lines • Healthy and tumor bearing animals
Intervention	• Naringin
Comparison	• Δ-changes between treatments (naringin/control/anticancer drug)
Outcome	• Effect of naringin on cancer cell growth inhibition and/or reduction of tumor size and volume
Study design	• *In vitro* studies • *In vivo* studies

including dietary phytochemicals, offers therapeutic and protective activities with low cytotoxicity (Reddy et al., 2003).

NARINGIN: SOURCES, CHEMISTRY, AND PHARMACOLOGY

Naringin, chemically known as 4′,5,7-trihydroxyflavanone-7-rhamnoglucoside ($C_{27}H_{32}O_{14}$, molecular weight: 580.5, **Figure 1**), is a flavone glycoside that is present in many plant species, particularly citrus fruits, with remarkable pharmacological and biological activities. It is one of the main active components of various Chinese herbal medicines, such as *Citrus medica L.* (CM) and *Citrus aurantium L.* (CA) (**Table 1**) (Alam et al., 2014; Zhang et al., 2014). The chemical structure of naringin was first annotated in 1928 by Inubuse and Asahina (EFSA, 2011). In one study, naringin was isolated from *C. aurantium* crude peel extract after HPLC separation and its structure was confirmed by electrospray ionization mass spectrometry. The predicted mass for naringin was 580 Da (Zhang et al., 2018a). Naringin is derived from naringenin and is responsible for the bitterness of citrus fruits and their products (Konno et al., 1982). It can be hydrolyzed by rhamnosidase activity of naringinase into prunin and rhamnose, which can be further hydrolyzed by the b-D-glucosidase component of naringinase, into naringenin and glucose (Real et al., 2007).

Naringin has been shown to modulate various enzyme and protein expressions, thus exerting potential therapeutic activities. Naringin has been demonstrated to significantly affect cell proliferation and osteogenic differentiation (Dai et al., 2009). Naringin has also been indicated to be effective in decreasing the expression of numerous signaling factors involved in the inflammatory response, e.g., interleukin-8 (IL-8), tumor necrosis factor-α (TNF-α), interleukin-6 (IL-6), inducible nitric oxide synthase (iNOS), and nuclear factor erythroid 2-related factor 2 (Nrf2) (Habauzit et al., 2011). It has also been reported to decrease metabolic syndrome through downregulation of the expression of key gluconeogenic enzymes and upregulation of AMP-activated protein kinase. Additionally, it decreases the activity of 3-hydroxy-3-methylglutaryl coenzyme A reductase and enhances the production of nitric oxide metabolites. Naringin also shows antigenotoxic actions and decreases DNA damage by controlling the generation of free radicals and the expression of oxidative mediators (Chen et al., 2016). It has beneficial effects on many central nervous system diseases, including epilepsy, Parkinson's disease, and Alzheimer's disease (Jäger and Saaby, 2011), and has been demonstrated to have dose-dependent radical scavenging activity and decreased oxidative stress (Rajadurai and Prince, 2007). Overall, naringin can be regarded as a promising natural compound that elicits various health benefits.

METHODOLOGY FOR LITERATURE SEARCH ON NARINGIN AND MALIGNANCIES

Search Strategy

The current systematic review was conducted following the Preferred Reporting Items for Systematic Reviews and Meta-Analysis (PRISMA) guidelines (Moher et al., 2009), employing several electronic databases (Science Direct, PubMed, and Scopus) and using the following keywords: "naringin" AND ("neoplasm" OR "cancer" OR "tumor" OR "carcinoma" OR "malignancy"). The information about populations, interventions, comparators, outcomes, and study designs (PICOS) criteria are presented in **Table 2**.

Inclusion Criteria

Experimental studies (*in vivo* and *in vitro*) up to September 2020 in the English language which assessed the anticancer effect of naringin (in any cancer cell line and/or animal model) were included.

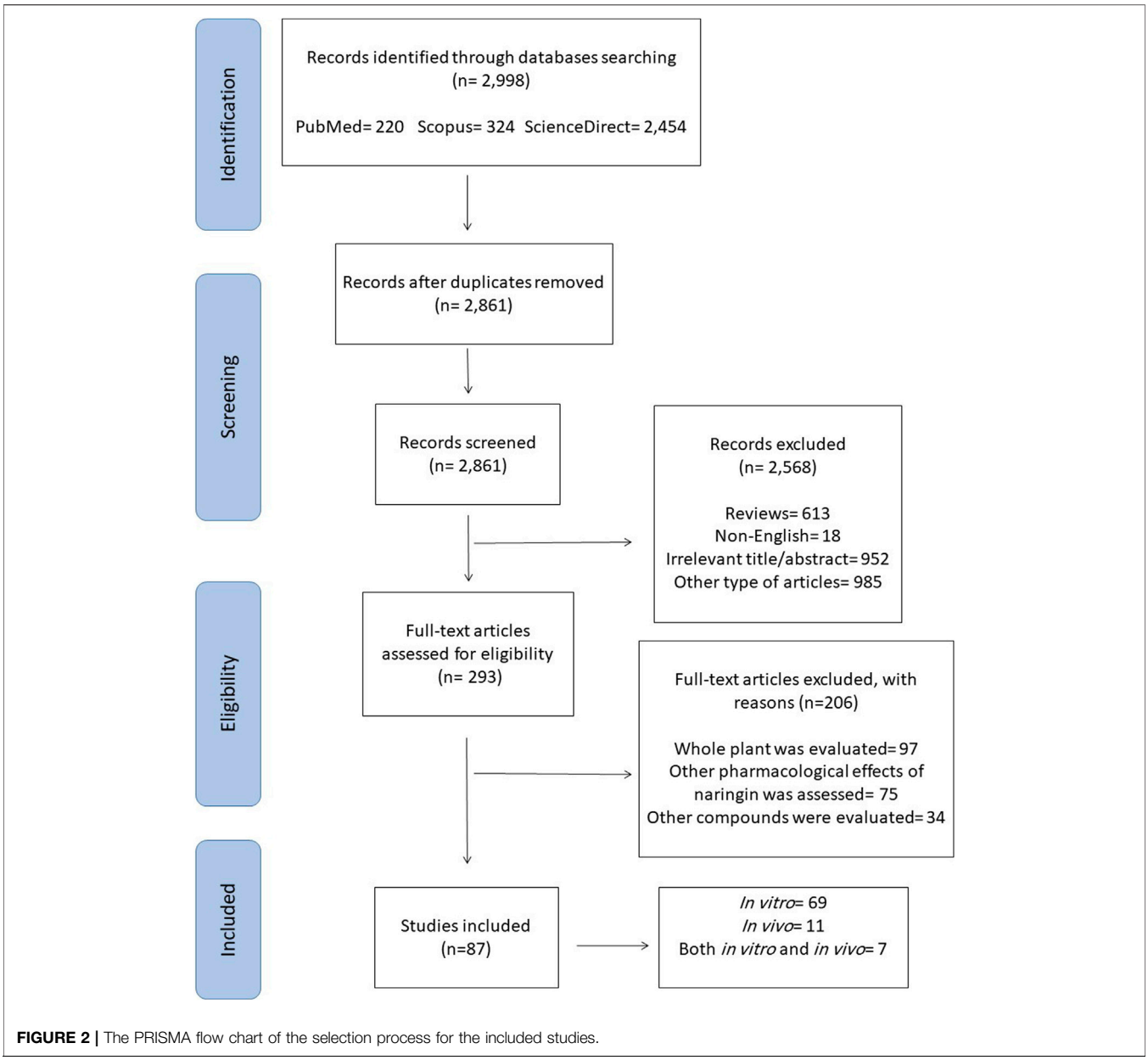

FIGURE 2 | The PRISMA flow chart of the selection process for the included studies.

Exclusion Criteria

We applied the following exclusion criteria: 1) conference abstracts, books, book chapters, and unpublished results; 2) non-English papers; 3) reviews, systematic reviews, meta-analysis, and letters; 4) primary research papers that do not involve tumor cell lines or animal tumor models.

Data Extraction

Among the initial 2,998 reports that were collected through electronic search, 137 were omitted due to duplicated results, 985 were ruled out because of the article type, 613 review articles were omitted, and 952 were deemed irrelevant based on abstract and/or title information. Besides, 18 were excluded because they were not in English language. Out of 293 retrieved reports, 97 were excluded as they evaluated the whole plant, 75 were ruled out as they examined other biological impacts of naringin rather than anticancer effects, and 34 were excluded because they concentrated on other compounds, not naringin.

Data Synthesis

Finally, 87 articles were included in this study as demonstrated in a flowchart of the literature search and selection process (**Figure 2**). It was envisioned that studies would be too heterogeneous to be combined. Hence, a narrative synthesis was conducted. The results are summarized according to type of cancer and outcome measures assessed. The magnitudes of effects on each outcome measure are reported.

TABLE 3 | Potential anticancer effects and related mechanisms of action of naringin based on *in vitro* studies.

Cancer type	Cell type	Conc	Source	Purity (%)	Quality control reported? (Y/N)	Duration	Anticancer effects	References
Bladder	T24 and 5,637 cell lines	50–150 μM	Wako pure chemical Industries, ltd. (Osaka, Japan)	ND	Y	24 h	↓Cell proliferation, ↓cell viability, ↓cell growth, ↑cell cycle arrest, ↑p21WAF1, ↑Ras, ↑Raf	Kim et al. (2008)
Bladder	TCC cell line	0.3–5 μM	Merck Chemical Co. (Darmstadt, Germany)	ND	Y	24–48 h	↓Cell proliferation, ↓cell viability	Karami et al. (2018)
Bladder	TCC cell line	75 μg/ml	Sigma-Aldrich (Munich, Germany)	ND	Y	24–72 h	↓Cell proliferation, ↓cell viability	Oršolić et al. (2009)
Blood (leukemia)	HL-60, Kasumi-1, and K562 cell lines	0.125–2 mg/ml	China Institute of drugs and Bioproducts (Beijing, China)	ND	Y-HPLC	24–48 h	↓Cell proliferation, ↑apoptosis, ↓Mcl-1	Dai et al. (2017)
Blood (leukemia)	U937 cell line	50–500 μM	Sigma-Aldrich (Lyon, France)	(90%)	Y	24 h	↓Cell proliferation, ↓cell growth, ↑cell death	Jin et al. (2009)
Blood (leukemia)	THP-1 cell line	50–400 μM	Gibco BRL (Gaithersburg, MD, United States)	ND	Y	48 h	↓Cell proliferation, ↓cell viability	Park et al. (2008)
Blood (leukemia)	HL-60 and THP-1 cell lines	40–80 μM	Sigma-Aldrich (Lyon, France)	ND	Y	6–24 h	No effect	Chen et al. (2003)
Blood (leukemia)	K562 cell line	5–500 μM	Quinabra Company (São José dos Campos, Brazil)	ND	Y	24–72 h	↓Cell number, ↓cell growth, ↑cell death, ↓DPPH	Pereira et al. (2007)
Blood (leukemia)	K562 cell line	1–100 μM	Fluka chemie GmbH (Buchs, Switzerland)	(≥95%)	Y- TLC and HPLC	20–100 h	↓VEGF	Mellou et al. (2006)
Blood (lymphoma)	P-388D1, L-1210 cell lines	1–2 mM	Sigma-Aldrich (St. Louis, MO, USA)	ND	Y	12 h	↑Cytotoxic activity, ↑anti-platelet aggregation activity, ↑trypsin inhibition	Kim et al. (1998)
Blood (lymphoma)	Raji cell line	10–1,000 μM	Extrasynthese-Genay (Lyon, France)	ND	Y	24 h	↓Cell proliferation, ↓cell growth	Ramanathan et al. (1992)
Brain	U-87cell line	5–30 μM	Sigma-Aldrich (Lyon, France)	(98%)	Y	24–48 h	↓Cell proliferation, ↓cell viability, ↓cell invasion, ↓tubulogenesis	Aroui et al. (2020)
Brain	U87 and U251 cell lines	10–40 μM	Invitrogen (Carlsbad, CA, USA)	ND	Y	12–48 h	↓Cell proliferation, ↓FAK/cyclin D1 pathway, ↑apoptosis, ↓cell invasion, ↓metastasis, ↓migration, ↓FAK/MMPs pathway, ↓kinase activity of FAK	Li et al. (2017)
Brain	U373 and U87 cell lines	5–100 μM	Sigma-Aldrich (Lyon, France)	ND	Y	12–24 h	↓Cell growth, ↓cell viability, ↓migration, ↓cell invasion, ↓MMP-9, ↓MMP-2, ↑MAPK signaling pathways, ↓metastasis	Aroui et al. (2016a)
Brain	U251 cell line	5–60 μM	Sigma-Aldrich (Lyon, France)	(98%)	Y	24 h	↓Cell proliferation, ↓cell viability, ↓cell invasion, ↓migration, ↓ MMP-9, ↓MMP-2, ↑TIMP-2, ↑TIMP-1, ↓p38 signal transduction pathways	Aroui et al. (2016b)

(Continued on following page)

TABLE 3 | (*Continued*) Potential anticancer effects and related mechanisms of action of naringin based on *in vitro* studies.

Cancer type	Cell type	Conc	Source	Purity (%)	Quality control reported? (Y/N)	Duration	Anticancer effects	References
Brain (Glioma)	U343 and U118 cell lines	0.1–100 μM	Sigma-Aldrich (Steinheim, Germany)	ND	Y	24 h	↓VEGF	Schindler and Mentlein (2006)
Breast	MCF-7 cell line	50–400 μg/ml	Sigma-Aldrich (Berlin, Germany)	ND	Y-HPLC	48–72 h	↓Cell proliferation, ↓cell growth, ↑apoptosis	Elansary et al. (2020)
Breast	MCF7 cell line	5 μM	Sigma-Aldrich (St. Louis, MO, USA)	ND	Y-HPLC	12–48 h	↓Cell proliferation, ↓cell viability	Puranik et al. (2019)
Breast	MCF7 and HCT116 cell lines	0.78–100 μg/ml	Purified by Basta et al., 2020	ND	Y-TLC	48 h	↓Cell proliferation, ↓cell viability	Basta et al. (2020)
Breast	MCF7 cell line	0.78–100 μg/ml	Purified by Atta et al., 2019	ND	Y-TLC	48 h	↓Cell viability, ↓cell growth, ↑apoptosis	Atta et al. (2019)
Breast	MCF-7 cell line	200 μM	Sigma-Aldrich (St. Louis, MO, United States)	(≥95%)	Y	72 h	↓Cell proliferation, ↓cell viability, ↑apoptosis	Fazary et al. (2017)
Breast	MCF7 cell line	0.3–5 μM	Merck Chemical Co. (Darmstadt, Germany)	ND	Y	24–48 h	↓Cell proliferation, ↓cell viability	Karami et al. (2018)
Breast	MCF7 cell line	20–100 μM	Sigma-Aldrich (St. Louis, MO, USA)	(97%)	Y-HPLC	1–48 h	↓Cell proliferation, ↓cell viability	Selvaraj et al. (2014)
Breast	MCF-7 and MDA-MB-231 cell lines	5–100 μM	Sigma-Aldrich (Poznań, Poland)	ND	Y	24–48 h	↓Cell viability, ↑cell cycle arrest, ↑apoptosis	Kabała-Dzik et al. (2018)
Breast	CMT-U27 cell line	20–1,000 μM	Sigma-Aldrich Chemical Co. (Steinheim, Germany)	ND	Y	48 h	↓Cell proliferation, ↓cell viability	Özyürek et al. (2014)
Breast	MDA-MB-231, MDA-MB-468, and BT-549 cell lines	50–200 μM	Sigma-Aldrich (St. Louis, MO, USA)	(≥95%)	Y-HPLC	24–48 h	↓Cell proliferation, ↓cell growth, ↑cell cycle arrest, ↓cell viability, ↑apoptosis, ↓β-catenin pathway	Li et al. (2013a)
Breast	Ehrlich ascites tumor cells	5–100 μM	Sigma-Aldrich (St. Louis, MO, USA)	ND	Y	3–24 h	↑Tumor cell death, ↓tumor cell growth	Menon et al. (1995)
Breast	MDA-MB-231 cell line	0.1–100 μM	Sigma-Aldrich (St. Louis, MO, USA)	ND	Y	24 h	↓VEGF	Schindler and Mentlein (2006)
Cervical	C33A, SiHa, and HeLa cell lines	10–10,000 μM	Sigma-Aldrich (St. Louis, MO, USA)	(≥95%)	Y-HPLC	24 h	↓Cell viability, ↑cell cycle arrest, ↑apoptosis, ↓Wnt/β-catenin pathway	Chen et al. (2020)
Cervical	SiHa cell line	250–2000 μM	Sigma–Aldrich (St. Louis, MO, United States)	ND	Y	24–48 h	↓Cell proliferation, ↓cell viability, ↑cell cycle arrest, ↑apoptosis, ↑caspases, ↑p53, ↑Bax, ↑Fas	Ramesh and Alshatwi (2013)
Cervical	HeLa cell line	200–2000 μM	Sigma-Aldrich (St. Louis, MO, United States)	ND	Y	24 h	↓Cell proliferation, ↓cell growth, ↑apoptosis	Liu et al. (2017)
Cervical	HeLa cell line	200–3200 μM	Nacalai tesque (Kyoto, Japan)	ND	Y	48 h	↓Cell growth, ↑apoptosis, ↓NEU3, ↑EGFR/ERK signaling	Yoshinaga et al. (2016)
Cervical	HeLa cell line	10–1,000 μM	Extrasynthese-Genay (Lyon, France)	ND	Y	24 h	↓Cell proliferation, ↓cell growth	Ramanathan et al. (1992)
Cervical	HeLa cell line	50–400 μg/ml	Sigma-Aldrich (Berlin, Germany)	ND	Y-HPLC	48–72 h	↓Cell proliferation, ↓cell growth, ↑apoptosis	Elansary et al. (2020)
Cervical	HeLa cell line	200–1,500 μmol/L	Sigma-Aldrich (St. Louis, MO, United States)	ND	Y	3–48 h	↓Cell viability, ↓cell growth, ↑apoptosis, ↓NF-κB/COX-2-caspase-1 pathway	Zeng et al. (2014)

(Continued on following page)

TABLE 3 | (*Continued*) Potential anticancer effects and related mechanisms of action of naringin based on *in vitro* studies.

Cancer type	Cell type	Conc	Source	Purity (%)	Quality control reported? (Y/N)	Duration	Anticancer effects	References
Colon	HT-29 cell line	50–400 μg/ml	Sigma-Aldrich (Berlin, Germany)	ND	Y-HPLC	48–72 h	↓Cell proliferation, ↓cell growth, ↑apoptosis	Elansary et al. (2020)
Colon	CT26 cell line	1–100 μg/ml	Purified by Zhou et al., 2018	ND	Y- HPLC		↓Cell proliferation, ↓cell viability, ↑apoptosis	Zhou et al. (2018)
Colon	SW480 cell line	12.5–200 μM	Sigma-Aldrich (St. Louis, MO, USA)	ND	Y	12–48 h	↓Cell proliferation, ↓cell viability	Chidambara Murthy et al. (2012)
Colorectal	HCT116 and SW620 cell lines	6–25 μg/ml	Beijing Solarbio Science and Technology Co., Ltd (Beijing, China)	ND	Y	12–72 h	↓Cell proliferation, ↑apoptosis, ↓PI3k/Akt/mTOR pathway	Cheng et al. (2020)
Colon	Colo 205 and Colo 320 cell lines	4–10 μg/ml	Purified by Ugocsai et al. (2005)	ND	Y	24 h	↑Apoptosis	Ugocsai et al. (2005)
Colon	COLO 320HSR, COLO 205, and HT 29 cell lines	200 μM	Sigma-Aldrich (St. Louis, MO, USA)	ND	Y	24 h	No effect	Shen et al. (2004)
Colon	HT29 cell line	10–250 μg/ml	Sigma-Aldrich (St. Louis, MO, USA)	ND	Y-HPLC and mass spectrometer	24–48 h	↓Cell proliferation, ↓cell growth	Ferreira et al. (2013)
Colon	HCT116 cell line	200 μM	Sigma Aldrich (St. Louis, MO, United States)	(≥95%)	Y	72 h	↓Cell proliferation, ↓cell viability, ↑apoptosis	Fazary et al. (2017)
Colon	HCT116 cell line	0.78–100 μg/ml	Purified by Basta et al., 2020	ND	Y-TLC	48 h	↓Cell proliferation, ↓cell viability	Basta et al. (2020)
Colon	SNU-C4 cell line	1–2 mM	Sigma-Aldrich (St. Louis, MO, USA)	ND	Y	12 h	↑Cytotoxic activity, ↑anti-platelet aggregation activity, ↑trypsin inhibition	Kim et al. (1998)
Colorectal	Caco-2 cell line	10–1,000 μM	Sigma-Aldrich (St. Louis, MO, USA)	ND	Y	24 h	↓Cell proliferation, ↓cell growth, ↓cell viability ↓GLO-I activity	Yadav et al. (2016)
Colon	HT-29 and Caco-2 cell lines	10–60 μM	Fluka Chemika-BioChemika (New York, USA)	(>95%)	Y	24–48 h	No effect	Kuo (1996)
Esophageal	YM1 cell line	300 μM	Sigma-Aldrich (St. Louis, MO, USA)	ND	Y	24 h	↓Cell proliferation, ↓cell viability	Tajaldini et al. (2020)
Head and Neck (laryngeal)	HEp2 cell line	3.8–500 μM	Sigma-Aldrich (St. Louis, MO, USA)	ND	Y	72 h	↓Cell viability, ↓lipid peroxidation, ↑CYP1A1	Durgo et al. (2007)
Liver	HepG2 cell line	12.5 μM–3.2 mM	Sigma–Aldrich (St. Louis, MO, United States)	(≥95%)	Y-HPLC	48 h	↓Cell viability, ↓cell growth, ↑apoptosis	Elsawy et al. (2020)
Liver	HepG2 cell line	5 μM	Sigma-Aldrich (St. Louis, MO, United States)	ND	Y	24 h	↓Cell proliferation, ↓cell viability	Syed et al. (2020)
Liver	HepG2 cell line	10–40 μM	Sigma-Aldrich (St. Louis, MO, USA)	ND	Y	24–72 h	↓Cell proliferation, ↑apoptosis, ↑Bax, ↓Bcl-2, ↑miR-19b	Xie et al. (2017)
Liver	HepG2 cell line	50–250 μg/ml	Sigma-Aldrich (St. Louis, MO, United States)	ND	Y	24 h	↓Cell proliferation, ↓cell viability, ↓cell growth, ↑apoptosis	Banjerdpongchai et al. (2016a)
Liver	HepG2 cell line	100 μg/ml	Sigma-Aldrich (St. Louis, MO, United States)	ND	Y	24 h	↓Cell proliferation, ↑apoptosis, ↑Bax, ↑Bak, ↓Bcl-xL, ↑tBid	Banjerdpongchai et al. (2016b)

(Continued on following page)

TABLE 3 | (*Continued*) Potential anticancer effects and related mechanisms of action of naringin based on *in vitro* studies.

Cancer type	Cell type	Conc	Source	Purity (%)	Quality control reported? (Y/N)	Duration	Anticancer effects	References
Liver	HepG2 cell line	1–100 μg/ml	Purified by Zhou et al., 2018	ND	Y- HPLC		↓Cell proliferation, ↓cell viability, ↑apoptosis	Zhou et al. (2018)
Liver	HepG2, Huh-7, and HA22T cell lines	25–100 μM	Sigma–Aldrich (St. Louis, MO, United States)	(>98%)	Y	8–24 h	↓Cell invasion, ↓migration, ↓metastasis, ↓MMP-9, ↓PI3K/Akt, ↓MAPK, ↓IκB	Yen et al. (2015)
Liver	HepG2 cell line	10–250 μg/ml	Sigma-Aldrich (St. Louis, MO, USA)	ND	Y-HPLC and mass spectrometer	24–48 h	↓Cell proliferation, ↓cell growth	Ferreira et al. (2013)
Liver	HepG2, MCF-7, and HCT116 cell lines	200 mM	Sigma-Aldrich (St. Louis, MO, United States)	(≥95%)	Y	72 h	↓Cell proliferation, ↓cell viability, ↑apoptosis	Fazary et al. (2017)
Liver	HA22T and SK-Hep1 cell lines	10–100 μM	Aldrich chem. Co. (Milwaukee, WI, United States)	ND	Y	24 h	↓Cell viability, ↓cell growth	Hsiao et al. (2007a)
Liver	HepG2 cell line	1–2 mM	Sigma-Aldrich (St. Louis, MO, USA)	ND	Y	12 h	↑Cytotoxic activity, ↑anti-platelet aggregation activity, ↑trypsin inhibition	Kim et al. (1998)
Liver	Hepa-1c1c7 cell line	50–100 μM	Sigma-Aldrich (St. Louis, MO, USA)	ND	Y	72 h	No effect	Campbell et al. (2006)
Lung	A549 cell line	3–1,000 μM	Purified by Nie et al., 2012	(>98.3%)	Y-determined by peak area normalization	24–96 h	↓Cell proliferation, ↓cell viability	Nie et al. (2012)
Lung	A549 and LLC cell lines	10–100 μM	Aldrich chem. Co. (Milwaukee, WI, United States)	ND	Y	24 h	↓Cell viability, ↓cell growth	Hsiao et al. (2007a)
Lung	H69AR cell line	6–25 μg/ml	ND	ND	ND	24 h	↓Cell proliferation, ↓cell growth, ↑apoptosis, ↑miR-126, ↓PI3K, ↓p-Akt, ↓p-mTOR, ↓VCAM-1, ↓NF-κB, ↓PI3K/Akt/mTOR pathway	Chen et al. (2018)
Lung	A549 cell line	10–50 μM	Aldrich chem. Co. (Milwaukee, WI, United States)	ND	Y	24 h	↓Cell viability, ↓cell invasion, ↓cell-matrix adhesion, ↓cellular motility	Hsiao et al. (2007b)
Lung	A549 cell line	1–2 mM	Sigma-Aldrich (St. Louis, MO, USA)	ND	Y	12 h	↑Cytotoxic activity, ↑anti-platelet aggregation activity, ↑trypsin inhibition	Kim et al. (1998)
Lung	A549 cell line	10–120 μg/ml	Sigma-Aldrich, (St. Louis, MO, United States)	ND	Y	6–24 h	↓Cell proliferation, ↓cell viability, ↑apoptosis	Garcia et al. (2019)
Lung	A549 cell line	0.78–100 μg/ml	Purified by Atta et al., 2019	ND	Y-TLC	48 h	↓Cell viability, ↓cell growth, ↑apoptosis	Atta et al. (2019)
Lung	HeLa and A549 cell lines	200–3200 μM	Nacalai Tesque, Inc. (Kyoto, Japan)	ND	Y	48 h	↓Cell growth, ↑apoptosis, ↓NEU3, ↑EGFR/ERK signaling	Yoshinaga et al. (2016)
Neuroblastoma	SH-SY5Y cell line	1–10 μM	Sigma-Aldrich (St. Louis, MO, USA)	ND	Y	24 h	↓Cell viability, ↑cell death	Kim et al. (2009)
Ovarian	SKOV3/CDDP cell line	10–40 μmol/L	Institute of pharmacology at Nanchang university (Nanchang, China)	ND	Y	48 h	↓NF-κB, ↓P-gp	Zhu et al. (2018)

(Continued on following page)

TABLE 3 | (*Continued*) Potential anticancer effects and related mechanisms of action of naringin based on *in vitro* studies.

Cancer type	Cell type	Conc	Source	Purity (%)	Quality control reported? (Y/N)	Duration	Anticancer effects	References
Ovarian	SKOV3/ CDDP cell line	10–40 μmol/L	Shandong Qilu Pharmaceutical Co., Ltd. (Shandong, China)	ND	Y	48 h	↓NF-κB, ↓COX-2	Zhu et al. (2017)
Ovarian	OVCAR-3 cell line	5–160 μM	Sigma-Aldrich (St. Louis, MO, USA)	ND	Y	24 h	No effect	Luo et al. (2008)
Prostate	PC-3 and LNCaP cell lines	2.5–300 μM	Selleck (Maple Valley, WA, USA)	ND	Y	24–48 h	↓Cell growth, ↓migration, ↓cell invasion, ↑apoptosis, ↑Bax, ↓p-↓STAT3, ↓survivin, ↓Bcl-2, ↓p-Akt	Wu et al. (2019)
Prostate	PC3, DU145, and LNCaP cell lines	3.9–500 μM	Sigma-Aldrich (St. Louis, MO, United States)	ND	Y	72 h	↓Cell survival, ↓cell viability, ↑apoptosis, ↑cell cycle arrest, ↑PTEN, ↓nuclear factor-κB p50 protein, ↓cell migration, ↓NF-κB signaling	Erdogan et al. (2018)
Prostate	DU145 cell line	50–250 μM	Sigma-Aldrich (Poznan, Poland)	ND	Y	24 h	↓Cell proliferation, ↓cell viability, ↓cell number, ↑oxidative stress, ↑apoptosis	Lewinska et al. (2015)
Sarcoma (osteosarcoma)	MG63 and U2OS cell lines	10–20 μmol/L	Beyotime Biotechnology (Shanghai, China)	ND	Y	24 h	↓Cell proliferation, ↓cell invasion, ↑apoptosis, ↓Zeb1, ↓cell migration, ↑cell cycle arrest	Ming et al. (2018)
Sarcoma (osteosarcoma)	MG-63 cell line	1–100 μg/ml	Purified by Zhang et al., 2018a	ND	Y-HPLC and Mass spectrometry	24–72 h	No effect	Zhang et al. (2018a)
Sarcoma (chondrosarcoma)	JJ012 cell line	3–30 μM	Sigma-Aldrich (St. Louis, MO, United States)	ND	Y	24–48 h	↓Cell invasion, ↓migration, ↓VCAM-1, ↑miR-126	Tan et al. (2014)
Skin (Melanoma)	A375 and A875 cell lines	10–40 μM	ND	ND	ND	12–60 h	↓Cell proliferation, ↓cancer metabolism, ↑cell cycle arrest, ↑apoptosis, ↓cell growth, ↓cell invasion, ↓migration, ↓c-Src	Guo et al. (2016)
Skin (Melanoma)	MO4 cell line	0.5 mM	Provided by dr. J, A. Attaway (department of citrus, state of Florida, United States)	ND	Y- Reversed-phase high-pressure liquid chromatography	4 days	↓Invasion	Bracke et al. (1991)
Skin (Melanoma)	B16F10 cell line	5–500 μM	Quinabra Company (São José dos Campos, Brazil)	ND	Y	24–72 h	↓Cell number, ↓cell growth, ↑cell death, ↓DPPH	Pereira et al. (2007)
Stomach (Gastric)	AGS cell line	1–3 mM	Sigma-Aldrich (St. Louis, MO, United States)	ND	Y	3–24 h	↑ROS, ↑ERK1/2-p38 MAPKs, ↑autophagy cell death	Raha et al. (2020)
Stomach (Gastric)	AGS cell line	10–100 μM	Aldrich Chemical Co. (Milwakee, WI, United States)	ND	Y	24 h	↓Cell viability, ↓cell growth	Hsiao et al. (2007a)

(Continued on following page)

TABLE 3 | (*Continued*) Potential anticancer effects and related mechanisms of action of naringin based on *in vitro* studies.

Cancer type	Cell type	Conc	Source	Purity (%)	Quality control reported? (Y/N)	Duration	Anticancer effects	References
Stomach (Gastric)	AGS cell line	1–3 mM	Sigma-Aldrich (St. Louis, MO, United States)	ND	Y	24–48 h	↓Cell proliferation, ↓cell growth, ↓PI3K/Akt/mTOR, ↑MAPKs, ↑$p21^{CIP1/WAF1}$, ↑autophagosome	Raha et al. (2015)
Stomach (Gastric)	SNU-1	1–2 mM	Sigma-Aldrich (St. Louis, MO, USA)	ND	Y	12 h	↑Cytotoxic activity, ↑anti-platelet aggregation activity, ↑trypsin inhibition	Kim et al. (1998)
Thyroid	TPC-1 and SW1736 cell lines	6–25 μg/ml	Beyotime Biotechnology (Shanghai, China)	ND	Y	24–72 h	↓Cell proliferation, ↑apoptosis, ↓PI3k/Akt pathway	Zhou et al. (2019)

Note: *A down arrow indicates a reduction or decrease and an up arrow indicates an increase. Bak, Bcl-2 homologous antagonist/killer; Bax, Bcl-2-associated X protein; Bcl-2, B-cell lymphoma 2; Bcl-xL, B-cell lymphoma-extra-large; COX-2, cyclooxygenase- 2; c-Src, proto-oncogene tyrosine-protein kinase Src; DPPH, diphenylpicrylhydrazyl radical; EGFR, epidermal growth factor receptor; ERK, extracellular signal-regulated kinase; FAK, focal adhesion kinase; GLO-I, glyoxalase-I; IκB, inhibitor of NF-κB; MMPs, matrix metallopeptidases; MAPK, mitogen-activated protein kinase; Mcl-1, myeloid cell leukemia 1; miR, microRNA; mTOR, mammalian target of rapamycin; ND, not determined; NEU3, plasma membrane-associated sialidase; NF-κB, nuclear factor-κB; p53, tumor protein p53; p38 MAPKs, p38 mitogen-activated protein kinases; p-Akt, phosphorylated Akt; P-gp, P-glycoprotein; PI3K, phosphatidylinositol-3-kinase; p-mTOR, phosphorylated mammalian target of rapamycin; p-STAT3, phosphorylated signal transducer and activator of transcription 3; ROS, reactive oxygen species; tBid, truncated BH3 interacting domain death agonist; TIMP, tissue inhibitor of metalloproteinase; VCAM-1, vascular cell adhesion molecule 1; VEGF, vascular endothelial growth factor; Zeb1, zinc finger E-box binding homeobox 1.*

Assessment of Bias and Errors

The primary search was conducted by two researchers, and they extracted the data independently, which limits the risk of bias and errors.

ANTICANCER ACTIVITIES OF NARINGIN

Naringin has been shown to inhibit various cancers via different mechanisms, including growth suppression of malignant cells, apoptosis induction and cell cycle arrest, and modulation of oxidative stress, inflammation, and angiogenesis, through the regulation of several cellular signaling cascades. The antitumor effects and associated mechanisms of naringin in various cancers are presented in the following sections.

Bladder Cancer

Bladder cancer includes a broad range of tumors, including transitional cell carcinoma, which is categorized into three types, namely superficial tumors, tumors confined to the bladder, and invasive tumors. In superficial bladder cancer, the risk of disease recurrence and/or progression to invasive diseases is high (Levi et al., 1993). For these cases, efficient preventive measures are required. One study determined a new mechanism of naringin anticancer activity observed in bladder cancer cell lines. Results demonstrated that naringin treatment suppressed cell viability and growth, and induced $p21^{WAF1}$ expression and cell cycle arrest in 5,637 and T24 bladder carcinoma cell lines, potentially through suppressing the Ras/Raf/extracellular signal-regulated kinase (ERK)-signaling pathway (**Table 3**) (Kim et al., 2008). Another study showed that treatment with mononuclear palladium (II) complexes of naringin decreased the viability and proliferation of TCC bladder carcinoma cell lines, and these complexes noticeably showed major and selective cytotoxicity toward bladder cancer cells (Karami et al., 2018). In another *in vitro* study, naringin reduced cell proliferation and viability in TCC Human urinary bladder transitional cell carcinoma cells (Oršolić et al., 2009).

Blood Cancer

Leukemia is one form of the hematological malignancies with particularly high mortality (Vardiman et al., 2009). At present, leukemia treatment relies on chemotherapies to abrogate malignant cells or to promote differentiation in leukemia cells. Conversely, the available chemotherapies commonly have severe adverse effect (Goldman and Melo, 2003). Accordingly, the discovery of novel therapeutic reagents with a magnificently safe profile is required. One study indicated that treatment of K562, HL-60, and Kasumi-1 human myeloid leukemia cells with naringin blocked cell proliferation and promoted their apoptosis in a time- and concentration-dependent way, via downregulation of Mcl-1 expression and activation of caspase and PARP pathway (Dai et al., 2017). Naringin treatment also enhanced cell death and decreased cell proliferation and growth in U937 (Jin et al., 2009) and THP-1 (Park et al., 2008) human leukemia cells. However, one study showed that naringin had no cytotoxic effect on THP-1 and HL-60 are leukemia cell lines (Chen et al., 2003). In another study, a naringin-derived copper (II) complex 1 was engineered, and its anticancer effect was investigated. Results showed that treatment of K562 human chronic myeloid leukemia cells with naringin–Cu (II) complex 1 or naringin reduced cell proliferation and growth, increased cell death, and decreased diphenylpicrylhydrazyl radical (DPPH). Results also showed that naringin–Cu (II) complex 1 had greater anti-inflammatory, antioxidant, and anticancer activities in comparison to free naringin without decreasing

TABLE 4 | Potential anticancer effects and related mechanisms of action of naringin based on *in vivo* studies.

Cancer type	Animal model	Dose	Source	Purity (%)	Quality control reported? (Y/N)	Duration	Anticancer effects	References
Brain	Athymic mice bearing U-87 tumor	60–180 mg/kg	Sigma-Aldrich (St. Louis, MO, USA)	(98%)	Y	7 days	↓Tumor size, ↓survival, ↓angiogenesis	Aroui et al. (2020)
Breast	SCID female mice bearing MDA-MB-231 tumor	100 mg/kg	Sigma-Aldrich (St. Louis, MO, USA)	(≥95%)	Y-HPLC	1–5 weeks	↓Tumor volume, ↓tumor weight	Li et al. (2013a)
Breast	Swiss albino mice bearing ehrlich ascites tumor cells	100 mg/kg	Sigma-Aldrich Chemie GmbH (Munich, Germany)	ND	Y	90 days	↑Survival, ↓tumor growth, ↓tumor cell proliferation, ↑tumor regression	Benkovic et al. (2007)
Breast	Swiss albino mice bearing ehrlich ascites tumor cells	100 mg/kg	Sigma–Aldrich chemie GmbH (Germany)	ND	Y	5 days	↓Tumor growth, ↑survival, ↓tumor cell proliferation	Oršolić et al. (2010)
Breast	Swiss albino mice bearing ehrlich ascites tumor cells	100 mg/kg	Sigma-Aldrich chemie GmbH (Munich, Germany)	ND	Y	5 days	↓Tumor growth, ↑survival, ↓tumor cell proliferation	Knežević et al. (2011)
Breast	Female Sprague-dawley rats with DMBA-induced breast tumors	500 mg/100 g diet	Provided by dr. W. Widmer (state of Florida dept. of citrus, United States)	ND	N	10 weeks	↓Tumor development, ↓tumor weight	So et al. (1996)
Cervix	Female athymic nude mice bearing HeLa tumors	20 mg/kg	Sigma-Aldrich (St. Louis, MO, United States)	ND	Y	20 days	↓Tumor growth, ↑apoptosis	Liu et al. (2017)
Colon	Male C57BL/6 mice with AOM/DSS-induced colon carcinogenesis	50–100 mg/kg	Sigma-Aldrich (St. Louis, MO, USA)	(≥98%)	Y	1–63 days	↓Tumor growth, ↓tumor size, ↓STAT3, ↓p-mTOR, ↓NF-κB	Zhang et al. (2018b)
Colon	Male Sprague–Dawley rats with AOM-induced colon carcinogenesis	200 mg/kg	Purified by Vanamala et al., 2006	ND	Y-Reverse phase liquid chromatography	10 weeks	↓Tumor cell proliferation, ↑apoptosis	Vanamala et al. (2006)
Esophagus	Male nude mice with YM1 xenograft tumors	50 mg/kg	Sigma-Aldrich (St. Louis, MO, USA)	ND	Y	14 days	↓Tumor size, ↓tumor growth	Tajaldini et al. (2020)
Head and neck (oral cavity)	Hamster cheek pouch oral cancer model	0.5–8.0 mg/kg	ND	ND	ND		↓Tumor growth, ↓tumor number, ↓tumor burden	Miller et al. (2008)
Liver	Male Wistar rats bearing DEN-induced hepatocellular carcinoma	40 mg/kg	Sigma-Aldrich (St. Louis, MO, USA)	ND	Y	6–16 weeks	↓Cell proliferation, ↑apoptosis, ↓AgNOR/nuclei	Thangavel and Vaiyapuri (2013)
Ovary	Female BALB/c nude mice bearing SKOV3 tumor	0.5–2 mg/kg	Merck KGaA (Darmstadt, Germany)	(>90%)	Y	10 days	↑Apoptosis, ↓tumor size, ↓tumor weight, ↓tumor growth, ↓Bcl-xL, ↓Bcl-2, ↓cyclin D1, ↓c-Myc, ↓ survivin, ↑caspase-3, ↑caspase-7	Cai et al. (2018)
Prostate	Male SCID mice bearing PC-3 and LNCaP tumors	50 mg/kg	Selleck (Maple Valley, WA, USA)	ND	Y	16 days	↓Tumors growth, ↑apoptosis	Wu et al. (2019)
Sarcoma (osteosarcoma)	Female, athymic nude BALB/c mice bearing MG63 tumor	5–10 mg/kg	Beyotime Biotechnology (Shanghai, China)	ND	Y	16 days	↓Invasion, ↓migration ↓cyclin D1, ↓MMP-2, ↓Bcl-2, ↓Zeb1	Ming et al. (2018)
Sarcoma	Male ddY mice bearing S180 tumor	30–300 mg/kg	Sigma-Aldrich (St. Louis, MO, USA)	ND	Y	5 days	↓Tumor growth	Kanno et al. (2005)

(Continued on following page)

TABLE 4 | (*Continued*) Potential anticancer effects and related mechanisms of action of naringin based on *in vivo* studies.

Cancer type	Animal model	Dose	Source	Purity (%)	Quality control reported? (Y/N)	Duration	Anticancer effects	References
Sarcoma (carcinosarcoma)	Male Wistar rats bearing W256 tumor	10–35 mg/kg	Sigma-Aldrich (St. Louis, MO, USA)	ND	Y	50 days	↓Tumor growth, ↑survival, ↓TNF-α, ↓IL-6	Camargo et al. (2012)
Skin (melanoma)	C57BL/6 female mice bearing B16FIO tumors	200 nmol/kg	Sigma-Aldrich (St. Louis, MO, USA)	ND	Y	10 days	↓Metastatic foci formation, ↑survival, ↓lung tumor nodules	Menon et al. (1995)

Note: *A down arrow indicates a reduction or decrease and an up arrow indicates an increase. AgNOR, argyrophilic nucleolar organizer region; Bcl-2, B-cell lymphoma 2; Bcl-xL, B-cell lymphoma-extra-large; DEN, diethylnitrosamine, DMBA, 7,12-dimethylbenz[a]anthracene; MMP-2, matrix metallopeptidase-2; mTOR, mammalian target of rapamycin; ND, not determined; NF-κB, nuclear factor-κB; STAT3, signal transducer and activator of transcription three; Zeb1, zinc finger E-box binding homeobox 1.*

cell viability (Pereira et al., 2007). One study demonstrated that *in vitro* naringin treatment reduced the VEGF production in K562 human leukemia cells (Mellou et al., 2006). Naringin also increased the inhibitory activity of trypsin and enhanced the antiplatelet aggregation activity and cytotoxic activity against P-388D1 (mouse lymphoid neoplasma) and L-1210 (mouse lymphocytic leukemia) cell lines (Kim et al., 1998). Another study also showed that *in vitro* naringin treatment suppressed cell proliferation and growth in Raji lymphoma cells (Ramanathan et al., 1992).

Brain Cancer

Gliomas are the most aggressive and frequent brain tumors, and regardless of progress in therapeutic management, they are still lethal. Accordingly, various therapeutic approaches are required to treat this aggressive disease (Martínez-Vélez et al., 2018). One study examined the antitumor effects of naringin treatment *in vitro* and *in vivo*. Results indicated that naringin had a toxic impact on the U-87 cell line and reduced cancer cell proliferation and viability in a concentration-dependent way. Moreover, naringin administration also suppressed tubulogenesis and angiogenesis and reduced tumor size and cell invasion U-87 mouse xenograft tumor model (**Table 4**) (Aroui et al., 2020). Another study demonstrated that naringin could specifically suppress the focal adhesion kinase (FAK) activity and inhibit the FAKp-Try397 and its downstream pathway in glioblastoma cells. Treatment of U87 and U251 glioblastoma cells with naringin blocked cell proliferation through suppression of the FAK/cyclin D1 pathway and induction of cell apoptosis via the FAK/Bad pathway. It also inhibited cell metastasis and invasion by suppressing the FAK/MMPs pathway (Li et al., 2017). Another study demonstrated that naringin had inhibitory impacts on the migration, adhesion, and invasion of U87 and U373 human glioblastoma cells in a concentration-dependent way. Additionally, naringin inhibited several aspects of the MAPK signaling pathways, including p38, ERK, and JNK, and led to the downregulation of the MMP-9 and MMP-2 expression and enzymatic activities, contributing to the suppression of metastasis of glioblastoma cells (Aroui et al., 2016a). Treatment with naringin also reduced cell proliferation and viability in U251 glioma cells. Additionally, naringin suppressed cell invasion and migration via the modulation of matrix metallopeptidase-9 (MMP-9) and MMP-2 expressions. Therefore, naringin might have therapeutic potential for the control of the invasiveness of malignant gliomas through suppressing the p38 signal transduction pathways (Aroui et al., 2016b). In an *in vitro* study, the treatment of U343 and U118 glioma cells with naringin showed a reduction in VEGF levels (Schindler and Mentlein, 2006). These findings have shown a new potential for exploring the capability of naringin as a promising therapeutic agent in gliomas.

Breast Cancer

Breast cancer is a heterogeneous group of tumors. Lately, a large number of personalized treatments for breast cancer have been introduced, with proven effectiveness (Cadoo et al., 2013). Natural products containing bioactive compounds are being used for both chemotherapy and cancer chemoprevention. Treatment with naringin suppressed proliferation and growth, and also increased apoptosis in MCF-7 cell lines (Puranik et al., 2019; Elansary et al., 2020). One study indicated that treatment with naringin alone or in combination with the sodium salt of carboxymethyl cellulose-phenyl alanine and sodium caseinate-phenyl alanine reduced viability and proliferation of MCF-7 cell line. Besides, naringin in hybrids had a greater cytotoxic effect in comparison to naringin alone (Basta et al., 2020). Moreover, treatment with naringin and its metal complexes decreased cell viability and proliferation and increased apoptosis in MCF-7 cell line (Atta et al., 2019). Based on the results, metal complexes of naringin demonstrated the highest cytotoxicity against cancer cells in comparison with naringin alone (Fazary et al., 2017). In another study, mononuclear palladium (II) complexes of naringin were synthesized, and the cytotoxic effect against MCF-7 cells was investigated. Results showed that naringin complexes reduced the viability and proliferation of breast cancer cells (Karami et al., 2018). Another study showed that treatment with naringin and its iron and copper complexes resulted in a reduction in the proliferation and viability of MCF-7 breast adenocarcinoma cell line (Selvaraj et al., 2014). One study, using different breast cancer cells (MCF-7 and MDA-MB-231), indicated that naringin reduced cell viability and promoted apoptosis and cycle arrest in breast cancer cells (Kabała-Dzik et al., 2018).

TABLE 5 | Anticancer effects of naringin-based nano-drug delivery systems.

Nano-formulation	Cancer type	Study type	Cell line/animal model	Dose/Conc	Source	Purity (%)	Quality control reported? (Y/N)	Duration	Outcomes	References
Gold-naringin nanoclusters	Lung	*In vitro*	A549 cell line	15–90 μg/ml	Sigma-Aldrich (St. Louis, MO, United States)	ND	Y	1–5 days	↓Cell viability	Sangubotla et al. (2020)
Naringin-reduced graphene oxide nanosheets	Colon	*In vitro*	HT-29 cell line	0.39–12.5 μM	KPI. (Shanghai, China)	ND	Y	24 h	↓Cell growth, ↓cell proliferation, ↑apoptosis	Han et al. (2020)
Ti-Naringin-PBA-ZnO nanoparticles	Osteosarcoma	*In vitro*	Saos-2 cell line	98.6 μg/ml	Aladdin industrial co. Ltd. (Shanghai, China)	ND	Y	1–7 days	↑Apoptosis, ↑ROS, ↑MAPK/ERK pathway	Yang et al. (2020)
Nanostructured lipid carrier-containing naringin and coix seed oil	Liver	*In vitro; In vivo*	HepG2 cell line; BALB-nu nude mice with HepG2 xenografts	0.39–25 μM; 20 mg/kg	Shanghai Standard Technology Co. Ltd. (Shanghai, China)	(>98%)	Y	1–10 days	↓Cell proliferation, ↑apoptosis, ↓cell viability, ↓tumor growth	Zhu et al. (2020)
PTX-NRG-MIC micelles	Breast	*In vitro*	MCF-7 cell line	15–100 mg/ml	Sigma-Aldrich (Taufkirchen, Germany)	ND	Y	4–24 h	↓Cell growth, ↓cell viability, ↑intracellular uptake	Jabri et al. (2019)
Naringin-PF68 micelles	Liver, breast and colorectal	*In vitro; In vivo*	Caco-2, HepG2, and MCF-7 cell lines; female Swiss albino mice with EAC cells	0.1–40 μM; 100 mg/kg	Sigma-Aldrich co. (St louis, MO, United States)	ND	Y-HPLC	1–7 days	↓Tumor growth, ↓cell viability, ↓cell proliferation, ↓Tumor size	Mohamed et al. (2018)
PLGA nanoparticles co-encapsulating naringin and celecoxib	Lung	*In vitro*	A549 cell line	0.78–100 μM	Sigma-Aldrich (St. Louis, MO, USA)	ND	Y	10–70 h	↓Cell viability, ↓cell proliferation, ↑apoptosis	Said-Elbahr et al. (2016)
Naringin-conjugated gold nanoparticles	Breast and prostate	*In vitro*	MCF-7, MDA-MB-231, T47D, and PC-3 cell lines	30–100 μg/ml	Sigma-Aldrich (Chandigarh, India)	ND	Y	24 h	↓Cell viability, ↓cell proliferation	Singh et al. (2016)

Note: *A down arrow indicates a reduction or decrease and an up arrow indicates an increase. EAC, Ehrlich ascites carcinoma; ERK, extracellular signal-regulated kinase pathway; MAPK, mitogen-activated protein kinase; ND, not determined; PLGA, poly D,L-lactide-co-glycolic acid copolymer; PTX-NRG-MIC, paclitaxel- and naringin-loaded mixed micelles; ROS, reactive oxygen species; Ti-naringin-PBA-ZnO, titanium-naringin-3-carboxyphenylboronic acid-zinc oxide.*

Recently, there has been an increased interest in polyphenolic antioxidants because of their health advantages, which has resulted in the evaluation of novel polyphenolic compounds with increased antioxidant activity, such as naringin oxime. Treatment with naringin oxime reduced cell viability and proliferation in CMT-U27 canine mammary carcinoma cells. New oxime-type antioxidants, such as naringin oxime, can be synthesized from various flavanones, and these derivatives may be used as anticancer and radioprotective agents (Özyürek et al., 2014). In another study, triple-negative breast cancer cell lines (MDA-MB-231, MDA-MB-468, and BT-549) were used to investigate the antitumor effect and related mechanisms of naringin. Results showed that naringin suppressed cell proliferation and increased G1 cycle arrest and apoptosis, accompanied by enhanced p21 and reduced survivin. Besides, the β-catenin signaling pathway was blocked by naringin treatment. Correspondingly, the anticancer potential of naringin was investigated in an *in vivo* condition, and naringin decreased tumor volume and weight in naringin-treated MDA-MB-231 xenograft mice (Li et al., 2013a).

Irinotecan is a semi-synthetic derivate of camptothecin that belongs to the class of topoisomerase I inhibitors and has significant activity against various cancers. *In vivo* studies showed that treatment with naringin alone or combined with irinotecan suppressed tumor growth and tumor cell proliferation and promoted survival in Ehrlich ascites tumor cell bearing-mice. Besides, naringin enhanced irinotecan-induced cytotoxicity to cancer cells in mice bearing Ehrlich ascites tumors, while protecting normal cells (Benkovic et al., 2007; Oršolić et al., 2010; Knežević et al., 2011). Another study also showed that

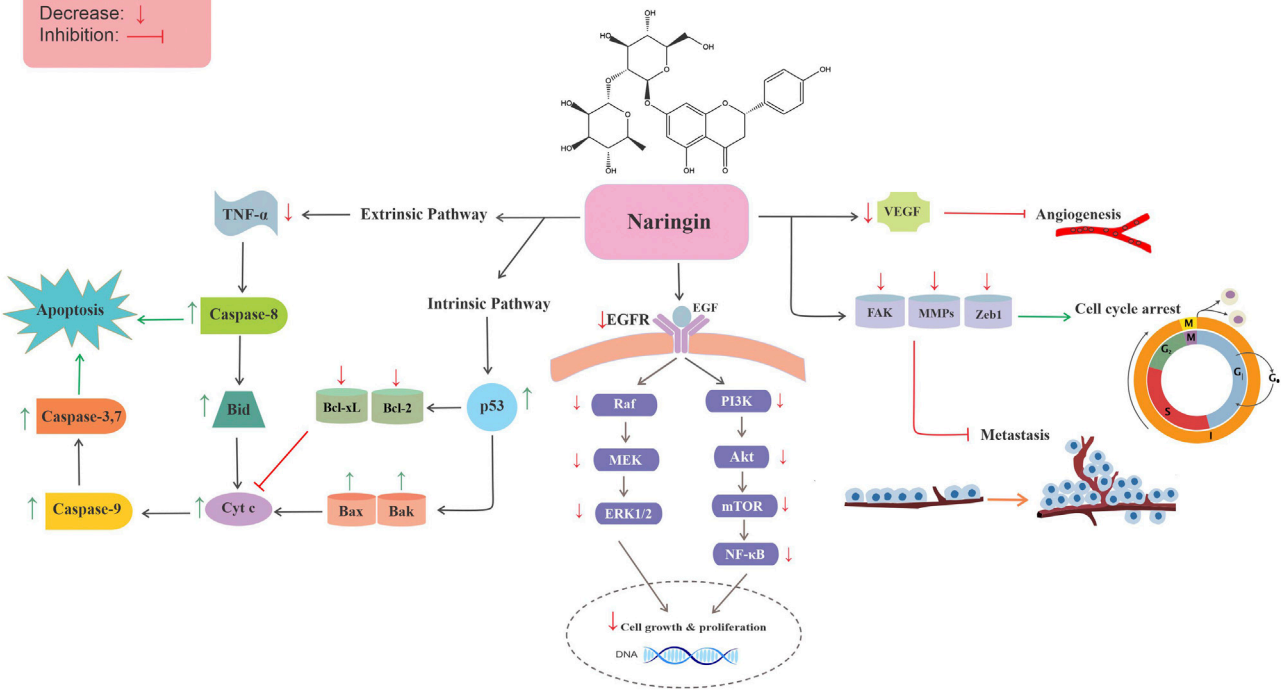

FIGURE 3 | Molecular mechanisms underlying anticancer effect of naringin. Bax, Bcl-2-associated X protein; Bak, Bcl-2 homologous antagonist/killer; Bcl-2, B-cell lymphoma 2; Bcl-xL, B-cell lymphoma-extra-large; Bid, BH3-interacting domain death agonist; cyt. c, cytochrome c; EGF, epidermal growth factor; EGFR, epidermal growth factor receptor; ERK1/2, extracellular signal-regulated kinase 1 and 2; FAK, focal adhesion kinase; MEK, mitogen-activated protein kinase; MMPs, matrix metallopeptidases; mTOR, mammalian target of rapamycin; NF-κB, nuclear factor-κB; p53, tumor protein p53; PI3K, phosphatidylinositol-3-kinase; Raf, rapidly accelerated fibrosarcoma; TNF-α, tumor necrosis factor-α; VEGF, vascular endothelial growth factor; Zeb1, zinc finger E-box binding homeobox 1.

naringin increased cell death in Ehrlich ascites tumor cells (Menon et al., 1995). Naringin treatment also inhibited the development of mammary tumors and decreased the tumor weight in Sprague-Dawley rats induced by 7,12-dimethylbenz [a]anthracene (DMBA) (So et al., 1996). Numerous solid tumors induce vascular proliferation through the production of angiogenic factors, especially vascular endothelial growth factor (VEGF). One study demonstrated that naringin treatment decreased the level of secreted VEGF from MDA-MB-231 cells (Schindler and Mentlein, 2006).

Cervical Cancer

Cervical cancer is the second-highest cause of death among women between the ages of 20 and 39 years (Fidler et al., 2017). Although chemotherapy is the standard therapeutic option, the survival rates of patients with cervical cancer are poor and need improvement via investigation of specific antitumor agents with less adverse effects on healthy cells (Pfaendler and Tewari, 2016). Hence, novel therapeutic targets are urgently required for the improvement of cervical cancer therapeutics. One study evaluated the antiproliferative effect and the associated mechanism of naringin-induced cell death in C33A, SiHa, and HeLa human cervical cancer cell lines. Results demonstrated that naringin treatment reduced cell viability and induced endoplasmic reticulum stress-mediated apoptosis. It also inhibited the Wnt/β-catenin pathway by reducing the protein expression and phosphorylation of glycogen synthase kinase-3β (Ser9) and β-catenin (Ser576), while simultaneously induced cell cycle arrest (Chen et al., 2020). *In vitro* treatment of SiHa cells with naringin decreased cell proliferation and viability by G2/M cell cycle arrest and induced apoptosis via DwM disruption, and intrinsic and extrinsic pathway activation (Ramesh and Alshatwi, 2013).

The doxorubicin (DOX) application in cervical cancer chemotherapy is severely hampered by the DOX side effects. The formation of DOX-iron complexes by oxygen free radicals plays an important role in DOX-induced toxicity (Myers, 1998). Fortunately, flavonoids have excellent radical scavenging and iron-chelating properties (Kaiserová et al., 2007), and they can act as an effective modulator for DOX-induced toxicity. Treatment with naringin, DOX, and their combination reduced cell proliferation in HeLa human cervical cancer cells and suppressed HeLa cervical tumor and induced cell apoptosis in tumor-bearing mice. More importantly, the combined treatment had a greater antitumor effect in comparison to either agent alone (Liu et al., 2017). Another study showed that naringin treatment suppressed plasma membrane-associated sialidase (NEU3), and the NEU3-inhibitory effect of naringin promoted GM3 accumulation in HeLa cells, resulting in epidermal growth factor receptor (EGFR)/ERK signaling

TABLE 6 | Anticancer effects of naringin based on google patents and US patents registry.

Patent NO	Cancer types	Subjects	Results	Major outcomes	References
ES2519040T3	Liver and lung cancers	Cell lines, animals, and humans	Inhibiting TGF-β1 signaling pathway; improving serum IFN-γ	Treating or preventing fibrosis and tumors	Liang et al. (2008)
US7326734B2	Bladder cancer	Cell lines	Inhibiting cell proliferation	Treating or preventing tumors	Zi et al. (2004)
US10307393B2	Pulmonary carcinoma, esophageal carcinoma, breast carcinoma, and mediastinum tumors	Cell lines and animals	Reducing the release of the inflammatory factors (IL-1β, IL-6, TNF-α, TGF-β, and IFN-γ)	Radiotherapy protection and treating tumors	Liang et al. (2016)
JP2005508312A	Colorectal, cervical, gastric, lung cancer, malignant glioma, ovarian, and pancreatic cancers	Cell lines, animals, and humans	Inhibiting MDR1 gene expression	Treating or preventing tumors	Gunther and Reinhold, (2005)
KR20060120101A	Prostate, colorectal, and liver cancers	Cell lines	Binding to EGR-1-like promoter sequences to modulate the expression of cancer related genes (p21 and p53)	Treating or preventing tumors	Wong et al. (2004)

EGR1, early growth response 1; IFN-γ, interferon-γ; IL-1β, interleukin-1β; IL-6; interleukin-6; MDR1, multi-drug resistance-1; TGF-β1, transforming growth factor-β1; TNF-α, tumor necrosis factor-α.

attenuation accompanied by a reduction in cell growth and enhancement of apoptotic cells (Yoshinaga et al., 2016). Additional studies demonstrated that naringin decreased proliferation and viability and also induced apoptosis of HeLa cervical adenocarcinoma cells (Ramanathan et al., 1992; Elansary et al., 2020) by blocking the NF-κB/cyclooxygenase-2 (COX-2)-caspase-1 pathway (Zeng et al., 2014).

Colon Cancer

Colorectal cancer (CRC) is one of the most frequent malignant tumors. The primary methods for CRC treatment are radiotherapy, chemotherapy, and surgery. However, because of the challenges rising from drug resistance, it is vital to explore additional effectual compounds targeting alternative signaling pathways (Van der Jeught et al., 2018). Studies show that naringin has antineoplastic activities and treatment with naringin can reduce proliferation, and viability, while also enhancing apoptosis in HT-29 colon adenocarcinoma (Elansary et al., 2020) and CT26 colorectal cancer cell lines (Zhou et al., 2018). Another study indicated that treatment of human colon tumor cell lines (HCT116 and SW620) with naringin suppressed the CRC cell viability and proliferation, and promoted apoptosis by suppressing the phosphoinositide-3 kinase (PI3K)/protein kinase-B (also known as Akt)/mammalian target of rapamycin (mTOR) signaling pathway (Chidambara Murthy et al., 2012; Cheng et al., 2020). Naringin treatment also induced apoptosis in Colo 205 and Colo 320 human colon cancer cells (Ugocsai et al., 2005). However, one study indicated that naringin had no inhibitory effect on cell growth of COLO 320HSR, COLO 205, and HT 29 colon cancer cells (Shen et al., 2004). In another study, naringin treatment interestingly abrogated cell growth and proliferation in human colon adenocarcinoma cells (HT29) in a concentration-dependent manner, and bio-transformed naringin showed significant antiproliferative activity (Ferreira et al., 2013). Also, treating HCT116 human colorectal carcinoma cells with naringin and synthesized binary and ternary platinum and vanadium metal complexes has shown moderate cytotoxic activities, with enhanced apoptosis and reduced cell viability and proliferation (Fazary et al., 2017). In another study, the antitumor effect of naringin was examined alone and in hybrids with SCMC-PA and SC-PA conjugates against the HCT116 colon cancer cells. Results showed that naringin, individually or in hybrids, reduced the proliferation and viability of colon cancer cell lines (Basta et al., 2020). Naringin also increased the inhibitory activity of trypsin and enhanced the antiplatelet aggregation activity and cytotoxic activity toward SNU-C4 human colon cancer cells (Kim et al., 1998).

In an *in vivo* study, the cytotoxic impacts of naringin on azoxymethane (AOM)/dextran sulfate sodium (DSS)-induced colorectal carcinogenesis and inflammation in C57BL/6 mice were investigated. Results indicated that naringin-treatment reduced tumor size and growth in C57BL/6 mice through inhibiting robust endoplasmic reticulum stress-induced autophagy in colorectal mucosal cells (Zhang et al., 2018b). Another study showed that naringin reduced tumor cell proliferation and promoted apoptosis in AOM-injected Sprague–Dawley rats (Vanamala et al., 2006). Glyoxalase-I (GLO-I), the ubiquitous detoxification system component, is involved in methylglyoxal (MG) conversion to D-lactate in the glycolytic pathway and has been shown to be regularly overexpressed in several cancer cells (Thornalley, 2008). One study showed that naringin reduced GLO-I activity and suppressed cell proliferation and viability in Caco-2 human epithelial colorectal adenocarcinoma cells (Yadav et al., 2016). However, naringin had no cytotoxic impact on Caco-2 and HT-29 human colon adenocarcinoma cells (Kuo, 1996).

Esophageal/Head and Neck Cancer

Esophageal carcinoma is a relatively rare cancer with a high death rate worldwide (Pennathur et al., 2013). DOX is an important chemotherapy agent that has been widely used as an antitumor agent (Hajjaji et al., 2012). Recent works demonstrated that the combination of herbal medicines and chemotherapy drugs have several advantages. One study showed that treatment with naringin alone or combined with DOX reduced cell viability

and proliferation in YM1 esophageal cancer cell line, and reduced tumor size in xenograft mice tumor model (Tajaldini et al., 2020). An *in vivo* study indicated that naringin treatment markedly reduced tumor size and growth, and also significantly decreased tumor burden in the hamster cheek pouch oral cancer model (Miller et al., 2008). A separate study demonstrated that *in vitro* treatment with naringin reduced cell viability in HEp2 human laryngeal carcinoma cells. Naringin also reduced lipid peroxidation and enhanced cytochrome P-450 (CYP) 1A1 expression in laryngeal cancer cell lines (Durgo et al., 2007).

Liver Cancer

Irrespective of the combined efforts of researchers and clinicians around the world, there has been a continuous increase in the incidence rate of hepatocellular carcinoma (HCC) over the last two decades (Alwhibi et al., 2017). In one study, HepG2 cell lines were used to examine the possible antiproliferative and cytotoxic effects of naringin and/or methotrexate (MTX). Naringin and/or MTX treatment exhibited cytotoxic and antiproliferative effects and induced apoptosis in HepG2 hepatocellular cancer cells via Bax activation and downregulation of Bcl-2 protein expression in a concentration-dependent way. Additionally, naringin potentiated the viability and cytotoxic effect of MTX in HepG2 cells (Elsawy et al., 2020). In another study, naringin substantially reduced the viability and proliferation of HepG2 cells (Syed et al., 2020). Naringin treatment also significantly suppressed proliferation, upregulated the expression of microRNA (miR)-19b, and promoted apoptosis in HepG2 cells. Additionally, it downregulated the Bcl-2 protein expression and upregulated the Bax protein expression to trigger apoptosis (Xie et al., 2017). Naringin blocked proliferation and enhanced early apoptosis of HepG2 cells via activation of Bid proteolysis mediated by caspase-8 and caspase-9. Therefore, the intrinsic and extrinsic pathways were linked in naringin-mediated apoptosis in HepG2 cells. Additionally, increased expression levels of pro-apoptotic Bak and Bax proteins and reduced levels of anti-apoptotic Bcl-xL protein were demonstrated, verifying the participation of the mitochondrial pathway (Banjerdpongchai et al., 2016b). Treatment with naringin reduced proliferation, viability, and growth and promoted apoptosis in HepG2 cells through extrinsic and intrinsic pathways (Banjerdpongchai et al., 2016a; Zhou et al., 2018). In another *in vitro* study, the cytotoxic effect of naringin in different hepatocellular carcinoma cells (Huh-7, HepG2, and HA22T) was investigated. Treatment with naringin inhibited MMP-9 transcription by suppressing NF-κB and activator protein-1 (AP-1) activity. It inhibited 12-O-tetradecanoylphorbol 13-acetate (TPA)-induced AP-1 activity by suppressing the phosphorylation of the c-Jun N-terminal kinase (JNK) and ERK signaling cascades, and it inhibited TPA-induced suppression of NF-κB nuclear translocation by IκB. This data demonstrates that naringin inhibits the metastasis and invasion of HCC cells by suppressing multiple signal transduction pathways (Yen et al., 2015). In another study, treatment with various concentrations of naringin hampered cell growth and cell proliferation of HepG2 cells and biotransformation with tannase significantly increased its antiproliferative activity (Ferreira et al., 2013).

Diethylnitrosamine (DEN) is one of the major environmental carcinogens and hepatotoxins (Sreepriya and Bali, 2005). In an *in vivo* experiment, the apoptotic and antiproliferative effect of naringin on DEN-induced liver carcinogenesis in male Wistar rat models was evaluated. Results showed that treatment with naringin significantly reduced the levels of proliferating cell nuclear antigen (PCNA) and the argyrophilic nucleolar organizer region (AgNOR)/nuclei. Naringin also suppressed proliferation and enhanced apoptosis in the liver cancer cells of rats (Thangavel and Vaiyapuri, 2013). In one study, cytotoxic actions of the synthesized binary and ternary platinum and vanadium metal complexes of naringin were evaluated using HepG2 cells. Results demonstrated that treatment with naringin and its metal complexes reduced cell viability and proliferation, and enhanced apoptosis in liver cancer cells. Additionally, metal complexes of naringin had a greater cytotoxic effect compared with naringin alone (Fazary et al., 2017). Moreover, naringin treatment of Hep1 and HA22T human liver cancer cells resulted in the suppression of cell viability and growth (Hsiao et al., 2007a). In another study, naringin treatment increased cytotoxic and antiplatelet aggregation activities and enhanced trypsin inhibition in HepG2 cells (Kim et al., 1998). However, at least one study demonstrated that naringin did not suppress cell growth in Hepa-1c1c7 mouse liver cancer cell line (Campbell et al., 2006).

Lung Cancer

Lung carcinoma is one of the main causes of cancer-related death worldwide (Jemal et al., 2002). The high death rate of lung cancer is possibly due to challenges associated with diagnosis and a high metastatic potential (Sangodkar et al., 2010). Consequently, it is essential to determine non-toxic alternative therapies to improve the responsiveness of lung cancers to chemotherapy. Treatment with naringin reduced viability and growth in the A549 human lung adenocarcinoma (Nie et al., 2012), and Lewis lung carcinoma (LLC) cell lines (Hsiao et al., 2007a). Naringin treatment also suppressed cell viability and proliferation, and promoted apoptosis in human small cell lung cancer cells (H69AR) by regulation of miR-126/Akt/mTOR/PI3K pathway via miR-126 overexpression and suppression of VCAM-1, p-Akt, PI3K, NF-κB, and p-mTOR pathways (Chen et al., 2018). In one study, the antimetastatic properties of naringin were evaluated, and results showed that treating A549 lung cancer cells with naringin resulted in a reduction of cell invasion, cellular motility, cell viability, and cell-matrix adhesion (Hsiao et al., 2007b). In a separate study, treatment with naringin increased the inhibitory activity of trypsin and enhanced its cytotoxic and anti-platelet aggregation activity against A549 cells (Kim et al., 1998).

Ruthenium is a great alternative to platinum due to its extensive variety of oxidation states and its capability to form complexes with bioactive ligands (Jayakumar et al., 2018). Naringin was used to fabricate a ruthenium complex with anticancer activity. Results showed that a naringin-ruthenium (II) complex reduced cell viability and proliferation, and promoted apoptosis in A549 human lung adenocarcinoma

(Garcia et al., 2019). Also, treatment with naringin alone and in combination with transition metal ions [Ag (I), Y (III), and Ru (III)] reduced cell growth and viability, and enhanced apoptosis in A549 human lung adenocarcinoma. Additionally, results showed that transition metal ions enhance the naringin activity when they are coordinated with each other (Atta et al., 2019). Another study showed that treatment of A549 cells with naringin promoted accumulation of GM3 through inhibition of NEU3 and resulted in the attenuation of ERK/EGFR signaling accompanied by a reduction in cell growth (Yoshinaga et al., 2016).

Neuroblastoma

Neuroblastoma is the most frequent extracranial solid tumor in children. There is an increasing interest in using plant-derived dietary compounds for the treatment of several solid tumors, including malignant neuroblastoma (Yamane and Kato, 2012). Naringin treatment reduced cell viability and promoted apoptosis in rotenone-treated SH-SY5Y human neuroblastoma cell line through suppression of P38 and JNK phosphorylation, as well as activation of caspase-3 and caspase-9 (Kim et al., 2009).

Ovarian Cancer

Ovarian cancer is a heterogeneous group of neoplasms, which is classified based upon type and degree of differentiation. It is one of the most deadly female reproductive system malignant tumors (Cho and Shih, 2009). The most efficient treatment for ovarian cancer is platinum-based chemotherapy and surgical cytoreduction (Jessmon et al., 2017). Resistance to platinum-based agents is one of the difficulties of ovarian cancer treatment using pharmacological agents (Choi et al., 2008). Therefore, investigating novel agents with low toxicity and high efficacy that can also reduce resistance to platinum-based agents, is very important. NF-κB is highly expressed in cisplatin-resistant ovarian cancer cell lines and has a crucial role in the drug resistance of ovarian cancer cells (Choi et al., 2008). One study demonstrated that the inhibitory effect of naringin was associated with inhibition of the NF-κB signaling pathway, and treatment with naringin significantly reduced P-glycoprotein (P-gp) and NF-κB expression in a concentration-dependent way in SKOV3/CDDP cisplatin-resistant human epithelial ovarian cancer cell line (Zhu et al., 2018). Another study also indicated that naringin downregulated COX-2 and NF-κB expression in a concentration-dependent way in SKOV3/CDDP cells (Zhu et al., 2017). In an *in vivo* study, treatment with naringin reduced ovarian tumor size and weight in tumor-bearing mice. Naringin also induced apoptosis by decreasing c-Myc, Bcl-2, surviving, cyclin D1, and Bcl-xL and increasing caspase-3 and caspase-7 levels in ovarian tumor cells. Such suppression may be related to the NF-κB signaling pathway regulation (Cai et al., 2018). Interestingly, at least one study indicated that naringin had no obvious inhibitory impact on cell growth and proliferation of OVCAR-3 human ovarian cancer cell line (Luo et al., 2008).

Prostate Cancer

Prostate cancer is the second most common cancer in men and the fourth most common cancer overall (Ferlay et al., 2015). The combined consumption of nutraceutical agents and chemotherapeutic drugs is a great approach for increasing the therapeutic anticancer impacts, as well as easing adverse effects of chemotherapy and drug resistance (de Oliveira Júnior et al., 2018). Atorvastatin, a 3-hydroxyl-3-methylglutaryl coenzyme A reductase inhibitor, has demonstrated antitumor activity in prostate cancer (Allott et al., 2017). One study examined the anticancer effect of naringin in combination with atorvastatin on PC-3 and LNCaP prostate cancer cell lines. Results demonstrated that combined treatment of atorvastatin and naringin synergistically induced apoptosis, reduced cell growth, suppressed invasion and migration, and potently inhibited AR, p-STAT3, survivin, p-Akt, and Bcl-2 expression levels. Additionally, treatment with naringin alone or combined with atorvastatin suppressed the tumor growth in tumor-bearing SCID mice, and the combined treatment demonstrated a greater inhibitory effect compared to either compound alone (Wu et al., 2019). In another study, PC3, DU145, and LNCaP cell lines were treated with different concentrations of naringin, paclitaxel, and their combinations. Treatment with naringin individually or combined with paclitaxel suppressed cell proliferation and cell survival in a concentration- and time-dependent way through induction of apoptosis and cycle arrest as well as decreased cell migration via inhibition of NF-κB, ERK, and Akt signaling and upregulation of phosphatase and tensin homologue (PTEN) expression. Taken together, naringin synergistically promoted the paclitaxel cytotoxic impact in PCa cell lines (Erdogan et al., 2018). In an *in vitro* study, treatment with naringin decreased cell viability and proliferation as well as enhanced apoptosis in DU145 prostate cancer cell line. Naringin also enhanced oxidative stress and had a genotoxic effect on prostate cancer cells (Lewinska et al., 2015).

Sarcoma

Even though adjuvant chemotherapy has led to the improved survival rates in osteosarcoma patients, the development of multidrug resistance has seriously influenced prognosis and limited the success of therapeutic attempts (Davis et al., 2018). Hence, novel and effective drugs for osteosarcoma treatment are required. One study showed that naringin treatment suppressed cell migration, invasion, and proliferation, and promoted apoptosis and cell cycle arrest in MG63 and U2OS human osteosarcoma cells through blockage of zinc finger E-box binding homeobox 1 (Zeb1), which plays a role in tumor metastasis. Additionally, naringin decreased tumor nodule formation and expression of MMP-2, Bcl-2, and cyclin D1 in the livers of mice bearing MG63 osteosarcoma cell line (Ming et al., 2018). However, another study indicated that naringin did not affect the MG-63 osteosarcoma cells' growth rate (Zhang et al., 2018a). *In vitro* treatment of JJ012 human chondrosarcoma cells with naringin reduced cell invasion and migration through the suppression of VCAM-1 expression by enhancing miR-126 expression (Tan et al., 2014).

In an *in vivo* study, naringin treatment demonstrated significant inhibition of tumor growth in male ddY mice bearing S180 sarcoma cancer cells (Kanno et al., 2005). *In vivo* treatment of naringin decreased TNF-α and IL-6 levels,

suppressed tumor growth, and increased the survival rate in Wistar rats bearing W256 carcinosarcoma cells (Camargo et al., 2012).

Skin Cancer

Melanoma is the leading cause of mortality from skin cancer (Siegel and Naishadham, 2013). Historically, melanoma has been refractive to chemotherapy which provides very low response rates and very few beneficial effects in overall survival. Therefore, multiple targeted therapeutic approaches have been examined (Ascierto et al., 2013). Treatment of A375 and A875 melanoma cell lines with naringin promoted cycle arrest and apoptosis, and also suppressed cell proliferation and growth in a concentration-dependent way. Naringin also suppressed c-Src and cancer cell metabolism through suppression of the c-Src/Akt signaling pathway, leading to a decrease in cell migration and invasion (Guo et al., 2016). Another study demonstrated that naringin treatment reduced the metastatic foci formation and increased the survival rate in mice bearing B16FlO melanoma cells (Menon et al., 1995). Another study also indicated that *in vitro* treatment of naringin reduced cell invasion in MO4 mouse melanoma cell line (Bracke et al., 1991). In an *in vitro* study, the anticancer effect of the naringin-derived copper (II) complex was investigated. The results showed that treatment of B16FlO melanoma with naringin or naringin-Cu (II) complex reduced cell proliferation and growth, increased cell death, and decreased diphenylpicrylhydrazyl radical (DPPH). Additionally, it demonstrated that the naringin-Cu (II) complex had higher anti-inflammatory, antioxidant, and anticancer activities in comparison to free naringin without decreasing cell viability (Pereira et al., 2007).

Stomach Cancer

Gastric cancer is the fourth most detrimental cancer-related death in the world (Torre et al., 2015). A large number of cancer cases and mortality could be avoided with early detection, using the phytomedicine intervention as an alternative to radiotherapy and chemotherapy. One study investigated the mechanism behind naringin-mediated autophagic cell death in AGS gastric cancer cell line. Naringin treatment promoted lysosomal membrane permeabilization through suppression of Akt/mTOR/PI3K signaling cascade, resulting in lysosomal cell death protein cathepsin D-mediated ERK1/2-p38 MAPKs activation through Bcl-xL decrease, and Bad, BH3, and ROS increase in autophagy-mediated cell death in AGS cell line. Additionally, rapamycin pre-treatment with naringin indicated a significant reduction in mTOR phosphorylation and enhancement in LC3B activation in AGS cells compared with naringin treatment alone (Raha et al., 2020). In another study, naringin treatment suppressed viability and growth in the AGS (human gastric epithelial 108 adenocarcinoma) cells (Hsiao et al., 2007a). Naringin treatment of AGS cells induced autophagy-mediated growth suppression through suppression of PI3K/Akt/mTOR cascade, and potentially via activation of MAPKs (Raha et al., 2015). Furthermore, treatment with naringin increased the inhibitory activity of trypsin and increased the cytotoxic activity and anti-platelet aggregation activity against SNU-1 human stomach cancer cells (Kim et al., 1998).

Thyroid Cancer

Thyroid cancer is the most frequent malignant tumor of the endocrine system (Kweon et al., 2014). The current approach for thyroid cancer treatment includes thyroid hormone inhibition therapy, surgical treatment, adjuvant radiotherapy, and isotope iodine-131 therapy. However, there are several disadvantages for these different types of treatment (Tang et al., 2017; Zivancevic-Simonovic et al., 2017). Hence, the development of low-toxic, effective, and new inhibitors is important in improving the survival rates of thyroid cancer patients. One study showed that *in vitro* treatment of SW1736 and TPC-1 thyroid cancer cells with naringin reduced cell proliferation and promoted apoptosis via suppression of PI3K/Akt pathway (Zhou et al., 2019).

NANOSTRUCTERED FORMULATIONS OF NARINGIN IN COMBATING MALIGNANCIES

In the past two decades, nanotechnology-based delivery systems have gained interest as a method to overcome the challenges associated with solubility, bioavailability, distribution, low therapeutic index, toxicity and targeting of conventional chemotherapeutic drugs as well as anticancer natural compounds (Feng and Mumper, 2013; Davatgaran-Taghipour et al., 2017; Kashyap et al., 2021; Lagoa et al., 2020). Naringin is one of the most fascinating phytopharmaceuticals that has been broadly examined for different biological activities. Yet, its suboptimal bioavailability, limited permeability, and low water solubility have restricted its use. A useful approach to overcome these difficulties is encapsulation of the agent into different nano-sized delivery vehicles (Mohamed et al., 2018).

Gold-naringin nanoclusters (GNNC) showed cytotoxic effects against A549 lung cancer cells and reduced the cell viability with increased concentrations of GNNC. At the same time, the WI-38 levels in lung normal cells remained elevated, even after treatment with high doses of GNNC (Sangubotla et al., 2020) (**Table 5**).

With advances in nanotechnology and the extensive use of graphene, it has become essential to evaluate the possible disadvantages of graphene. Thus, most of the current studies are focused on different modified graphene. Naringin-reduced graphene oxide nanosheets (rGO@Nar), promotes cytotoxicity in the colon cancer cells (HT-29) through increased apoptosis and reduced cell viability and proliferation. The rGO@Nar plus naringin is more efficient toward colon cancer in comparison to rGO@Nar or naringin alone. Additionally, it has been shown that rGO@Nar together with naringin and rGO@Nar can efficiently eliminate tumor cells without affecting normal cells (Han et al., 2020). rGO@Nar may be a promising agent for assessment in the *in vivo* models of colon cancers.

After bone tumor resection, the large deficits are normally reconstructed with titanium (Ti)-based metallic endoprosthesis. When applied in osteosarcoma resection, Ti implant-related infection and tumor recurrence were determined as two crucial factors for failure of implantation. Ti-naringin-3-carboxyphenylboronic acid (PBA)-zinc oxide (ZnO)

nanoparticles reduce infection and tumor recurrence and induce Saos-2 osteosarcoma cells apoptosis through activation of ROS/ERK signaling. *In vitro* cellular experiments showed that these nanoparticles could promote the proliferation and growth of osteoblasts (Yang et al., 2020). Nevertheless, *in vivo* experiments are required for understanding the anticancer properties of Ti-Naringin-PBA-ZnO nanoparticles in osteosarcoma.

Lipid-based nanoparticles are another delivery system that has particular benefits due to their unique properties, such as biodegradation, biological compatibility, multiple routes of administration, and convenient and easy industrial scale-up process (Rout et al., 2018). Nanostructured lipid carriers containing naringin and coix seed oil (NCNLCs) were successfully fabricated, and their cytotoxic activity was evaluated. NCNLCs reduced proliferation and viability and promoted apoptosis in HepG2 liver cancer cells and had a greater cytotoxic effect compared with free naringin, NONLCs, and NDNLCs. Moreover, the *in vivo* synergistic anticancer efficacy was evaluated in NCNLCs in xenograft tumor mice models and results showed that NCNLCs upregulated the IL-10 and IL-6 expression in the serum of tumor-bearing mice and inhibited tumor growth (Zhu et al., 2020).

The development of multidrug resistance (MDR) has restricted the efficacy of chemotherapeutic agents. Co-delivery of natural flavonoids with anticancer drugs in polymeric micelles is a potentially significant approach for overwhelming MDR and enhancing their anticancer efficacy. Paclitaxel co-encapsulation with naringin in mixed polymeric micelles increased *in vitro* cytotoxicity toward MCF-7 breast cancer cell line. Paclitaxel- and naringin-loaded mixed (PTX-NRG-MIC) micelles synergistically reduced the growth and viability of MCF-7 cell line and increased their intracellular uptake. Additionally, PTX-NRG-MIC micelles are more effective toward breast cancer when compared to naringin or paclitaxel (Jabri et al., 2019). Yet, *in vivo* experiments are required to confirm the active targeted delivery of PTX-NRG-MIC micelles.

Naringin polymeric micelles based on pluronic F68 were fabricated and their *in vitro* cytotoxicity was assessed against different cancer cell lines. Naringin-PF68 micelles reduced the viability and proliferation of Caco-2, HepG2, and MCF-7 cells. Furthermore, Swiss albino mice were used to evaluate the anticancer activity of naringin-PF68 micelles compared to the free drug. Results showed that PF68 micelles of naringin reduced tumor size and inhibited tumor growth in tumor-bearing mice. Naringin-PF68 micelles had a greater cytotoxic effect when compared with free naringin (Mohamed et al., 2018).

In another study, poly D,L-lactide-co-glycolic acid copolymer (PLGA) nanoparticles co-encapsulating celecoxib and naringin were synthesized and induced apoptosis and inhibited proliferation in the A549 cells in a concentration-dependent manner. They also showed greater cytotoxic activity on A549 cells in comparison to the combination of free drugs, while exhibiting significant safety on healthy lung tissues (Said-Elbahr et al., 2016).

In another study, gold nanoparticles (AuNPs) were synthesized using naringin as a reducing and stabilizing agent to create nano-theranostic agents. Naringin-conjugated gold nanoparticles (N-AuNPs) were evaluated with cytotoxicity and hemolysis assays, which showed their biocompatibility with MDA-MB-231 cell lines and normal red blood cells, while also demonstrating their potential to induce cell death in T47D, PC-3, and MCF-7 cell lines. *In vivo* studies must be conducted to confirm the active targeted delivery of N-AuNPs in cancer (Singh et al., 2016).

Taken together, results show that the nano-drug delivery systems have the capability to overwhelm the pharmacokinetic restrictions of naringin, highlighting its impacts on cancer therapy. Further research is required for designing surface-modified nano-formulations of naringin to achieve adjusted drug delivery systems.

PHARMACOKINETICS AND TOXICITY OF NARINGIN

After a single oral administration (42 mg/kg) of naringin in aged rats, minor differences were shown in the area under the plasma concentration-time curve (AUC) of total naringenin and naringin gained in the gastrointestinal tract, stomach, liver, muscle, kidney, and brain between male and female aged rats. It must be mentioned that the AUC of naringin in the trachea (3,140%) and lung (1,250%) of female rats in comparison to male rats were considerably higher, indicating that naringin may exhibit gender differences in the treatment of respiratory diseases in elderly individuals (Zeng et al., 2019). In multiple-dose studies, no considerable accumulation of naringenin was detected in rats, dogs, and humans. In single-dose studies, various pharmacokinetic parameters in females, including the elimination half-life ($t_{1/2}$) (naringenin, rats, oral, 42 mg/kg), AUC (naringin, humans, 160 mg (high-fat diet); naringin, rats, oral, 21 mg/kg; and naringenin, humans, 40 mg), peak plasma concentration (C_{max}) (naringenin, humans, 40 mg), and time to reach C_{max} (T_{max}) (naringenin, rats, oral, 168 mg/kg) were considerably higher than those of males, while a small number of pharmacokinetic parameters in females, including AUC (naringin, humans, 40 mg) and C_{max} (naringenin, rats, i.v., 42 mg/kg) were significantly lower than those of males. In multiple-dose studies, considerably greater female parameters were only detected in rats (naringenin, accumulation index, 1.79 ± 0.457 and naringin, T_{max}, 2.70 ± 1.48 h) (Bai et al., 2020). The plasma drug concentration-time curves indicate that the oridonin AUC 0–24 h value was nearly three times larger compared to naringin, while the naringin dose was approximately four times larger compared to oridonin, indicating that the oridonin absorption in rats is higher than naringin (Jin et al., 2015). Naringin administration (15 mg/kg) suppressed the P-gp function and considerably enhanced the candesartan intestinal absorption by 3.2 times (Surampalli et al., 2015). After administration of 600 and 1,000 mg/kg naringin through the duodenal cannula, the naringin average C_{max} in portal plasma was measured at 18.8 ± 3.8 min, while the naringin absorption ratios in lymph fluid and portal plasma were nearly 4.1 and 95.9, respectively. This suggests that naringin may be

absorbed through portal blood and concentrations may be reduced via bile excretion (Tsai and Tsai, 2012). In membrane toxicity studies, naringin administration (15 mg/kg, w/w) did not cause any toxicity; but, it insignificantly increased the protein release from the intestinal membrane (Surampalli et al., 2015). The sub-chronic and acute toxicology of naringin was indicated to be almost non-toxic for Sprague-Dawley rats, and the naringin no-observed-adverse-effect-level (NOAEL) in rats was larger than 1,250 mg per kg per day after oral administration for 13 weeks (Li et al., 2013b). No intestinal membrane impairment was noted in the naringin presence through measurement of the alkaline phosphatase and protein release (Surampalli et al., 2015).

CONCLUSIONS AND FUTURE DIRECTIONS

Natural products have played an important part in the treatment of human diseases and most notably, in cancer therapies. Naringin, a flavone glycoside, is promising for the treatment of many diseases due to its low cost, broad availability, long history of use, and variety of pharmacological actions, with the predominant evidence currently focusing on its anticancer impacts. Naringin alone, or combined with other drugs may be useful for treating cancers. Emerging studies showed that naringin-metal complexes have greater anticancer activities compared to free naringin. Naringin can impact several cancer types, including glioblastoma, hepatocellular carcinoma, lung adenocarcinoma, breast cancer, prostate cancer, melanoma, leukemia, colon cancer, gastric cancer, oral cancer, brain cancer, bladder cancer, and ovarian cancer. It has been demonstrated that naringin employs multiple mechanisms to hamper cancer initiation, promotion, and progression via modulation of several dysregulated signaling cascades implicated in inflammation, proliferation, cell survival, apoptosis, autophagy, angiogenesis, invasion, and metastasis (**Figure 3**). In particular, the cancer-inhibitory effects of naringin have been linked to the regulation of various signaling pathways, such as Nrf2, NF-κB, PI3K/Akt/mTOR, JNK, ERK, and p38 MAPK. Naringin intervenes with the function of various signaling molecules, such as caspases, Bax, TNF-α, Bcl-2, VEGF, and ILs. Various patents have shown that naringin can specifically affect desired targets (**Table 6**), making it possible to use naringin and its formulations for further investigations for targeted therapies.

The biggest obstacle concerning naringin as a novel therapeutic agent is that current naringin anticancer evidence is focused on *in vitro* models of cancers, and there are few detailed *in vivo* studies. Another challenge is related to bioavailability of naringin and selection of a dose range for clinical/therapeutic application based on available preclinical studies. Nevertheless, according to completed and undergoing clinical studies on naringin, bioavailability and effective concentration may not be barrier for exploring its therapeutic benefits. Moreover, since all studies presented in this review utilized pure compounds obtained from various sources, providing a full taxonomic validation of the material under investigation is one of the challenges. The possible restrictions with naringin pharmacokinetics highlight the necessity for the development of novel delivery systems. In particular, further experimental and technological approaches are needed for designing surface-modified naringin-nanostructures to attain targeted drug delivery systems toward cancer. The result of research findings as evaluated here might offer substantial support for further development of naringin as a multi-targeted agent for the prevention and intervention of human malignancies.

DATA AVAILABILITY STATEMENT

The original contributions presented in the study are included in the article/Supplementary Material, further inquiries can be directed to the corresponding authors.

AUTHOR CONTRIBUTIONS

MF conceived and designed the study. MG-M and MF collected and reviewed the literature as well as extracted and analyzed the data. MGM prepared the first draft of the manuscript and created the figures. MG-M and MF collected additional literature, refined mechanistic figures, edited the manuscript, and suggested improvements. GJ edited the manuscript. AB coordinated this project as well as reviewed and edited the manuscript. All authors have read and approved the final manuscript.

REFERENCES

Abdulla, M., and Gruber, P. (2000). Role of diet modification in cancer prevention. *Biofactors* 12, 45–51. doi:10.1002/biof.5520120108

Abotaleb, M., Samuel, S. M., Varghese, E., Varghese, S., Kubatka, P., Liskova, A., et al. (2019). Flavonoids in cancer and apoptosis. *Cancers (Basel).* 11, 28. doi:10.3390/cancers11010028

Alam, M. A., Subhan, N., Rahman, M. M., Uddin, S. J., Reza, H. M., and Sarker, S. D. (2014). Effect of citrus flavonoids, naringin and naringenin, on metabolic syndrome and their mechanisms of action. *Adv. Nutr.* 5, 404–417. doi:10.3945/an.113.005603

Allott, E. H., Howard, L. E., Vidal, A. C., Moreira, D. M., Castro-Santamaria, R., Andriole, G. L., et al. (2017). Statin use, serum lipids, and prostate inflammation in men with a negative prostate biopsy: results from the REDUCE trial. *Cancer Prev. Res.* 10, 319–326. doi:10.1158/1940-6207.capr-17-0019

Alwhibi, M. S., Khalil, M. I. M., Ibrahim, M. M., El-Gaaly, G. A., and Sultan, A. S. (2017). Potential antitumor activity and apoptosis induction of Glossostemon bruguieri root extract against hepatocellular carcinoma cells. *Evid Based Complement Alternat Med.* 2017, 7218562. doi:10.1155/2017/7218562

Amin, A. R. M. R., Kucuk, O., Khuri, F. R., and Shin, D. M. (2009). Perspectives for cancer prevention with natural compounds. *Jco*, 27, 2712. doi:10.1200/JCO.2008.20.6235

Aroui, S., Aouey, B., Chtourou, Y., Meunier, A.-C., Fetoui, H., and Kenani, A. (2016a). Naringin suppresses cell metastasis and the expression of matrix metalloproteinases (MMP-2 and MMP-9) via the inhibition of ERK-P38-JNK signaling pathway in human glioblastoma. *Chem. Biol. Interact.* 244, 195. doi:10.1016/j.cbi.2015.12.011

Aroui, S., Fetoui, H., and Kenani, A. (2020). Natural dietary compound naringin inhibits glioblastoma cancer neoangiogenesis. *BMC Pharmacol. Toxicol.* 21, 46. doi:10.1186/s40360-020-00426-1

Aroui, S., Najlaoui, F., Chtourou, Y., Meunier, A.-C., Laajimi, A., Kenani, A., et al. (2016b). Naringin inhibits the invasion and migration of human glioblastoma cell via downregulation of MMP-2 and MMP-9 expression and inactivation of p38 signaling pathway. *Tumor Biol.* 37, 3831. doi:10.1007/s13277-015-4230-4

Ascierto, P. A., Grimaldi, A. M., Acquavella, N., Borgognoni, L., Calabrò, L., Cascinelli, N., et al. (2013). Future perspectives in melanoma research. *J. Transl. Med.* 14, 323. doi:10.1186/s12967-016-1070-y

Atta, E. M., Hegab, K. H., Abdelgawad, A. A. M., and Youssef, A. A. (2019). Synthesis, characterization and cytotoxic activity of naturally isolated naringin-metal complexes. *Saudi Pharm. J.* 27, 584. doi:10.1016/j.jsps.2019.02.006

Ávila-Gálvez, M. Á., Giménez-Bastida, J. A., Espín, J. C., and González-Sarrías, A. (2020). Dietary phenolics against breast cancer. A critical evidence-based review and future perspectives. *Ijms* 21, 5718. doi:10.3390/ijms21165718

Bai, Y., Peng, W., Yang, C., Zou, W., Liu, M., Wu, H., et al. (2020). Pharmacokinetics and metabolism of naringin and active metabolite naringenin in rats, dogs, humans, and the differences between species. *Front. Pharmacol.* 11, 364. doi:10.3389/fphar.2020.00364

Banjerdpongchai, R., Wudtiwai, B., and Khawon, P. (2016b). Induction of human hepatocellular carcinoma HepG2 cell apoptosis by naringin. *Asian Pac. J. Cancer Prev.* 17, 3289–3294. doi:10.14456/apjcp.2016.90/APJCP.2016.17.7.3289

Banjerdpongchai, R., Wudtiwai, B., Khaw-on, P., Rachakhom, W., Duangnil, N., and Kongtawelert, P. (2016a). Hesperidin from Citrus seed induces human hepatocellular carcinoma HepG2 cell apoptosis via both mitochondrial and death receptor pathways. *Tumor Biol.* 37, 227. doi:10.1007/s13277-015-3774-7

Basta, A. H., Lotfy, V. F., Ghaly, N. S., Nabil, M., and Mohamed, K. M. (2020). Bioactivity evaluation of amino acid-conjugates with protein versus cellulose based conjugates and extracted flavonoids. *J. Drug Deliv. Sci. Tech.* 60, 101924. doi:10.1016/j.jddst.2020.101924

Basu, P., and Maier, C. (2018). Phytoestrogens and breast cancer: in vitro anticancer activities of isoflavones, lignans, coumestans, stilbenes and their analogs and derivatives. *Biomed. Pharmacother.* 107, 1648. doi:10.1016/j.biopha.2018.08.100

Benkovic, V., Horvat Knezevic, A., Brozovic, G., Knezevic, F., Đikic, D., Bevanda, M., et al. (2007). Enhanced antitumor activity of irinotecan combined with propolis and its polyphenolic compounds on Ehrlich ascites tumor in mice. *Biomed. Pharmacother.* 61, 292. doi:10.1016/j.biopha.2007.02.012

Bharti, S., Rani, N., Krishnamurthy, B., and Arya, D. (2014). Preclinical evidence for the pharmacological actions of naringin: a review. *Planta Med.* 80, 437. doi:10.1055/s-0034-1368351

Bishayee, A., and Sethi, G. (2016). Bioactive natural products in cancer prevention and therapy: progress and promise. *Semin. Cancer Biol.* 40-41, 1. doi:10.1016/j.semcancer.2016.08.006

Bracke, M., Vyncke, B., Opdenakker, G., Foidart, J.-M., De Pestel, G., and Mareel, M. (1991). Effect of catechins and citrus flavonoids on invasionin vitro. *Clin. Exp. Metast* 9, 13. doi:10.1007/BF01831706

Cadoo, K. A., Fornier, M. N., and Morris, P. G. (2013). Biological subtypes of breast cancer: current concepts and implications for recurrence patterns. *Q. J. Nucl. Med. Mol. Imaging* 57, 312–321.

Cai, L., Wu, H., Tu, C., Wen, X., and Zhou, B. (2018). Naringin inhibits ovarian tumor growth by promoting apoptosis: an *in vivo* study. *Oncol. Lett.* 16, 59–64. doi:10.3892/ol.2018.8611

Camargo, C. A., Gomes-Marcondes, M. C., Wutzki, N. C., and Aoyama, H. (2012). Naringin inhibits tumor growth and reduces interleukin-6 and tumor necrosis factor α levels in rats with Walker 256 carcinosarcoma. *Anticancer Res.* 32, 129.

Campbell, J. K., King, J. L., Harmston, M., Lila, M. A., and Erdman, J. W. (2006). Synergistic effects of flavonoids on cell proliferation in Hepa-1c1c7 and LNCaP cancer cell lines. *J. Food Sci.* 71, S358. doi:10.1111/j.1750-3841.2006.00013.x

Chen, M., Peng, W., Hu, S., and Deng, J. (2018). miR-126/VCAM-1 regulation by naringin suppresses cell growth of human non-small cell lung cancer. *Oncol. Lett.* 16, 4754–4760. doi:10.3892/ol.2018.9204

Chen, R., Qi, Q.-L., Wang, M.-T., and Li, Q.-Y. (2016). Therapeutic potential of naringin: an overview. *Pharm. Biol.* 54, 3203–3210. doi:10.1080/13880209.2016.1216131

Chen, S., Lin, R., Hu, X., Shi, Q., and Chen, H. (2020). Naringin induces endoplasmic reticulum stress-mediated apoptosis, inhibits β-catenin pathway and arrests cell cycle in cervical cancer cells. *Acta Biochim. Pol.* 67, 181–188. doi:10.18388/abp.2020_5182

Chen, Y. C., Shen, S. C., and Lin, H. Y. (2003). Rutinoside at C7 attenuates the apoptosis-inducing activity of flavonoids. *Biochem. Pharmacol.* 66, 1139. doi:10.1016/S0006-2952(03)00455-6

Cheng, H., Jiang, X., Zhang, Q., Ma, J., Cheng, R., Yong, H., et al. (2020). Naringin inhibits colorectal cancer cell growth by repressing the PI3K/AKT/mTOR signaling pathway. *Exp. Ther. Med.* 19, 3798–3804. doi:10.3892/etm.2020.8649

Chidambara Murthy, K. N., Kim, J., Vikram, A., and Patil, B. S. (2012). Differential inhibition of human colon cancer cells by structurally similar flavonoids of citrus. *Food Chem.* 132, 27. doi:10.1016/j.foodchem.2011.10.014

Cho, K. R., and Shih, I.-M. (2009). Ovarian cancer. *Annu. Rev. Pathol. Mech. Dis.* 4, 287–313. doi:10.1146/annurev.pathol.4.110807.092246

Choi, J., Lee, D.-H., Jang, H., Park, S.-Y., and Seol, J.-W. (2020). Naringenin exerts anticancer effects by inducing tumor cell death and inhibiting angiogenesis in malignant melanoma. *Int. J. Med. Sci.* 17, 3049. doi:10.7150/ijms.44804

Choi, M., Fuller, C. D., Thomas, C. R., Jr., and Wang, S. J. (2008). Conditional survival in ovarian cancer: results from the SEER dataset 1988–2001. *Gynecol. Oncol.* 109, 203–209. doi:10.1016/j.ygyno.2008.01.033

Cragg, G. M., and Pezzuto, J. M. (2016). Natural products as a vital source for the discovery of cancer chemotherapeutic and chemopreventive agents. *Med. Princ. Pract.* 25, 41–59. doi:10.1159/000443404

Dai, K., Yan, S., Yan, W., Chen, D., and Xu, Z. (2009). Effects of naringin on the proliferation and osteogenic differentiation of human bone mesenchymal stem cell. *Eur. J. Pharmacol.* 607, 1–5. doi:10.1016/j.ejphar.2009.01.035

Dai, T.-y., Wang, B., Lin, S.-y., Jiang, J.-p., Wu, L.-q., and Qian, W.-b. (2017). Pure total flavonoids from Citrus paradisi Macfad induce leukemia cell apoptosis *in vitro*. *Chin. J. Integr. Med.* 23, 370. doi:10.1007/s11655-016-2593-z

Davatgaran-Taghipour, Y., Masoomzadeh, S., Farzaei, M. H., Bahramsoltani, R., Karimi-Soureh, Z., Rahimi, R., et al. (2017). Polyphenol nanoformulations for cancer therapy: experimental evidence and clinical perspective. *Ijn*, 12, 2689. doi:10.2147/IJN.S131973

Davis, J. C., Daw, N. C., Navid, F., Billups, C. A., Wu, J., Bahrami, A., et al. (2018). 18F-FDG uptake during early adjuvant chemotherapy predicts histologic response in pediatric and young adult patients with osteosarcoma. *J. Nucl. Med.* 59, 25–30. doi:10.2967/jnumed.117.190595

de Lourdes Mata Bilbao, M., Andreslacueva, C., Jáuregui, O., and Lamuelaraventos, R. (2007). Determination of flavonoids in a Citrus fruit extract by LC-DAD and LC-MS. *Food Chem.* 101, 1742. doi:10.1016/j.foodchem.2006.01.032

de Oliveira Júnior, R. G., Christiane Adrielly, A. F., da Silva Almeida, J. R. G., Grougnet, R., Thiéry, V., and Picot, L. (2018). Sensitization of tumor cells to chemotherapy by natural products: a systematic review of preclinical data and molecular mechanisms. *Fitoterapia* 129, 383–400. doi:10.1016/j.fitote.2018.02.025

Dhuique-Mayer, C., Caris-Veyrat, C., Ollitrault, P., Curk, F., and Amiot, M.-J. (2005). Varietal and interspecific influence on micronutrient contents in citrus from the mediterranean area. *J. Agric. Food Chem.* 53, 2140. doi:10.1021/jf0402983

Durgo, K., Vuković, L., Rusak, G., Osmak, M., and Čolić, J. F. (2007). Effect of flavonoids on glutathione level, lipid peroxidation and cytochrome P450 CYP1A1 expression in human laryngeal carcinoma cell lines. *Food Technol. Biotechnol.* 45, 69–79.

EFSA (2011). Scientific Opinion on the safety and efficacy of naringin when used as a sensory additive for all animal species. *EFSA J.* 9, 2444. doi:10.2903/j.efsa.2011.2444

Elansary, H. O., Szopa, A., Kubica, P., Ekiert, H., Klimek-Szczykutowicz, M., El-Ansary, D. O., et al. (2020). Polyphenol profile and antimicrobial and cytotoxic activities of natural Mentha x piperita and Mentha longifolia populations in Northern Saudi Arabia. *Processes* 8, 479. doi:10.3390/PR8040479

Elsawy, H., Algefare, A. I., Alfwuaires, M., Khalil, M., Elmenshawy, O. M., Sedky, A., et al. (2020). Naringin alleviates methotrexate-induced liver injury in male albino rats and enhances its antitumor efficacy in HepG2 cells. *Biosci. Rep.* 40, BSR20193686. doi:10.1042/BSR20193686

Erdogan, S., Doganlar, O., Doganlar, Z. B., and Turkekul, K. (2018). Naringin sensitizes human prostate cancer cells to paclitaxel therapy. *Prostate Int.* 6, 126. doi:10.1016/j.prnil.2017.11.001

Fazary, A. E., Ju, Y.-H., Al-Shihri, A. S., Bani-Fwaz, M. Z., Alfaifi, M. Y., Alshehri, M. A., et al. (2017). Platinum and vanadate bioactive complexes of glycoside naringin and phenolates. *Open Chem.* 15, 189. doi:10.1515/chem-2017-0022

Feng, L., and Mumper, R. J. (2013). A critical review of lipid-based nanoparticles for taxane delivery. *Cancer Lett.* 334, 157–175. doi:10.1016/j.canlet.2012.07.006

Ferlay, J., Soerjomataram, I., Dikshit, R., Eser, S., Mathers, C., Rebelo, M., et al. (2015). Cancer incidence and mortality worldwide: sources, methods and major patterns in GLOBOCAN 2012. *Int. J. Cancer* 136, E359–E386. doi:10.1002/ijc.29210

Ferreira, L. R., Macedo, J. A., Ribeiro, M. L., and Macedo, G. A. (2013). Improving the chemopreventive potential of orange juice by enzymatic biotransformation. *Food Res. Int.* 51, 526. doi:10.1016/j.foodres.2013.01.018

Fidler, M. M., Gupta, S., Soerjomataram, I., Ferlay, J., Steliarova-Foucher, E., and Bray, F. (2017). Cancer incidence and mortality among young adults aged 20–39 years worldwide in 2012: a population-based study. *Lancet Oncol.* 18, 1579–1589. doi:10.1016/s1470-2045(17)30677-0

Garcia, J. P., Lakshmi, B. A., and Kim, S. (2019). Potential anticancer applications of the novel naringin-based ruthenium (II) complex. *3 Biotech.* 9, 181. doi:10.1007/s13205-019-1718-4

Goldman, J. M., and Melo, J. V. (2003). Chronic myeloid leukemia—advances in biology and new approaches to treatment. *N. Engl. J. Med.* 349, 1451–1464. doi:10.1056/nejmra020777

Gullett, N. P., Ruhul Amin, A. R. M., Bayraktar, S., Pezzuto, J. M., Shin, D. M., Khuri, F. R., et al. (2010). Cancer prevention with natural compounds. *Semin. Oncol.*, 37, 258. doi:10.1053/j.seminoncol.2010.06.014

Gunther, H., and Reinhold, K. (2005). Means and methods for improved cancer treatment based on MDR1. Japan Patent NO JP2005508312A. Japan Patent Office.

Guo, B., Zhang, Y., Hui, Q., Wang, H., and Tao, K. (2016). Naringin suppresses the metabolism of A375 cells by inhibiting the phosphorylation of c-Src. *Tumor Biol.* 37, 3841. doi:10.1007/s13277-015-4235-z

Habauzit, V., Sacco, S. M., Gil-Izquierdo, A., Trzeciakiewicz, A., Morand, C., Barron, D., et al. (2011). Differential effects of two citrus flavanones on bone quality in senescent male rats in relation to their bioavailability and metabolism. *Bone* 49, 1108–1116. doi:10.1016/j.bone.2011.07.030

Hajjaji, N., Couet, C., Besson, P., and Bougnoux, P. (2012). DHA effect on chemotherapy-induced body weight loss: an exploratory study in a rodent model of mammary tumors. *Nutr. Cancer* 64, 1000–1007. doi:10.1080/01635581.2012.714832

Han, L., Tan, J., Li, J., Meng, T., Wang, Y., and Wang, S. (2020). Structurally improved reduced graphene oxide nanocluster structured assembly with Naringin for the effective photothermal therapy of colon tumour patients and nursing care management. *Mol. Phys.* 118, e1736674. doi:10.1080/00268976.2020.1736674

Hsiao, Y.-C., Hsieh, Y.-S., Kuo, W.-H., Chiou, H.-L., Yang, S.-F., Chiang, W.-L., et al. (2007a). The tumor-growth inhibitory activity of flavanone and 2′-OH flavanone *in vitro* and *in vivo* through induction of cell cycle arrest and suppression of cyclins and CDKs. *J. Biomed. Sci.* 14, 107. doi:10.1007/s11373-006-9117-3

Hsiao, Y.-C., Kuo, W.-H., Chen, P.-N., Chang, H.-R., Lin, T.-H., Yang, W.-E., et al. (2007b). Flavanone and 2′-OH flavanone inhibit metastasis of lung cancer cells via down-regulation of proteinases activities and MAPK pathway. *Chem. Biol. Interact.*, 167, 193. doi:10.1016/j.cbi.2007.02.012

Jabri, T., Imran, M., Aziz, A., Rao, K., Kawish, M., Irfan, M., et al. (2019). Design and synthesis of mixed micellar system for enhanced anticancer efficacy of Paclitaxel through its co-delivery with Naringin. *Drug Development Ind. Pharm.* 45, 703. doi:10.1080/03639045.2018.1550091

Jäger, A., and Saaby, L. (2011). Flavonoids and the CNS. *Molecules* 16, 1471–1485. doi:10.3390/molecules16021471

Jayakumar, T., Hsu, C.-Y., Khamrang, T., Hsia, C.-H., Hsia, C.-W., Manubolu, M., et al. (2018). Possible molecular targets of novel ruthenium complexes in antiplatelet therapy. *Ijms* 19, 1818. doi:10.3390/ijms19061818

Jemal, A., Thomas, A., Murray, T., and Thun, M. (2002). Cancer statistics, 2002. *CA: A Cancer J. Clinicians* 52, 23–47. doi:10.3322/canjclin.52.1.23

Jessmon, P., Boulanger, T., Zhou, W., and Patwardhan, P. (2017). Epidemiology and treatment patterns of epithelial ovarian cancer. *Expert Rev. Anticancer Ther.* 17, 427–437. doi:10.1080/14737140.2017.1299575

Jin, C.-Y., Park, C., Lee, J.-H., Chung, K. T., Kwon, T. K., Kim, G.-Y., et al. (2009). Naringenin-induced apoptosis is attenuated by Bcl-2 but restored by the small molecule Bcl-2 inhibitor, HA 14-1, in human leukemia U937 cells. *Toxicol. Vitro* 23, 259. doi:10.1016/j.tiv.2008.12.005

Jin, Y., Tian, T., Ma, Y., Xu, H., and Du, Y. (2015). Simultaneous determination of ginsenoside Rb1, naringin, ginsenoside Rb2 and oridonin in rat plasma by LC-MS/MS and its application to a pharmacokinetic study after oral administration of Weifuchun tablet. *J. Chromatogr. B* 1000, 112–119. doi:10.1016/j.jchromb.2015.06.027

Joshi, R., Kulkarni, Y. A., and Wairkar, S. (2018). Pharmacokinetic, pharmacodynamic and formulations aspects of Naringenin: an update. *Life Sci.* 215, 43. doi:10.1016/j.lfs.2018.10.066

Kabała-Dzik, A., Rzepecka-Stojko, A., Kubina, R., Iriti, M., Wojtyczka, R. D., Buszman, E., et al. (2018). Flavonoids, bioactive components of propolis, exhibit cytotoxic activity and induce cell cycle arrest and apoptosis in human breast cancer cells MDA-MB-231 and MCF-7-A comparative study. *Cell. Mol. Biol.* 64, 1–10. doi:10.14715/cmb/2018.64.8.1

Kaiserová, H., Šimůnek, T., Van Der Vijgh, W. J. F., Bast, A., and Kvasničková, E. (2007). Flavonoids as protectors against doxorubicin cardiotoxicity: role of iron chelation, antioxidant activity and inhibition of carbonyl reductase. *Biochim. Biophys. Acta (BBA)—Mol. Basis Disease* 1772, 1065–1074. doi:10.1016/j.bbadis.2007.05.002

Kanno, S.-i., Tomizawa, A., Hiura, T., Osanai, Y., Shouji, A., Ujibe, M., et al. (2005). Inhibitory effects of naringenin on tumor growth in human cancer cell lines and sarcoma S-180-implanted mice. *Biol. Pharm. Bull.* 28, 527. doi:10.1248/bpb.28.527

Karami, K., Mehri Lighvan, Z., Farrokhpour, H., Dehdashti Jahromi, M., and Momtazi-borojeni, A. A. (2018). Synthesis and spectroscopic characterization study of new palladium complexes containing bioactive O,O-chelated ligands: evaluation of the DNA/protein BSA interaction, *in vitro* antitumoural activity and molecular docking. *J. Biomol. Struct. Dyn.* 36, 3324. doi:10.1080/07391102.2017.1391125

Kashyap, D., Tuli, H. S., Yerer, M. B., Sharma, A., Sak, K., Srivastava, S., et al. (2021). Natural product-based nanoformulations for cancer therapy: opportunities and challenges. *Semin. Cancer Biol.* 69, 5–23. doi:10.1016/j.semcancer.2019.08.014

Kawaii, S., Tomono, Y., Katase, E., Ogawa, K., and Yano, M. (1999). HL-60 differentiating activity and flavonoid content of the readily extractable fraction prepared fromCitrusJuices. *J. Agric. Food Chem.* 47, 128. doi:10.1021/jf9805101

Kim, D.-H., Jung, E.-A., Sohng, I.-S., Han, J.-A., Kim, T.-H., and Han, M. J. (1998). Intestinal bacterial metabolism of flavonoids and its relation to some biological activities. *Arch. Pharm. Res.* 21, 17. doi:10.1007/BF03216747

Kim, D.-I., Lee, S.-J., Lee, S.-B., Park, K., Kim, W.-J., and Moon, S.-K. (2008). Requirement for Ras/Raf/ERK pathway in naringin-induced G1-cell-cycle arrest via p21WAF1 expression. *Carcinogenesis* 29, 1701. doi:10.1093/carcin/bgn055

Kim, H.-J., Song, J. Y., Park, H. J., Park, H.-K., Yun, D. H., and Chung, J.-H. (2009). Naringin protects against rotenone-induced apoptosis in human neuroblastoma SH-SY5Y cells. *Korean J. Physiol. Pharmacol.* 13, 281. doi:10.4196/kjpp.2009.13.4.281

Knežević, A. H., Dikić, D., Lisičić, D., Kopjar, N., Oršolić, N., Karabeg, S., et al. (2011). Synergistic effects of irinotecan and flavonoids on Ehrlich ascites tumour-bearing mice. *Basic Clin. Pharmacol. Toxicol.* 109, 343–349. doi:10.1111/j.1742-7843.2011.00735.x

Konno, A., Misaki, M., Toda, J., Wada, T., and Yasumatsu, K. (1982). Bitterness reduction of naringin and limonin by .BETA.-cyclodextrin. *Agric. Biol. Chem.* 46, 2203–2208. doi:10.1271/bbb1961.46.2203

Krishnakumar, N., Sulfikkarali, N., RajendraPrasad, N., and Karthikeyan, S. (2011). Enhanced anticancer activity of naringenin-loaded nanoparticles in human cervical (HeLa) cancer cells. *Biomed. Prev. Nutr.* 1, 223. doi:10.1016/j.bionut.2011.09.003

Kuo, S. M. (1996). Antiproliferative potency of structurally distinct dietary flavonoids on human colon cancer cells. *Cancer Lett.* 110, 41. doi:10.1016/S0304-3835(96)04458-8

Kweon, K. H., Lee, C. R., Jung, S. J., Ban, E. J., Kang, S.-W., Jeong, J. J., et al. (2014). Sirt1 induction confers resistance to etoposide-induced genotoxic apoptosis in thyroid cancers. *Int. J. Oncol.* 45, 2065–2075. doi:10.3892/ijo.2014.2585

Lagoa, R., Silva, J., Rodrigues, J. R., and Bishayee, A. (2020). Advances in phytochemical delivery systems for improved anticancer activity. *Biotechnol. Adv.* 38, 107382. doi:10.1016/j.biotechadv.2019.04.004

Le Marchand, L., Murphy, S. P., Hankin, J. H., Wilkens, L. R., and Kolonel, L. N. (2000). Intake of flavonoids and lung cancer. *J. Natl. Cancer Inst.* 92, 154. doi:10.1093/jnci/92.2.154

Lee, K. W., Bode, A. M., and Dong, Z. (2011). Molecular targets of phytochemicals for cancer prevention. *Nat. Rev. Cancer* 11, 211. doi:10.1038/nrc3017

Levi, F., Vecchia, C. L., Randimbison, L., and Franceschi, S. (1993). Incidence of infiltrating cancer following superficial bladder carcinoma. *Int. J. Cancer* 55, 419–421. doi:10.1002/ijc.2910550316

Lewinska, A., Siwak, J., Rzeszutek, I., and Wnuk, M. (2015). Diosmin induces genotoxicity and apoptosis in DU145 prostate cancer cell line. *Toxicol. Vitro* 29, 417. doi:10.1016/j.tiv.2014.12.005

Li, H., Yang, B., Huang, J., Xiang, T., Yin, X., Wan, J., et al. (2013a). Naringin inhibits growth potential of human triple-negative breast cancer cells by targeting β-catenin signaling pathway. *Toxicol. Lett.* 220, 219. doi:10.1016/j.toxlet.2013.05.006

Li, J., Dong, Y., Hao, G., Wang, B., Wang, J., Liang, Y., et al. (2017). Naringin suppresses the development of glioblastoma by inhibiting FAK activity. *J. Drug Target.* 25, 41. doi:10.1080/1061186X.2016.1184668

Li, P., Wang, S., Guan, X., Liu, B., Wang, Y., Xu, K., et al. (2013b). Acute and 13 weeks subchronic toxicological evaluation of naringin in Sprague-Dawley rats. *Food Chem. Toxicol.* 60, 1–9. doi:10.1016/j.fct.2013.07.019

Liang, W., Du, G., Zhang, H., Jin, L., Lv, H., Wang, W., et al. (2008). Use of naringenin and naringin as inhibitors of the signaling pathway of transforming growth factor beta1. European patent NO ES2519040T3. European Patent Office.

Liang, W., Zhang, C. L., Zeng, W., Zhang, C., and Wang, L. (2016). Application of naringenin and naringin in tumor radiotherapy. U.S. Patent NO US10307393B2. U.S. Patent and Trademark Office.

Liu, X., Yang, X., Chen, F., and Chen, D. (2017). Combined application of doxorubicin and naringin enhances the antitumor efficiency and attenuates the toxicity of doxorubicin in HeLa cervical cancer cells. *Int. J. Clin. Exp. Pathol.* 10, 7303–7311.

Luo, H., Jiang, B.-H., King, S. M., and Chen, Y. C. (2008). Inhibition of cell growth and VEGF expression in ovarian cancer cells by flavonoids. *Nutr. Cancer* 60, 800. doi:10.1080/01635580802100851

Martínez-Vélez, N., Gomez-Manzano, C., Fueyo, J., Patiño-García, A., and Alonso, M. M. (2018). "Oncolytic virotherapy for gliomas: a preclinical and clinical summary," in *Gene therapy in neurological disorders* (Amsterdam, Netherlands: Elsevier), 357–384.

Meiyanto, E., Hermawan, A., and Anindyajati, A. (2012). Natural products for cancer-targeted therapy: citrus flavonoids as potent chemopreventive agents. *Asian Pac. J. Cancer Prev.* 13, 427. doi:10.7314/APJCP.2012.13.2.427

Mellou, F., Loutrari, H., Stamatis, H., Roussos, C., and Kolisis, F. N. (2006). Enzymatic esterification of flavonoids with unsaturated fatty acids: effect of the novel esters on vascular endothelial growth factor release from K562 cells. *Process Biochem.* 41, 2029. doi:10.1016/j.procbio.2006.05.002

Memariani, Z., Abbas, S. Q., ul Hassan, S. S., Ahmadi, A., and Chabra, A. (2020). Naringin and naringeninin as anticancer agents and adjuvants in cancer combination therapy; efficacy and molecular mechanisms of action, a comprehensive narrative review. *Pharmacol. Res.*, 105264. doi:10.1016/j.phrs.2020.105264

Menichini, F., Tundis, R., Loizzo, M. R., Bonesi, M., D'Angelo, D., Lombardi, P., et al. (2016). Citrus medica L. cv Diamante (Rutaceae) peel extract improves glycaemic status of Zucker diabetic fatty (ZDF) rats and protects against oxidative stress. *J. Enzyme Inhib. Med. Chem.* 31, 1270. doi:10.3109/14756366.2015.1115400

Menon, L. G., Kuttan, R., and Kuttan, G. (1995). Inhibition of lung metastasis in mice induced by B16F10 melanoma cells by polyphenolic compounds. *Cancer Lett.* 95, 221. doi:10.1016/0304-3835(95)03887-3

Miller, E. G., Peacock, J. J., Bourland, T. C., Taylor, S. E., Wright, J. M., Patil, B. S., et al. (2008). Inhibition of oral carcinogenesis by citrus flavonoids. *Nutr. Cancer* 60, 69. doi:10.1080/01635580701616163

Ming, H., Chuang, Q., Jiashi, W., Bin, L., Guangbin, W., and Xianglu, J. (2018). Naringin targets Zeb1 to suppress osteosarcoma cell proliferation and metastasis. *Aging* 10, 4141. doi:10.18632/aging.101710

Mohamed, E., Abu Hashim, I., Yusif, R., Shaaban, A., El-Sheakh, A., Hamed, M., et al. (2018). Polymeric micelles for potentiated antiulcer and anticancer activities of naringin. *IJN* 13, 1009. doi:10.2147/IJN.S154325

Moher, D., Liberati, A., Tetzlaff, J., Altman, D. G., and Group, P. (2009). Preferred reporting items for systematic reviews and meta-analyses: the PRISMA statement. *Plos Med.* 6, e1000097. doi:10.1371/journal.pmed.1000097

Myers, C. (1998). The role of iron in doxorubicin-induced cardiomyopathy. *Semin. Oncol.* 25, 10.

Neuhouser, M. L. (2004). Review: dietary flavonoids and cancer risk: evidence from human population studies. *Nutr. Cancer* 50, 1–7. doi:10.1207/s15327914nc5001_1

Newman, D. J., and Cragg, G. M. (2012). Natural products as sources of new drugs over the 30 years from 1981 to 2010. *J. Nat. Prod.* 75, 311. doi:10.1021/np200906s

Newman, D. J., and Cragg, G. M. (2020). Natural products as sources of new drugs over the nearly four decades from 01/1981 to 09/2019. *J. Nat. Prod.* 83, 770. doi:10.1021/acs.jnatprod.9b01285

Nie, Y.-c., Wu, H., Li, P.-b., Xie, L.-m., Luo, Y.-l., Shen, J.-g., et al. (2012). Naringin attenuates EGF-induced MUC5AC secretion in A549 cells by suppressing the cooperative activities of MAPKs-AP-1 and IKKs-IκB-NF-κB signaling pathways. *Eur. J. Pharmacol.* 690, 207. doi:10.1016/j.ejphar.2012.06.040

Ooghe, W. C., Ooghe, S. J., Detavernier, C. l. M., and Huyghebaert, A. (1994). Characterization of orange juice (Citrus sinensis) by flavanone glycosides. *J. Agric. Food Chem.* 42, 2183–2190. doi:10.1021/jf00046a020

Oršolić, N., Benković, V., Lisičić, D., Dikić, D., Erhardt, J., and Knežević, A. H. (2010). Protective effects of propolis and related polyphenolic/flavonoid compounds against toxicity induced by irinotecan. *Med. Oncol.* 42, 1346–1358. doi:10.1007/s12032-009-9387-5

Oršolić, N., Štajcar, D., and Bašić, I. (2009). Propolis and its flavonoid compounds cause cytotoxicity on human urinary bladder transitional cell carcinoma in primary culture. *Period. Biol.* 111, 113–121.

Özyürek, M., Akpınar, D., Bener, M., Türkkan, B., Güçlü, K., and Apak, R. (2014). Novel oxime based flavanone, naringin-oxime: synthesis, characterization and screening for antioxidant activity. *Chem. Biol. Interact.* 212, 40. doi:10.1016/j.cbi.2014.01.017

Park, J. H., Jin, C.-Y., Lee, B. K., Kim, G.-Y., Choi, Y. H., and Jeong, Y. K. (2008). Naringenin induces apoptosis through downregulation of Akt and caspase-3 activation in human leukemia THP-1 cells. *Food Chem. Toxicol.* 46, 3684. doi:10.1016/j.fct.2008.09.056

Pennathur, A., Gibson, M. K., Jobe, B. A., and Luketich, J. D. (2013). Oesophageal carcinoma. *The Lancet* 381, 400–412. doi:10.1016/s0140-6736(12)60643-6

Pereira, R., Andrades, N., Paulino, N., Sawaya, A., Eberlin, M., Marcucci, M., et al. (2007). Synthesis and characterization of a metal complex containing naringin and Cu, and its antioxidant, antimicrobial, antiinflammatory and tumor cell cytotoxicity. *Molecules* 12, 1352. doi:10.3390/12071352

Persky, M. J., Persky, V., Setchell, K. D., and Barnes, S. (1994). Soy intake and cancer risk: a review of the *in vitro* and *in vivo* data. *Nutr. Cancer* 21, 113. doi:10.1080/01635589409514310

Pfaendler, K. S., and Tewari, K. S. (2016). Changing paradigms in the systemic treatment of advanced cervical cancer. *Am. J. Obstet. Gynecol.* 214, 22–30. doi:10.1016/j.ajog.2015.07.022

Puranik, N. V., Srivastava, P., Bhatt, G., John Mary, D. J. S., Limaye, A. M., and Sivaraman, J. (2019). Determination and analysis of agonist and antagonist potential of naturally occurring flavonoids for estrogen receptor (ERα) by various parameters and molecular modelling approach. *Sci. Rep.* 9, 7450. doi:10.1038/s41598-019-43768-5

Raha, S., Kim, S. M., Lee, H. J., Yumnam, S., Saralamma, V. V., Ha, S. E., et al. (2020). Naringin induces lysosomal permeabilization and autophagy cell death in AGS gastric cancer cells. *Am. J. Chin. Med.* 48, 679. doi:10.1142/S0192415X20500342

Raha, S., Yumnam, S., Hong, G. E., Lee, H. J., Saralamma, V. V. G., Park, H.-S., et al. (2015). Naringin induces autophagy-mediated growth inhibition by downregulating the PI3K/Akt/mTOR cascade via activation of MAPK pathways in AGS cancer cells. *Int. J. Oncol.* 47, 1061. doi:10.3892/ijo.2015.3095

Rajadurai, M., and Stanely Mainzen Prince, P. (2007). Preventive effect of naringin on isoproterenol-induced cardiotoxicity in Wistar rats: an *in vivo* and *in vitro* study. *Toxicology* 232, 216–225. doi:10.1016/j.tox.2007.01.006

Rajamani, S., Radhakrishnan, A., Sengodan, T., and Thangavelu, S. (2018). Augmented anticancer activity of naringenin-loaded TPGS polymeric nanosuspension for drug resistive MCF-7 human breast cancer cells. *Drug Development Ind. Pharm.* 44, 1752. doi:10.1080/03639045.2018.1496445

Ramanathan, R., Tan, C. H., and Das, N. P. (1992). Cytotoxic effect of plant polyphenols and fat-soluble vitamins on malignant human cultured cells. *Cancer Lett.* 62, 217. doi:10.1016/0304-3835(92)90099-H

Ramesh, E., and Alshatwi, A. A. (2013). Naringin induces death receptor and mitochondria-mediated apoptosis in human cervical cancer (SiHa) cells. *Food Chem. Toxicol.* 51, 97. doi:10.1016/j.fct.2012.07.033

Ravishankar, D., Rajora, A. K., Greco, F., and Osborn, H. M. I. (2013). Flavonoids as prospective compounds for anti-cancer therapy. *Int. J. Biochem. Cell Biol.* 45, 2821–2831. doi:10.1016/j.biocel.2013.10.004

Real, H. J. V., Alfaia, A. J., Calado, A. R. T., and Ribeiro, M. H. L. (2007). High pressure-temperature effects on enzymatic activity: naringin bioconversion. *Food Chem.* 102, 565–570. doi:10.1016/j.foodchem.2006.05.033

Reddy, L., Odhav, B., and Bhoola, K. D. (2003). Natural products for cancer prevention: a global perspective. *Pharmacol. Ther.* 99, 1–13. doi:10.1016/s0163-7258(03)00042-1

Rivoira, M. A., Rodriguez, V., Talamoni, G., and de Talamoni, N. T. (2020). New perspectives in the pharmacological potential of naringin in medicine. *Curr. Med. Chem.* doi:10.2174/0929867327666200604171351

Romagnolo, D. F., and Selmin, O. I. (2012). Flavonoids and cancer prevention: a review of the evidence. *J. Nutr. Gerontol. Geriatr.* 31, 206–238. doi:10.1080/21551197.2012.702534

Rout, G. K., Shin, H.-S., Gouda, S., Sahoo, S., Das, G., Fraceto, L. F., et al. (2018). Current advances in nanocarriers for biomedical research and their applications. *Artif. Cell Nanomedicine, Biotechnol.* 46, 1053–1062. doi:10.1080/21691401.2018.1478843

Said-Elbahr, R., Nasr, M., Alhnan, M. A., Taha, I., and Sammour, O. (2016). Nebulizable colloidal nanoparticles co-encapsulating a COX-2 inhibitor and a herbal compound for treatment of lung cancer. *Eur. J. Pharm. Biopharm.* 103, 1. doi:10.1016/j.ejpb.2016.03.025

Sangodkar, J., Katz, S., Melville, H., and Narla, G. (2010). Lung adenocarcinoma: lessons in translation from bench to bedside. *Mt Sinai J. Med.* 77, 597–605. doi:10.1002/msj.20226

Sangubotla, R., Anantha Lakshmi, B., Kim, S., and Kim, J. (2020). Bio-inspired green fluorescent gold-naringin nanoclusters as a dual-functional optical probe for bio-imaging and intracellular sensing applications. *Appl. Surf. Sci.* 510, 145417. doi:10.1016/j.apsusc.2020.145417

Schindler, R., and Mentlein, R. (2006). Flavonoids and vitamin E reduce the release of the angiogenic peptide vascular endothelial growth factor from human tumor cells. *J. Nutr.* 136, 1477. doi:10.1093/jn/136.6.1477

Selvaraj, S., Krishnaswamy, S., Devashya, V., Sethuraman, S., and Krishnan, U. M. (2014). Investigations on the membrane interactions of naringin and its complexes with copper and iron: implications for their cytotoxicity. *RSC Adv.* 4, 46407. doi:10.1039/c4ra08157a

Seyfried, T. N., and Shelton, L. M. (2010). Cancer as a metabolic disease. *Nutr. Metab.* 7, 7. doi:10.1186/1743-7075-7-7

Sheikh, I., Sharma, V., Tuli, H. S., Aggarwal, D., Sankhyan, A., Vyas, P., et al. (2021). Cancer chemoprevention by flavonoids, dietary polyphenols and terpenoids. *Biointerface Res. Appl. Chem.* 11, 8502–8537. doi:10.33263/BRIAC111.85028537

Shen, S.-C., Ko, C. H., Tseng, S.-W., Tsai, S.-H., and Chen, Y.-C. (2004). Structurally related antitumor effects of flavanones *in vitro* and *in vivo*: involvement of caspase 3 activation, p21 gene expression, and reactive oxygen species production. *Toxicol. Appl. Pharmacol.* 197, 84. doi:10.1016/j.taap.2004.02.002

Siegel, R., Naishadham, D., and Jemal, A. (2013). Cancer statistics, 2013. *CA: A Cancer J. Clinicians* 63, 11–30. doi:10.3322/caac.21166

Singh, B., Rani, M., Singh, J., Moudgil, L., Sharma, P., Kumar, S., et al. (2016). Identifying the preferred interaction mode of naringin with gold nanoparticles through experimental, DFT and TDDFT techniques: insights into their sensing and biological applications. *RSC Adv.* 6, 79470. doi:10.1039/c6ra12076h

So, F. V., Guthrie, N., Chambers, A. F., Moussa, M., and Carroll, K. K. (1996). Inhibition of human breast cancer cell proliferation and delay of mammary tumorigenesis by flavonoids and citrus juices. *Nutr. Cancer* 26, 167. doi:10.1080/01635589609514473

Sreepriya, M., and Bali, G. (2005). Chemopreventive effects of embelin and curcumin against N-nitrosodiethylamine/phenobarbital-induced hepatocarcinogenesis in Wistar rats. *Fitoterapia* 76, 549–555. doi:10.1016/j.fitote.2005.04.014

Steiner, C., Arnould, S., Scalbert, A., and Manach, C. (2008). Isoflavones and the prevention of breast and prostate cancer: new perspectives opened by nutrigenomics. *Br. J. Nutr.* 99, ES78–ES108. doi:10.1017/s0007114508965788

Surampalli, G., K. Nanjwade, B., and Patil, P. A. (2015). Corroboration of naringin effects on the intestinal absorption and pharmacokinetic behavior of candesartan cilexetil solid dispersions usingin-siturat models. *Drug Development Ind. Pharm.* 41, 1057–1065. doi:10.3109/03639045.2014.925918

Syed, A. A., Reza, M. I., Shafiq, M., Kumariya, S., Singh, P., Husain, A., et al. (2020). Naringin ameliorates type 2 diabetes mellitus-induced steatohepatitis by inhibiting RAGE/NF-κB mediated mitochondrial apoptosis. *Life Sci.* 257, 118118. doi:10.1016/j.lfs.2020.118118

Tajaldini, M., Samadi, F., Khosravi, A., Ghasemnejad, A., and Asadi, J. (2020). Protective and anticancer effects of orange peel extract and naringin in doxorubicin treated esophageal cancer stem cell xenograft tumor mouse model. *Biomed. Pharmacother.*, 121, 109594. doi:10.1016/j.biopha.2019.109594

Tan, T.-W., Chou, Y.-E., Yang, W.-H., Hsu, C.-J., Fong, Y.-C., and Tang, C.-H. (2014). Naringin suppress chondrosarcoma migration through inhibition vascular adhesion molecule-1 expression by modulating miR-126. *Int. Immunopharmacol.* 22, 107. doi:10.1016/j.intimp.2014.06.029

Tang, J., Kong, D., Bu, L., and Wu, G. (2017). Surgical management for follicular variant of papillary thyroid carcinoma. *Oncotarget* 8, 79507. doi:10.18632/oncotarget.18525

Thangavel, P., and Vaiyapuri, M. (2013). Antiproliferative and apoptotic effects of naringin on diethylnitrosamine induced hepatocellular carcinoma in rats. *Biomed. Aging Pathol.* 3, 59. doi:10.1016/j.biomag.2013.01.006

Thornalley, P. J. (2008). Protein and nucleotide damage by glyoxal and methylglyoxal in physiological systems-role in ageing and disease. *Drug Metabol. Drug Interact.* 23, 125. doi:10.1515/dmdi.2008.23.1-2.125

Torre, L. A., Bray, F., Siegel, R. L., Ferlay, J., Lortet-Tieulent, J., and Jemal, A. (2015). Global cancer statistics, 2012. *CA: A Cancer J. Clinicians* 65, 87–108. doi:10.3322/caac.21262

Tsai, Y.-J., and Tsai, T.-H. (2012). Mesenteric lymphatic absorption and the pharmacokinetics of naringin and naringenin in the rat. *J. Agric. Food Chem.* 60, 12435–12442. doi:10.1021/jf301962g

Ugocsai, K., Varga, A., Molnár, P., Antus, S., and Molnár, J. (2005). Effects of selected flavonoids and carotenoids on drug accumulation and apoptosis induction in multidrug-resistant colon cancer cells expressing MDR1/LRP. *In vivo* 60, 433–438.

Van der Jeught, K. V. d., Xu, H.-C., Li, Y.-J., Lu, X.-B., and Ji, G. (2018). Drug resistance and new therapies in colorectal cancer. *Wjg* 24, 3834. doi:10.3748/wjg.v24.i34.3834

Vanamala, J., Leonardi, T., Patil, B. S., Taddeo, S. S., Murphy, M. E., Pike, L. M., et al. (2006). Suppression of colon carcinogenesis by bioactive compounds in grapefruit. *Carcinogenesis* 27, 1257. doi:10.1093/carcin/bgi318

Vardiman, J. W., Thiele, J., Arber, D. A., Brunning, R. D., Borowitz, M. J., Porwit, A., et al. (2009). The 2008 revision of the World Health Organization (WHO) classification of myeloid neoplasms and acute leukemia: rationale and important changes. *Blood* 114, 937–951. doi:10.1182/blood-2009-03-209262

Wong, N., Tucker, J., and Mccaffrey, D. R. (2006). Treatment of diseases associated with the egr-1 enhancer element. South Korea Patent NO KR20060120101A Office. doi:10.7591/9781501711480

Wu, X., Huang, Z., Liu, J., Chen, Y., Huang, H., He, Y., et al. (2019). Effects and mechanism of inhibition of naringin in combination with atorvastatin on prostate cancer cells *in vitro* and *in vivo*. *Phytochemistry Lett.* 32, 168. doi:10.1016/j.phytol.2019.06.008

Xie, D., Yuan, P., Wang, D., Jin, H., and Chen, H. (2017). Effects of naringin on the expression of miR-19b and cell apoptosis in human hepatocellular carcinoma. *Oncol. Lett.* 14, 1455–1459. doi:10.3892/ol.2017.6278

Yadav, A., Kumar, R., Sunkaria, A., Singhal, N., Kumar, M., and Sandhir, R. (2016). Evaluation of potential flavonoid inhibitors of glyoxalase-I based on virtual screening and *in vitro* studies. *J. Biomol. Struct. Dyn.* 34, 993. doi:10.1080/07391102.2015.1064830

Yamane, K., and Kato, Y. (2012). *Handbook on flavonoids: dietary sources, properties and health benefits*. Hauppauge, NY: Nova Science Publishers.

Yang, C. S., Landau, J. M., Huang, M.-T., and Newmark, H. L. (2001). Inhibition ofcarcinogenesis bydietarypolyphenoliccompounds. *Annu. Rev. Nutr.*, 21, 381. doi:10.1146/annurev.nutr.21.1.381

Yang, Y., Tao, B., Gong, Y., Chen, R., Yang, W., Lin, C., et al. (2020). Functionalization of Ti substrate with pH-responsive naringin-ZnO nanoparticles for the reconstruction of large bony after osteosarcoma resection. *J. Biomed. Mater. Res.* 108, 2190. doi:10.1002/jbm.a.36977

Yen, H.-R., Liu, C.-J., and Yeh, C.-C. (2015). Naringenin suppresses TPA-induced tumor invasion by suppressing multiple signal transduction pathways in human hepatocellular carcinoma cells. *Chem. Biol. Interact.* 235, 1. doi:10.1016/j.cbi.2015.04.003

Yoshinaga, A., Kajiya, N., Oishi, K., Kamada, Y., Ikeda, A., Chigwechokha, P. K., et al. (2016). NEU3 inhibitory effect of naringin suppresses cancer cell growth by attenuation of EGFR signaling through GM3 ganglioside accumulation. *Eur. J. Pharmacol.* 782, 21. doi:10.1016/j.ejphar.2016.04.035

Zeng, L., Zhen, Y., Chen, Y., Zou, L., Zhang, Y., Hu, F., et al. (2014). Naringin inhibits growth and induces apoptosis by a mechanism dependent on reduced activation of NF-κB/COX-2-caspase-1 pathway in HeLa cervical cancer cells. *Int. J. Oncol.* 45, 1929. doi:10.3892/ijo.2014.2617

Zeng, X., Su, W., Zheng, Y., He, Y., He, Y., Rao, H., et al. (2019). Pharmacokinetics, tissue distribution, metabolism, and excretion of naringin in aged rats. *Front. Pharmacol.* 10, 34. doi:10.3389/fphar.2019.00034

Zhang, J., Gao, W., Liu, Z., Zhang, Z., and Liu, C. (2014). Systematic analysis of main constituents in rat biological samples after oral administration of the methanol extract of fructus aurantii by HPLC-ESI-MS/MS. *Iran J. Pharm. Res.* 13, 493.

Zhang, L., Xu, X., Jiang, T., Wu, K., Ding, C., Liu, Z., et al. (2018a). Citrus aurantium naringenin prevents osteosarcoma progression and recurrence in the patients who underwent osteosarcoma surgery by improving antioxidant capability. *Oxid. Med. Cell. Longevity* 2018, 8713263. doi:10.1155/2018/8713263

Zhang, Y.-S., Wang, F., Cui, S.-X., and Qu, X.-J. (2018b). Natural dietary compound naringin prevents azoxymethane/dextran sodium sulfate-induced chronic colorectal inflammation and carcinogenesis in mice. *Cancer Biol. Ther.* 19, 735. doi:10.1080/15384047.2018.1453971

Zhou, J.-L., Fang, X.-Y., Wang, J.-Q., Zhao, L.-G., Li, Y., Tang, F., et al. (2018). Structures and bioactivities of seven flavonoids from Osmanthus fragrans "Jinqiu" essential oil extraction residues. *Nat. Product Res.* 32, 588. doi:10.1080/14786419.2017.1318387

Zhou, J., Xia, L., and Zhang, Y. (2019). Naringin inhibits thyroid cancer cell proliferation and induces cell apoptosis through repressing PI3K/AKT pathway. *Pathol. Res. Pract.* 215, 152707. doi:10.1016/j.prp.2019.152707

Zhu, H., Gao, J., Wang, L., Qian, K. J., and Cai, L. P. (2018). *In vitro* study on reversal of ovarian cancer cell resistance to cisplatin by naringin via the nuclear factor-κB signaling pathway. *Exp. Ther. Med.* 14, 2643–2648. doi:10.3892/etm.2018.5695

Zhu, H., Zou, X., Wan, J., Wang, L., Qian, K.-J., Cai, L.-P., et al. (2017). Reversal of cisplatin resistance in ovarian cancer cells mediated by naringin-induced COX-2 expression through the NF-κB signaling pathway. *Int. J. Clin. Exp. Med.* 10, 7590–7596.

Zhu, J., Huang, Y., Zhang, J., Feng, Y., and Shen, L. (2020). Formulation, preparation and evaluation of nanostructured lipid carrier containing naringin and coix seed oil for anti-tumor application based on "unification of medicines and excipients". *DDDT* 14, 1481. doi:10.2147/DDDT.S236997

Zi, X., and Simoneau, R. (2004). Treatment of bladder and urinary tract cancers. U.S. Patent NO US7326734B2. U.S. Patent and Trademark Office.

Zivancevic-Simonovic, S., Mihaljevic, O., Kostic, I., Ilic, N., Mihajlovic, D., Vasiljevic, D., et al. (2017). Eosinophil cationic protein in patients with differentiated thyroid cancer treated with radioactive iodine 131. *Ann. Clin. Lab. Sci.* 47, 541–545.

Conflict of Interest: The authors declare that the research was conducted in the absence of any commercial or financial relationships that could be construed as a potential conflict of interest.

frontiers in Pharmacology

ORIGINAL RESEARCH
published: 12 April 2021
doi: 10.3389/fphar.2021.594833

Computational and *In Vitro* Analysis of Plumbagin's Molecular Mechanism for the Treatment of Hepatocellular Carcinoma

Yanfei Wei[†], *Yuning Lin*[†], *Wanjun Chen*[†], *Shasha Liu, Lijie Jin and Delun Huang*[*]

Department of Physiology, Guangxi University of Chinese Medicine, Nanning, China

Hepatocellular carcinoma (HCC) is the fifth most common malignant tumor and the second leading cause of cancer-related death in the world. Plumbagin (PL) is a small molecule naphthoquinone compound isolated from *Plumbago zeylanica* L. that has important anticancer properties, but its mechanism requires further investigation. In this study, we used a comprehensive network pharmacology approach to study the mechanism of action of PL for the treatment of HCC. The method includes the construction of multiple networks; moreover, Gene Ontology (GO) and Kyoto Encyclopedia of Genes and Genomes (KEGG) analyses were performed to identify biological processes and signaling pathways. Subsequently, *in vitro* experiments were performed to verify the predicted molecular mechanisms obtained from the network pharmacology-based analysis. Network pharmacological analysis showed that PL may exert anti-HCC effects by enhancing reactive oxygen species (ROS) production to generate oxidative stress and by regulating the PI3K/Akt and MAPK signaling pathways. *In vitro* experiments confirmed that PL mainly mediates the production of ROS, regulates the PI3K/Akt and MAPK signaling pathways to promote apoptosis and autophagy, and shows significant therapeutic effects on HCC. In conclusion, our work proposes a comprehensive systems pharmacology approach to explore the potential mechanism of PL for the treatment of HCC.

Keywords: plumbagin, hepatocellular carcinoma, network pharmacology, ROS, PI3K/Akt pathway, MAPK pathway

OPEN ACCESS

Edited by:
Marcus Scotti,
Federal University of Paraíba, Brazil

Reviewed by:
Xianbin Zhang,
Shenzhen University, China
Yashi Mi,
University of Arizona, United States

***Correspondence:**
Delun Huang
huangdelun0621@foxmail.com

[†]*These authors have contributed equally to this work*

Specialty section:
This article was submitted to Ethnopharmacology, a section of the journal Frontiers in Pharmacology

Received: *14 August 2020*
Accepted: *18 February 2021*
Published: *12 April 2021*

Citation:
Wei Y, Lin Y, Chen W, Liu S, Jin L and Huang D (2021) Computational and In Vitro Analysis of Plumbagin's Molecular Mechanism for the Treatment of Hepatocellular Carcinoma. Front. Pharmacol. 12:594833. doi: 10.3389/fphar.2021.594833

INTRODUCTION

Hepatocellular carcinoma (HCC) comprises a group of malignant tumors that seriously threaten human life. Surgical treatment is currently the accepted treatment of choice, but the high recurrence and high metastatic characteristics of HCC severely restrict the survival prognosis of HCC patients (Farazi and Depinho, 2006). In recent years, studies have found that traditional Chinese medicine can inhibit the growth and proliferation of HCC cells in various ways and has a prominent role in HCC treatment (Franco and Usatoff, 2001; Belghiti and Fuks, 2012). Therefore, it is a feasible research direction to search for potential liver cancer treatment drugs by screening and selecting biologically active ingredients that can effectively reduce liver cancer mortality (Su et al., 2019).

East Asian (China, Japan, and South Korea) and traditional Chinese medicine (TCM) have been widely used for disease prevention and treatment for more than two thousand years. Chinese herbal medicine is an important part of Chinese medicine, including plant medicine, animal medicine

and mineral medicine. In recent years, Chinese medicine has received increasing attention (Lam et al., 2015). Plumbagin (PL) is a natural naphthoquinone compound isolated and purified from *Plumbago zeylanica* L., a traditional Chinese medicinal plant from China (Tilak et al., 2004; Sakamoto et al., 2011). A large number of studies have shown that PL has antitumor, anti-liver fibrosis, anti-hepatitis B virus, antiplatelet activity, anti-atherosclerosis and other effects (Panda and Kamble, 2016). Studies have shown that PL has significant inhibitory effects on leukemia, lung cancer, prostate cancer, melanoma, breast cancer and other malignant tumors (Subramaniya et al., 2011; Tian et al., 2011; Liu et al., 2017). Previous experimental studies have shown that PL can induce HCC SMMC-7721 cell apoptosis by inhibiting the epithelial-mesenchymal transition (EMT) and inhibit HCC cell angiogenesis and proliferation through the SDF-1-CXCR4/CXCR7 axis (Wei et al., 2019; Zhong et al., 2019).

However, more detailed therapeutic targets and signaling mechanisms of PL acting on HCC have not been revealed. Therefore, to further explore the relevant mechanisms of PL acting on HCC, this study aimed to identify therapeutic targets and signaling mechanisms through network pharmacology based on bioinformatics and verify them through relevant experiments *in vitro*. Network pharmacology is an emerging new method to explore the systemic mechanism of therapeutic compounds in diseases (Kohl et al., 2011; Szklarczyk et al., 2016a). The workflow is shown in **Figure 1**. Using network pharmacology to determine herbal targets and potential mechanisms is becoming increasingly important to save money, effort and time required for drug discovery and design (Győrffy et al., 2013; Zhang et al., 2013). Indeed, network pharmacology has successfully led to the construction and visualization of drug-disease-target networks, which are helpful for evaluating drug mechanisms from multiple perspectives (Gao et al., 2016; Fang et al., 2017). Therefore, network pharmacology can be used to determine the pharmacological target and mechanism of action of PL in HCC and provide guidance and evidence for future research on the use of PL to treat HCC.

MATERIALS AND METHODS

Network Pharmacology-Based Analysis

Identifying PL Targets

The predicted genes were obtained by searching the keyword "plumbagin" in the STITCH database (http://stitch.embl.de) (Szklarczyk et al., 2016b). The chemical structural formula of PL was entered into the SuperPred database (http://prediction.charite.de) (Mathias et al., 2008) and the PhamMapper database (http://lilab.ecust.edu.cn/pharmmapper/help.php) (Li et al., 2017). Additionally, the UniProt database (https://www.UniProt.org/) was combined with the literature to collect PL-predictive genes (Rolf et al., 2004), and the Swiss Target Prediction database (http://www.swisstargetprediction.ch/) (Antoine et al., 2019) was used to supplement the gene prediction information. We predicted the target genes of the compound by selecting the compound with the highest "Tanimoto score" and set the "minimum required interaction score" to "high confidence (0.700)" in STITCH. The threshold of "gene probability" was set to >0.6, and the related genes of the predicted compounds in the "Swiss Target Forecast" were selected.

Identification of HCC Prediction Genes

The significant prediction genes of HCC were retrieved from OncoDB.HCC (http://oncodb.hcc.ibms.sinica.edu.tw/) (Su et al., 2007) and the GeneCards database (https://www.genecards.org/) (Marilyn et al., 2010). OncoDB.HCC can effectively integrate data sets in public references, provide a multidimensional view of current HCC research, and is the first comprehensive HCC genome database. Potential genes associated with HCC were collected from GeneCards with the keyword "Hepatocellular carcinoma."

Construction of the Components–Targets–Disease Network

Venny2.1.0 (http://bioinfogp.cnb.csic.es/tools/venny/) (Shade and Handelsman, 2012) was used to screen common targets related to PL and HCC. The Cytoscape v3.7.1 (Shannon et al., 2003) software was used to establish target disease and component-target network models, and the merge function was used to build component-target-disease network models. The results were analyzed to determine the relationships in the network model. The proteins were sorted according to their degree of binding.

Gene Ontology and KEGG Pathway Analysis

Gene Ontology and KEGG pathway analyses can clarify the role of potential targets by gene function and signaling pathways. The Bioconductor package "org.Hs.eg.db" was installed and run in the R software (Stoll et al., 2005). The drug-disease common targets were converted into Entrez IDs, and then the "clusterProfiler" package was installed in the R software. According to the converted Entrez IDs, enrichment analysis of key target gene GO functions and analysis of KEGG signaling pathways were performed with $p < 0.05$. The results were output in the form of bar and bubble charts.

EXPERIMENTAL VALIDATION

Chemicals and Reagents

Plumbagin (PL) was purchased from Sigma-Aldrich (St. Louis, MO, United States) with purity ≥98%; the Acridine Orange (AO)/Ethidium bromide (EB) Double Stain Kit was from Solable Technology (Beijing, China); N-acetyl-l-cysteine, SB203580, and SB202190 were from Sigma-Aldrich (St. Louis, MO, United States); SC-79, MEK2206, 3-MA, and Z-VAD-FMK were from Selleck (Texas, United States); the BCA Protein Assay Kit, ROS Assay Kit, Annexin V-FITC Apoptosis Detection Kit and Cell lysis buffer for Western were all obtained from Beyotime Biotechnology (Shanghai, China); antibodies against Akt, phospho-Akt, mTOR, phospho-mTOR, p38 MAPK, phospho-p38 MAPK, PI3K, phospho-PI3K, LC3B, cleave-RP, and cleave-caspase 3 were

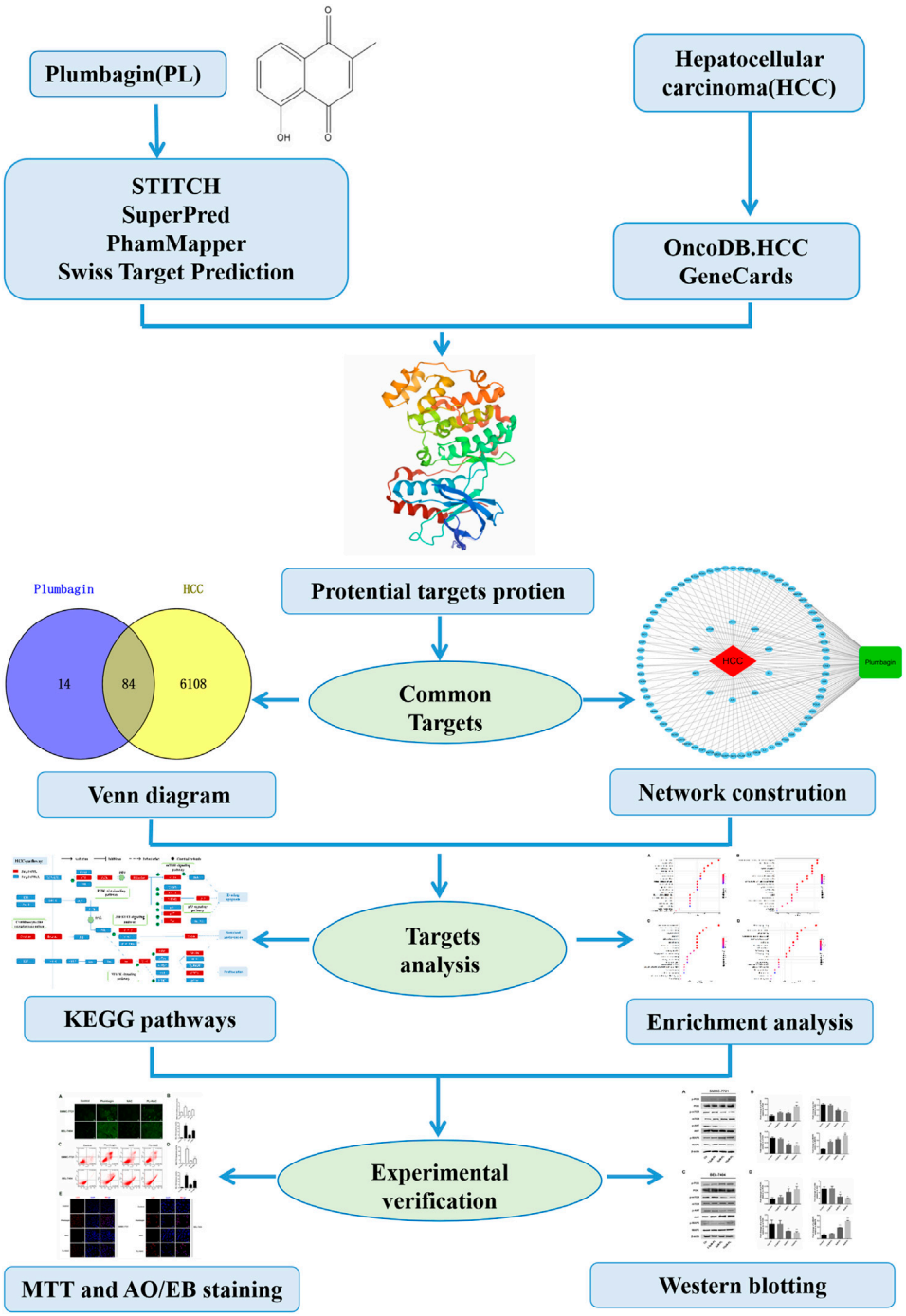

FIGURE 1 | Systems pharmacology approach workflow.

from Cell Signaling Technology, Inc. (Boston, MA, United States); and β-p38 MAPK was purchased from Boster Technology (Wuhan, China).

Cell Lines and Culture

The human HCC cell lines SMMC-7721 and BEL-7404 were purchased from the Shanghai Institute of Biological Sciences (Shanghai, China). The DMEM high-glucose medium required for human HCC SMMC-7721 cell culture and the RPMI-1640 medium required for human HCC BEL-7404 cells were from Thermo Fisher Scientific (MA, United States). The complete culture medium contained 10% fetal bovine serum (FBS), 100 μg/ml penicillin and 100 μg/ml streptomycin, which were obtained from Invitrogen (CA, United States). The cells

were cultured in an incubator at 37°C with a humidified atmosphere of 5% CO_2.

Cell Viability Assay

Cell operations were performed on an ultraclean workbench. After the cells were recovered, SMMC-7721 and BEL-7404 cells at 80% confluence were digested into seed plates and seeded in 96-well plates at a density of 5×10^3 cells/well. After 24 h, the cells were completely attached to the wall and then synchronized. Each group was equipped with four auxiliary holes. A negative control well was set up without seeding cells. After treatment with various concentrations of PL (0.5, 3, 6, and 10 μM) for 6, 12 or 24 h in a 5% CO_2 incubator at 37°C, 20 μL of 5 mg/ml MTT solution was added to each well, the plates were wrapped in foil and protected from light, and then placed in an incubator to continue incubation for an additional 3–4 h. The absorbance value of each well was measured using a continuous spectrum scanning microplate reader (Thermo Fisher, MA, United States) at a wavelength of 560 nm.

AO/EB Staining

SMMC-7721 and BEL-7404 cells in logarithmic growth phase were digested and plated. Three multi-wells were set up and inoculated into a 24-well culture plate according to the standard of 500 μL per well, after which a moderate concentration of PL was added to stimulate the cells for 24 h. The supernatant was discarded after the intervention, a final concentration of 1 μg/ml AO/EB was added, and the plate was incubated for 10 min in the dark. Observation by fluorescence microscopy (Olympus, Tokyo, Japan) revealed that AO produces green fluorescence in the cytosol and the nuclear compartment (emission peak between 530 and 550 nm). Fluorescence microscopy showed four cell morphologies. The nuclear chromatin of living cells was green and showed a normal structure; the nuclear chromatin of early apoptotic cells was green, though the shape was shrunken or rounded; the nuclear spot material of late apoptotic cells was orange-red, and the shape was solid or as round beads; and the nuclear chromatin of nonapoptotic dead cells was orange-red, with normal cell morphology.

Detection of ROS

ROS production was determined using a 2′,7′-dichlorodihydrofluorescein diacetate (DCFH-DA) assay (Beyotime, Shanghai, China). After treatment, SMMC-7721 and BEL-7404 cells were incubated with DCFH-DA for 30 min at 37°C in the dark. The cells were then harvested and suspended in PBS. The fluorescence intensity in each well was detected by an LSM 700 confocal microscope (Zeiss, Hamburg, Germany).

Flow Cytometry for Apoptosis Analysis

The instructions of the Annexin V-FITC Apoptosis Detection Kit were strictly followed to process each group of cells. The cells were digested with trypsin without EDTA and washed twice with prechilled PBS, and $10–50 \times 10^4$ cells were collected. The cells were then resuspended in 100 μL of 1×Binding Buffer, and then 5 μL each of Annexin V-FITC and PI staining solution were added. The lysates were then mixed gently and incubated at room temperature in the dark for 10 min. The cells were detected by flow cytometry within 1 h. Apoptosis rate = (number of apoptotic cells/total number of cells observed) × 100%.

Immunofluorescence Staining

The cells were fixed with 4% paraformaldehyde for 15 min and permeabilized with 0.1% Triton X-100 for 10 min. The cells were then blocked with 2% bovine serum albumin (BSA) at 37°C for 30 min, after which the cells were incubated with anti-LC3B (1:100, Cell Signaling Technology, Boston, United States) overnight at 4°C. The cells were then incubated with the corresponding secondary antibodies for 1 h at room temperature. The nuclei were stained with DAPI for 10 min and washed twice with PBS, and then images were captured using an LSM 700 confocal microscope (Zeiss, Hamburg, Germany).

Western Blotting

SMMC-7721 and BEL-7404 cells treated with the preset intervention conditions were collected and proteins were extracted. After using BSA to measure the absorbance, a standard curve was prepared versus the standard, and the protein concentration of the sample was determined according to the standard curve. The samples were prepared according to the instructions for the BCA protein quantitation kit. Depending on the relative molecular weights of the proteins, 7.5–12.5% PAGE-SDS gel electrophoresis was performed, and the proteins were then transferred to PVDF membranes. The PVDF membranes were blocked with 5% skimmed milk powder for 1 h at room temperature. Then, the following appropriately diluted primary antibodies were added: anti-β-actin (1:200), PI3K (1:1000), p-PI3K (1:500), Akt (1:2000), p-Akt (1:500), mTOR (1:1000), p-mTOR (1:1000), p38 MAPK (1:1000), p-p38 MAPK (1:500), cleave-caspase 3 (1:1000), cleave-PARP (1:1000), and LC3B (1:1000). Next, the blots were incubated at 4°C overnight. After washing three times with PBS, the corresponding secondary antibody was added and incubated for 2 h at room temperature. After incubating with the luminescent solution from the ECL kit, the film was exposed in the cassette, the protein bands were developed, and Band Scan software was used to scan grayscale images.

Statistical Analysis

Data are expressed as the means ± standard deviation (SD). Statistical analysis was performed using SPSS 22.0. One-way ANOVA was used for comparisons between groups, and the difference was statistically significant at $p < 0.05$.

RESULTS

Screening Results of PL Targets and HCC Disease Targets

The 3D chemical structure of PL was imported into the chemical substance interaction search tool STITCH and the SuperPred and PhamMapper databases for retrieval; the Swiss Target Prediction database was used to supplement the target information. Then, the corresponding targets were input into

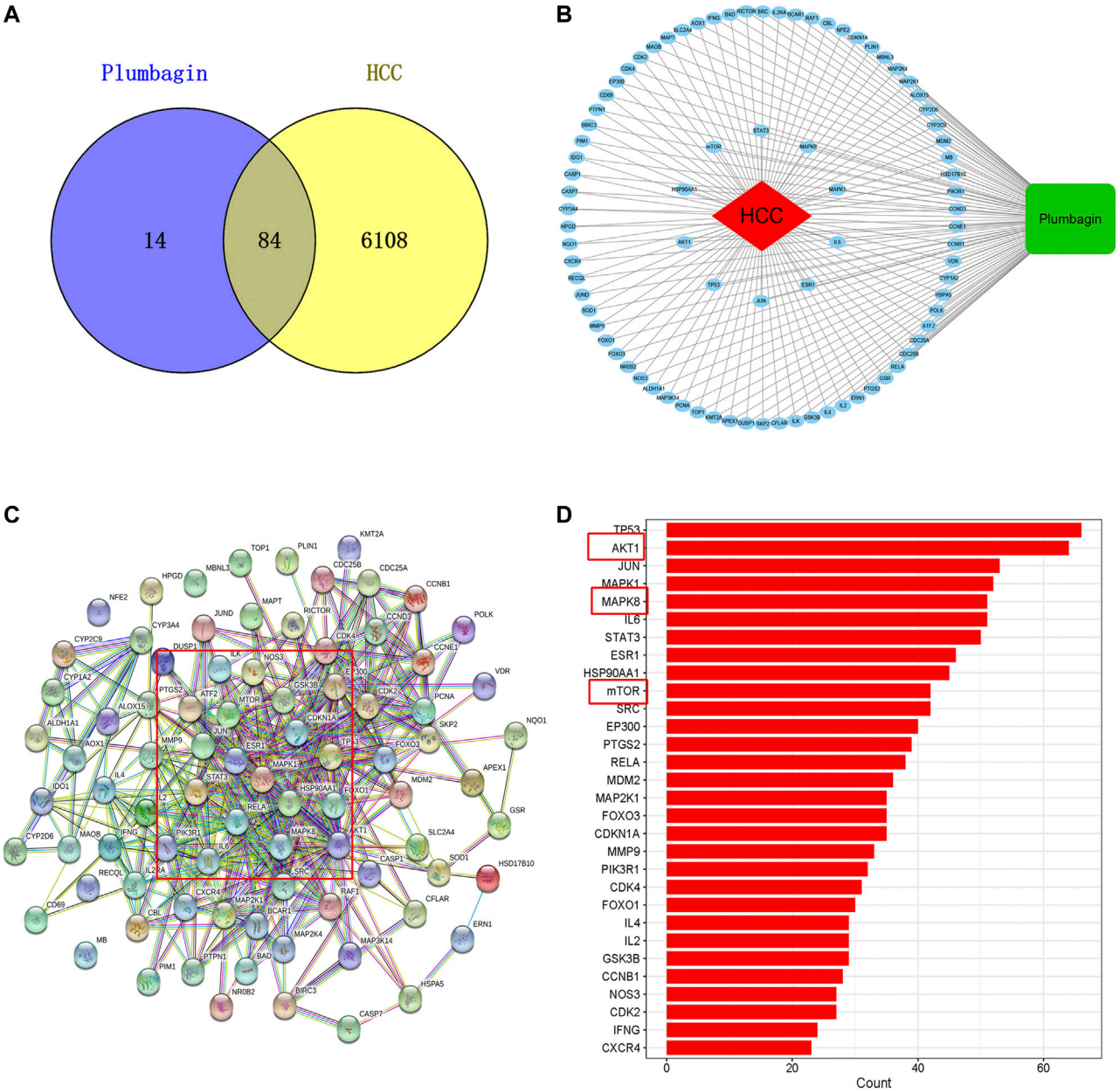

FIGURE 2 | (A) Venn diagram of common targets of plumbagin (PL) in HCC. **(B)** Network of PL targets and HCC targets. The rectangle represents the compound PL, the ellipse represents 84 common targets, and the diamond represents HCC. The protein-protein interaction (PPI) network based on targets of PL in HCC. **(C)** Nodes represent different proteins. Edges represent protein-protein associations, and the line thickness indicates the strength of data support. **(D)** Bar plot of the protein-protein interaction (PPI) network. The X-axis represents the number of neighboring proteins of the target protein. The Y-axis represents the target proteins.

the UniProt database, and after removing the duplicates, 98 targets of PL were obtained; the list of targeted genes is shown in **Supplementary Table S1**. Potential genes related to HCC were collected from GeneCards with the keyword "hepatocellular carcinoma." In addition, the potential targets of HCC were retrieved from the OncoDB.HCC database, and after removing the duplicates, 6192 targets related to HCC were obtained; the list of targeted genes is shown in **Supplementary Table S2**.

Network Construction

Among the 6192 HCC-related targets discovered, 84 targets were common targets corresponding to PL. Through Venny 2.1.0, AKT1, ALDH1A1, MTOR, NR0B2, FOXO3, FOXO1, MMP9, SOD1, JUND, RECQL, CXCR4, NQO1 and other common targets were obtained (**Figure 2A** and **Table 1**). The 84 drug-disease common targets of PL and HCC were input into the Cytoscape 3.7.1 software, and a network diagram of the "component-target-disease" interaction was drawn

TABLE 1 | Common targets between PL and HCC.

Gene name	Gene symbol	Uniprot ID
Histone acetyltransferase p300	EP300	Q09472
Indoleamine 2,3-dioxygenase	IDO1	P14902
Dual specificity phosphatase Cdc25B	CDC25B	P30305
Serine/threonine-protein kinase PIM1	PIM1	P11309
Dual specificity protein phosphatase 1	DUSP1	P28562
Monoamine oxidase B	MAOB	P27338
Glutathione reductase	GSR	P00390
Serine/threonine-protein kinase/endoribonuclease IRE1	ERN1	O75460
Myoglobin	MB	P02144
C-X-C chemokine receptor type 4	CXCR4	P61073
RAC-alpha serine/threonine-protein	AKT1	P31749
Mitogen-activated protein kinase 8	MAPK8	P45983
Superoxide dismutase [Cu-Zn]	SOD1	P00441
Transcription factor NF-E2	NFE2	Q16621
Solute carrier family 2	SLC2A4	P14672
Proto-oncogene tyrosine-protein kinase	SRC	P12931
Cyclin-dependent kinase inhibitor 1	CDKN1A	P38936
DNA topoisomerase I	TOP1	P11387
RAF proto-oncogene serine/threonine-protein kinase	RAF1	P04049
Tumor suppressor p53/oncoprotein Mdm2	TP53	P04637
Vitamin D receptor	VDR	P11473
15-Hydroxyprostaglandin dehydrogenase [NAD+]	HPGD	P15428
78 kDa glucose-regulated protein	HSPA5	P11021
Aldehyde dehydrogenase 1A1	ALDH1A1	P00352
Arachidonate 15-lipoxygenase	ALOX15	P16050
ATP-dependent DNA helicase Q1	RECQL	P46063
Caspase-1	CASP1	P29466
Caspase-7	CASP7	P55210
DNA polymerase kappa	POLK	Q9UBT6
Dual specificity mitogen-activated protein kinase kinase	MAP2K1	Q02750
Endoplasmic reticulum-associated amyloid beta-peptide-binding protein	HSD17B10	Q99714
Microtubule-associated protein tau	MAPT	P10636
Mitogen-activated protein kinase kinase kinase 14	MAP3K14	Q99558
Mitogen-activated protein kinase; ERK1/ERK2	MAPK1	P28482
Nuclear factor NF-kappa-B p65 subunit	RELA	Q04206
Transcription factor AP-1	JUN	P05412
Transcription factor jun-D	JUND	P17535
Estrogen receptor, ER	ESR1	P03372
Dual specificity mitogen-activated protein kinase kinase 4	MAP2K4	P45985
Signal transducer and activator of transcription 3	STAT3	P40763
Tyrosine-protein phosphatase non-receptor type 1	PTPN1	P18031
E3 ubiquitin-protein ligase CBL	CBL	P22681
Nuclear receptor subfamily 0 group B member 2	NR0B2	Q15466
E3 ubiquitin-protein ligase Mdm2	MDM2	Q00987
Serine/threonine-protein kinase mTOR	MTOR	P42345
Heat shock protein HSP 90-alpha	HSP90AA1	P07900
Cyclin-dependent kinase 2	CDK2	P24941
S-phase kinase-associated protein 2	SKP2	Q13309
E3 ubiquitin-protein ligase CCNB1IP1	CCNB1	Q9NPC3
G1/S-specific cyclin-E1	CCNE1	P24864
G1/S-specific cyclin-D3	CCND3	P30281
Cyclin-dependent kinase 4	CDK4	P11802
Glycogen synthase kinase-3 beta	GSK3B	P49841
Cyclic AMP-dependent transcription factor ATF-2	ATF2	P15336
Integrin-linked protein kinase	ILK	Q13418
Rapamycin-insensitive companion of mTOR	RICTOR	Q6R327
Nitric oxide synthase, endothelial	NOS3	P29474
Zinc finger protein Gfi-1	CDKNIA	Q99684
PCNA-associated factor	PCNA	Q15004
Forkhead box protein O3	FOXO3	O43524
Forkhead box protein O1	FOXO1	Q12778
Breast cancer anti-estrogen resistance protein 1	BCAR1	P56945
Baculoviral IAP repeat-containing protein 3	BIRC3	Q13489
Interleukin-6	IL6	P05231

(Continued on following page)

TABLE 1 | (*Continued*) Common targets between PL and HCC.

Gene name	Gene symbol	Uniprot ID
Phosphatidylinositol 3-kinase regulatory subunit alpha	PIK3R1	P27986
Bcl2-associated agonist of cell death	BAD	Q92934
Histone-lysine N-methyltransferase 2A	KMT2A	Q03164
Interleukin-4	IL4	P05112
Early activation antigen CD69	CD69	Q07108
M-phase inducer phosphatase 1	CDC25A	P30304
CASP8 and FADD-like apoptosis regulator	CFLAR	O15519
Matrix metalloproteinase-9	MMP9	P14780
Prostaglandin G/H synthase 2	PTGS2	P35354
DNA-(apurinic or apyrimidinic site) lyase	APEX1	P27695
Perilipin-1	PLIN1	O60240
Muscleblind-like protein 3	MBNL3	Q9NUK0
Interleukin-2	IL2	P60568
Interleukin-2 receptor subunit alpha	IL2RA	P01589
Cytochrome P450 1A2	CYP1A2	P05177
Ubiquinol oxidase 1a	AOX1	Q39219
Cytochrome P450 3A4	CYP3A4	P08684
Cytochrome P450 2C9	CYP2C9	P11712
Cytochrome P450 2D6	CYP2D6	P10635
Interferon gamma	IFNG	P01579
NAD(P)H dehydrogenase [quinone] 1	NQO1	P15559

(**Figure 2B**). The above 84 common targets were entered into the STRING database, and the PPI network of protein interactions was analyzed (**Figure 2C**). The ranking of the top 30 targets is shown in **Figure 2D**.

GO and KEGG Pathway Analyses

GO enrichment analysis was used to further study the biological processes, cellular components and molecular functions of the 84 common targets. As shown in **Figure 3A**, the intersection genes were enriched in 1,560 biological processes, and there were 164 biological processes with a number of enriched genes >10. The results indicated that the top 20 GO items with significant abundance ($p < 0.001$) are mainly related to biological processes such as oxidative stress, reactive oxygen synthesis, cell proliferation, and peptidyl-serine phosphorylation. Intersect gene enrichment analysis of the expression processes of the 27 cell components revealed that they are mainly related to transferase complex, transferring phosphorus-containing groups, transcription factor complex, and membrane raft (**Figure 3B**). The intersection genes were enriched in 100 processes related to molecular function, mainly related to protein serine/threonine kinase activity and phosphatase binding (**Figure 3C**). The above results indicate that PL correlates highly with anticancer activity, and PL may exert anti-HCC effects by participating in oxidative stress and reactive oxygen synthesis, regulating protein kinase phosphorylation.

Furthermore, of the 84 common targets, 78 genes participate in 154 KEGG pathways with adjusted *p*-values <0.01; after sorting the adjusted *p*-values, the top 20 pathways were analyzed (**Figure 3D**). The results show that the common targets of PL and HCC are mainly enriched in the PI3K-Akt, mTOR and MAPK signaling pathways. Then, considering the complex mechanism of PL to treat HCC, a complete "HCC pathway" was constructed by integrating the key pathways obtained through KEGG network analysis, as shown in **Figure 3E**. The results indicate that these integration pathways involve multiple pathophysiological modules, such as cell survival, proliferation, apoptosis, and angiogenesis. The PI3K/AKT pathway is responsible for regulating cell proliferation and apoptosis, and the mTOR/p38 MAPK pathway is responsible for regulating cell autophagy. Therefore, we performed *in vitro* experiments to validate that PL promotes apoptosis and autophagy through the PI3K-Akt/p38 MAPK signaling pathway, thereby explaining the potential therapeutic mechanism of PL in HCC treatment.

Experimental Validation

PL Inhibits HCC Cell Proliferation

The MTT assay was found that PL inhibited BEL-7404 and SMMC-7721 cell proliferation (Lin et al., 2018). And the inhibitory effect of PL on BEL-7404 and SMMC-7721 cell proliferation was concentration- and time-dependent. After treatment with different concentrations of PL (0–10 μM) at three time points (6, 12 and 24 h), the cell proliferation rate decreased significantly ($p < 0.05$). Within the dose range of 3–10 μM, the cell growth inhibition rate reached greater than 50% within 24 h (**Figures 4A,C**). The half-inhibitory concentrations (IC50) of PL on BEL-7404 hepatocellular carcinoma cells were 4.689 μM at 6 h, 2.770 μM at 12 h, and 2.457 μM at 24 h (**Figure 4B**). The half-inhibitory concentrations (IC50) of PL on SMMC-7721 HCC cells were 36.05 μM at 6 h, 5.41 μM at 12 h, and 2.43 μM at 24 h (**Figure 4D**) (Lin et al., 2018).

PL Mediated Reactive Oxygen Generation in HCC Cells

Oxidative stress mediates the pathogenesis of liver cancer. The network pharmacology GO analysis results indicate that PL may mediate oxidative stress by activating the production of ROS and may have an anti-liver cancer effect. In our *in vitro* validation experiments, we treated BEL-7404 and SMMC-7721 cells with PL, the antioxidant NAC and PL+NAC and then detected levels of ROS in the cells using fluorescent probe technology. The results are shown in **Figure 4E**. After PL treatment, ROS expression levels in the two cell groups were significantly increased. Statistical analysis showed that after treatment with PL+NAC antioxidants, ROS expression levels

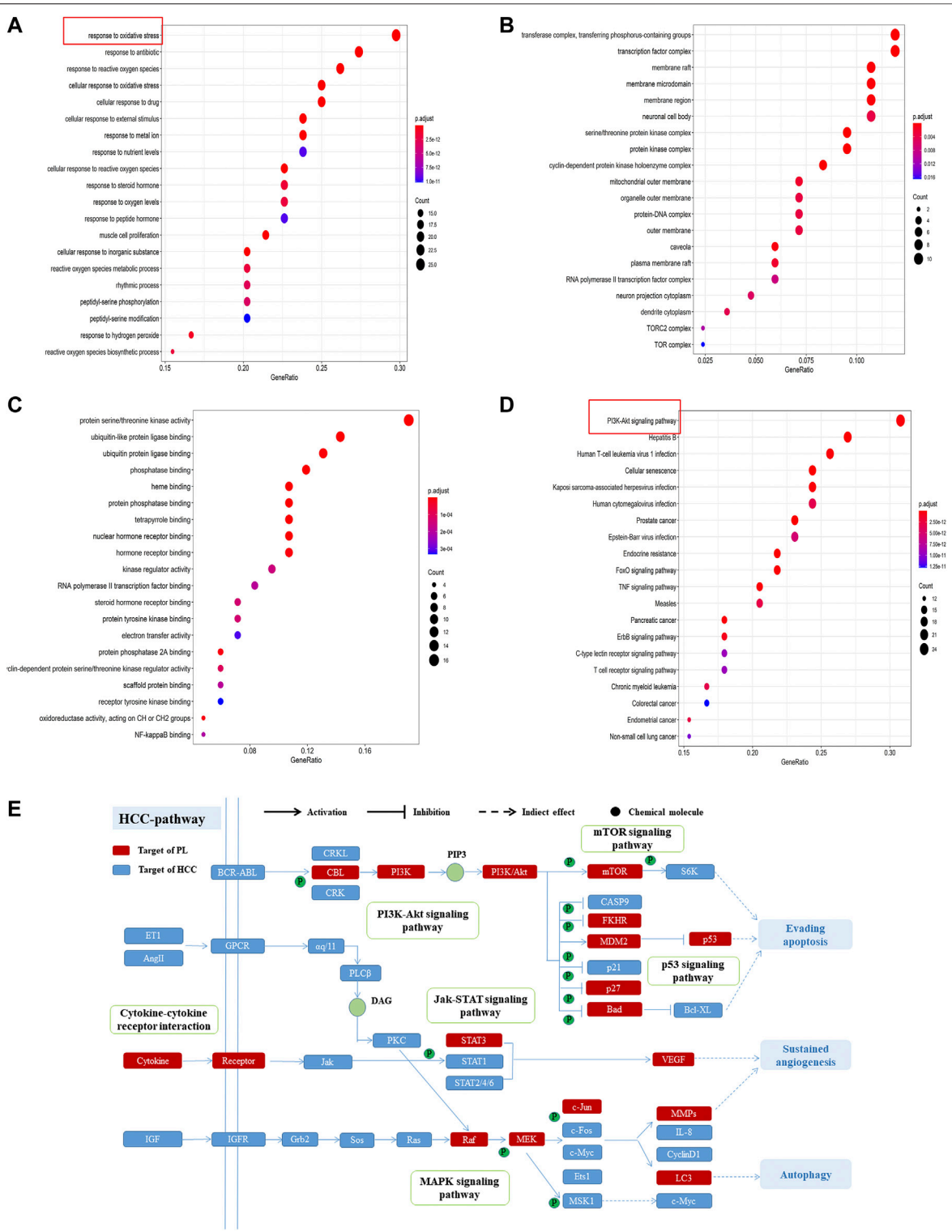

FIGURE 3 | (A) GO enrichment analysis of biological processes of common targets of PL and HCC. The Y-axis represents significant GO biological processes, and the X-axis represents the counts of enriched targets. The gradient of color represents the different adjusted *p* values. **(B)** GO enrichment analysis of cell components of common targets of PL and HCC. The Y-axis represents significant cell components, and the X-axis represents the counts of enriched targets. The gradient of color represents the different adjusted *p* values. **(C)** GO enrichment analysis of the molecular functions of common targets of PL and HCC. The Y-axis represents significant GO molecular functions, and the X-axis represents the counts of enriched targets. The gradient of color represents the different adjusted *p* values. **(D)** KEGG analysis for common targets of PL and HCC. The Y-axis represents significant KEGG pathways, and the X-axis represents the ratio of enriched targets in a pathway to all common targets. The size of the nodes shows the count of targets, and the gradient of color represents the adjusted *p* value. **(E)** Distribution of target proteins of PL on the compressed "HCC pathway." Five pathways form the tubular HCC pathway. Arrows show activation activity, T-arrows show inhibition activity, and segments represent indirect activation effects or inhibition effects.

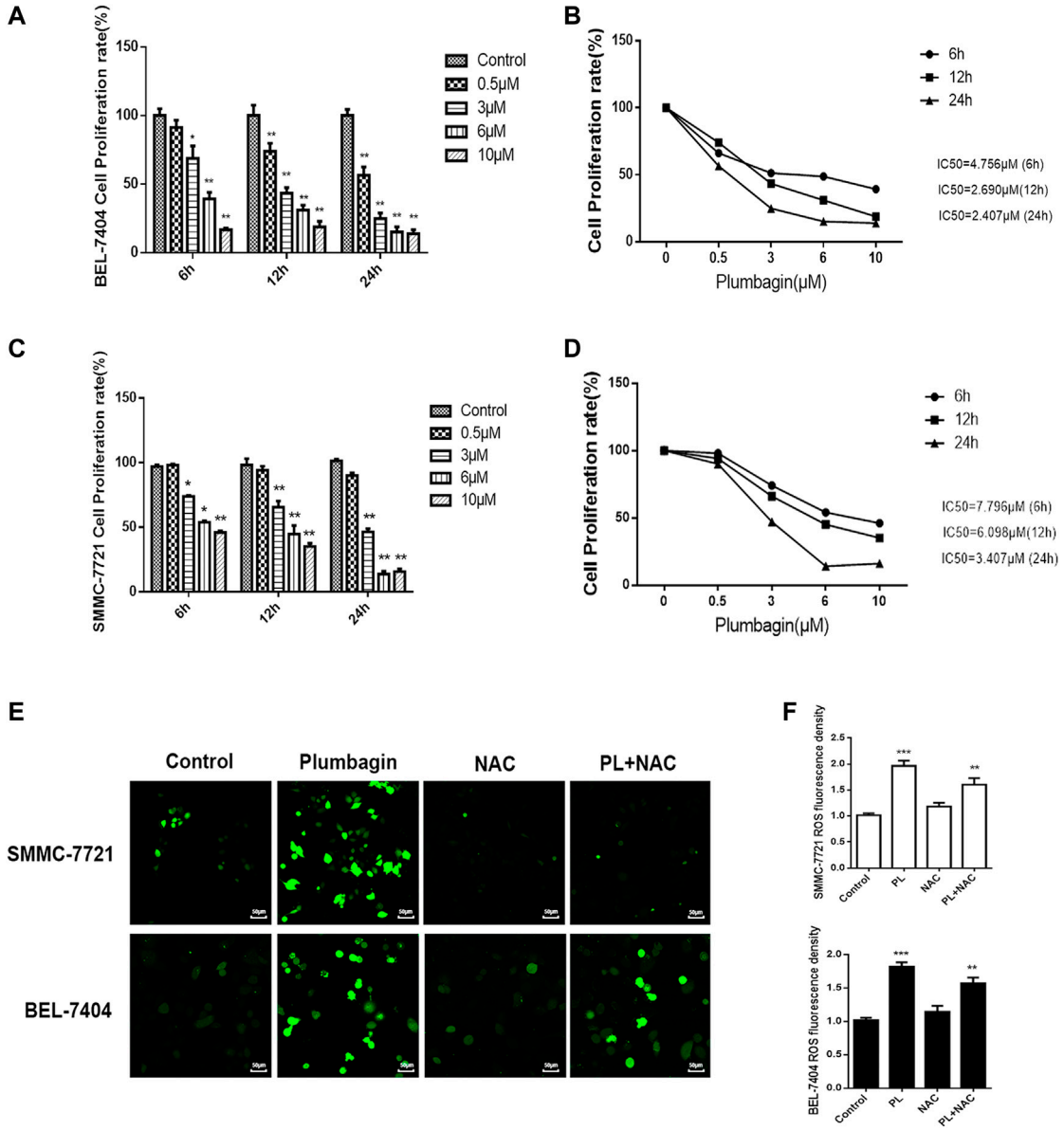

FIGURE 4 | (A) Cell viability of BEL-7404 cells treated with various concentrations of PL (0.5, 3, 6, and 10 μM) for 6, 12 or 24 h *; $p < 0.05$, **; $p < 0.01$ ***; $p < 0.001$, compared with the 0 μM group. **(B)** The 50% inhibitory concentrations (IC50) of BEL-7404 cells were 4.756 μM at 6 h, 2.690 μM at 12 h, and 2.407 μM at 24 h. **(C)** Cell viability of SMMC-7721 cells treated with various concentrations of PL (0.5, 3, 6, and 10 μM) for 6, 12 or 24 h; $p < 0.05$, **; $p < 0.01$ ***; $p < 0.001$, compared with the 0 μM group. **(D)** The 50% inhibitory concentrations (IC50) of SMMC-7721 cells were 7.796 μM at 6 h, 6.098 μM at 12 h, and 3.407 μM at 24 h. **(E)** The production of ROS was measured by DCFH-DA to assess the level of oxidative stress. SMMC-7721 and BEL-7404 cells were pretreated with 10 mM NAC for 30 min and were then treated with 5 μM PL for 24 h, and fluorescence was detected by confocal fluorescence microscopy. Scale bar, 50 μm. **(F)** For statistical analysis, the mean DCFH-DA fluorescence intensity (representing cellular ROS level) was measured from 9 random fields for each culture. All values represent the mean ± SEM of three independent experiments. *$p < 0.05$, **$p < 0.01$ vs. normal control group, respectively.

were lower than in the PL group but higher than in the NAC group (**Figure 4F**). These findings indicate that PL may mediate oxidative stress through the production of ROS and may promote an anti-liver cancer effect.

PL Promotes Apoptosis by Mediating the Generation of ROS in HCC Cells

SMMC-7721 and BEL-7404 cells were subjected to AO/EB staining (Lin et al., 2018). Observation under a fluorescence microscope showed that cells in the PL group emitted green fluorescence after AO staining. The nuclei presented one to several bead-shaped bodies of varying sizes, called apoptotic bodies, which are characterized by smooth and clear edges, and the fluorescence under the excitation of a fluorescence microscope is enhanced and uniform. These findings are consistent with the nuclear morphological features of apoptosis. In addition, the cell membrane may display a "budding" phenomenon. Late apoptotic cells with damaged cell membranes were simultaneously stained by EB and showed the same nuclear morphological characteristics, but the

fluorescence showed orange-red, the green fluorescence of cells in the PL+NAC group decreased after AO staining, and the formation of apoptotic bodies was reduced, while the green fluorescence intensity was stronger than that of the NAC group alone (**Figures 5A,B**). These results indicate that PL may mediate apoptosis through ROS.

Moreover, we used flow cytometry to further verify that PL may mediate apoptosis through ROS. As shown in **Figures 5C,D**, after PL treatment, the percentage of apoptosis increased significantly compared with the control group, mainly with regard to the percentage of late apoptotic cells. The level of apoptosis in the PL+NAC group was significantly reduced. Therefore, these findings further indicate that PL may mediate apoptosis through ROS.

PL Induces Autophagy by Mediating the Production of ROS in HCC Cells

The expression level of the autophagy marker LC3 in BEL-7404 and SMMC-7721 cells after PL treatment was assessed by immunofluorescence detection. As depicted in **Figure 5E**, the red fluorescence of the autophagy marker LC3 in the PL group showed a concentrated state, the fluorescence dot density increased, and the fluorescence intensity increased, indicating that the expression level of LC3 protein increased. In contrast, the fluorescence intensity decreased in the PL+NAC antioxidant group. These findings indicate that PL may induce autophagy by mediating the generation of ROS in HCC cells, thereby playing a role in the treatment of liver cancer.

PI3K/Akt/ and mTOR/p38 MAPK Pathway Verification

Western blotting revealed no significant difference in expression of Akt and mTOR phosphorylated protein in the PL low concentration group compared with the control group in SMMC-7721 cells ($p > 0.05$). After intervention, the medium- and high-concentration groups of PL showed significantly reduced expression of PI3K Akt and mTOR phosphorylated proteins and upregulated expression of p38 MAPK phosphorylated proteins (**Figure 6A**). As shown in **Figure 6B**, when using PI3K, MAPK, Akt, and mTOR as internal reference total proteins for gray value analysis, the difference was statistically significant ($p < 0.05$). For BEL-7404 cells, there was no significant difference in expression levels of PI3K, MAPK, Akt and mTOR phosphorylated proteins in the PL low-concentration group compared with the control group ($p > 0.05$). Additionally, PI3K, Akt, and mTOR phosphorylated protein expression was significantly downregulated in the PL medium- and high-concentration groups, with increased expression of p38 MAPK phosphorylated protein (**Figure 6C**). As shown in **Figure 6D**, the difference was statistically significant when using PI3K, MAPK, Akt, and mTOR as internal reference total proteins for gray value analysis ($p < 0.05$).

PL Promotes Apoptosis Through the PI3K/Akt Signaling Pathway

We employed Western blotting to verify that PL mediates apoptosis through regulation of the PI3K/Akt signaling pathway. The results showed that for the SMMC-7721 liver cancer cell line, expression of phosphorylated Akt was significantly downregulated in the PL group compared with the control group. At the same time, protein expression levels of cleave-caspase 3 and cleave-PARP were upregulated, but caspase 3 and PARP total proteins were decreased, as shown in **Figures 7A,B**. After pretreatment with the Akt agonist SC-79 and apoptosis-targeting Caspase inhibitor Z-VAD-FMK for 1 h followed by PL treatment for 24 h, p-Akt levels increased, and the levels of cleave-caspase 3 and cleave-PARP were reduced; however, caspase 3 and PARP total protein levels remained unchanged. Interestingly, after pretreatment with the Akt inhibitor MEK2206 for 1 h followed by PL incubation for 24 h, there was no significant difference in protein expression levels of p-Akt, cleave-caspase 3 and cleave-PARP compared with the PL treatment group alone.

In the BEL-7404 liver cancer cell line, pretreatment with the Akt agonist SC-79 and the apoptosis-targeting Caspase inhibitor Z-VAD-FMK for 1 h followed by PL treatment for 24 h upregulated p-Akt expression. Protein expression levels of cleave-caspase 3 and cleave-PARP were downregulated, which was consistent with the results for SMMC-7721 cells (**Figures 7C,D**). The above results indicate that PL mediates apoptosis by regulating the PI3K/Akt signaling pathway.

PL Induces Autophagy Through the mTOR/p38 MAPK Signaling Pathway

The experimental results showed that in SMMC-7721 cells, both PL and the autophagy agonist rapamycin upregulated the expression level of the autophagy marker protein LC3 and the phosphorylation level of p-p38 compared with the control group, and the difference was significant. In addition, the autophagy inhibitor 3-MA and the p38 MAPK inhibitors SB202190 and SB203580 jointly interfered in SMMC-7721 cells treated with PL. Compared with the PL treatment alone group, levels of LC3 were significantly downregulated in the p-p383-MA+PL group. These expression levels indicated suppression of PL-induced autophagy. In the SB202190+PL and SB203580+PL groups, LC3 expression was increased, whereas that of p-p38 was significantly decreased (**Figures 8A,B**).

In BEL-7404 cells, expression levels of the autophagy marker protein LC3 in the PL and autophagy agonist rapamycin groups were significantly increased compared with the blank control group. In addition, the autophagy inhibitor 3-MA and the p38 MAPK inhibitors SB202190 and SB203580 acted in BEL-7404 cells treated with PL. Compared with the PL treatment group, the 3-MA+PL group showed significantly decreased levels of LC3 and p-p38. LC3 expression levels were increased in the SB202190+PL and SB203580+PL groups, while p38 phosphorylation expression levels were significantly reduced in the SB203580+PL group (**Figures 8C,D**). The above results indicate that PL may simultaneously upregulate the phosphorylation of the p38 MAPK protein and induce autophagy in HCC cells.

DISCUSSION

HCC is a malignant tumor with high morbidity and mortality in China and worldwide (Orcutt and Anaya, 2018 Jan-Mar). Due to its rapid proliferation and high metastasis and recurrence rates, it is not sensitive to the characteristics of conventional chemotherapy drugs and is prone to drug resistance; thus, treatment of HCC is facing a severe test. Although the current treatments for HCC include surgical resection, arterial intubation chemotherapy, radiotherapy and local treatment, the effects are not satisfactory. Moreover, substantial progress in the diagnosis and treatment of HCC has failed to greatly improve its efficacy. Therefore, international interest in finding new ways to treat HCC is also increasing. The

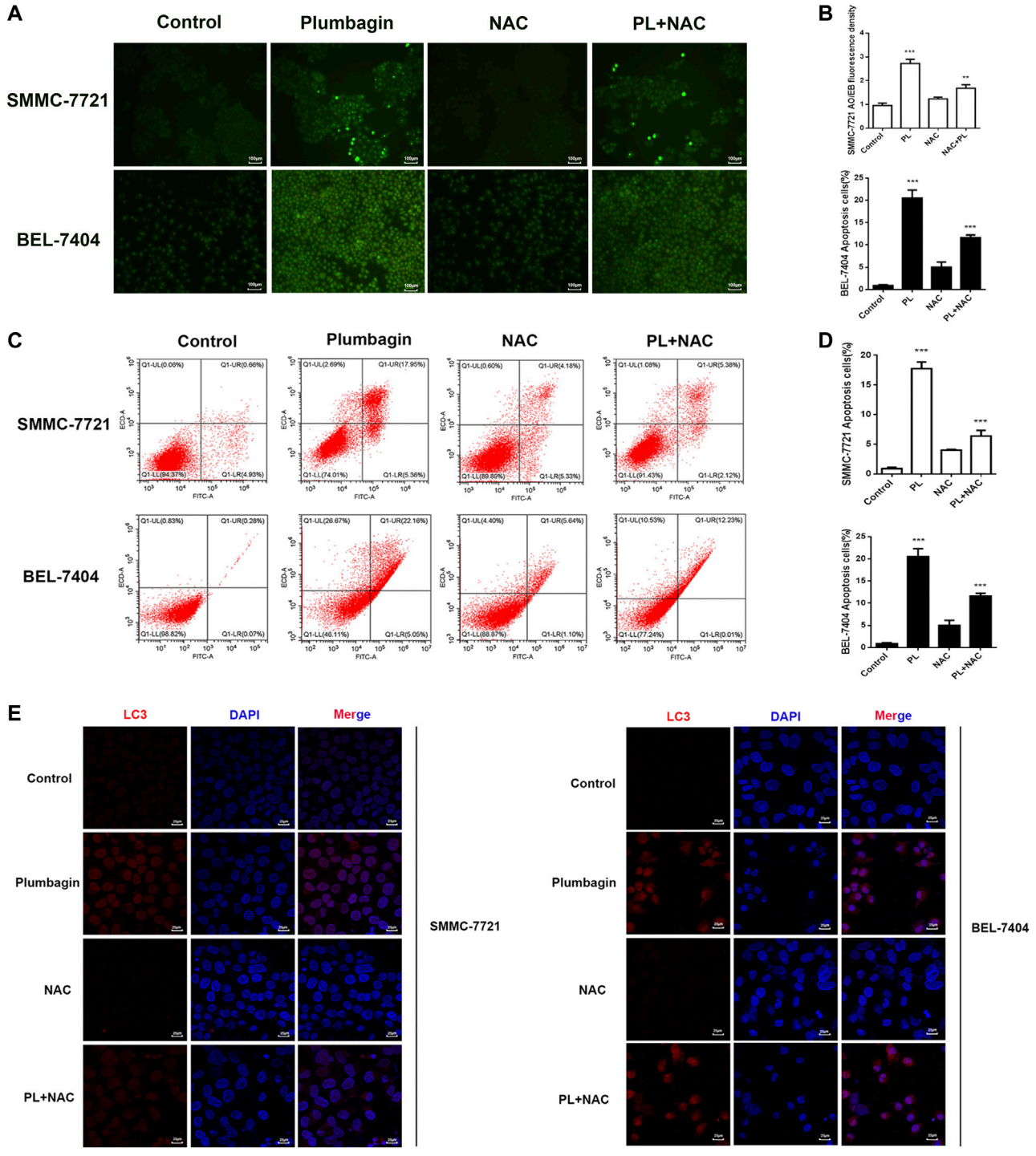

FIGURE 5 | (A) AO/EB staining to detect the formation of PL-induced BEL-7404 cells and SMMC-7721 apoptotic bodies. Scale bar, 100 μm. All data are representative of at least three independent experiments. **(B)** Data were shown as the mean ± SD. *$p < 0.05$, **$p < 0.01$ vs. the normal control group. **(C)** SMMC-7721 and BEL-7404 cells were pretreated with 10 mM NAC for 30 min and were then treated with 5 μM PL for 24 h. Then, the ratio of apoptosis was measured and analyzed by Annexin V-FITC/PI staining and flow cytometry. **(D)** Data are shown as the mean ± SD. *$p < 0.05$, **$p < 0.01$ vs. the normal control group. **(E)** SMMC-7721 and BEL-7404 cells were pretreated with 10 mM NAC for 30 min and were then treated with 5 μM PL for 24 h. Immunofluorescence detection of LC3 expression. The expression of LC3 (red) was significantly higher. The morphology of SMMC-7721 and BEL-7404 cells had a fusiform shape rather than a rounded shape. Cell nuclei were defined by DAPI (blue). Scale bar, 25 μm.

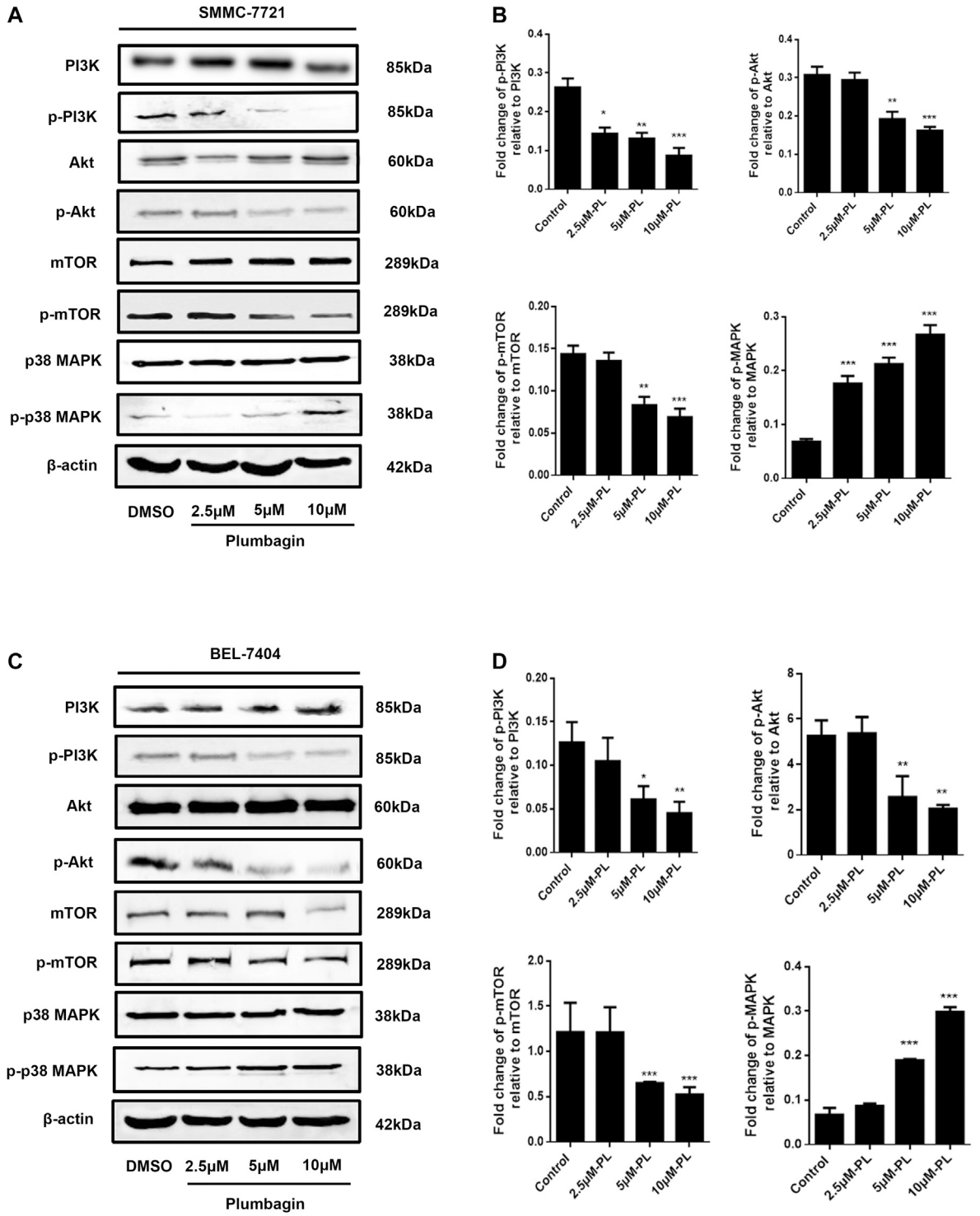

FIGURE 6 | (A) Protein expression levels of PI3K, p-PI3K, Akt, p-Akt, mTOR, p-mTOR, MAPK, and p-MAPK in SMMC-7721 cells measured by Western blot after treatment with various concentrations of PL (0.5, 2.5, 5, and 10 μM). **(B)** PI3K, MAPK, Akt, and mTOR were used as internal reference total proteins for gray value analysis. Each bar represents the mean value ± standard deviation (SD) of the intensity of PL-induced cells across triplicate experiments. $^{*}p < 0.05$, $^{**}p < 0.01$ $^{***}p < 0.001$, compared with the control group. **(C)** Protein expression levels of PI3K, p-PI3K, AKT, p-AKT, mTOR, p-mTOR, MAPK, and p-MAPK in BEL-7404 cells measured by Western blot after treatment with various concentrations of PL (0.5, 2.5, 5, and 10 μM). **(D)** PI3K, MAPK, Akt, and mTOR were used as internal reference total proteins for gray value analysis. Each bar represents the mean value ± standard deviation (SD) of the intensity of PL-induced cells across triplicate experiments. $^{*}p < 0.05$, $^{**}p < 0.01$ $^{***}p < 0.001$, compared with the control group.

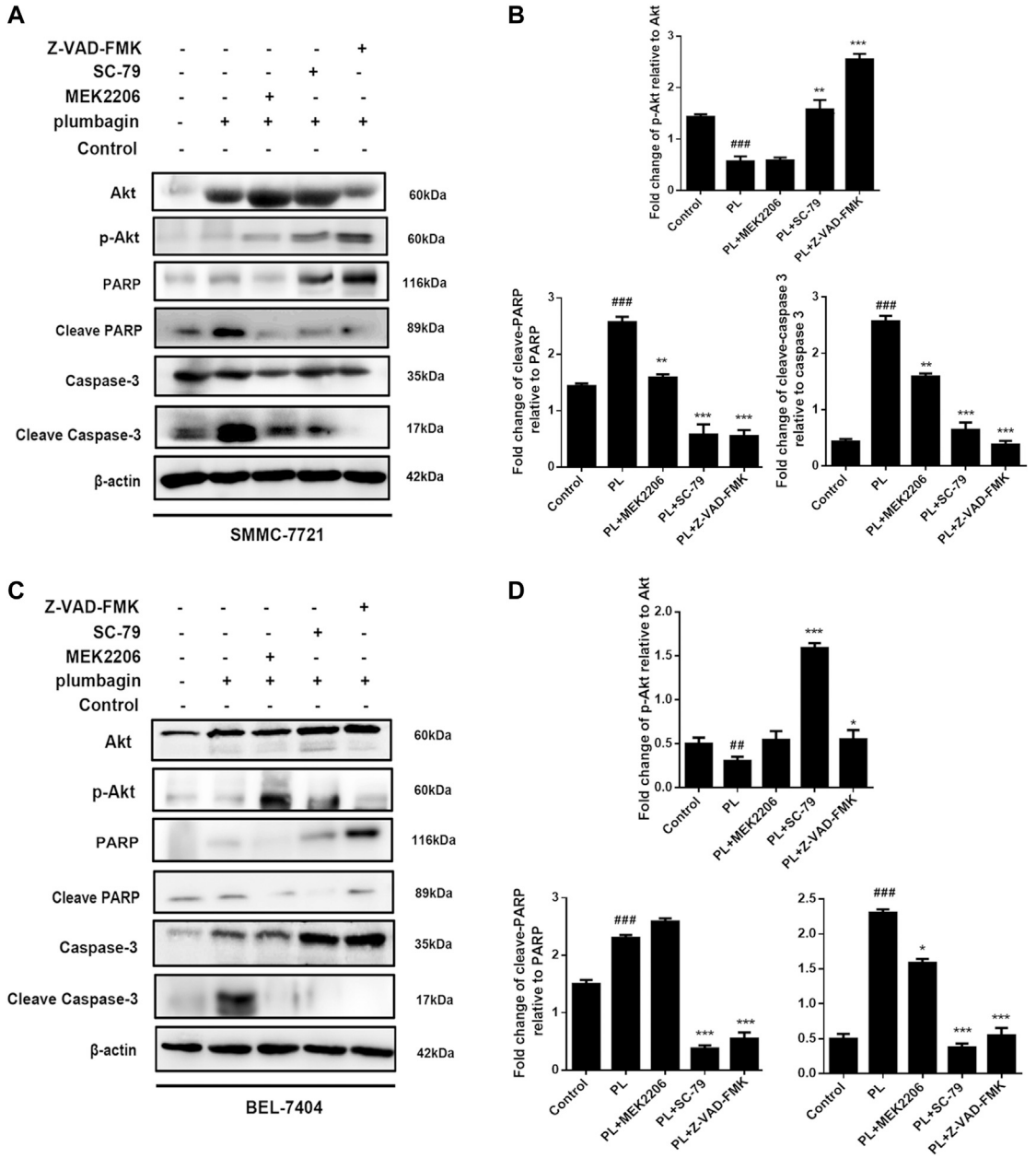

FIGURE 7 | (A) Protein expression levels of p-Akt, Akt, PARP, cleaved PARP, caspase 3, and cleaved caspase 3 in SMMC-7721 cells measured by Western blot after treatment with 5 μM PL, 10 μM SC79 Akt agonist, 10 μM MEK2206 Akt inhibitor and 10 μM Z-VAD-FMK caspase inhibitor. **(B)** p-Akt, Akt, PARP, cleaved PARP, caspase 3, and cleaved caspase 3 were used as internal reference total proteins for gray value analysis. *$p < 0.05$, **$p < 0.01$ ***$p < 0.001$, compared with the PL group. #$p < 0.05$, ##$p < 0.01$ vs. the control group, respectively. **(C)** Protein expression levels of p-Akt, Akt, PARP, cleaved PARP, caspase 3, and cleaved caspase 3 in BEL-7404 cells measured by Western blot after treatment with 5 μM PL, 10 μM SC79 Akt agonist, 10 μM MEK2206 Akt inhibitor and 10 μM Z-VAD-FMK caspase inhibitor. **(D)** p-Akt, Akt, PARP, cleaved PARP, caspase 3, and cleaved caspase 3 were used as internal reference total proteins for gray value analysis. *$p < 0.05$, **$p < 0.01$ ***$p < 0.001$, compared with the PL group. #$p < 0.05$, ##$p < 0.01$ ###$p < 0.001$ vs. the control group.

development and application of new drugs is important for tumor treatment. The search for safe and effective anti-cancer drugs is a major research topic in the treatment of HCC. By exploring the regulation of multichannel signaling pathways, network pharmacology can improve the efficacy of drugs and the success rate of clinical trials, reducing the cost of drug discovery (Zhang et al., 2013). In this study, network pharmacology results from the network databases revealed core gene targets, and we explored the biological functions, pathways, and mechanisms of PL in HCC. The potential targets and signaling pathways of PL acting on HCC were further explored and verified through *in vitro* experiments. These findings indicate that PL is a promising resource with specific therapeutic effects on HCC.

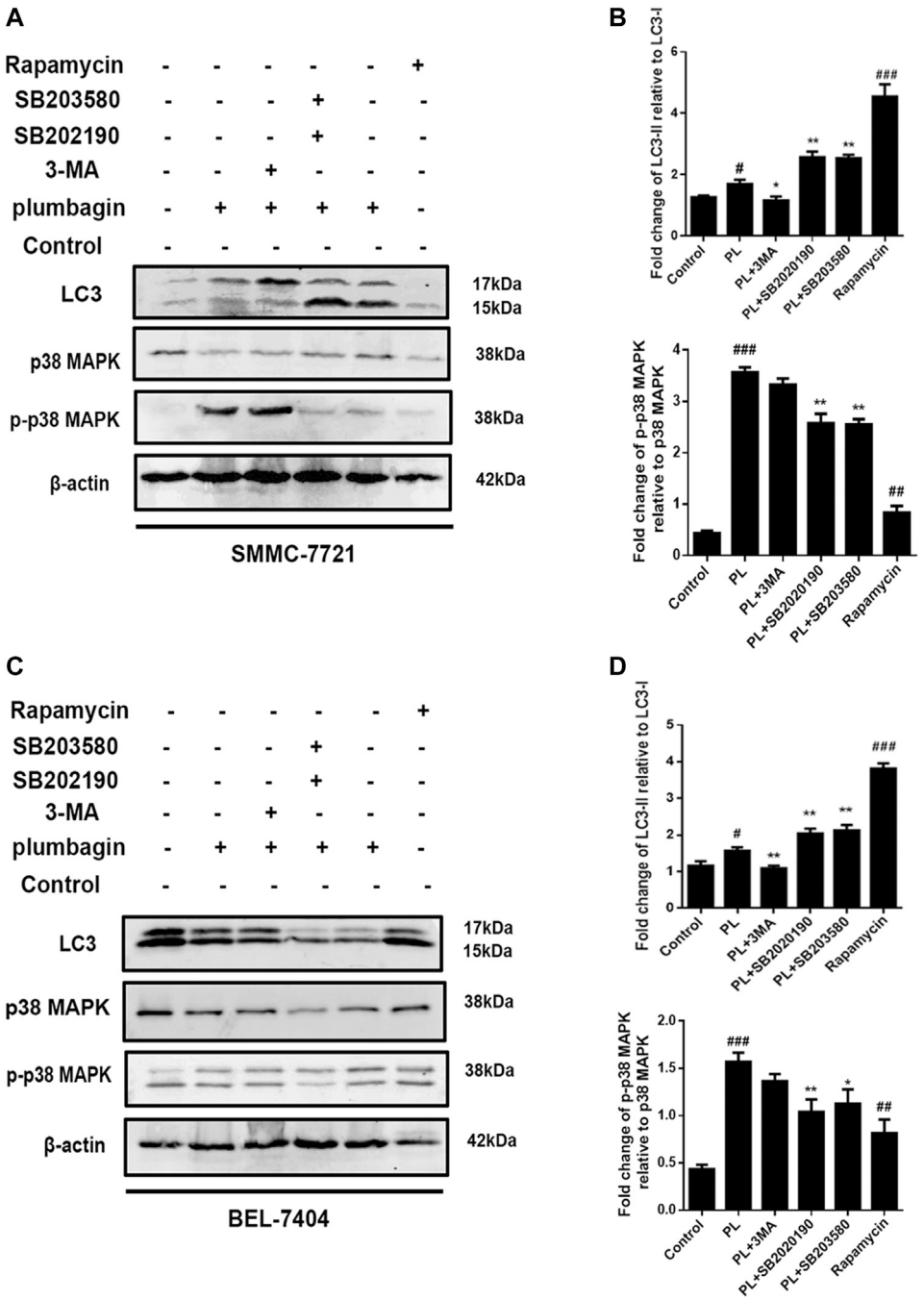

FIGURE 8 | (A) Protein expression levels of LC3-I, LC3-II, p38 MAPK, and p-p38 MAPK in SMMC-7721 cells measured by Western blot after treatment with 5 μM PL, 10 μM 3-MA autophagy inhibitor, 10 μM rapamycin autophagy agonist, 10 μM SB202190, and 10 μM SB203580 p38 MAPK inhibitor. **(B)** LC3-I, LC3-II, p38 MAPK, and p-p38 MAPK were used as internal reference total proteins for gray value analysis. $^{*}p < 0.05$, $^{**}p < 0.01$ $^{***}p < 0.001$, compared with the PL group. $\#p < 0.05$, $\#\#p < 0.01$ $\#\#\#p < 0.001$ vs. the control group. **(C)** Protein expression levels of LC3-I, LC3-II, p38 MAPK, and p-p38 MAPK in BEL-7404 cells measured by Western blot after treatment with 5 μM PL, 10 μM 3-MA autophagy inhibitor, 10 μM rapamycin autophagy agonist, 10 μM SB202190, and 10 μM SB203580 p38 MAPK inhibitor. **(D)** LC3-I, LC3-II, p38 MAPK, and p-p38 MAPK were used as internal reference total proteins for gray value analysis. $^{*}p < 0.05$, $^{**}p < 0.01$ $^{***}p < 0.001$, compared with the PL group. $\#p < 0.05$, $\#\#p < 0.01$ $\#\#\#p < 0.001$ vs. the control group.

In various human cancer cell lines, ROS is involved in autophagy, apoptosis and cell cycle arrest (Zou et al., 2017). Studies have shown that c-Jun induced by ROS is activated and regulated in HeLa cells, leading to apoptosis (Lo and Wang, 2013). In breast cancer MDA-MB-231 and MCF-7 cells, ROS-induced JNK activation induces apoptosis through mitochondrial membrane depolarization (Lebelo et al., 2020). In addition, antioxidant N-acetylcysteine (NAC) restored the depleted GSH contents of the new polyphenol

conjugate DPP-23 in pancreatic cancer MIAPaCa-2 cells, further confirming that apoptosis and oxidation induced by DPP-23 stress are closely related. These findings also show that oxidative stress is an upstream event that induces apoptosis (Shin et al., 2014). Studies have shown that the anticancer effects of PL are mainly related to ROS generation, mitochondrial function, apoptosis and autophagy and related signaling pathways (Zhou et al., 2015). In our study, GO analysis results showed that the biological functions affected by the common targets of PL and HCC are mainly related to oxidative stress and ROS generation, and KEGG pathway analysis showed that the targets are mainly concentrated in the PI3K/Akt/and mTOR/MAPK signaling pathways. Our *in vitro* cell experiments confirmed that PL can mediate the generation of ROS and promote apoptosis. In addition, the phosphorylation levels of PI3K, Akt and mTOR proteins in the PI3K/Akt signaling pathway were downregulated. Our study also found that PL mainly mediates apoptosis through the mitochondrial apoptotic pathway. These results indicate that PL-induced apoptosis of human liver cancer cells is closely related to the increase in intracellular ROS, and ROS may be an upstream factor that regulates the PI3K/Akt/mTOR pathway. The interaction between PL-induced autophagy and apoptosis varies with different cell types, external stimuli and environments. Some studies have suggested that autophagy is a potential partner, antagonist or promoter of apoptosis. Our study found that the autophagy inhibitor 3-MA can attenuate PL-induced apoptosis of HCC cells. Therefore, we speculate that PL-induced autophagy can enhance apoptosis to a certain extent, and when autophagy is weakened by autophagy inhibitors, apoptosis will also be affected.

The p38 MAPK signaling pathway is thought to regulate autophagy. p38 mitogen-activated protein kinase (p38 MAPK) is a well-known kinase that is phosphorylated and participates in amino acid signal transduction in bacterial lipopolysaccharide, heat shock, osmotic stress and other environmental stress responses (Webber, 2010; Gupta et al., 2014). Recent studies have shown interaction between the p38α type of p38 MAPK and a new ATG9 binding partner, p38IP, to control the level of starvation-induced autophagy (Webber and Tooze, 2010). p38 MAPK has a dual role in autophagy: it is both a positive and a negative regulator. Importantly, phosphorylation of p38α leads to increased expression of the autophagy protein marker LC3 (Moruno-Manchón et al., 2013). Our study found that consistency between PL-induced autophagy in HCC cells and the positive effect of p38α in autophagy control. Overall, PL acts on SMMC-7721 and BEL-7404 cells to increase the phosphorylation level of p38α, thereby inducing autophagy.

Studies have also shown that the pyridinimidazole compound SB203580 is an inhibitor of p38 MAPK. It can inhibit the expression of p38 and can induce autophagy when acting on colorectal cancer cells. Prolonged inhibition can lead to cell death with autophagy characteristics (Lim et al., 2006). Our research also found that after co-intervention of the p38 MAPK inhibitors SB203580 and SB202190 with PL, the expression levels of LC3 increased, indicating that the level of autophagy increased. In addition, expression of p-p38/p38 was significantly reduced. These results indicate that using p38 MAPK inhibitors to reduce the phosphorylation levels of p38 can also induce autophagy, suggesting that this may be a potential mechanism that limits the degree of autophagy that cells can withstand and that p38α activity may determine the balance between cell survival and cell death during cell stress. As autophagy is becoming an important factor affecting many neurodegenerative diseases and cancers, p38 in the p38 MAPK signaling pathway may become a clinical target for autophagy control.

CONCLUSION

In conclusion, this study identified key targets of effects of PL against HCC through network pharmacology. *In vitro* experiments were conducted to verify the effective molecular mechanism by which PL targets HCC. This study shows that PL can promote apoptosis and induce autophagy through ROS-mediated PI3K/Akt and mTOR/MAPK signaling pathways and suggests that PL may exert anti-HCC effects through multiple targets and signaling pathways. This study also demonstrates that network pharmacology is of great significance for target screening and pathway prediction of drugs and diseases.

DATA AVAILABILITY STATEMENT

The raw data supporting the conclusions of this article will be made available by the authors, without undue reservation.

AUTHOR CONTRIBUTIONS

DL, YF, YN, and WJ are the major contributors to this manuscript. YN conducted the analysis, wrote the first version of the manuscript, and finalized the manuscript. WJ downloaded the references and developed the graphs and tables in the manuscript. SS and LJ collected the data. DL (corresponding author) conceived and coordinated the study and critically evaluated the data. All authors read and approved the final manuscript.

FUNDING

The authors gratefully acknowledge financial support by the National Natural Science Foundation of China (No. 81760757), the Key projects of Guangxi Natural Science Foundation (2019JJD140032), and the Guangxi first-class discipline construction key project (2018XK020), The second batch of "Qihuang Project" high-level talent team cultivation project of Guangxi University of Traditional Chinese Medicine (2021001).

ACKNOWLEDGMENTS

All the authors thank all the people who helped and provided comments to complete this research.

SUPPLEMENTARY MATERIAL

The Supplementary Material for this article can be found online at: https://www.frontiersin.org/articles/10.3389/fphar.2021.594833/full#supplementary-material.

REFERENCES

Antoine, D., Olivier, M., and Vincent, Z. S. (2019). Updated data and new features for efficient prediction of protein targets of small molecules. *Nucleic Acids Res.*47, W357. doi:10.1093/nar/gkz382

Belghiti, J., and Fuks, D. (2012). Liver resection and transplantation in hepatocellular carcinoma. *Liver Cancer* 1, 71–82. doi:10.1159/000342403

Fang, J., Wang, L., Wu, T., Yang, C., Gao, L., Cai, H., et al. (2017). Network pharmacology-based study on the mechanism of action for herbal medicines in alzheimer treatment. *J. Ethnopharmacol* 196, 281–292. doi:10.1016/j.jep.2016.11.034

Farazi, P. A., and Depinho, R. A. (2006). Hepatocellular carcinoma pathogenesis: from genes to environment. *Nat. Rev. Cancer* 6, 674–687. doi:10.1038/nrc1934

Franco, D., and Usatoff, V. (2001). Resection of hepatocellular carcinoma. *Hepatogastroenterology* 48, 33–36. doi:10.1007/978-1-4615-0547-1_1

Gao, L., Wang, X., Niu, Y., Duan, D., Yang, X., Hao, J., et al. (2016). Molecular targets of Chinese herbs: a clinical study of hepatoma based on network pharmacology. *Sci. Rep.* 6, 24944. doi:10.1038/srep24944

Gupta, J., del Barco Barrantes, I., Igea, A., Sakellariou, S., Pateras, I. S., Gorgoulis, V. G., et al. (2014). Dual function of p38α MAPK in colon cancer: suppression of colitis-associated tumor initiation but requirement for cancer cell survival. *Cancer cell* 25, 484–500. doi:10.1016/j.ccr.2014.02.019

Győrffy, B., Surowiak, P., Budczies, J., and Lánczky, A. (2013). Online survival analysis software to assess the prognostic value of biomarkers using transcriptomic data in non-small-cell lung cancer. *PLOS ONE* 8, e82241. doi:10.1371/journal.pone.0082241

Kohl, M., Wiese, S., and Warscheid, B. (2011). Cytoscape: software for visualization and analysis of biological networks. *Methods Mol. Biol.* 696, 291–303. doi:10.1007/978-1-60761-987-1_18

Lam, W., Jiang, Z., Guan, F., Huang, X., Hu, R., Wang, J., et al. (2015). Phy906(kd018), an adjuvant based on a 1800-year-old Chinese medicine, enhanced the anti-tumor activity of sorafenib by changing the tumor microenvironment. *Sci. Rep.* 5, 9384. doi:10.1038/srep09384

Lebelo, M. T., Joubert, A. M., and Visagie, M. H. (2020). Sulphamoylated estradiol analogue induces reactive oxygen species generation to exert its antiproliferative activity in breast cancer cell lines. *Molecules* 25, 4337. doi:10.3390/molecules25184337

Li, D., Ling, C., and Zhu, D. (2007). [Study on the quantitative evaluation on the degree of TCM basic syndromes often encountered in patients with primary liver cancer]. *Zhongguo Zhong Xi Yi Jie He Za Zhi.* 27, 602–5.

Li, Y., Chang, N., Han, Y., Zhou, M., Gao, J., Hou, Y., et al. (2017). Anti-inflammatory effects of Shufengjiedu capsule for upper respiratory infection via the ERK pathway. *Biomed. Pharmacother.* 94, 758–766. doi:10.1016/j.biopha.2017.07.118

Lim, S. J., Lee, Y. J., and Lee, E. (2006). P38mapk inhibitor sb203580 sensitizes human snu-c4 colon cancer cells to exisulind-induced apoptosis. *Oncol. Rep.* 16, 1131–1135.

Lin, Y., Chen, Y., Wang, S., Ma, J., Peng, Y., Yuan, X., et al. (2018). Plumbagin induces autophagy and apoptosis of smmc-7721 cells *in vitro* and *in vivo*. *J. Cell Biochem.* 120, 9820-9830. doi:10.1002/jcb.28262

Liu, Y., Cai, Y., He, C., Chen, M., and Li, H. (2017). Anticancer properties and pharmaceutical applications of plumbagin: a review. *Am. J. Chin. Med.* 45, 423–441. doi:10.1142/S0192415X17500264

Lo, Y. L., and Wang, W. (2013). Formononetin potentiates epirubicin-induced apoptosis via ros production in hela cells *in vitro*. *Chem. Biol. Interact* 205, 188–197. doi:10.1016/j.cbi.2013.07.003

Marilyn, S., Irina, D., Justin, A., Naomi, R., Tsippi, I. S., Michael, S., et al. (2010). Genecards version 3: the human gene integrator. *Database (Oxford).* 2010, baq020. doi:10.1093/database/baq020

Mathias, D., Stefan, G., Jessica, A., Burghardt, W., and Robert, P. (2008). Superpred: Drug classification and target prediction. *Nucleic Acids Res.* 36 (suppl_2), W55-9. doi:10.1093/nar/gkn307

Moruno-Manchón, J. F., Pérez-Jiménez, E., and Knecht, E. (2013). Glucose induces autophagy under starvation conditions by a p38 mapk-dependent pathway. *Biochem. J.* 449, 497–506. doi:10.1042/bj20121122

Orcutt, S. T., and Anaya, D. A. (2018). Liver resection and surgical strategies for management of primary liver cancer. *Cancer Control* 25, 1073274817744621. doi:10.1177/1073274817744621

Panda, S., and Kamble, A. (2016). Genotypic and seasonal variation of plumbagin content from different populations of plumbago zeylanica L. In India. *Proc. Natl. Acad. Sci., India, Sect. B.* 86, 165–169. doi:10.1007/s40011-014-0432-6

Rolf, A., Amos, B., Wu, C. H., Barker, W. C., Brigitte, B., Serenella, F., et al. (2004). Uniprot: the universal protein knowledgebase. *Nuclc Acids Res.* 32, D115–D119. doi:10.1093/nar/gkh131

Sakamoto, S., Tanizaki, Y., Pongkitwitoon, B., Tanaka, H., and Morimoto, S. (2011). A chimera of green fluorescent protein with single chain variable fragment antibody against ginsenosides for fluorescence-linked immunosorbent assay. *Protein Expr. Purif.* 77, 124–130. doi:10.1016/j.pep.2011.01.010

Shade, A., and Handelsman, J. (2012). Beyond the venn diagram: the hunt for a core microbiome. *Environ. Microbiol.* 14, 4–12. doi:10.1111/j.1462-2920.2011.02585.x

Shannon, P., Markiel, A., Ozier, O., Baliga, N. S., Wang, J. T., Ramage, D., et al. (2003). Cytoscape: a software environment for integrated models of biomolecular interaction networks. *Genome Res.* 13, 2498–2504. doi:10.1101/gr.1239303

Shin, S. Y., Lee, J. M., Lee, M. S., Koh, D., Jung, H., Lim, Y., et al. (2014). Targeting cancer cells via the reactive oxygen species-mediated unfolded protein response with a novel synthetic polyphenol conjugate. *Clin. Cancer Res.* 20, 4302–4313. doi:10.1158/1078-0432.CCR-14-0424

Stoll, H., King, G., and Zeng, L. (2005). Whatif: R software for evaluating counterfactuals. *J. Stat. Softw.* 015. doi:10.18637/jss.v015.i04

Su, M., Guo, C., Liu, M., Liang, X., and Yang, B. (2019). Therapeutic targets of vitamin c on liver injury and associated biological mechanisms: a study of network pharmacology. *Int. Immunopharmacol* 66, 383–387. doi:10.1016/j.intimp.2018.11.048

Su, W., Chao, C., Yeh, S., Chen, D., Chen, P., and JouOncodb, Y. (2007). OncoDB.HCC: an integrated oncogenomic database of hepatocellular carcinoma revealed aberrant cancer target genes and loci. *Nucleic Acids Res.* 35, D727–D731. doi:10.1093/nar/gkl845

Subramaniya, B. R., Srinivasan, G., Sadullah, S. S., Davis, N., Subhadara, L. B., Halagowder, D., et al. (2011). Apoptosis inducing effect of plumbagin on colonic cancer cells depends on expression of cox-2. *PLOS ONE.* 6, e18695. doi:10.1371/journal.pone.0018695

Szklarczyk, D., Morris, J. H., Cook, H., Kuhn, M., Wyder, S., Simonovic, M., et al. (2016a). The STRING database in 2017: quality-controlled protein-protein association networks, made broadly accessible. *Nucleic Acids Res.* 45, D362–D368. doi:10.1093/nar/gkw937

Szklarczyk, D., Santos, A., Von Mering, C., Jensen, L. J., Bork, P., and Kuhn, M. (2016b). Stitch 5: augmenting protein-chemical interaction networks with tissue and affinity data. *Nucleic Acids Res.* 44, D380–D384. doi:10.1093/nar/gkv1277

Tian, L., Yin, D., Ren, Y., Gong, C., Chen, A., and Guo, F. (2011). Plumbagin induces apoptosis via the p53 pathway and generation of reactive oxygen species in human osteosarcoma cells. *Mol. Med. Rep.* 5, 126–132. doi:10.3892/mmr.2011.624

Tilak, J. C., Adhikari, S., and Devasagayam, T. P. (2004). Antioxidant properties of plumbago zeylanica, an indian medicinal plant and its active ingredient, plumbagin. *Redox Rep.* 9, 219–227. doi:10.1179/135100004225005976

Webber, J. L. (2010). Regulation of autophagy by p38alpha MAPK. *Autophagy* 6, 292–293. doi:10.4161/auto.6.2.11128

Webber, J. L., and Tooze, S. A. (2010). Coordinated regulation of autophagy by p38alpha MAPK through mAtg9 and p38IP. *EMBO J.* 29, 27–40. doi:10.1038/emboj.2009.321

Wei, Y., Lv, B., Xie, J., Zhang, Y., Lin, Y., Wang, S., et al. (2019). Plumbagin promotes human hepatoma smmc-7721 cell apoptosis via caspase-3/vimentin signal-mediated Emt. *Drug Des Devel Ther.* Vol. 13, 2343–2355. doi:10.2147/dddt.s204787

Zhang, G. B., Li, Q. Y., Chen, Q. L., and Su, S. B. (2013). Network pharmacology: a new approach for Chinese herbal medicine research. *Evid. Based Complement. Alternat Med.* 2013, 621423–621429. doi:10.1155/2013/621423

Zhong, J., Li, J., Wei, J., Huang, D., Huo, L., Zhao, C., et al. (2019). Plumbagin restrains hepatocellular carcinoma angiogenesis by stromal cell-derived factor (sdf-1)/cxcr4-cxcr7 axis. *Med. Sci. Monit.* 25, 6110–6119. doi:10.12659/MSM.915782

Zhou, Z. W., Li, X. X., He, Z. X., Pan, S. T., Yang, Y., Zhang, X., et al. (2015). Induction of apoptosis and autophagy via sirtuin1- and PI3K/Akt/mTOR-mediated pathways by plumbagin in human prostate cancer cells. *Drug Des. Devel Ther.* 9, 1511. doi:10.2147/DDDT.S75976

Zou, Z., Chang, H., Li, H., and Wang, S. (2017). Induction of reactive oxygen species: an emerging approach for cancer therapy. *Apoptosis* 22, 1321–1335. doi:10.1007/s10495-017-1424-9

Conflict of Interest: The authors declare that the research was conducted in the absence of any commercial or financial relationships that could be construed as a potential conflict of interest.

frontiers in Pharmacology

REVIEW
published: 07 May 2021
doi: 10.3389/fphar.2021.639628

Phytochemicals as a Complement to Cancer Chemotherapy: Pharmacological Modulation of the Autophagy-Apoptosis Pathway

Md. Ataur Rahman[1,2†], Md. Abdul Hannan[3,4†], Raju Dash[3], MD. Hasanur Rahman[5,9], Rokibul Islam[7,8], Md Jamal Uddin[6,9], Abdullah Al Mamun Sohag[4], Md. Habibur Rahman[10] and Hyewhon Rhim[1,11*]*

[1]Center for Neuroscience, Korea Institute of Science and Technology (KIST), Seoul, South Korea, [2]Global Biotechnology & Biomedical Research Network (GBBRN), Department of Biotechnology and Genetic Engineering, Faculty of Biological Sciences, Islamic University, Kushtia, Bangladesh, [3]Department of Anatomy, Dongguk University College of Medicine, Gyeongju, South Korea, [4]Department of Biochemistry and Molecular Biology, Bangladesh Agricultural University, Mymensingh, Bangladesh, [5]Department of Biotechnology and Genetic Engineering, Bangabandhu Sheikh Mujibur Rahman Science and Technology University, Gopalganj, Bangladesh, [6]ABEx Bio-Research Center, Dhaka, Bangladesh, [7]Department of Biotechnology and Genetic Engineering, Faculty of Biological Sciences, Islamic University, Kushtia, Bangladesh, [8]Department of Biochemistry, College of Medicine, Hallym University, Chuncheon-si, South Korea, [9]Graduate School of Pharmaceutical Sciences, College of Pharmacy, Ewha Womans University, Seoul, South Korea, [10]Department of Global Medical Science, Wonju College of Medicine, Yonsei University, Seoul, South Korea, [11]Division of Bio-Medical Science and Technology, KIST School, Korea University of Science and Technology (UST), Seoul, South Korea

Bioactive plant derived compounds are important for a wide range of therapeutic applications, and some display promising anticancer properties. Further evidence suggests that phytochemicals modulate autophagy and apoptosis, the two crucial cellular pathways involved in the underlying pathobiology of cancer development and regulation. Pharmacological targeting of autophagy and apoptosis signaling using phytochemicals therefore offers a promising strategy that is complementary to conventional cancer chemotherapy. In this review, we sought to highlight the molecular basis of the autophagic-apoptotic pathway to understand its implication in the pathobiology of cancer, and explore this fundamental cellular process as a druggable anticancer target. We also aimed to present recent advances and address the limitations faced in the therapeutic development of phytochemical-based anticancer drugs.

Keywords: phytochemicals, pharmacology, apoptosis, autophagy, anticancer

OPEN ACCESS

Edited by:
Supratik Kar,
Jackson State University,
United States

Reviewed by:
Prakash P. Praharaj,
National Institute of Technology Rourkela, India
Natália Cruz-Martins,
Universidade do Porto, Portugal
Sujit Kumar Bhutia,
National Institute of Technology Rourkela, India

***Correspondence:**
Md. Ataur Rahman
ataur1981rahman@hotmail.com
Hyewhon Rhim
hrhim@kist.re.kr

†These authors have contributed equally to this work

Specialty section:
This article was submitted to Ethnopharmacology, a section of the journal Frontiers in Pharmacology

Received: *09 December 2020*
Accepted: *18 March 2021*
Published: *07 May 2021*

Citation:
Rahman MA, Hannan MA, Dash R, Rahman MDH, Islam R, Uddin MJ, Sohag AAM, Rahman MH and Rhim H (2021) Phytochemicals as a Complement to Cancer Chemotherapy: Pharmacological Modulation of the Autophagy-Apoptosis Pathway. Front. Pharmacol. 12:639628. doi: 10.3389/fphar.2021.639628

INTRODUCTION

Cancer is responsible for 9.6 million deaths in 2018 and is listed as the second leading cause of death globally. Cancer thus poses a pivotal public health concern worldwide (WHO, 2018). During the 20th century, the cancer death rate was found to markedly increase, primarily because of abnormal lifestyles, such as excessive tobacco use (Siegel et al., 2020), physical and chemical carcinogens (Bhatia et al., 2020), alcohol use (Sanford et al., 2020), unhealthy diet (Khaltaev and Axelrod, 2020), and biological carcinogens (Hartwig et al., 2020). Delaying cancer treatment initiation increases patient mortality (Hanna et al., 2020). However, increased awareness about the need for lifestyle modification, early detection, and treatment may have contributed to a decline in cancer prevalence (i.e., by 1.5%, on average, per year from 2013 to 2017) (Henley et al., 2020). Cancer treatment options,

such as chemotherapy, radiation therapy, hormone therapy, gene therapy, immunotherapy, photodynamic therapy, targeted therapy, surgery, palliative care, and a combination of these, are increasing in both number and efficiency across multiple types of cancer and for various patients (Markham et al., 2020). The main goal of cancer therapy is to stimulate the death of abnormal cells and preserve normal cells (Schirrmacher, 2019). Chemotherapy is the backbone of many cancer treatments. It aids in the reduction of tumor size and kills cancer cells at primary sites or metastasizing sites (Sak, 2012; Alfarouk et al., 2015). However, response to treatment varies substantially according to the type of cancer or even with the same type of cancer (Sak, 2012). Resistance to chemotherapeutic agents poses a major problem in cancer treatment, ultimately limiting the efficiency of anticancer drugs, which causes therapeutic failure and eventually death (Alfarouk et al., 2015). Chemotherapy resistance can be attributed to numerous mechanisms, including multi-drug resistance, alterations of cell death mechanisms (autophagy and apoptosis), changes in drug metabolism, epigenetic and drug targets, enhanced DNA repair and gene amplification, tumor cell heterogeneity, drug efflux and metabolism, and tumor microenvironment stress-induced genetic or epigenetic alterations as a cellular response to drug exposure (Wang et al., 2019). Among these mechanisms, alterations in autophagy ('self-eating') and apoptosis ('self-killing'), which are two self-destructive processes that have propelled scientific innovation, are the vital causes of chemotherapy resistance (Thorburn et al., 2014). Autophagy, an evolutionarily conserved and regulated cellular recycling mechanism, has emerged as a key player in metabolic and therapeutic stresses. In fact, this mechanism attempts to maintain or restore metabolic homeostasis via the catabolic degradation of unnecessary proteins and injured or aged organelles (Santana-Codina et al., 2017). The role of autophagy in cancer treatment is paradoxical; it may act as a pro-survival or pro-death mechanism to counteract or mediate the cytotoxic effect of anticancer agents (Santana-Codina et al., 2017). Autophagy primarily functions as a tumor suppressor by modulating reactive oxygen species (ROS) within cells and maintaining genetic instability (Levine and Kroemer, 2008). Moreover, accumulating evidence suggests that faulty autophagy is linked to malignant transformation of cancer stem cells (Moosavi et al., 2018). Under these conditions, autophagy stimulation might be a critical approach to halt early tumor formation and development (Moosavi et al., 2018). However, autophagy can promote the growth and survival of current tumors during migration and epithelial-to-mesenchymal transition. Further, this process can help cancer stem cells escape immune surveillance and make cancer cells resistant to anoikis (Moosavi et al., 2018; Rahman et al., 2020). In this regard, inhibition of autophagy increases chemotherapy-induced cytotoxicity. Therefore, autophagy, a double-edge sword that works in a context-dependent manner, blocks the early stages of tumorigenesis while becoming a driver of tumor invasion and metastasis at later stages (Moosavi et al., 2018). The molecular mechanisms regulating the switch between these different modes of action are poorly understood (Kardideh et al., 2019). Nonetheless, the interplay between apoptosis and autophagy can be leveraged to improve cancer therapy (Tompkins and Thorburn, 2019). Cancer cells become chemotherapy-resistant by escaping some of the potential apoptotic mechanisms, such as downregulated pro-apoptotic signals, upregulated anti-apoptotic signals, and faulty apoptosis initiation and implementation. However, the functional relationship between apoptosis and autophagy is complex and has recently been deciphered at the molecular level. Therefore, modulating the key factors in the autophagic and apoptotic pathways may be a novel therapeutic strategy for enhancing chemotherapy efficiency.

The potential roles of phytochemicals in the modulation of autophagy and apoptosis have recently been reviewed (Deng et al., 2019). However, autophagy and apoptosis induction and/or inhibition are extremely complex processes that require thorough exploration. Nevertheless, a better understanding of the crosstalk between autophagy and apoptosis will enable further developments of novel anticancer therapeutic strategies. In this review, we summarize the molecular mechanisms of autophagy and apoptosis in cancer. Given the pivotal role of phytochemicals in cancer therapy, we sought to discuss various phytochemicals that could regulate autophagy and apoptosis-related signaling pathways to enhance cancer chemotherapy outcomes.

METHODS

A literature-based search was accomplished to collect published databases and relevant methodological contributions of the molecular mechanism of phytochemicals in autophagy-apoptosis modulation and cancer prevention has been conducted using PubMed, Scopus, Google Scholar, Web of Science, and Google that includes all original research articles written in English on multifunctional role of phytochemicals. Searching was conducted using various keywords including autophagy, apoptosis, natural compounds, cancer, phytochemical, neurodegenerative diseases, solid tumors and lymphomas, heart/cardiovascular diseases, perspectives role autophagy in cancer therapy and so on. All figures were generated using Adobe Illustrator software.

MOLECULAR MECHANISM OF AUTOPHAGY IN CANCER

Autophagy is a cellular process that breaks down or degrades unwanted or aggregated dysfunctional cellular components through fusion with lysosomes; this cellular process is known to play an essential role in maintaining cellular function as well as homeostasis (Krishnan et al., 2020). Autophagy preserves an active interlink in cell defense as well as a cytostatic link in cancer cell progression (Rahman and Rhim, 2017). Generally, the process of autophagy might be introduced by the generation of pre-autophagosomal structures known as phagophore assembly sites (PAS) (Hurley and Young, 2017; Rahman and Rhim, 2017). Phosphatidylinositol 3-phosphate (PI3K), which is associated with

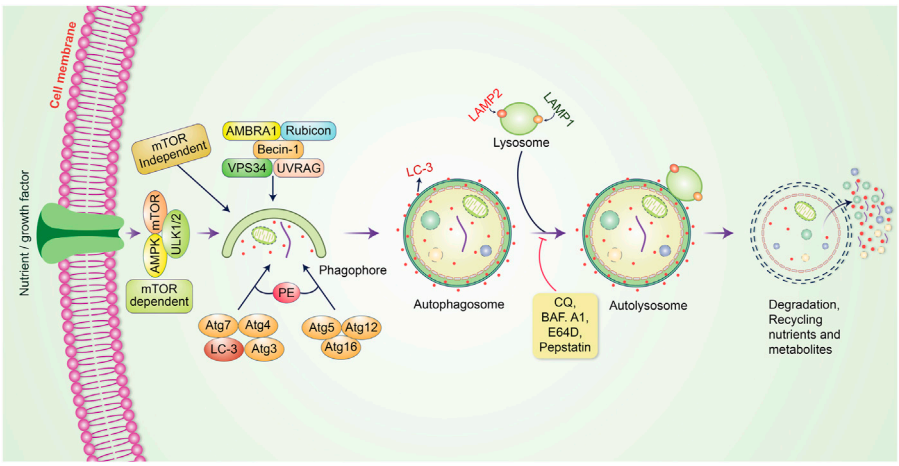

FIGURE 1 | Molecular mechanism of the autophagic pathway. Autophagy is initiated by the formation of a pre-autophagosomal structure. PI3K-AMPK and mammalian target of rapamycin (mTOR) contribute to the formation of the pre-autophagosomal structure. ULK1, Vps34 and the Beclin-1 complex help to activate phagophore formation. After phagophore nucleation is elongated, subsequent binding to autophagosome occurs. Binding between mature autophagosome and lysosome results in autolysosome formation. Finally, autolysosomes are eliminated through acid hydrolases, which produce nutrients and recycling metabolites.

the endoplasmic reticulum (ER), plays an essential role in the initiation of PAS formation (Kotani et al., 2018). AMP-activated protein kinase (AMPK), mammalian target of rapamycin (mTOR), and unc-51 like autophagy activating kinase-1 (ULK1) have been demonstrated to facilitate phagophore formation during autophagy induction (Alers et al., 2012), with Vps34, Vps15/p150, and Beclin-1 as recruiters for phagophore formation (Velazquez and Jackson, 2018). After phagophores are formed, phagocytosis occurs. This process is subsequently followed by expansion and sealing to elongate the membrane for autophagosome formation (Rubinsztein et al., 2012). Mature autophagosomes bind to lysosomes, resulting in autolysosome formation (Kardideh et al., 2019). Eventually, autolysosomes containing inner cargos are degraded by acid hydrolases and produce nutrients; other recycling metabolites subsequently preserve cellular homeostasis (**Figure 1**). The fate of cancer cells is thus dependent on autophagy (Wei and Huang, 2019). Autophagy decides whether the cancer is suppressed or promoted under certain conditions. mTOR plays an important role in protecting or activating oncogenic cells through the induction of autophagy. However, chemotherapy drugs have been found to suppress tumor cells by modulating autophagic pathways. Furthermore, inhibition of this pathway regulates cancer progression, and the influence of autophagy becomes either a cellular survival or death function (Jung et al., 2020). The metabolism of malignant cells is intensely altered to retain their proliferation and survival under adverse microenvironmental conditions. Autophagy plays an essential role in maintaining metabolic adaptations in cancer cells (Goldsmith et al., 2014). Although autophagy is recognized to sustain neoplastic cell metabolism under stress, the mutual association between cancer cell metabolism and autophagy remains unknown. mTOR and AMPK have been identified as the main signaling components that modulate autophagy via the regulation of amino acid and glucose levels (Alers et al., 2012). However, specific metabolites, ROS, growth factors, palmitate, oxygen concentration, ATP to ADP ratio, specific amino acid levels, and oncogenes regulate autophagy initiation and autophagosome formation. Further, they regulate this fine balance by assimilating these autophagy-related signals in cancer (Singh and Cuervo, 2011; Panda et al., 2015). Prominently, autophagy has been frequently identified to play a "dual role" as it can either hinder or stimulate cancer initiation and progression (Patra et al., 2020; Rahman et al., 2020a). In the present review, we outline the dual role of autophagy in tumorigenesis and emphasize our recent understanding of autophagy regulation of cancer cell activation and metabolism to control tumor growth and progression.

MOLECULAR MECHANISM OF APOPTOSIS IN CANCER

Apoptosis or programmed cell death is one of the predominant strategies for blocking or avoiding cancer or cancer formation (Lopez and Tait, 2015). Focusing on apoptosis is most effective for different cancer types because escaping apoptosis is a trademark of cancer and is indifferent to the type of cancer. Apoptosis is generally a central pathway that is associated with intrinsic and extrinsic pathways (Elmore, 2007). However, these extrinsic and intrinsic pathways could be involved in the same station, which is known as the execution pathway (Goldar et al., 2015) (**Figure 2**). To initiate apoptosis in apoptotic cells, the extrinsic pathway uses extracellular signals to induce apoptosis *via* stimulation of Fas ligand, tumor necrosis factor (TNF), and TNF-related apoptosis-inducing ligand (TRAIL), which interact with the extracellular transmembrane domain of death receptors (DR) (Guicciardi and Gores, 2009). Finally, caspases participate in the extrinsic pathway and are generally typified as starter, stimulator, or executioner caspases owing to their involvement and participation in the apoptotic signaling pathways. The intrinsic apoptotic pathway is directly involved in mitochondria-mediated proteins. Different stimuli, such as adequate Ca^{2+}, impaired DNA molecules,

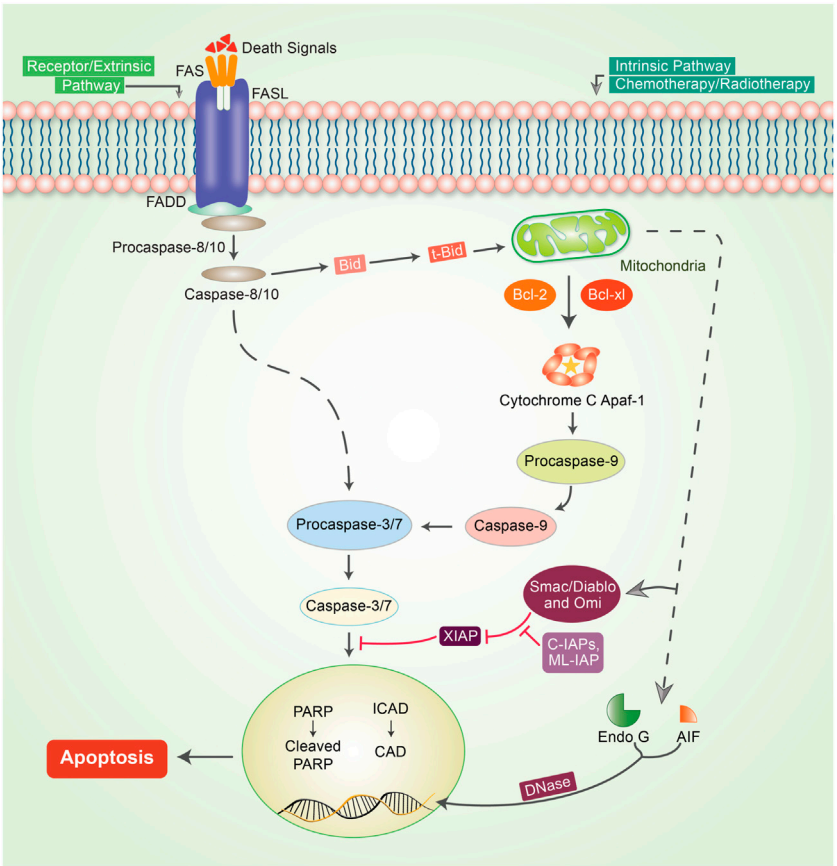

FIGURE 2 | Mechanism of the apoptotic pathway in cancer. To initiate apoptosis, two central pathways are involved in this mechanism: the intrinsic pathway and extrinsic pathway. The extrinsic pathway of apoptosis is well defined by the TNF-α/TNFR1 and FasL/FasR models. Herein, the death receptor is induced by an adaptor protein; adaptor proteins are comprised of FADD (Fas-associated death domain) and TRADD (TNF receptor-associated death domain). The signaling that occurs through the extrinsic pathway causes the attachment of DRs to specific death ligands (DLs), thereby forming a death-inducing signaling cascade (DISC). The complex pathway of caspase-8 activation follows a predefined system that actively enables caspase-8 to detach from the DISC, whether or not the pro-domain of caspase-8 is retained as part of the DISC to initiate the signaling phases of apoptosis. However, in most apoptotic cells, proteins are customarily engaged in intrinsic phases that involve caspase-9, SMAC/DIABLO, Bcl-2, Bcl-w, Aven, Nox, and MYC. Mitochondrial dysfunction is followed by the loss of inner membrane mitochondrial potential, adequate formation of superoxide ions, impaired mitochondrial biogenesis formation, release of intra-membrane proteins, and matrix calcium glutathione burst, which enumerate the important potential for cancer therapeutic strategies by triggering the intrinsic phases of apoptosis in tumor cells. The execution phase of apoptosis initiator caspases, such as caspase-8/-9 or caspase-activated dnase (CAD), Poly (ADP-ribose polymerase (PARP), and other caspases such as caspase-3, -6, -7, and caspase-10, are typified as upregulator or executioner caspases. Caspase-3 is the most essential and effective of all effector caspases because it can be activated by all initiator caspases.

oxidative stress (OS), surplus oxidants, deprivation of growth factors, and drug treatment and irradiation, have been associated with this pathway (Ghavami et al., 2004; Hassan et al., 2020). When Bax/Bak is incorporated into the mitochondrial membrane, it triggers the release of cytochrome c from the mitochondrial inner membrane into the cytosol (Kim, 2005). The intrinsic pathway of cell death is caused by Bcl-2 family proteins, which are pro-apoptotic and anti-apoptotic proteins, including Bcl-2 and Bcl-xL (Ghobrial et al., 2005). Apaf-1 and procaspase-9 combine with cytochrome c to form an apoptosome. Both mitochondria-dependent (intrinsic) and independent (extrinsic) pathways are connected at the same point, called the execution pathway (Elmore, 2007). The extrinsic and intrinsic phases are linked at the same point after caspase-8 is triggered. Activated caspase-8 in the extrinsic mechanism regulates the activation of BH3 interacting-domain (BID), a pro-apoptotic protein alternatively called BH3-only protein. BID then stimulates and oligomerizes the pro-apoptotic proteins, BAX and BAK, resulting in an intrinsic apoptotic phase (Green and Llambi, 2015).

PHYTOCHEMICALS MODULATE AUTOPHAGY-APOPTOSIS SIGNALING IN SEVERAL CANCERS

Autophagy plays an essential role in cancer treatment, especially in chemotherapy, by removing dysfunctional organelles and intracellular components and inducing lysosomal degradation. This self-digestion mechanism strengthens cellular defense to protect cells from various intracellular and extracellular stresses

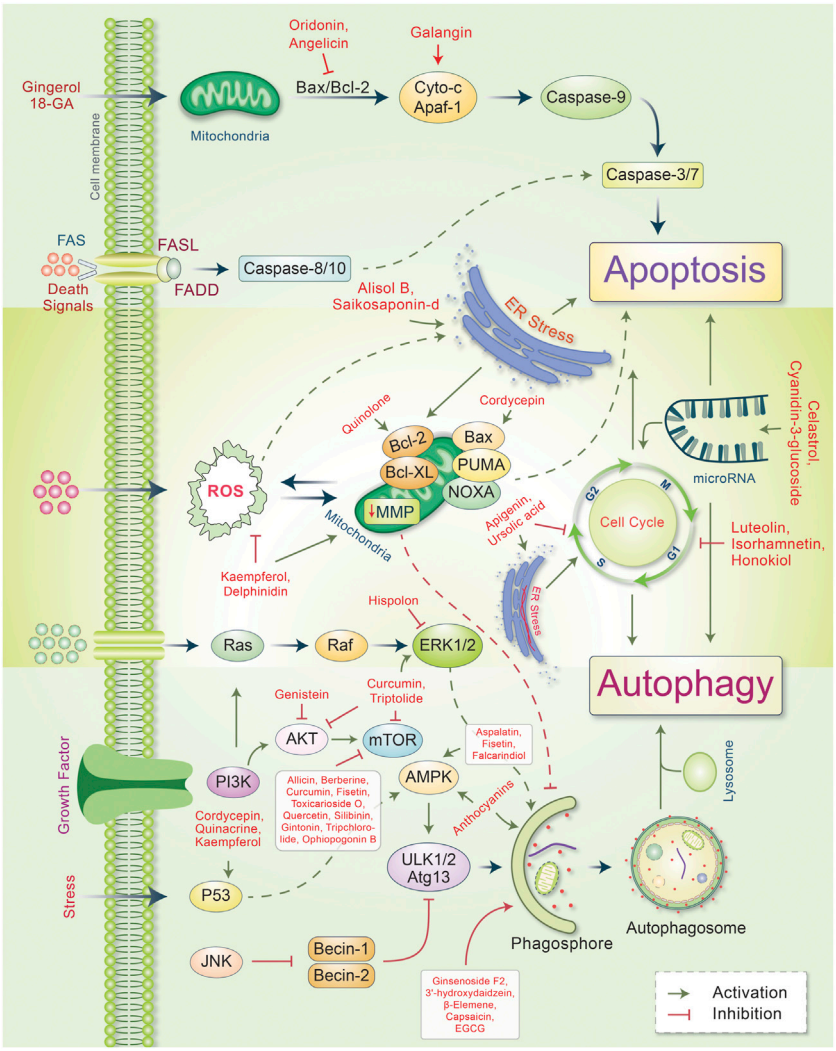

FIGURE 3 | Major phytochemicals induce the signal transduction pathways that regulate autophagic and apoptotic cell death in cancer. Phytochemicals have been found to activate both the intrinsic and extrinsic apoptotic pathways by inducing a dysfunction in mitichrondria-caspase-9 and FAS-ligand-caspase-8 mediated apoptotic cell death, respectively. Phytochemicals induce ER stress and apoptotic cell death. However, some phytochemicals modulate mitichrondrial biogenesis and ensure apoptosis-autophagic cell death. Phytochemicals regulate the cell cycle and microRNA as well as cause apoptosis-autophagic cell death in cancer cells. Some phytochemicals activate autophagic signaling and inhibits cell growth and autophagy. For a detailed explanation, see the text.

and regulate redox balance to provide genomic and cytoplasmic stability. Emerging evidence supports the dual role of autophagy in cancer (i.e., as a promoter and an inhibitor of tumor development). However, the induction of autophagy in cancer is still a potential strategy; this is because it induces type II programmed cell death. During cancer initiation, autophagy regulators, such as mTOR and AMPK, are negatively modulated by tumor-suppressing factors, which cause autophagy induction (Comel et al., 2014). However, these autophagy regulators are activated by several oncogenes that suppress autophagy and promote cancer formation (Choi et al., 2013). Autophagy also suppresses carcinogenesis by regulating ROS, and excessive ROS production promotes tumor generation (Ávalos et al., 2014; Filomeni et al., 2015). Owing to their multifaceted therapeutic activities, phytochemicals have proven to be promising for treating many cancers (Mitra and Dash, 2018). In some cases, metabolites and synthetic products from natural compounds have demonstrated better chemopreventive effects than their original compounds (Aung et al., 2017). Our model and emerging evidence indicate that phytochemicals targeting the autophagic-apoptotic pathways are promising agents for cancer treatment for both pathways, or are dependent- and -independent of target-specific molecular mechanisms in cancer cells (**Figure 3**). Several phytochemicals and their autophagic-apoptotic effects are summarized in **Table 1**.

Phytochemicals in Autophagy Signaling

Apigenin is a flavonoid derivative that modulates several kinase pathways and inhibits the cell cycle at the G2/M phase. Studies

TABLE 1 | Phytochemicals that activate autophagy and apoptosis in various *in vitro* and *in vivo* cancer models.

Phytochemicals	Doses/ Conc	Cancer model	Molecular effects	References
Resveratrol	10–100 μM	Human colon carcinoma cell lines SW480, SW620, B103, and HCT116	Activate procaspase-3, 8/FADD	Delmas et al. (2003); Rahman et al. (2012a)
Eriocalyxin B (EriB)	1.4 μM	Human pancreatic cancer cellPANC-1, SW1990 CAPAN-2, and CAPAN-1	Caspase 8,9 activation and downstream regulation of caspases 3, 7, PARP	Li et al. (2012)
β-Elemene	10 μM	Human breast cancer cell lines Bcap37, MBA-MD-231	Conservation of LC3-I to LC3-II	Guan et al. (2014)
Oblongifolin C	15 μM	Human breast carcinoma cell lines HeLa or MEF	Activation of CASP3 and cleaved PARP	Lao et al. (2014)
Apigenin	10 μM	Colorectal cancer cells HCT-116, SW480, HT-29 and LoVo	Activate NAG-1, p53, p21	Zhong et al. (2010)
Allicin	1 μg/ml	Human gastric cancer cell line MGC-803, BGC-823 and SGC-7901	Increase expression of p38 and cleaved Of caspase 3	Zhang et al. (2015)
Anthocyanins	50 μM	Breast cancer cell lines MCF-MDA-MB-231 and MDA-MB-453	Inhibit the expression of VEGF, suppressed the MMP-9,MMP-2 and uPA expression	Hui et al. (2010)
Aspalathin	0.2 μM	Ovarian cancer cell Caov-3	Inhibit Dox, decrease expression of p53 and induce AMPK and Foxo1	Lin et al. (2017)
Baicalein	200 μM	Human HCC cell lines SMMC-772 and Bel-7402	Downregulate Bcl 2, increase ER stress	Wang et al. (2014)
Berberine	100 nM	Human glioma cell lines U251 and U87 GBM	Inhibition of AMPK/mTOR/ULK1	Peng et al. (2008); Wang et al. (2010); Yu et al. (2014); Guamán Ortiz et al. (2015); Wang et al. (2016a)
Capsaicin	150 μM	Human nasopharyngeal carcinoma cell line NPC-TW01	Downstream of PI3K/Akt/mTOR, increase caspase-3 activity	Lin et al. (2017b)
Celastrol	1.5 μM	Human prostate cancer cell lines LNCaP, 22Rv1, DU145 and PC-3	Upstream of miR-101	Guo et al. (2015)
Cordycepin	200 μM	Human brain cancer cellSH-SY5Y and U-251	Upregulates ROS, p53, and LC3II	Chaicharoenaudomrung et al. (2018)
Curcumin	25 μM	Malignant mesotheloma cancer cell line MM-B1, H-Meso-1, and MM-F1	Increase Bax/bcl-2 ratio, p53 expression, activation of caspase 9, cleavage of PARP-1	Masuelli et al. (2017)
Epigallocatechin gallate (EGCG)	100 nM	Vascular endothelial cell line U-937	Reduce TNF-α, inhibit VCAM1, LC3A, LC3B	Yamagata et al. (2015)
Evodiamine	10 μM	Gastric cancer cell line SGC-7901	Activates beclin-2, Bax, downregulates Bcl-2	Rasul et al. (2012)
Fisetin	40–120 μM	Prostate cancer cell lines PC3 and DU145	Supressed Mtor and inhibit Akt, activate AMPK	Suh et al. (2010)
Genistein	50–100 μM	Ovarian cancer cell line A2780	Reduces Akt/mTOR phosphorylation	Gossner et al. (2007)
Gingerol	300 μM	Human colon cancer cell lines SW-480 and HCT116	Inhibition of JNK, ERK1-2, and P38 MAPK	Shukla and Singh, (2007); Baliga et al. (2011); Radhakrishnan et al. (2014)
Ginsenoside F2	100 μM	Breast cancer cell lines MCF-7	Elevated Atg-7 Cleaved PARP	Mai et al. (2012)
Hispolon	25–100 μM	Cervical cancer cell lines Hela and SiHa	Downregulated lysosomal protease Cathepsin S(CTSS)	Chen et al. (2012)
3′-hydroxydaidzein (3′-ODI)	100 μM	Mouse melanoma cell line B16F1	Reduce the α-MSH	Kim et al. (2013)
Toxicarioside O	50 nM	Human colorectal cancer cell lines HCT116 and SW480	Inhibition of the Akt/mTOR Upstream SIRT1↑	Huang et al. (2017)
Falcarindiol	6 μM	Human breast cancer cell lines MDA-MB-231,MDA-MB-468 and Her2	FAD induce expression of GRP78	Minto and Blacklock, (2008); Jin et al. (2012); Lu et al. (2017)
Oleanolic acid	100 μg/ml	Human pancreatic cancer cell line Panc-28	Modulate JNK and mTOR pathway	Pollier and Goossens, (2012); Liu et al. (2014)
Honokiol	40 μM	Human glioblastoma cell lines LN229, GBM8401 and U373	Reduction of p-PI3K, p-Akt and Ki67	Cheng et al. (2016)
Magnolol	40 μM	Human glioblastoma cell lines LN229, GBM8401 and U373	Reduction of p-PI3K, p-Akt and Ki67	Cheng et al. (2016)
Alisol B	30 μM	Breast cancer cell lines MCF-7, SK-BR-3, and HeLa	Activation of Ca2+/AMPK/Mtor	Law et al. (2010)

(Continued on following page)

TABLE 1 | (*Continued*) Phytochemicals that activate autophagy and apoptosis in various *in vitro* and *in vivo* cancer models.

Phytochemicals	Doses/ Conc	Cancer model	Molecular effects	References
Luteolin	100 μM	Human liver cancer SMMC-7721	Increase expression of caspase-8, decrease bcl-2	Cao et al. (2017)
α-Mangostin	5–10 μM	Human brain cancer cell lines, GBM8401 and DBTRG05MG	Activation of AMPK	Chao et al. (2011)
Oridonin	8–32 μmol/L	Human hepatocellular carcinoma cell line BEL-7402	Activation of caspase-3 Down-regulation of Bcl-2 and Up-regulation of Bax	Zhang et al. (2006)
Quercetin	15 μM	Lymphoma cell lines BC3, BCBL1 and BC1	Inhibits PI3K/Akt/mTOR and Wnt/β-catenin	Granato et al. (2017)
Rottlerin	1–2 μM	Breast cancer cell lines CD44/ CD24	Enhance expression of LC3	Kumar et al. (2013)
6-Shogaol	55.4 μM	Lung cancer cell line A549	Inhibition af Akt and mTOR downstream	Hung et al. (2009)
Silibinin (silybin)	50 μM	RCC cell lines ACHN and 786-O	Inhibit mTOR and activate AMPK	Li et al. (2015)
Sulforaphane	40 μM	Human pancreatic cancer cell lines MIA PaCa-2,Panc-1	Increase ROS level	Naumann et al. (2011)
γ-tocotrienol	10 μmol/L	Breast cancer cell lines MCF-7 and MDA-MB-231	Activate AMPK, down regulate Ang-1/Tie-2	Ling et al. (2012); Tang et al. (2019)
Thymoquinone	40–60 μM	Oral cancer cell lines SASVO3,SCC-4, OCT,SAS	Increase expression of LC3-II, Bax expression	Chu et al. (2014)
Tripchlorolide	200 nM	Lung cancer cell line A549/DDP	Inhibition of PI3K/Akt/mTOR	Chen et al. (2017a)
Tetrandrine	0–4 μM	Hepatocellular carcinoma cell lines Huh7, HCCLM9 and Hep3B	Inhibits Wnt/β-catenin Decreases MTA1	Zhang et al. (2018)
N-desmethyldauricine	150 μM	Lung cancer cell line H1299	Inhibition of Ulk-1/PERK/AMPK/ mTOR	Law et al. (2017)
Quinacrine	15 μM	Colon cancer cell lines HCT-116/ HCT-116/HCT-116	Activation of p53, p21, and inhibition of topoisomerase	Mohapatra et al. (2012)
Chloroquine	50 μM	Pancreatic cancer cell line MiaPaCa2 and S2VP10	Decrease the level of O_2	Frieboes et al. (2014)
Tangeritin	10 μM	Breast cancer cell lines MCF7, MDA–MB–468 and MCF10A	Induce CYP1 and CYP1A1/CYP1B1 protein expression	Surichan et al. (2018)
Myricetin	100 μM/L	Prostate cancer cell lines PC3, DU145	Knockdown the interaction between P1M1/CXCR4	Ye et al. (2018)
Galangin	15 μM	Human kidney cancer cell line A498	Inhibition of PI3K/Akt/mTOR signaling	Zhu et al. (2018)
Isorhamnetin	100 μM	Colon cancer cell lines HCT116 and SW480	Increase ROS	Wu et al. (2018)
Hesperetin	350 μM	Lung cancer cell line H522	Knockdown caspase-3/9,p53,Bax Upregulate Fas, FADD and caspase-8	Elango et al. (2018)
Delphinidin	80 μM	Breast cancer cell lines MDA-MB-453 and BT474	Suppression of mTOR Activation of the AMPK	Chen et al. (2018)
Epigallocatechingallate (EGCG)	500 μM	Human glioblastoma cell lines T98G and U87MG	Increase ROS	Grube et al. (2018)
Epicatechin-3-*O*-gallate (ECG)	36 μM	Prostate cancer cell lines LNCaP and PC-3	Diminished the progression of carcinofenic cell	Siddiqui et al. (2011); Stadlbauer et al. (2018)
Cyanidin-3-glucoside (C3G)	20 μM	Human breast cancer MDA-MB-231 and Hs-578T	Inhibiting STAT3/VEGF and *miR*124 mediated downregulation STAT3	Ma and Ning, (2019)
Benzyl isothiocyanate (BITC)	6.5 μM	Pancreatic cell lines BxPC-3 and PanC-1	Decrease the phosphorylation of PI3K/Akt/FOXO1/PDK1/mTOR/ FOXO3a	Boreddy et al. (2011)
Phenethyl isothiocyanates (PEITC)	10 μM	Breast cancer cell lines MDA-MB-231 and MCF-7	Reduction of HER2, EGFR and STAT3 expression	Gupta and Srivastava, (2012)
Piperlongumine (PL)	6 μM	Lung cancer cell lines A549 and A549/DTX	Regulate PI3K/Akt/mTOR	Bezerra et al. (2008); Raj et al. (2011); Wang et al. (2015)
Saikosaponin-d	10 μM	Breast cancer cell lines HeLa and MCF-7	Calcium mobilization, induce CaMKKβ-AMPK-mTOR	Hsu et al. (2004); Tundis et al. (2009); Wong et al. (2013)
Guttiferone K	20 μM	Human HCCs HuH7 and HepG2	Reduce phosphorylation of Akt /mTOR, increase ROS	Xu et al. (2008) Wu et al. (2015)
Licochalcone A	20 or 50 μM	Breast cancer cell line MCF-7	Suppression of PI3K/Akt/mTOR pathway	Xue et al. (2018)
Ophiopogonin B	10 μM	Lung cancer (NSCLC) cell lines NCI-H157 and NCI-H460	Inhibition of PI3K, Akt, mTOR	Chen et al. (2013a)

(Continued on following page)

TABLE 1 | (*Continued*) Phytochemicals that activate autophagy and apoptosis in various *in vitro* and *in vivo* cancer models.

Phytochemicals	Doses/ Conc	Cancer model	Molecular effects	References
Norcantharidin	40 μM	Human MHCC-97H (97H) and HepG2 HCC cells	Inhibition of c-Met, mTOR	Sun et al. (2017a)
Juglanin	10 μM	Breast cancer cell lines MCF-7 and SKBR3	Regulation of ROS, JNK	Sun et al. (2017b)
Isoliquiritigenin	25 μM	Human ovarian cancer cell lines, OVCAR5 and ES-2	Cleaved caspase-3, increased LC3B-II, and Beclin-1 level	Chen et al. (2017b)
Cucurbitacin B	200 μM	Breast cancer cell line MCF-7	Increase γH_2AX, phosphorylation of ATM/ATR, ROS	Chen et al. (2005); Ren et al. (2015)
Carnosol	25 μM	Human breast cancer cell line MDA-MB-231	Increase p21/WAF1 and downregulate p27	Al Dhaheri et al. (2014)
Kaempferol	50 or 100 μM	Colorectal cancer cell lines HCT116, HCT15, and SW480	Generated ROS and p53 signal	Choi et al. (2018)
Ursolic acid	10–40 μM	Prostate cancer cell lines PC3	Increases Beclin-1/Atg5 and inhibits Akt/mTOR	Shin et al. (2012)
Triptolide	200 nM	Human pancreatic cancer cell line S2-013, S2-VP10, and Hs766T	Inhibits of Akt-mTOR-P70S6K	Mujumdar et al. (2010)

have shown that apigenin can inhibit cell growth and induce autophagy in time-and dose-dependent manners in HepG2 cells (Zhong et al., 2010). Autophagy was also found to be mediated *via* the inhibition of the PI3K/Akt/mTOR pathway in HepG2 cells (Yang et al., 2018). An organic sulfur compound, allicin, acts as an antitumor agent that activates autophagic cell death by inhibiting the PI3K/mTOR signaling pathway (Sak, 2012). Allicin also inhibits the expression of p53 and Bcl-2, and upregulates the Beclin-1 signaling and AMPK/TSC2 signaling pathways (Chu et al., 2012). Anthocyanins (ACNs) present in black soybeans induce autophagy; however, their underlying mechanism have yet to be determined (Choe et al., 2012). Aspalathin is a polyphenolic dihydrochalcone C-glucoside that plays a critical role in inhibiting Dox-induced cardiotoxicity and decreasing P53 expression. Aspalatin triggered autophagy-related genes and decreased p62 by inducing the AMPK and Fox pathways (Johnson et al., 2017). Berberine is an isoquinoline alkaloid that exerts anticancer activity for autophagy induction by inhibiting the AMPK/mTOR/ULK1 pathway (Wang et al., 2016a). Celastrol is another triterpenoid that is effective against human prostate cancer. Celastrol blocks the AR signaling pathway, which induces autophagy and downregulates the expression of miR-101 (Guo et al., 2015). Cordycepin generates ROS in cancer cells and enhances p53 and LC3I/II expression, thereby modulating autophagy (Chaicharoenaudomrung et al., 2018). Cordycepin inhibits renal carcinoma in the migration of the Caki-1 cell line by reducing microRNA-21 expression and Akt phosphorylation, and increasing PTEN phosphatase levels (Yang et al., 2017). In addition, cordycepin induces autophagy *via* Bax activation in ovarian cancer cell lines, including SKOV-3 and OVCAR-3 (Jang et al., 2019). Curcumin has been shown to increase ROS and DNA damage in cancer cells. Further, curcumin increased the phosphorylation of ERK1/2 and p38 MAPK, inhibited Akt and P54 JNK (Masuelli et al., 2017), and eventually induced autophagy in NSLCA549 cells (Liu et al., 2018). Evodiamine, a quinolone alkaloid, mediates autophagy activation by upregulating Beclin-1 and Bax expression and downregulating Bcl-2 (Rasul et al., 2012). Fisetin is a naturally occurring flavonoid that is reported to suppress the mTOR signaling pathway *via* the inhibition of Akt and activation of AMPK, and autophagic programmed cell death in prostate cancer cells (Suh et al., 2010). Similarly, genistein displayed chemopreventive and chemotherapeutic effects in cancer cells. Treating ovarian cancer cells with genistein led to a reduction in Akt phosphorylation and induced autophagy, thereby contributing to glucose uptake reduction in cancer cells (Gossner et al., 2007). Ginsenoside F2 showed anti-proliferative activity and initiated the autophagic process in breast cancer stem cells. Concurrently, ginsenoside F2 elevated Atg-7 levels, induced the formation of acidic vascular organelles, and recruited GFP-tagged LC3-II to autophagosomes (Mai et al., 2012). Hispolon, a phenolic compound isolated from *Phellinus igniarius* (L.) Quél., exhibited apoptotic and anti-tumor effects in cervical cancer cell lines and notably induced autophagy. Treatment with hispolon inhibited metastasis by downregulating lysosomal protease cathepsin S (CTSS) (Chen et al., 2012). Further, hispolon was found to mechanistically block the ERK pathway and enhance LC3 conversion and acidic vesicular organelle formation (Hsin et al., 2017). 3′-hydroxydaidzein (3′-ODI) is another phytochemical derivative that induces autophagy. In fact, it was found to significantly reduce α-MSH-mediated melanogenesis in melanoma cells (Kim et al., 2013). Toxicarioside O, a natural product derived from the *Antira toxicaria* Lesch., showed anticancer potency through autophagy induction *via* the subsequent reduction of the Akt/mTOR pathway (Huang et al., 2017). Falcarindiol (FAD), a natural polyene (Minto and Blacklock, 2008) promotes autophagy in response to ER stress (Jin et al., 2012) while α-mangostin mediates autophagic cell death *via* AMPK activation in human glioblastoma cells (Chao et al., 2011). The bioflavonoid, quercetin, possesses anticancer and anti-inflammatory properties. In hyperactive primary effusion lymphoma (PEL), quercetin reduced the release of cytokines and inhibited PI3K/Akt/mTOR and STAT3 pathway-induced autophagy, ultimately resulting in PEL cell death (Granato

et al., 2017). In breast cancer steam cells, rottlerin (Rott) enhanced the expression of LC3, Beclin-1, and Atg12 aggregation during autophagy. Silibinin (silybin) is a chemoprotective flavonoid that might exhibit anti-metastatic effects on renal cell carcinoma (RCC). Silibinin increased the expression of LC3-II, which not only suppressed mTOR regulation but also activated the AMPK pathway (Li et al., 2015). Sulforaphane (SFN) is a group of phytochemicals that are referred to as isothiocyanates (Uddin et al., 2020). Multiple studies have shown that autophagy in SFN-induced cell death eliminates highly resistant pancreatic carcinoma cells by releasing ROS, without exhibiting cytotoxic effects (Naumann et al., 2011; Uddin et al., 2020). Gintonin has been found to stimulate autophagic flux *via* the Akt/mTOR/p70S6K-mediated pathway in primary cortical astrocytes (Rahman et al., 2020b). Ursolic acid (UA), a pentacyclic triterpenoid, showed anti-proliferative effects *via* G1 phase arrest and induced autophagy regulation through the beclin-1 and Akt/mTOR pathways (Shin et al., 2012). Tripchlorolide is present in tripterygium. Treatment with tripchlorolide was found to attenuate the expression of the PI3K/Akt/mTOR signaling pathway (Chen et al., 2017a). Tetrandrine is a bisbenzylisoquinoline alkaloid isolated from the Chinese medicinal herb, *Stephania tetrandra* S. Moore. Tetrandrine plays an important role in the suppression of human hepatocellular carcinoma, inhibits the Wnt/β-catenin pathway, and reduces MTA1 expression, which eventually causes autophagy (Zhang et al., 2018). N-desmethyldauricine is a novel inducer of autophagy that is mediated by the inhibition of Ulk-1/PERK/AMPK mTOR and causes calcium accumulation, leading to autophagic cell death (Law et al., 2017). Quinacrine displayed anticancer properties in breast cancer cells by enhancing p53 and p21 regulation and inhibiting topoisomerase activity (Mohapatra et al., 2012). The anti-proliferative activity of tangeritin initiates anticancer activity by modulating autophagy and inducing the CYP1 enzyme and CYP1A1/CYP1B1 proteins in MDA-MB-468 and MCF-7 cells (Surichan et al., 2018). Multiple studies have indicated that licochalcone A treatment activates the LC3-II signaling pathway and suppresses the PI3K/Akt/mTOR pathway to promote autophagy in MCF-7 cells (Xue et al., 2018). In addition, ophiopogonin B was found to induce autophagy by inhibiting the PI3K/Akt/mTOR signaling pathway (Chen et al., 2013a). Anticancer activity was also exhibited by juglanin, which is generally extracted from green husks. Juglanin-mediated treatment attenuated G2/M phase arrest and induced autophagy by regulating the ROS/JNK signaling pathway in human breast cancer (Sun et al., 2017a). Cucurbitacin B (Cuc B) is another natural tetracyclic triterpene compound that is generally used as an anti-inflammatory drug (Chen et al., 2005). Treatment with Cuc B increases γH_2AX protein expression, promotes DNA damage through phosphorylation of ATM/ATR, and concurrently increases the level of ROS that induces autophagy in MCF-7 cells (Ren et al., 2015).

Phytochemicals in Apoptosis Signaling

Angelica polymorpha Maxim, which contains angelicin, increases cellular cytotoxicity and induces apoptosis by decreasing the expression of anti-apoptotic proteins, including Bcl-xL, Bcl-2, and Mcl-1 in SH-SY5Y human neuroblastoma cells (Rahman et al., 2012b; Rahman et al., 2012b). As FAD-induced cell death is known to be caused by caspase-dependent modulation, FAD is suggested to have a synergistic effect on several approved cancer drugs designed to kill cancer cells (Lu et al., 2017). Alisol B induces autophagy by modulating the CaMKK-AMPK-mTOR signaling pathway, calcium mobilization, and enhanced ER stress, leading to apoptotic cell death (Law et al., 2010). Luteolin is a flavonoid found in various plants and is known to play a leading role in hepatocellular carcinoma cell lines through G0/G1 phase cell cycle arrest. Studies have shown that treatment with luteolin induces apoptosis by increasing caspase-8 expression, reducing Bcl-2 at the mRNA level, improving the conversion of LC3B-I to LC3B-II, and decreasing the viability of SMMC-7721 cells (Cao et al., 2017). In the human carcinoma BEL-7402 cell line, oridonin-mediated apoptosis was found to be driven by the activation of caspase-3 as well as reduced Bcl-2 expression and Bax upregulation, which can inhibit cell growth (Zhang et al., 2006). Prolonged treatment with Rott in breast CSCs suppressed the phosphorylation of Akt and mTOR, and upregulated the phosphorylation of AMPK, eventually upregulating apoptosis (Kumar et al., 2013). Several natural plant extracts derived from *Dioscorea nipponica* Makino, *Melandrium firmum* (Sieb. & Zucc.) Rohrb., and *Saussurea lappa* (Decne.) Sch. Bip. have been found to induce anti-proliferative effects and apoptotic cell death in human neuroblastoma cells (Rahman et al., 2013; Rahman et al., 2014; Rahman et al., 2015). γ-Tocotrienol, a vitamin E isomer (Ling et al., 2012), is known to target Ang-1/Tie-2 and exert anti-cancer effects through the activation of AMPK signaling, leading to apoptotic cell death in human prostate cancer cell lines (Tang et al., 2019). Triptolide induced apoptosis in pancreatic cancer cells, causing the inactivation of Akt/mTOR/p70S6K and upregulation of the ERK1/2 pathway (Mujumdar et al., 2010). Kaempferol is a flavonoid compound that generates ROS and p53 signals and regulates p38 phosphorylation as well as caspase activation, thereby inducing apoptosis of colorectal cancer cells (Choi et al., 2018). Myricetin is a natural flavonoid found in various fruits and vegetables. A previous report suggested that myricetin attenuated tumor cell growth by promoting apoptotic cell death (Cao et al., 2018). Myricetin exerts pro-apoptotic and cytotoxic effects on prostate cancer cells by inhibiting P1M1 and downregulating the interaction between P1M1 and CXCR4 (Ye et al., 2018). Galangin induced apoptosis in kidney cancer cells by increasing the expression of Bax and Cyt-c and decreasing Bcl-2 expression (Zhu et al., 2018). In a human breast cancer cell line, isorhamnetin inhibited tumor growth by inducing cell cycle arrest in the S-phase and displayed strong cytotoxic effects *via* the ROS-dependent apoptotic pathway (Wu et al., 2018). In H522 cells, Hesperet induced apoptotic cell death by downregulating caspase-3/9, p53, and Bax expression and upregulating Fas, FADD, and caspase-8 expression (Elango et al., 2018). Cyanidin-3-glucoside (C3G) is an ACN found in fruits. C3G exerts anti-inflammatory properties and induces *miR*-124 expression. Concurrently, *miR*-124 regulation downregulates STAT3 and inhibits angiogenesis induced by C3G in human

breast cancer (Ma and Ning, 2019). Benzyl isothiocyanate (BITC) is present in cruciferous vegetables. Administering BITC to mice caused decreased phosphorylation of PI3K/Akt/FOXO1/PDK1/mTOR/FOXO3a, which suppressed pancreatic cancer cell growth and induced apoptosis (Boreddy et al., 2011). Several studies have reported that glucosinolate-derived phenethyl isothiocyanates (PEITC) are promising anti-tumorigenic agents. In fact, PEITC-treated mice were found to exhibit reduced expression of HER2, EGFR, and STAT3, and enhanced apoptosis through the cleavage of caspase 3 and PARP (Gupta and Srivastava, 2012). NCTD inhibits c-Met and mTOR and exhibits anticancer properties (Sun et al., 2017b).

Phytochemicals in Autophagic-Apoptotic Signaling

β-Elemene is a natural chemical compound collected from different medicinal plants, such as Curcuma WenYuJin (Edris, 2009). β-Elemene exerts cytoprotective activity by converting LC3-I into LC3-II to form autolysosomes that activate autophagy and significantly reduce the *in vitro* growth of human breast cancer cells *via* apoptosis (Guan et al., 2014). Capsaicin is another naturally occurring phytochemical that exerts antitumor potency by downregulating the PI3K/Akt/mTOR pathway. Capsaicin instigates the autophagy process by increasing the expression of the autophagy markers, LC3-II and Atg5, and enhances the degradation of p62 and Fap-1, while increasing caspase-3 activity (Lin et al., 2017a). The *Morus alba* L. root extract containing oxyresveratrol was previously found to accumulate ROS and induce autophagic and apoptotic cell death *via* the FOXO-Caspase-3 pathway in human neuroblastoma cells (Kwon et al., 2015; Rahman et al., 2017). Gingerol possesses antioxidant, anti-inflammatory, and anti-tumor properties (Shukla and Singh, 2007; Baliga et al., 2011), and inhibits colon cancer cell proliferation by activating the caspase-dependent pathway and concurrently cleaving PARP, which induces autophagy (Radhakrishnan et al., 2014). Concurrent treatment with honokiol (Hono) and magnolol (Mag) decreased the expression of cyclin A, D1, and cyclin-dependent kinase, which arrests cell cycle progression and reduces p-PI3K, p-Akt, and Ki67 expression in U87MG and LN229 human glioma cells. Both Hono-and Mag-mediated treatments exert synergistic anti-tumor effects by inhibiting cell proliferation. Accordingly, they induce autophagy and apoptosis in human GMB cells (Cheng et al., 2016). 6-Shogaol disrupts the Akt/mTOR mediated signaling pathway; blocking of Akt is beneficial to apoptotic cell death. 6-Shogaol induces autophagy through the inhibition of Akt overexpression and exhibits anticancer activity against non-small cell lung cancer (Hung et al., 2009). Thymoquinone (TQ), a major component of black cumin, exhibits potent cytotoxic effects in several cancer cell lines. In SASVO3 cells, TQ was found to mediate cell death caused by the enhancement of Bax expression and increase autophagic vacuoles and LC3-II protein expression following apoptosis and autophagy (Chu et al., 2014). In our previously published study, we revealed that the gap-junction inhibitor, 18α-Glycyrrhetinic acid (18-GA), induces apoptosis and autophagy. 18-GA-induced autophagy has been shown to induce Atg5, Atg7, and LC3II accumulation through p62 degradation (Rahman et al., 2016b). 18-GA was also found to destabilize the Bcl-2/Beclin-1 interaction and the cleavage of Beclin-1, ultimately highlighting the occurrence of mitochondrial-mediated apoptosis in SH-SY5Y cells (**Figure 4**). 18-GA is also known to activate several MAPKs and arrest the cell cycle, which leads to the activation of apoptosis. 18-GA may thus be used as a therapeutic target for the apoptosis-autophagy pathway in neuroblastoma.

Delphinidin is an anthocyanidin monomer with strong anti-oxidative characteristics. In HER-2 positive breast cancer cells, delphinidin enhances apoptosis and autophagy by suppressing mTOR and activating the AMPK signaling pathway (Chen et al., 2018). Emerging evidence has shown that epicatechin-3-O-gallate (EGCG) promotes autophagy and apoptosis in different cancer lines (Siddiqui et al., 2011; Grube et al., 2018; Stadlbauer et al., 2018). Previously, OxyR was found to simultaneously activate apoptosis and autophagy in NB. OxyR also reduces PI3K/Akt/mTOR signaling and enhances cytotoxicity by increasing autophagy levels (**Figure 5**) (Rahman et al., 2017). OxyR-induced cell death was found to occur independent of apoptosis induction due to alterations in the levels of PI3K/Akt/mTOR and p38 MAPK activity in SH-SY5Y cells.

Saikosaponin-d is reported to induce intracellular calcium accumulation and autophagy by activating the CaMKKβ-AMPK-mTOR pathway. Nonetheless, ER stress and UPR activation by saikosaponin-d have been demonstrated to trigger apoptosis and autophagic cell death (Wong et al., 2013). Isoliquiritigenin (ISL) hinders the viability of ovarian cancer cell lines (OVCAR5) and the ES-2 model. ISL also induced autophagy in OVCAR5 *via* cell cycle arrest at the G2/M phase, cleaved caspase-3, and increased LC3B-II and Beclin-1 expression (Chen et al., 2017b). Guttiferone K (GUTK) isolated from *garcinia yunnanensis* Hu (Xu et al., 2008) was found to reduce Akt phosphorylation and inhibit the mTOR pathway. GUTK also enhanced ROS and triggered the phosphorylation of JNK in EBSS, which induced autophagy and apoptosis under nutrient-deficient conditions (Wu et al., 2015).

PHYTOCHEMICALS MODULATE AUTOPHAGY-APOPTOSIS THROUGH ROS SIGNALING

ROS, such as $O_2^{\bullet-}$, H_2O_2, and $^{\bullet}OH$, are generated as metabolic by-products by biological systems; such generation may trigger detrimental as well as useful health outcomes (Covarrubias et al., 2008; Sena and Chandel, 2012). An optimum level of ROS is required for different biological processes, such as cell signaling, activation of proteins, immune function and transcriptional factors, and the regulation of apoptosis and differentiation (Rajendran et al., 2014). However, overproduction of ROS may have damaging effects on various proteins, lipids, and nucleic acids (Wu et al., 2013). Thus, an imbalance in ROS levels may be the cause of several diseases, such as cancer. Cellular ROS levels are also critical for cancer progression (Aggarwal et al., 2019). ROS-mediated DNA damage may play

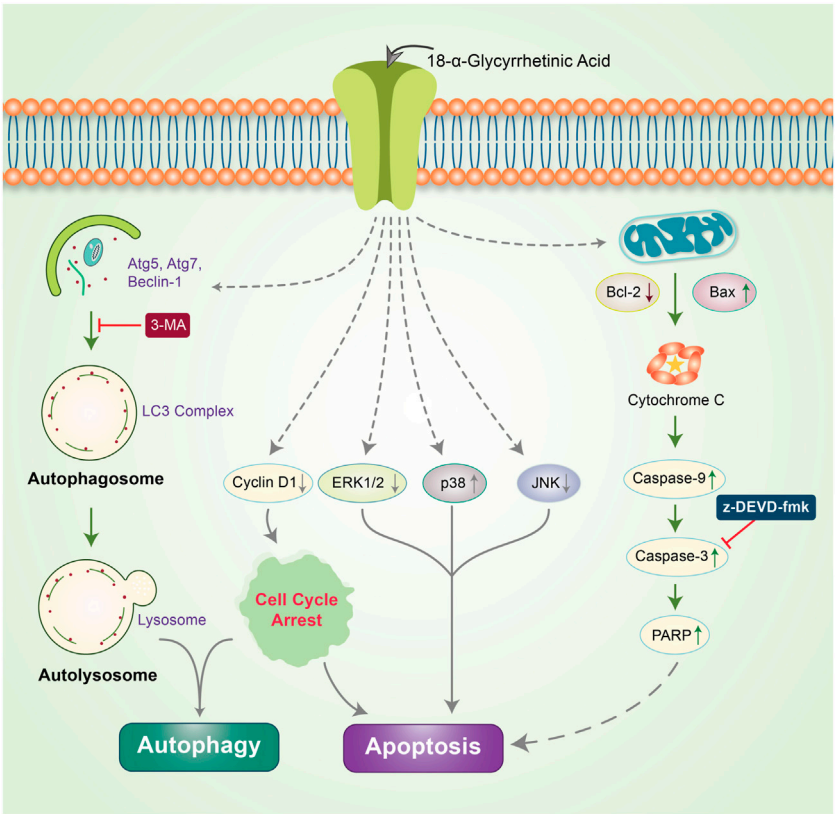

FIGURE 4 | Anticancer effects of 18-GA in autophagy-apoptosis modulation in neuroblastoma cells. 18-GA encouraged caspase-induced apoptosis by depolarizing the mitochondria membrane potential (MMP). 18-GA also induced early autophagy through Atg5 and Atg7 activation and converted LC3I to LC3II. The autophagy inhibitor, 3-MA, inhibited 18-GA-mediated autophagy. Nonetheless, 18-GA caused the downregulation of ERK1/2, JNK, and cyclinD1 protein and the upregulation of p38 MAPK, which activated apoptosis in neuroblastoma cancer.

a critical role in the initiation and progression of carcinogenesis. Reversible DNA damage may allow an internal repair system to normalize the adverse effects of ROS. However, irreversible damage may not permit the proper functioning of the repair system. As a result, the cells undergo apoptosis, which has a considerable effect in cancer therapy (Aggarwal et al., 2019).

As antioxidant phytochemicals can inhibit the growth of different cancer cells, they could serve as good candidates for anticancer therapy (Barrajón-Catalán et al., 2010; Sak, 2014). Depending on the concentration, exposure time, and ability of oxidative stress-inducing compounds, ROS signaling may act as an autophagic activator or apoptotic initiator in target cancer cells (Chirumbolo et al., 2018). EGCG is the most abundant polyphenol in green tea. EGCG has been found to induce apoptosis and autophagy in human mesothelioma cell death through prompting ROS (Satoh et al., 2013). Ha et al. represented that ROS generation is important in quercetin-meiated apoptotic cell death in Jurkat T cells has been targeted *via* BCL-XL antiapoptotic action protein (Ha et al., 2019). Epicatechins as shown to modulate autophagy and endoplasmic reticulum (ER) stress-induced apoptostic cell death of human various diseases (Zhang et al., 2020a). Gallic acid, 3,4,5-trihydroxy-benzoic acid found in red wine and grapes, acts as an auto-oxidation in addition to produce H_2O_2 and O_2^- lead to intrinsic mitochondria-mediated apoptosis in prostate cancer cells (Russell Jr et al., 2012). Gallic acid prevents lung cancer cell growth *via* elevating ROS level as well as GSH depleting (Wang et al., 2016b). Gallic acid additionally encourages apoptosis through ROS-mediated activation of JNK pathways (Chen et al., 2013b). Oxidation of catechin-derived quinone has also been observed to result in anti-tumor activities in several human cancer cells through apoptotic as well as autophagic cell death *via* modulating ROS (Saibu et al., 2014; Lee et al., 2017). Thus, activation of oxidative stress signaling may not always be associated with unexpected side effects. A high dose of EGCG exerts pro-oxidant effects, which ultimately leads to autophagy activation and increased antitumor activity (Yang et al., 1998; Tsai et al., 2018; Bimonte et al., 2019). EGCG induces apoptosis in cancer cells through different mechanisms, including the suppression of PI3K/Akt signaling (Liu et al., 2016), reduction in mitochondrial membrane potential (Li et al., 2009) and expression of anti-apoptotic proteins, including Bcl-2, xIAP, and Bcl-xl (Wu et al., 2009). Previously, quercetin was found to promote ROS-stimulated apoptosis and autophagy in different cancers (Choi et al., 2008; Bi et al., 2016) by activating caspase-3 and inhibiting anti-apoptotic proteins, such as Bcl-2 and Bcl-xl. Additionally, quercetin reduces apoptosis in addition to decrease intervertebral disc degeneration through SIRT-mediated autophagy induction (Wang et al., 2020). In

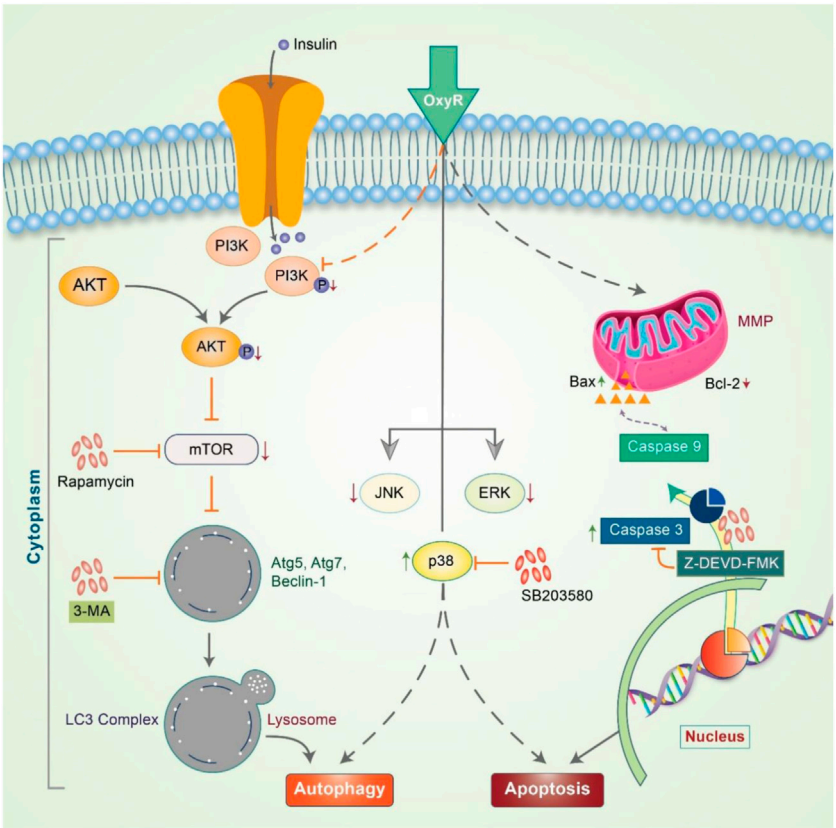

FIGURE 5 | Oxyresveratrol controls the autophagy-apoptosis signal to modulate neuroblastoma cells. OxyR activates PI3K/Akt/mTOR and the inhibition of mTOR by rapamycin blocks autophagy, indicating an mTOR-dependent autophagic pathway. OxyR led to arrest at the G2/M phase of the cell cycle and activated mitochondria-mediated caspase-3 dependent apoptosis. OxyR was also revealed to increase Bax/Bcl-2 ratio without generating ROS or activating p53. When the p38 inhibitor, SB203580, was applied, OxyR was found to activate autophagy-apoptosis signaling in neuroblastoma cells.

cancer cells, curcumin enhances TRAIL-induced apoptosis *via* ROS-mediated DR5 upregulation (Jung et al., 2005) and activates autophagy through the ROS-ERK1/2-p38 MAPK signaling pathway (Lee et al., 2011). Resveratrol has also been demonstrated to possess beneficial effects (Moni et al., 2018) it promotes apoptosis *via* ROS-dependent caspase activation (Shankar et al., 2007) and Bax/caspase-3 (Whitlock and Baek, 2012) and induces apoptosis associated with mitochondrial dysfunction in cancer cells (Lin et al., 2012). As depicted in **Figure 6**, phytochemicals are important modulators of cancer cell control owing to the autophagy-apoptosis pathways.

THERAPEUTIC TARGETS OF PHYTOCHEMICALS IN AUTOPHAGY-APOPTOSIS MODULATION FOR CANCER PREVENTION

Phytochemicals and naturally occurring compounds are well-known to ameliorate several human diseases owing to their pharmacological activities (Hannan et al., 2020; Rahman et al., 2020b). The most well-known anticancer agents, including taxol, resveratrol, vincristine, quercetin, vinblastine, tetrandrine, and arteannuin, modulate the autophagy-apoptosis pathway (Sun et al., 2019). Polyphenolic compounds and alkaloids are particularly dominant among all other cancer therapeutics (Newman and Cragg, 2016). Polyphenols play a greater role in apoptotic, autophagic, and cytostatic activities owing to their antioxidant properties, thereby serving as preventative cancer therapies (Focaccetti et al., 2019). Polyphenols can easily bind to cell membranes and trigger numerous signaling pathways, including caspases, epidermal growth factor (EGF), Bcl-2 family proteins, mitogen-activated protein kinase (MAPK), microRNAs (*miR*NAs), nuclear factor (NF)-κB, phosphatidylinositol-3-kinase PI3K/Akt/mTOR, and epidermal growth factor receptor (EGFR) (Sun et al., 2019). MicroRNAs (*miR*NAs) have also been demonstrated to regulate gene expression and are targeted as novel therapeutic approaches to control cancer; phytochemicals, such as resveratrol, silibinin, curcumin, genistein, and EGCG can be employed as apoptotic inducers, autophagy modulators, and cell cycle inhibitors (Lancon et al., 2012; Estrela et al., 2017; Jahanafrooz et al., 2018). *miR*NAs have been predicted to be critical for modulating cancer cell differentiation, invasion, proliferation, autophagy, and apoptosis *via* the regulation of oncogenic gene

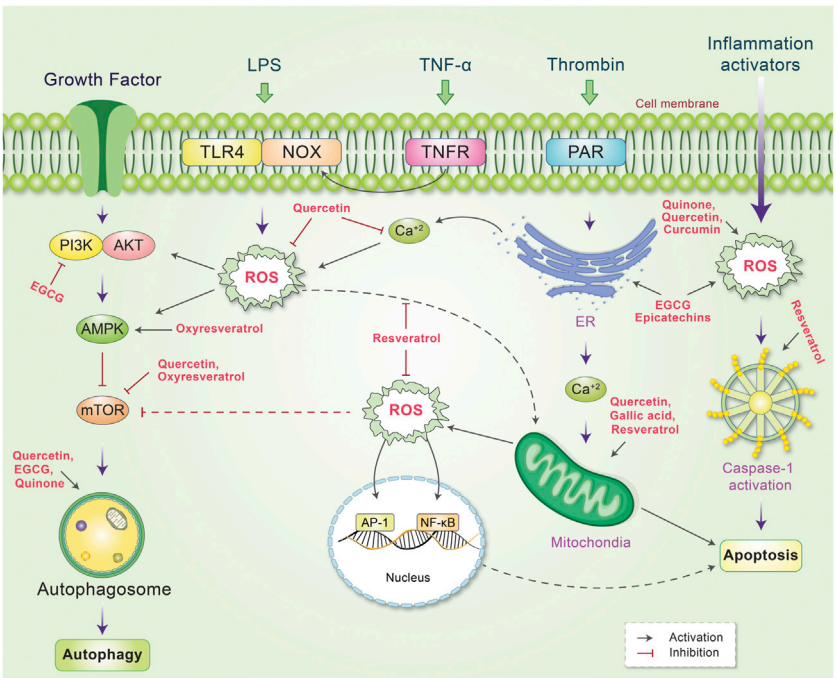

FIGURE 6 | Schematic representation of the mechanism of action of phytochemicals and reactive oxygen species (ROS), which lead to the control of several signaling pathways. ROS is produced by several internal and external stimuli. Extranally, ROS is activated through growth factors, LPS, TNF-α, thrombin, and inflammation. Different phytochemicals have been found to scavenge or decrease cellular ROS level by inhibiting or stimulating their action. Internally, phytochemicals inhibit PI3K or mTOR, which activates autophagy and reduces ROS production. Some phytochemicals have also been found to activate mitochrondrial ROS production while other phytochemicals scavenge ROS and protect against DNA damage. ROS production mediated by ER and inflammation activators is also reduced by phytochemicals, which modulate the autophagy-apoptosis pathways.

expression (Karius et al., 2012). Further, the MAPK and PI3K/Akt/mTOR signaling pathways have been shown to activate NF-κB in numerous cancer cell lines by modulating several phytochemicals in the autophagy-apoptosis pathway (Chao et al., 2017). Matrix metalloproteinase (MMP)-2 and MMP-9 modulate the autophagy-apoptosis pathway and control cancer through the action of different polyphenols (Balli et al., 2016).

Based on scientific evidence, phytochemicals present substantial anticancer potential for bench to bedside drug development. In fact, preclinical screening models can be used to assess their preliminary toxicity, safety, pharmacokinetics, and efficacy, which may serve as useful information for clinical trials (Zhang et al., 2020b). The preclinical efficacy of several phytochemicals, including ursolic acid, baicalein, genistein, 6-Shogaol, apigenin, thymoquinone, allicin, dicumarol, epigallocatechin, alpinumisoflavone, sulforaphane, curcumin, emodin, withaferin A, resveratrol, gingerol, physapubescin B, nimbolide, licochalcone A, glycyrrhizin, and hispidulin, has been demonstrated using numerous animal models (Choudhari et al., 2020). Despite several assessments of phytochemicals against cancer in the clinical trial setting, most trials continue to be in the early stage as numerous anti-cancer chemicals are currently being investigated. The most important phytochemicals under clinical trial investigation for various cancers include sulforaphane, resveratrol, lycopene, epigallocatechin, curcumin, and berberine; these phytochemicals aim to target the autophagy-apoptosis pathway (Choudhari et al., 2020).

LIMITATIONS OF TARGETING THE AUTOPHAGY-APOPTOSIS CROSSTALK USING PHYTOCHEMICALS IN ANTICANCER DRUG DEVELOPMENT

Increasing evidence suggests that phytochemicals could exhibit anticancer effects by modulating various signaling pathways, such as autophagy and apoptosis (**Figure 3**). These two significant cellular pathways are largely responsible for determining the fate of cancerous cells (Su et al., 2013). However, such finding is mainly based on *in vitro* and preclinical *in vivo* investigations that may not necessarily guarantee clinical outcomes. Moreover, many phytochemicals target multiple signaling pathways that may be shared among multiple cellular systems. These multitargeted effects of phytochemicals may generate positive outcomes, but can also lead to unanticipated effects, thereby challenging the development of phytochemical-based anticancer drugs. Although many phytochemicals are not specific in their action and exert multitarget effects, it is uncertain whether their anticancer effects are autophagy-dependent or merely a response to mitigate the adverse conditions that support the survival of

cells in the tumor microenvironment (Patra et al., 2020). Although autophagy and apoptosis are two critical cellular pathways in cancer biology, their specific roles remain unclear. However, because autophagy plays a critical role in cellular protein homeostasis and other quality control systems, modulating this crucial pathway may hamper cellular physiology. As autophagy is considered to be a double-edge sword, targeting this pathway may result in unprecedented outcomes.

CONCLUSION AND FUTURE PERSPECTIVES

As the incidence of cancer increases on a daily basis, new strategies are being discovered to ensure this fatal disease is managed therapeutically. The major challenge in developing target-specific anticancer drugs is inextricably linked to the complexity of cancer pathobiology. Autophagy and apoptosis are two vital cellular pathways involved in cancer development and regulation. In addition, crosstalk is known to occur across signaling pathways, including those associated with autophagy and apoptosis. Many cancer types are becoming resistant to chemotherapy due to defects in signaling pathways, particularly apoptosis. As an alternative cell fate mechanism, autophagy could be explored for the development of target-specific anticancer drugs. Further investigations, both *in vitro* and *in vivo*, are however necessary to better understand cancer pathobiology, which will enable the full potential of autophagy-apoptosis-targeted drug design to be exploited.

Scientists have always been interested in the use of plant products and their derivatives as successful sources of anticancer therapeutics. In fact, there is increasing evidence suggesting the emerging anticancer potential of phytochemicals that modulate several signaling pathways, including autophagy and apoptosis. The anticancer effects of phytochemicals have been observed to be selective and specific to cancer cells, and involve the modulation of autophagy and apoptosis. As a result, many phytochemicals are promising sources of anticancer drugs. The most notable phytochemicals that have exerted their anticancer potential *in vitro* and *in vivo* through modulating the autophagy-apoptosis pathway (i.e., sulforaphane, resveratrol, lycopene, epigallocatechin, curcumin, and berberine) are currently being investigated in clinical trials for different cancer types.

Because autophagy plays a context-dependent role in cancer patients, targeting this crucial cellular pathway may not always be beneficial. Furthermore, several phytochemicals target multiple signaling pathways that may be shared among multiple cellular systems, thereby posing a challenge to the development of phytochemical-based anticancer drugs. This issue could however be resolved through *in vitro* and *in vivo* studies on phytochemical-mediated autophagy-apoptosis modulation. In addition, an integrated system pharmacology and computational approach could be employed to better understand the anticancer effects of phytochemicals. As the clinical application of phytochemicals is limited by their poor bioavailability, improvements can be achieved by employing nanotechnology-based drug delivery. Based on the highlights in this review, the potential as well as the challenges of phytochemical-mediated targeting of autophagy and apoptosis could unravel new approaches and strategies for the development of novel anticancer therapeutics to treat several cancer types.

Eventually, upcoming challenges as well as possible perspectives have been demonstrated in the hope of improving anticancer effectiveness in addition to accelerate the translational improvement of precise nanomedicine or nanotechnology for targeted cancer therapy based on autophagy-apoptosis pathway. Nanoparticle-based drug delivery systems (NDDSs) have been comprehensively used in the diagnosis, therapy, as well as cancer imaging because of their features of extraordinary cancer-targeting efficiency and low toxic properties. Nevertheless, because of the problems of poor patient prognosis, high variability, as well as multidrug resistance (MDR), NDDSs have currently been challenged remarkable experiments. Indeed, combined targets of nanoscience along with naturally occurring bioactive compounds are very attractive as well as developing rapidly in recent times in combination with conventional drugs for improving clinical outcomes. Therefore, it would be urgently required to necessary with designing novel treatment approaches to investigate in-depth the early diagnosis and pathogenesis of cancer thereby targeting phytochemicals through autophagy-apoptosis pathway.

AUTHOR CONTRIBUTIONS

Idea and conceptualization by MAR. Figures are drawing by MHR. Writing and original draft preparation by MAH, RD, RI, MJU, AAMS, and MHR. Visualization and supervision by HR. All authors have read and agreed to the published version of the manuscript.

FUNDING

This work was supported by NRF Research Program (2016M3C7A1913845) and the Korea Research Fellowship (KRF) Program (M.A.R. 2016H1D3A1908615; M.A.H. 2018H1D3A1A01074712 to.; R.I. 2020H1D3A1A04104782), and additionally supported by (M.J.U. 2020R1I1A1A01072879 and 2020H1D3A2A02110924) funded by the Ministry of Science and ICT, Republic of Korea, and the KIST Institutional Programs (2E30962).

REFERENCES

Aggarwal, V., Tuli, H. S., Varol, A., Thakral, F., Yerer, M. B., Sak, K., et al. (2019). Role of reactive oxygen species in cancer progression: molecular mechanisms and recent advancements. *Biomolecules*. 9, 735. doi:10.3390/biom9110735

Al Dhaheri, Y., Attoub, S., Ramadan, G., Arafat, K., Bajbouj, K., Karuvantevida, N., et al. (2014). Carnosol induces ROS-mediated beclin1-independent autophagy and apoptosis in triple negative breast cancer. *PLoS One*. 9, e109630. doi:10.1371/journal.pone.0109630

Alers, S., Loffler, A. S., Wesselborg, S., and Stork, B. (2012). Role of AMPK-mTOR-ulk1/2 in the regulation of autophagy: cross talk, shortcuts, and feedbacks. *Mol. Cell Biol.* 32, 2–11. doi:10.1128/Mcb.06159-11

Alfarouk, K. O., Stock, C.-M., Taylor, S., Walsh, M., Muddathir, A. K., Verduzco, D., et al. (2015). Resistance to cancer chemotherapy: failure in drug response from ADME to P-gp. *Cancer Cel Int.* 15, 71. doi:10.1186/s12935-015-0221-1

Aung, T. N., Qu, Z. P., Kortschak, R. D., and Adelson, D. L. (2017). Understanding the effectiveness of natural compound mixtures in cancer through their molecular mode of action. *Int. J. Mol. Sci.* 18, 656. doi:10.3390/ijms18030656

Ávalos, Y., Canales, J., Bravo-Sagua, R., Criollo, A., Lavandero, S., and Quest, A. F. G. (2014). Tumor suppression and promotion by autophagy. *Biomed. Res. Int.* 2014, 1. doi:10.1155/2014/603980

Baliga, M. S., Haniadka, R., Pereira, M. M., D'Souza, J. J., Pallaty, P. L., Bhat, H. P., et al. (2011). Update on the chemopreventive effects of ginger and its phytochemicals. *Crit. Rev. Food Sci. Nutr.* 51, 499–523. doi:10.1080/10408391003698669

Balli, U., Cetinkaya, B. O., Keles, G. C., Keles, Z. P., Guler, S., Sogut, M. U., et al. (2016). Assessment of MMP-1, MMP-8 and TIMP-2 in experimental periodontitis treated with kaempferol. *J. Periodontal Implan*. 46, 84–95. doi:10.5051/jpis.2016.46.2.84

Barrajón-Catalán, E., Fernández-Arroyo, S., Saura, D., Guillén, E., Fernández-Gutiérrez, A., Segura-Carretero, A., et al. (2010). Cistaceae aqueous extracts containing ellagitannins show antioxidant and antimicrobial capacity, and cytotoxic activity against human cancer cells. *Food Chem. Toxicol.* 48, 2273–2282. doi:10.1016/j.fct.2010.05.060

Bezerra, D. P., Pessoa, C., Moraes, M. O., Alencar, N. M., Mesquita, R. O., Lima, M. W., et al. (2008). *In vivo* growth inhibition of sarcoma 180 by piperlonguminine, an alkaloid amide from the Piper species. *J Appl Toxicol.* 28, 599–607. doi:10.1002/jat.1311

Bhatia, K., Bhumika, and Das, A. (2020). Combinatorial drug therapy in cancer - new insights. *Life Sci.* 258, 118134. doi:10.1016/j.lfs.2020.118134

Bi, Y., Shen, C., Li, C., Liu, Y., Gao, D., Shi, C., et al. (2016). Inhibition of autophagy induced by quercetin at a late stage enhances cytotoxic effects on glioma cells. *Tumour Biol.* 37, 3549–3560. doi:10.1007/s13277-015-4125-4

Bimonte, S., Albino, V., Piccirillo, M., Nasto, A., Molino, C., Palaia, R., et al. (2019). Epigallocatechin-3-gallate in the prevention and treatment of hepatocellular carcinoma: experimental findings and translational perspectives. *Drug Des. Dev. Ther.* 13, 611–621. doi:10.2147/DDDT.S180079

Boreddy, S. R., Pramanik, K. C., and Srivastava, S. K. (2011). Pancreatic tumor suppression by benzyl isothiocyanate is associated with inhibition of PI3K/AKT/FOXO pathway. *Clin Cancer Res.* 17, 1784–1795. doi:10.1158/1078-0432.ccr-10-1891

Cao, Z., Zhang, H., Cai, X., Fang, W., Chai, D., Wen, Y., et al. (2017). Luteolin promotes cell apoptosis by inducing autophagy in hepatocellular carcinoma, cellular physiology and biochemistry. *Int. J. Exp. Cell. Physiol. Biochem. Pharmacol.* 43, 1803–1812. doi:10.1159/000484066

Cao, J., Chen, H., Lu, W., Wu, Y., Wu, X., Xia, D., et al. (2018). Myricetin induces protective autophagy by inhibiting the phosphorylation of mTOR in HepG2 cells, anatomical record (hoboken, N. *Anat Rec (Hoboken).* 301, 786–795. doi:10.1002/ar.23754

Chaicharoenaudomrung, N., Jaroonwitchawan, T., and Noisa, P. (2018). Cordycepin induces apoptotic cell death of human brain cancer through the modulation of autophagy. *Toxicol. Vitro.* 46, 113–121. doi:10.1016/j.tiv.2017.10.002

Chao, A. C., Hsu, Y. L., Liu, C. K., and Kuo, P. L. (2011). α-Mangostin, a dietary xanthone, induces autophagic cell death by activating the AMP-activated protein kinase pathway in glioblastoma cells. *J. Agric. Food Chem.* 59, 2086–2096. doi:10.1021/jf1042757

Chao, W., Deng, J. S., Li, P. Y., Liang, Y. C., and Huang, G. J. (2017). 3,4-Dihydroxybenzalactone suppresses human non-small cell lung carcinoma cells metastasis via suppression of epithelial to mesenchymal transition, ROS-mediated PI3K/AKT/MAPK/MMP and NF kappa B signaling pathways. *Molecules.* 22, 537. doi:10.3390/molecules22040537

Chen, J. C., Chiu, M. H., Nie, R. L., Cordell, G. A., and Qiu, S. X. (2005). Cucurbitacins and cucurbitane glycosides: structures and biological activities. *Nat. Prod. Rep.* 22, 386–399. doi:10.1039/b418841c

Chen, K.-L., Chang, W.-S. W., Cheung, C. H. A., Lin, C.-C., Huang, C.-C., Yang, Y.-N., et al. (2012). Targeting cathepsin S induces tumor cell autophagy via the EGFR-ERK signaling pathway. *Cancer Lett.* 317, 89–98. doi:10.1016/j.canlet.2011.11.015

Chen, C. Y., Chen, K. C., Yang, T. Y., Liu, H. C., and Hsu, S. L. (2013a). Gallic acid induces a reactive oxygen species-provoked c-jun NH2-terminal kinase-dependent apoptosis in lung fibroblasts. *Evid. Based Complement. Alternat Med.* 2013, 613950. doi:10.1155/2013/613950

Chen, M., Du, Y., Qui, M., Wang, M., Chen, K., Huang, Z., et al. (2013b). Ophiopogonin B-induced autophagy in non-small cell lung cancer cells via inhibition of the PI3K/Akt signaling pathway. *Oncol. Rep.* 29, 430–436. doi:10.3892/or.2012.2131

Chen, H. Y., Huang, T. C., Shieh, T. M., Wu, C. H., Lin, L. C., and Hsia, S. M. (2017a). Isoliquiritigenin induces autophagy and inhibits ovarian cancer cell growth. *Int. J. Mol. Sci.* 18, 2025. doi:10.3390/ijms18102025

Chen, L. M., Song, T. J., Xiao, J. H., Huang, Z. H., Li, Y., and Lin, T. Y. (2017b). Tripchlorolide induces autophagy in lung cancer cells by inhibiting the PI3K/AKT/mTOR pathway and improves cisplatin sensitivity in A549/DDP cells. *Oncotarget*. 8, 63911–63922. doi:10.18632/oncotarget.19201

Chen, J., Zhu, Y., Zhang, W., Peng, X., Zhou, J., Li, F., et al. (2018). Delphinidin induced protective autophagy via mTOR pathway suppression and AMPK pathway activation in HER-2 positive breast cancer cells. *BMC Cancer*. 18, 342. doi:10.1186/s12885-018-4231-y

Cheng, Y. C., Hueng, D. Y., Huang, H. Y., Chen, J. Y., and Chen, Y. (2016). Magnolol and honokiol exert a synergistic anti-tumor effect through autophagy and apoptosis in human glioblastomas. *Oncotarget*. 7, 29116–29130. doi:10.18632/oncotarget.8674

Chirumbolo, S., Bjørklund, G., Lysiuk, R., Vella, A., Lenchyk, L., and Upyr, T. (2018). Targeting cancer with phytochemicals via their fine tuning of the cell survival signaling pathways. *Int. J. Mol. Sci.* 19. doi:10.3390/ijms19113568

Choe, Y.-J., Ha, T. J., Ko, K.-W., Lee, S.-Y., Shin, S. J., and Kim, H.-S. (2012). Anthocyanins in the black soybean (*Glycine* max L.) protect U2OS cells from apoptosis by inducing autophagy via the activation of adenosyl monophosphate-dependent protein kinase. *Oncol. Rep.* 28, 2049–2056. doi:10.3892/or.2012.2034

Choi, E. J., Bae, S. M., and Ahn, W. S. (2008). Antiproliferative effects of quercetin through cell cycle arrest and apoptosis in human breast cancer MDA-MB-453 cells. *Arch. Pharm. Res.* 31, 1281–1285. doi:10.1007/s12272-001-2107-0

Choi, A. M. K., Ryter, S. W., and Levine, B. (2013). Autophagy in human health and disease. *N. Engl. J. Med.* 368, 651–662. doi:10.1056/NEJMra1205406

Choi, J. B., Kim, J. H., Lee, H., Pak, J. N., Shim, B. S., and Kim, S. H. (2018). Reactive oxygen species and p53 mediated activation of p38 and caspases is critically involved in kaempferol induced apoptosis in colorectal cancer cells. *J. Agric. Food Chem.* 66, 9960–9967. doi:10.1021/acs.jafc.8b02656

Choudhari, A. S., Mandave, P. C., Deshpande, M., Ranjekar, P., and Prakash, O. (2020). Phytochemicals in cancer treatment: from preclinical studies to clinical practice. *Front. Pharmacol.* 10, 1614. doi:10.3389/fphar.2019.01614

Chu, Y.-L., Ho, C.-T., Chung, J.-G., Rajasekaran, R., and Sheen, L.-Y. (2012). Allicin induces p53-mediated autophagy in hep G2 human liver cancer cells. *J. Agric. Food Chem.* 60, 8363–8371. doi:10.1021/jf301298y

Chu, S. C., Hsieh, Y. S., Yu, C. C., Lai, Y. Y., and Chen, P. N. (2014). Thymoquinone induces cell death in human squamous carcinoma cells via caspase activation-dependent apoptosis and LC3-II activation-dependent autophagy. *PLoS One*. 9, e101579. doi:10.1371/journal.pone.0101579

Comel, A., Sorrentino, G., Capaci, V., and Del Sal, G. (2014). The cytoplasmic side of p53's oncosuppressive activities. *FEBS Lett.* 588, 2600–2609. doi:10.1016/j.febslet.2014.04.015

Covarrubias, L., Hernández-García, D., Schnabel, D., Salas-Vidal, E., and Castro-Obregón, S. (2008). Function of reactive oxygen species during animal

development: passive or active? *Developmental Biol.* 320, 1–11. doi:10.1016/j.ydbio.2008.04.041

Delmas, D., Rébé, C., Lacour, S., Filomenko, R., Athias, A., Gambert, P., et al. (2003). Resveratrol-induced apoptosis is associated with Fas redistribution in the rafts and the formation of a death-inducing signaling complex in colon cancer cells. *J. Biol. Chem.* 278, 41482–41490. doi:10.1074/jbc.M304896200

Deng, S., Shanmugam, M. K., Kumar, A. P., Yap, C. T., Sethi, G., and Bishayee, A. (2019). Targeting autophagy using natural compounds for cancer prevention and therapy. *Cancer*. 125, 1228–1246. doi:10.1002/cncr.31978

Edris, A. E. (2009). Anti-cancer properties of Nigella spp. essential oils and their major constituents, thymoquinone and beta-elemene. *Curr. Clin. Pharmacol.* 4, 43–46. doi:10.2174/157488409787236137

Elango, R., Athinarayanan, J., Subbarayan, V. P., Lei, D. K. Y., and Alshatwi, A. A. (2018). Hesperetin induces an apoptosis-triggered extrinsic pathway and a p53-independent pathway in human lung cancer H522 cells. *J. Asian Nat. Prod. Res.* 20, 559–569. doi:10.1080/10286020.2017.1327949

Elmore, S. (2007). Apoptosis: a review of programmed cell death. *Toxicol. Pathol.* 35, 495–516. doi:10.1080/01926230701320337

Estrela, J. M., Mena, S., Obrador, E., Benlloch, M., Castellano, G., Salvador, R., et al. (2017). Polyphenolic phytochemicals in cancer prevention and therapy: bioavailability versus bioefficacy. *J. Med. Chem.* 60, 9413–9436. doi:10.1021/acs.jmedchem.6b01026

Filomeni, G., De Zio, D., and Cecconi, F. (2015). Oxidative stress and autophagy: the clash between damage and metabolic needs. *Cell Death Differ*. 22, 377–388. doi:10.1038/cdd.2014.150

Focaccetti, C., Izzi, V., Benvenuto, M., Fazi, S., Ciuffa, S., Giganti, M. G., et al. (2019). Polyphenols as immunomodulatory compounds in the tumor microenvironment: friends or foes? *Int. J. Mol. Sci.* 20, 1714. doi:10.3390/ijms20071714

Frieboes, H. B., Huang, J. S., Yin, W. C., and McNally, L. R. (2014). Chloroquine-mediated cell death in metastatic pancreatic adenocarcinoma through inhibition of autophagy. *JOP*. 15, 189–197. doi:10.6092/1590-8577/1900

Ghavami, S., Kerkhoff, C., Los, M., Hashemi, M., Sorg, C., and Karami-Tehrani, F. (2004). Mechanism of apoptosis induced by S100A8/A9 in colon cancer cell lines: the role of ROS and the effect of metal ions. *J. Leukoc. Biol.* 76, 169–175. doi:10.1189/jlb.0903435

Ghobrial, I. M., Witzig, T. E., and Adjei, A. A. (2005). Targeting apoptosis pathways in cancer therapy. *CA Cancer J Clin.* 55, 178–194. doi:10.3322/canjclin.55.3.178

Goldar, S., Khaniani, M. S., Derakhshan, S. M., and Baradaran, B. (2015). Molecular mechanisms of apoptosis and roles in cancer development and treatment. *Asian Pac. J. Cancer Prev.* 16, 2129–2144. doi:10.7314/apjcp.2015.16.6.2129

Goldsmith, J., Levine, B., and Debnath, J. (2014). Autophagy and cancer metabolism. *Method Enzymol.* 542, 25–57. doi:10.1016/B978-0-12-416618-9.00002-9

Gossner, G., Choi, M., Tan, L., Fogoros, S., Griffith, K., Kuenker, M., et al. (2007). Genistein-induced apoptosis and autophagocytosis in ovarian cancer cells. *Gynecol. Oncol.* 105, 23–30. doi:10.1016/j.ygyno.2006.11.009

Granato, M., Rizzello, C., Gilardini Montani, M. S., Cuomo, L., Vitillo, M., Santarelli, R., et al. (2017). Quercetin induces apoptosis and autophagy in primary effusion lymphoma cells by inhibiting PI3K/AKT/mTOR and STAT3 signaling pathways. *J. Nutr. Biochem.* 41, 124–136. doi:10.1016/j.jnutbio.2016.12.011

Green, D. R., and Llambi, F. (2015). Cell death signaling. *Cold Spring Harbor Perspect. Biol.* 7, a00608. doi:10.1101/cshperspect.a006080

Grube, S., Ewald, C., Kögler, C., Lawson McLean, A., Kalff, R., and Walter, J. (2018). Achievable central nervous system concentrations of the green tea catechin EGCG induce stress in glioblastoma cells *in Vitro*. *Nutr. Cancer*. 70, 1145–1158. doi:10.1080/01635581.2018.1495239

Guamán Ortiz, L. M., Croce, A. L., Aredia, F., Sapienza, S., Fiorillo, G., Syeda, T. M., et al. (2015). Effect of new berberine derivatives on colon cancer cells. *Acta Biochim. Biophys. Sinica*. 47, 824–833. doi:10.1093/abbs/gmv077

Guan, C., Liu, W., Yue, Y., Jin, H., Wang, X., and Wang, X.-J. (2014). Inhibitory effect of β-elemene on human breast cancer cells. *Int. J. Clin. Exp. Pathol.* 7, 3948

Guicciardi, M. E., and Gores, G. J. (2009). Life and death by death receptors. *FASEB j.* 23, 1625–1637. doi:10.1096/fj.08-111005

Guo, J., Huang, X., Wang, H., and Yang, H. (2015). Celastrol induces autophagy by targeting AR/miR-101 in prostate cancer cells. *PLoS One*. 10, e0140745. doi:10.1371/journal.pone.0140745

Gupta, P., and Srivastava, S. K. (2012). Antitumor activity of phenethyl isothiocyanate in HER2-positive breast cancer models. *BMC Med.* 10, 80. doi:10.1186/1741-7015-10-80

Ha, E. J., Kim, K. Y., Kim, C. E., Jun, D. Y., and Kim, Y. H. (2019). Enhancement of quercetin-induced apoptosis by cotreatment with autophagy inhibitor is associated with augmentation of BAK-dependent mitochondrial pathway in Jurkat T cells. *Oxid Med. Cel Longev*. 2019, 7989276. doi:10.1155/2019/7989276

Hanna, T. P., King, W. D., Thibodeau, S., Jalink, M., Paulin, G. A., Harvey-Jones, E., et al. (2020). Mortality due to cancer treatment delay: systematic review and meta-analysis. *BMJ*. 371, m4087. doi:10.1136/bmj.m4087

Hannan, M. A., Dash, R., Haque, M. N., Mohibbullah, M., Sohag, A. A., Rahman, M. A., et al. (2020). Neuroprotective potentials of marine algae and their bioactive metabolites: pharmacological insights and therapeutic advances. *Mar. Drugs*. 18, 347. doi:10.3390/md18070347

Hartwig, A., Arand, M., Epe, B., Guth, S., Jahnke, G., Lampen, A., et al. (2020). Mode of action-based risk assessment of genotoxic carcinogens. *Arch. Toxicol.* 94, 1787–1877. doi:10.1007/s00204-020-02733-2

Hassan, M., Watari, H., AbuAlmaaty, A., Ohba, Y., and Sakuragi, N. (2020). Apoptosis and molecular targeting therapy in cancer, BioMed Research International. 2020, 2451249. doi:10.1155/2020/2451249

Henley, S. J., Ward, E. M., Scott, S., Ma, J., Anderson, R. N., Firth, A. U., et al. (2020). Annual report to the nation on the status of cancer, part I: National cancer statistics. *Cancer*. 126, 2225–2249. doi:10.1002/cncr.32802

Hsin, M. C., Hsieh, Y. H., Wang, P. H., Ko, J. L., Hsin, I. L., and Yang, S. F. (2017). Hispolon suppresses metastasis via autophagic degradation of cathepsin S in cervical cancer cells. *Cell Death Dis*. 8. 3089. doi:10.1038/cddis.2017.459

Hsu, Y. L., Kuo, P. L., Chiang, L. C., and Lin, C. C. (2004). Involvement of p53, nuclear factor kappaB and Fas/Fas ligand in induction of apoptosis and cell cycle arrest by saikosaponin d in human hepatoma cell lines. *Cancer Lett.* 213, 213–221. doi:10.1016/j.canlet.2004.03.044

Huang, Y.-H., Sun, Y., Huang, F.-Y., Li, Y.-N., Wang, C.-C., Mei, W.-L., et al. (2017). Toxicarioside O induces protective autophagy in a sirtuin-1-dependent manner in colorectal cancer cells. *Oncotarget*. 8, 52783. doi:10.18632/oncotarget.17189

Hui, C., Bin, Y., Xiaoping, Y., Long, Y., Chunye, C., Mantian, M., et al. (2010). Anticancer activities of an anthocyanin-rich extract from black rice against breast cancer cells *in vitro* and *in vivo*. *Nutr. Cancer*. 62, 1128–1136. doi:10.1080/01635581.2010.494821

Hung, J. Y., Hsu, Y. L., Li, C. T., Ko, Y. C., Ni, W. C., Huang, M. S., et al. (2009). 6-Shogaol, an active constituent of dietary ginger, induces autophagy by inhibiting the AKT/mTOR pathway in human non-small cell lung cancer A549 cells. *J. Agric. Food Chem.* 57, 9809–9816. doi:10.1021/jf902315e

Hurley, J. H., and Young, L. N. (2017). Mechanisms of autophagy initiation. *Annu. Rev. Biochem.* 86, 225–244. doi:10.1146/annurev-biochem-061516-044820

Jahanafrooz, Z., Motamed, N., Rinner, B., Mokhtarzadeh, A., and Baradaran, B. (2018). Silibinin to improve cancer therapeutic, as an apoptotic inducer, autophagy modulator, cell cycle inhibitor, and microRNAs regulator. *Life Sci.* 213, 236–247. doi:10.1016/j.lfs.2018.10.009

Jang, H. J., Yang, K. E., Hwang, I. H., Huh, Y. H., Kim, D. J., Yoo, H. S., et al. (2019). Cordycepin inhibits human ovarian cancer by inducing autophagy and apoptosis through Dickkopf-related protein 1/β-catenin signaling. *Am. J. Transl Res.* 11, 6890–6906.

Jin, H. R., Zhao, J., Zhang, Z., Liao, Y., Wang, C. Z., Huang, W. H., et al. (2012). The antitumor natural compound falcarindiol promotes cancer cell death by inducing endoplasmic reticulum stress. *Cel Death Dis.* 3, e376. doi:10.1038/cddis.2012.122

Johnson, R., Shabalala, S., Louw, J., Kappo, A. P., and Muller, C. J. F. (2017). Aspalathin reverts doxorubicin-induced cardiotoxicity through increased autophagy and decreased expression of p53/mTOR/p62 signaling. *Molecules*. 22. 1589. doi:10.3390/molecules22101589

Jung, E. M., Lim, J. H., Lee, T. J., Park, J. W., Choi, K. S., and Kwon, T. K. (2005). Curcumin sensitizes tumor necrosis factor-related apoptosis-inducing ligand (TRAIL)-induced apoptosis through reactive oxygen species-mediated upregulation of death receptor 5 (DR5). *Carcinogenesis*. 26, 1905–1913. doi:10.1093/carcin/bgi167

Jung, S., Jeong, H., and Yu, S.-W. (2020). Autophagy as a decisive process for cell death. *Exp. Mol. Med.* 52, 921–930. doi:10.1038/s12276-020-0455-4

Kardideh, B., Samimi, Z., Norooznezhad, F., Kiani, S., and Mansouri, K. (2019). Autophagy, cancer and angiogenesis: where is the link? *Cell Biosci*. 9, 65. doi:10.1186/s13578-019-0327-6

Karius, T., Schnekenburger, M., Dicato, M., and Diederich, M. (2012). MicroRNAs in cancer management and their modulation by dietary agents. *Biochem. Pharmacol.* 83, 1591–1601. doi:10.1016/j.bcp.2012.02.004

Khaltaev, N., and Axelrod, S. (2020). Global lung cancer mortality trends and lifestyle modifications: preliminary analysis. *Chin. Med J-Peking.* 133, 1526–1532. doi:10.1097/Cm9.0000000000000918

Kim, E. S., Shin, J. H., Seok, S. H., Kim, J. B., Chang, H., Park, S. J., et al. (2013). Autophagy mediates anti-melanogenic activity of 3′-ODI in B16F1 melanoma cells. *Biochem. Biophysical Res. Commun.* 442, 165–170. doi:10.1016/j.bbrc.2013.11.048

Kim, R. (2005). Recent advances in understanding the cell death pathways activated by anticancer therapy. *Cancer*. 103, 1551–1560. doi:10.1002/cncr.20947

Kotani, T., Kirisako, H., Koizumi, M., Ohsumi, Y., and Nakatogawa, H. (2018). The Atg2-Atg18 complex tethers pre-autophagosomal membranes to the endoplasmic reticulum for autophagosome formation. *Proc. Natl. Acad. Sci. USA*. 115, 10363–10368. doi:10.1073/pnas.1806727115

Krishnan, S., Shrestha, Y., Jayatunga, D. P. W., Rea, S., Martins, R., and Bharadwaj, P. (2020). Activate or inhibit? Implications of autophagy modulation as a therapeutic strategy for alzheimer's disease. *Int. J. Mol. Sci.* 21, 6739 doi:10.3390/ijms21186739

Kumar, D., Shankar, S., and Srivastava, R. K. (2013). Rottlerin-induced autophagy leads to the apoptosis in breast cancer stem cells: molecular mechanisms. *Mol. Cancer*. 12, 171. doi:10.1186/1476-4598-12-171

Kwon, Y. H., Bishayee, K., Rahman, M. A., Hong, J. S., Lim, S. S., and Huh, S. O. (2015). Morus alba accumulates reactive oxygen species to initiate apoptosis via FOXO-caspase 3-dependent pathway in neuroblastoma cells. *Mol. Cell*. 38, 630–637. doi:10.14348/molcells.2015.0030

Lancon, A., Kaminski, J., Tili, E., Michaille, J. J., and Latruffe, N. (2012). Control of MicroRNA expression as a new way for resveratrol to deliver its beneficial effects. *J. Agr Food Chem.* 60, 8783–8789. doi:10.1021/jf301479v

Lao, Y., Wan, G., Liu, Z., Wang, X., Ruan, P., Xu, W., et al. (2014). The natural compound oblongifolin C inhibits autophagic flux and enhances antitumor efficacy of nutrient deprivation. *Autophagy*. 10, 736–749. doi:10.4161/auto.28034

Law, B. Y., Wang, M., Ma, D. L., Al-Mousa, F., Michelangeli, F., Cheng, S. H., et al. (2010). Alisol B, a novel inhibitor of the sarcoplasmic/endoplasmic reticulum Ca(2+) ATPase pump, induces autophagy, endoplasmic reticulum stress, and apoptosis. *Mol. Cancer Ther.* 9, 718–730. doi:10.1158/1535-7163.mct-09-0700

Law, B. Y. K., Mok, S. W. F., Chen, J., Michelangeli, F., Jiang, Z. H., Han, Y., et al. (2017). N-desmethyldauricine induces autophagic cell death in apoptosis-defective cells via Ca(2+) mobilization. *Front. Pharmacol.* 8, 388. doi:10.3389/fphar.2017.00388

Lee, Y. J., Kim, N.-Y., Suh, Y.-A., and Lee, C. (2011). Involvement of ROS in curcumin-induced autophagic cell death. *Korean J. Physiol. Pharmacol.* 15, 1–7. doi:10.4196/kjpp.2011.15.1.1

Lee, E. B., Cheon, M. G., Cui, J., Lee, Y. J., Seo, E. K., and Jang, H. H. (2017). The quinone-based derivative, HMNQ induces apoptotic and autophagic cell death by modulating reactive oxygen species in cancer cells. *Oncotarget*. 8, 99637–99648. doi:10.18632/oncotarget.21005

Levine, B., and Kroemer, G. (2008). Autophagy in the pathogenesis of disease. *Cell.* 132, 27–42. doi:10.1016/j.cell.2007.12.018

Li, W., Nie, S., Yu, Q., and Xie, M. (2009). (-)-Epigallocatechin-3-gallate induces apoptosis of human hepatoma cells by mitochondrial pathways related to reactive oxygen species. *J. Agric. Food Chem.* 57, 6685–6691. doi:10.1021/jf901396f

Li, L., Yue, G. G., Lau, C. B., Sun, H., Fung, K. P., Leung, P. C., et al. (2012). Eriocalyxin B induces apoptosis and cell cycle arrest in pancreatic adenocarcinoma cells through caspase-and p53-dependent pathways. *Toxicol. Appl. Pharmacol.* 262, 80–90.

Li, F., Ma, Z., Guan, Z., Chen, Y., Wu, K., Guo, P., et al. (2015). Autophagy induction by silibinin positively contributes to its anti-metastatic capacity via AMPK/mTOR pathway in renal cell carcinoma. *Int. J. Mol. Sci.* 16, 8415–8429. doi:10.3390/ijms16048415

Lin, X., Wu, G., Huo, W.-Q., Zhang, Y., and Jin, F.-S. (2012). Resveratrol induces apoptosis associated with mitochondrial dysfunction in bladder carcinoma cells. *Int. J. Urol.* 19, 757–764. doi:10.1111/j.1442-2042.2012.03024.x

Lin, C.-M., Chen, H.-H., Lin, C.-A., Wu, H.-C., Sheu, J. J.-C., and Chen, H.-J. (2017a). Apigenin-induced lysosomal degradation of β-catenin in Wnt/β-catenin signaling. *Scientific Rep.* 7, 1–17. doi:10.1038/s41598-017-00409-z

Lin, Y.-T., Wang, H.-C., Hsu, Y.-C., Cho, C.-L., Yang, M.-Y., and Chien, C.-Y. (2017b). Capsaicin induces autophagy and apoptosis in human nasopharyngeal carcinoma cells by downregulating the PI3K/AKT/mTOR pathway. *Int. J. Mol. Sci.* 18, 1343. doi:10.3390/ijms18071343

Ling, M. T., Luk, S. U., Al-Ejeh, F., and Khanna, K. K. (2012). Tocotrienol as a potential anticancer agent. *Carcinogenesis*. 33, 233–239. doi:10.1093/carcin/bgr261

Liu, J., Zheng, L., Zhong, J., Wu, N., Liu, G., and Lin, X. (2014). Oleanolic acid induces protective autophagy in cancer cells through the JNK and mTOR pathways. *Oncol. Rep.* 32, 567–572. doi:10.3892/or.2014.3239

Liu, S., Xu, Z. L., Sun, L., Liu, Y., Li, C. C., Li, H. M., et al. (2016). (-)-Epigallocatechin-3-gallate induces apoptosis in human pancreatic cancer cells via PTEN. *Mol. Med. Rep.* 14, 599–605. doi:10.3892/mmr.2016.5277

Liu, F., Gao, S., Yang, Y., Zhao, X., Fan, Y., Ma, W., et al. (2018). Antitumor activity of curcumin by modulation of apoptosis and autophagy in human lung cancer A549 cells through inhibiting PI3K/Akt/mTOR pathway. *Oncol. Rep.* 39, 1523–1531. doi:10.3892/or.2018.6188

Lopez, J., and Tait, S. W. G. (2015). Mitochondrial apoptosis: killing cancer using the enemy within. *Br. J. Cancer*. 112, 957–962. doi:10.1038/bjc.2015.85

Lu, T., Gu, M., Zhao, Y., Zheng, X., and Xing, C. (2017). Autophagy contributes to falcarindiol-induced cell death in breast cancer cells with enhanced endoplasmic reticulum stress. *PLoS One*. 12, e0176348. doi:10.1371/journal.pone.0176348

Ma, X., and Ning, S. (2019). Cyanidin-3-glucoside attenuates the angiogenesis of breast cancer via inhibiting STAT3/VEGF pathway. *Phytotherapy Res.* 33, 81–89. doi:10.1002/ptr.6201

Mai, T. T., Moon, J., Song, Y., Viet, P. Q., Phuc, P. V., Lee, J. M., et al. (2012). Ginsenoside F2 induces apoptosis accompanied by protective autophagy in breast cancer stem cells. *Cancer Lett.* 321, 144–153. doi:10.1016/j.canlet.2012.01.045

Markham, M. J., Wachter, K., Agarwal, N., Bertagnolli, M. M., Chang, S. M., Dale, W., et al. (2020). Clinical cancer advances 2020: annual report on progress against cancer from the American society of clinical oncology. *Jco*. 38, 1081. doi:10.1200/jco.19.03141

Masuelli, L., Benvenuto, M., Stefano, E. D., Mattera, R., Fantini, M., Feudis, G. D., et al. (2017). Curcumin blocks autophagy and activates apoptosis of malignant mesothelioma cell lines and increases the survival of mice intraperitoneally transplanted with a malignant mesothelioma cell line. *Oncotarget*. 8, 34405. doi:10.18632/oncotarget.14907

Minto, R. E., and Blacklock, B. J. (2008). Biosynthesis and function of polyacetylenes and allied natural products. *Prog. lipid Res.* 47, 233–306. doi:10.1016/j.plipres.2008.02.002

Mitra, S., and Dash, R. (2018). Natural products for the management and prevention of breast cancer, evidence-based complementary and alternative medicine, *Evid Based Complement Alternat Med.* 2018, 8324696. doi:10.1155/2018/8324696

Mohapatra, P., Preet, R., Das, D., Satapathy, S. R., Choudhuri, T., Wyatt, M. D., et al. (2012). Quinacrine-mediated autophagy and apoptosis in colon cancer cells is through a p53- and p21-dependent mechanism. *Oncol. Res.* 20, 81–91. doi:10.3727/096504012x13473664562628

Moni, A., Iqbal, A., and Uddin, M. J. (2018). Resveratrol attenuates inflammation through tristetraprolin expression in human hepatocytes. *J. Adv. Biotechnol. Exp. Ther.* 1, 78–82. doi:10.5455/jabet.2018.d14

Moosavi, M. A., Haghi, A., Rahmati, M., Taniguchi, H., Mocan, A., Echeverría, J., et al. (2018). Phytochemicals as potent modulators of autophagy for cancer therapy. *Cancer Lett.* 424, 46–69. doi:10.1016/j.canlet.2018.02.030

Mujumdar, N., Mackenzie, T. N., Dudeja, V., Chugh, R., Antonoff, M. B., Borja-Cacho, D., et al. (2010). Triptolide induces cell death in pancreatic cancer cells by apoptotic and autophagic pathways. *Gastroenterology*. 139, 598–608. doi:10.1053/j.gastro.2010.04.046

Naumann, P., Fortunato, F., Zentgraf, H., Büchler, M. W., Herr, I., and Werner, J. (2011). Autophagy and cell death signaling following dietary sulforaphane act independently of each other and require oxidative stress in pancreatic cancer. *Int. J. Oncol.* 39, 101–109. doi:10.3892/ijo.2011.1025

Newman, D. J., and Cragg, G. M. (2016). Natural products as sources of new drugs from 1981 to 2014. *J. Nat. Prod.* 79, 629–661. doi:10.1021/acs.jnatprod.5b01055

Panda, P. K., Mukhopadhyay, S., Das, D. N., Sinha, N., Naik, P. P., and Bhutia, S. K. (2015). Mechanism of autophagic regulation in carcinogenesis and cancer therapeutics. *Semin. Cel Developmental Biol.* 39, 43–55. doi:10.1016/j.semcdb.2015.02.013

Patra, S., Mishra, S. R., Behera, B. P., Mahapatra, K. K., Panigrahi, D. P., Bhol, C. S., et al. (2020). Autophagy-modulating phytochemicals in cancer therapeutics: current evidences and future perspectives. *Semin. Cancer Biol.* doi:10.1016/j.semcancer.2020.05.008

Peng, P. L., Kuo, W. H., Tseng, H. C., and Chou, F. P. (2008). Synergistic tumor-killing effect of radiation and berberine combined treatment in lung cancer: the contribution of autophagic cell death. *Int. J. Radiat. Oncol. Biol. Phys.* 70, 529–542. doi:10.1016/j.ijrobp.2007.08.034

Pollier, J., and Goossens, A. (2012). *Oleanolic acid, Phytochemistry*. 77, 10–15. doi:10.1016/j.phytochem.2011.12.022

Radhakrishnan, E., Bava, S. V., Narayanan, S. S., Nath, L. R., Thulasidasan, A. K. T., Soniya, E. V., et al. (2014). [6]-Gingerol induces caspase-dependent apoptosis and prevents PMA-induced proliferation in colon cancer cells by inhibiting MAPK/AP-1 signaling. *PloS one*. 9, e104401. doi:10.1371/journal.pone.0104401

Rahman, M. A., and Rhim, H. (2017). Therapeutic implication of autophagy in neurodegenerative diseases. *BMB Rep.* 50, 345–354. doi:10.5483/BMBRep.2017.50.7.069

Rahman, M. A., Kim, N. H., Kim, S. H., Oh, S. M., and Huh, S. O. (2012a). Antiproliferative and cytotoxic effects of resveratrol in mitochondria-mediated apoptosis in rat B103 neuroblastoma cells. *Korean J. Physiol. Pha.* 16, 321–326. doi:10.4196/kjpp.2012.16.5.321

Rahman, M. A., Kim, N. H., Yang, H., and Huh, S. O. (2012b). Angelicin induces apoptosis through intrinsic caspase-dependent pathway in human SH-SY5Y neuroblastoma cells. *Mol. Cell Biochem.* 369, 95–104. doi:10.1007/s11010-012-1372-1

Rahman, M. A., Kim, N. H., and Huh, S. O. (2013). Cytotoxic effect of gambogic acid on SH-SY5Y neuroblastoma cells is mediated by intrinsic caspase-dependent signaling pathway. *Mol. Cel Biochem.* 377, 187–196. doi:10.1007/s11010-013-1584-z

Rahman, M. A., Yang, H., Kim, N. H., and Huh, S. O. (2014). Induction of apoptosis by *Dioscorea* nipponica Makino extracts in human SH-SY5Y neuroblastoma cells via mitochondria-mediated pathway. *Anim. Cell Syst.* 18, 41–51. doi:10.1080/19768354.2014.880372

Rahman, M. A., Hong, J. S., and Huh, S. O. (2015). Antiproliferative properties of Saussurea lappa Clarke root extract in SH-SY5Y neuroblastoma cells via intrinsic apoptotic pathway. *Anim. Cell Syst* 19, 119–126. doi:10.1080/19768354.2015.1008041

Rahman, M. A., Bishayee, K., Habib, K., Sadra, A., and Huh, S. O. (2016a). 18 alpha-Glycyrrhetinic acid lethality for neuroblastoma cells via de-regulating the Beclin-1/Bcl-2 complex and inducing apoptosis. *Biochem. Pharmacol.* 117, 97–112. doi:10.1016/j.bcp.2016.08.006

Rahman, M. A., Bishayee, K., and Huh, S. O. (2016b). Angelica polymorpha Maxim induces apoptosis of human SH-SY5Y neuroblastoma cells by regulating an intrinsic caspase pathway. *Mol. Cell.* 39, 119–128. doi:10.14348/molcells.2016.2232

Rahman, M. A., Bishayee, K., Sadra, A., and Huh, S. O. (2017). Oxyresveratrol activates parallel apoptotic and autophagic cell death pathways in neuroblastoma cells. *Biochim. Biophys. Acta Gen. Subj.* 1861, 23–36. doi:10.1016/j.bbagen.2016.10.025

Rahman, M. A., Hwang, H., Nah, S. Y., and Rhim, H. (2020). Gintonin stimulates autophagic flux in primary cortical astrocytes. *J. Ginseng Res.* 44, 67–78. doi:10.1016/j.jgr.2018.08.004

Rahman, M. A., Rahman, M. H., Hossain, M. S., Biswas, P., Islam, R., Uddin, M. J., et al. (2020a). Molecular insights into the multifunctional role of natural compounds: autophagy modulation and cancer prevention. *Biomedicines*. 8. 517. doi:10.3390/biomedicines8110517

Rahman, M. A., Rahman, M. R., Zaman, T., Uddin, M. S., Islam, R., Abdel-Daim, M. M., et al. (2020b). Emerging potential of naturally occurring autophagy modulators against neurodegeneration. *Curr. Pharm. Des.* 26, 772–779. doi:10.2174/1381612826666200107142541

Raj, L., Ide, T., Gurkar, A. U., Foley, M., Schenone, M., Li, X., et al. (2011). Selective killing of cancer cells by a small molecule targeting the stress response to ROS. *Nature*. 475, 231–234. doi:10.1038/nature10167

Rajendran, P., Nandakumar, N., Rengarajan, T., Palaniswami, R., Gnanadhas, E. N., Lakshminarasaiah, U., et al. (2014). Antioxidants and human diseases. *Clin. Chim. Acta* 436, 332–347. doi:10.1016/j.cca.2014.06.004

Rasul, A., Yu, B., Zhong, L., Khan, M., Yang, H., and Ma, T. (2012). Cytotoxic effect of evodiamine in SGC-7901 human gastric adenocarcinoma cells via simultaneous induction of apoptosis and autophagy. *Oncol. Rep.* 27, 1481–1487. doi:10.3892/or.2012.1694

Ren, G., Sha, T., Guo, J., Li, W., Lu, J., and Chen, X. (2015). Cucurbitacin B induces DNA damage and autophagy mediated by reactive oxygen species (ROS) in MCF-7 breast cancer cells. *J. Nat. medicines*. 69, 522–530. doi:10.1007/s11418-015-0918-4

Rubinsztein, D. C., Shpilka, T., and Elazar, Z. (2012). Mechanisms of autophagosome biogenesis. *Curr. Biol.* 22, R29–R34. doi:10.1016/j.cub.2011.11.034

Russell, L. H., Jr., Mazzio, E., Badisa, R. B., Zhu, Z. P., Agharahimi, M., Oriaku, E. T., et al. (2012). Autoxidation of gallic acid induces ROS-dependent death in human prostate cancer LNCaP cells. *Anticancer Res.* 32, 1595–1602.

Saibu, M., Sagar, S., Green, I., Ameer, F., and Meyer, M. (2014). Evaluating the cytotoxic effects of novel quinone compounds. *Anticancer Res.* 34, 4077–4086.

Sak, K. (2012). Chemotherapy and dietary phytochemical agents, Chemotherapy research and practice. *Chemother Res Pract.* 2012, 282570. doi:10.1155/2012/282570

Sak, K. (2014). Site-specific anticancer effects of dietary flavonoid quercetin. *Nutr. Cancer*. 66, 177–193. doi:10.1080/01635581.2014.864418

Sanford, N. N., Sher, D. J., Xu, X., Ahn, C., D'Amico, A. V., Aizer, A. A., et al. (2020), Alcohol use among patients with cancer and survivors in the United States, 2000-2017, *J. Natl. Compr. Canc Ne*. 18, 69. doi:10.6004/jnccn.2019.7341

Santana-Codina, N., Mancias, J. D., and Kimmelman, A. C. (2017). The role of autophagy in cancer. *Annu. Rev. Cancer Biol.* 1, 19–39. doi:10.1146/annurev-cancerbio-041816-122338

Satoh, M., Takemura, Y., Hamada, H., Sekido, Y., and Kubota, S. (2013). EGCG induces human mesothelioma cell death by inducing reactive oxygen species and autophagy. *Cancer Cel Int.* 13, 19. doi:10.1186/1475-2867-13-19

Schirrmacher, V. (2019). From chemotherapy to biological therapy: a review of novel concepts to reduce the side effects of systemic cancer treatment (Review). *Int. J. Oncol.* 54, 407–419. doi:10.3892/ijo.2018.4661

Sena, Laura. A., and Chandel, Navdeep. S. (2012). Physiological roles of mitochondrial reactive oxygen species. *Mol. Cel*. 48, 158–167. doi:10.1016/j.molcel.2012.09.025

Shankar, S., Chen, Q., Siddiqui, I., Sarva, K., and Srivastava, R. K. (2007). Sensitization of TRAIL-resistant LNCaP cells by resveratrol (3, 4', 5 tri-hydroxystilbene): molecular mechanisms and therapeutic potential. *J. Mol. Signal.* 2, 7. doi:10.1186/1750-2187-2-7

Shin, S. W., Kim, S. Y., and Park, J. W. (2012). Autophagy inhibition enhances ursolic acid-induced apoptosis in PC3 cells. *Biochim. Biophys. Acta*. 1823, 451–457. doi:10.1016/j.bbamcr.2011.10.014

Shukla, Y., and Singh, M. (2007). *Cancer* preventive properties of ginger: a brief review. *Food Chem Toxicol.* 45, 683–690. doi:10.1016/j.fct.2006.11.002

Siddiqui, I. A., Asim, M., Hafeez, B. B., Adhami, V. M., Tarapore, R. S., and Mukhtar, H. (2011). Green tea polyphenol EGCG blunts androgen receptor function in prostate cancer. *FASEB J. : official Publ. Fed. Am. Societies Exp. Biol.* 25, 1198–1207. doi:10.1096/fj.10-167924

Siegel, R. L., Miller, K. D., and Jemal, A. (2020). *Cancer* statistics, 2020. *CA A. Cancer J. Clin.* 70, 7–30. doi:10.3322/caac.21590

Singh, R., and Cuervo, A. M. (2011). Autophagy in the cellular energetic balance. *Cel Metab.* 13, 495–504. doi:10.1016/j.cmet.2011.04.004

Stadlbauer, S., Steinborn, C., Klemd, A., Hattori, F., Ohmori, K., Suzuki, K., et al. (2018). Impact of green tea catechin ECG and its synthesized fluorinated analogue on prostate cancer cells and stimulated immunocompetent cells. *Planta Med.* 84, 813–819. doi:10.1055/s-0044-102099

Su, M., Mei, Y., and Sinha, S. (2013). Role of the crosstalk between autophagy and apoptosis in cancer. *J. Oncol.* 2013, 102735. doi:10.1155/2013/102735

Suh, Y., Afaq, F., Khan, N., Johnson, J. J., Khusro, F. H., and Mukhtar, H. (2010). Fisetin induces autophagic cell death through suppression of mTOR signaling pathway in prostate cancer cells. *Carcinogenesis*. 31, 1424–1433. doi:10.1093/carcin/bgq115

Sun, C. Y., Zhu, Y., Li, X. F., Tang, L. P., Su, Z. Q., Wang, X. Q., et al. (2017a). Norcantharidin alone or in combination with crizotinib induces autophagic cell death in hepatocellular carcinoma by repressing c-Met-mTOR signaling. *Oncotarget*. 8, 114945–114955. doi:10.18632/oncotarget.22935

Sun, Z. L., Dong, J. L., and Wu, J. (2017b). Juglanin induces apoptosis and autophagy in human breast cancer progression via ROS/JNK promotion. *Biomed. Pharmacother.* 85, 303–312. doi:10.1016/j.biopha.2016.11.030

Sun, L. R., Zhou, W., Zhang, H. M., Guo, Q. S., Yang, W., Li, B. J., et al. (2019). Modulation of multiple signaling pathways of the plant-derived natural products in cancer. *Front. Oncol.* 9, 1153. doi:10.3389/fonc.2019.01153

Surichan, S., Arroo, R. R., Tsatsakis, A. M., and Androutsopoulos, V. P. (2018). Tangeretin inhibits the proliferation of human breast cancer cells via CYP1A1/CYP1B1 enzyme induction and CYP1A1/CYP1B1-mediated metabolism to the product 4' hydroxy tangeretin. *Toxicol In Vitro.* 50, 274–284. doi:10.1016/j.tiv.2018.04.001

Tang, K. D., Liu, J., Russell, P. J., Clements, J. A., and Ling, M. T. (2019). Gamma-tocotrienol induces apoptosis in prostate cancer cells by targeting the ang-1/tie-2 signalling pathway. *Int. J. Mol. Sci.* 20, 1164. doi:10.3390/ijms20051164

Thorburn, A., Thamm, D. H., and Gustafson, D. L. (2014). Autophagy and cancer therapy. *Mol. Pharmacol.* 85, 830–838. doi:10.1124/mol.114.091850

Tompkins, K. D., and Thorburn, A. (2019). Regulation of apoptosis by autophagy to enhance cancer therapy. *Yale J. Biol. Med.* 92, 707–718.

Tsai, C.-Y., Chen, C.-Y., Chiou, Y.-H., Shyu, H.-W., Lin, K.-H., Chou, M.-C., et al. (2018). Epigallocatechin-3-gallate suppresses human herpesvirus 8 replication and induces ROS leading to apoptosis and autophagy in primary effusion lymphoma cells. *Int. J. Mol. Sci.* 19, 16. doi:10.3390/ijms19010016

Tundis, R., Bonesi, M., Deguin, B., Loizzo, M. R., Menichini, F., Conforti, F., et al. (2009). Cytotoxic activity and inhibitory effect on nitric oxide production of triterpene saponins from the roots of Physospermum verticillatum (Waldst & Kit) (Apiaceae). *Bioorg. Med. Chem.* 17, 4542–4547. doi:10.1016/j.bmc.2009.05.006

Uddin, M. S., Al Mamun, A., Jakaria, M., Thangapandiyan, S., Ahmad, J., Rahman, M. A., et al. (2020). Emerging promise of sulforaphane-mediated Nrf2 signaling cascade against neurological disorders. *Sci. Total Environ.* 707, 135624. doi:10.1016/j.scitotenv.2019.135624

Velazquez, A. F. C., and Jackson, W. T. (2018). So many roads: the multifaceted regulation of autophagy induction. *Mol. Cel Biol.* 38, e00303-18. doi:10.1128/MCB.00303-18

Wang, N., Feng, Y., Zhu, M., Tsang, C. M., Man, K., Tong, Y., et al. (2010). Berberine induces autophagic cell death and mitochondrial apoptosis in liver cancer cells: the cellular mechanism. *J. Cell. Biochem.* 111, 1426–1436. doi:10.1002/jcb.22869

Wang, Z., Jiang, C., Chen, W., Zhang, G., Luo, D., Cao, Y., et al. (2014). Baicalein induces apoptosis and autophagy via endoplasmic reticulum stress in hepatocellular carcinoma cells. *Biomed Res Int.* 2014, 732516. doi:10.1155/2014/732516

Wang, F., Mao, Y., You, Q., Hua, D., and Cai, D. (2015). Piperlongumine induces apoptosis and autophagy in human lung cancer cells through inhibition of PI3K/Akt/mTOR pathway. *Int. J. immunopathology Pharmacol.* 28, 362–373. doi:10.1177/0394632015598849

Wang, J., Qi, Q., Feng, Z., Zhang, X., Huang, B., Chen, A., et al. (2016a). Berberine induces autophagy in glioblastoma by targeting the AMPK/mTOR/ULK1-pathway. *Oncotarget*. 7, 66944. doi:10.18632/oncotarget.11396

Wang, R., Ma, L., Weng, D., Yao, J., Liu, X., and Jin, F. (2016b). Gallic acid induces apoptosis and enhances the anticancer effects of cisplatin in human small cell lung cancer H446 cell line via the ROS-dependent mitochondrial apoptotic pathway. *Oncol. Rep.* 35, 3075–3083. doi:10.3892/or.2016.4690

Wang, X., Zhang, H., and Chen, X. (2019). Drug resistance and combating drug resistance in cancer. *Cancer Drug Resist.* 2, 141–160. doi:10.20517/cdr.2019.10

Wang, D., He, X., Wang, D., Peng, P., Xu, X., Gao, B., et al. (2020). Quercetin suppresses apoptosis and attenuates intervertebral disc degeneration via the SIRT1-autophagy pathway. *Front Cel Dev Biol.* 8, 613006. doi:10.3389/fcell.2020.613006

Wei, Y., and Huang, J. (2019). Role of estrogen and its receptors mediated-autophagy in cell fate and human diseases. *J. Steroid Biochem.* 191, 105380. doi:10.1016/j.jsbmb.2019.105380

Whitlock, N. C., and Baek, S. J. (2012). The anticancer effects of resveratrol: modulation of transcription factors. *Nutr. Cancer*. 64, 493–502. doi:10.1080/01635581.2012.667862

WHO (2018). https://www.who.int/news-room/fact-sheets/detail/cancer

Wong, V. K., Li, T., Law, B. Y., Ma, E. D., Yip, N. C., Michelangeli, F., et al. (2013). Saikosaponin-d, a novel SERCA inhibitor, induces autophagic cell death in apoptosis-defective cells. *Cel Death Dis.* 4, e720. doi:10.1038/cddis.2013.217

Wu, P. P., Kuo, S. C., Huang, W. W., Yang, J. S., Lai, K. C., Chen, H. J., et al. (2009). (-)-Epigallocatechin gallate induced apoptosis in human adrenal cancer NCI-H295 cells through caspase-dependent and caspase-independent pathway. *Anticancer Res.* 29, 1435–1442.

Wu, J. Q., Kosten, T. R., and Zhang, X. Y. (2013). Free radicals, antioxidant defense systems, and schizophrenia. *Prog Neuropsychopharmacol Biol Psychiatry.* 46, 200–206. doi:10.1016/j.pnpbp.2013.02.015

Wu, M., Lao, Y., Xu, N., Wang, X., Tan, H., Fu, W., et al. (2015). Guttiferone K induces autophagy and sensitizes cancer cells to nutrient stress-induced cell death. *Phytomedicine*. 22, 902–910. doi:10.1016/j.phymed.2015.06.008

Wu, Q., Kroon, P. A., Shao, H., Needs, P. W., and Yang, X. (2018). Differential effects of quercetin and two of its derivatives, isorhamnetin and isorhamnetin-3-glucuronide, in inhibiting the proliferation of human breast-cancer MCF-7 cells. *J. Agric. Food Chem.* 66, 7181–7189. doi:10.1021/acs.jafc.8b02420

Xu, G., Feng, C., Zhou, Y., Han, Q. B., Qiao, C. F., Huang, S. X., et al. (2008). Bioassay and ultraperformance liquid chromatography/mass spectrometry guided isolation of apoptosis-inducing benzophenones and xanthone from the pericarp of *Garcinia* yunnanensis Hu. *J. Agric. Food Chem.* 56, 11144–11150. doi:10.1021/jf802690g

Xue, L., Zhang, W. J., Fan, Q. X., and Wang, L. X. (2018). Licochalcone A inhibits PI3K/Akt/mTOR signaling pathway activation and promotes autophagy in breast cancer cells. *Oncol. Lett.* 15, 1869–1873. doi:10.3892/ol.2017.7451

Yamagata, K., Xie, Y., Suzuki, S., and Tagami, M. (2015). Epigallocatechin-3-gallate inhibits VCAM-1 expression and apoptosis induction associated with LC3 expressions in TNFα-stimulated human endothelial cells. *Phytomedicine*. 22, 431–437. doi:10.1016/j.phymed.2015.01.011

Yang, G.-Y., Liao, J., Kim, K., Yurkow, E. J., and Yang, C. S. (1998). Inhibition of growth and induction of apoptosis in human cancer cell lines by tea polyphenols. *Carcinogenesis*. 19, 611–616. doi:10.1093/carcin/19.4.611

Yang, C., Zhao, L., Yuan, W., and Wen, J. (2017). Cordycepin induces apoptotic cell death and inhibits cell migration in renal cell carcinoma via regulation of microRNA-21 and PTEN phosphatase. *Biomed. Res.* 38, 313–320. doi:10.2220/biomedres.38.313

Yang, J., Pi, C., and Wang, G. (2018). Inhibition of PI3K/Akt/mTOR pathway by apigenin induces apoptosis and autophagy in hepatocellular carcinoma cells. *Biomed. Pharmacother.* 103, 699–707. doi:10.1016/j.biopha.2018.04.072

Ye, C., Zhang, C., Huang, H., Yang, B., Xiao, G., Kong, D., et al. (2018). The natural compound myricetin effectively represses the malignant progression of prostate cancer by inhibiting PIM1 and disrupting the PIM1/CXCR4 interaction, cellular physiology and biochemistry. *Cell Physiol Biochem.* 48, 1230–1244. doi:10.1159/000492009

Yu, R., Zhang, Z. Q., Wang, B., Jiang, H. X., Cheng, L., and Shen, L. M. (2014). Berberine-induced apoptotic and autophagic death of HepG2 cells requires AMPK activation. *Cancer Cel. Int.* 14, 49. doi:10.1186/1475-2867-14-49

Zhang, J. F., Liu, J. J., Liu, P. Q., Lin, D. J., Li, X. D., and Chen, G. H. (2006). Oridonin inhibits cell growth by induction of apoptosis on human hepatocelluar carcinoma BEL-7402 cells. *Hepatol. Res.* 35, 104–110. doi:10.1016/j.hepres.2006.03.007

Zhang, X., Zhu, Y., Duan, W., Feng, C., and He, X. (2015). Allicin induces apoptosis of the MGC-803 human gastric carcinoma cell line through the p38 mitogen-activated protein kinase/caspase-3 signaling pathway. *Mol. Med. Rep.* 11, 2755–2760. doi:10.3892/mmr.2014.3109

Zhang, Z., Liu, T., Yu, M., Li, K., and Li, W. (2018). The plant alkaloid tetrandrine inhibits metastasis via autophagy-dependent Wnt/β-catenin and metastatic tumor antigen 1 signaling in human liver cancer cells. *J. Exp. Clin. Cancer Res.* 37, 7. doi:10.1186/s13046-018-0678-6

Zhang, S., Cao, M., and Fang, F. (2020a). The role of epigallocatechin-3-gallate in autophagy and endoplasmic reticulum stress (ERS)-Induced apoptosis of human diseases. *Med. Sci. Monit.* 26, e924558. doi:10.12659/MSM.924558

Zhang, Z., Zhou, L., Xie, N., Nice, E. C., Zhang, T., Cui, Y. P., et al. (2020b), Overcoming cancer therapeutic bottleneck by drug repurposing. *Signal Transduct Target Ther.* 5, 113. doi:10.1038/s41392-020-00213-8

Zhong, Y., Krisanapun, C., Lee, S.-H., Nualsanit, T., Sams, C., Peungvicha, P., et al. (2010). Molecular targets of apigenin in colorectal cancer cells: involvement of p21, NAG-1 and p53. *Eur. J. Cancer* 46, 3365–3374. doi:10.1016/j.ejca.2010.07.007

Zhu, Y., Rao, Q., Zhang, X., and Zhou, X. (2018). Galangin induced antitumor effects in human kidney tumor cells mediated via mitochondrial mediated apoptosis, inhibition of cell migration and invasion and targeting PI3K/AKT/mTOR signalling pathway. *J BUON.* 23, 795–799.

Conflict of Interest: The authors declare that the research was conducted in the absence of any commercial or financial relationships that could be construed as a potential conflict of interest.

frontiers in Pharmacology

SYSTEMATIC REVIEW
published: 07 July 2021
doi: 10.3389/fphar.2021.702487

Antitumor Effects of Carvacrol and Thymol: A Systematic Review

Laeza Alves Sampaio[1], *Lícia Tairiny Santos Pina*[2], *Mairim Russo Serafini*[3], *Débora dos Santos Tavares*[4] *and Adriana Gibara Guimarães*[3]*

[1]Graduate Program of Applied Sciences to Health, Federal University of Sergipe, Lagarto, Brazil, [2]Graduate Program in Health Sciences, Federal University of Sergipe, Aracaju, Brazil, [3]Department of Pharmacy, Federal University of Sergipe, São Cristóvão, Brazil, [4]Department of Health Education, Federal University of Sergipe, Lagarto, Brazil

Background: It is estimated that one in five people worldwide faces a diagnosis of a malignant neoplasm during their lifetime. Carvacrol and its isomer, thymol, are natural compounds that act against several diseases, including cancer. Thus, this systematic review aimed to examine and synthesize the knowledge on the antitumor effects of carvacrol and thymol.

Methods: A systematic literature search was carried out in the PubMed, Web of Science, Scopus and Lilacs databases in April 2020 (updated in March 2021) based on the PRISMA 2020 guidelines. The following combination of health descriptors, MeSH terms and their synonyms were used: carvacrol, thymol, antitumor, antineoplastic, anticancer, cytotoxicity, apoptosis, cell proliferation, *in vitro* and *in vivo*. To assess the risk of bias in *in vivo* studies, the SYRCLE Risk of Bias tool was used, and for *in vitro* studies, a modified version was used.

Results: A total of 1,170 records were identified, with 77 meeting the established criteria. The studies were published between 2003 and 2021, with 69 being *in vitro* and 10 *in vivo.* Forty-three used carvacrol, 19 thymol, and 15 studies tested both monoterpenes. It was attested that carvacrol and thymol induced apoptosis, cytotoxicity, cell cycle arrest, antimetastatic activity, and also displayed different antiproliferative effects and inhibition of signaling pathways (MAPKs and PI3K/AKT/mTOR).

Conclusions: Carvacrol and thymol exhibited antitumor and antiproliferative activity through several signaling pathways. *In vitro*, carvacrol appears to be more potent than thymol. However, further *in vivo* studies with robust methodology are required to define a standard and safe dose, determine their toxic or side effects, and clarify its exact mechanisms of action.

This systematic review was registered in the PROSPERO database (CRD42020176736) and the protocol is available at https://www.crd.york.ac.uk/prospero/display_record.php?RecordID=176736.

Keywords: carvacrol, thymol, cancer, antitumor, anticancer

OPEN ACCESS

Edited by:
Supratik Kar,
Jackson State University,
United States

Reviewed by:
Simone Carradori,
University "G. d'Annunzio" of Chieti-Pescara, Italy
Xiaoxiao Huang,
Shenyang Pharmaceutical University, China

***Correspondence:**
Adriana Gibara Guimarães
adrianagibara@hotmail.com
adrianagibara@academico.ufs.br

Specialty section:
This article was submitted to Ethnopharmacology, a section of the journal Frontiers in Pharmacology

Received: *29 April 2021*
Accepted: *22 June 2021*
Published: *07 July 2021*

Citation:
Sampaio LA, Pina LTS, Serafini MR, Tavares DdS and Guimarães AG (2021) Antitumor Effects of Carvacrol and Thymol: A Systematic Review. Front. Pharmacol. 12:702487. doi: 10.3389/fphar.2021.702487

INTRODUCTION

It is estimated that one in five people worldwide faces the diagnosis of some malignant neoplasm during their lifetime, and the number of people with cancer is forecast to double by the year 2040 (World Health Organization, 2020). In fact, cancer is a major global public health problem, and it is one of the four main causes of premature death (before 70 years old) in most countries, resulting in 8.8 million deaths per year (National Cancer Institute, 2019). The antineoplastic agents available on the market have different mechanisms of action that impair cell proliferation and/or cause cell death, thereby increasing patient survival rate (Powell et al., 2014; Lee and Park, 2016). However, the toxicity and side effects of many treatments can worsen the quality of life of these individuals (Weingart et al., 2018; Hassen et al., 2019; Lu et al., 2019). Thus, despite being the subject of research for many years, cancer still remains a major concern and an important area of study in the search for a cure.

There is, therefore, an ongoing search for substances that can be used to develop more effective treatments, with less side effects, to use against cancer; one promising group of substances are natural products (NPs). There are many medicinal plants whose pharmacological properties have already been described and scientifically proven (Nelson, 1982; Mishra and Tiwari, 2011; Carqueijeiro et al., 2020). However, the enormous diversity of nature still holds many plant compounds without sufficient studies, particularly in the oncology area (Gordaliza, 2007; Asif, 2015). Historically, secondary plant metabolites have made important contributions to cancer therapy, such as, the vinca alkaloids (vinblastine and vincristine) and the paclitaxel terpene that was obtained from the *Taxus brevifolia* Nutt. species (Martino et al., 2018). More recently, other compounds, such as perillyl alcohol and limonene -monoterpenes found in aromatic plant species, have been widely studied due to their antitumor potential, and have been included in clinical phase studies (Shojaei et al., 2014; Arya and Saldanha, 2019).

In this context, carvacrol (5-isopropyl-2-methylphenol) and its thymol isomer (2-isopropyl-5-methylphenol), classified as natural multi-target compounds, deserve attention. Both are monoterpenoid phenols, the main components present in essential oils obtained from several plant species of the Lamiaceae and Verbenaceae families, such as oregano (*Origanum vulgare* L.), thyme (*Thymus vulg*aris L.) and "alecrim-da-chapada" (*Lippia gracilis*) (Santos et al., 2016; Salehi et al., 2018; Sharifi-Rad et al., 2018; Baj et al., 2020), which have already been reported to exhibit beneficial effects against many diseases (Silva et al., 2018), including cancer (Elbe et al., 2020; Pakdemirli et al., 2020). In addition, these compounds present anti-inflammatory (Li et al., 2018; Chamanara et al., 2019) and antioxidant (Arigesavan and Sudhandiran, 2015; Sheorain et al., 2019) activities that enable the reduction of inflammation and an increase in enzymatic and non-enzymatic antioxidants in the tumor environment (Gouveia et al., 2018). Hence, this systematic review aims to examine and synthesize knowledge about the antitumor and antiproliferative effect of carvacrol and thymol, as well as to report the main mechanisms of action already described for the two compounds against cancer. to provide guidance for future research.

METHODS

Question and PICOS Strategy

The purpose of this systematic review was to answer the following question: Do carvacrol and thymol exhibit an anti-tumor effect on cancer cells (*in vitro*) or in animal models of cancer? The review followed the guidelines of the Preferred Reporting Items for Systematic Reviews and Meta-Analyses (PRISMA) (Page et al., 2021).

A PICOS strategy (patient or pathology, intervention, control, and other outcomes and type of study) was used based on: P: Animals with cancer or tumor cells; I: Treatment with carvacrol or thymol; C: No treatment, healthy cells or placebo (vehicle); O: Cytotoxic and antitumor effects, induction of apoptosis and inhibition of proliferation; S: Pre-clinical studies *in vitro* and *in vivo*.

Data Sources and Literature Search

The research was carried out in the databases PubMed, Web of Science, Scopus and Lilacs in April 2020 (updated in March 2021) using a combination of health descriptors, MeSH terms and their synonyms, such as antitumor, antineoplastic, anticancer, cytotoxicity, apoptosis, cell proliferation, *in vitro*, *in vivo*, carvacrol or 5-isopropyl-2-methylphenol and thymol or 5-methyl-2-propan-2-ylphenol (**Supplementary Table S1**, contains a complete list of these search terms).

Study Selection and Eligibility Criteria

Two independent reviewers (L.A.S. and L.T.S.P.) analyzed the research results and selected potentially relevant studies after reading their title and abstract, using the systematic review application, Rayyan (Ouzzani et al., 2016). We used the Kappa statistical test to measure the inter-rater reliability (Landis and Koch, 1977). Disagreements were resolved through a consensus between the reviewers, and the decision was supported by the assistance of a third reviewer when necessary (AGG). The following inclusion criteria were applied: Administration of carvacrol or pure thymol vs. placebo; *in vitro* studies of cancer cell lines, *in vivo* study of animals with cancer; cytotoxic effect, antitumor effect, inhibition of proliferation and apoptosis and experimental studies (*in vitro* and *in vivo*). The exclusion criteria were: experiments with derivatives of the carvacrol or thymol, association of the two compounds with other substances or in mixtures composing essential oils and extracts, animals with other diseases in addition to cancer, review articles, meta-analyses, abstracts, conference articles, editorials/letters and case reports. A manual search of the reference lists of all selected studies was also conducted, in order to identify additional primary studies for inclusion.

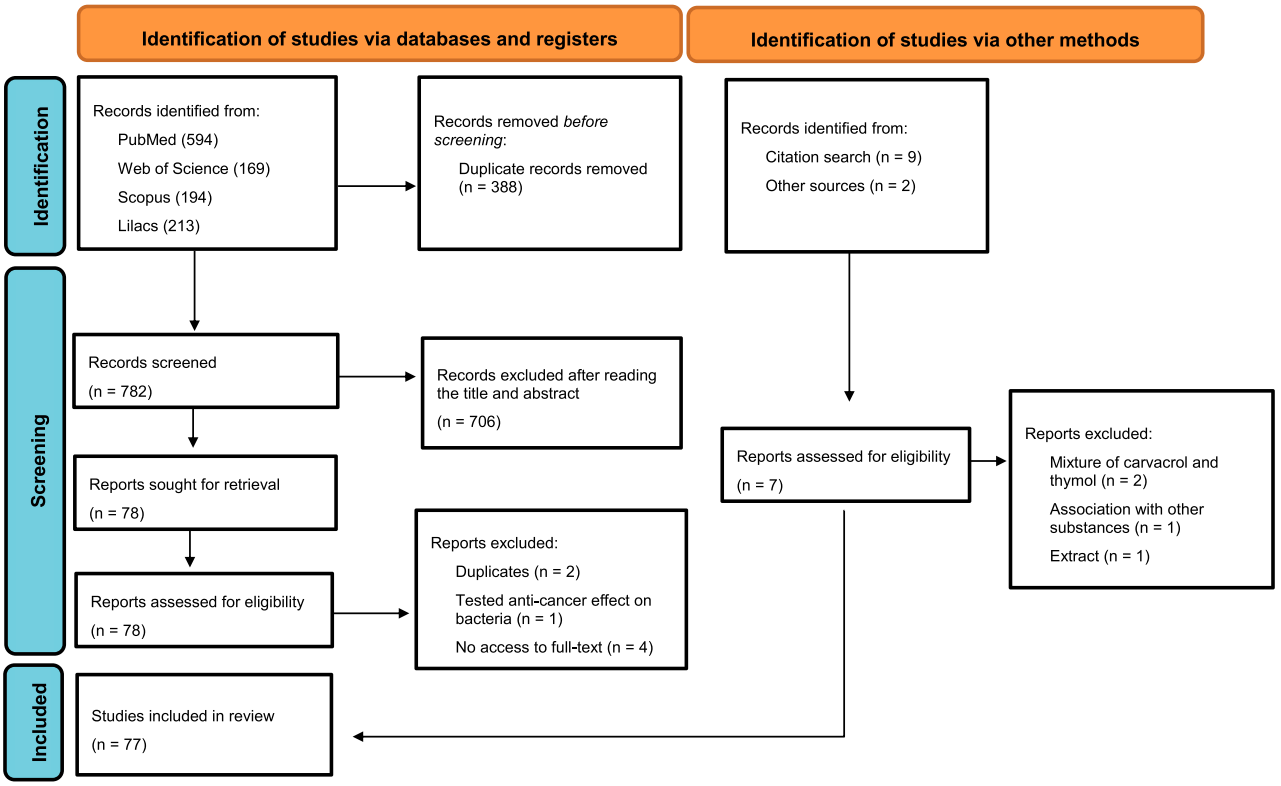

FIGURE 1 | Flowchart of included studies.

Data Extraction and Risk of Bias Assessment

We extracted the following data from the included articles: author, year, country, data about the monoterpene (source, obtention method), concentration and/or dose, type of animal or cell line, results (cytotoxicity, cell proliferation, apoptosis, cell cycle, histology), proposed mechanisms involved in the antitumor effect and conclusion. The authors of the included studies were contacted when necessary (whenever any data or article was not available).

The SYRCLE Risk of Bias tool was used to assess the risk of bias of all *in vivo* experimental studies (Hooijmans et al., 2014). We analyzed the following ten domains: sequence generation, allocation concealment and random accommodation (selection bias), random accommodation and concealment (performance bias), random evaluation and concealment of results (detection bias), incomplete result data (bias of attrition), selective report of results (report bias) and other sources of bias, such as inappropriate influence from financiers. An adapted protocol of the SYRCLE Risk of Bias tool was used to evaluate the methodological quality of *in vitro* studies, as described by Chan et al. (2017). The methodological quality was classified as low, unclear or high, according to the established criteria (Hooijmans et al., 2014).

Statistical Analysis

IC_{50} values determined 24 h after the incubation of the studied cells with carvacrol or thymol were compiled, submitted to the standardization of the unit (μM) (**Supplementary Table S2**) and were expressed as mean ± standard error of the mean (SEM).

RESULTS

Study Selection

The initial search resulted in 1,170 records, of which 594, 169, 194, and 213 were found in PubMed, Web of Science, Scopus and Lilacs, respectively. Of these, 388 were excluded due to duplication. After screening the title and abstract, 706 reports were excluded, and 1 report was sought for retrieval, as it met the criteria after reading the full text, resulting in 77 studies. Of these, three were excluded after reading the full text (two for presenting the same results and one that tested the anti-cancer effect on bacteria) and four for not having access to the full text, resulting in 70 articles. In addition, 9 studies were identified after a manual search of the references and two studies obtained from other sources, but only seven studies were added (two studies were excluded for having a mixture between carvacrol and thymol, one for being associated with other substances, and one that studied the extract of a plant rich in thymol), finally resulting in 77 included studies (**Figure 1**). There was almost perfect (Landis and Koch, 1977) reliability/agreement (κ = 0.813) among the reviewers, after selecting the titles and abstracts.

TABLE 1 | Detailed description of the studies that used carvacrol, included in the systematic review.

Model	Concentration/ incubation time	Experimental methods for testing IC50 values	Results/targets			Conclusion	Authors (Year), Country
			Increase	Decrease	IC_{50}		
Monoterpene carvacrol *In vitro* studies							
CO25	1–150 µg/mL 24, 48, 72 h of incubation	MTT assay	$p21^{N-ras}$	Tumor growth DNA synthesis level	60 µg/mL–24 h	Carvacrol has a cytotoxic effect and an antiproliferative effect	Zeytinoglu et al. (2003), Turkey
A549	100–1,000 µM 24 h of incubation	—	Apoptosis induction	Cell viability Cell proliferation	—	Carvacrol may have an anticancer effect and be used as a drug substance to cure cancer	Koparal and Zeytinoglu (2003), Turkey
HepG2 Caco-2	25–900 µmol 24 of incubation	—	Cytotoxic effects	DNA damage level	—	HepG2 cells were slightly more sensitive to the effects	Horváthová et al. (2006), Slovakia
Leiomyosarcoma	10–4,000 µM 24 and 48 h of incubation	Trypan Blue	Antiproliferative effects	Cell growth	90 µM–24 h 67 µM–48 h	Carvacrol has anticarcinogenic, antiproliferative and antiplatelet properties	Karkabounas et al. (2006), Greece
K-562	200–1,000 µM 24 or 48 h of incubation	Trypan blue exclusion	Cytotoxic effects	DNA damage level	220 µM–24 h	Carvacrol has cytotoxic, antioxidant effects and has a protective action against DNA damage	Horvathova et al. (2007), Slovakia
P-815	0.004–0.5% v/v 48 h of incubation	MTT assay	—	—	<0.004% v/v–48 h	Carvacrol is cytotoxic	Jaafari et al. (2007), Morocco
HepG2 Caco-2	100–1,000 µM 24 h of incubation	Trypan blue exclusion	Cytotoxic effects	Cell proliferation	HepG2 - 350 µM–24 h Caco-2 - 600 µM–24 h	Carvacrol has antiproliferative and antioxidant effects	Slamenová et al. (2007), Slovakia
MDA-MB 231	20–100 µM 24 or 48 h of incubation	MTT assay	Apoptosis induction Caspase activation Sub-stage G0/G1 Cyt C Bax	Cell growth S-phase cells Mitochondrial membrane potential Bcl-2	100 µM–48 h	Carvacrol can be a potent antitumor molecule against breast cancer metastatic cells	Arunasree, (2010), India
5RP7 CO25	0.0002–0.1 mg/mL 24 or 48 h of incubation	MTT assay and Trypan Blue exclusion	Cytotoxic effects Apoptotic cells	—	5RP7 - 0.04 mg/mL–24/48 h CO25–0.1 mg/mL–24 h 0.05 mg/mL–48 h	Carvacrol promoted a cytotoxic effect, induced apoptosis and can be used in cancer therapy	Akalin and Incesu, (2011), Turkey
SiHa HeLa	25–500 µg/mL 48 h of incubation	MTT and LDH assay	Apoptosis induction	Cell proliferation	SiHa - 50 ± 3.89 mg/L HeLa - 50 ± 5.95 mg/L	Carvacrol is a potent anticancer compound that exhibits cytotoxic effects and induces the inhibition of cell proliferation in both human cervical cancer cells	Mehdi et al. (2011), India
HepG2	20–200 µg/mL 24 h of incubation	CellTiter-Blue® cell viability assay	Cytotoxic effects Antiproliferative effects	Membrane damage Cell viability	53.09 µg/mL	Carvacrol exhibits antioxidant activity and anticancer effects on cells	Özkan and Erdogan (2011), Turkey
P-815 CEM K-562 MCF-7 MCF-7 gem	0.05–1.25 µM 48 h of incubation	MTT assay	Cytotoxic effects	Interruption of cell cycle progression in the S phase	P-815–0.067 µM CEM - 0.042 µM K-562–0.067 µM MCF-7 - 0.125 µM MCF-7 gem - 0.067 µM	Carvacrol showed a cytotoxic effect in all strains tested	Jaafari et al. (2012), Morocco
DBTRG-05MG	200–1,000 µM 24 h of incubation	—	Generation of ROS Caspase-3	Cell viability	—	Carvacrol was cytotoxic and induced cell death in human glioblastoma cells	Liang and Lu, (2012), China
H1299	25–1800 µM 24 and 48 h of incubation	CellTiter-Blue® cell viability assay	MDA 8-OHdG	Membrane and DNA damage	380 µM–24 h 244 µM–48 h	Carvacrol exhibited cytotoxic and antioxidant effects	Ozkan and Erdogan (2012), Turkey

(Continued on following page)

TABLE 1 | (*Continued*) Detailed description of the studies that used carvacrol, included in the systematic review.

Model	Concentration/ incubation time	Experimental methods for testing IC50 values	Results/targets			Conclusion	Authors (Year), Country
			Increase	Decrease	IC_{50}		
B16-F10	Not reported 24 h of incubation	Trypan blue assay and MTT assay	Cytotoxic effects	Cell viability Relative melanogenesis Relative melanin cell	550 μM	Carvacrol showed an antitumor effect with moderate cytotoxicity	Satooka and Kubo (2012), United States
HepG2	0.05–0.4 mmol/L 24 h of incubation	MTT assay	p-p38 MAPK Caspase-3	Cell viability p-ERK 1/2 Bcl-2	0.4 mmol/L–24 h	Carvacrol caused inhibition of cell proliferation, inhibition of tumor cell growth and induction of apoptosis	Yin et al. (2012), China
OC2	200–1,000 μM 24 h of incubation	—	Generation of ROS Caspase-3	Cell viability	—	Carvacrol exhibited a cytotoxic effect and induced apoptosis in human oral cancer cells	Liang et al. (2013), China
MCF-7	140–450 μM 24 and 48 of incubation	MTT and LDH assay	Caspase-3, -6 and -9 Bax p53	Cell viability Bcl-2	244.7 ± 0.71μM–48 h	Carvacrol induces cytotoxicity and apoptosis in MCF-7 cells and may be a potential chemotherapeutic agent against cancer	Al-Fatlawi and Ahmad (2014), India
N2a	10–400 mg/L 24 h of incubation	—	TAC TOS	—	—	Carvacrol has antioxidant and anticancer properties in N2a cells at concentrations of 200 and 400 mg/L	Aydın et al. (2014), Turkey
Caco-2	100–2,500 μM 24 and 48 h of incubation	MTS assay	Apoptosis induction	Cell viability	460 ± 3.6 μM–24 h 343 ± 7.4 μM–48 h	Carvacrol exhibited cytotoxic effects and induction of apoptosis	Llana-Ruiz-Cabello et al. (2014), Spain
HepG2	25–1,000 μM 24 h of incubation	Trypan Blue exclusion and MTT assay	Apoptosis induction	Cell growth SsDNA breaks Oxidative DNA lesions	425 μM–24 h	Carvacrol can be used as an anti-tumor molecule against cancer cells	Melusova et al. (2014), Slovakia
HepG2	100–600 μM 24 h of incubation	—	Cells in G1 phase	S-phase cells	—	Carvacrol caused induction of apoptosis and slowed cell division, resulting in cell death	Melušová et al. (2014), Slovakia
U87	125–1,000 μM 24, 48 or 72 h of incubation	MTT assay	Apoptosis induction Caspase-3	Cell viability Cell proliferation PI3K/Akt MAPK TRPM7 MMP-2	561.3 μM–24 h	Carvacrol has therapeutic potential for the treatment of glioblastomas by inhibiting TRPM7 channels	Chen et al. (2015), Canada
HCT116 LoVo	100–900 μmol/L 48 h of incubation	MTT assay	Apoptosis induction Bax p-JNK	Cell growth Cell migration and invasion Bcl-2 MMP-2 and -9 Cyclin B1 p-ERK p-Akt PI3K/Akt Cell cycle stop in phase G2/M	HCT116–544.4 μmol/L–48 h LoVo - 530.2 μmol/L–48 h	Carvacrol can be a promising natural product in the management colon cancer	Fan et al. (2015), China
AGS	0.01–6 mg/mL 48 h of incubation	MTT assay	Cytotoxic effects	Cell viability	30 μg/mL–48 h	Carvacrol exhibited a cytotoxic effect against gastric cancer cells	Maryam et al. (2015), Iran
HL-60 Jurkat	10–200 μM 24 h of incubation	MTT assay	Apoptosis induction Cytotoxic effects Generation of ROS Caspase-3 Bax	Cell viability MMP Bcl-2	HL-60–100 μM–24 h Jurkat - 50 μM–24 h	Carvacrol effectively blocked the proliferation of cancer cells *in vitro*	Bhakkiyalakshmi et al. (2016), India

(Continued on following page)

TABLE 1 | (*Continued*) Detailed description of the studies that used carvacrol, included in the systematic review.

Model	Concentration/ incubation time	Experimental methods for testing IC50 values	Results/targets			Conclusion	Authors (Year), Country
			Increase	Decrease	IC_{50}		
Tca-8113 SCC-25	10–80 μM 24 and 48 h of incubation	—	Apoptosis induction p21 Bax	Cell proliferation S-Phase cells CCND1 CDK4 Bcl-2 MMP-2 and -9 COX-2	—	Carvacrol is a powerful new natural anti-cancer drug for human OSCC	Dai et al. (2016), China
A549 HepG2 Hep3B	1–1,000 μM 72 h of incubation	SRB assay	Antiproliferative effects Cytotoxic effects	—	A549–0.118 ± 0.0012 mM–72 h HepG2 - 0.344 ± 0.0035 mM–72 h Hep3B- 0.234 ± 0.017 mM–72 h	Carvacrol exhibited antiproliferative and antioxidant effects. In addition, it exhibited more potent cytotoxicity against cells (A549). The cells (Hep3B) were more resistant to treatment and the cells (HepG2) were less sensitive	Fitsiou et al. (2016), Greece
PC-3 DU 145	250–750 μM 24, 48 and 72 h of incubation	CCK-8 Kit	—	Cell viability Cell proliferation Cell migration Wound healing MMP-2 PI3K/Akt and MAPK Cell invasion TRPM7	PC-3 - 498.3 ± 12.2 μM–24 h DU 145–430.6 ± 21.9 μM–24 h	Carvacrol treatment suppresses cell proliferation, migration and invasion, indicating that it has antiprostatic effects *in vitro*	Luo et al. (2016), China
A549	0–250 μM 24 h of incubation	—	Cytotoxic effects	Cell viability	—	Carvacrol has cytotoxic activity	Coccimiglio et al. (2016), Canada
U87 MDA-MB 231	1–10,000 μM 24 h of incubation	MTT assay	Anticancer activity Antiproliferative activity Antioxidant activity	—	U87–322 μM–24 h MDA-MB 231–199 μM–24 h	Carvacrol exerted anticancer and antiproliferative activity with greater effect against the breast cancer cell line	Baranauskaite et al. (2017), Lithuania
HepG2	0.01–0.25 μg/μL 24 h of incubation	MTT assay	—	Cell viability Hepatocarcinoma cells	48 mg/L–24 h	Carvacrol has therapeutic potential in tumor cells without adverse effects in healthy cells	Elshafie et al. (2017), Italy
PC-3	100–800 μM 24 h of incubation	—	Cytotoxic effects	Cell viability	—	Carvacrol is cytotoxic	Horng et al. (2017), China
DU 145	10–500 μM 24 and 48 h of incubation	MTT assay	Cytotoxic effects Apoptosis induction Caspase-3 Generation of ROS Cells in phase G0/G1	Cell viability Cell proliferation Mitochondrial membrane potential Cell cycle stop Cells in S and G2/M phases	84.39 μM–24 h 42.06 μM–48 h	Carvacrol has antiproliferative potential and can act as a chemopreventive agent in prostate cancer	Khan et al. (2017), India
SiHa HepG2	140–450 μM 24 and 48 h of incubation	MTT assay and LDH	Cytotoxic effects Apoptosis induction Caspase-3, -6 and -9 Bax p53	Cell viability Bcl-2	SiHa - 424.22 μmol –24 h and 339.13 μmol–48 h HepG2 - 576.52 μmol –24 h and 415.19 μmol –48 h	Carvacrol exhibited antiproliferative effects and may be a potential chemotherapeutic agent against cancer	Abbas and Al-Fatlawi (2018), Iraq
A375	3.906–1,000 μg/mL 24 of incubation	MTT assay	Apoptosis induction Sub-G1 phase	Cell viability Cell growth Bcl-2 Cell cycle stop Cells in phase G0/G1 and G2/M	40.41 ± 0.044 μg/mL–24 h	Carvacrol exhibits antiproliferative effects	Govindaraju and Arulselvi (2018), India

(Continued on following page)

TABLE 1 | (*Continued*) Detailed description of the studies that used carvacrol, included in the systematic review.

Model	Concentration/ incubation time	Experimental methods for testing IC50 values	Results/targets			Conclusion	Authors (Year), Country
			Increase	Decrease	IC_{50}		
AGS	10–600 μM 24 h of incubation	CellTiter-Glo Luminescent cell viability assay	Apoptotic effects Necrosis Bax Caspase-3 and -9 Generation of ROS Genotoxic effect	Cell viability Bcl-2 GSH levels	82.57 ± 5.58 μM–24 h	Carvacrol has cytotoxic effects, apoptotic, genotoxic effects and dose-dependent ROS generators	Günes-Bayir et al. (2018), Turkey
AGS	10–600 μM 48 h of incubation	CellTiter-Glo Luminescent cell viability assay	Cytotoxic effects Apoptosis induction Bax Caspase-3 e -9 Generation of ROS Genotoxic effect	Cell viability Bcl-2 GSH levels	82.57 ± 5.5 μM–48 h	Carvacrol inhibited cell proliferation and induced cytotoxicity in cancer cells	Günes-Bayir et al. (2018), Turkey
MCF-7 MDA-MB 231	10–200 μg/mL 24 h of incubation	MTT assay	—	Cell viability	MCF-7 - 46.5 μg/mL–24 h MDA-MB 231–53 μg/mL– 24 h	Carvacrol has a cytotoxic effect and can cause inhibition of cell growth	Jamali et al. (2018), Iran
A549 H460	30–300 μM 24 h of incubation	—	—	Cell viability Cell proliferation AXL expression Cell migration	-	Carvacrol suppressed cell proliferation and migration and its inhibitory effect was attenuated in NSCLC cells with overexpression of AXL	Jung et al. (2018), Republic of Korea
JAR JEG3	50–300 μM 48 h of incubation	—	Apoptosis induction Sub-G1 phase Generation of ROS p-JNK p-p38	Cell proliferation Cell viability PI3K/AKT p-ERK1/2 MMP	—	Carvacrol may be a possible new therapeutic agent or supplement for the control of human choriocarcinomas	Lim et al. (2019), Republic of Korea
HeLa	100–800 μM 24 h of incubation	XTT Reduction assay	Induction of cytotoxicity and apoptosis ERK1/2 Caspase-9 p21	Cyclin D1	556 ± 39 μM–24 h	Carvacrol can be used to treat cervical cancer, however, it should be avoided during cisplatin chemotherapy	Potočnjak et al. (2018), Croatia
PC-3	100–800 μM 48 h of incubation	MTT assay	Cell death	Cell viability Cell proliferation Tumor cell invasion IL-6 p-STAT3 p-ERK1/2 p-AKT	360 μM–48 h	Carvacrol inhibited the ability to invade and migrate PC3 cells and can be considered an anticancer agent	Heidarian and Keloushadi (2019), Iran
PC-3	10–500 μM 24 and 48 h of incubation	MTT assay	Apoptosis induction Caspases -8 e -9 Generation of ROS Bax	Cell viability Cell proliferation Cell migration Cell cycle stop at G0/G1 Cells in S and G2/M phases Bcl-2 Notch-1 mRNA Jagged-1	46.71 μM–24 h 39.81 μM–48 h	Carvacrol is a chemopreventive agent and has an antiproliferative effect on prostate cancer cells	Khan et al. (2019), India
MCF-7 PC-3 DU 145	31.2–500 μg/mL 48 h of incubation	AlamarBlue® assay	Apoptosis induction Cytotoxic effects Bax	Cell proliferation Cell viability	MCF-7 - 266.8 μg/mL–48 h PC-3 - >500 μg/mL– 48 h DU 145–21.11 μg/mL– 48 h	Carvacrol had the most cytotoxic effect among the other components studied	Tayarani-Najaran et al. (2019), Iran

(Continued on following page)

TABLE 1 | (*Continued*) Detailed description of the studies that used carvacrol, included in the systematic review.

Model	Concentration/ incubation time	Experimental methods for testing IC50 values	Results/targets			Conclusion	Authors (Year), Country
			Increase	Decrease	IC_{50}		
PC-3	25–200 µg/mL 24 and 48 h of incubation	—	Cytotoxic effects	Cell viability	—	At the lowest concentration tested (25 µg/ml), carvacrol did not exhibit cytotoxicity to cancer cells	Trindade et al. (2019), Brazil
HCT116 HT-29 MCF-7	25–200 µM 48 h of incubation 25–250 µmol/L 24 and 48 of incubation	xCELLigence Real-time cell Analysis MTT and LDH assay	— Apoptosis induction Cells in phase G0/G1 Bax	Cell proliferation Cell viability Cells in S and G2 phase CDK4 and 6 Cyclin D1 Bcl-2 PI3K/p-AKT	HCT116–92 µM–48 h HT-29–42 µM–48 h 200 µmol/L–24/48 h	Carvacrol has an antiproliferative effect on both cell lines, but is more efficient against HT-29 compared to the HCT116 cell line Carvacrol can be used in a new approach for the treatment of breast cancer	Pakdemirli et al. (2020), Turkey Mari et al. (2020), India
SKOV-3	100, 200, 400, 600 µM 24 and 48 h of incubation	MTT assay	Apoptosis induction	Cell viability	322.50 µM–24 h 289.54 µM–48 h	Carvacrol was cytotoxic to the ovarian cancer cell line	Elbe et al. (2020), Turkey
Kelly SH-SY5Y	12.5, 25, 50 µM 24 h of incubation	—	Antiproliferative effects	—	—	Carvacrol can be used to inhibit neuroblastoma cell proliferation	Kocal and Pakdemirli (2020), Turkey
BT-483 BT-474 MCF-7 MDA-MB 231 MDA-MB 453	25–500 µM 24 h of incubation	—	Apoptosis induction Cells in G1/G0 phase Cyclin C, D and E	Cell viability S-phase and G2/M cells Cell proliferation Cyclin A e B CDK 4	—	Carvacrol suppresses breast cancer cells by regulating the cell cycle and the TRPM7 pathway is one of the pharmacological mechanisms	Li et al. (2021), China
KG1 K-562 HL-60	100, 200, 300, 400 µM 24 and 48 h of incubation	—	Cell death	Cell viability	—	KG1 cell lines were very sensitive to 300 µM carvacrol compared to the HL60 line, while the K562 line showed resistance after 48 h of treatment with 400 µM carvacrol	Bouhtit et al. (2021), Belgium

Model	Dose	Results/targets		Conclusion	Authors (Year), Country
		Increase	Decrease		
In vivo studies					
Chemical carcinogenesis induced by B [a]P in male wistar rats	20 mL of carvacrol (ε = 976 mg/mL) mixed with 200mg of B [a]P	Anticarcinogenic effects Animal survival time	30% tumor incidence B [a]P carcinogenic potency	Carvacrol has anticarcinogenic, antiproliferative and antiplatelet properties	Karkabounas et al. (2006), Greece
Male wistar rats induced with hepatocarcinogenesis providing 0.01% DEN through drinking water for 16 weeks	Pre-treatment: (15 mg/kg b.wt) of carvacrol orally one week before DEN administration and up to 16 weeks Post-treatment: (15 mg/kg b.wt) of carvacrol orally for 6 weeks after administration of DEN for 10 weeks	Final body weight Chemopreventive effect apoptosis induction GPx, GR, GSH, SOD, CAT	Pre-treatment: Number of nodules; neoplastic transformations; liver weight Post-treatment: Persistent but tiny nodules; architecture; Likely to spread through intrahepatic veins AST, ALT, ALP, LDH, cGT	Carvacrol has the ability to cause apoptosis in cancer cells and has a potent elimination of free radicals and antioxidant activities	Jayakumar et al. (2012), India
Liver carcinogenesis chemically induced by NDEA in male wistar rats orally (dissolved in 0.9% normal saline), in a dose of 20 mg/kg body weight, five times a week, for 6 weeks	15 mg/kg of carvacrol orally, five times a week for 15 weeks, after NDEA administration for 6 weeks	Antiproliferative effect Apoptosis induction Marked improvement in histological characteristic of liver tissue	AFP VEGF AFU GGT	Carvacrol may have an antitumor effect through its antiangiogenic capacity, antiproliferative effect and apoptotic activity against tumor cells *in vivo*	Ahmed et al. (2013), Egypt

(Continued on following page)

TABLE 1 | (*Continued*) Detailed description of the studies that used carvacrol, included in the systematic review.

Model	Dose	Results/targets		Conclusion	Authors (Year), Country
		Increase	Decrease		
Male wistar rats induced with hepatocarcinogenesis providing 0.01% DEN through drinking water for 16 weeks	Pre-treatment: (15 mg/kg b.wt) of carvacrol orally one week before DEN administration and up to 16 weeks Post-treatment: (15 mg/kg b.wt) of carvacrol orally for 6 weeks after administration of DEN for 10 weeks	–	Cell proliferation Tumor markers Mast cell density PCNA MMP-2 and -9 AgNORs	Carvacrol attenuates hepatocellular carcinoma by inhibiting cell proliferation and tumor metastases	Subramaniyan et al. (2014), India
DMH-induced colon carcinogenesis in male Wistar rats who received subcutaneous injections of DMH (20 mg/kg b.wt) in the right thigh, once a week for the first 4 weeks of the experiment (four injections)	20, 40 or 80 mg/kg every day from the day of the carcinogen treatment till the end of the 16th week	Weight gain Growth rate GPx, GR, GSH, SOD, CAT	Incidence of tumors Growth of neoplastic polyps	Carvacrol has antiproliferative, anticarcinogenic and chemopreventive potential and its effects were better observed at a dose of 40 mg/kg b.wt	Sivaranjani et al. (2016), India
C57BL/6 mice induced with DEN hepatocellular carcinoma injected intraperitoneally at a dose of 100 mg/kg	– Intragastrically 20 weeks	Intrastromal and peritumor lymphocytes DAPK1	Tumor growth Tumor cells Mitotic phase PPP2R2A	The direct regulation relationship between DAPK1 and PPP2R2A may be the biological mechanism of tumorigenesis and progression of hepatocellular carcinoma	Li et al. (2019), China
DMBA-induced breast cancer in female Holztman mice in a single administration of DMBA by oral gavage at a dose of 80 mg /kg body weight	50, 100 and 200 mg/kg/day Oral gavage 14 weeks	Tumor latency	Number of tumors 75% in the frequency of tumors 67% in the incidence of tumors Average volume	Carvacrol had an antitumor effect on breast cancer *in vivo* and it is likely that this effect may be due to its antioxidant activity	Rojas-Armas et al. (2020), Peru

Overview of Included Studies

The selected studies were carried out in different countries: India (n = 14), China (n = 14), Turkey (n = 13), the Republic of Korea (n = 5), Slovakia (n = 5), Iran (n = 5), Morocco (n = 2), Brazil (n = 2), Greece (n = 2), Iraq (n = 2), The United States of America (n = 2), Canada (n = 2), Egypt (n = 2), Croatia (n = 1), Lithuania (n = 1), Italy (n = 1), Spain (n = 1), The United Kingdom (n = 1), Peru (n = 1), Belgium (n = 1). Asia (51.9%) was the continent with the largest number of publications on the subject, followed by Europe (33.7%), the Americas (9.3%) and Africa (5.1%), with a greater trend of publications on this subject in the last three years (**Supplementary Figure S1**). Among the selected articles, 69 (89.6%) reported *in vitro* experiments and 10 (12.9%) were *in vivo* studies. Likewise, 43, 19, and 15 publications tested only carvacrol, thymol and both compounds, respectively. They were mostly obtained commercially, provided by Sigma Aldrich (n = 52), Fluka (n = 5), Aldrich Chemical (n = 2), Western Chemical (n = 1), Agolin SA (n = 1), Alfa Aesar (n = 1). In only five studies were the compounds isolated from essential oils. Remarkably, ten studies did not report the source of the tested compounds. A detailed description of the included studies is shown in **Tables 1** and **2**. A narrative summary of the results is presented below, divided into *in vitro* and *in vivo* studies.

Description of *In Vitro* Studies with Carvacrol and Thymol

Carcinomas

Carvacrol (500 and 1,000 μM) was able to inhibit the viability and proliferation of lung cancer cells (A549 cell line), in addition to inducing early apoptotic characteristics (Koparal and Zeytinoglu, 2003) and reducing the viability of the A549, H460 (Jung et al., 2018) and H1299 cells lines, the latter being resistant to epirubicin (Ozkan and Erdogan, 2012). These effects occurred mainly through the inhibition of tyrosine kinase receptor (AXL) expression and an increase in malondialdehyde (MDA) and 8-hydroxy-2′-deoxyguanosine levels (8-OHdG) (Ozkan and Erdogan, 2012; Jung et al., 2018).

In relation to hepatocarcinomas (HepG2 cell line), carvacrol exhibited anticancer effects, provoking cell death and antiproliferative effects in a concentration-dependent manner (Özkan and Erdogan, 2011; Melusova et al., 2014). The inhibition of cell proliferation and apoptosis induction occurred via the mitochondria-mediated pathway, accompanied by caspase-3 activation and Bcl-2 inhibition (Yin et al., 2012). The via extracellular signal-regulated kinases (ERK) protein, and mitogen-activated protein kinases (p38) apoptotic pathways may also be involved (Yin et al., 2012). Similarly, Melušová et al. (2014) demonstrated a marked apoptotic effect of carvacrol at a concentration of 650 μM after 24 h of incubation, and an accumulation of cells in the G1 phase, together with a reduction of cells in the S phase, slowing cell cycle/mitosis and provoking cell death.

Colorectal cancer (Caco-2 cell line) also exhibited reduced cell viability and a significant increase of early apoptotic cells after carvacrol incubation (115 μM) (Llana-Ruiz-Cabello et al., 2014). There was also inhibition of HCT116, LoVo and HT-29 cells

TABLE 2 | Detailed description of the studies that used thymol, included in the systematic review.

Model	Concentration/ Incubation time	Experimental methods for testing IC50 values	Results/targets			Conclusion	Authors (Year), Country
			Increase	Decrease	IC_{50}		
Monoterpene thymol *In vitro* studies							
HepG2 Caco-2	150–900 µmol 24 of incubation	–	Cytotoxic effects	DNA damage level	–	HepG2 cells were slightly more sensitive to the effects	Horváthová et al. (2006), Slovakia
K-562	200, 400, 600, 800, 1,000 µM 24 or 48 h of incubation	Trypan blue exclusion	Cytotoxic effects	DNA damage level	500 µM–24 h	Thymol has cytotoxic, antioxidant effects and has a protective action against DNA damage	Horvathova et al. (2007), Slovakia
P-815	0.004–0.5% v/v 48 h of incubation	MTT assay	Cytotoxic effects	–	0.015% v/v–48 h	Thymol is cytotoxic	Jaafari et al. (2007), Morocco
HepG2 Caco-2	150–1,000 µM 24 of incubation	Trypan blue exclusion	Cytotoxic effects Resistance to harmful DNA effects (antioxidant properties)	Cell proliferation	HepG2 - 400 µM–24 h Caco-2 - 700 µM–24 h	Thymol has antiproliferative and protective effects	Slamenová et al. (2007), Slovakia
HeLa Hep	15, 30.5, 61, 122, 244 ng/mL 72 h of incubation	–	Cytotoxic effects	Cell survival	–	Thymol has strong antitumor activity against the HeLa cell line	Abed, (2011), Iraq
MG63	100, 200, 400, 600 µmol/L 24 h of incubation	–	Cytotoxic effects Apoptosis induction Generation of ROS	Cell viability	–	Thymol showed antitumor activity in MG63 cells, moreover, its apoptotic effect is related to the pronounced antioxidant activity	Chang et al. (2011), China
HL-60	5, 25, 50, 75, 100 µM 24 h of incubation	–	Cytotoxic effects Apoptosis induction Cells in sub phase G0/G1 generation of ROS Caspase-9, -8 and -3	Cell viability Cells in phases G0/G1, S and G2/M Cell cycle stop in phase G0/G1 Bcl-2	–	Apoptosis induced by thymol in HL-60 cells involves the dependent and independent pathways of caspase	Deb et al. (2011), India
DBTRG-05MG	200, 300, 400, 500, 600, 800 µM 24 h of incubation	–	Cytotoxic effects Apoptosis induction and necrosis	Cell viability	–	Thymol induces cell death in human glioblastoma cells	Hsu et al. (2011), China
HepG2	20–200 µg/mL 24 h of incubation	CellTiter-Blue® cell viability assay	Cytotoxic effects Antiproliferative effects	Membrane damage	60.01 µg/mL–24 h	Thymol exhibits antioxidant activities and anti-cancer effects on cells	Özkan and Erdogan, (2011), Turkey
P-815 CEM K-562 MCF-7 $MCF\text{-}7_{gem}$	0.05–1.25 µM 48 h of incubation	MTT assay	Cytotoxic effects	Cell cycle stop in phase G0/G1	P-815–0.15 µM–48 h CEM - 0.31 µM–48 h K-562–0.44 µM–48 h MCF-7 - 0.48 µM–48 h $MCF\text{-}7_{gem}$ -	Thymol showed relevant cytotoxic effects in all tested strains	Jaafari et al. (2012), Morocco

(Continued on following page)

TABLE 2 | (*Continued*) Detailed description of the studies that used thymol, included in the systematic review.

Model	Concentration/ Incubation time	Experimental methods for testing IC50 values	Results/targets			Conclusion	Authors (Year), Country
			Increase	Decrease	IC_{50}		
H1299	10–2,000 µM 24 and 48 of incubation	CellTiter-Blue® cell viability assay	Cytotoxic effects MDA 8-OHdG	Membrane and DNA damage	497 µM–24 h 266 µM–48 h	Thymol exhibited a cytotoxic and antioxidant effect	Ozkan and Erdogan, (2012), Turkey
B16-F10	75, 150, 300, 600, 1,200 µM 24 h of incubation	Trypan blue and MTT assay	Cytotoxic effects Generation of ROS	Cell viability Density of melanoma cells	400 µM	Thymol showed antitumor effect with moderate cytotoxicity	Satooka and Kubo, (2012), United States
HepG2 K-562 B16-F10	1.56–50 µg/mL 72 h of incubation	Trypan blue assay	Cytotoxicity only for B16-F10 cells Apoptosis induction in HepG2 cells Induction of caspase-3-dependent apoptotic cell death in HepG cells	–	HepG2 - > 25 µg/mL K-562–72 h B16-F10–18.23 µg/mL–72 h	Thymol showed cytotoxicity to B16-F10 cells	Ferraz et al. (2013), Brazil
PC-3 MDA-MB 231 A549 MCF-7 HL-60	10, 30.50, 70, 100 µg/mL 48 h of incubation	MTT assay	Cytotoxic effects Apoptosis induction DNA fraction sub G0 TNF-R1 Bax Caspase-8 and 9	Cell viability Cell proliferation PI3K/AKT/mTOR Bcl-2	PC-3 - 18 µg/mL–48 h MDA-MB 231–15 µg/mL–48 h A549–52 µg/mL–48 h MCF-7 - 10 µg/mL–48 h HL-60–45 µg/mL–48 h	Thymol exhibited cytotoxicity and induced apoptosis	Pathania et al. (2013), India
Caco-2	100–2,500 µM 24 and 48 h of incubation	–	–	–	–	The cells exposed to thymol remained unchanged and did not produce any cytotoxic, apoptotic or necrotic effects at any of the tested concentrations	Llana-Ruiz-Cabello et al. (2014), Spain
A549 HepG2 Hep3B	1–1.000 µM 72 h of incubation	SRB assay	Cytotoxic effects Antiproliferative effects	–	A549–0.187 ± 0.061 m⊠–72 h HepG2 - 0.390 ± 0.01 m⊠–72 h Hep3B- 0.181 ± 0.016 m⊠–72 h	Thymol exhibited more effective cytotoxicity against cells (Hep3B), while cells (A549) were less sensitive to treatment and cells (HepG2) were more resistant	Fitsiou et al. (2016), Greece
AGS	100, 200, 400 µM 6, 12, 24 h of incubation	–	Cytotoxic effects Apoptosis induction Sub-G1 phase Generation of ROS Bax Caspase-8, -7 and -9	Cell viability Cell growth MMP	–	Thymol has potent anticancer effects on gastric cancer cells	Kang et al. (2016), Republic of Korea
C6	0.1, 0.3, 1, 3, 10, 30, 100, 200 µM 24 h of incubation	–	–	Cell viability Cell migration p-ERK1/2 MMP-2 and -9	–	Thymol is a potential candidate for the treatment of malignant gliomas	Lee et al. (2016), Republic of Korea
A549	0–250 µM	–	Cytotoxic effects	Cell viability	–		

(Continued on following page)

TABLE 2 | (*Continued*) Detailed description of the studies that used thymol, included in the systematic review.

Model	Concentration/ Incubation time	Experimental methods for testing IC50 values	Results/targets			Conclusion	Authors (Year), Country
			Increase	Decrease	IC_{50}		
	24 h of incubation					Thymol has cytotoxic and antioxidant activity and its cytotoxic effect was greater than that of carvacrol	Coccimiglio et al. (2016), Canada
HCT-116	100, 150, 200 µg/mL 24 h of incubation	–	Cytotoxic effects Apoptosis induction Generation of ROS Caspase-3 p-JNK Cyt C	Cell proliferation Clonogenic potential	–	Thymol can be used as a potent drug against colon cancer due to its lower toxicity	Chauhan et al. (2018), Republic of Korea
HepG2	0.06, 0.11, 0.22, 0.45, 0.90 µg/µL 24 h of incubation	MTT assay	–	Cell viability Hepatocarcinoma cells	289 mg/L–24 h	Thymol has therapeutic potential in tumor cells without adverse effects on healthy cells	Elshafie et al. (2017), Italy
T24 SW780 J82	25, 50, 100, 150 µM 24 h of incubation or 100 µM – 6, 12, 24, 36 h of incubation	MTT assay	Cytotoxic effects Apoptosis induction p21 Caspase-3 and -9 p-JNK p-p38 MAPK Generation of ROS	Cell viability Cell cycle stop in phase G2/M Cyclin A and B1 CDK2 PI3K/Akt	T24–90.1 ± 7.6 µM–24 h SW780–108.6 ± 11.3 µM–24 h J82–130.5 ± 10.8 µM–24 h	Thymol can be used as a promising anticancer agent against bladder cancer	Li et al. (2017), China
PC-3	100, 300, 500, 700, 900 µM 24 h of incubation	–	Cytotoxic effects Induction of cell death	Cell viability	–	Thymol was cytotoxic to PC-3 cells	Yeh et al. (2017), China
Cal7 SCC4 SCC9 HeLa H460 MDA-231 PC-3	200–800 µM 48 h of incubation	Cell Titer 96 ® Aqueous non-Radioactive cell Proliferation assay	Cytotoxic effects	Cell viability	350 µM–500 µM	Thymol had cytotoxic, antiproliferative and antitumor effects	De La Chapa et al. (2018), United States
AGS	10, 20, 30, 50, 100, 200, 400, 600 µM 24 h of incubation	CellTiter-Glo Luminescent cell viability assay	Apoptotic effects Necrosis Bax Caspase-3 and -9 Generation of ROS Genotoxic effect	Cell viability Bcl-2 GSH levels	75.63 ± 4.01 µM–24 h	Thymol has cytotoxic, apoptotic, genotoxic and dose-dependent ROS-generating effects	Günes-Bayir et al. (2018), Turkey
MCF-7 MDA-MB 231	10, 15, 30, 50, 80, 100, 200 µg/mL 24 h of incubation	MTT assay	Cytotoxic effects Antiproliferative effect Apoptosis induction	Bcl-2	MDA-MB 231–56 µg/mL–24 h MCF-7 - 47 µg/mL–24 h	Thymol has antiproliferative effects	Jamali et al. (2018), Iran

(Continued on following page)

TABLE 2 | (*Continued*) Detailed description of the studies that used thymol, included in the systematic review.

Model	Concentration/ Incubation time	Experimental methods for testing IC50 values	Results/targets			Conclusion	Authors (Year), Country
			Increase	Decrease	IC_{50}		
			Caspase-3 Bax Generation of ROS Sub-G1 phase	Interruption of cell cycle progression in the S phase			
MCF-7	5, 10, 20, 30, 40, 50, 75, 100 g/mL 48 and 72 h of incubation	MTT assay	Cytotoxic effects p53 p21	Number of cancer cells Cell cycle arrest induction	54 µg/mL - 48 h 62 µg/mL - 72 h	Thymol can induce the process of apoptosis in MCF-7 and, therefore, can be considered an anticancer agent	Seresht et al. (2019), Iran
HT-29	62.5, 125, 250, 500, 750, 1,000 ppm 24 h of incubation	Trypan Blue exclusion assay	Cytotoxic effects Genoprotective effects	–	152.1 ± 18.0 ppm–24 h	Thymol induces cytotoxicity and provides genoprotective effects	Thapa et al. (2019), United Kingdom
MDA-MB 231 PC-3 DU 145 KLN 205	100, 200, 400, 600, 800 µM 24, 48 and 72 h of incubation	MTT assay	Cytotoxic effects Antiproliferative effect Apoptosis induction	–	MDA-MB 231–208.36 µM–72 h; PC-3 - 711 µM–24 h, 601 µM–48 h and 552 µM–72 h; DU 145–799 µM–24 h, 721 µM–48 h and 448 µM–72 h KLN 205–421 µM–48 h and 229.68 µM–72 h	Thymol has apoptotic and antiproliferative properties and can serve as a potential therapeutic agent	Elbe et al. (2020), Turkey
SKOV-3	100, 200, 400, 600 µM 24 and 48 h of incubation	MTT assay	Apoptosis induction	Cell viability	316.08 µM–24 h 258.38 µM–48 h	Thymol was cytotoxic to the ovarian cancer cell line and it was more potent than carvacrol	Elbe et al. (2020), Turkey
HCT116 LoVo	10, 20, 40, 80, 120 µg/mL 24, 48 and 72 h of incubation	CCK-8 Kit	Apoptosis induction Bax Caspase-3 and PARP Cells in phase G0/G1	Proliferative capacity Cell migration and invasion Cell cycle stop Bcl-2 Cells in S and G2/M phases	LoVo - 41.46 µg/mL - 48 h HCT116–46.74 µg/mL - 48 h	Thymol treatment reduced the proliferative capacity of cells and suppressed cell migration and invasion	Zeng et al. (2020), China
AGS	0–600 µM 24 h of incubation	CellTiter-Glo Luminescent cell viability assay	Cytotoxic effects Generation of ROS Apoptosis induction Bax Caspase-3 and -9 DNA damage	Cell viability GSH levels Bcl-2	75.63 ± 4.01 µM–24 h	Thymol has cytotoxic and antioxidant effects in gastric adenocarcinoma	Günes-Bayir et al. (2020), Turkey
A549	25–200 µg/mL 12 and 24 h of incubation	MTT assay	Antiproliferative effect Apoptosis induction DNA damage	Cell viability MMP Bcl-2	745 µM–24 h	Thymol can act as a safe and potent therapeutic agent to treat non-small cell lung cancer	Balan et al. (2021), India

(Continued on following page)

TABLE 2 | (*Continued*) Detailed description of the studies that used thymol, included in the systematic review.

Model	Concentration/ Incubation time	Experimental methods for testing IC50 values	Results/targets			Conclusion	Authors (Year), Country
			Increase	Decrease	IC_{50}		
			Generation of ROS Caspase-3 and -9 Bax Cells in phase G0/G1 TBARBS CARBONIL	SOD			
KG1 K-562 HL-60	25, 50, 100 μM 24 and 48 h of incubation	–	Cell death	Cell viability	–	KG1 cells treated with 50 μM thymol were more sensitive compared to the other two lines. At 100 μM, thymol induced complete cell death of KG1 and HL60 cells, while about 50% of K562 cells resisted cell death after 48 h of treatmentl	Bouhtit et al. (2021), Belgium

Model	Concentration	Results/Targets		Conclusion	Authors (Year), country
		Increase	Decrease		
In vivo studies					
Female athymic nude rats were injected subcutaneously in the right flank with 3×10^6 Cal27 or HeLa cells in 0.1 mL of sterile PBS	4.3 mM thymol (32 μg diluted in 50 μl sterile saline with a final concentration of 0.25% DMSO)	Apoptotic cells	Tumor volume reduction Proliferative cells	Thymol had cytotoxic, antiproliferative and antitumor effects	De La Chapa et al. (2018), United States
Xenograft model: BALB/c male nude mice were injected subcutaneously with HCT116 cells (1×10^7 cells in 0.2 mL of PBS) on the back Lung metastasis model: HCT116 cells (1×10^6) were intravenously injected into the tail vein of each mouse	Xenograft model and lung metastasis model: Intraperitoneal injection for 30 days with thymol at 75 mg/kg 1x on alternate days or thymol at 150 mg/kg 1x on alternate days	Necrotic lesions Bax Caderina-E	Tumor growth and metastasis Average number of tumor nodules on the surface of the lungs Ki-67 expression level Cell proliferation Bcl-2 Wnt/β-catenin signaling pathway Vimentina Cyclin D1 C-myc Survivin	Thymol inhibits the growth and metastasis of colorectal cancer *in vivo* by suppressing Wnt/β-catenin signaling and the EMT program	Zeng et al. (2020), China

(Continued on following page)

TABLE 2 | (*Continued*) Detailed description of the studies that used thymol, included in the systematic review.

Model	Concentration	Results/Targets		Conclusion	Authors (Year), country
		Increase	Decrease		
Male Wistar rats injected with DMH (40 mg/kg intraperitoneally, twice a week) for 16 consecutive weeks	20 mg/kg/day, orally, for 16 weeks	Final body weight Weight gain Growth rate NRF2 GST, GSH, SOD, CAT	Mortality Incidence of ACF Serum CEA levels Serum levels of CA19-9 Caspase-3 TNF-α NF-κB IL-6 Tissue content of MDA (colon lipid peroxidation)	Thymol administration had promising preclinical protective efficacy by promoting inhibition of oxidative stress, inflammation and induction of apoptosis	Hassan et al. (2021), Egypt

Abbreviations: 5RP7, Mouse embryonic fibroblast with transformation of H-ras oncogenes; 8-OHdG, 8-hydroxy-2′-deoxyguanosine; A375, Melanoma (skin) cancer cell line; A549, Lung Carcinoma Cell Line; ACF, Aberrant crypt foci; AFP, Alpha-fetoprotein serum; AFU, Alpha l-fucosidase; AgNORs, Proteins Associated with the Argyrophilic Nucleolar Organizing Region; AGS, Human gastric carcinoma cell line; ALP, Alkaline Phosphatase; ALT, Alanine transaminase; AST, Aspartate transaminase; AXL, Tyrosine Kinase Receptor; B[a]P, 3.4 benzopurene; B16-F10, Mouse melanoma cells; BT-474, Breast ductal carcinoma; BT-483, Breast ductal carcinoma; C6, Glioma cell line; Caco-2, Cell line derived from human colon carcinoma; CA 19–9, Tumor markers carbohydrate antigen 19–9; Cal27, Cell line of the squamous cell carcinoma of the tongue; CAT, Catalase; CEA, Carcinoembryonic antigen; CCK-8, Cell Counting Kit-8; CCND1, Gene encoding the cyclin D1 protein; CDK4 or 6, Cyclin-dependent kinases; cGT, Glutamyl transpeptidase Range; CyT C, Cytochrome C; c-Myc, Proto-oncogene; CO25, Mouse muscle cell line; COX-2, Cyclooxygenase; DAPK1, Protein kinase 1 associated with death; DBTRG-05MG, Human Glioblastoma Cells; DEN, Diethylnitrosamine; DMH, 1,2-dimethylhydrazine; DMBA, 7,12-dimethylbenz[a]anthracene; DMSO, Dimethylsulfoxide; DNA, Deoxyribonucleic acid; DU 145, Human Prostate Cancer Cell Line; EC50, Half of the maximum effective concentration; EMF, Acute T Lymphoblastoid Leukemia; EMT, Epithelial-mesenchymal transition; ERK 1/2, Kinase 1/2 regulated by extracellular signal; ERO, Reactive Oxygen Species; GGT, Gamma-Glutamyltransferase; GPx, Glutathione Peroxidase; GR, Glutathione reductase; GSH, Reduced Glutathione; H1299, Parental and Drug Resistant Human Lung Cancer Cell Line; H460, Non-small cell lung cancer cell line; HCT116, Colorectal adenocarcinoma cell line; HeLa, Human Cervical Cancer Cell Line; Hep, Human Laryngeal Squamous Cell Carcinoma; Hep3B, Human Hepatocellular Carcinoma Cell Line; HepG2, Human Hepatocellular Carcinoma Cell Line; HL-60, Human Acute Promyelocytic Leukemia Cell Line; HT-29, Colorectal adenocarcinoma cell line; IC50, Half of the maximum inhibitory concentration; IL-6, Interleukin-6; J82, Bladder Cancer Cell Line; Jagged-1, Jagged Canonical Notch Ligand 1; JAR, Human Choriocarcinoma Cell Line; JEG3, Human Choriocarcinoma Cell Line; Jurkat, Lymphocytes derived from T-cell lymphoma; KG1 and K-562, Human Myelogenous Leukemia Cell Line; Kelly, Neuroblastoma cell line; Ki-67, Antigen, biomarker; KLN 205, Non-small cell lung cancer; LDH, Lactate dehydrogenase; LoVo, Colorectal Adenocarcinoma Cell Line; MAPK, Protein kinase activated by mitogen; MTT, Methyl Tetrazolium Test; MTS, Tetrazolium salt reduction; MCF-7, Human breast cancer cell line; MCF-7gem, Gemcitabine-resistant human breast adenocarcinoma; MDA, Malondialdehyde; MDA-MB 231, Human metastatic breast adenocarcinoma cell line; MDA-MB 453, Human metastatic breast adenocarcinoma cell line; MDPK, Myotonic dystrophy protein kinase; MG63, Human Osteosarcoma Cell Line; MMP, Potential of the mitochondrial membrane; MMP-2 or 9, Metalloproteinase-2 or 9 of the matrix; N2a, Rat neuroblastoma cell line; NDEA, N-nitrosodiethylamine; Notch-1, Signaling path; NSCLC, Non-small cell lung cancer; OC2, Human oral cancer cells; OSCC, Human oral squamous cell carcinoma; p21, WAF1 encoding gene; p38, Mitogen-activated protein kinases; p53, tumor protein; P-815, Murine Mastocytoma Cell Line; p-AKT, Phospho-protein kinase B; PBS, Sterile phosphate buffered saline; PC-3, Human Prostate Cancer Cell Line; PCNA, Proliferating Cell Nuclear Antigen; PI3K/AKT/mTOR, Phosphoinositide-3-kinase/Akt/mammalian target; PI3K/Akt, Phosphoinositide-3-kinase-Akt; p-JNK, Fosto-c-Jun N-terminal kinase; p-p38, Phospho-p38; PPP2R2A, Serine/threonine-protein phosphatase 2A; p-STAT3, Phospho-signal transducer and transcription activator; SRB, Sulforhodamine B; SCC-25, Human squamous cell carcinoma cell line; SCC4 and SCC9, Human oral squamous cell carcinoma cell line; SH-SY5Y, Neuroblastoma cell line; SiHa, Human Cervical Cancer Cell Line; SKOV-3, Ovarian cancer cell line; SOD, Superoxide dismutase; SW780, Bladder cancer cell line; T24, Bladder Cancer Cell Line; TAC, Total antioxidant capacity; TBARS, Thiobarbituric Acid Reactive Substances; TCA-8113, Human tongue squamous cell carcinoma cell line; TNF-α, Tumor Necrosis Factor-Alpha; TNFR1, Tumor necrosis factor 1 receptor; TOS, Total oxidant status; TRPM7, Subfamily M of the cation channel of the potential transient receptor Member 7; U87, Human glioblastoma cell line; VEGF, Vascular endothelial growth factor; XXT, 2.3-bis(2-methoxy-4-nitro-5-sulfophenyl)-2H-tetrazolium-5-carboxanilide inner salt.

proliferation (Fan et al., 2015; Pakdemirli et al., 2020). Carvacrol also promoted a decrease in Bcl-2, metalloproteinase-2 and -9 (MMP-2 and MMP-9), p-ERK, p-Akt, cyclin B1 levels and an increase in p-JNK, Bax levels, resulting in cell cycle arrest at the G2/M phase (Fan et al., 2015).

In respect of breast cancer, treatment with carvacrol decreases MDA-MB231 (Jamali et al., 2018; Li et al., 2021) and MCF-7 cells line viability (Al-Fatlawi and Ahmad, 2014; Jamali et al., 2018; Tayarani-Najaran et al., 2019; Li et al., 2021). At 200 μM, the MDA-MB-231 cell line was the most sensitive and MCF-7 was the least sensitive, indicating that the effectiveness of carvacrol may vary according to the types of breast cancer cell. In addition, the TRPM7 pathway is one of the suggested pharmacological mechanisms of action (Li et al., 2021). Carvacrol was more cytotoxic compared to thymol (Jamali et al., 2018), α-thujone, 4-terpineol, 1,8-cineol, bornyl acetate and camphor (Tayarani-Najaran et al., 2019). Tayarani-Najaran et al. (2019) also reported an apoptotic effect marked by an increased level of Bax protein, and cleaved both poly [ADP-ribose] polymerase 1 (PARP-1) and caspase-3. The antiproliferative activity of carvacrol was 1.2 times higher against MDA-MB231 cells compared to U87 cells (Baranauskaite et al., 2017). MDA-MB 231 cell proliferation slowed after treatment with carvacrol, accompanied by apoptosis induction with increased levels of Bax, decreased mitochondrial membrane potential, cytochrome C release, caspase activation, PARP cleavage, increased sub-phase G0/G1 of the cell cycle and a reduced number of cells in the S phase (Arunasree, 2010). The viability of MCF-7 cells was reduced after carvacrol treatment (200 μmol/L), with a significant increase in the number of early and late apoptotic cells, accompanied by a negative regulation of Bcl2 and positive regulation of Bax protein. An accumulation of cells in the G0/G1 phase was observed, along with a reduction of cells in the S and G2 phases, mainly through the reduced expressions of CDK4, CDK6, retinoblastoma protein (pRB), cyclin D and phosphoinositide-3-kinase-Akt (PI3K/p-AKT) (Mari et al., 2020).

It was also observed that the administration of carvacrol provoked cytotoxic and apoptotic effects on HeLa and SiHa cervical cell lines (Mehdi et al., 2011). In fact, Potočnjak et al. (2018) demonstrated that the cytotoxicity exhibited by carvacrol against HeLa cells occurred through the suppression of the cell cycle and induction of apoptosis, the latter accompanied by an increase in caspase-9, PARP cleavage, and activation of ERK, increasing the expression of phospho-ERK1/2. In SiHa cells, the reduction in viability and apoptosis induction occurred through p53 activation and Bax, caspase-3, -6, -9 expression, along, with negative regulation of Bcl-2 gene (Abbas and Al-Fatlawi, 2018). Furthermore, another study demonstrated that carvacrol and thymol were cytotoxic against ovarian cancer (SKOV-3 cell line) exhibiting apoptotic and antiproliferative properties (Elbe et al., 2020).

Carvacrol also induced cytotoxicity and apoptosis (via caspase-3 and reactive oxygen species—ROS) of human oral squamous cell carcinoma (OC2 cell line) in a concentration-dependent manner (Liang et al., 2013). In tongue cancer (Tca-8113, SCC-25 cell lines), Dai et al. (2016) reported that carvacrol effectively inhibited cell proliferation through the negative regulation of CCND1 and CDK4 expression, and the positive regulation of p21 expression, resulting in a significant decrease of cells in the S phase, in addition to inhibiting the migration and invasion abilities of Tca-8113 cells via phospho-focal adhesion kinase (p-FAK), p-catenin, ZEB1 and MMP-2 and -9 reduction. Apoptosis was marked by a reduction of anti-apoptotic Bcl-2 proteins expression and an increase of proapoptotic Bax proteins levels (Dai et al., 2016).

In a prostate cancer cell line (DU 145), carvacrol showed a significant reduction of cell viability and proliferation in a concentration and time dependent manner, marked by a cell cycle arrest, resulting in the accumulation of cells in the G0/G1 phase, and apoptosis, related to the increased activity of caspase-3, production of ROS and loss of mitochondrial membrane potential (Khan et al., 2017). PC-3 cells also exhibited cytotoxicity and decreased cell viability in a concentration dependent manner after carvacrol treatment (Horng et al., 2017). A blockade of TRPM7 channels, reduced expression of MMP-2 and F-actin, was also observed, together with the inhibition of PI3K/Akt and MAPK (Mitogen-activated protein kinases) signaling pathways was also observed (Luo et al., 2016). Similarly, Heidarian and Keloushadi (2019) reported that this monoterpene acts through the negative regulation of pERK1/2, pSTAT3 and pAKT expression, suggesting that inhibition of interleukin-6 (IL-6) signaling pathways can be a promising target for prostate cancer treatment. The induction of PC-3 cells apoptosis was mostly through the intrinsic pathway, associated with the production of ROS and mediated by the increase expression of caspase-3, -8 and -9 and Bcl-2/Bax. There was also a G0/G1 phase arrest of cell cycle, together with a considerable decrease of cells in the S and G2/M phase (Khan et al., 2019). Similarly, Tayarani-Najaran et al. (2019) demonstrated decreased cell viability in a concentration dependent manner and also marked apoptosis (mitochondrial pathway), accompanied by cleavage of PARP-1 and caspase-3 and an increased Bax protein level.

Günes-Bayir et al. (2018), Günes-Bayir et al. (2018), and Maryam et al. (2015) reported cytotoxic effects of carvacrol on gastric cancer (AGS cell line) significantly reducing cell viability in a manner dependent on concentration. There was also an induction of apoptosis with a reduction of Bcl-2 protein levels, and an increase in Bax, caspase-3 and -9 protein levels, besides the production of ROS. In their most recent study, Günes-Bayir et al. (2020) also identified the cytotoxic effects of thymol on AGS cell viability, in addition to inducing apoptosis, by increasing ROS, Bax, Caspase-3, -9 levels and reducing Bcl-2 and GSH levels.

Regarding human choriocarcinoma (JAR and JEG3 cell lines), carvacrol was able to inhibit proliferation and induce cell cycle arrest. The results showed that carvacrol reduced cell proliferation and provoked apoptosis mediated by mitochondrial membrane potential depolarization, increased mitochondrial calcium and activation of Bax and Cytochrome C expression. In addition, treatment with this monoterpene promoted an accumulation of cells in the sub-G1 phase, indicating that changes in intracellular calcium and ROS generation are related to the antiproliferative effects observed. Additionally, there was a marked phosphorylation of ERK1/2 and

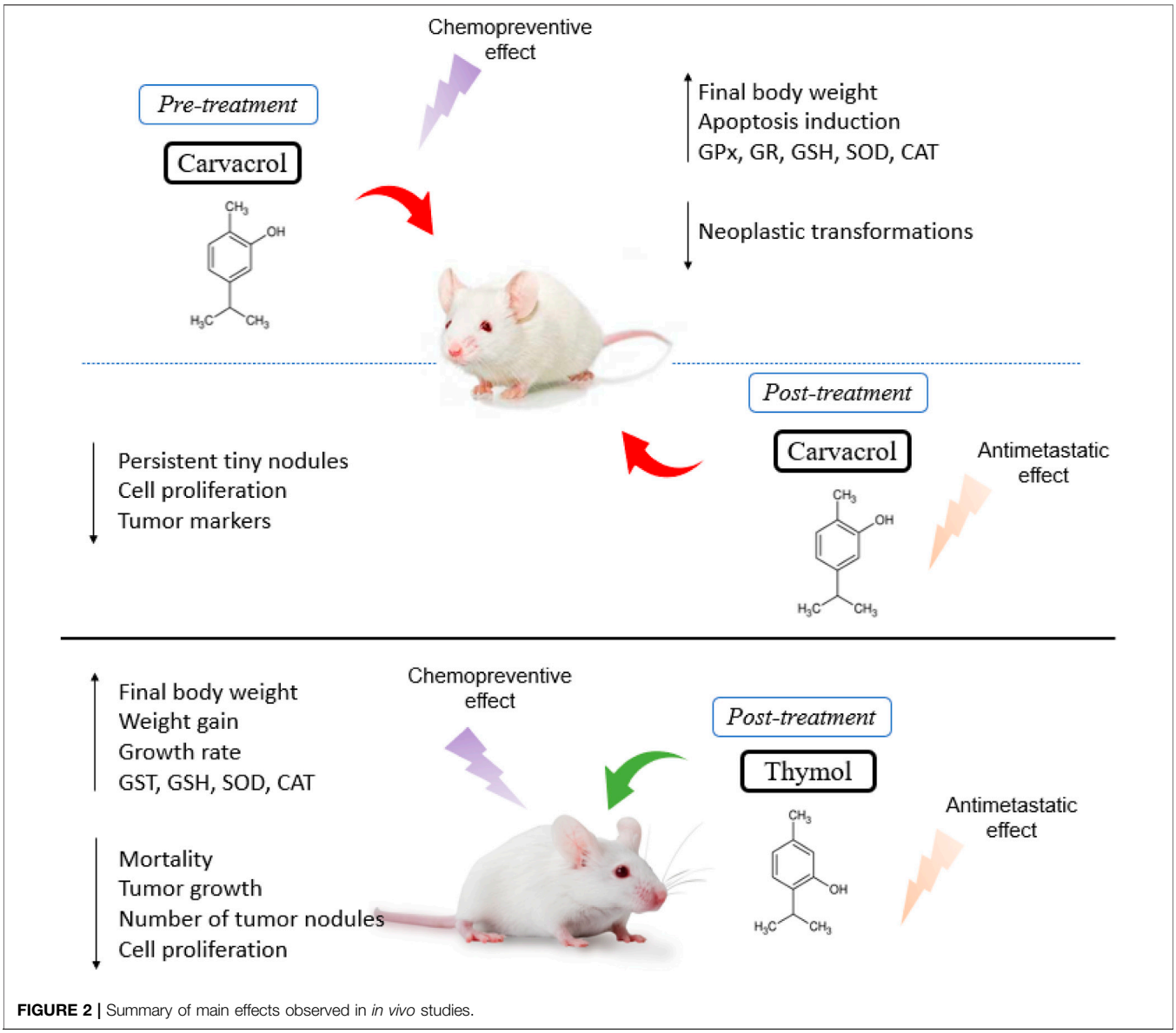

FIGURE 2 | Summary of main effects observed in *in vivo* studies.

also inhibition of the PI3K/AKT signaling pathway, indicating that carvacrol regulates signaling pathways by inhibiting MAPK and PI3K (Lim et al., 2019).

In murine B16-F10 and A375 melanoma cell lines, carvacrol reduced cell viability and induced cytotoxicity (Satooka and Kubo, 2012; Ferraz et al., 2013; Govindaraju and Arulselvi, 2018). The antiproliferative effect was confirmed by Govindaraju and Arulselvi (2018), who reported marked cell cycle arrest, attested by the accumulation of G1 phase cells, a reduction in the number of G2/M cells and apoptosis through the mitochondria-mediated pathway and PARP cleavage/activation, together with a reduced expression of the anti-apoptotic protein Bcl-2.

Similarly, the administration of thymol to lung cancer cells promoted a reduction in cell viability in the A549, H460 and H1299 cell lines (Pathania et al., 2013; Coccimiglio et al., 2016; De La Chapa et al., 2018; Balan et al., 2021). Likewise, the cytotoxic effect of thymol on A549 cells was higher than carvacrol cytotoxicity (Coccimiglio et al., 2016). Thymol also promoted cytotoxicity and apoptosis of KLN 205 cells with an IC_{50} of 421 and 229.68 μM in 48 and 72 h, respectively (Elbe et al., 2020). In liver carcinoma cells (HepG2), thymol exhibited antioxidant activity at lower ($<IC_{50}$ = 60.01 μg/mL) concentrations and antitumor effects (apoptosis and inhibition of cell proliferation) at higher concentrations ($>IC_{50}$ = 60.01 μg/mL) (Özkan and Erdogan, 2011). Elshafie et al. (2017) reported HepG2 cell death, decreased cell viability and a selective action of thymol against these tumor cells.

Thymol also showed concentration-dependent cytotoxic effects and reduced the proliferation of Caco-2 cells (Horváthová et al., 2006). In contrast, Llana-Ruiz-Cabello et al. (2014) reported that Caco-2 cells exposed to thymol did not

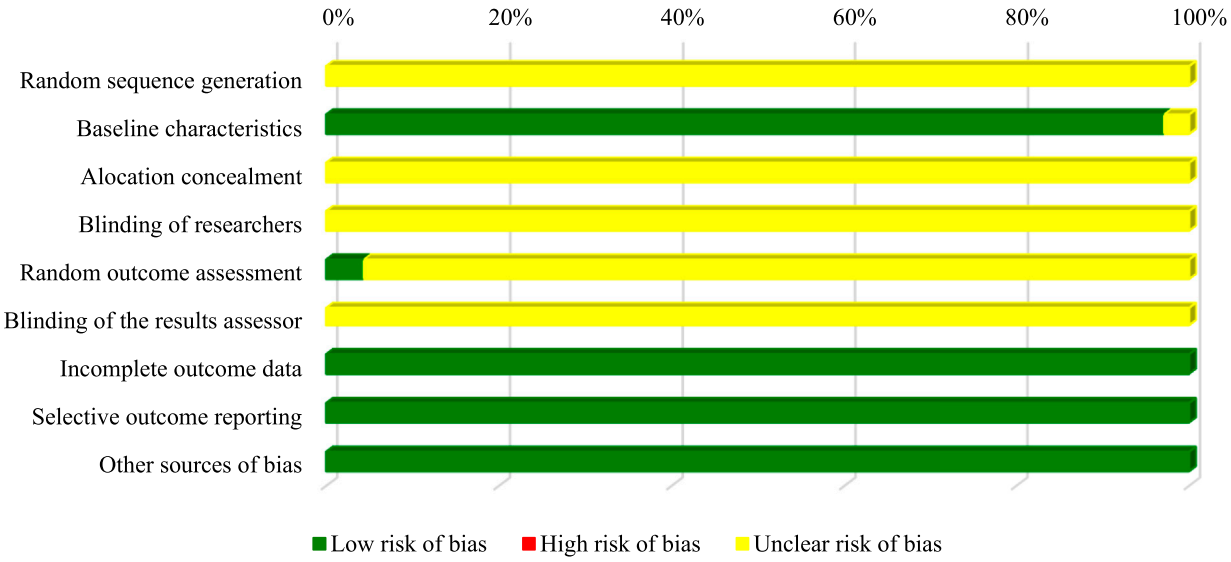

FIGURE 3 | Assessment of *in vitro* studies risk of bias.

exhibit any cytotoxic, apoptotic or necrotic effects in any of the tested concentrations. HCT-116 and HT-29 cells, after thymol administration, displayed a cell number reduction, cell apoptosis by disrupting mitochondrial membrane potential and ROS production (Chauhan et al., 2018; Thapa et al., 2019). These effects may have been caused by the positive regulation of the caspase-3, PARP-1, p-JNK and Cytochrome C expression (Chauhan et al., 2018).

Breast cancer cells (MDA-MB 231 cell line) also exhibited a reduction in cell viability after thymol treatment (Pathania et al., 2013; De La Chapa et al., 2018; Elbe et al., 2020). The inhibition of cell proliferation and apoptosis on MDA-MB231 and MCF-7 cell lines occurred via the mitochondrial pathway and induction of oxidative damage to DNA through Bax/Bcl-2 modulation, decreased levels of procaspase-8, -9, -3, increased levels of cleaved caspase-3 and ROS, and also cell cycle arrest at S-phase (Jamali et al., 2018). According to the results found by Seresht et al. (2019), thymol produced cytotoxic effects and reduced the number of MCF-7 cells, suggesting that this monoterpene induces cell cycle arrest, probably due to p21 overexpression. Thymol also promoted a marked antitumor effect on cervical cancer (HeLa cell line), through cytotoxic effects on the concentration of 30.5 ng/mL (Abed, 2011). De La Chapa et al. (2018) also reported decreased viability of HeLa cells and induction of apoptosis by PARP cleavage, suggesting that the anticancer effect of thymol is caused by mitochondrial dysfunction and subsequent apoptosis.

The administration of thymol to bladder cancer (T24, SW780, J82 cell lines) provoked inhibition of cell proliferation and decreased the cell viability in a concentration and time dependent manner, along with marked cell cycle arrest in the G2/M phase and induction of apoptosis through the intrinsic pathway, together with the activation of caspase-3 and -9, JNK and p38, release of cytochrome C, negative regulation of Bcl-2 family proteins and production of ROS. In addition, a considerable decrease in the expression of cyclin A, B1 and CDK2, as well as an increase in the expression of p21 were observed after treatment with thymol, suggesting that its antitumor effect occurs by inhibiting the PI3K/Akt signaling pathway, via MAPKs, and generation of ROS (Li et al., 2017). In human laryngeal squamous cell carcinomas (Hep), thymol showed a pronounced reduction of cell proliferation and also apoptosis, at a concentration of 30.5 ng/mL. According to De La Chapa et al. (2018) thymol exhibited cytotoxicity and decreased cell viability in a concentration dependent manner on Cal27, SCC4 and SCC9 cell lines. However, this cytotoxicity was reversed by the N-acetyl-cysteine (NAC) antioxidant addition, providing evidence that the anticancer mechanism of action of thymol involves mitochondrial dysfunction, and generation of ROS, culminating in apoptosis (De La Chapa et al., 2018). Thymol also caused a decrease in cell viability of prostate cancer (PC-3 cell line), and provoked cytotoxic effects (Pathania et al., 2013; Yeh et al., 2017; De La Chapa et al., 2018). PC-3 cells demonstrated greater sensitivity to treatment with thymol compared to DU145 cells. In addition, the induction of apoptosis in both cell lines occurred in a concentration-dependent manner (Elbe et al., 2020). Similarly, thymol suppressed the viability of melanoma (B16-F10 cell line), also in a concentration-dependent manner, by reducing the cell number and provoking cytotoxic effects. These effects seem to be related to the oxidative damage observed after the increase of ROS levels (Satooka and Kubo, 2012).

Central Nervous System Cancers

Human glioblastoma cells (DBTRG-05MG) showed reduced viability in a concentration-dependent manner when treated with carvacrol (200–600 μM), induced apoptosis and necrosis

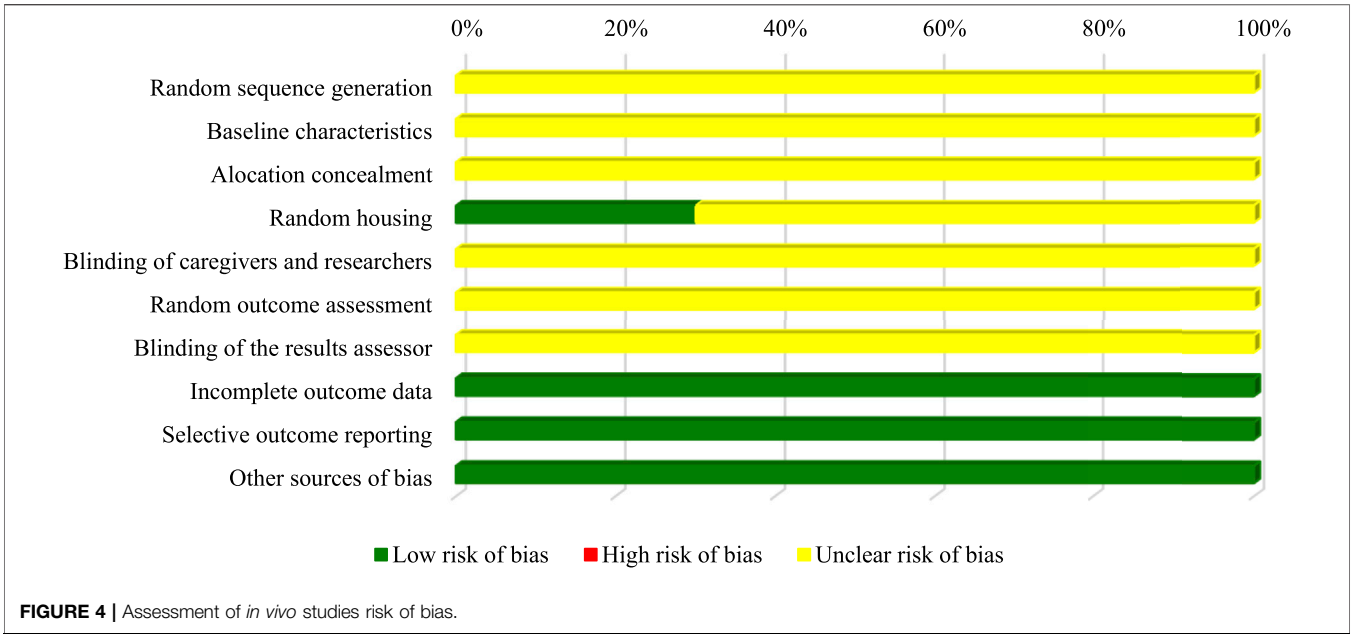

FIGURE 4 | Assessment of *in vivo* studies risk of bias.

by ROS production and caspase-3 activity (Liang and Lu, 2012). In a rat neuroblastoma (N2a cell line), treatment with carvacrol (200–400 mg/L) exhibited cytotoxic and antiproliferative effects, along with antioxidant activity (Aydın et al., 2014). Kelly and SH-SY5Y neuroblastoma cells also exhibited a reduced proliferation rate after exposure to carvacrol (Kocal and Pakdemirli, 2020). In glioblastoma (cell line U87), carvacrol induced apoptosis by increasing the levels of caspase-3 cleavage, moreover, its antitumor mechanism of action seems to be related to the inhibition of PI3K/Akt signaling pathways, activation of mitogen/protein kinase by extracellular signals (via MAPK/ERK) and decreased levels of MMP-2 protein (Chen et al., 2015).

Regarding thymol, treatment at concentrations of 100 and 200 μM induced a significant reduction in cell viability and inhibited the migration of glioma cells (C6 cell line) through phosphorylation of PKCα and ERK1/2, that resulted in decreased expression of MMP-9 and MMP-2 (Lee et al., 2016). In addition, in DBTRG-05MG cells, thymol exhibited a cytotoxic effect in a concentration-dependent manner, by reducing cell viability and inducing apoptosis. The 400–600 μM range of concentrations promoted cell necrosis and the 800 μM concentration killed all cultivated cells (Hsu et al., 2011).

Sarcomas

Treatment with carvacrol in leiomyosarcoma cells exhibited antiproliferative effects in a concentration dependent manner and also inhibition of cell growth (Karkabounas et al., 2006). In addition, carvacrol showed a greater cytotoxicity compared to thymol against murine mast cell cells (P-815 cell line) (Jaafari et al., 2007; Jaafari et al., 2012), with accumulation of cells in the S phase (Jaafari et al., 2012).

In relation to thymol, there were concentration-dependent cytotoxic effects and interruption of the cell cycle progression in the G0/G1 phase in P-815 cells (Jaafari et al., 2012). In human osteosarcoma cells (MG63 cell line), thymol reduced cell viability, induced cytotoxic effects and apoptosis, which occurred in a concentration-dependent manner. Additionally, there was an increase in the production of ROS and cell death (Chang et al., 2011).

Leukemias

Carvacrol showed cytotoxic effects against human myeloid leukemia cells (K-562 cell line) (Horvathova et al., 2007; Jaafari et al., 2012) and against T-cell acute lymphoblastic leukemia (CEM cell line) (Jaafari et al., 2012). Carvacrol was more cytotoxic than thymol, inducing accumulation of cells in the S phase (Jaafari et al., 2012). It was shown that carvacrol produced cytotoxic effects and reduced cell viability in human acute promyelocytic leukemia (HL-60 cell line) and lymphocytes derived from T-cell lymphoma (Jurkat cell line). Treatment with carvacrol (100 μM) showed early and late apoptotic cells accompanied by a reduction of mitochondrial membrane potential levels, suggesting that apoptosis was mediated by the mitochondrial pathway, with a significant increase of Bax pro-apoptotic proteins, decreased expression of the anti-apoptotic proteins Bcl2 and an increased caspase-3 protein level (Bhakkiyalakshmi et al., 2016).

Analyzing the effects of thymol on K-562 and CEM cells, Jaafari et al. (2012) revealed that the latter was more sensitive to thymol effects, resulting in the accumulation of cells in the G0/G1 phase. In addition, treatment with thymol also reduced HL-60 cell viability, exhibiting cytotoxicity with concentrations above 50 μM (Deb et al., 2011). Cell cycle arrest was observed in the G0/G1 phase, with decreased Bcl-2 protein levels and interruption of mitochondrial homeostasis; increased ROS production, mitochondrial production of H_2O_2, and Bax protein levels; and activation of caspase-8, -9, -3 and PARP (Deb et al.,

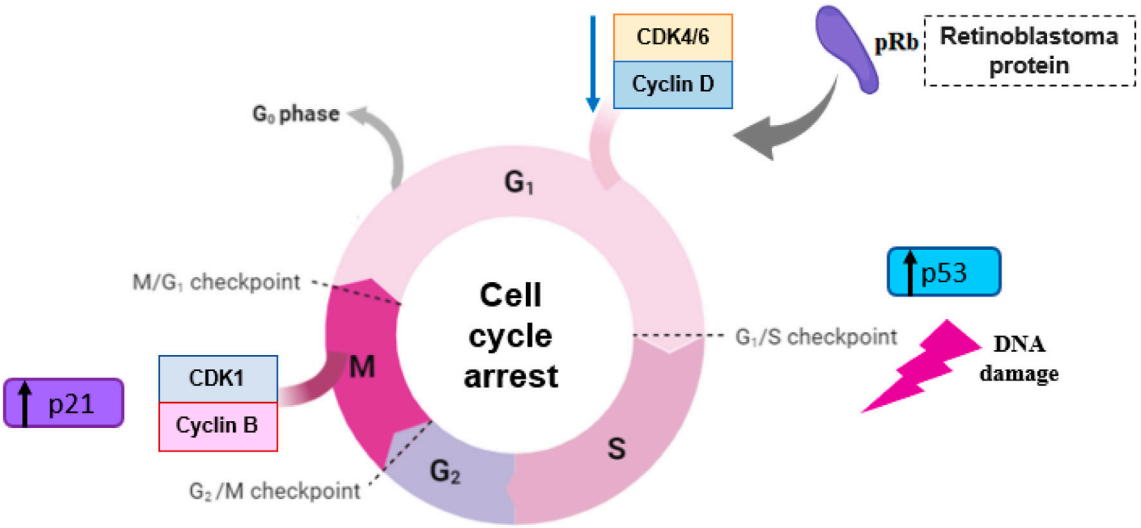

FIGURE 5 | Cell cycle involvement in cancer treatment with carvacrol and thymol.

2011). Thus, inhibition of the PI3K/Akt/mTOR signaling pathway may be a possible mechanism involved behind the effects of thymol on HL-60 cells (Pathania et al., 2013).

It was observed by Bouhtit *et al.* (2021) that at a concentration of 300 μM of carvacrol the KG1 cell lines were more sensitive compared to the HL60 cell line, and at 400 μM the K-562 cell line showed resistance after 48 h of treatment. Regarding thymol (50 μM), the KG1 cell line was also more sensitive when compared to the other two and at the 100 μM dose, thymol was able to induce complete cell death in the KG1 and HL60 cell lines (Bouhtit et al., 2021).

Transformed Cell Lines

When using mouse myoblast cells (CO25 cell line) transformed with human N-RAS oncogene, Zeytinoglu et al. (2003) showed that the concentrations of 1, 5, and 10 μg/mL of carvacrol provoked cytotoxic effects. The same effects were also observed for 5RP7 and CO25 cells transformed by H-RAS and N-RAS oncogenes, respectively, as well as apoptotic morphological changes in both cell lines. However, the fragmentation of internucleosomal DNA and the initial apoptotic determinants were observed only in the cell line 5RP7 cell line. In addition, H-RAS-transformed 5RP7 cells were more sensitive to carvacrol than N-RAS-transformed CO25 cells (Akalin and Incesu, 2011).

Based on these data, we compiled the IC_{50} (μM) values determined 24 h after the incubation of the studied cells with carvacrol or thymol. It was possible to verify that, in general, carvacrol (336.7 ± 35.0, n = 21) is more potent than thymol (527.1 ± 146.6, n = 11), with difference between means of 103.8 (±106.9). The lowest IC_{50} values for carvacrol were against prostate carcinoma (PC-3 IC_{50} = 46.71 μM, Khan et al., 2019; DU 145 IC_{50} = 84.39 μM, Khan et al., 2017) and gastric carcinoma (AGS IC_{50} = 82.57 μM, Günes-Bayir et al., 2018), whereas thymol appears to be more selective for gastric cancer carcinoma (AGS, IC_{50} = 75.63 μM, Günes-Bayir et al., 2018) as seen in **Supplementary Table S2**.

Description of *In Vivo* Studies with Carvacrol and Thymol

Anticarcinogenic effects were observed after treatment with carvacrol in Wistar rats, depicted by a reduction in the incidence of tumors, increased survival rate, and a reduced carcinogenic potency of the substance in inducing malignant tumors (Karkabounas et al., 2006). The pre- and post-treatment with carvacrol in animals with liver cancer induced by diethylnitrosamine (DEN) revealed a decrease in the number of nodules, a final body weight increase and a reduction in liver weight. In fact, carvacrol pre-treatment caused the disappearance of most tumoral foci and nodules, characterized by few neoplastic cells, suggesting a chemopreventive effect. In contrast, post-treatment with carvacrol demonstrated the presence of small persistent nodules, loss of cellular architecture and a lower tendency to spread through the intrahepatic veins. Moreover, carvacrol was able to increase the levels of superoxide dismutase (SOD), catalase (CAT), glutathione peroxidase (GPx), glutathione reductase (GR) and glutathione (GSH), along with a reduction of lipid peroxides and the enzymes AST, ALT, ALP, LDH and γGT in the serum (Jayakumar et al., 2012).

Similarly, Subramaniyan et al. (2014) also evaluated the effect of carvacrol pre- and post-treatment on a DEN-induced hepatocarcinogenesis rat model and observed a stability in tumor marker levels, a reduced mast cell density and inhibition of cell proliferation. Furthermore, supplementation with carvacrol significantly restored the activities of liver microsomal xenobiotic metabolizing enzymes to normal, with a reduced expression of proliferative nuclear cell antigen (PCNA), MMP-2 and -9, and thereby prevented the local spread of carcinogenic cells, showing an antimetastatic effect

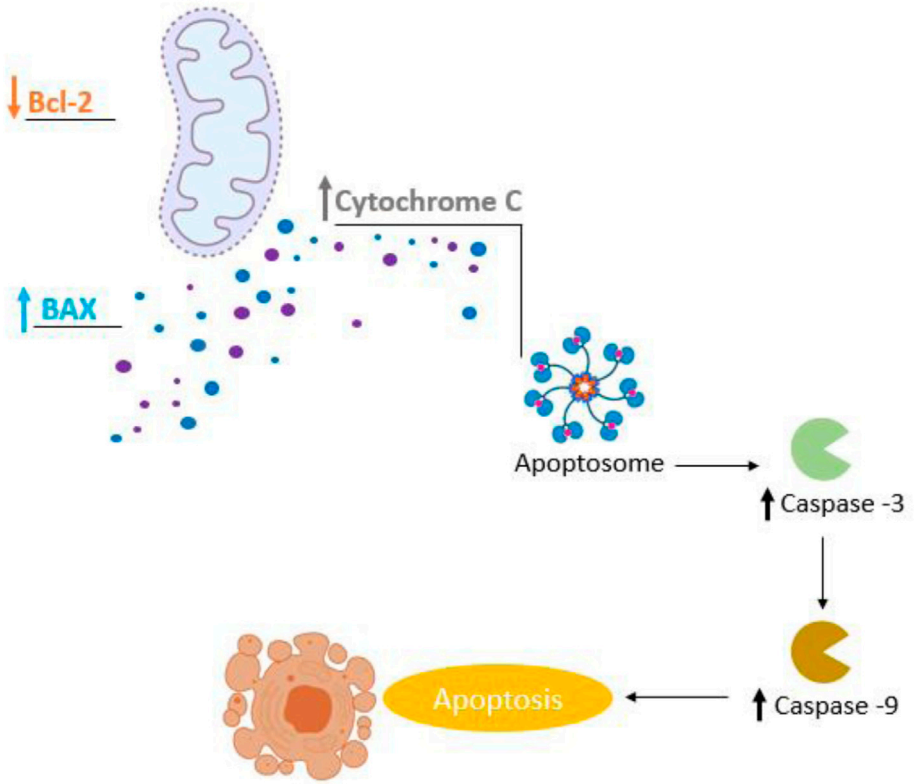

FIGURE 6 | Involvement of apoptosis in carvacrol and thymol treatment in cancer.

(Subramaniyan et al., 2014). Hence, in a rat model of hepatocellular carcinoma induced by diethylnitrosamine (DEN), carvacrol treatment promoted DNA fragmentation indicating its potential as an apoptotic agent. In addition, carvacrol showed a reduction in serum levels of alpha-fetoprotein (AFP), alpha L-fucosidase (AFU), vascular endothelial growth factor (VEGF) and decreased expression of the gamma glutamyl transferase (GGT) gene (Ahmed et al., 2013).

Carvacrol supplementation significantly improved the weight gain and growth rate of animals with colon cancer induced by 1,2-dimethylhydrazine (DMH), exhibiting a lower incidence of tumors and pre-neoplastic lesions, along with a reduction in oxidative stress damage (higher levels of GSH, GPx, GR, SOD and CAT), suggesting that carvacrol presents chemopreventive effects (Sivaranjani et al., 2016).

Li et al. (2019) showed that tumor growth in mice with DEN-induced hepatocarcinoma and treated with carvacrol was limited, revealing tumor cell reduction, rare mitotic figures, normal arrangement of cells, few microvessels, a central necrotic area on tumor tissue and a reduction of intrastromal and peritumor lymphocytes. Likewise, there was an increased expression of the death-associated protein kinase 1 (DAPK1) and decreased expression of serine/threonine-protein phosphatase 2A (PPP2R2A) in tumor tissues (Li et al., 2019). More recently, Rojas-Armas et al. (2020) showed a better effect of carvacrol at a dose of 100 mg/kg/day compared to the other doses tested (50 and 200 mg/kg/day) in female Holztman rats with breast cancer induced by 7,12-dimethylbenzanthracene (DMBA), showing a reduction of 4 (of 16) tumors, in addition to a 75% reduction in the frequency of tumors, a 67% reduction in incidence, an increase in tumor latency and a reduction in the average tumor volume and cumulative tumor volume (Rojas-Armas et al., 2020).

De La Chapa et al. (2018), after treating female athymic nude mice injected with tongue squamous cell carcinoma (Cal27 cell line) and cervical cancer (HeLa cell line), reported a significant inhibition of tumor growth and volume, besides a significant reduction in the number of proliferative cells, with thymol increasing the quantity of apoptotic cells. In a later study, Zeng et al. (2020) established two *in vivo* models to investigate the effect of thymol on cancer progression. For the colorectal cancer model, HCT116 xenograft was injected (i.p.) into BALB/c mice, which after 7–10 days (when the tumors grew to approximately 100 mm^3) were treated with thymol (75 or 150 mg/kg every other day). A significant reduction in cancer growth, a greater number of necrotic lesions and a lower level of Ki-67 expression were observed, which reflects cell proliferation. As for the lung metastasis model, HCT116 cells were injected into the tail vein of each mouse and then received treatment with thymol (75 or 150 mg/kg every other day). After 6 weeks, they found that the average number of tumor nodules on the lung surface of the two treatment groups was significantly lower, revealing an anti-metastatic effect, probably due to the

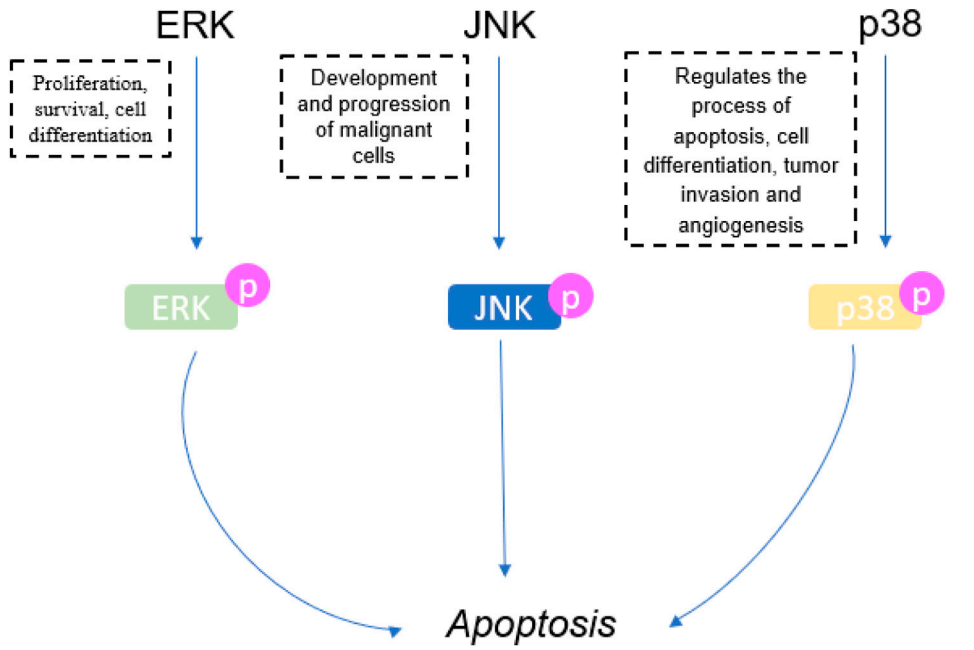

FIGURE 7 | Involvement of the MAPK pathway in carvacrol and thymol treatment in cancer.

inhibition of the Wnt/β-catenin signaling pathway (Zeng et al., 2020).

It was revealed in the study by Hassan et al. (2021) that the administration of thymol (20 mg/kg/day, p. o.) in male Wistar rats provided promising protective activity against colon cancer by significantly reducing elevated serum levels of colon-related tumor markers, carbohydrate antigen 19-9 (CA 19-9) and carcinoembryonic antigen (CEA), as well as the apoptotic marker, caspase-3 compared to the colon cancer group. In addition, it promoted the reduction of oxidative stress by increasing the enzymatic antioxidants SOD, CAT, GSH and GST, inhibiting inflammation by decreasing TNF-α, NF-κB and IL-6 (Hassan et al., 2021). **Figure 2** shows a summary of the main effects observed in the *in vivo* studies.

Risk of Bias and Quality of Included Studies

Almost all studies did not present enough data to allow the judgment of the domains related to the generation of the random sequence, concealment of the allocation, blinding of the researchers and evaluators of the results. Only 4.3% (n = 3) of the studies recorded reported randomness when taking photos of selected areas regarding apoptotic activity assays. However, 97% of the studies applied the same conditions (temperature and incubation time, and purity, stability) for *in vitro* assays, ensuring a low risk of bias (**Figure 3**).

Similarly, most of the SYRCLE tool domains for animal studies (random sequence generation; baseline characteristics; allocation concealment; blinding of caregivers and researchers; random evaluation of results; blinding of the results evaluator) were classified as uncertain due to the lack of information in the articles. In contrast, 30% (n = 3) record random allocation of the animals in the study (**Figure 4**).

DISCUSSION

Through the scientific evidence compiled in this systematic review, it was possible to verify the preventive and therapeutic effects of carvacrol and thymol in cancer in addition to the antimetastatic activity that these compounds were able to exert due to their cytotoxic and antiproliferative effects. Most studies have demonstrated the effect of these compounds on carcinomas, as they are one of the most common types of cancer (Neville, 2011).

Medicinal plants and their bioactive compounds have been an important source of recent drug discoveries (Van Wyk and Wink, 2018). Our review identified a considerable number of reports (77 studies) published in the last two decades, with an increasing trend over recent years. In fact, phytochemicals have great pharmaceutical significance due to their diverse structures (with more than 100,000 being described so far) and their pharmacological properties (Srivastav et al., 2020), and have already made an important contribution to cancer treatments (Ashraf, 2020). Our review also showed that carvacrol and its thymol isomer are capable of restraining growth and combating different tumor strains *in vitro*.

In Asia, the continent with the largest number of publications on the subject, the use of traditional, popular medicine continues to grow (De Boer and Cotingting, 2014) due to the low costs, easy access, the frequent reduced side effects and toxicity, and their

better biodegradable properties (Soković et al., 2013). This is often reinforced by difficulties in accessing health services and obtaining essential medicines (WHO, 2007-2017; Ozawa et al., 2019). Moreover, India and China have, historically, made important contributions to knowledge about medicinal plants, being responsible for some of the most ancient reports about this issue, that were written approximately 5,000 and 4,000 years ago, respectively (Wiart, 2007; Kelly, 2009).

Neoplasia can be described as a disease of unchecked cell division, and its progression is related to abnormal activity of cell cycle regulators. The cell cycle consists of four discrete phases in which the cell increases in size and cellular content is duplicated (gap 1 or G1 phase), DNA is replicated (synthesis, or S phase), it prepares to divide (gap 2, or G2 phase), and then divides, creating two identical daughter cells (mitosis, or M phase). As a cell moves through each phase, stimulated by growth and transcription factors, it passes through several checkpoints, which ensure that mitosis occurs only when the cellular genome has been precisely replicated, avoiding mutations and generation of transformed cells (Hamilton and Infante, 2016; Ingham and Schwartz, 2017). The cell cycle is controlled mainly by cyclin-dependent kinases (CDKs) (Ingham and Schwartz, 2017) CDK4/6 are the kinases responsible for the inactivation/phosphorylation of retinoblastoma protein, at the G1/S phase transition checkpoint. In this review, it was noted that three *in vitro* studies (4.4%) reported that carvacrol decreased CDK4 protein expression in human tongue squamous cell carcinoma (Tca-8113 cells) (Dai et al., 2016) and in breast cancer (MCF-7 cells) (Mari et al., 2020; Li et al., 2021) and only one (1.4%) reported a decrease in CDK6 in MCF-7 cells (Mari et al., 2020). CDK inhibitor drugs are being used in some cancer types (Mari et al., 2020), such as acute myeloid leukemia (Lee and Zeidner, 2019) and breast cancer (Pernas et al., 2018). In addition, cell cycle arrest, reported in 14.7% (n = 10) of *in vitro* studies also represents a promising target of cancer treatment, since natural compounds can act as modulators, interrupting the cell cycle and, therefore, killing cancer cells (Bailon-Moscoso et al., 2017). The uncontrolled proliferation of cancer cells occurs due to their ability to prevent programmed cell death (apoptosis) (Olsson and Zhivotovsky, 2011; Dabrowska et al., 2016; Kim and Kim, 2018), that is responsible for eliminating aberrant proliferating cells or those with DNA damage/mutations (Dabrowska et al., 2016) (**Figure 5**). In this review, 55% (n = 38) of the studies reported induction of apoptosis after treatment with carvacrol or thymol in their *in vitro* studies and only 40% (n = 4) in *in vivo* studies.

The tumor suppressor TP53 gene, also called "the guardian of the genome", is activated in response to stress signals (DNA damage) and can interrupt DNA replication and cell division through cell cycle arrest (G1/S checkpoint), in order to restore genetic integrity, thereby preventing genetically transformed cell proliferation (Harris and Levine, 2005; Belyi et al., 2010; Georgakilas et al., 2017). When repair is not possible, p53 causes programmed cell death, interacting with the Bcl-2 family of proteins, triggering genes involved in apoptosis, such as Bax (Gottlieb and Oren, 1998; Song et al., 2014). In addition, evidence indicates that when there is a deficiency of p53, the p21 gene can act as an oncogenic factor, causing the cell cycle to be interrupted (Georgakilas et al., 2017). Treatment with carvacrol increased p53 expression in breast cancer (Al-Fatlawi and Ahmad, 2014), cervical and liver cancer cells (Abbas and Al-Fatlawi, 2018). Meanwhile, administration of thymol increased p21expression in bladder cancer cells (Li et al., 2017) and increased expression of both p53 and p21 in breast cancer cells (Seresht et al., 2019). In fact, TP53 genetic alterations are commonly observed in clinical tumor samples, since most mutations lead to function loss, in which cells can escape the destruction and repair process, resulting in a malignant transformation through favorable natural selection (Olsson and Zhivotovsky, 2011).

During cancer, overexpression of anti-apoptotic genes and under expression of pro-apoptotic genes can lead to the failure of the programmed cell death mechanism (Olsson and Zhivotovsky, 2011; Zhang et al., 2000). The expression of proapoptotic proteins, such as Bax (Li et al., 2017; Basu and Haldar, 1998), is an important mechanism of tumor regression (Backus et al., 2002). It triggers apoptosis by forming pores within the outer mitochondrial membrane, releasing cytochrome C that activates proteases such as caspase-9 and -3, that dismantle and destroy the cell (apoptosis) (Olsson and Zhivotovsky, 2011). Our results showed that 24.6% of *in vitro* studies (n = 17) and 10% of *in vivo* studies showed an increase in Bax levels after treatment with carvacrol or thymol. Additionally, 26% (n = 18) of *in vitro* studies reported negative regulation of the anti-apoptotic protein Bcl-2 (Swanton et al., 1999; Kroemer et al., 1998). Caspases are central apoptosis regulators and executors, and thus attractive targets for the development of therapeutic strategies for cancer treatment (Ghavami et al., 2009; Hensley et al., 2013; Fiandalo and Kyprianou, 2012; Shalini et al., 2015). Hence, positive expression of caspases increases tumor sensitization to treatment (Hensley et al., 2013) (**Figure 6**). In this review, 33.3% (n = 23) of *in vitro* studies reported an increase of caspase activity, more specifically caspase-3 (Deb et al., 2011; Liang and Lu, 2012; Yin et al., 2012; Ferraz et al., 2013; Liang et al., 2013; Al-Fatlawi and Ahmad, 2014; Chen et al., 2015; Bhakkiyalakshmi et al., 2016; Khan et al., 2017; Li et al., 2017; Abbas and Al-Fatlawi, 2018; Chauhan et al., 2018; Günes-Bayir et al., 2018; Günes-Bayir et al., 2018; Tayarani-Najaran et al., 2019), -6 (Al-Fatlawi and Ahmad, 2014; Abbas and Al-Fatlawi, 2018), -7 (Kang et al., 2016), -8 (Deb et al., 2011; Pathania et al., 2013; Kang et al., 2016; Khan et al., 2019) and -9 (Deb et al., 2011; Pathania et al., 2013; Al-Fatlawi and Ahmad, 2014; Kang et al., 2016; Li et al., 2017; Abbas and Al-Fatlawi, 2018; Günes-Bayir et al., 2018; Günes-Bayir et al., 2018; Potočnjak et al., 2018; Khan et al., 2019). It is noteworthy that the positive regulation of caspase-3 propagates and amplifies the apoptosis signal, and its loss of expression promotes tumorigenesis (Fiandalo and Kyprianou, 2012). Shalini et al. (2015) reported that high caspase-3 expression caused apoptosis of tumor cells, and is significantly associated with better prognosis in patients with non-small cell lung cancer (Yoo et al., 2004) and hepatocellular carcinomas (Huang et al., 2010). However, there is very little knowledge about the role of caspases-6 and -7 during cancer (Ghavami et al., 2009). In this review, caspase-6 and -7 expression was reported in only three studies. Overexpression of caspase-8

has been reported in prostate cancer cells treated with carvacrol (Khan et al., 2019) and in studies that tested thymol on promyelocytic leukemia (Deb et al., 2011; Pathania et al., 2013) and gastric cancer (Kang et al., 2016). The literature reveals that the activation of caspase-8 plays an important role in the initiation phase of apoptosis (Soung et al., 2005), as well as in suppressing oncogenic transformation, confirmed by an increased susceptibility to spontaneous mutations in its absence (Olsson and Zhivotovsky, 2011). Krelin et al. (2018) reported that caspase-8 deficient cells exhibit resistance to death, facilitating tumorigenic transformation (Krelin et al., 2008). The expression of caspase-9 was the second most reported in this review, due to its crucial role in apoptosis initiation among various types of cancer (Kim et al., 2015). Previous studies have reported that caspase-9 regulates the apoptosis process of cancer cells through interactions with signaling molecules (Bou-Hanna et al., 2015; Thakor et al., 2017). Natural compounds can regulate caspase-9 expression, and, therefore, favor apoptosis in cancer (Kim et al., 2015). Pre-treatment with caspase inhibitors caused a significant reduction in cytotoxicity and attenuation of apoptosis induced by carvacrol, observed in prostate cancer cells (Khan et al., 2019).

Another very important cell cycle regulator is MAPK. It controls cell growth, proliferation, differentiation and apoptosis, and represents one of the main signaling pathways involved in extracellular signals transduction (Binétruy et al., 2007; Kim and Choi, 2015; Li et al., 2018). In particular, JNK, ERK and p38 are the main proteins of MAPK pathways when approaching cancer. ERK is generally associated with cell proliferation, while JNK and p38 are closely related to the cell death process (Wagner and Nebreda, 2009). JNK is proven to be related to the development and progression of malignant cells (Wu et al., 2019). In this review, 5.7% (n = 4) of the studies that tested carvacrol or thymol showed that they were able to increase *in vitro* JNK phosphorylation in colon cancer (Fan et al., 2015; Chauhan et al., 2018), choriocarcinoma (Lim et al., 2019) and bladder cancer (Li et al., 2017). Studies showed that phosphorylation/activation of p38, MAPK and JNK contributes to cancer cell apoptosis (Liu et al., 2014; Wang et al., 2014) and that the p38 regulates apoptosis process, cycle growth progression and cell differentiation (Zarubin and Han, 2005; Krens et al., 2006). P38 can also directly affect tumor invasion and angiogenesis (Wagner and Nebreda, 2009). Herein, 4.3% (n = 3) of the studies *in vitro* induced phosphorylation of p38 in hepatocarcinoma cells (Yin et al., 2012), cancer bladder cells (Li et al., 2017) and choriocarcinoma cell (Lim et al., 2019). In fact, Li et al., (2017) suggested that the activation of JNK and p38 were pivotal to the cytotoxicity exhibited by thymol against cancer cells. In addition, the level of phosphorylated ERK decreased in hepatocarcinoma, colon cancer, choriocarcinoma and prostate cancer cells, after treatment with carvacrol, and p-ERK1/2 levels decreased after thymol treatment in glioma cells (Yin et al., 2012; Fan et al., 2015; Heidarian and Keloushadi, 2019; Lim et al., 2019). This corroborated the findings of Wang et al. (2018) who reported that patients with tumors with low p-ERK (activated form) had a higher survival rate (Low and Zhang, 2016) (**Figure 7**).

The PI3K/AKT/mTOR signaling pathway is also studied in cancer since it regulates cell proliferation, growth, metabolism and motility (Song et al., 2019; O'Donnell et al., 2018). Its inhibition induces a pronounced anticancer activity (Li et al., 2016). In addition, some inhibitors of this signaling pathway have already been approved by the Food and Drug Administration for cancer treatment (Alzahrani, 2019). PI3k belongs to a family of lipid kinases, involved in extracellular signals transduction and cell growth promotion (Wullschleger et al., 2006; Alzahrani, 2019). AKT, also known as protein kinase B (PKB), is an oncogenic protein that regulates cell survival, proliferation, growth, apoptosis and glycogen metabolism (Alzahrani, 2019; Song et al., 2019). Excessive activation of mTOR (mammalian target of rapamycin), a serine/threonine kinase, is associated with the activation of hypoxia inducible factor (HIF) that regulates angiogenesis and tumor growth (Semenza, 2003). Its inhibition was identified by 2.8% (n = 2) of *in vitro* studies using thymol in human promyelocytic leukemia cell lines (Pathania et al., 2013) and bladder cancer cells (Li et al., 2017), and by 7.2% (n = 5) of *in vitro* studies that used carvacrol in colon cancer (Fan et al., 2015), glioblastoma (Chen et al., 2015), prostate cancer (Luo et al., 2016), choriocarcinoma (Lim et al., 2019) and breast cancer cells (Mari et al., 2020).

The mechanism of action reported in *in vivo* studies involves slightly more complex processes. Starting with Ahmed et al. (2013), the only authors of this review who reported in *in vivo* models a reduction in serum levels of AFP, AFU, VEGF and reduced GGT gene expression after treatment with carvacrol. The literature reveals that AFP, besides being one of the most useful biomarkers for the detection of hepatocellular carcinoma, also serves to monitor the response to anticancer therapy (high levels indicate tumor progression) (Bei and Mizejewski, 2011; Wong et al., 2015; Wang and Wang, 2018). On the other hand, AFU indicates clinical prognosis of several malignant tumors and helps to diagnose primary hepatocarcinoma (Giardina et al., 1992), colorectal cancer (Ayude et al., 2000), ovarian cancer (Abdel-Aleem et al., 1996), and was recently identified as an effective new biomarker for squamous cell carcinoma of the early esophagus (Yu et al., 2019). In addition, high levels of GGT influence proliferation and apoptosis and contribute to tumor progression (Koss and Greengard, 1982; Pompella et al., 2006; Zhang et al., 2006) serving as a biomarker in various types of cancer (Paolicchi et al., 1996; Whitfield, 2001; Pompella et al., 2006). The increased expression of VEGF during cancer, along with other pro-angiogenic factors, is responsible for new vascularization, representing a strategic point in the treatment (Collins and Hurwitz, 2005; Riaz et al., 2015; Siveen et al., 2017). The decrease in serum levels of these biomarkers in animals treated with carvacrol may prove to be an important antitumor characteristic that deserves attention and further studies to elucidate this mechanism (Ahmed et al., 2013). Together with VEGF, other enzymes collaborate for neoplastic invasion, such as mitochondrial membrane potential. They are matrix degradation enzymes (such as MMP), responsible for the degradation of the main constituents of basement membrane and extracellular matrix, facilitating the invasion of tumor cells and favoring the spread of cancer cells and metastases (Nagase et al., 2006; Shuman Moss et al., 2012; Jabłońska-Trypuć et al., 2016). High MMP-2 and -9 levels were associated with esophageal carcinomas

(Koyama et al., 1990) and breast (Alrehaili et al., 2020), oral (Lin et al., 2004), bladder (Fouad et al., 2019), skin (Fundyler et al., 2004), larynx (Liu et al., 2005) cancer. In this systematic review, only one *in vivo* study (10%) reported a decrease in the levels of MMP-2 and MMP-9 in liver cancer after treatment with carvacrol (Subramaniyan et al., 2014), the majority 8.6% (n = 6) were *in vitro* studies. It is important to note that carvacrol prevented metastasis *in vivo*, demonstrated by tumors less likely to spread through intrahepatic veins (Jayakumar et al., 2012) and preventing local spread of cancer cells by suppressing the expression of MMP-2 and MMP-9 proteins (Subramaniyan et al., 2014), and thymol decreased the number of lung metastatic lesions *in vivo*, suppressing the Wnt/β-catenin signaling pathway (Zeng et al., 2020). However, there is almost nothing about this topic documented in the literature, and further studies are required to address this outcome.

Considering reactive oxygen species (ROS), these are a group of molecules that contain reduced forms of oxygen with short life and that are more energetically reactive than molecular oxygen (Srinivas et al., 2019). The generation of ROS inside the cell contributes to the antitumor process in order to induce DNA damage and slow the progression of the cell cycle, preventing cells with DNA damage (cancer cells) from continuing with cell division (Allawzi et al., 2019; Srinivas et al., 2019). *In vitro*, carvacrol and thymol increased the generation of reactive oxygen species in 24.63% (n = 17) of the studies, a fact that is also observed in chemotherapeutics such as doxorubicin (Conklin, 2004), cisplatin (Marullo et al., 2013) and bleomycin (Allawzi et al., 2019), which also increase ROS levels. Regarding *in vivo* studies, the pretreatment with carvacrol in colon cancer (Sivaranjani et al., 2016) and hepatocellular carcinoma (Jayakumar et al., 2012) increased the levels of enzymatic antioxidants such as GPx, SOD, CAT, GR, and GSH, revealing a chemopreventive effect of carvacrol and prevention of cell proliferation (Jayakumar et al., 2012; Sivaranjani et al., 2016). Similarly, thymol had a promising protective efficacy, revealing a chemopreventive effect against colon cancer observed by the increase in GST, GSH, SOD and CAT levels, in addition to inhibiting oxidative stress (Hassan et al., 2021). However, these results should be interpreted with caution, as low levels of ROS can be beneficial in preventing the development of cancer cells, since they can promote cancer (Prasad et al., 2017). In this sense, anticancer therapies can follow two paths; using compounds that prevent the formation of ROS, and thereby preventing carcinogenesis; or using compounds that have as their action mechanism the increase of ROS, promoting oxidative stress within the tumor (de Sá Junior et al., 2017). Further studies are needed to clarify this issue.

Post-treatment with carvacrol also promoted an increase in the expression of the DAPK1 gene and a decrease in the enzyme PPP2R2A (Li et al., 2019). DAPK1 is a serine/threonine kinase, a tumor suppressor protein that promotes apoptosis (Agodi et al., 2015; Zhai et al., 2019), while PPP2R2A, a regulatory subunit of protein phosphatase 2A (PP2A), controls the pathway of AKT signaling associated with tumor growth (Wang et al., 2016; Zeng et al., 2016). In fact, both may be involved in a possible antitumor mechanism of carvacrol, but it is still not very clear, requiring further studies (Li et al., 2019).

Through *in vitro* studies, we found that carvacrol proves to be more potent than thymol, and appears to have a greater cytotoxic effect for some cell lines, such as carcinomas (prostate and stomach) (Khan et al., 2017; Günes-Bayir et al., 2018; Khan et al., 2019). Thymol seems to act more against gastric cancer carcinoma (AGS, IC_{50} = 75.63 μM, Günes-Bayir et al., 2018). In fact, two recent studies published by Sisto et al. (2020) and Sisto et al. (2021) demonstrated the potential of these monoterpenes in the control of gastric carcinoma by reducing the viability of AGC cells.

In *in vivo* studies, on the other hand, the effect of carvacrol has been predominantly studied against hepatocarcinoma, with few studies for breast and colon cancer. In a way, it can be seen that the studies in this area do not seem to evolve toward a specific target, with low complementarity of the screenings carried out *in vitro* for the studies developed with experimental animals. This is a great barrier advances in this area of knowledge and helps to explain the discrepancy in the number of studies published *in vitro* (n = 69) and *in vivo* (n = 10) over the last two decades, as well as the absence of clinical trials. Thus, it is necessary to consider the studies already carried out for these compounds before conducting new primary studies on this topic, in order to evolve the research stages to the next level of drug development: *in vivo* studies and clinical trials.

As for security, some studies have suggested that normal cells tolerate exposure to carvacrol (Koparal and Zeytinoglu, 2003; Yin et al., 2012; Khan et al., 2017; Lim et al., 2019) and thymol (Deb et al., 2011; Ferraz et al., 2013; Chauhan et al., 2018; Balan et al., 2021) in different concentration ranges well. However, some studies have demonstrated the action of these compounds, in a negative way, in some normal cells, such as human fibroblast cells (WS-1; IC_{50} of 138.1 ± 8.7 μM of carvacrol (Günes-Bayir et al., 2018); breast epithelial cells (fR2; IC_{50} of 86 μg/mL of thymol; (Pathania et al., 2013), normal lymphocyte (PBMC; IC_{50} > 25 μg/ml of thymol; (Ferraz et al., 2013); rat embryonic fibroblasts (mild toxicity of 20.94% after thymol 5, 30.5, 61, 122, 244 ng/mL; (Abed, 2011). Moreover, it has been shown that at concentrations of 0.5% (v/v) carvacrol and thymol exhibited a proliferative effect on normal human PBMC cells (Jaafari et al., 2007), and a lower concentration (10 μM) of carvacrol also caused a statistically significant proliferation of WS-1 cells (Günes-Bayir et al., 2018). In their most recent study, Günes-Bayir et al. (2020) reported that high doses of thymol can act on cancerous and healthy cells, while low doses seem to protect healthy cells but harm cancer cells. Moreover, genotoxic effects have been shown to be exhibited by carvacrol (Günes-Bayir et al., 2018) and thymol (Günes-Bayir et al., 2018), and it was also shown that a high concentration of carvacrol (460 μM) exhibited mutagenic and genotoxic effects causing DNA damage (Llana-Ruiz-Cabello et al., 2015). *In vivo*, Suntres et al. (2015) reported that the average lethal dose of carvacrol after intravenous administration in dogs was 310 mg/kg, for rats it was 810 mg/kg when administered orally and 80 and 73 mg/kg when injected intravenously or intraperitoneally, respectively. In mice, the lethal dose was 110–233.3 mg/kg, after inducing ataxia and drowsiness (Suntres et al., 2015). However, a phase I randomized clinical trial conducted in healthy subjects treated with carvacrol (1 or 2 mg/kg daily, p.o., during one month)

revealed that this monoterpene did not lead to clinically significant changes, and did not cause any adverse effects, showing clinical safety and tolerability for this agent (Ghorani et al., 2021). Thus, the dose-response relationship must be considered in more detail, so that further studies in more advanced stages are developed to assess the antitumor effects of these compounds.

The methodological quality of the studies included revealed many items classified as "unclear" or "uncertain" indicating that the report—and presumably the experimental design—of these studies can be improved, especially with regard to the generation of the random sequence, the concealment of allocation and the blinding of researchers and evaluators, important factors in respect of a reliable result. Therefore, future studies need to improve their methodological quality, particularly in respect of risk of bias, in order to produce more reliable results. Even after almost two decades of research in this field, there has been no progress in research in humans, possibly due limitations of preclinical studies and the lack of knowledge about pharmacokinetics and toxicity of carvacrol and thymol. These factors limit the introduction of these compounds as a therapeutic option, and highlight the new for innovative studies to be undertaken.

Seven studies used a positive control to compare the antitumor effect of carvacrol (Jaafari et al., 2007; Maryam et al., 2015; Tayarani-Najaran et al., 2019) and/or thymol (Deb et al., 2011; Ferraz et al., 2013; Kang et al., 2016; Zeng et al., 2020) in their studies. *In vitro*, methotrexate and vincristine (0.5 μg/100 μL) (Jaafari et al., 2007), 5-fluorouracil (5-FU) (2.6 μg/μM) (Maryam et al., 2015), doxorubicin (0.5, 5, 10, and 20 μg/mL) (Tayarani-Najaran et al., 2019) (1.0 μg/mL) (Ferraz et al., 2013) and (2 μM) (Kang et al., 2016), camptothecin (5 μM) (Deb et al., 2011) and *in vivo*, doxorubicin (2 mg/kg) (Zeng et al., 2020), were the main substances used to compare the potential therapeutic effect of these monoterpenes. We emphasize here the importance of using a standard substance as a positive control as a parameter for comparing the effect of new candidates for cancer treatment.

In summary, we observed that more *in vivo* studies, particularly in respect of thymol, are needed. Further studies are required to help unravel and define the mechanisms of action of the two compounds against cancer cells, as well as studies that further explore their chemopreventive and anti-metastatic effects. It is of note that several studies suggested that signaling pathways (PI3K/AKT/mTOR and MAPKs) may be the main mechanism of action of these monoterpenoids, but more advanced studies are needed to elucidate this issue. There is also still a wide variation in the doses used, requiring the establishment of a consensus in respect of defining potentially effective and safe doses. In addition, further studies are also needed to clarify the effects of these two compounds on normal/healthy cells *in vitro,* and in appropriate *in vivo* models.

CONCLUSION

The knowledge obtained through the reviewed studies provides strong evidence of the antitumor and antiproliferative activity promoted by carvacrol and thymol. However, there are still gaps regarding the standard or ideal dose, the exact mechanism of action and safety of the two compounds, revealing challenges for future studies. In addition, it was found through *in vitro* studies that carvacrol seems more potent than thymol, and was shown to have a greater cytotoxic effect for some cell lines. Moreover, further animal studies should be encouraged, as they have as yet made limited progress, and most of the current results are based on *in vitro* studies.

DATA AVAILABILITY STATEMENT

The original contributions presented in the study are included in the article/**Supplementary Material**, further inquiries can be directed to the corresponding author.

AUTHOR CONTRIBUTIONS

Conception and design: AG, DT, and LS. Data acquisition: LS and LP. Analysis and interpretation of data: LS and LP. Elaboration of the manuscript: LS. Review of intellectual content: MS, AG, and DT. Final approval of the completed manuscript: AG and DT.

FUNDING

Financial support was provided by the Fundação de Apoio à Pesquisa e Inovação Tecnológica do Estado de Sergipe (FAPITEC/SE), the Conselho Nacional de Desenvolvimento Científico e Tecnológico (CNPq/Brazil), the Coordenação de Aperfeiçoamento de Pessoal de Nível Superior (CAPES/Brazil) and Federal University of Sergipe.

SUPPLEMENTARY MATERIAL

The Supplementary Material for this article can be found online at: https://www.frontiersin.org/articles/10.3389/fphar.2021.702487/full#supplementary-material

REFERENCES

Abbas, A., and Al-Fatlawi, A. (2018). Anti-proliferative and Pro-apoptotic Activity of Carvacrol on Human Cancer Cells. *Int. J. Pharm. Res.* 10 (2), 174–180. doi:10.3892/or.2012.1877

Abdel-Aleem, H., Ahmed, A., Sabra, A. M., Zakhari, M., Soliman, M., and Hamed, H. (1996). Serum Alphal-Fucosidase Enzyme Activity in Ovarian and Other Female Genital Tract Tumors. *Int. J. Gynecol. Obstet.* 55 (3), 273–279. doi:10.1016/s0020-7292(96)02770-1

Abed, R. (2011). Cytotoxic, Cytogenetics and Immunomodulatory Effects of Thymol from *Thymus Vulgaris* on Cancer and Normal Cell Lines *In Vitro* and *In Vivo*. *Al-mustansiriyah J. Sci.* 22 (5), 41–53. doi:10.3403/30303631

Agodi, A., Barchitta, M., Quattrocchi, A., Maugeri, A., and Vinciguerra, M. (2015). DAPK1 Promoter Methylation and Cervical Cancer Risk: A Systematic Review

and a Meta-Analysis. *PLoS ONE* 10 (8), e0135078. doi:10.1371/journal.pone.0135078

Ahmed, H., Shousha, W., El-Mezayen, H., Ismaiel, N., and Mahmoud, N. (2013). *In Vivo* antitumor Potential of Carvacrol against Hepatocellular Carcinoma in Rat Model. *World J. Pharm. Pharm. Sci.* 2 (5), 2367–2396. doi:10.3748/wjg.v8.i3.464

Akalin, G., and Incesu, Z. (2011). The Effect of Carvacrol on Apoptosis of H-RAS and N-RAS Transformed Cell Lines. *Turk J. Pharm. Sci.* 8 (2), 105–116. doi:10.1007/978-1-4757-1235-3_13

Al-Fatlawi, A., and Ahmad, A. (2014). Cytotoxicity and Pro-apoptotic Activity of Carvacrol on Human Breast Cancer Cell Line MCF-7. *World J. Pharm. Sci.* 2 (10), 1218–1223. doi:10.3923/pjbs.2021.646.655

Allawzi, A., Elajaili, H., Redente, E. F., and Nozik-Grayck, E. (2019). Oxidative Toxicology of Bleomycin: Role of the Extracellular Redox Environment. *Curr. Opin. Toxicol.* 13 (13), 68–73. doi:10.1016/j.cotox.2018.08.001

Alrehaili, A. A., Gharib, A. F., Karam, R. A., Alhakami, R. A., El Sawy, W. H., and Abd Elrahman, T. M. (2020). Clinical Significance of Plasma MMP-2 and MMP-9 Levels as Biomarkers for Tumor Expression in Breast Cancer Patients in Egypt. *Mol. Biol. Rep.* 47 (2), 1153–1160. doi:10.1007/s11033-019-05216-5

Alzahrani, A. S. (2019). PI3K/Akt/mTOR Inhibitors in Cancer: At the Bench and Bedside. *Semin. Cancer Biol.* 59, 125–132. doi:10.1016/j.semcancer.2019.07.009

Arigesavan, K., and Sudhandiran, G. (2015). Carvacrol Exhibits Anti-oxidant and Anti-inflammatory Effects against 1, 2-dimethyl Hydrazine Plus Dextran Sodium Sulfate Induced Inflammation Associated Carcinogenicity in the colon of Fischer 344 Rats. *Biochem. Biophysical Res. Commun.* 461 (2), 314–320. doi:10.1016/j.bbrc.2015.04.030

Arunasree, K. M. (2010). Anti-proliferative Effects of Carvacrol on a Human Metastatic Breast Cancer Cell Line, MDA-MB 231. *Phytomedicine* 17 (8–9), 581–588. doi:10.1016/j.phymed.2009.12.008

Arya, R., and Saldanha, S. N. (2019). "Dietary Phytochemicals, Epigenetics, and Colon Cancer Chemoprevention," in *Epigenetics of Cancer Prevention*. Editors A. Bishayee and D. Bhatia (Cambridge: Academic Press), 205–229. doi:10.1016/B978-0-12-812494-9.00010-X

Ashraf, M. A. (2020). Phytochemicals as Potential Anticancer Drugs: Time to Ponder Nature's Bounty. *Biomed. Res. Int.* 2020, e8602879. doi:10.1155/2020/8602879

Asif, M. (2015). Role of Fruit and Vegetable in the Treatment of Cancer. *Curr. Sci. Perspect.* 1 (1), 33–40. doi:10.1533/9781845694296.4.272

Aydın, E., Türkez, H., and Keleş, M. S. (2014). The Effect of Carvacrol on Healthy Neurons and N2a Cancer Cells: Some Biochemical, Anticancerogenicity and Genotoxicity Studies. *Cytotechnology* 66 (1), 149–157. doi:10.1007/s10616-013-9547-5

Ayude, D., Fernández-Rodríguez, J., Rodríguez-Berrocal, F. J., Martínez-Zorzano, V. S., De Carlos, A., Gil, E., et al. (2000). Value of the Serum Alpha-L-Fucosidase Activity in the Diagnosis of Colorectal Cancer. *Oncology* 59 (4), 310–316. doi:10.1159/000012188

Backus, H. H. J., Van Groeningen, C. J., Vos, W., Dukers, D. F., Bloemena, E., Wouters, D., et al. (2002). Differential Expression of Cell Cycle and Apoptosis Related Proteins in Colorectal Mucosa, Primary colon Tumours, and Liver Metastases. *J. Clin. Pathol.* 55 (3), 206–211. doi:10.1136/jcp.55.3.206

Bailon-Moscoso, N., Cevallos-Solorzano, G., Romero-Benavides, J., and Ramirez Orellana, M. (2017). Natural Compounds as Modulators of Cell Cycle Arrest: Application for Anticancer Chemotherapies. *Curr. Genomics* 18 (2), 106–131. doi:10.2174/1389202917666160808125645

Baj, T., Biernasiuk, A., Wróbel, R., and Malm, A. (2020). Chemical Composition and *In Vitro* Activity of *Origanum Vulgare* L., Satureja Hortensis L., Thymus Serpyllum L. And *Thymus Vulgaris* L. Essential Oils towards Oral Isolates of Candida Albicans and Candida Glabrata. *Open Chem.* 18 (1), 108–118. doi:10.1515/chem-2020-0011

Balan, D. J., Rajavel, T., Das, M., Sathya, S., Jeyakumar, M., and Devi, K. P. (2021). Thymol Induces Mitochondrial Pathway-Mediated Apoptosis via ROS Generation, Macromolecular Damage and SOD Diminution in A549 Cells. *Pharmacol. Rep.* 73 (1), 240–254. doi:10.1007/s43440-020-00171-6

Baranauskaite, J., Kubiliene, A., Marksa, M., Petrikaite, V., Vitkevičius, K., Baranauskas, A., et al. (2017). The Influence of Different Oregano Species on the Antioxidant Activity Determined Using HPLC Postcolumn DPPH Method and Anticancer Activity of Carvacrol and Rosmarinic Acid. *Biomed. Res. Int.* 2017, 1681392. doi:10.1155/2017/1681392

Basu, A., and Haldar, S. (1998). The Relationship between BcI2, Bax and P53: Consequences for Cell Cycle Progression and Cell Death. *Mol. Hum. Reprod.* 4 (12), 1099–1109. doi:10.1093/molehr/4.12.1099

Bei, R., and Mizejewski, G. J. (2011). Alpha Fetoprotein Is More Than a Hepatocellular Cancer Biomarker: from Spontaneous Immune Response in Cancer Patients to the Development of an AFP-Based Cancer Vaccine. *Curr. Mol. Med.* 11 (7), 564–581. doi:10.2174/156652411800615162

Belyi, V. A., Ak, P., Markert, E., Wang, H., Hu, W., Puzio-Kuter, A., et al. (2010). The Origins and Evolution of the P53 Family of Genes. *Cold Spring Harbor Perspect. Biol.* 2 (6), a001198. doi:10.1101/cshperspect.a001198

Bhakkiyalakshmi, E., Suganya, N., Sireesh, D., Krishnamurthi, K., Saravana Devi, S., Rajaguru, P., et al. (2016). Carvacrol Induces Mitochondria-Mediated Apoptosis in HL-60 Promyelocytic and Jurkat T Lymphoma Cells. *Eur. J. Pharmacol.* 772, 92–98. doi:10.1016/j.ejphar.2015.12.046

Binétruy, B., Heasley, L., Bost, F., Caron, L., and Aouadi, M. (2007). Concise Review: Regulation of Embryonic Stem Cell Lineage Commitment by Mitogen-Activated Protein Kinases. *Stem Cells* 25 (5), 1090–1095. doi:10.1634/stemcells.2006-0612

Bou-Hanna, C., Jarry, A., Lode, L., Schmitz, I., Schulze-Osthoff, K., Kury, S., et al. (2015). Acute Cytotoxicity of MIRA-1/NSC19630, a Mutant P53-Reactivating Small Molecule, against Human normal and Cancer Cells via a Caspase-9-dependent Apoptosis. *Cancer Lett.* 359 (2), 211–217. doi:10.1016/j.canlet.2015.01.014

Bouhtit, F., Najar, M., Moussa Agha, D., Melki, R., Najimi, M., Sadki, K., et al. (2021). New Anti-leukemic Effect of Carvacrol and Thymol Combination through Synergistic Induction of Different Cell Death Pathways. *Molecules* 26 (2), 410. doi:10.3390/molecules26020410

Carqueijeiro, I., Langley, C., Grzech, D., Koudounas, K., Papon, N., O'Connor, S. E., et al. (2020). Beyond the Semi-synthetic Artemisinin: Metabolic Engineering of Plant-Derived Anti-cancer Drugs. *Curr. Opin. Biotechnol.* 65, 17–24. doi:10.1016/j.copbio.2019.11.017

Chamanara, M., Abdollahi, A., Rezayat, S. M., Ghazi-Khansari, M., Dehpour, A., Nassireslami, E., et al. (2019). Thymol Reduces Acetic Acid-Induced Inflammatory Response through Inhibition of NF-kB Signaling Pathway in Rat colon Tissue. *Inflammopharmacol* 27 (6), 1275–1283. doi:10.1007/s10787-019-00583-8

Chan, H., Ho, J., Liu, X., Zhang, L., Wong, S. H., Chan, M., et al. (2017). Potential and Use of Bacterial Small RNAs to Combat Drug Resistance: a Systematic Review. *Infect. Drug Resist.* 10, 521–532. doi:10.2147/IDR.S148444

Chang, H.-T., Hsu, S.-S., Chou, C.-T., Cheng, J.-S., Wang, J.-L., Lin, K.-L., et al. (2011). Effect of Thymol on Ca2+ Homeostasis and Viability in MG63 Human Osteosarcoma Cells. *Pharmacology* 88 (3–4), 201–212. doi:10.1159/000331864

Chauhan, A. K., Bahuguna, A., Paul, S., and Kang, S. C. (2018). Thymol Elicits HCT-116 Colorectal Carcinoma Cell Death through Induction of Oxidative Stress. *Acamc* 17 (14), 1942–1950. doi:10.2174/1871520617666170327121228

Chen, W.-L., Barszczyk, A., Turlova, E., Deurloo, M., Liu, B., Yang, B. B., et al. (2015). Inhibition of TRPM7 by Carvacrol Suppresses Glioblastoma Cell Proliferation, Migration and Invasion. *Oncotarget* 6 (18), 16321–16340. doi:10.18632/oncotarget.3872

Coccimiglio, J., Alipour, M., Jiang, Z.-H., Gottardo, C., and Suntres, Z. (2016). Antioxidant, Antibacterial, and Cytotoxic Activities of the Ethanolic*Origanum vulgare* Extract and its Major Constituents. *Oxidative Med. Cell. longevity* 2016, 1404505. doi:10.1155/2016/1404505

Collins, T. S., and Hurwitz, H. I. (2005). Targeting Vascular Endothelial Growth Factor and Angiogenesis for the Treatment of Colorectal Cancer. *Semin. Oncol.* 32 (1), 61–68. doi:10.1053/j.seminoncol.2004.09.026

Conklin, K. A. (2004). Chemotherapy-associated Oxidative Stress: Impact on Chemotherapeutic Effectiveness. *Integr. Cancer Ther.* 3 (4), 294–300. doi:10.1177/1534735404270335

Dabrowska, C., Li, M., and Fan, Y. (2016). Apoptotic Caspases in Promoting Cancer: Implications from Their Roles in Development and Tissue Homeostasis. *Adv. Exp. Med. Biol.* 930, 89–112. doi:10.1007/978-3-319-39406-0_4

Dai, W., Sun, C., Huang, S., and Zhou, Q. (2016). Carvacrol Suppresses Proliferation and Invasion in Human Oral Squamous Cell Carcinoma. *Onco Targets Ther.* 9, 2297–2304. doi:10.2147/OTT.S98875

De Boer, H. J., and Cotingting, C. (2014). Medicinal Plants for Women's Healthcare in Southeast Asia: A Meta-Analysis of Their Traditional Use,

Chemical Constituents, and Pharmacology. *J. Ethnopharmacology* 151 (2), 747–767. doi:10.1016/j.jep.2013.11.030

De La Chapa, J. J., Singha, P. K., Lee, D. R., and Gonzales, C. B. (2018). Thymol Inhibits Oral Squamous Cell Carcinoma Growth via Mitochondria-Mediated Apoptosis. *J. Oral Pathol. Med.* 47 (7), 674–682. doi:10.1111/jop.12735

de Sá Junior, P. L., Câmara, D. A. D., Porcacchia, A. S., Fonseca, P. M. M., Jorge, S. D., Araldi, R. P., et al. (2017). The Roles of ROS in Cancer Heterogeneity and Therapy. *Oxidative Med. Cell. longevity* 2017, 2467940. doi:10.1155/2017/2467940

Deb, D. D., Parimala, G., Saravana Devi, S., and Chakraborty, T. (2011). Effect of Thymol on Peripheral Blood Mononuclear Cell PBMC and Acute Promyelotic Cancer Cell Line HL-60. *Chemico-Biological Interactions* 193 (1), 97–106. doi:10.1016/j.cbi.2011.05.009

Elbe, H., Yigitturk, G., Cavusoglu, T., Baygar, T., Ozgul Onal, M., and Ozturk, F. (2020). Comparison of Ultrastructural Changes and the Anticarcinogenic Effects of Thymol and Carvacrol on Ovarian Cancer Cells: Which Is More Effective? *Ultrastructural Pathol.* 44 (2), 193–202. doi:10.1080/01913123.2020.1740366

Elbe, H., Yigitturk, G., Cavusoglu, T., Uyanikgil, Y., and Ozturk, F. (2020). Apoptotic Effects of Thymol, a Novel Monoterpene Phenol, on Different Types of Cancer. *Bratisl Lek Listy* 121 (2), 122–128. doi:10.4149/BLL_2020_016

Elshafie, H., Armentano, M., Carmosino, M., Bufo, S., De Feo, V., and Camele, I. (2017). Cytotoxic Activity of *Origanum Vulgare* L. On Hepatocellular Carcinoma Cell Line HepG2 and Evaluation of its Biological Activity. *Molecules* 22 (9), 1435. doi:10.3390/molecules22091435

Fan, K., Li, X., Cao, Y., Qi, H., Li, L., Zhang, Q., et al. (2015). Carvacrol Inhibits Proliferation and Induces Apoptosis in Human colon Cancer Cells. *Anticancer Drugs* 26 (8), 813–823. doi:10.1097/CAD.0000000000000263

Ferraz, R. P. C., Bomfim, D. S., Carvalho, N. C., Soares, M. B. P., da Silva, T. B., Machado, W. J., et al. (2013). Cytotoxic Effect of Leaf Essential Oil of Lippia Gracilis Schauer (Verbenaceae). *Phytomedicine* 20 (7), 615–621. doi:10.1016/j.phymed.2013.01.015

Fiandalo, M. V., and Kyprianou, N. (2012). Caspase Control: Protagonists of Cancer Cell Apoptosis. *Exp. Oncol.* 34 (3), 165–175.

Fitsiou, E., Anestopoulos, I., Chlichlia, K., Galanis, A., Kourkoutas, I., Panayiotidis, M. I., et al. (2016). Antioxidant and Antiproliferative Properties of the Essential Oils of Satureja Thymbra and Satureja Parnassica and Their Major Constituents. *Anticancer Res.* 36 (11), 5757–5764. doi:10.21873/anticanres.11159

Fouad, H., Salem, H., Ellakwa, D. E. S., and Abdel-Hamid, M. (2019). MMP-2 and MMP-9 as Prognostic Markers for the Early Detection of Urinary Bladder Cancer. *J. Biochem. Mol. Toxicol.* 33 (4), e22275. doi:10.1002/jbt.22275

Fundyler, O., Khanna, M., and Smoller, B. R. (2004). Metalloproteinase-2 Expression Correlates with Aggressiveness of Cutaneous Squamous Cell Carcinomas. *Mod. Pathol.* 17 (5), 496–502. doi:10.1038/modpathol.3800066

Georgakilas, A. G., Martin, O. A., and Bonner, W. M. (2017). p21: A Two-Faced Genome Guardian. *Trends Mol. Med.* 23 (4), 310–319. doi:10.1016/j.molmed.2017.02.001

Ghavami, S., Hashemi, M., Ande, S. R., Yeganeh, B., Xiao, W., Eshraghi, M., et al. (2009). Apoptosis and Cancer: Mutations within Caspase Genes. *J. Med. Genet.* 46 (8), 497–510. doi:10.1136/jmg.2009.066944

Ghorani, V., Alavinezhad, A., Rajabi, O., Mohammadpour, A. H., and Boskabady, M. H. (2021). Safety and Tolerability of Carvacrol in Healthy Subjects: a Phase I Clinical Study. *Drug Chem. Toxicol.* 44 (2), 177–189. doi:10.1080/01480545.2018.1538233

Giardina, M. G., Matarazzo, M., Varriale, A., Morante, R., Napoli, A., and Martino, R. (1992). Serum Alpha-L-Fucosidase. A Useful Marker in the Diagnosis of Hepatocellular Carcinoma. *Cancer* 70 (5), 1044–1048. doi:10.1002/1097-0142(19920901)70:5<1044::aid-cncr2820700506>3.0.co;2-u

Gordaliza, M. (2007). Natural Products as Leads to Anticancer Drugs. *Clin. Transl Oncol.* 9 (12), 767–776. doi:10.1007/s12094-007-0138-9

Gottlieb, T. M., and Oren, M. (1998). p53 and Apoptosis. *Semin. Cancer Biol.* 8 (5), 359–368. doi:10.1006/scbi.1998.0098

Gouveia, D. N., Costa, J. S., Oliveira, M. A., Rabelo, T. K., Silva, A. M. d. O. e., Carvalho, A. A., et al. (2018). α-Terpineol Reduces Cancer Pain via Modulation of Oxidative Stress and Inhibition of iNOS. *Biomed. Pharmacother.* 105, 652–661. doi:10.1016/j.biopha.2018.06.027

Govindaraju, S., and Arulselvi, P. I. (2018). Characterization ofColeus Aromaticusessential Oil and its Major Constituent Carvacrol Forin Vitroantidiabetic and Antiproliferative Activities. *J. Herbs, Spices Med. Plants* 24 (1), 37–51. doi:10.1080/10496475.2017.1369483

Günes-Bayir, A., Kocyigit, A., Güler, E. M., Bilgin, M. G., Ergün, İ. S., and Dadak, A. (2018). Effects of Carvacrol on Human Fibroblast (WS-1) and Gastric Adenocarcinoma (AGS) Cells *In Vitro* and on Wistar Rats *In Vivo*. *Mol. Cel Biochem.* 448 (5), 237–249. doi:10.1007/s11010-018-3329-5

Günes-Bayir, A., Kocyigit, A., Guler, E. M., and Dadak, A. (2020). *In Vitro* Hormetic Effect Investigation of Thymol on Human Fibroblast and Gastric Adenocarcinoma Cells. *Molecules* 25 (14), 3270. doi:10.3390/molecules25143270

Günes-Bayir, A., Kocyigit, A., and Güler, E. M. (2018). *In Vitro* effects of Two Major Phenolic Compounds from the Family Lamiaceae Plants on the Human Gastric Carcinoma Cells. *Toxicol. Ind. Health* 34 (8), 525–539. doi:10.1177/0748233718761698

Hamilton, E., and Infante, J. R. (2016). Targeting CDK4/6 in Patients with Cancer. *Cancer Treat. Rev.* 45, 129–138. doi:10.1016/j.ctrv.2016.03.002

Harris, S. L., and Levine, A. J. (2005). The P53 Pathway: Positive and Negative Feedback Loops. *Oncogene* 24 (17), 2899–2908. doi:10.1038/sj.onc.1208615

Hassan, H. F. H., Mansour, A. M., Salama, S. A., and El-Sayed, E.-S. M. (2021). The Chemopreventive Effect of Thymol against Dimethylhydrazine And/or High Fat Diet-Induced colon Cancer in Rats: Relevance to NF-Kb. *Life Sci.* 274, 119335. doi:10.1016/j.lfs.2021.119335

Hassen, A. M., Taye, G., Gizaw, M., and Hussien, F. M. (2019). Quality of Life and Associated Factors Among Patients with Breast Cancer under Chemotherapy at Tikur Anbessa Specialized Hospital, Addis Ababa, Ethiopia. *PLoS ONE* 14 (9), e0222629. doi:10.1371/journal.pone.0222629

Heidarian, E., and Keloushadi, M. (2019). Antiproliferative and Anti-invasion Effects of Carvacrol on PC3 Human Prostate Cancer Cells through Reducing pSTAT3, pAKT, and pERK1/2 Signaling Proteins. *Int. J. Prev. Med.* 10, 156. doi:10.4103/ijpvm.IJPVM_292_17

Hensley, P., Mishra, M., and Kyprianou, N. (2013). Targeting Caspases in Cancer Therapeutics. *Biol. Chem.* 394 (7), 831–843. doi:10.1515/hsz-2013-0128

Hooijmans, C. R., Rovers, M. M., De Vries, R. B., Leenaars, M., Ritskes-Hoitinga, M., and Langendam, M. W. (2014). SYRCLE's Risk of Bias Tool for Animal Studies. *BMC Med. Res. Methodol.* 14, 43. doi:10.1186/1471-2288-14-43

Horng, C.-T., Chou, C., Sun, T., Liang, W., Kuo, C., Wang, J., et al. (2017). Effect of Carvacrol on Ca(2+) Movement and Viability in PC3 Human Prostate Cancer Cells. *Chin. J. Physiol.* 60 (5), 275–283. doi:10.4077/cjp.2017.bag506

Horvathova, E., Turcaniova, V., and Slamenova, D. (2007). Comparative Study of DNA-Damaging and DNA-Protective Effects of Selected Components of Essential Plant Oils in Human Leukemic Cells K562. *Neoplasma* 54 (6), 478–483.

Horváthová, E., Sramková, M., Lábaj, J., and Slamenová, D. (2006). Study of Cytotoxic, Genotoxic and DNA-Protective Effects of Selected Plant Essential Oils on Human Cells Cultured *In Vitro*. *Neuro Endocrinol. Lett.* 27 (Suppl. 2), 44–47. doi:10.4172/2167-0412.1000170

Hsu, S.-S., Lin, K.-L., Chou, C.-T., Chiang, A.-J., Liang, W.-Z., Chang, H.-T., et al. (2011). Effect of Thymol on Ca2+ Homeostasis and Viability in Human Glioblastoma Cells. *Eur. J. Pharmacol.* 670 (1), 85–91. doi:10.1016/j.ejphar.2011.08.017

Huang, H., Zhang, X.-F., Zhou, H.-J., Xue, Y.-H., Dong, Q.-Z., Ye, Q.-H., et al. (2010). Expression and Prognostic Significance of Osteopontin and Caspase-3 in Hepatocellular Carcinoma Patients after Curative Resection. *Cancer Sci.* 101 (5), 1314–1319. doi:10.1111/j.1349-7006.2010.01524.x

Ingham, M., and Schwartz, G. K. (2017). Cell-Cycle Therapeutics Come of Age. *J. Clin. Oncol.* 35 (25), 2949–2959. doi:10.1200/JCO.2016.69.0032

Jaafari, A., Mouse, H. A., Rakib, E. M., M'barek, L. A., Tilaoui, M., Benbakhta, C., et al. (2007). Chemical Composition and Antitumor Activity of Different Wild Varieties of Moroccan Thyme. *Rev. Bras. Farmacogn.* 17 (4), 477–491. doi:10.1590/S0102-695X2007000400002

Jaafari, A., Tilaoui, M., Mouse, H. A., M'bark, L. A., Aboufatima, R., Chait, A., et al. (2012). Comparative Study of the Antitumor Effect of Natural Monoterpenes: Relationship to Cell Cycle Analysis. *Rev. Bras. Farmacogn.* 22 (3), 534–540. doi:10.1590/S0102-695X2012005000021

Jabłońska-Trypuć, A., Matejczyk, M., and Rosochacki, S. (2016). Matrix Metalloproteinases (MMPs), the Main Extracellular Matrix (ECM) Enzymes

in Collagen Degradation, as a Target for Anticancer Drugs. *J. Enzyme Inhib. Med. Chem.* 31 (Suppl. 1), 177–183. doi:10.3109/14756366.2016.1161620

Jamali, T., Kavoosi, G., Safavi, M., and Ardestani, S. (2018). *In-vitro* Evaluation of Apoptotic Effect of OEO and Thymol in 2D and 3D Cell Cultures and the Study of Their Interaction Mode with DNA. *Sci. Rep.* 8 (1), 15787. doi:10.1038/s41598-018-34055-w

Jayakumar, S., Madankumar, A., Asokkumar, S., Raghunandhakumar, S., Gokula dhas, K., Kamaraj, S., et al. (2012). Potential Preventive Effect of Carvacrol against Diethylnitrosamine-Induced Hepatocellular Carcinoma in Rats. *Mol. Cel Biochem.* 360 (1–2), 51–60. doi:10.1007/s11010-011-1043-7

Jung, C. Y., Kim, S. Y., and Lee, C. (2018). Carvacrol Targets AXL to Inhibit Cell Proliferation and Migration in Non-small Cell Lung Cancer Cells. *Anticancer Res.* 38 (1), 279–286. doi:10.21873/anticanres.12219

Kang, S.-H., Kim, Y.-S., Kim, E.-K., Hwang, J.-W., Jeong, J.-H., Dong, X., et al. (2016). Anticancer Effect of Thymol on AGS Human Gastric Carcinoma Cells. *J. Microbiol. Biotechnol.* 26 (1), 28–37. doi:10.4014/jmb.1506.06073

Karkabounas, S., Kostoula, O. K., Daskalou, T., Veltsistas, P., Karamouzis, M., Zelovitis, I., et al. (2006). Anticarcinogenic and Antiplatelet Effects of Carvacrol. *Exp. Oncol.* 28 (2), 121–125. doi:10.1080/01913123.2020.1740366

Kelly, K. (2009). *The History of Medicine. The Middle Ages*. Medicine: Stonehenge, 500–1450.

Khan, F., Khan, I., Farooqui, A., and Ansari, I. A. (2017). Carvacrol Induces Reactive Oxygen Species (ROS)-mediated Apoptosis along with Cell Cycle Arrest at G0/G1 in Human Prostate Cancer Cells. *Nutr. Cancer* 69 (7), 1075–1087. doi:10.1080/01635581.2017.1359321

Khan, F., Singh, V. K., Saeed, M., Kausar, M. A., and Ansari, I. A. (2019). Carvacrol Induced Program Cell Death and Cell Cycle Arrest in Androgen-independent Human Prostate Cancer Cells via Inhibition of Notch Signaling. *Anticancer Agents Med. Chem.* 19 (13), 1588–1608. doi:10.2174/1871520619666190731152942

Kim, B., Srivastava, S. K., and Kim, S.-H. (2015). Caspase-9 as a Therapeutic Target for Treating Cancer. *Expert Opin. Ther. Targets* 19 (1), 113–127. doi:10.1517/14728222.2014.961425

Kim, C., and Kim, B. (2018). Anti-Cancer Natural Products and Their Bioactive Compounds Inducing ER Stress-Mediated Apoptosis: A Review. *Nutrients* 10 (8), 1021. doi:10.3390/nu10081021

Kim, E. K., and Choi, E.-J. (2015). Compromised MAPK Signaling in Human Diseases: an Update. *Arch. Toxicol.* 89 (6), 867–882. doi:10.1007/s00204-015-1472-2

Kocal, G., and Pakdemirli, A. (2020). Antiproliferative Effects of Carvacrol on Neuroblastoma Cells. *J. Dr Behcet Uz Child. Hosp.* 10 (1), 61–64. doi:10.5222/buchd.2020.59251

Koparal, A. T., and Zeytinoglu, M. (2003). Effects of Carvacrol on a Human Non-small Cell Lung Cancer (NSCLC) Cell Line, A549. *Cytotechnology* 43 (1–3), 149–154. doi:10.1023/b:cyto.0000039917.60348.45

Koss, B., and Greengard, O. (1982). Effect of Neoplasms on the Content and Activity of Alkaline Phosphatase and Gamma-Glutamyl Transpeptidase in Uninvolved Host Tissues. *Cancer Res.* 42 (6), 2146–2158.

Koyama, H., Iwata, H., Kuwabara, Y., Iwase, H., Kobayashi, S., and Fujii, Y. (1990). Gelatinolytic Activity of Matrix Metalloproteinase-2 and -9 in Oesophageal Carcinoma; a Study Using *In Situ* Zymography. *Eur. J. Cancer* 36 (16), 2164–2170. doi:10.1016/s0959-8049(00)00297-5

Krelin, Y., Zhang, L., Kang, T.-B., Appel, E., Kovalenko, A., and Wallach, D. (2008). Caspase-8 Deficiency Facilitates Cellular Transformation *In Vitro*. *Cell Death Differ.* 15 (9), 1350–1355. doi:10.1038/cdd.2008.88

Krens, S. F. G., Spaink, H. P., and Snaar-Jagalska, B. E. (2006). Functions of the MAPK Family in Vertebrate-Development. *FEBS Lett.* 580 (21), 4984–4990. doi:10.1016/j.febslet.2006.08.025

Kroemer, G., Dallaporta, B., and Resche-Rigon, M. (1998). The Mitochondrial Death/life Regulator in Apoptosis and Necrosis. *Annu. Rev. Physiol.* 60, 619–642. doi:10.1146/annurev.physiol.60.1.619

Landis, J. R., and Koch, G. G. (1977). The Measurement of Observer Agreement for Categorical Data. *Biometrics* 33 (1), 159–174. doi:10.2307/2529310

Lee, D. J., and Zeidner, J. F. (2019). Cyclin-dependent Kinase (CDK) 9 and 4/6 Inhibitors in Acute Myeloid Leukemia (AML): a Promising Therapeutic Approach. *Expert Opin. Investig. Drugs* 28 (11), 989–1001. doi:10.1080/13543784.2019.1678583

Lee, H. S., and Park, S. W. (2016). Systemic Chemotherapy in Advanced Pancreatic Cancer. *Gut Liver* 10 (3), 340–347. doi:10.5009/gnl15465

Lee, K. P., Kim, J.-E., Park, W.-H., and Hong, H. (2016). Regulation of C6 Glioma Cell Migration by Thymol. *Oncol. Lett.* 11 (4), 2619–2624. doi:10.3892/ol.2016.4237

Li, D., Yang, M., Liao, A., Zeng, B., Liu, D., Yao, Y., et al. (2018). Linc00483 as ceRNA Regulates Proliferation and Apoptosis through Activating MAPKs in Gastric Cancer. *J. Cel Mol Med.* 22 (8), 3875–3886. doi:10.1111/jcmm.13661

Li, H., Hu, J., Wu, S., Wang, L., Cao, X., Zhang, X., et al. (2016). Auranofin-mediated Inhibition of PI3K/AKT/mTOR axis and Anticancer Activity in Non-small Cell Lung Cancer Cells. *Oncotarget* 7 (3), 3548–3558. doi:10.18632/oncotarget.6516

Li, L., He, L., Wu, Y., and Zhang, Y. (2021). Carvacrol Affects Breast Cancer Cells through TRPM7 Mediated Cell Cycle Regulation. *Life Sci.* 266, 118894. doi:10.1016/j.lfs.2020.118894

Li, S., Zhao, H., and Bao, L. (2019). Preliminary Study on the Mechanism of Carvacrol Regulating Hepatocellular Carcinoma Based on Network Pharmacology. *Lett. Drug Des. Discov.* 16 (11), 1286–1295. doi:10.2174/1570180816666190516105906

Li, Y., Wen, J.-m., Du, C.-j., Hu, S.-m., Chen, J.-x., Zhang, S.-g., et al. (2017). Thymol Inhibits Bladder Cancer Cell Proliferation via Inducing Cell Cycle Arrest and Apoptosis. *Biochem. Biophysical Res. Commun.* 491 (2), 530–536. doi:10.1016/j.bbrc.2017.04.009

Li, Y., Xu, J. z., Gu, C. x., Liu, G. l., and Tian, K. (2018). Carvacrol Suppresses Inflammatory Responses in Rheumatoid Arthritis Fibroblast-like Synoviocytes. *J. Cel Biochem.* 120 (5), 8169–8176. doi:10.1002/jcb.28098

Liang, W.-Z., Chou, C.-T., Lu, T., Chi, C.-C., Tseng, L.-L., Pan, C.-C., et al. (2013). The Mechanism of Carvacrol-Evoked [Ca2+]i Rises and Non-ca2+-triggered Cell Death in OC2 Human Oral Cancer Cells. *Toxicology* 303, 152–161. doi:10.1016/j.tox.2012.10.026

Liang, W. Z., and Lu, C. H. (2012). Carvacrol-induced [Ca2+]i Rise and Apoptosis in Human Glioblastoma Cells. *Life Sci.* 90 (17–18), 703–711. doi:10.1016/j.lfs.2012.03.027

Lim, W., Ham, J., Bazer, F. W., and Song, G. (2019). Carvacrol Induces Mitochondria-Mediated Apoptosis via Disruption of Calcium Homeostasis in Human Choriocarcinoma Cells. *J. Cel Physiol.* 234 (2), 1803–1815. doi:10.1002/jcp.27054

Lin, S.-C., Lo, S.-S., Liu, C.-J., Chung, M.-Y., Huang, J.-W., and Chang, K.-W. (2004). Functional Genotype in Matrix Metalloproteinases-2 Promoter Is a Risk Factor for Oral Carcinogenesis. *J. Oral Pathol. Med.* 33 (7), 405–409. doi:10.1111/j.1600-0714.2004.00231.x

Liu, J., Wu, N., Ma, L.-N., Zhong, J.-T., Liu, G., Zheng, L.-H., et al. (2014). p38 MAPK Signaling Mediates Mitochondrial Apoptosis in Cancer Cells Induced by Oleanolic Acid. *Asian Pac. J. Cancer Prev.* 15 (11), 4519–4525. doi:10.7314/apjcp.2014.15.11.4519

Liu, W.-W., Zeng, Z.-Y., Wu, Q.-L., Hou, J.-H., and Chen, Y.-Y. (2005). Overexpression of MMP-2 in Laryngeal Squamous Cell Carcinoma: a Potential Indicator for Poor Prognosis. *Otolaryngol. Head Neck Surg.* 132 (3), 395–400. doi:10.1016/j.otohns.2004.09.050

Llana-Ruiz-Cabello, M., Gutiérrez-Praena, D., Pichardo, S., Moreno, F. J., Bermúdez, J. M., Aucejo, S., et al. (2014). Cytotoxicity and Morphological Effects Induced by Carvacrol and Thymol on the Human Cell Line Caco-2. *Food Chem. Toxicol.* 64, 281–290. doi:10.1016/j.fct.2013.12.005

Llana-Ruiz-Cabello, M., Gutiérrez-Praena, D., Puerto, M., Pichardo, S., Jos, Á., and Cameán, A. M. (2015). *In Vitro* pro-oxidant/antioxidant Role of Carvacrol, Thymol and Their Mixture in the Intestinal Caco-2 Cell Line. *Toxicol. Vitro* 29 (4), 647–656. doi:10.1016/j.tiv.2015.02.006

Low, H. B., and Zhang, Y. (2016). Regulatory Roles of MAPK Phosphatases in Cancer. *Immune Netw.* 16 (2), 85–98. doi:10.4110/in.2016.16.2.85

Lu, L. C., Tsay, S. L., Chang, S. Y., Chen, C. M., and Liu, C. Y. (2019). Daily Activity, Mood, and Quality of Life in Colorectal Cancer Patients with Chemotherapy-induced Peripheral Neuropathy: A Mediation Effect Analysis. *Cancer Med.* 8 (3), 963–971. doi:10.1002/cam4.1976

Luo, Y., Wu, J.-Y., Lu, M.-H., Shi, Z., Na, N., and Di, J.-M. (2016). Carvacrol Alleviates Prostate Cancer Cell Proliferation, Migration, and Invasion through Regulation of PI3K/Akt and MAPK Signaling Pathways. *Oxidative Med. Cell Longevity* 2016, 1–11. doi:10.1155/2016/1469693

Mari, A., Mani, G., Nagabhishek, S. N., Balaraman, G., Subramanian, N., Mirza, F. B., et al. (2020). Carvacrol Promotes Cell Cycle Arrest and Apoptosis through

PI3K/AKT Signaling Pathway in MCF-7 Breast Cancer Cells. *Chin. J. Integr. Med.* 12, 133. doi:10.1007/s11655-020-3193-5

Martino, E., Casamassima, G., Castiglione, S., Cellupica, E., Pantalone, S., Papagni, F., et al. (2018). Vinca Alkaloids and Analogues as Anti-cancer Agents: Looking Back, Peering Ahead. *Bioorg. Med. Chem. Lett.* 28 (17), 2816–2826. doi:10.1016/j.bmcl.2018.06.044

Marullo, R., Werner, E., Degtyareva, N., Moore, B., Altavilla, G., Ramalingam, S. S., et al. (2013). Cisplatin Induces a Mitochondrial-ROS Response that Contributes to Cytotoxicity Depending on Mitochondrial Redox Status and Bioenergetic Functions. *PloS one* 8 (11), e81162. doi:10.1371/journal.pone.0081162

Maryam, K., Shakeri, S., and Kiani, K. (2015). Preparation and *In Vitro* Investigation of Antigastric Cancer Activities of Carvacrol-loaded Human Serum Albumin Nanoparticles. *IET nanobiotechnol.* 9 (5), 294–299. doi:10.1049/iet-nbt.2014.0040

Mehdi, S., Ahmad, A., Irshad, M., Manzoor, N., and Rizvi, M. (2011). Cytotoxic Effect of Carvacrol on Human Cervical Cancer Cells. *Biol. Med.* 3 (2), 307–312. doi:10.26226/morressier.5770e29ad462b80290b4ba57

Melušová, M., Jantová, S., and Horváthová, E. (2014). Carvacrol and Rosemary Oil at Higher Concentrations Induce Apoptosis in Human Hepatoma HepG2 Cells. *Interdiscip. Toxicol.* 7 (4), 189–194. doi:10.2478/intox-2014-0027

Melusova, M., Slamenova, D., Kozics, K., Jantova, S., and Horvathova, E. (2014). Carvacrol and Rosemary Essential Oil Manifest Cytotoxic, DNA-Protective and Pro-apoptotic Effect Having No Effect on DNA Repair. *Neoplasma* 61 (6), 690–699. doi:10.4149/neo_2014_084

Mishra, B. B., and Tiwari, V. K. (2011). Natural Products: an Evolving Role in Future Drug Discovery. *Eur. J. Med. Chem.* 46 (10), 4769–4807. doi:10.1016/j.ejmech.2011.07.057

Nagase, H., Visse, R., and Murphy, G. (2006). Structure and Function of Matrix Metalloproteinases and TIMPs. *Cardiovasc. Res.* 69 (3), 562–573. doi:10.1016/j.cardiores.2005.12.002

National Cancer Institute (2019). National Cancer Institute. Available at: https://www.inca.gov.br/estimativa/introducao (Acesseced November 13, 2020).

Nelson, R. L. (1982). The Comparative Clinical Pharmacology and Pharmacokinetics of Vindesine, Vincristine, and Vinblastine in Human Patients with Cancer. *Med. Pediatr. Oncol.* 10 (2), 115–127. doi:10.1002/mpo.2950100202

Neville, B. (2011). *Patologia Oral e Maxilofacial*. Amsterdam: Elsevier Brasil, 3475.

O'Donnell, J. S., Massi, D., Teng, M. W. L., and Mandala, M. (2018). PI3K-AKT-mTOR Inhibition in Cancer Immunotherapy, Redux. *Semin. Cancer Biol.* 48, 91–103. doi:10.1016/j.semcancer.2017.04.015

Olsson, M., and Zhivotovsky, B. (2011). Caspases and Cancer. *Cel Death Differ* 18 (9), 1441–1449. doi:10.1038/cdd.2011.30

Ouzzani, M., Hammady, H., Fedorowicz, Z., and Elmagarmid, A. (2016). Rayyan-a Web and mobile App for Systematic Reviews. *Syst. Rev.* 5 (1), 1–10. doi:10.1186/s13643-016-0384-4

Ozawa, S., Shankar, R., Leopold, C., and Orubu, S. (2019). Access to Medicines through Health Systems in Low- and Middle-Income Countries. *Health Policy Plan* 34, iii1–iii3. doi:10.1093/heapol/czz119

Özkan, A., and Erdogan, A. (2011). A Comparative Evaluation of Antioxidant and Anticancer Activity of Essential Oil from Origanum Onites (Lamiaceae) and its Two Major Phenolic Components. *Turk J. Biol.* 35 (2011), 735–742. doi:10.1016/j.toxlet.2010.03.459

Ozkan, A., and Erdogan, A. (2012). A Comparative Study of the Antioxidant/prooxidant Effects of Carvacrol and Thymol at Various Concentrations on Membrane and DNA of Parental and Drug Resistant H1299 Cells. *Nat. Prod. Commun.* 7 (12), 1557–1560. doi:10.1177/1934578x1200701201

Page, M. J., McKenzie, J. E., Bossuyt, P. M., Boutron, I., Hoffmann, T. C., Mulrow, C. D., et al. (2021). The PRISMA 2020 Statement: an Updated Guideline for Reporting Systematic Reviews. *Plos Med.* 18 (3), e1003583. doi:10.1371/journal.pmed.1003583

Pakdemirli, A., Karaca, C., Sever, T., Daşkin, E., Leblebici, A., Yiğitbaşi, T., et al. (2020). Carvacrol Alters Soluble Factors in HCT-116 and HT-29 Cell Lines. *Turk J. Med. Sci.* 50 (1), 271–276. doi:10.3906/sag-1907-173

Paolicchi, A., Pompella, A., Tonarelli, P., Gadducci, A., Genazzani, A. R., Zunino, F., et al. (1996). Gamma-glutamyltranspeptidase Activity in Human Ovarian Carcinoma. *Anticancer Res.* 16 (5B), 3053–3058.

Pathania, A. S., Guru, S. K., Verma, M. K., Sharma, C., Abdullah, S. T., Malik, F., et al. (2013). Disruption of the PI3K/AKT/mTOR Signaling cascade and Induction of Apoptosis in HL-60 Cells by an Essential Oil from Monarda Citriodora. *Food Chem. Toxicol.* 62, 246–254. doi:10.1016/j.fct.2013.08.037

Pernas, S., Tolaney, S. M., Winer, E. P., and Goel, S. (2018). CDK4/6 Inhibition in Breast Cancer: Current Practice and Future Directions. *Ther. Adv. Med. Oncol.* 10, 175883591878645. doi:10.1177/1758835918786451

Pompella, A., De Tata, V., Paolicchi, A., and Zunino, F. (2006). Expression of γ-glutamyltransferase in Cancer Cells and its Significance in Drug Resistance. *Biochem. Pharmacol.* 71 (3), 231–238. doi:10.1016/j.bcp.2005.10.005

Potočnjak, I., Gobin, I., and Domitrović, R. (2018). Carvacrol Induces Cytotoxicity in Human Cervical Cancer Cells but Causes Cisplatin Resistance: Involvement of MEK-ERK Activation. *Phytother Res.* 32 (6), 1090–1097. doi:10.1002/ptr.6048

Powell, H. A., Tata, L. J., Baldwin, D. R., Potter, V. A., Stanley, R. A., Khakwani, A., et al. (2014). Treatment Decisions and Survival for People with Small-Cell Lung Cancer. *Br. J. Cancer* 110 (4), 908–915. doi:10.1038/bjc.2013.812

Prasad, S., Gupta, S. C., and Tyagi, A. K. (2017). Reactive Oxygen Species (ROS) and Cancer: Role of Antioxidative Nutraceuticals. *Cancer Lett.* 387, 95–105. doi:10.1016/j.canlet.2016.03.042

Riaz, S. K., Iqbal, Y., and Malik, M. F. A. (2015). Diagnostic and Therapeutic Implications of the Vascular Endothelial Growth Factor Family in Cancer. *Asian Pac. J. Cancer Prev.* 16 (5), 1677–1682. doi:10.7314/apjcp.2015.16.5.1677

Rojas-Armas, J. P., Arroyo-Acevedo, J. L., Palomino-Pacheco, M., Herrera-Calderón, O., Ortiz-Sánchez, J. M., Rojas-Armas, A., et al. (2020). The Essential Oil of Cymbopogon Citratus Stapt and Carvacrol: An Approach of the Antitumor Effect on 7,12-Dimethylbenz-[α]-Anthracene (DMBA)-Induced Breast Cancer in Female Rats. *Molecules* 25 (14), 3284. doi:10.3390/molecules25143284

Salehi, B., Mishra, A. P., Shukla, I., Sharifi-Rad, M., Contreras, M. d. M., Segura-Carretero, A., et al. (2018). Thymol, Thyme, and Other Plant Sources: Health and Potential Uses. *Phytotherapy Res.* 32 (9), 1688–1706. doi:10.1002/ptr.6109

Santos, C. P. d., Pinto, J. A. O., Santos, C. A. d., Cruz, E. M. O., Arrigoni-Blank, M. d. F., Andrade, T. M., et al. (2016). Harvest Time and Geographical Origin Affect the Essential Oil of Lippia Gracilis Schauer. *Ind. Crops Prod.* 79, 205–210. doi:10.1016/j.indcrop.2015.11.015

Satooka, H., and Kubo, I. (2012). Effects of Thymol on B16-F10 Melanoma Cells. *J. Agric. Food Chem.* 60 (10), 2746–2752. doi:10.1021/jf204525b

Semenza, G. L. (2003). Targeting HIF-1 for Cancer Therapy. *Nat. Rev. Cancer* 3 (10), 721–732. doi:10.1038/nrc1187

Seresht, H. R., Albadry, B. J., Al-mosawi, A. K. M., Gholami, O., and Cheshomi, H. (2019). The Cytotoxic Effects of Thymol as the Major Component of Trachyspermum Ammi on Breast Cancer (MCF-7) Cells. *Pharm. Chem. J.* 53 (2), 101–107. doi:10.1007/s11094-019-01961-w

Shalini, S., Dorstyn, L., Dawar, S., and Kumar, S. (2015). Old, New and Emerging Functions of Caspases. *Cel Death Differ* 22 (4), 526–539. doi:10.1038/cdd.2014.216

Sharifi-Rad, M., Varoni, E. M., Iriti, M., Martorell, M., Setzer, W. N., Del Mar Contreras, M., et al. (2018). Carvacrol and Human Health: A Comprehensive Review. *Phytotherapy Res.* 32 (9), 1675–1687. doi:10.1002/ptr.6103

Sheorain, J., Mehra, M., Thakur, R., Grewal, S., and Kumari, S. (2019). *In Vitro* anti-inflammatory and Antioxidant Potential of Thymol Loaded Bipolymeric (Tragacanth Gum/chitosan) Nanocarrier. *Int. J. Biol. Macromolecules* 125, 1069–1074. doi:10.1016/j.ijbiomac.2018.12.095

Shojaei, S., Kiumarsi, A., Moghadam, A. R., Alizadeh, J., Marzban, H., and Ghavami, S. (2014). "Perillyl Alcohol (Monoterpene Alcohol), Limonene," in *The Enzymes Natural Products and Cancer Signaling: Isoprenoids, Polyphenols and Flavonoids*. Editors S. Zahra Bathaie and F. Tamanoi (Cambridge: Academic Press), 1–258. doi:10.1016/B978-0-12-802215-3.00002-1

Shuman Moss, L. A., Jensen-Taubman, S., and Stetler-Stevenson, W. G. (2012). Matrix Metalloproteinases. *Am. J. Pathol.* 181 (6), 1895–1899. doi:10.1016/j.ajpath.2012.08.044

Silva, E. R., de Carvalho, F. O., Teixeira, L. G. B., Santos, N. G. L., Felipe, F. A., Santana, H. S. R., et al. (2018). Pharmacological Effects of Carvacrol in *In Vitro* Studies: A Review. *Curr. Pharm. Des.* 24 (29), 3454–3465. doi:10.2174/1381612824666181003123400

Sisto, F., Carradori, S., Guglielmi, P., Spano, M., Secci, D., Granese, A., et al. (2021). Synthesis and Evaluation of Thymol-Based Synthetic Derivatives as Dual-Action Inhibitors against Different Strains of *H. pylori* and AGS Cell Line. *Molecules* 26 (7), 1829. doi:10.3390/molecules26071829

Sisto, F., Carradori, S., Guglielmi, P., Traversi, C. B., Spano, M., Sobolev, A. P., et al. (2020). Synthesis and Biological Evaluation of Carvacrol-Based Derivatives as Dual Inhibitors of *H. pylori* Strains and AGS Cell Proliferation. *Pharmaceuticals* 13 (11), 405. doi:10.3390/ph13110405

Sivaranjani, A., Sivagami, G., and Nalini, N. (2016). Chemopreventive Effect of Carvacrol on 1,2-dimethylhydrazine Induced Experimental colon Carcinogenesis. *J. Cancer Res. Ther.* 12 (2), 755–762. doi:10.4103/0973-1482.154925

Siveen, K. S., Prabhu, K., Krishnankutty, R., Kuttikrishnan, S., Tsakou, M., Alali, F. Q., et al. (2017). Vascular Endothelial Growth Factor (VEGF) Signaling in Tumour Vascularization: Potential and Challenges. *Curr. Vasc. Pharmacol.* 15 (4), 339–351. doi:10.2174/1570161115666170105124038

Slamenová, D., Horváthová, E., Sramková, M., and Marsálková, L. (2007). DNA-protective Effects of Two Components of Essential Plant Oils Carvacrol and Thymol on Mammalian Cells Cultured *In Vitro*. *Neoplasma* 54 (2), 108–112. doi:10.7287/peerj.9626v0.1/reviews/1

Soković, M., Glamoclija, J., and Ciric, A. (2013). *Natural Products from Plants and Fungi as Fungicides. Fungicides—Showcases of Integrated Plant Disease. Management from Around the World. Chapter: Natural Products from Plants and Fungi as Fungicides*. Berlin: Springer, 185–232. doi:10.5772/50277

Song, H.-Y., Deng, X.-H., Yuan, G.-Y., Hou, X.-F., Zhu, Z.-D., Zhou, L., et al. (2014). Expression of Bcl-2 and P53 in Induction of Esophageal Cancer Cell Apoptosis by ECRG2 in Combination with Cisplatin. *Asian Pac. J. Cancer Prev.* 15 (3), 1397–1401. doi:10.7314/apjcp.2014.15.3.1397

Song, M., Bode, A. M., Dong, Z., and Lee, M.-H. (2019). AKT as a Therapeutic Target for Cancer. *Cancer Res.* 79 (6), 1019–1031. doi:10.1158/0008-5472.CAN-18-2738

Soung, Y. H., Lee, J. W., Kim, S. Y., Jang, J., Park, Y. G., Park, W. S., et al. (2005). CASPASE-8 Gene Is Inactivated by Somatic Mutations in Gastric Carcinomas. *Cancer Res.* 65 (3), 815–821. doi:10.1038/sj.onc.1208244

Srinivas, U. S., Tan, B. W. Q., Vellayappan, B. A., and Jeyasekharan, A. D. (2019). ROS and the DNA Damage Response in Cancer. *Redox Biol.* 25, 101084. doi:10.1016/j.redox.2018.101084

Srivastav, V. K., Egbuna, C., and Tiwari, M. (2020). Plant Secondary Metabolites as lead Compounds for the Production of Potent Drugs. *Phytochemicals as Lead Comp. New Drug* 14, 3–14. doi:10.1016/B978-0-12-817890-4.00001-9

Subramaniyan, J., Krishnan, G., Balan, R., Mgj, D., Ramasamy, E., Ramalingam, S., et al. (2014). Carvacrol Modulates Instability of Xenobiotic Metabolizing Enzymes and Downregulates the Expressions of PCNA, MMP-2, and MMP-9 during Diethylnitrosamine-Induced Hepatocarcinogenesis in Rats. *Mol. Cel Biochem.* 395 (1), 65–76. doi:10.1007/s11010-014-2112-5

Suntres, Z. E., Coccimiglio, J., and Alipour, M. (2015). The Bioactivity and Toxicological Actions of Carvacrol. *Crit. Rev. Food Sci. Nutr.* 55 (3), 304–318. doi:10.1080/10408398.2011.653458

Swanton, E., Savory, P., Cosulich, S., Clarke, P., and Woodman, P. (1999). Bcl-2 Regulates a Caspase-3/caspase-2 Apoptotic cascade in Cytosolic Extracts. *Oncogene* 18 (10), 1781–1787. doi:10.1038/sj.onc.1202490

Tayarani-Najaran, Z., Akaberi, M., Hassanzadeh, B., Shirazi, N., Asili, J., Al-Najjar, H., et al. (2019). Analysis of the Essential Oils of Five Artemisia Species and Evaluation of Their Cytotoxic and Proapoptotic Effects. *Mini Rev. Med. Chem.* 19 (11), 902–912. doi:10.2174/1389557519666190311155021

Thakor, P., Subramanian, R. B., Thakkar, S. S., Ray, A., and Thakkar, V. R. (2017). Phytol Induces ROS Mediated Apoptosis by Induction of Caspase 9 and 3 through Activation of TRAIL, FAS and TNF Receptors and Inhibits Tumor Progression Factor Glucose 6 Phosphate Dehydrogenase in Lung Carcinoma Cell Line (A549). *Biomed. Pharmacother.* 92, 491–500. doi:10.1016/j.biopha.2017.05.066

Thapa, D., Richardson, A. J., Zweifel, B., Wallace, R. J., and Gratz, S. W. (2019). Genoprotective Effects of Essential Oil Compounds against Oxidative and Methylated DNA Damage in Human Colon Cancer Cells. *J. Food Sci.* 84 (7), 1979–1985. doi:10.1111/1750-3841.14665

Trindade, G. G. G., Thrivikraman, G., Menezes, P. P., França, C. M., Lima, B. S., Carvalho, Y. M. B. G., et al. (2019). Carvacrol/β-cyclodextrin Inclusion Complex Inhibits Cell Proliferation and Migration of Prostate Cancer Cells. *Food Chem. Toxicol.* 125, 198–209. doi:10.1016/j.fct.2019.01.003

Van Wyk, B., and Wink, M. (2018). *Medicinal Plants of the World*. Germany: CABI. University of Johannesburg, South Africa, Heidelberg University.

Wagner, E. F., and Nebreda, Á. R. (2009). Signal Integration by JNK and P38 MAPK Pathways in Cancer Development. *Nat. Rev. Cancer* 9 (8), 537–549. doi:10.1038/nrc2694

Wang, C., Jin, H., Gao, D., Lieftink, C., Evers, B., Jin, G., et al. (2018). Phospho-ERK Is a Biomarker of Response to a Synthetic Lethal Drug Combination of Sorafenib and MEK Inhibition in Liver Cancer. *J. Hepatol.* 69 (5), 1057–1065. doi:10.1016/j.jhep.2018.07.004

Wang, J., Su, B., Zhu, H., Chen, C., and Zhao, G. (2016). Protective Effect of Geraniol Inhibits Inflammatory Response, Oxidative Stress and Apoptosis in Traumatic Injury of the Spinal Cord through Modulation of NF-Kb and P38 MAPK. *Exp. Ther. Med.* 12 (6), 3607–3613. doi:10.3892/etm.2016.385010.3892/etm.2016.3850

Wang, X., and Wang, Q. (2018). Alpha-Fetoprotein and Hepatocellular Carcinoma Immunity. *Can. J. Gastroenterol. Hepatol.* 2018, e9049252. doi:10.1155/2018/9049252

Wang, Y., He, Q.-Y., and Chiu, J.-F. (2014). Dioscin Induced Activation of P38 MAPK and JNK via Mitochondrial Pathway in HL-60 Cell Line. *Eur. J. Pharmacol.* 735, 52–58. doi:10.1016/j.ejphar.2014.04.018

Weingart, S., Zhang, L., Sweeney, M., and Hassett, M. (2018). Chemotherapy Medication Errors. *Lancet Oncol.* 19 (4), 191–199. doi:10.1016/S1470-2045(18)30094-9

Whitfield, J. B. (2001). Gamma Glutamyl Transferase. *Crit. Rev. Clin. Lab. Sci.* 38 (4), 263–355. doi:10.1080/20014091084227

WHO (2007-2017). Ten Years in Public Health 2007-2017. World Health Organization; Report on Cancer: Setting Priorities, Investing Wisely and Providing Care for All. Available at: http://www.who.int/publications/10-year-review/en/ (Acesseced November 20, 2020).

Wiart, C. (2007). Ethnopharmacology of Medicinal Plants—Asia and the Pacific | Christophe Wiart | Springer. Available at: https://www.springer.com/gp/book/9781588297488 (Acesseced December 21, 2020).

Wong, R. J., Ahmed, A., and Gish, R. G. (2015). Elevated Alpha-Fetoprotein. *Clin. Liver Dis.* 19 (2), 309–323. doi:10.1016/j.cld.2015.01.005

World Health Organization (2020). Report on Cancer: Setting Priorities, Investing Wisely and Providing Care for All. Available at: https://www.who.int/publications/i/item/who-report-on-cancer-setting-priorities-investing-wisely-and-providing-care-for-all (Acesseced November 13, 2020).

Wu, Q., Wu, W., Fu, B., Shi, L., Wang, X., and Kuca, K. (2019). JNK Signaling in Cancer Cell Survival. *Med. Res. Rev.* 39 (6), 2082–2104. doi:10.1002/med.21574

Wullschleger, S., Loewith, R., and Hall, M. N. (2006). TOR Signaling in Growth and Metabolism. *Cell* 124 (3), 471–484. doi:10.1016/j.cell.2006.01.016

Yeh, J.-H., Chou, C-T., Chen, I-S., Lu, T., Lin, K-L., Yu, C-C., et al. (2017). Effect of Thymol on Ca̋(2+) Homeostasis and Viability in PC3 Human Prostate Cancer Cells. *Chin. J. Physiol.* 60 (1), 32–40. doi:10.4077/CJP.2017.BAF447

Yin, Q.-h., Yan, F.-x., Zu, X.-Y., Wu, Y.-h., Wu, X.-p., Liao, M.-c., et al. (2012). Anti-proliferative and Pro-apoptotic Effect of Carvacrol on Human Hepatocellular Carcinoma Cell Line HepG-2. *Cytotechnology* 64 (1), 43–51. doi:10.1007/s10616-011-9389-y

Yoo, J. y., Kim, C. H., Song, S. H., Shim, B. Y., Jeong, Y. J., Ahn, M. I., et al. (2004). Expression of Caspase-3 and C-Myc in Non-small Cell Lung Cancer. *Cancer Res. Treat.* 36 (5), 303–307. doi:10.4143/crt.2004.36.5.303

Yu, X., Zhang, R., Yang, T., Zhang, M., Xi, K., Lin, Y., et al. (2019). Alpha-l-fucosidase: a Novel Serum Biomarker to Predict Prognosis in Early Stage Esophageal Squamous Cell Carcinoma. *J. Thorac. Dis.* 11 (9), 3980–3990. doi:10.21037/jtd.2019.08.92

Zarubin, T., and Han, J. (2005). Activation and Signaling of the P38 MAP Kinase Pathway. *Cell Res.* 15 (1), 11–18. doi:10.1038/sj.cr.7290257

Zeng, L. P., Hu, Z. M., Li, K., and Xia, K. (2016). miR-222 Attenuates Cisplatin-induced Cell Death by Targeting the PPP 2R2A/Akt/mTOR Axis in Bladder Cancer Cells. *J. Cel. Mol. Med.* 20 (3), 559–567. doi:10.1111/jcmm.12760

Zeng, Q., Che, Y., Zhang, Y., Chen, M., Guo, Q., and Zhang, W. (2020). Thymol Isolated from *Thymus Vulgaris* L. Inhibits Colorectal Cancer Cell Growth and Metastasis by Suppressing the Wnt/β-Catenin Pathway. *Drug Des. Devel Ther.* 14, 2535–2547. doi:10.2147/DDDT.S25421810.2147/dddt.s254218

Zeytinoglu, H., Incesu, Z., and Baser, K. H. C. (2003). Inhibition of DNA Synthesis by Carvacrol in Mouse Myoblast Cells Bearing a Human N-RAS Oncogene. *Phytomedicine* 10 (4), 292–299. doi:10.1078/094471103322004785

Zhai, C.-L., Tang, G.-M., Qian, G., Hu, H.-L., Wang, S.-J., Yin, D., et al. (2019). MicroRNA-98 Attenuates Cardiac Ischemia-Reperfusion Injury through Inhibiting DAPK1 Expression. *IUBMB Life* 71 (2), 166–176. doi:10.1002/iub.1879

Zhang, H., Liu, H., Iles, K. E., Liu, R.-M., Postlethwait, E. M., Laperche, Y., et al. (2006). 4-Hydroxynonenal Induces Rat γ-Glutamyl Transpeptidase through Mitogen-Activated Protein Kinase-Mediated Electrophile Response Element/ Nuclear Factor Erythroid 2-Related Factor 2 Signaling. *Am. J. Respir. Cel Mol Biol* 34 (2), 174–181. doi:10.1165/rcmb.2005-0280OC

Zhang, L., Yu, J., Park, B., Kinzler, K., and Vogelstein, B. (2000). Role of BAX in the Apoptotic Response to Anticancer Agents. *Science* 290 (5493), 989–992. doi:10.1126/science.290.5493.989

Conflict of Interest: The authors declare that the research was conducted in the absence of any commercial or financial relationships that could be construed as a potential conflict of interest.

frontiers in Pharmacology

ORIGINAL RESEARCH
published: 04 August 2021
doi: 10.3389/fphar.2021.713332

Crotoxin Inhibits Endothelial Cell Functions in Two- and Three-dimensional Tumor Microenvironment

Ellen Emi Kato[1†], Luciana Araújo Pimenta[1†], Maíra Estanislau Soares de Almeida[1], Vanessa Olzon Zambelli[2], Marinilce Fagundes dos Santos[3] and Sandra Coccuzzo Sampaio[1,4]*

[1]Laboratory of Pathophysiology, Butantan Institute, São Paulo, Brazil, [2]Special Laboratory of Pain and Signaling, Butantan Institute, São Paulo, Brazil, [3]Institute of Biomedical Sciences, Department of Cell and Developmental Biology, University of São Paulo, São Paulo, Brazil, [4]Institute of Biomedical Sciences, Department of Pharmacology, University of São Paulo, São Paulo, Brazil

Antitumor property of Crotoxin (CTX), the major toxin from *Crotalus durissus terrificus* snake venom, has been demonstrated in experimental animal models and clinical trials. However, the direct action of this toxin on the significant events involved in neovascularization, which are essential for tumor growth and survival, has not been confirmed. This study investigated the effects of CTX on the key parameters of neovascularization in two- and three-dimensional culture models. Murine endothelial cell lines derived from thymus hemangioma (t.End.1) were treated at different concentrations of CTX (6.25–200 nM). Endothelial cell proliferation, cell adhesion, and actin cytoskeletal dynamics on laminin (10 µg/ml), type I collagen (10 µg/ml), and fibronectin (3 µg/ml) were evaluated along with the endothelial cell migration and formation of capillary-like tubes in 3D Matrigel. CTX concentration of 50 nM inhibited tube formation on 3D Matrigel and impaired cell adhesion, proliferation, and migration under both culture medium and tumor-conditioned medium. These actions were not accountable for the loss of cell viability. Inhibition of cell adhesion to different extracellular matrix components was related to the reduction of αv and α2 integrin distribution and cytoskeletal actin polymerization (F-actin), accompanied by inhibition of focal adhesion kinase (FAK), Rac1 (GTPase) signaling proteins, and actin-related protein 2/3 (Arp 2/3) complex. This study proved that CTX inhibits the major events involved in angiogenesis, particularly against tumor stimuli, highlighting the importance of the anti-angiogenic action of CTX in inhibition of tumor progression.

Keywords: crotoxin, endothelial cells, extracellular matrix, adhesion, migration

OPEN ACCESS

Edited by:
Rajeev K. Singla, Sichuan University, China

Reviewed by:
Guang Hu, Chongqing University of Technology, China
Xiaonan Zheng, Sichuan University, China
Shikha Joon, Sichuan University, China

****Correspondence:***
Sandra Coccuzzo Sampaio
Sandra.coccuzzo@butantan.gov.br

[†]These authors have contributed equally to this work

Specialty section:
This article was submitted to Ethnopharmacology, a section of the journal Frontiers in Pharmacology

Received: *22 May 2021*
Accepted: *22 July 2021*
Published: *04 August 2021*

Citation:
Kato EE, Pimenta LAújo, Almeida MESde, Zambelli VO, Santos MFdos and Sampaio SC (2021) Crotoxin Inhibits Endothelial Cell Functions in Two- and Three-dimensional Tumor Microenvironment. Front. Pharmacol. 12:713332. doi: 10.3389/fphar.2021.713332

INTRODUCTION

Angiogenesis is a complex process involving the formation of new blood vessels from preexisting endothelium and is regulated under both physiological and pathological conditions, by a range of anti-angiogenic and proangiogenic factors (Folkman and Haudenschild, 1980; Folkman 1995; Fierro, 2005). The overexpression of angiogenic factors and down-regulation of angiogenic inhibitors, known as the "angiogenic switch," is particularly essential for tumor progression (Folkman, 2002; Dass et al., 2007). Besides growth factors, tumor angiogenesis is also regulated by cell-cell and cell-

extracellular matrix interactions mediated by adhesion receptors like cadherins and integrins (Eliceiri and Cheresh, 1998). Intracellular signaling, based on a microenvironment-induced modulation, coordinates the different cellular functions, including proliferation, differentiation, and migration (McCarty, 2020). Integrins are transmembrane receptors for several extracellular matrix (ECM) components such as laminin, collagen, and fibronectin connecting the ECM to the cytoskeleton; integrins also mediate this signaling (Barczyk et al., 2010; Schlie-Wolter et al., 2013; McCarty, 2020). The endothelial cell-ECM interaction mediated by integrins promotes intracellular signal transduction, cytoskeleton reorganization, and alterations in cell behavior, such as stimulation of endothelial cell proliferation, migration, and invasion (Varinska et al., 2017; Viallard and Larrivee, 2017). The literature reports that endothelial cells proliferate 50–200 times faster in a tumor microenvironment and express specific molecules, which may become a pharmacological target, without affecting the integrity of healthy vessels. A single vessel can support about 100 tumor cells. Thus, destroying this structure may eradicate a considerable number of tumor cells (Dass et al., 2007).

Additionally, endothelial cells in the tumor microenvironment are genetically stable and are less likely to accumulate mutations that allow drug resistance (Boehm et al., 1997). Thus, targeting tumor neovascularization is an attractive strategy for cancer therapy (Hood et al., 2002). Several animal venoms have been identified as an alternative strategy for anticancer therapies (Varinska et al., 2017). Venoms are a complex mixture of bioactive chemical substances, mainly proteins, and peptides rich in disulfide, with several pharmacological actions, making it an efficient anticancer agent. Also, venoms exhibit specificity and possess the ability to modify their molecular targets, making them good therapeutic candidates (Chatterjee, 2018). Snake venoms are a natural source of molecules that modulate cell-ECM interaction orchestrated by integrins; two large Viper venom molecules considered integrin antagonists include disintegrins and C-type lectin proteins (Marcinkiewicz, 2013). However, phospholipases A2 (PLA2-EC: 3.1.1.4) derived from snake venoms possess antitumor activity owing to their inhibitory action against several tumor cells (Rudrammaji and Gowda, 1998; Kang et al., 2000; Rodrigues et al., 2009). The cell-cell interactions (Kang et al., 2000), along with cell adhesion and migration functions (Zouari-Kessentini et al., 2009), are not necessarily dependent on their catalytic activity (Stabeli et al., 2006).

Crotoxin (CTX) is the most abundant toxin (nearly 60% of the total venom) in *Crotalus durissus terrificus* (Laurenti, 1768) venom (CdtV). It is a heterodimeric β-neurotoxin, formed by the non-covalent association of two different subunits: an acid denominated as CA (Crotoxin A) or crotapotin and a base named CB (Crotoxin B) or phospholipase A2. Several studies have shown that CTX has immunomodulatory, anti-inflammatory, antimicrobial, analgesic, and antitumor effects (Sampaio et al., 2010; Sartim et al., 2018). Antitumor activity of CTX has been demonstrated particularly on tumor cells, in both *in vitro* and *in vivo* experimental trials, as well as in clinical trials (Rodrigues et al., 2009; Sampaio et al., 2010). CTX has shown significant regression of various tumors, particularly solid tumors, in clinical trials, besides pain relief and improvement in overall clinical status (Costa et al., 1998; Cura et al., 2002). This inhibitory activity has also been evidenced in experimental models aimed at characterizing the mechanisms involved in the antitumor effects of CTX. *In vitro* studies have highlighted that CTX incubation in different tumor cell lines induces significant inhibition on the proliferation of murine and human tumor cells, including decreased expression of receptors for growth factors, cytotoxic activity, mitochondrial membrane potential, necrosis, and autophagy (Newman et al., 1993; Rudd et al., 1994; Donato et al., 1996; Kang et al., 2000; Papo and Shai, 2003; Yamazaki et al., 2005). On the other hand, *in vivo* experimental models have indicated that the prolonged inhibitory action of CTX promotes the reduction of solid tumors (Faiad, 2012; Brigatte et al., 2016) and ascites tumor (Nunes et al., 2010; Neves et al., 2019). The significance of CTX immunomodulatory activity on macrophages in the tumor microenvironment has been demonstrated as the most marked inhibitory effect on solid tumor development and progression (de Araujo Pimenta et al., 2019). The inhibitory effect of CTX on neovascularization induced by the tumor could significantly contribute to the antitumor action described for this toxin. The present study is the first to demonstrate the direct action of CTX on endothelial cell functions with specificities of the tumor microenvironment, confirming the notable contribution of the anti-angiogenic action to the antitumor effect of this toxin.

MATERIALS AND METHODS

Isolation of Crotoxin

Purification and phospholipase activity of the CTX was performed as described in previous studies (Fraenkel-Conrat and Singer, 1956; Laemmli, 1970; Lobo de Araujo and Radvanyi, 1987; Faure and Bon, 1988; Sampaio et al., 2003; Sampaio et al., 2006a; Sampaio et al., 2006b; Brigatte et al., 2016; de Araujo Pimenta et al., 2019). Briefly, crude venom solution (CdtV) was subjected to anion-exchange chromatography, using a Mono-Q HR 5/5 column in an FPLC system (Pharmacia, Uppsala, Sweden). The fractions (1 ml/min) were eluted using a linear gradient of NaCl (0–1 mol/L in 50 mmol/L Tris-HCl, pH 7.0). Three peaks (p1, p2 and p3) were obtained: p2 corresponded to the pure CTX fraction (about 60% of the crude venom); peaks 1 and 3 included the other CdtV toxins. Before pooling, the fractions containing CTX were tested for homogeneity by non-reducing sodium dodecyl sulphate-polyacrylamide gel electrophoresis (12.5%) and the phospholipase A2 activity was assessed by a colorimetric assay using a synthetic chromogenic substrate.

Cell Culture

Murine endothelial cells derived from thymus hemangioma (t.End.1) were obtained by courtesy of Dr. Ana Maria Moura (Laboratory of Immunopathology, Butantan Institute, Brazil). The cell line t.End.1 was derived from a thymic hemangioma expressing the polyoma middle T antigen, which is highly tumorigenic and bears functional characteristics similar to

those found in angiogenic endothelial cells (Aurrand-Lions et al., 2004; Bussolino et al., 1991; Williams et al., 1988). Cells were cultivated in 75 cm^2 flasks in the presence of RPMI 1640 (Gibco, Grand Island, NY, United States) media supplemented with 10% fetal bovine serum (FBS), 2 mM L-glutamine, 100 U/mL penicillin, 100 U/mL streptomycin (all Gibco) having a pH 7.4, incubated at 37°C enriched with 5% CO_2. In all experiments, t.End.1 cells were used between the second and fourth cell passage.

Human breast adenocarcinoma cell line MCF-7 (ATCC® HTB22) were seeded at a density of 1×10^6 in 75 cm^2 flasks in the presence of RPMI 1640 (Gibco, Grand Island, NY, United States) media supplemented with 10% FBS, 2 mM L-glutamine, 100 U/mL penicillin, 100 U/mL streptomycin (all Gibco), at a pH 7.4, incubated at 37°C, enriched with 5% CO_2 for growth and semiconfluence. Cells were rinsed twice in phosphate-buffered saline (PBS) and incubated in RPMI 1640 medium containing 2% FBS. Three days later, MCF-7 conditioned medium (MCF-7-CM) was collected, centrifuged for 10 min at 1200 rpm, filtered through a 0.22 µm pore size filter and stored at −20°C until use. In all experiments, MCF-7 cells were used in the second or third cell passage.

Cell Proliferation and Viability

t.End.1 cells (5×10^4/ml/well) were seeded into a six-well plate in the presence of RPMI 1640 medium and 10% FBS and left overnight at 37°C. Unattached cells were removed after washing with PBS, attached cells were treated with CTX at concentrations of 6.25, 12.5, 25, 50, 100, and 200 nM (corresponding to 0.15, 0.3, 0.6, 1.2, 2.4, and 4.8 µg/ml, respectively), for 24 or 1 h followed by 24 h incubation in fresh culture medium. The cells were then removed from the plate using 0.25% trypsin-EDTA. Cell viability was measured by the dye exclusion method using Trypan Blue. A Neubauer chamber was utilized to determine cell proliferation by cell counting.

Cell Adhesion Assay

96-well plates were coated with fibronectin (3 µg/ml), type I collagen (10 µg/ml), and laminin (10 µg/ml; Invitrogen, Carlsbad, CA, United States) and left overnight at 4°C. Wells were then washed thrice with PBS and blocked with 1% bovine serum albumin (BSA) in PBS for 2 h at 37°C. For all matrix components evaluated, a negative control (adhesion cells in BSA coating alone) was used to assess adherence to non-specific substrates. t.End.1 cells previously treated with CTX (50 nM) for 1 h in a single cell suspension (1×10^6/ml) were added to the wells and allowed to adhere to the substrate for 1 h at 37°C with 5% CO_2. After incubation, unattached cells were eliminated by rinsing the well with PBS, while the attached cells were incubated with 5 mg/ml MTT for 3 h at 37°C. Formazan crystals obtained by MTT reduction were dissolved by the addition of 100 µl PBS containing 10% SDS and 0.01 M HCl (18 h, 37°C, 5% CO_2). The absorbance was read at 595 nm in an ELISA plate reader (Multiskan EX, LabSystem). The number of cells was estimated using the absorbance of a standard curve of known number of fresh live cells added to the plates just before staining (Costa et al., 2013).

Cell Scratch Wound Healing Assay

A confluent monolayer of t.End.1 (1×10^6) was formed on the coverslips in 24-well plates previously coated with type I collagen (10 µg/ml), and a wound was made using a sterile cell lifter. Next, t.End.1 cells were incubated for 1 h in the presence of CTX (6.25–100 nM). The cells were then washed with PBS and further incubated in the presence of RPMI media containing 1% FBS. After 6, 12 and 24 h of incubation, migrated endothelial cells were stained with Rosenfeld and photographed and quantified with ImageJ software by measuring the area of the cell that moved beyond the reference line. For counting the migrating cells in the field induced by the probe, the images were inserted into the rules on the left and right edges of the field, based on the image obtained in the T0 coverslip. After insertion of dashed lines, the count of migrating cells in the field was performed (de Araujo Pimenta et al., 2019).

Chemotaxis in the Transwell Model

Transwell inserts (6.5 mm diameter) with an 8 µm pore (Costar, Cambridge, MA, United States) were used to assess the *in vitro* directional migration of t.End.1 cells in response to a gradient of soluble chemoattractants. The membranes were hydrated with serum-free culture media for 45 min at 37°C, containing 5% CO_2. Next, t.End.1 cells (1×10^5) previously treated with CTX (50 nM) for 1 h were added to the upper side of the inserts in 200 µl serum-free media. The lower chamber was filled with 600 µl of RPMI media supplemented with 2% FBS or MCF-7-CM, which holds high secretory activity for various substances, including chemokines (Garrido et al., 1995; Shih et al., 2012). After 5 h of cell migration at 37°C with 5% CO_2, non-migrated cells were removed from the upper side of the membrane by cotton swabs. Cells migrated to the lower side were fixed with methanol for 15 min and stained with 0.5% crystal violet for 15 min. After several washing steps with PBS to remove excess amounts of crystal violet dye, cell migration was quantified, and cells were counted from photographs taken under phase contrast microscope in five random fields per insert.

Capillary-Like Structure Formation Assay on 3D-Matrigel

According to the method described by Arnaoutova and Kleinman (2010), 50 µl of Matrigel (9.3 mg/ml; BD Biosciences, New Bedford, MA, United States) was added to a 96-well culture plate and allowed to polymerize for 45 min at 37°C. Subsequently, t.End.1 cells previously treated with CTX (50 nM) were plated on top of the Matrigel at a density of 1.5×10^4/well in the RPMI medium comprising 2% FBS and incubated for 6 h at 37°C. Tube formation was observed through an inverted phase-contrast microscope (Nikon Eclipse TS100) and photographed with a DS-Fi2 camera, using the Nis-Element D software. Quantification was carried out by counting all branches in five random fields from each well.

Cell Migration Assays by Time-Lapse Video Microscopy

TTP® 24-well plates were coated with type I collagen (10 μg/100 μl) for 30 min at 37°C. The plates were then washed thrice using PBS, and 1×10^3 cells/well were plated and incubated in RPMI media for 24 h. Next, cells were incubated in the absence (control) or presence of CTX (50 nM) for 1 h. Subsequently, the cells were washed and incubated only in the presence of a fresh culture medium. The plates were incubated and coupled to the IN Cell Analyzer GE 2200 equipment in a ×10 air objective lens; for at least 18 h, eight fields/well (six wells for every treatment) were recorded every 5 min to evaluate t.End.1 cell speed, relative distance, and directionality. Image acquisition was performed using Analyzer 2200, version 1.6.3. The ImageJ plugin manual tracking was employed to track cell nuclei. Hence, the velocity of the cells was analyzed; the net distances per hour were calculated and summed up to determine the total cell path length (Hauff et al., 2015; de Araujo Pimenta et al., 2019). Since the trajectory of individual cells was monitored, directionality was evaluated by calculating the D/T ratio (0–1), which is the ratio between the smallest distance between the initial and final position of the cell (D) by the total distance traveled (T). The effectiveness of migration is improved when directionality is high.

Confocal Microscopy Analysis of Integrins Distribution and Actin Cytoskeleton Arrangement

Coverslips, previously coated with fibronectin (3 μg/ml), type I collagen (10 μg/ml), and laminin (10 μg/ml) were plated by CTX treated t.End.1 cells (5×10^4/well) and incubated overnight at 37°C with 5% CO_2 in the presence of MCF-7-CM or RPMI media supplemented with 10% FBS. Subsequently, the cells were fixed in 4% paraformaldehyde and 5% sucrose in PBS buffer for 10 min, rehydrated with PBS (3 × 10 min) and then permeabilized with 0.2% Triton X-100 for 10 min. Unspecific binding sites were blocked with 2% BSA diluted in PBS for 1 h at room temperature (RT). After that, t.End.1 cells were incubated with primary rabbit antibodies against αv integrin for fibronectin coating and α2 integrin for type I collagen coating (both antibodies from Millipore, Billerica, MA, United States) for 1 h at RT. After washing, secondary antibodies (Goat anti-rabbit Alexa 488, 1: 800; Invitrogen, Carlsbad, CA, United States) and rhodamine phalloidin (1:800; Molecular Probes, Burlington, CA, United States) were applied for 1 h at RT. Negative controls consisted of the absence of primary antibodies. The coverslips were washed twice in PBS, mounted with Vectashield® (Vector Labs, Burlingame, CA, United States) and observed using a Zeiss confocal inverted microscope (Zeiss LSM-510) (Butantan Institute, São Paulo, Brazil).

SDS/PAGE and Western Blot Analysis

The t.End.1 cells previously treated with 50 nM of CTX for 1 h were harvest and lysed in Radioimmunoprecipitation assay (RIPA) buffer (R0278; Thermo Scientific) containing 1:300 protease and phosphatase inhibitor cocktail (P8340, P5726, P0044; Sigma-Aldrich) and incubated on ice for 30 min. Cell lysates were homogenized and then centrifuged at 16,000 × g at 4°C for 20 min. The supernatant was collected and protein concentration was measured using BCA Protein Assay. Protein extracts (30 μg) were denatured in Laemmli buffer, incubated at 95°C for 4 min and then, were separated into 4–20% polyacrylamide gels (Bio-Rad). After electrophoresis, samples were transferred to a nitrocellulose membrane (Bio-Rad). The membranes were blocked in Tris Buffered Saline with 0.1% Tween® 20 (TBST) containing 5% BSA for 2 h at RT and then incubated with anti-FAK antibody (1:1000; BD Biosciences), anti-Arp2/3 (1:1000; Abcam), anti-F-actin (1:500; Abcam), anti-Rac1 (1:1000; Abcam), anti-MMP-2 (1:2000; Millipore) and anti-MMP-9 (1:2000; Millipore) overnight at 4°C The membranes were then incubated in the peroxidase-conjugated secondary antibody (1:5000; anti-rabbit or anti-mouse) for 2 h at RT. Enhanced Chemoluminescence kit (Thermo Scientific) was used for detection. The signals were detected using an image acquisition system (Uvitec mod Alliance 9.7; Uvitec, Cambridge, United Kingdom). Band intensities were measured using ImageJ (NIH) software. Targeted bands were normalized to the GAPDH antibody (1:5000; Abcam).

Measurement of VEGF, MMP-2 and Pro-MMP-9

Endothelial cells were treated with 50 nM CTX and then incubated in RPMI or MCF-7 tumor-conditioned media for 24 h. The supernatant was collected, and the concentration of the VEGF, MMP-2 and pro-MMP-9 thus secreted, was measured using an enzyme-linked immunosorbent assay (ELISA, Abcam Elisa Kit).

Statistical Analysis

GraphPad InStat software version 3.01 (GraphPad Software Inc., San Diego, CA, United States) was used (Glantz, 1997) for the statistical analyses. Multiple comparisons analyses (for all pairs of groups) were performed using one-way analysis of variance (ANOVA) followed by Tukey's post test. Results from other assays were analyzed using ANOVA and then Bonferroni's test for multiple comparisons against a single control. An unpaired Student's t-test or Mann Whitney test was performed to compare two groups. A p-value <0.05 was considered statistically significant. The results have been demonstrated as mean value ± standard errors of means.

RESULTS

CTX Inhibits Proliferation and Adhesion of t.End.1 Cells to Different Extracellular Matrix Ligands

Initially, the proliferative capacity of t.End.1 cells were evaluated 24 h after incubation in the presence of CTX at different concentrations. A significant inhibition of endothelial cell growth was observed at concentrations of 12.5 nM (29%),

25 nM (38%), 50 nM (62%), 100 nM (44%), and 200 nM (24%), compared to the control group, consisting of t.End-1 cells incubated only in the presence of RPMI 1640 medium, under the same experimental conditions. Only the 6.25 nM concentration did not affect the number of cells (**Figure 1A**). To evaluate whether short incubation in the presence of CTX would have the same inhibitory effect as observed in long incubation, t.End.1 cells were pretreated with CTX for 1 h at the same concentrations and subsequently washed and incubated only in the presence of fresh culture medium for 24 h. The results demonstrated that CTX significantly inhibited the proliferative capacity of t.End.1 cells at concentrations of 25 nM (39%), 50 nM (61%), 100 nM (51%), and 200 nM (27%) compared to the control group, consisting of t.End-1cells incubated only in the presence of RPMI 1640 medium, under the same experimental conditions. CTX concentrations of 6.25 and 12.5 nM showed inhibition of 17 and 18%, respectively, but were not considered statistically significant in comparison to the control group, incubated only in the presence of RPMI culture medium (**Figure 1B**). Cell viability test (1% Trypan blue exclusion) was performed after the assays, both on cells incubated with culture medium (control) and CTX. The viability of all cells was more than 98% (data not shown). Based on these results, for the accomplishment of other assays t.End.1 cells were treated with CTX beforehand for 1 h.

To investigate the action of CTX on t.End.1 cell adhesion on different natural ligands, main concentrations of the toxin that induced inhibition on the proliferation of t.End.1 cells were utilized. CTX at concentrations of 25, 50, and 100 nM inhibited (47, 64, and 72%, respectively) cell adhesion to type I collagen (10 μg/ml) significantly as compared to the control group (**Figure 1C**). On the other hand, endothelial cell adhesion on fibronectin coating (3 μg/ml) was significantly affected at CTX concentrations of 50 nM (33%) and 100 nM (28%), in comparison to the control group (**Figure 1D**). Unlike other matrix components, t.End.1 cells showed a lesser adhesion to

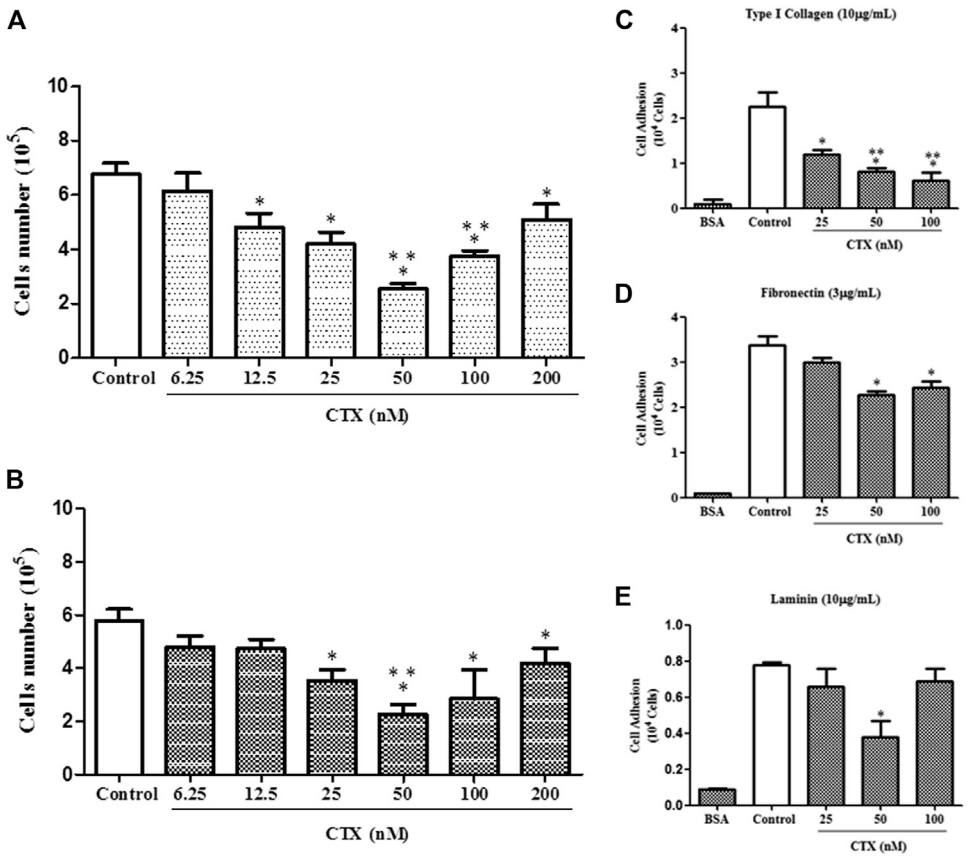

FIGURE 1 | Effect of CTX on t.End.1 cell proliferation and adhesion to extracellular matrix ligands. t.End.1 cells (5×10^4 cells/well) were incubated in the presence of different CTX concentrations (6.25, 12.5, 25, 50, 100 and 200 nM) for 24 h **(A)** or were previously incubated with the different concentrations for only 1 h and then washed and incubated for another 24 h only in fresh culture medium **(B)**. Cell proliferation was assessed after 24 h by cell counting. The data are presented from three distinct experiments run in octoplicate and are expressed as mean ± s.e.m. $^*p < 0.05$ compared to control group, $^{**}p < 0.05$ compared to other CTX concentrations. For adhesion assay, t.End.1 cells pretreated for 1 h with CTX (25, 50 and 100 nM) were washed and added (100 μl) to Maxsorp plates (Nunc®) containing 96 wells, previously sensitized with the different ligands of matrix: type I collagen (10 μg/ml) **(C)**; fibronectin (3 μg/ml) **(D)** and laminin (10 μg/ml) **(E)**. After 1 h, adhered cells were evaluated by MTT assay. The values obtained were fed into GraphPad INSTAT program V2.01 for conversion of optical density (OD) in the number of adhered cells. The data are presented from three distinct experiments run in sextuplicate and are expressed as mean ± s.e.m. $^*p < 0.05$, compared to control group and $^{**}p < 0.01$, significantly different from mean values for groups to their respective CTX-treated cells.

laminin (10 μg/ml) coating (**Figure 1E**). Furthermore, the inhibitory effect of CTX was observed only at a concentration of 50 nM (55%), relative to the control. Negative control (BSA coating) demonstrated that cell adhesion was ECM protein-dependent (**Figures 1C–E**).

CTX Decreases Migration in Wound Healing Model

Wound healing assay was used to evaluate the directional endothelial cell movement onto an empty field created by an interruption in the cell monolayer. After that, t.End.1 cells were treated with different concentrations of CTX (6.25–100 nM) for 1 h. Subsequently, cells were incubated in culture medium for 6, 12, and 24 h. The significant inhibitory action of CTX on t.End.1 cell migration was observed at concentrations of 50 and 100 nM (59 and 33%, respectively) after 6 h, as compared to the control cells (**Figure 2A**). As compared to other concentrations (6.25 nM: 55%, 25 nM: 54%, 50 nM: 46%, and 100 nM: 39%), CTX significantly inhibited cell migration at a concentration of 50 nM within 6 h (**Figure 2A**). In the 12 h period, the inhibitory action of CTX at concentrations of 50 and 100 nM was again significant, in comparison to the control cells (35 and 21%, respectively) and with the other concentrations (6.25 nM: 49 and 38%, respectively and 12.5 nM: 49 and 39%, respectively) (**Figure 2A**). Following 24 h of incubation, cell migration was significantly inhibited when pretreated at concentrations of 50 and 100 nM (47%), in comparison to the control cells, and the concentration of 6.25 nM (**Figure 2A**). **Figure 2B** depicts the results obtained over the 24 h culture period, after 1 h pretreatment with 50 nM CTX. The time 0 h corresponds to the period in which the monolayer was interrupted. After 24 h, inhibited migration of t.End.1 cells into the empty field was observed following pretreatment with CTX.

CTX Prevents Capillary Structure Formation by t.End.1 Cells Grown in 3D-Matrigel and Compromises the t.End.1-Migratory Behavior on Type I Collagen in a 2D Assay Analyzed by Time-Lapse Method

The effect of CTX on the formation of endothelial cell capillary structures was evaluated in 3D-Matrigel (**Figure 3**). Control cells showed capillary structure formation after the second hour of incubation (data not shown). After 6 h, the t.End.1 cellular network thus formed presented fine, elongated structures, and cell-cell contact was established (**Figures 3A,B**, Panel Control). On the other hand, t.End.1 cells pretreated with CTX (50 nM) for 1 h demonstrated a 66% reduction in the ability to form capillary-like structures compared to control cells at the same incubation period. This result suggests that CTX promoted loss of cell-cell contact, possibly accompanied by cytoskeleton retraction, contributing to the reduction of capillary-like structures (**Figures 3A,B**, panel CTX).

A detailed analysis of the endothelial cell dynamic behavior during migration was analyzed by time-lapse microscopy, which allows measurement of individual parameters such as cell velocity, distance traveled (relative distance), and directionality. A 2D assay was performed where t.End.1 cells at low density were plated on dishes previously coated with a mixture of type I collagen (10 μg/ml) and 1% fibronectin (3 μg/ml). It was found that after 8 h of incubation, CTX reduced 25% of t.End.1 migration velocity at basal stimulus compared to the control group (22.95 ± 1.61 vs. 30.8 ± 3.7) (**Figure 3C**). Besides, CTX also decreased relative distance (**Figure 3D**) and directionality (**Figure 3E**) of t.End.1 cells (53 and 43%, respectively). **Figure 3F** represents the results obtained in the 8 h culture period, after pretreatment with 50 nM CTX for 1 h,

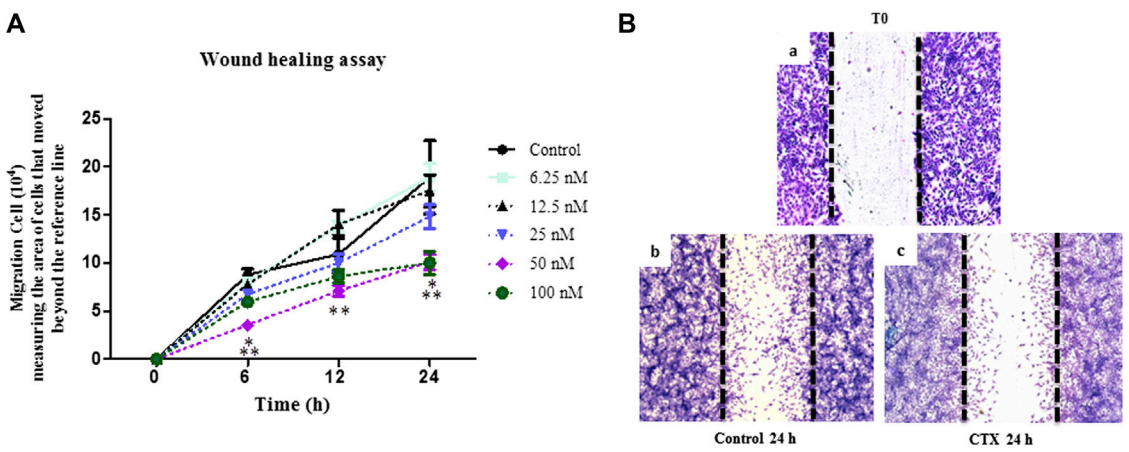

FIGURE 2 | Effect of CTX on t.End.1 migration in the Wound healing model at different treatment periods. Wound healing assay performed in t.End.1 cells treated with different CTX concentrations (6.25, 12.5, 25, 50, 100 and 200 nM) for 0, 6, 12 and 24 h at 37°C and 5% CO_2. **(A)** Results are expressed as Number of Migrated Cells and represent the mean ± s.e.m. The data are presented from three distinct experiments run in at least in triplicate each group. *$p < 0.05$ compared to the control group, **$p < 0.05$ compared to other CTX concentrations. **(B)** Photomicrographs obtained at time 0 and 24 h at ×10 magnification. The images were collected under an Olympus BX 51 microscope, using the Image-Pro Plus 5.1 software, in a ×10 objective.

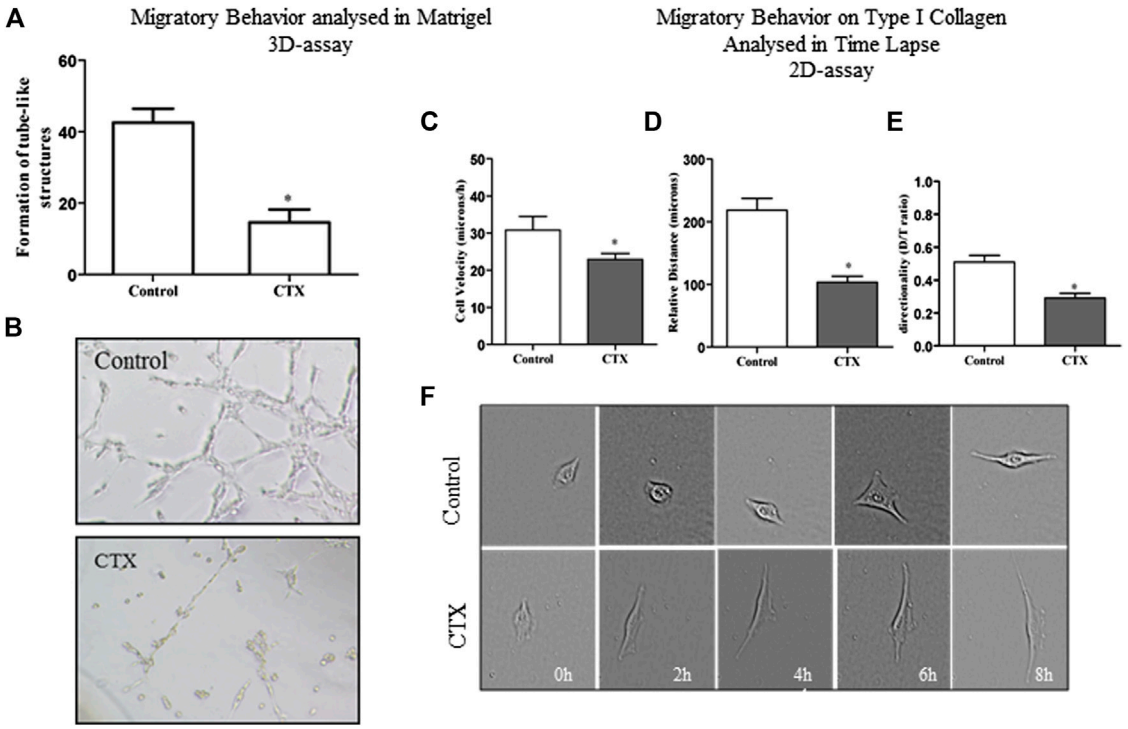

FIGURE 3 | Effect of CTX on the formation of tubule-like structures in 3D-matrigel and migratory behavior on type 2D-type I collagen evaluated in Time Lapse. CTX-pretreated t.End.1 cells were added on polymerized Matrigel in 96-well plates and incubated for 6 h. The results are expressed in a number of tubular structures and represent the count of five fields from triplicates of each group. The data are presented from three distinct experiments. *$p < 0.0001$, compared to the control group **(A)**. Photomicrograph of representative tube formation. Images obtained at the ×40 objective **(B)**. For the 2D-assay, time lapse images obtained from CTX pretreated t.End.1 cells migrating under collagen coating in In Cell Analyzer GE 2200 equipment in a ×10 objective for 18 h. The t.End.1 cell velocity **(C)**, relative distance **(D)**, and directionality **(E)** were measured. These parameters were evaluated using Image J software. Data are mean ± s.e.m. *$p < 0.05$ by comparison with the control group (n = 29) and CTX (n = 33). The graphs were plotted from the data collected during three independent experiments.

and control cells stimulated with RPMI 1640 medium supplemented with 2% FBS.

The Supplementary Material (**Supplementary Videos S1,S2**) projects the migratory capacity through time-lapse assay of the t.End.1 cells in a 2D-matrix of type I collagen and fibronectin mixture, cultured in the presence of the RPMI medium supplemented with 2% FBS for 8 h (**Supplementary Videos S1,S2**). The images depict that t.End.1 cells treated with CTX (**Supplementary Video S2**) exhibited altered migratory behavior and changed the cytoskeletal dynamics and the formation of lamellipodium-like structures, compromising cytoskeleton displacement and directionality *via* 2D coating.

CTX Impairs t.End.1 Migration Properties in MCF-7-Conditioned Medium

Migration in Wound Healing Model

Under basal stimulus (RPMI supplemented with 2% FBS), t.End.1 cells previously treated with CTX (50 nM) and incubated for 24 h demonstrated a significant reduction (52%) in endothelial cell migration (**Figures 4A,B**, a,b [if subparts are of B]). However, under tumor-derived factors stimulus by the use of tumor conditioned medium at the same experimental conditions, a 59% increase in the migratory capacity of t.End.1 cells was demonstrated compared to the basal stimulus group (**Figures 4A,B**, a,c [if subparts are of B]). Surprisingly, t.End.1 cells pretreated with CTX and subjected to the migration assay under tumor conditioned medium stimulus demonstrated a marked inhibitory effect (81%) compared to that in the control cells pretreated with RPMI supplemented with 2% FBS alone (**Figures 4A,B**, c,d [if subparts are of B]).

Migration in Transwell Model

As illustrated in **Figure 4C**, the control group demonstrated an increased cell migration (35%) under conditioned media with MCF-7 stimulus, in comparison to the control group stimulated with RPMI media having 2% FBS (**Figures 4C,D**, a,c [if subparts are of D]). Furthermore, t.End.1 cells treated with CTX (50 nM) for 1 h supported 41% inhibition of cell migration against the control group stimulated with MCF-7 conditioned medium (**Figures 4C,D**, c,d [if subparts are of D]). Regarding basal stimulus, although CTX showed 21% inhibition of the number of migrated cells, this difference was not statistically significant when compared to the control group (**Figures 4C,D**, a,b [if subparts are of D]).

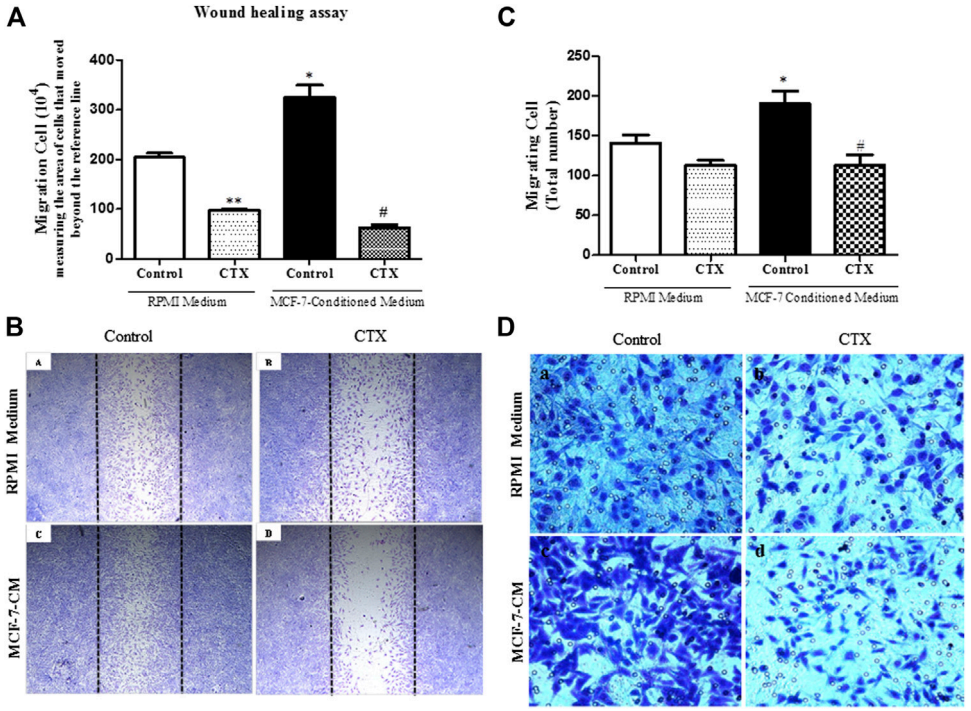

FIGURE 4 | Effect of the CTX on migration assay induced by MCF-7-Conditioned medium. **(A)** Wound healing assay performed in CTX-pretreated t.End.1 cells in the presence of RPMI medium containing 10% FBS (control) or in the presence of MCF-7-conditioned medium (chemotactic stimulation) for a period of 24 h. After this time, cells were fixed by the Rosenfeld panchromic method. A total of five random fields per coverslip were counted under a brightfield microscope (Standard 25; Carl Zeiss, Germany) using a ×10 objective. The results are expressed as Number of Migrated Cells and represent the mean ± s.e.m. The data are presented from three distinct experiments run in quadruplicate of each group. *p < 0.001 compared to RPMI control group. **p < 0.001 compared to RPMI control group. #p < 0.001 compared to MCF-7-CM control group. The images represented in **(B)** in Panels **(a–d)** were obtained in a ×5 objective. Panel **(a)** represents control cells incubated in RPMI 1640 medium with 10% FBS; Panel **(b)** represents cells treated with CTX and incubated in RPMI 1640 medium with 10% FBS; Panel **(c)** represents control cells incubated in MCF-7-CM and Panel **(d)** represents CTX treated cells and incubated in MCF-7-CM. For the Transwell assay, in **(C)** the number of migrating cells was determined by counting in five random fields per membrane using light microscopy. The results are expressed as Migrant Cells and represent the mean ± s.e.m. *p < 0.001 compared to RPMI control group. #p < 0.01 compared to MCF-7-CM control group. **(D)** The panels are representative of t.End.1 cell chemotaxis: **(a)** control in response to RPMI 1640 medium with 2% FBS; **(b)** CTX in response to RPMI 1640 medium with 2% FBS; **(c)** control in response to MCF-7-CM; **(d)** CTX in response to conditioned medium from MCF-7 tumor cells. The images were collected under an Olympus BX 51 microscope using the Image-Pro Plus 5.1 program, using a ×40 objective. The data are presented from three distinct experiments.

CTX Inhibits MMP-2 and VEGF Secretion and MMP-2 and MMP-9 Expression

CTX significantly inhibited the concentration of VEGF in t.End.1 cells in the presence of basal media and tumor conditioned media compared to the control (52 and 49%, respectively) (**Figure 5A**). The MMP-2 and MMP-9, which are related to the degradation of the basement membrane in the process of angiogenesis, demonstrated that CTX inhibited MMP-2 secretion under both the stimuli compared to its respective control (50 and 47%, respectively) (**Figure 5B**). Conversely, CTX did not have any effect on pro-MMP-9 secretion (data not shown). Western blotting analysis has shown the effect of CTX on MMP-9 and MMP-2 protein levels. Similar results were found on MMP-2 where CTX also inhibited MMP-2 expression by 37 and 41% under basal and tumor stimuli, respectively. Regarding MMP-9 protein expression, the anti-MMP-9 antibody detected both pro-MMP-9 and active MMP-9 as breakdown products, there is no detection of pro-MMP-9 expression level in the RPMI group and there is a mild expression in the TCM group which can be correlated to the finding of ELISA assay. However, the active MMP-9 expression levels were detected and were inhibited by CTX under both basal and tumoral stimuli (29 and 32%, respectively). (**Figures 5C,D**).

CTX Interferes in t.End.1 Filamentous Actin Organization Under Different Stimuli by Inhibiting Proteins Involved in the Signaling Pathway of Different Integrins

The filamentous actin (F-actin) cytoskeleton of t.End.1 cells, incubated overnight in RPMI medium with 2% FBS on both fibronectin (**Figure 6A**, a [if subparts are of A]) and type I collagen (**Figure 6B**, a [if subparts are of B]) showed a distinct cell cortex, a few actomyosin stress fibers (structures responsible for the production and transmission of mechanical stress) and, most notably, multiple projections in different directions (filopodia and lamellipodia). In the presence of MCF-7-CM control cells

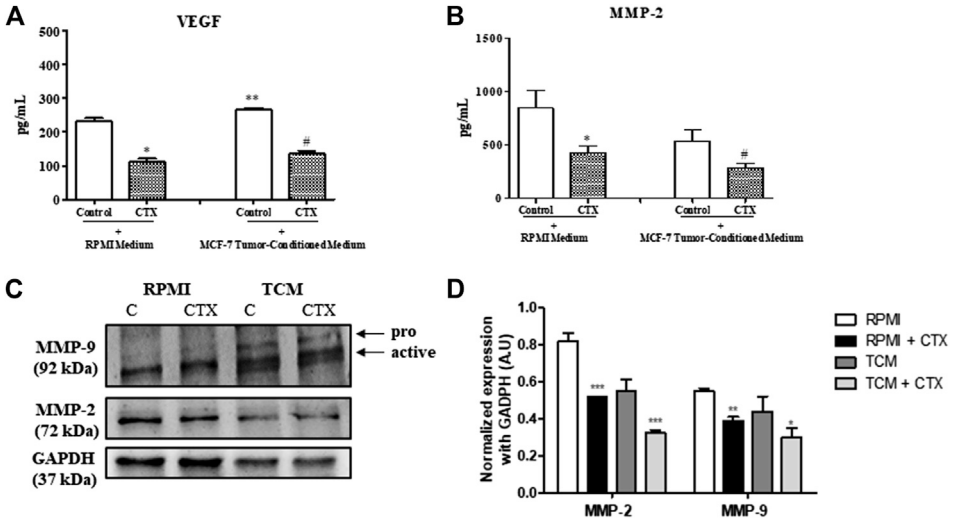

FIGURE 5 | Effect of CTX on the VEGF and MMPs. CTX-pretreated t.End.1 cells were incubated for 24 h in the presence of the fresh medium. Then, the supernatants were collected 99 for measurement of VEGF **(A)** and MMP-2 **(B)** concentrations by means of enzyme immunoassay (EIA) using a commercial kit. Data are mean ± s.e.m. Data are the average of four samples of each group ± s.e.m and represent two distinct trials. *$p < 0.01$, compared to RPMI control group. **$p < 0.05$, compared to RPMI control group, #$p < 0.01$, compared to MCF-7-CM. Western blotting analysis of protein expression levels of MMP-2 and MMP-9 **(C)**. The values were normalized by GAPDH expression and band intensities were quantified by densitometry of the homogenate Western blots **(D)** and represented the mean ± s.e.m. for three samples per group and represent three independent assays. *$p < 0.05$ by comparison with the respective control groups. **$p < 0.01$ by comparison with the respective control groups. ***$p < 0.001$ by comparison with the respective control groups.

showed a marked increase of stress fibers (SFs), becoming more contractile; on fibronectin, cells were apparently more polarized, showing a morphology that favors directional migration (**Figures 6A,B**, c [if subparts are of both A and B]). Treatment with CTX led to F-actin disorganization, dissolution of stress fibers and retraction of cellular projections, especially on fibronectin, under both the experimental conditions (RPMI-1640 and MCF-7-CM) (**Figures 6A,B**, b,d [if subparts are of B]).

The distribution of αv integrins on control and MCF-7-CM treated cells plated on fibronectin showed their presence in focal adhesions to the extracellular matrix, where stress fibers were inserted (**Figure 6A**, a,c [if subparts are of A]). Treatment with CTX on both experimental conditions (control and MCF-7-CM), maybe due to its collapsing effect on the F-actin cytoskeleton, led to an intracellular localization of this integrin subunit, with concentration in the perinuclear region (**Figure 6A**, b,d [if subparts are of A]).

Regarding the signaling proteins, CTX inhibited FAK (58%) and Rac1 (49%) expression with no effects on the levels of Arp2/3 (a Rac1 effector protein) and G-actin expression at basal condition. (**Figures 6C,D**). The Rac2 and Rac3 proteins have similar molecular weight, both being 21 kDa. Therefore, the other bands observed in the gel may be the product degradation of Rac 1 (**Figure 6C**). The effects of tumor-conditioned medium on control cells were a quite pronounced reduction on the expression of FAK and Arp 2/3 proteins, with no significant changes in Rac1 and actin filaments (**Figures 6C,D**). Cells pretreated with CTX and incubated in MCF-7-CM compared to MCF-7-CM control, showed higher inhibition of Arp2/3 (63%); the expression of Rac1, not previously affected by the tumor conditioned medium, was also reduced by CTX (43%) (**Figures 6C,D**). Science Identifiers (LSIDs) for ZOOBANK registered names or nomenclatural acts should be listed in the manuscript before the keywords with the following format:

DISCUSSION

The study demonstrated that CTX interferes with the functions of endothelial cells involved in tumor angiogenesis. The evaluation of whether this toxin could alter angiogenic events like the proliferation, adhesion, and migration activities of t.End.1 cells revealed that the presence of CTX affected the proliferative capacity of endothelial cells. The inhibitory effect was mainly observed at intermediate concentrations (25, 50, and 100 nM). These results have already been observed in other experimental models, where the median concentrations of the curve were found to be the most potent (Faiad et al., 2008). However, the inhibitory activity is probably not due to any cytotoxic effect of CTX on endothelial cells.

Cell proliferation depends on the degree of adhesion between the cell and its extracellular matrix ligand. It was noted that t.End.1 cells showed good adhesion to type I collagen and fibronectin, with values similar to those reported previously in the literature (Schlie-Wolter et al., 2013), and unlike that observed with these matrix components, the adhesiveness of t.End.1 was lower to laminin. Cell adhesion depends on the isoform of both integrin and laminin for specificity and affinity (Nishiuchi et al., 2006). Cell migration is an essential part of tumor progression. All CTX concentrations were assessed for endothelial cell migration. As the study was conducted in a wound healing model, it was possible to observe the inhibitory

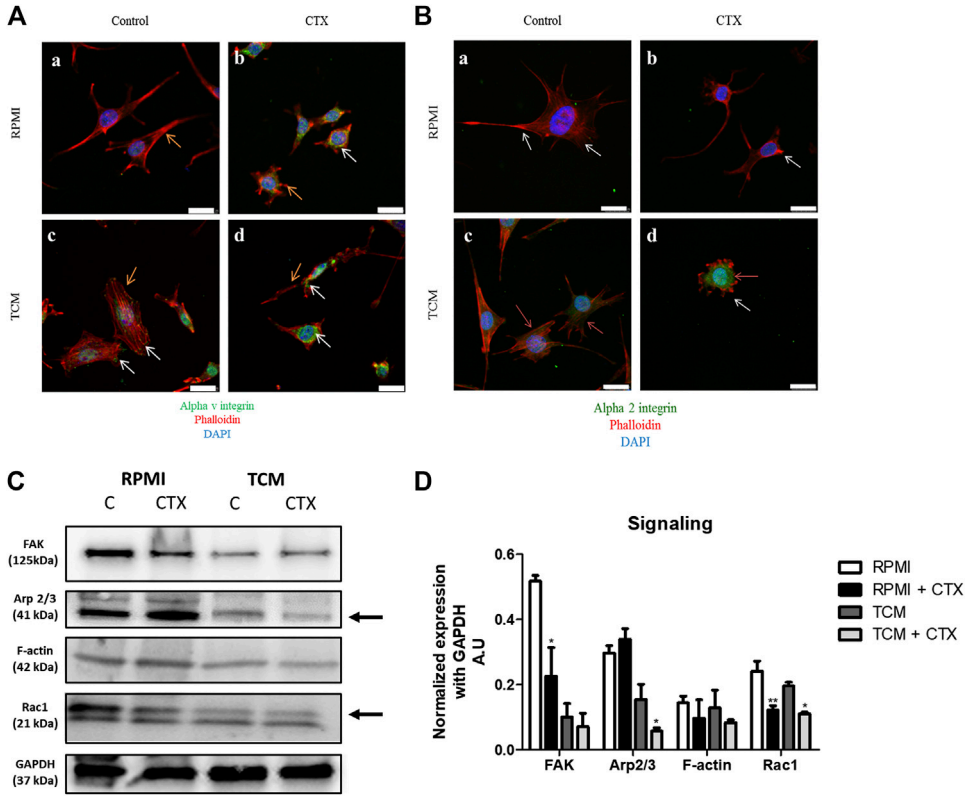

FIGURE 6 | Effect of CTX on actin cytoskeleton, intracellular signaling and integrin expression in t.End.1 endothelial cells in the different microenvironments. In **(A)**, marking of αv subunit (green) and F-actin (red) of control cells incubated with RPMI 1640 medium **(a)** or MCF-7-CM **(b)**. CTX-treated cells are labeled in **(b**,**d)**. In **(B)**, marking of α2 subunit (green) and F-actin (red) of control cells incubated with RPMI 1640 medium **(a)** or MCF-7-CM **(b)**. CTX-treated cells are labeled in **(b**,**d).** Orange arrows represent the expression of αv and α2 in the cell (green); White arrows represent the cytoskeleton protrusions (red). For details of the experiments, please see the Materials and Methods section. Scale bar: 25 μm. Western blotting was performed for the analysis shown in **(C)**, integrin-mediated signaling: FAK, Arp2/3, F-actin and Rac-1 expression levels. The values were normalized by GAPDH expression and band intensities were quantified by densitometry of the homogenate western blots and represented the mean ± s.e.m. for three samples per group and represent three separate assays **(D)**. $^{*}p < 0.05$ by comparison with the respective control groups. $^{**}p < 0.01$ by comparison with the respective control groups. $^{***}p < 0.001$ by comparison with the respective control groups.

capacity of CTX concentrations, particularly the 50 nM concentration, on cell migration induced in type I collagen coating. The results obtained after cell proliferation and migration tests in the wound healing model defined the use of 50 nM concentration for other experimental assays. Contributing to this negative effect on cell migration, CTX reduced cellular adhesion to collagen type I, fibronectin and laminin. Lowered expression of important integrins and cytoskeletal changes were related to reduced migration, with consequences to the ability of endothelial cells to form new vessels.

The capillary-like structure formation is an essential step in the angiogenesis process. Matrigel, a reconstituted basement membrane, was used to study *in vitro* angiogenesis as it allows rapid formation of capillary-like structures in a 3D system, being a simple and easily quantifiable technique (Arnaoutova et al., 2009; Bazaa et al., 2010). The presence of CTX also affected the formation of capillary-like structures. The toxin CTX altered endothelial cell morphology by preventing its projection to Matrigel. It can be suggested that Matrigel, derived from EHS murine sarcoma, provides conditions like those in the tumor microenvironment, allowing the rapid formation of tubular structures, as observed in this study. The results of this assay corroborate the data obtained in the adhesion and cell migration assays, which proposes that CTX affects the significant processes that depend directly on cytoskeleton reorganization.

The actin cytoskeleton is directly associated with the adhesive and migratory behavior of endothelial cells anchored to integrins that are adhesion molecules with bidirectional communication. Integrins allow the interaction between cells and extracellular matrix components (Weis and Cheresh, 2011), support the actin cytoskeleton's reorganization, and consequently, the cell migration, thus thriving the angiogenic process. Pretreatment with CTX reduced velocity and persistence in cells migrating on collagen type I, resulting in smaller distances traveled, corroborating the results observed using the wound healing assay. CTX also disorganized the actin cytoskeleton, and cells showed less stress fibers, shorter filopodia and smaller lamellipodia – all cellular processes important for cell migration.

The inhibitory action of CTX on the tumor stimulus was assessed by performing a migration assay using two *in vitro* models: wound healing and transwell system for chemotaxis. In the Wound healing test, migration is directional (stimulated by

the simulated wound), compared with the transwell model, which is directional migration stimulated by chemotaxis. At basal condition (in the presence of RPMI 1640 medium supplemented with 2% FBS), CTX at concentrations of 50 and 100 nM significantly inhibited cell migration from the 6thh onwards, 12thh, and the 24thh. Twenty-four hours is the maximum period analyzed in the wound healing model in all studies to date (Denker and Barber, 2002; Hotchkiss et al., 2002; Durham and Herman, 2009). The concentration of 50 nM caused the most remarkable inhibitory action among all. CTX entails its most striking actions at median doses in different cells (Faiad et al., 2008; Faiad et al., 2008; Lima et al., 2012; Costa et al., 2013). Thus, 50 nM concentration was used for the mediated supernatant wound healing assay obtained from tumor cells. At this concentration, CTX significantly inhibited cell migration induced by the MCF-7-CM. Similar results were obtained in the chemotaxis assay, demonstrating that CTX, at the concentration used, significantly inhibits the migration of endothelial cells against tumor stimulus. However, when basal conditions were used as a stimulus, no significant inhibition was observed. Notably, the conditioned medium used in the chemotactic factor migration assay was derived from a highly invasive human breast tumor line (MCF-7) owing to its ability to secrete various growth factors, including chemokines (Uddin et al., 2018), which are pro-inflammatory and modulate the angiogenic process (Romagnani et al., 2004).

Once the inhibitory action of CTX on functional events, like adhesion, proliferation, and migration of endothelial cells, including the tumor microenvironment was estimated, the mechanisms involved in this inhibitory activity were analyzed. Angiogenic functions of the endothelial cell involve the participation of integrins and their signaling pathways, coordinating both, the functions linked to the cytoskeleton, and the production and secretion of mediators (Bianconi et al., 2016; Guerrero and McCarty, 2018).

Accordingly, the concentrations of MMPs (MMP-2 and MMP-9) and VEGF were measured from the t.End.1 endothelial cell supernatants irrespective of whether they were pretreated with CTX (50 nM). It was revealed that CTX significantly reduced MMP-2 and VEGF secretion. An association between the MMP-2 and αvβ3 integrin was identified, suggesting the co-localization between these proteins on the membrane surface of endothelial cells (van Hinsbergh et al., 2006). Alternatively, this integrin captures latent MMP-2 to initiate extracellular matrix degradation (Brooks et al., 1996). Hence, it is proposed that the inhibitory action of CTX on αv subunit expression and distribution may contribute to the decreased secretion of this metalloproteinase by endothelial cells. The same inhibitory potential of CTX on MMP-2 secretion was observed against tumor stimulation. Although different studies have revealed the significance of MMP2 and MMP-9 in angiogenesis, mainly related to the tumor, the inhibitory action of CTX on pro-MMP-9 secretion was not observed in this study (data not shown). On the other hand, the expression levels of MMP-2 and active MMP-9 detected by western blotting demonstrated the significant inhibitory action of CTX and thus, reinforcing the capacity of this toxin in inhibiting crucial angiogenic-mediators.

As reported in the literature, αvβ3 integrin (RGD-recognizing integrins) can bind to different matrix components, including fibronectin and collagen I; this integrin is directly related to tumor angiogenesis (Hood and Cheresh, 2002; Bazaa et al., 2010). The integrin αvβ3 is expressed on the surface of endothelial cells (Aurrand-Lions et al., 2004; Davis and Senger, 2005). The main integrins responsible for the interaction between endothelial cell and collagen are α1β1 (preferentially recognizing type IV collagen) and α2β1 integrins, which mainly bind to type I collagen (Arlinghaus et al., 2013; Guerrero and McCarty, 2018) and laminin. After adhesion, these integrins alter the shape of these cells to promote cell migration (Languino et al., 1989; Davis and Senger, 2005; Guerrero and McCarty, 2018).

The immunofluorescence assay verified that CTX-treated endothelial cells altered the distribution of αv (fibronectin coating) and α2 (type I collagen and laminin coating) integrin subunits, in comparison to the control. Consequently, this alteration may have triggered changes in the actin cytoskeleton, promoting disruption in cell projection under laminin coating, disorganization, and reduction of SFs under collagen and fibronectin coating, respectively, compromising cytoskeleton contraction. Besides, punctual actin accumulation was observed in collagen and fibronectin coating. So, these actin cytoskeleton modulations and protrusions, promoted by the presence of CTX, may have been due to decreased migration-related intracellular signaling (Ridley et al., 2003) and possibly, decreased expression of integrin subunits. Consequently, low adhesion between endothelial cells and the matrix component prevented the generation of sufficient tensile force for efficient migration (Hood and Cheresh, 2002). In conditions stimulating the tumor, αv and α2 integrin subunits, in the presence of CTX, resulted in inhibition of endothelial cell projection, presenting a round shape and membrane ruffles with actin marked these immature adhesions. The α2 subunit distribution in collagen and laminin coating exhibited lower intensity accompanied by more significant retraction of the cell body, without the regular formation of protrusions; this characteristic corroborated the data obtained in the wound healing assay with tumor stimulation, which inhibited migration by 81%.

Binding of integrins to their ligands in the extracellular matrix changes the endothelial cell cytoskeleton conformation, and consequently, cell migration. This is modulated by intracellular signaling pathways like focal adhesion kinase (FAK), leading to activation of Rho GTPases proteins and phosphorylation of myosin light chain, responsible for cell contractility (Bryan and D'Amore, 2007; Bloom and Zaman, 2014). Inhibition of Rac1 stimulates RhoA activity (implicated with SFs), thus inhibiting the formation of lamellipodia and filopodia (structures associated with the cytoskeleton projections on the front and rear parts of the cell, respectively) (Bloom and Zaman, 2014; Burridge and Guilluy, 2016). The development of lamellipodium protrusions is dependent on the rapid polymerization of actin in filaments. The 2/3rd protein complex related to actin (Arp2/3) is a crucial regulator of this process, which is responsible for the nucleation of new actin

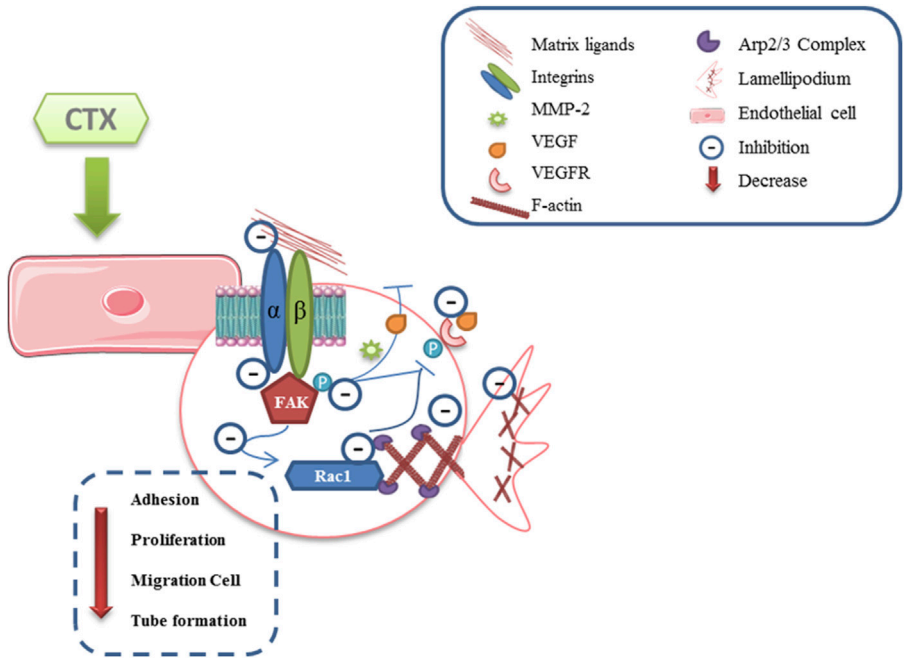

FIGURE 7 | Scheme proposed for anti-angiogenic effect directly induced by CTX. CTX exerts its inhibitory effect by decreasing endothelial cell adhesion to their matrix ligands and, consequently, interferes with FAK kinase phosphorylation, which may lead to the inhibition of Rho GTPases Rac1, since these effector proteins activate the regulation of cell proliferation, migration, and invasion. Moreover, the inhibitory action on signaling molecules such as FAK may lead to a significant decrease in the secretion of critical mediators for the development of angiogenesis, MMP-2, while reducing speed and persistence of migration in 3D matrices, and of the VEGF, in turn decrease the stimulus on the same receivers. Furthermore, both of inhibited αv and α2 subunits of the integrins, and the decrease in VEGF binding to VEGFR lead to the inhibition of the Arp2/3 complex, a key regulator in actin polymerization and stress fiber formation (Scheme based in Lamalice et al., 2015). Supplementary Material should be uploaded separately on submission, if there are Supplementary Figures, please include the caption in the same file as the figure. Supplementary Material templates can be found in the Frontiers Word Templates file.

filaments by providing the necessary force for membrane protrusion to enlarge the existing filaments (Pollard and Borisy, 2003; Pollard 2007; Burridge and Guilluy, 2016). Also, marked inhibitory activity of CTX (50 nM) on Rac1 and FAK expression and the Arp2/3 complex in endothelial cells was observed, which explains the inhibitory action on the cytoskeleton morphology and dynamics evidenced in immunofluorescence, Western Blotting, and time-lapse assays performed in this study.

CTX inhibited VEGF secretion in t.End.1 cells, irrespective of whether t.End.1 cells were incubated in the presence of culture medium or stimulated with tumor conditioned media. Decreased CTX secretion of VEGF may be a consequence of FAK inhibition as VEGF, a signaling molecule, is involved in the production of this mediator (Wary et al., 2012). Just as decreased VEGF secretion contributes to the inhibition of α2 subunit expression, and αv in particular, besides the fact that this mediator activates these integrins during angiogenic and lymphangiogenic processes (Avraamides et al., 2008), it may, therefore, generate negative feedback. Thus, the inhibitory action of CTX on FAK expression is crucial for the diminution of endothelial cell events associated with angiogenesis. These results, along with those obtained in immunofluorescence analyses, such as morphology, cytoskeleton polymerization, and cell extension, are strongly correlated with FAK inhibition, protein kinase capable of stimulating actin polymerization, and filopodia formation involving regulation of the proteins from the Rho GTPases family (Schlie-Wolter et al., 2013; Hohmann and Dehghani 2019). This hypothesis is based on data from previous studies that demonstrated that CTX could inhibit the expression of Rho GTPases in both the macrophages, inhibiting the translocation of RhoA and Rac1, interfering with the cytoskeleton efficiency in capturing particles to be phagocytized (Sampaio et al., 2006b). In tumor cells of the WRC 256 strain, CTX inhibited RhoA and FAK kinase (Faiad et al., 2008), thereby compromising the actin filament polymerization of these cells involved in the proliferation and adhesion of the tumor cell. As future perspectives, *in vivo* studies using tumor models will be necessary to confirm the mechanisms involved in CTX-induced inhibitory effect on endothelial cells functions, specially on the emergence of new vessels.

CONCLUDING REMARKS

The present study showed that CTX inhibits cell adhesion on different extracellular matrix components (**Figure 7**). This inhibition was related to the reduction of αv and α2 integrin distribution, and cytoskeletal actin polymerization (F-actin), accompanied by inhibition of FAK, Rac1 (GTPase) signaling

proteins. This was because these effector proteins activate the regulation of cell proliferation, migration, and invasion (Bryan and D'Amore, 2007; Hohmann and Dehghani, 2019). Furthermore, FAK inhibition induces a decrease in MMP-2 and VEGF secretion and MMP-2 and MMP-9 expression, while reducing the speed and persistence of migration in 3D matrices (Kim et al., 2008) and also inhibits the Arp 2/3 complex, an essential regulator for the polymerization of actin and the formation of lamellipodia (Lamalice et al., 2007). This study is the first to describe the direct inhibitory action of CTX on the critical events involved in angiogenesis and, therefore, contributes significantly to increasing knowledge on the mechanisms involved in the antitumor action of this toxin.

DATA AVAILABILITY STATEMENT

The original contributions presented in the study are included in the article/**Supplementary material**, further inquiries can be directed to the corresponding author/s.

AUTHOR CONTRIBUTIONS

LP carried out the cell migration studies, data collection and statistical analysis. MA and VZ participated in the molecular biology experiments. MS and SS helped in critically revising the draft for important intellectual content. All authors have checked and approved the final manuscript and agreed to be accountable for all aspects of the work in ensuring that questions related to the accuracy or integrity of any part of the work are appropriately investigated and resolved.

FUNDING

This work was supported by São Paulo Research Foundation (FAPESP) - Grants 2012/51241–5, 2013/07467-1 and 2007/52447. This study was financed in part by the Coordenação de Aperfeiçoamento de Pessoal de Nível Superior–Brasil (CAPES); National Council for Scientific and Technological Development – CNPq-Productivity grant (301685/2017-7) and fellowships CNPq and CNPq/PIBIC: 132761/2012–2 and Code 119030/2011-0, respectively.

ACKNOWLEDGMENTS

The authors gratefully acknowledge the financial support by São Paulo Research Foundation, Conselho Nacional de Desenvolvimento Científico e Tecnológico (CNPq) and Coordenação de Aperfeiçoamento de Pessoal de Nível Superior (CAPES). The authors also thank technical support of Mario Costa Cruz from CEFAP-USP, São Paulo, Brazil, for confocal microscopy and Incell Analyzer and Alexsander S. de Souza from Cellular Biology Laboratory, Butantan Institute, São Paulo, Brazil, for confocal microscopy.

SUPPLEMENTARY MATERIAL

The Supplementary Material for this article can be found online at: https://www.frontiersin.org/articles/10.3389/fphar.2021.713332/full#supplementary-material

REFERENCES

Arlinghaus, F. T., Momic, T., Ammar, N. A., Shai, E., Spectre, G., Varon, D., et al. (2013). Identification of α2β1 Integrin Inhibitor VP-I with Anti-Platelet Properties in the Venom of Vipera Palaestinae. *Toxicon.* 64, 96–105. doi:10.1016/j.toxicon.2013.01.001

Arnaoutova, I., George, J., Kleinman, H. K., and Benton, G. (2009). The Endothelial Cell Tube Formation Assay on Basement Membrane Turns 20: State of the Science and the Art. *Angiogenesis* 12 (3), 267–274. doi:10.1007/s10456–009–9146–410.1007/s10456-009-9146-4

Arnaoutova, I., and Kleinman, H. K. (2010). In Vitro Angiogenesis: Endothelial Cell Tube Formation on Gelled Basement Membrane Extract. *Nat. Protoc.* 5 (4), 628–635. doi:10.1038/nprot.2010.6

Aurrand-Lions, M., Johnson-Leger, C., Pepper, M. S., and Imhof, B. A. (2004). Haemangiomas Are Formed by Cells Expressing High Levels Of αvβ3 Integrin and Lacking Acetylated LDL Uptake. *J. Pathol.* 203 (2), 700–709. doi:10.1002/path.1571

Avraamides, C. J., Garmy-Susini, B., and Varner, J. A. (2008). Integrins in Angiogenesis and Lymphangiogenesis. *Nat. Rev. Cancer* 8 (8), 604–617. doi:10.1038/nrc2353

Barczyk, M., Carracedo, S., and Gullberg, D. (2010). Integrins. *Cell Tissue Res.* 339 (1), 269–280. doi:10.1007/s00441-009-0834-6

Bazaa, A., Pasquier, E., Defilles, C., Limam, I., Kessentini-Zouari, R., Kallech-Ziri, O., et al. (2010). MVL-PLA2, A Snake Venom Phospholipase A2, Inhibits Angiogenesis Through an Increase in Microtubule Dynamics and Disorganization of Focal Adhesions. *PLoS One* 5 (4), e10124. doi:10.1371/journal.pone.0010124

Bianconi, D., Unseld, M., and Prager, G. (2016). Integrins in the Spotlight of Cancer. *Int. J. Mol. Sci.* 17 (12), 2037. doi:10.3390/ijms17122037

Bloom, A. B., and Zaman, M. H. (2014). Influence of the Microenvironment on Cell Fate Determination and Migration. *Physiol. Genomics* 46 (9), 309–314. doi:10.1152/physiolgenomics.00170.2013

Boehm, T., Folkman, J., Browder, T., and O'Reilly, M. S. (1997). Antiangiogenic Therapy of Experimental Cancer Does Not Induce Acquired Drug Resistance. *Nature* 390 (6658), 404–407. doi:10.1038/37126

Brigatte, P., Faiad, O. J., Ferreira Nocelli, R. C., Landgraf, R. G., Palma, M. S., Cury, Y., et al. (2016). Walker 256 Tumor Growth Suppression by Crotoxin Involves Formyl Peptide Receptors and Lipoxin A4. *Mediators Inflamm.* 2016, 1–11. doi:10.1155/2016/2457532

Brooks, P. C., Strömblad, S., Sanders, L. C., von Schalscha, T. L., Aimes, R. T., Stetler-Stevenson, W. G., et al. (1996). Localization of Matrix Metalloproteinase MMP-2 to the Surface of Invasive Cells by Interaction with Integrin αvβ3. *Cell* 85 (5), 683–693. doi:10.1016/s0092-8674(00)81235-0

Bryan, B. A., and D'Amore, P. A. (2007). What Tangled Webs They Weave: Rho-GTPase Control of Angiogenesis. *Cell. Mol. Life Sci.* 64 (16), 2053–2065. doi:10.1007/s00018-007-7008-z

Burridge, K., and Guilluy, C. (2016). Focal Adhesions, Stress Fibers and Mechanical Tension. *Exp. Cel. Res.* 343 (1), 14–20. doi:10.1016/j.yexcr.2015.10.029

Bussolino, F., De Rossi, M., Sica, A., Colotta, F., Wang, J. M., Bocchietto, E., et al. (1991). Murine Endothelioma Cell Lines Transformed by Polyoma Middle T Oncogene as Target for and Producers of Cytokines. *J. Immunol.* 147 (7), 2122–2129. doi:10.1016/0192-0561(91)90283-d

Chatterjee, B. (2018). Animal Venoms Have Potential to Treat Cancer. *Curr. Top. Med. Chem.* 18 (30), 2555–2566. doi:10.2174/1568026619666181221120817

Costa, E. S., Faiad, O. J., Landgraf, R. G., Ferreira, A. K., Brigatte, P., Curi, R., et al. (2013). Involvement of Formyl Peptide Receptors in the Stimulatory Effect of Crotoxin on Macrophages Co-cultivated with Tumour Cells. *Toxicon.* 74, 167–178. doi:10.1016/j.toxicon.2013.08.057

Costa, L. A., Miles, H., Araujo, C. E., González, S., and Villarrubia, V. G. (1998). Tumor Regression of Advanced Carcinomas Following Intra-and/or Peri-Tumoral Inoculation with VRCTC-310 in Humans: Preliminary Report of Two Cases. *Immunopharmacol. Immunotoxicol.* 20 (1), 15–25. doi:10.3109/08923979809034806

Cura, J. E., Blanzaco, D. P., Brisson, C., Cura, M. A., Cabrol, R., Larrateguy, L., et al. (2002). Phase I and Pharmacokinetics Study of Crotoxin (Cytotoxic PLA(2), NSC-624244) in Patients with Advanced Cancer. *Clin. Cancer Res.* 8 (4), 1033–1041.

Dass, C. R., Tran, T. M. N., and Choong, P. F. M. (2007). Angiogenesis Inhibitors and the Need for Anti-Angiogenic Therapeutics. *J. Dent Res.* 86 (10), 927–936. doi:10.1177/154405910708601005

Davis, G. E., and Senger, D. R. (2005). Endothelial Extracellular Matrix. *Circ. Res.* 97 (11), 1093–1107. doi:10.1161/01.RES.0000191547.64391.e3

de Araújo, A. L., and Radvanyi, F. (1987). Determination of Phospholipase A2 Activity by a Colorimetric Assay Using a pH Indicator. *Toxicon.* 25 (11), 1181–1188. doi:10.1016/0041-0101(87)90136-x

de Araújo Pimenta, L., de Almeida, M. E. S., Bretones, M. L., Cirillo, M. C., Curi, R., and Sampaio, S. C. (2019). Crotoxin Promotes Macrophage Reprogramming Toward an Anti-Angiogenic Phenotype. *Sci. Rep.* 9 (1), 4281. doi:10.1038/s41598-019-40903-0

Denker, S. P., and Barber, D. L. (2002). Cell Migration Requires Both Ion Translocation and Cytoskeletal Anchoring by the Na-H Exchanger NHE1. *J. Cel. Biol.* 159 (6), 1087–1096. doi:10.1083/jcb.200208050

Donato, N. J., Martin, C. A., Perez, M., Newman, R. A., Vidal, J. C., and Etcheverry, M. (1996). Regulation of Epidermal Growth Factor Receptor Activity by Crotoxin, A Snake Venom Phospholipase A2 Toxin. *Biochem. Pharmacol.* 51 (11), 1535–1543. doi:10.1016/0006-2952(96)00097-4

Durham, J. T., and Herman, I. M. (2009). Inhibition of Angiogenesis In Vitro: A central Role for β-actin Dependent Cytoskeletal Remodeling. *Microvasc. Res.* 77 (3), 281–288. doi:10.1016/j.mvr.2008.12.003

Eliceiri, B. P., and Cheresh, D. A. (1998). The Role of αv Integrins During Angiogenesis. *Mol. Med.* 4 (12), 741–750. doi:10.1007/bf03401768

Faiad, O. J., Della-Casa, M. S., and Sampaio, S. C. (2008). "Lipoxin A4 Contributes to Inhibitory Effect of Crotoxin on Growth of Walker 256 Tumor," in X Annual Scientific Meeting, São Paulo, Brazil at Instituto Butantan, December 6th, 2008 (São Paulo: Instituto Butantan).

Faiad, O. J. (2012). *Efeito da Crotoxina sobre função e o metabolismo de glicose e glutamina de macrófagos durante a progressão tumoral*. São Paulo: Mestre, Departamento de Farmacologia, Instituto de Ciências Biomédicas, Universidade de São Paulo.

Faure, G., and Bon, C. (1988). Crotoxin, a Phospholipase A2 Neurotoxin from the South American Rattlesnake *Crotalus durissus* Terrificus: Purification of Several Isoforms and Comparison of Their Molecular Structure and of Their Biological Activities. *Biochemistry* 27 (2), 730–738. doi:10.1021/bi00402a036

Fierro, I. M. (2005). Angiogenesis and Lipoxins. *Prostaglandins, Leukot. Essent. Fatty Acids* 73 (3–4), 271–275. doi:10.1016/j.plefa.2005.05.016

Folkman, J. (1995). Angiogenesis in Cancer, Vascular, Rheumatoid and Other Disease. *Nat. Med.* 1 (1), 27–30. doi:10.1038/nm0195-27

Folkman, J., and Haudenschild, C. (1980). Angiogenesis In Vitro. *Nature* 288 (5791), 551–556. doi:10.1038/288551a0

Folkman, J. (2002). Role of Angiogenesis in Tumor Growth and Metastasis. *Semin. Oncol.* 29 (6 Suppl. 16), 15–18. doi:10.1053/sonc.2002.3726310.1016/s0093-7754(02)70065-1

Fraenkel-Conrat, H., and Singer, B. (1956). Fractionation and Composition of Crotoxin. *Arch. Biochem. Biophys.* 60 (1), 64–73. doi:10.1016/0003–9861(56)90397–610.1016/0003-9861(56)90397-6

Garrido, T., Riese, H., Aracil, M., and Pérez-Aranda, A. (1995). Endothelial Cell Differentiation into Capillary-like Structures in Response to Tumour Cell Conditioned Medium: A Modified Chemotaxis Chamber Assay. *Br. J. Cancer* 71 (4), 770–775. doi:10.1038/bjc.1995.149

Glantz, S. A. (1997). *Primer of Bio-Statistics*. New York, NY: McGraw Hill.

Guerrero, P. A., and McCarty, J. H. (2018). Integrins in Vascular Development and Pathology. *Adv. Pharmacol.* 81, 129–153. doi:10.1016/bs.apha.2017.08.011

Hauff, K., Zambarda, C., Dietrich, M., Halbig, M., Grab, A. L., Medda, R., et al. (2015). Matrix-Immobilized BMP-2 on Microcontact Printed Fibronectin as an In Vitro Tool to Study BMP-Mediated Signaling and Cell Migration. *Front. Bioeng. Biotechnol.* 3, 62. doi:10.3389/fbioe.2015.00062

Hohmann, T., and Dehghani, F. (2019). The Cytoskeleton-A Complex Interacting Meshwork. *Cells* 8 (4), 362. doi:10.3390/cells8040362

Hood, J. D., Bednarski, M., Frausto, R., Guccione, S., Reisfeld, R. A., Xiang, R., et al. (2002). Tumor Regression by Targeted Gene Delivery to the Neovasculature. *Science* 296 (5577), 2404–2407. doi:10.1126/science.1070200

Hood, J. D., and Cheresh, D. A. (2002). Role of Integrins in Cell Invasion and Migration. *Nat. Rev. Cancer* 2 (2), 91–100. doi:10.1038/nrc727

Hotchkiss, K. A., Ashton, A. W., Mahmood, R., Russell, R. G., Sparano, J. A., and Schwartz, E. L. (2002). Inhibition of Endothelial Cell Function In Vitro and Angiogenesis In Vivo by Docetaxel (Taxotere): Association with Impaired Repositioning of the Microtubule Organizing center. *Mol. Cancer Ther.* 1 (13), 1191–1200.

Kang, I.-C., Kim, D.-S., Jang, Y., and Chung, K.-H. (2000). Suppressive Mechanism of Salmosin, A Novel Disintegrin in B16 Melanoma Cell Metastasis. *Biochem. Biophysical Res. Commun.* 275 (1), 169–173. doi:10.1006/bbrc.2000.3130

Kim, H.-D., Guo, T. W., Wu, A. P., Wells, A., Gertler, F. B., and Lauffenburger, D. A. (2008). Epidermal Growth Factor-Induced Enhancement of Glioblastoma Cell Migration in 3D Arises from an Intrinsic Increase in Speed but an Extrinsic Matrix- and Proteolysis-dependent Increase in Persistence. *Mol. Biol. Cel.* 19 (10), 4249–4259. doi:10.1091/mbc.e08-05-0501

Laemmli, U. K. (1970). Cleavage of Structural Proteins during the Assembly of the Head of Bacteriophage T4. *Nature* 227 (5259), 680–685. doi:10.1038/227680a0

Lamalice, L., Le Boeuf, F., and Huot, J. (2007). Endothelial Cell Migration During Angiogenesis. *Circ. Res.* 100 (6), 782–794. doi:10.1161/01.RES.0000259593.07661.1e

Languino, L. R., Gehlsen, K. R., Wayner, E., Carter, W. G., Engvall, E., and Ruoslahti, E. (1989). Endothelial Cells Use Alpha 2 Beta 1 Integrin as a Laminin Receptor. *J. Cel. Biol.* 109 (5), 2455–2462. doi:10.1083/jcb.109.5.2455

Lima, T. S., Cataneo, S. C., Iritus, A. C. C., Sampaio, S. C., Della-Casa, M. S., and Cirillo, M. C. (2012). Crotoxin, A Rattlesnake Toxin, Induces A Long-Lasting Inhibitory Effect on Phagocytosis by Neutrophils. *Exp. Biol. Med. (Maywood)* 237 (10), 1219–1230. doi:10.1258/ebm.2012.012010

Marcinkiewicz, C. (2013). Applications of Snake Venom Components to Modulate Integrin Activities in Cell-Matrix Interactions. *Int. J. Biochem. Cel. Biol.* 45 (9), 1974–1986. doi:10.1016/j.biocel.2013.06.009

McCarty, J. H. (2020). αvβ8 Integrin Adhesion and Signaling Pathways in Development, Physiology and Disease. *J. Cel. Sci.* 133 (12), jcs239434. doi:10.1242/jcs.239434

Neves, C. L., Mauro, E. F. L., and Sampaio, S. C. (2019). *Crotoxin Modulates the Phenotypic Reprogramming of Quiescent Macrophages or Stimulated by Tumor Microenvironment*. São Pedro: XV Congress of the Brazilian Society of Toxinology.

Newman, R. A., Vidal, J. C., Viskatis, L. J., Johnson, J., and Etcheverry, M. A. (1993). VRCTC-310 ? A Novel Compound of Purified Animal Toxins Separates Antitumor Efficacy from Neurotoxicity. *Invest. New Drugs* 11 (2–3), 151–159. doi:10.1007/bf00874149

Nishiuchi, R., Takagi, J., Hayashi, M., Ido, H., Yagi, Y., Sanzen, N., et al. (2006). Ligand-binding Specificities of Laminin-Binding Integrins: A Comprehensive Survey of Laminin-Integrin Interactions Using Recombinant α3β1, α6β1, α7β1 and α6β4 Integrins. *Matrix Biol.* 25 (3), 189–197. doi:10.1016/j.matbio.2005.12.001

Nunes, F. P. B., Zychar, B. C., Della-Casa, M. S., Sampaio, S. C., Gonçalves, L. R. C., and Cirillo, M. C. (2010). Crotoxin Is Responsible for the Long-Lasting Anti-inflammatory Effect of *Crotalus durissus* Terrificus Snake Venom: Involvement of Formyl Peptide Receptors. *Toxicon.* 55 (6), 1100–1106. doi:10.1016/j.toxicon.2009.12.011

Papo, N., and Shai, Y. (2003). New Lytic Peptides Based on Thed,l-Amphipathic Helix Motif Preferentially Kill Tumor Cells Compared to Normal Cells†. *Biochemistry* 42 (31), 9346–9354. doi:10.1021/bi027212o

Pollard, T. D., and Borisy, G. G. (2003). Cellular Motility Driven by Assembly and Disassembly of Actin Filaments. *Cell* 112 (4), 453–465. doi:10.1016/s0092-8674(03)00120-x

Pollard, T. D. (2007). Regulation of Actin Filament Assembly by Arp2/3 Complex and Formins. *Annu. Rev. Biophys. Biomol. Struct.* 36, 451–477. doi:10.1146/annurev.biophys.35.040405.101936

Ridley, A. J., Schwartz, M. A., Burridge, K., Firtel, R. A., Ginsberg, M. H., Borisy, G., et al. (2003). Cell Migration: Integrating Signals from Front to Back. *Science* 302 (5651), 1704–1709. doi:10.1126/science.1092053

Rodrigues, R., Izidoro, L. F., de Oliveira Jr., R., Soares, A., Rodrigues, V., and Sampaio, S. (2009). Snake Venom Phospholipases A2: A New Class of Antitumor Agents. *Protein Pept. Lett.* 16 (8), 894–898. doi:10.2174/092986609788923266

Romagnani, P., Lasagni, L., Annunziato, F., Serio, M., and Romagnani, S. (2004). CXC Chemokines: The Regulatory Link Between Inflammation and Angiogenesis. *Trends Immunol.* 25 (4), 201–209. doi:10.1016/j.it.2004.02.006

Rudd, C. J., Viskatis, L. J., Vidal, J. C., and Etcheverry, M. A. (1994). In Vitro Comparison of Cytotoxic Effects of Crotoxin Against Three Human Tumors and a Normal Human Epidermal Keratinocyte Cell Line. *Invest. New Drugs* 12 (3), 183–184. doi:10.1007/bf00873958

Rudrammaji, L. M. S., and Gowda, T. V. (1998). Purification and Characterization of Three Acidic, Cytotoxic Phospholipases A2 from Indian Cobra (Naja naja naja) Venom. *Toxicon.* 36 (6), 921–932. doi:10.1016/s0041-0101(97)00097-4

Sampaio, S. C., Alba-Loureiro, T. C., Brigatte, P., Landgraf, R. G., Dos Santos, E. C., Curi, R., et al. (2006a). Lipoxygenase-Derived Eicosanoids Are Involved in the Inhibitory Effect of *Crotalus durissus* Terrificus Venom or Crotoxin on Rat Macrophage Phagocytosis. *Toxicon.* 47 (3), 313–321. doi:10.1016/j.toxicon.2005.11.008

Sampaio, S. C., Brigatte, P., Sousa-e-Silva, M. C. C., dos-Santos, E. C., Rangel-Santos, A. C., Curi, R., et al. (2003). Contribution of Crotoxin for the Inhibitory Effect of *Crotalus durissus* Terrificus Snake Venom on Macrophage Function. *Toxicon.* 41 (7), 899–907. doi:10.1016/s0041-0101(03)00069-2

Sampaio, S. C., Hyslop, S., Fontes, M. R. M., Prado-Franceschi, J., Zambelli, V. O., Magro, A. J., et al. (2010). Crotoxin: Novel Activities for a Classic β-neurotoxin. *Toxicon.* 55 (6), 1045–1060. doi:10.1016/j.toxicon.2010.01.011

Sampaio, S. C., Santos, M. F., Costa, E. P., Rangel-Santos, A. C., Carneiro, S. M., Curi, R., et al. (2006b). Crotoxin Induces Actin Reorganization and Inhibits Tyrosine Phosphorylation and Activity of Small GTPases in Rat Macrophages. *Toxicon.* 47 (8), 909–919. doi:10.1016/j.toxicon.2006.03.004

Sartim, M. A., Menaldo, D. L., and Sampaio, S. V. (2018). Immunotherapeutic Potential of Crotoxin: Anti-inflammatory and Immunosuppressive Properties. *J. Venom Anim. Toxins Incl. Trop. Dis.* 24, 39. doi:10.1186/s40409-018-0178-3

Schlie-Wolter, S., Ngezahayo, A., and Chichkov, B. N. (2013). The Selective Role of ECM Components on Cell Adhesion, Morphology, Proliferation and Communication In Vitro. *Exp. Cel. Res.* 319 (10), 1553–1561. doi:10.1016/j.yexcr.2013.03.016

Shih, Y.-T., Wang, M.-C., Peng, H.-H., Chen, T.-F., Chen, L., Chang, J.-Y., et al. (2012). Modulation of Chemotactic and Pro-inflammatory Activities of Endothelial Progenitor Cells by Hepatocellular Carcinoma. *Cell Signal.* 24 (3), 779–793. doi:10.1016/j.cellsig.2011.11.013

Stábeli, R. G., Amui, S. F., Sant'Ana, C. D., Pires, M. G., Nomizo, A., Monteiro, M. C., et al. (2006). Bothrops Moojeni Myotoxin-II, a Lys49-Phospholipase A2 Homologue: An Example of Function Versatility of Snake Venom Proteins. *Comp. Biochem. Physiol. C: Toxicol. Pharmacol.* 142 (3–4), 371–381. doi:10.1016/j.cbpc.2005.11.020

Uddin, M. M., Zou, Y., Sharma, T., Gatla, H. R., and Vancurova, I. (2018). Proteasome Inhibition Induces IKK-Dependent Interleukin-8 Expression in Triple Negative Breast Cancer Cells: Opportunity for Combination Therapy. *PLoS One* 13 (8), e0201858. doi:10.1371/journal.pone.0201858

van Hinsbergh, V. W. M., Engelse, M. A., and Quax, P. H. A. (2006). Pericellular Proteases in Angiogenesis and Vasculogenesis. *Atvb* 26 (4), 716–728. doi:10.1161/01.ATV.0000209518.58252.17

Varinska, L., Kubatka, P., Mojzis, J., Zulli, A., Gazdikova, K., Zubor, P., et al. (2017). Angiomodulators in Cancer Therapy: New Perspectives. *Biomed. Pharmacother.* 89, 578–590. doi:10.1016/j.biopha.2017.02.071

Viallard, C., and Larrivée, B. (2017). Tumor Angiogenesis and Vascular Normalization: Alternative Therapeutic Targets. *Angiogenesis* 20 (4), 409–426. doi:10.1007/s10456-017-9562-9

Wary, K. K., Kohler, E. E., and Chatterjee, I. (2012). Focal Adhesion Kinase Regulation of Neovascularization. *Microvasc. Res.* 83 (1), 64–70. doi:10.1016/j.mvr.2011.05.002

Weis, S. M., and Cheresh, D. A. (2011). v Integrins in Angiogenesis and Cancer. *Cold Spring Harbor Perspect. Med.* 1 (1), a006478. doi:10.1101/cshperspect.a006478

Williams, R. L., Courtneidge, S. A., and Wagner, E. F. (1988). Embryonic Lethalities and Endothelial Tumors in Chimeric Mice Expressing Polyoma Virus Middle T Oncogene. *Cell* 52 (1), 121–131. doi:10.1016/0092-8674(88)90536-3

Yamazaki, Y., Tokunaga, Y., Takani, K., and Morita, T. (2005). C-terminal Heparin-Binding Peptide of Snake Venom VEGF Specifically Blocks VEGF-Stimulated Endothelial Cell Proliferation. *Pathophysiol. Haemos. Thromb.* 34 (4–5), 197–199. doi:10.1159/000092423

Zouari-Kessentini, R., Luis, J., Karray, A., Kallech-Ziri, O., Srairi-Abid, N., Bazaa, A., et al. (2009). Two Purified and Characterized Phospholipases A2 from Cerastes Cerastes Venom, that Inhibit Cancerous Cell Adhesion and Migration. *Toxicon.* 53 (4), 444–453. doi:10.1016/j.toxicon.2009.01.003

Conflict of Interest: The authors declare that the research was conducted in the absence of any commercial or financial relationships that could be construed as a potential conflict of interest.

frontiers in Pharmacology

REVIEW
published: 17 August 2021
doi: 10.3389/fphar.2021.702611

Advanced Computational Methodologies Used in the Discovery of New Natural Anticancer Compounds

Vivek P. Chavda[1], Yavuz Nuri Ertas[2,3], Vinayak Walhekar[4†], Dharti Modh[4†], Avani Doshi[5], Nirav Shah[6], Krishna Anand[7] and Mahesh Chhabria[8]*

[1]Department of Pharmaceutics and Pharmaceutical Technology, L.M. College of Pharmacy, Ahmedabad, India, [2]Department of Biomedical Engineering, Erciyes University, Kayseri, Turkey, [3]ERNAM-Nanotechnology Research and Application Center, Erciyes University, Kayseri, Turkey, [4]Department of Medicinal Chemistry, Bharati Vidyapeeth's Poona College of Pharmacy, Pune, India, [5]Department of Chemistry, SAL Institute of Pharmacy, Ahmedabad, India, [6]Department of Pharmaceutics, SAL Institute of Pharmacy, Ahmedabad, India, [7]Faculty of Health Sciences and National Health Laboratory Service, Department of Chemical Pathology, School of Pathology, University of the Free State, Bloemfontein, South Africa, [8]Department of Pharmaceutical Chemistry, L.M. College of Pharmacy, Ahmedabad, India

OPEN ACCESS

Edited by:
Rajeev K. Singla, Sichuan University, China

Reviewed by:
Mark Pfuhl, King's College London, United Kingdom
Godwin Upoki Anywar, Makerere University, Uganda

***Correspondence:**
Vivek P. Chavda
vivek7chavda@gmail.com
https://orcid.org/0000-0002-7701-8597

[†]These authors have contributed equally to this work

Specialty section:
This article was submitted to Ethnopharmacology, a section of the journal Frontiers in Pharmacology

Received: *29 April 2021*
Accepted: *21 July 2021*
Published: *17 August 2021*

Citation:
Chavda VP, Ertas YN, Walhekar V, Modh D, Doshi A, Shah N, Anand K and Chhabria M (2021) Advanced Computational Methodologies Used in the Discovery of New Natural Anticancer Compounds. Front. Pharmacol. 12:702611. doi: 10.3389/fphar.2021.702611

Natural chemical compounds have been widely investigated for their programmed necrosis causing characteristics. One of the conventional methods for screening such compounds is the use of concentrated plant extracts without isolation of active moieties for understanding pharmacological activity. For the last two decades, modern medicine has relied mainly on the isolation and purification of one or two complicated active and isomeric compounds. The idea of multi-target drugs has advanced rapidly and impressively from an innovative model when first proposed in the early 2000s to one of the popular trends for drug development in 2021. Alternatively, fragment-based drug discovery is also explored in identifying target-based drug discovery for potent natural anticancer agents which is based on well-defined fragments opposite to use of naturally occurring mixtures. This review summarizes the current key advancements in natural anticancer compounds; computer-assisted/fragment-based structural elucidation and a multi-target approach for the exploration of natural compounds.

Keywords: natural anticancer compounds, theranostics, multi-target approach, fragment-based screening, drug antibody conjugate, drug repurposing, personalized medicine

INTRODUCTION

Cancer is a disorder in which cells proliferate abnormally deprived of control. These cancerous cells can attack other nearby tissues and transfer to other body parts *via* lymph and blood. Numerous types of cancers exist such as carcinoma (cancer of the skin or internal organs covering the tissues), leukemia (cancer of tissue that forms blood like, bone marrow, which leads to the production of too many defected blood cells), sarcoma (cancer of muscle, bone, fat, cartilage, blood vessels or other connective tissues or supportive tissues), lymphoma and multiple myeloma (cancer of the immune system cells) (NIH, 2021). Healthy cells can change into tumor cells by following the multiple-stage processes resulting from the interaction between genetic factors of the person and external parameters. These external parameters include physical carcinogens, for example, UV and ionizing radiation, chemical carcinogens like asbestos, constituents of tobacco smoke, food

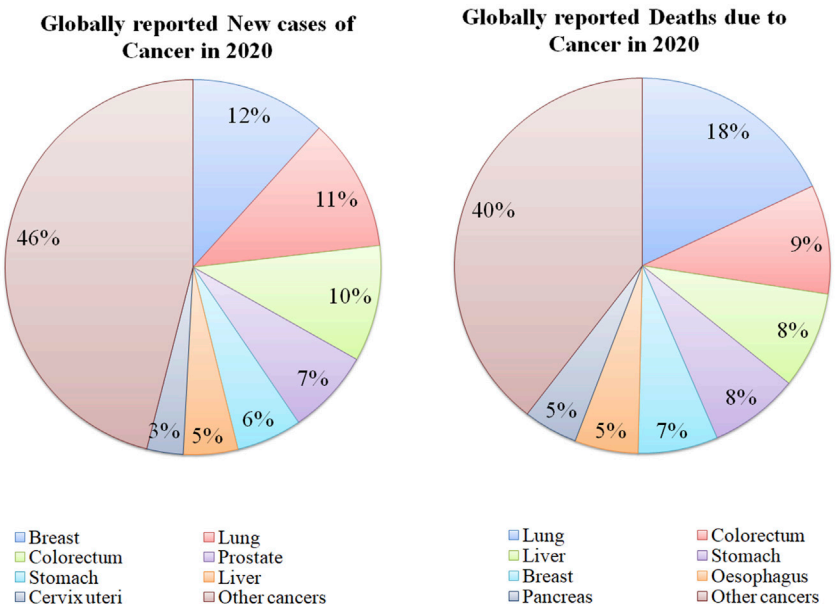

FIGURE 1 | Statistics of globally reported cases and deaths due to various types of cancers in 2020 [Data Collected from (WHO, 2021a)].

contaminants (aflatoxin), drinking water contaminants (arsenic), and biological carcinogens such as infection of virus, bacteria, or parasites (Setlow, 2001). Globally, cancer is the second major reason for mortality with an estimate of 10 million deaths in 2020 (**Figure 1**) among which, breast, lung, colon, rectal, prostate, skin, and stomach cancers were the most frequently observed. Lung cancer was responsible for the majority of cancer-related deaths in 2020 (WHO, 2021b). Throughout the globe, about 1 out of 6 deaths occur because of cancer each year. In low and middle-income countries, almost 70% of the deaths arise due to cancer, out of which, one-third of fatalities are caused by consumption of tobacco and alcohol, high body mass index, less intake of fruits and vegetables, and insufficient physical activity (Wogan et al., 2004). Several infections including human papillomavirus, *H. pylori,* Epstein-Barr virus, hepatitis B virus, and hepatitis C virus (HBV and HCV) can also become indirect risk factors for cancer.

Advancements in multimodal imaging, 3D visual technology, combinational therapy, and the use of nanomedicine have improvized the effectiveness of cancer treatment in the past 2 decades (Shi et al., 2017; Chavda et al., 2019). Progress in cancer immunotherapy, chemotherapy, gene therapy, and epigenome therapy enables substantial improvement in cancer management. Apart from that surgeries including plastic surgery, robotic laparoscopy, radiotherapy, hormonal (mainly for breast and prostate cancer), and photothermal (laser) therapy has revolutionized cancer management (Kumar, 2018). The discovery of targeted drugs, monoclonal antibodies, checkpoint inhibitors, cancer vaccines (prophylactic and therapeutic), cytokines (interferon and interleukins), and chimeric antigen receptor T-cell (CAR-T cell) therapy is proven to be safe and effective in cancer management. Proton therapy is effective in the treatment of several cancer types such as brain, prostate, liver, lung, esophagus, breast, colon, eye, neck, and head. Advancements in robotic surgery enabled the treatment of certain cancers such as kidney, bladder, prostate, ovaries, throat, and uterus (Charmsaz et al., 2018). Many trials and research are ongoing in oncology for enhancing the efficacy of the treatment with minimum side effects.

Targeted drug delivery has proven effective in the treatment of various cancers with fewer side effects. Trastuzumab is used for breast cancers with human epidermal growth factor receptor 2 (HER-2) gene mutation. Afatinib and cetuximab block epidermal growth factor receptor (EGFR), which supports the development of colorectal and lung cancers. Dabrafenib and vemurafenib treat melanomas having mutated BRAF genes. Even though such targeted therapies are promising, currently they are used in very few types of cancers. Research towards improving such therapies is ongoing (Charmsaz et al., 2018). Multi-target therapy (either in sequential order or in combination) is also a widely used approach especially in the cases of intrinsic and acquired resistance towards anti-cancer compounds (Holohan et al., 2013). Drugs such as sunitinib, sorafenib, vandetanib, pazopanib, and axitinib are examples of multi-target treatment of cancer. Sunitinib is approved to treat gastrointestinal stromal tumors and renal cancer. Similarly, sorafenib is approved for renal cancer and liver cancer, where both drugs have the potential to target multiple sites. Vandetanib, pazopanib, and axitinib are used for treating non-small-cell lung cancer (NSCLC) and breast cancer. Vandetanib is effective in thyroid cancer, pazopanib in ovarian and kidney cancer, and axitinib in renal and pancreatic cancer (Petrelli and Valabrega, 2009).

Approximately 60% of effective anticancer drugs are obtained from natural sources (Newman and Cragg, 2012). Campothesins, nucleosides, taxanes, and vinca alkaloids are widely used anticancer drugs obtained from natural origin, and these can provide potential clinical efficiency with diminished toxicity. Another important chemotherapeutic anticancer role is offered by combining potent cytotoxic natural compounds with monoclonal antibodies,

TABLE 1 | Pharmacological and Pharmacognostic details of the naturally occurring anticancer compounds.

Active chemical constituents	Plant name and (plant family)	Mechanism of action	Biological target	References
Shikonin	*Lithospermum erythrorhizon* Siebold and Zucc. (Boraginaceae)	Cell proliferation and cell death	Inhibition of CDC25 and CDK1	Zhang et al. (2019)
Columbianadin	Angelica decursiva (Miq.) Franch. & Sav. (Apiaceae or Umbelliferae)	Angiogenesis	Inhibition of VEGF,EGF,PDGF, TNF-α	Majnooni et al. (2019)
Polyphyllin D	*Paris polyphylla* Sm. (Melanthiaceae)	Apoptosis	Inducing DNA fragmentation and phosphatidyl-serine (PS) externalization	Cheung et al. (2005)
Tanshinol A	*Salviae miltiorrhizae* Bunge (Lamiaceae)	Inducing autophagy and apoptosis and inhibiting cell growth and migration	Activating AMPK and inhibiting Pl3K/Akt/mTOR signaling pathway	Tay et al. (2019)
Artesunate	*Artemisia annua* L. (Asteraceae)	Apoptosis, arrest of the cell cycle at G_0/G_1, and oxidative stress	Regulating the pathway of NK-B, survivin, NOXA, hypoxia-inducible factor-1α, and BMI-1	Das (2015)
Dihydroartemisinin	*Artemisia annua* L. (Asteraceae)	Inhibition of tumor hypoxia	Altering the ROS- dependent apoptosis which summarises the activation of pro-apoptotic Bcl-2 family member Bax, and caspase-activation	Ontikatze et al. (2014)
Phenethyl isothiocyan	*Cruciferous vegetables* (Cruciferouceae)	Inhibition of the progression of tumorigenesis	Pathway alteration of Akt, JNK, XIAP, MCl1, BCL2, BCL-XL, BAD, BAX	Gupta et al. (2014)
Piperlongumine	*Piper longum* L. (Piperaceae)	Cell cycle arrest, inhibition of angiogenesis, metastasis pathways, and autophagy pathways	Key regulatory proteins, including Pl3K, AKT, mTOR, NF-kβ, STATs, and cyclin D1	Tripathi and Biswal (2020)
Metformin	*Galega officinalis* L. (Fabaceae or Leguminosae)	Inhibition of tumor development	Triggering AMPK pathway	Aljofan and Riethmacher (2019)
Gossypol	*genus Gossypium* (Malvaceae)	Inhibition of tumor necrosis	Inhibition of TNF- α and NF-κB	Lu et al. (2017)
Anthocyanin	*Brassica oleracea var* (Brassicaceae)	Suppression of angiogenesis	Inhibition of TNF- α, inducing VEGF expression	Wang and Stoner (2008)
Paclitaxel	*Taxus brevifolia* Nutt. (Taxaceae)	Arrest cells in the G2/M phase of the cell cycle	Inhibition of EGFR	Barbuti and Chen (2015)
Curcumin	*Curcuma longa* L. (Zingiberaceae)	Inducing apoptosis and inhibiting proliferation	Strong inhibition of TNF-α	Barbuti and Chen (2015)
Dimethoxy curcumin	*Curcuma longa* L. (Zingiberaceae)	Anti-tumor effect	Inhibition of EGFR, epithelial-mesenchymal transition, and VEGFR	Chen et al. (2016)
Curcuminoid B63	*Curcuma longa* L. (Zingiberaceae)	Inducing cell proptosis	Targeted TrxR1 protein and increases (ROS) level which responsible for MAPK pathway activation.	Chen et al. (2019)
Celastrol	*Tripterygium wilfordii* Hook.f. (Celastraceae)	Suppressing the development and progression of tumor	Multiple signaling pathways inhibition such as reactive oxygen species (ROS)/JNK and Akt/mTOR, NF-κb, STAT3/JAK2, HSP90, Cdc37, p23, Iκκb, p-Akt, ERα	Shi et al. (2020)
Ginsenoside Rh2	*Panax spp* (Araliaceae)	Inhibition of cell proliferation, cell cycle, cell invasion, and metastasis	Signaling pathway inhibition Akt/mTOR, NF-κb, STAT3	Li et al. (2020)
Hesperidin	Citrus aurantium *L* (Rutaceae)	Responsible for autophagy and apoptosis cell death,	The regulatory protein of Caspase3 and Aurora-A kinase	Korga et al. (2019)
γ-tocotrienol, delta-tocotrienol	*Elaeis guineensis* Jacq. (Arecaceae)	Inhibition of angiogenesis	Downregulation of NF-kappa B pathway and VEGF	Ling et al. (2012)
Withaferin A	Withania somnifera (L.) Dunal (Solanaceae)	Inhibition of angiogenesis and inducing intratumoral apoptosis	Encouraging the expression of pro-apoptotic protein Bax and NF-κB pathway inhibiting by caspase-3 protein	Lee and Choi (2016)
6-Shogaol	*Zingiber officinale* Roscoe (Zingiberaceae)	Inducing apoptosis	Blocking of NF-κB	Ling et al. (2010)
Berberine	*Berberis aetnesis* aetnensis C.Presl (Berberidaceae)	Inhibition of cell proliferation	Suppressing EMT and downregulating signaling pathways (ROS, inhibiting mTOR and Akt phosphorylation, AMPK)	Wang et al. (2020)
Honokiol	*Magnolia virginiana* L. (Magnoliaceae)	Regulation of cellular homeostasis	Downregulating signaling pathway AMPK/mTOR	Lee et al. (2019)
Sanguinarine	*Argemone mexicana* L. (Papaveraceae)	Inducing apoptosis and programmed cell death	Inhibition of Bax and Bcl-2 proteins	Xu et al. (2012)

Abbreviations: CDC, Complement-dependent cytotoxicity; CDK, Cyclin-dependent kinase; VEGF, Vascular endothelial growth factor; EGF, Endothelial growth factor; PDGF, Platelet-derived growth factor; TNF-α, Tumor necrosis factor-alpha; AMPK, AMP-activated protein kinase; mTOR, The mechanistic target of rapamycin; DNA, Deoxyribonucleic acid; BMI-1, Polycomb complex protein; ROS, Reactive oxygen species; Akt, Protein kinase B; JNK, c-Jun N-terminal kinases; STATs, signal transducer and activator of transcription proteins; MAPK, mitogen-activated protein kinase; NF—κB, nuclear factor kappa-light-chain-enhancer of activated B cells.

TABLE 2 | Novel natural anticancer drug development approaches.

Methods	Natural ligands	Targeted PDB[a]	Activity	Analytical tools/Methodology	References
Structure-based and Ligand-based	Porphyrin derivatives	Interaction with Bcl2 active site (PDB: 1XJ)	Antitumor activity	Molecular dynamics (MD), Structure-based pharmacophore modeling, Molecular simulation (MS)	Arba et al. (2018)
	Curcuminoids, thiotryptophan, and 4-phenoxyphenol derivative	PDB of EGFR, MMP-9, mTOR, PKC AKR1B10 (PDB:1ZUA)	Antitumor activity	Molecular docking	Parsai et al. (2014)
	Pheophytin [high affinity human mitochondrial translocator protein (TSPO) ligand]	Inhibit mitochondrial membrane Potential in adenocarcinoma A549 cells	Cell survival	Molecular docking	Shailaja et al. (2019)
	4-Methylpteridinones (berberin)	PI3K/mTOR (PDB: 3OAW)	Cell survival	Molecular dynamics	Liu et al. (2010)
Fragment-based	Trypanosomabrucei, Trypanosomacruzi, Leishmaniainfantum, and Plasmodium falciparum.	Thioredoxin peroxidase 2 (Trx-Px2)	Antitumor activity	Molecular docking	Boucher et al. (2006)
Drug repositioning and purposing based	Metformin and Aspirin	*In-Vivo* cell line MCF-7, VEGFR-2 (PDB: 3ewz)	Inhibition of breast cancer cells	Molecular dynamics and Molecular simulation	Amaral et al. (2018)
	Mushrooms	Inhibition of Histone deacetylase (HDAC) (PDB: 3C10)	Inhibition of breast cancer cells (MCF-7 cell line inhibition)	Molecular docking	Maruca et al. (2020)
Antibody-drug conjugation	Gemtuzumab ozogmicin	Calichemicin monoclonal antibody	Inhibition of cytotoxic tumor	Disulfide-thiol exchange	Mullard (2014b)
Molecularly targeted drug	Hematoxylin analogs	Protein tyrosine kinase inhibitor (VEGFR-r PDB: 4ASD)	Inhibition of angiogenesis	Molecular dynamics and molecular simulation	Ortiz-Hidalgo and Pina-Oviedo (2019)
Leveraging cutting-edge technologies	Withaferin A	Cysteine 377	Inhibition of breast cancer	*In silico* approaches	Sivasankarapillai et al. (2020)

[a]*PDB: Protein Data Bank*

particularly targeting antigenic determinant sites of tumors (**Table 1**) (Cragg and Pezzuto, 2016). Chemo-preventive and tumor-suppressive activities exerted by certain natural agents such as resveratrol, curcumin, indole-3-carbinol, (-)-epigallocatechin-3-gallate, and vitamin D have been reported in multiple studies (Weng et al., 2008; Chakraborti, 2011; Ko et al., 2017; Kwak et al., 2017; Tomeh et al., 2019).

Some natural products are also used to prevent severe side effects of chemotoxic agents which include nausea, vomiting, loss of appetite, diarrhea, constipation, fatigue, skin irritation, etc. Hence, the natural compounds obtained from plants, marine sources, bacteria, fungi, and animals have great potential to effectively target carcinogenic cells with minimal side effects. In this review, we discuss the potential of phytochemicals as anticancer agents followed by new computational approaches like multi-target and fragment-based approaches for the natural anticancer discovery and at last, we discuss theranostic role of natural anticancer agents.

NATURAL ANTI-CANCER COMPOUNDS AND CURRENT RESEARCH

Having extraordinary diversity in nature, the plant-derived compounds are recognized as rich sources of bioactives with some of them also possesses theranostic potential. In the past four decades, many efforts have been made to isolate new chemical entities (NCE) from natural sources like plants, marine, and microorganisms to develop anti-cancer agents. Since 1981, around 25% of new anticancer molecules are derived from natural sources but most of the targeted small molecules were launched after the year 1990 (Beck et al., 2017). Different approaches for the development of novel natural anticancer drugs are summarized in **Table 2**.

a. Antibody-Drug conjugates

The development of antibody-drug conjugation (ADCs) therapy in the early 1990's that integrates monoclonal antibody (mAb) and potent chemotherapeutic agents in a single chemical moiety by a chemical linker has paved the way for the next-generation cancer therapeutics. This advanced approach explores targeting a mAb to improve tumor-specific drug delivery by the antigen-antibody interaction with enhanced anti-cancer activity. Physical and biological properties that are necessary for the ADCs are as follows: 1) Drug loading requires a suitable modified site for conjugation with mAb, 2) Appropriate solubility in water is crucial for desired antibody reaction, and 3) Considerably, higher toxicity (IC_{50} between 0.01 and 0.1 nM) than the standard chemotherapeutic agents is required (Abdollahpour-Alitappeh et al., 2019). Gemtuzumab ozogamicin was the first approved conjugate of humanized

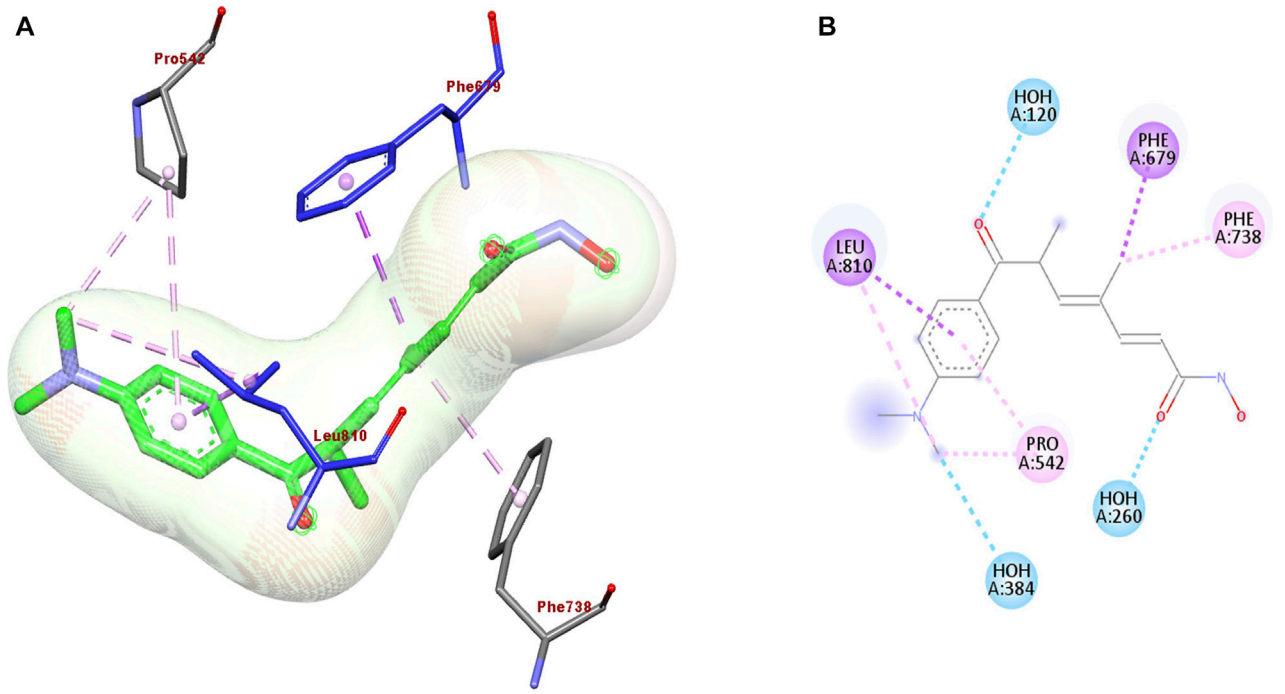

FIGURE 2 | (A) 3D and **(B)** 2D representation of the best re-docking pose of Trichostatin A (TSA) against HDAC7 (PDB code 3C10) receptor obtained using the Glide-SP algorithm.

anti-CD33 monoclonal antibody which is covalently attached to the cytotoxic antitumor antibiotic calicheamicin, but it was withdrawn from the market in 2010 due to fatal adverse events like hemorrhage, infection, and/or acute respiratory distress syndrome. In 2011, brentuximab vedotin was approved for treating Hodgkin lymphoma and anaplastic large cell lymphoma (Mullard, 2014a).

b. Structure-based drug design for natural products

The structure-based drug design is a new approach that can be applied to naturally occurring molecules for the discovery of new anticancer agents. The application of such approaches, resulted in a substantial compilation of natural remedies with potential therapeutic activities against cancer which, while mostly immature as drug candidates, provide highly heterogeneous substrates for lead compounds. This is the most reliable approach for natural lead development. Hematoxylin and its analogs sourced from the heartwood of *Haematoxylon campechianum* L. manifested tyrosine kinase inhibitory potential (Lin et al., 2008).

c. Drug mechanism-based evaluation of novel natural anticancer

Cutting-edge technologies incorporated with chemoproteomics and multi-omics help to overcome challenges in the mechanistic investigation of naturally occurring drugs. Grossman et al. reported the use of chemoproteomics for the discovery of anti-cancer natural product withaferin A that targets cysteine 377 on the regulatory subunit PPP2R1A of the tumor suppressor protein phosphatase 2A complex, and impair breast cancer cell proliferation (Ward et al., 2019).

d. Drug repositioning and repurposing

The discovery of novel anticancer agents from natural sources remains a challenging task. Therefore, many of the currently used natural anticancer drugs are derived from already existing drugs used for the treatment of different diseases as a part of drug repurposing. Drug repositioning approaches include structure-based and ligand-based drug designs. Mushrooms display antifungal, antimicrobial, antiviral, antitumor, and antioxidant activities. The antifungal activity of the mushrooms also inhibits histone deacetylase (HDAC) resulting in anti-proliferative activity against human breast cancer cell line MCF-7. As demonstrated in **Figure 2**, Trichostatin A docking with HDAC 7 crystal structure of the protein (PDB: 3C10) shows interaction with LEU 810, PRO 542, PHE 738, PHE 679, HOH 260, and HOH 384 aminoacids by hydrogen and π-π bond interaction (Maruca et al., 2020). Trichostatin A inhibits HDAC, resulting in anti-proliferative activity against the human breast cancer cell line, MCF-7.

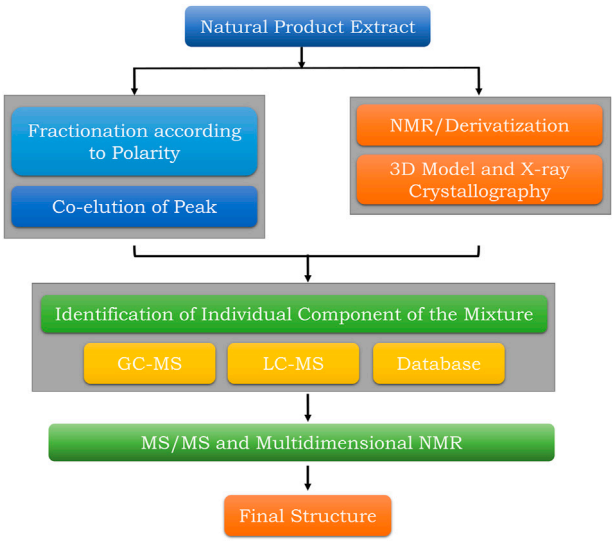

FIGURE 3 | Summary of stepwise structural elucidation techniques of natural products.

COMPUTER ASSISTED STRUCTURAL ELUCIDATION OF NATURAL ANTICANCER COMPOUNDS AND OTHER BIOINFORMATICS APPROACHES

The isolation and identification of natural compounds is a tedious task for chemists because natural compounds have more than one stereo-center, high molecular weight, and complicated chemical scaffolds (Koos et al., 2020). CASE strategies that are dependent on chromatographic and spectroscopic approaches are recently explored for structural elucidation of natural anticancer compounds (Elyashberg and Argyropoulos, 2020). However, to date, only a few spectral data are available for natural compounds, therefore structure elucidation remains a challenge. The spectroscopic and crystallographic analysis techniques accelerated the process of structural elucidation of natural molecules and helped in broadening the spectrum of structural elucidation that could be applied as a tool in the discovery of new drug entities (Nugroho and Morita, 2019).

Numerous advances in Mass Spectrometry (MS) and Nuclear Magnetic Resonance (NMR) over the last 2 decades have enabled structural elucidation processes for complex natural product mixtures (**Figure 3**). Qualitative analysis like MS gives information about the molecular weight and fragments of the sample. Recent scenarios of hyphenated techniques like LC-MS, GC-MS, GC-FID, GC-MSMS, and LC-MSMS are used for high-resolution molecular weight determination with a decrease in the total number of overlapping m/z ratios (Rinschen et al., 2019). Orthodox chromatographic approaches take a long time to identify or forecast the key chemical components found in a natural product mixture. The restricted compound references often render identifying or predicting each constituent in a mixture quite troublesome. As a result, an effective algorithm for solving the symmetric cone complementarity problem (CSCCP) is needed. Similarly, sensitive techniques like NMR spectroscopy give an essence of type and number of protons (H^1), carbon (C^{13}), phosphorous (P^{31}), and fluorine (F^{19}) content in the natural organic compounds. NMR spectrometric analysis alone cannot elucidate the structure of the natural organic compounds independently, therefore hyphenated techniques namely LC–NMR–MS and LC–UV–solid-phase extraction–NMR–MS are used. An IR spectrum can tell a lot about the existence or absence of such functional groups, but it does not give information about their environment in the compound (Elyashberg et al., 2009). It was suggested that 2D NMR data can be routinely generated, even in automation and a multitude of data are available as inputs to CASE systems like HSQC (HMQC), ^{1}H-^{1}H COSY (TOCSY), and HMBC methods (Elyashberg et al., 2009). Nowadays, 2D NMR spectroscopy is used for the structural elucidation and verification of natural organic molecules (Soong et al., 2020). A logical review of 2D NMR data often reveals the existence of "nonstandard" duration of COSY and HMBC correlations. Fuzzy structure generation allows for the right solution even though an uncertain number of nonstandard associations of unknown duration is present in the spectra (Su et al., 2017).

A new computer-aided software engineering (CASE) algorithm, known as the NP-Structure predictor, predicts individual components in a natural product mixture by using information acquired from LC-MS experiments (Harn et al., 2017). This is accomplished by comparing a list of known scaffolds with a list of weighted side groups to generate a list of potential molecules subject to defined structural constraints. They also mentioned an iterative DP algorithm with a wide range of potential sets of positions (Nk) that can be connected by the side chains upon its seed scaffolds, which may result in a challenging execution period for the algorithm (Kind and Fiehn, 2010; Harn et al., 2017). Expert system structure elucidator for the natural organic anticancer compound includes molecular connectivity diagram, structure generation, and verification and selection of the most probable structure. The fuzzy logic structure elucidator, which is based on spectral data, can easily identify large and complicated molecules consisting of up to 100 or more atoms with topological conceit. The beneficial predictions produced by computational models combined with empirical validations could help to accelerate the production of anti-cancer drugs from natural origin.

FRAGMENT-BASED SCREENING OF NATURAL ANTICANCER COMPOUNDS

Fragment-based drug discovery (FBDD) will have wide applications in the field of natural products in the upcoming years because extraction, isolation, and purification of the active constituents from the natural sources are quite tedious and time-consuming (Khalifa et al., 2019). Application of *in-silico* techniques may expedite the process of development of potent and semisynthetic compounds that were originally isolated from natural sources. FBDD of the natural compounds is challenging

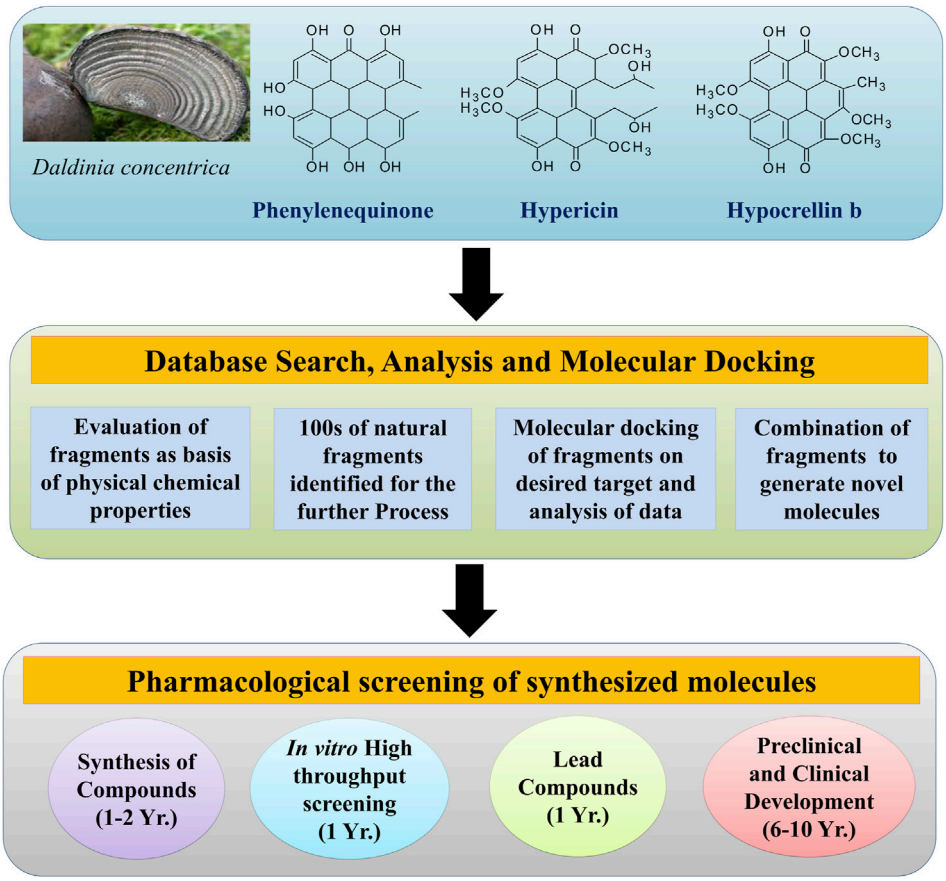

FIGURE 4 | Procedure for fragment-based screening.

because it is not yet largely explored for natural compounds manifesting anticancer activity (Murray and Rees, 2009). The natural chemical compounds that exhibit anticancer activity include alkaloids, polyphenolic compounds, etc. FBDD mainly depends on the molecular modeling strategy for the identification of the potential fragment for the anticancer agent. This involves the binding of the small fragments in the active site of the target (protein) to analyze the interaction of the small fragments with the target protein that helps the medicinal chemists and pharmacologists to design novel anticancer molecules. Natural anticancer compounds are sourced from plants, animals, and marine sources. The fragments are analyzed by various spectroscopic techniques and crystallographic techniques (David et al., 2020). Fragment-based screening (**Figure 4**) (Li, 2020) involves the following steps:

1. Collection of the compounds from the database
2. Filtration of the compounds from the database
3. Spectroscopic and crystallographic analysis of fragments
4. Molecular docking of the identified small fragments
5. Anti-cancer screening of the fragments.

Vemurafenib was the first drug discovered by the FBDD approach that consists of pyrollopyridine as a fragment for anticancer activity. Similarly, there is ample potential for various natural compounds to be screened as novel anticancer agents by applying the FBDD approach (Liu and Quinn, 2019). If a target has been established, bioinformatics can be used to comprehend the structure, which can be achieved by X-ray crystallography or other approaches such as homology modeling. The target protein would then be overexpressed. If the isotopically labeled protein is quickly purified and exhibits scattered cross-peaks in the 1H-15N-HSQC spectrum, this protein-based NMR can be used in screening. Otherwise, fragment scanning can be performed using DSF or 19F-NMR. If the target can be conveniently crystallized, X-ray crystallography would be the first tool to be used in screening. Where a target framework is open, the virtual screening will still be performed. An appropriate library would be chosen from a large number of sources, which is not a restriction. Structural, biophysical, and biochemical approaches can be used to validate the hits. Finally, appropriate techniques can be used to exploit fragment development (**Figure 4**). Role of medicinal chemists would be crucial in this phase.

Curcumin is an active constituent of *Curcuma longa* L. (Family: Zingiberaceae), which exhibits anticancer activity. It consists of the active fragment of β-diketone. Curcumin's anticancer activities are due to its direct or indirect control of

signal transduction pathways, *via* its effect on cell division, the p53 tumor suppressor gene, and transcription factors Nrf2 and NFB, as well as modulation of inflammatory signaling cascades. Similarly, for the designing of novel COX-2 inhibitors like diketone, is a pharmacophore for developing anticancer agent (Kljun and Turel, 2017).

Potential natural anticancer compounds which act on p21-activated kinase (PAK1) were reported by using computational methodologies (Shahinozzaman et al., 2020). 42 fragments of herbal compounds were identified from drugs such as triptolide, cucurbitacin I (C-I), nymphaeol A (NA), and staurosporine (SPN). Pharmacokinetic properties like absorption, distribution, metabolism, and excretion (ADMET) and molecular docking studies suggested that inhibitors C-I, NA, and SPN fit in the catalytic region of p21 activated kinase with promising pharmacological and pharmacokinetic parameters (Shahinozzaman et al., 2020). Molecular dynamic simulation studies revealed that NA shows tight binding with the PAK1 enzyme and can be considered to be safe while toxicity was manifested by SPN and C-I (Abdollahpour-Alitappeh et al., 2019).

AlAjmi et al. identified novel natural molecules as polo-like kinase (PLK-1) inhibitors with an anticancer activity using a computational modeling approach like FBDD (AlAjmi et al., 2018). Selleck's library of natural compounds was screened against PLK-1 with the aid of a molecular docking approach. Docking studies identified eight bioactive natural molecules (Apigenine, Dihydromyrecetion, Hesperidin, Hesperitine, Naringenin, Phlorizi, and Quesertine) as PLK-1 inhibitors. Molecular Mechanics-Generalized Born Surface Area (MM-GBSA) calculations showed that hesperidin was found to be a potent inhibitor of PLK-1 by the formation of a sturdy complex with Tyrosine-protein kinase (TLK) and confirmed with the help of molecular dynamics simulation studies. The generated data provide ample evidence and confirmed that hesperidin is a potential PLK-1 inhibitor by following parameters as molecular weight (610.56 g/mol), 8 H-bond donors, 15 H-bond acceptors, 234 Å TpSA, 0 net charges, and 7 rotatable bonds. These results were more significant as compared to other natural inhibitors of PLK-1 as an anti-cancer agent. Similarly, optimization of natural compound Itampoli A as p38α inhibitor by application of FBDD approach was reported elsewhere (Liang et al., 2019). Itampoli A which is effective against lung cancer was isolated from *Iotrochota purpurea,* a marine sponge. Itampoli was modified with the aid of the FBDD strategy. A total of 45 brominated tyramine analogs were synthesized as fragments. *In-vitro* enzyme inhibition assay of 45 analogs was performed against the p38α enzyme. The inhibitory study revealed that (−)-itampolin A potentially inhibited p38α with an IC50 value of 7.9 ± 1.7 nM. (−)-itampolin A also inhibited cell proliferation in the lung cancer cell line (A549) at a concentration of 0.66 mM. Molecular docking revealed that (−)-itampolin A fit in the active site of p38α by forming 3H-bonds with GLU71 and ASP168. On the other hand, the 3D QSAR approach revealed that the tyrosine skeleton was essential for the p38α inhibitory activity which was mainly contributed by the ureoid moiety in (−)-itampolin A (Liang et al., 2019).

Therefore, FBDD is one of the attractive tools for the medicinal scientists in order to explore natural anticancer agents and further identify hit fragments from the reported natural anticancer agents and model a new anticancer molecule (Koos et al., 2020).

MULTI-TARGET APPROACH FOR THE EXPLORATION OF NATURAL ANTICANCER COMPOUNDS

The conventional drug discovery approach was applied for the discovery of novel drugs. Even until 2000, scientists developed drugs separately for different targets of the same disease. This approach leads to an increase in the number of drugs and their corresponding side effects (**Table 3**). To avoid this, scientists focused on developing drugs that can target multiple sites of the same disease that can ultimately reduce the number of drugs in the chemical space and also the corresponding cost to develop them (**Figure 5**) (Ramsay et al., 2018). The blockbuster drug Sorafenib was developed by Bayers and Onyx which gained approval from USFDA in 2007. Sorafenib inhibited different kinases namely VEGFR-2, VEGFR-3, PDGFRβ, c-Kit, and Raf, that play a crucial role in cancer progression and angiogenesis at a low nanomolar concentration. Similarly, in Indian traditional medicine, curcumin is a natural active constituent of crude drug turmeric and its semisynthetic analogs are used in the treatment of several types of cancers. In the last 3–4 decades, various drugs were developed which act by binding to diverse biological targets, resulting in desired pharmacological activity (Cragg and Pezzuto, 2016).

There are various targets for the treatment of different diseases like tyrosine kinase for cancer, cyclooxygenases (COX) for inflammation, and DNA gyrase for bacterial infection and tuberculosis. Marine plants are the main source of anticancer agents, and they can target more than one disease. Methanolic extract of *Artemia salina* is a marine brine shrimp that shows both anticancer as well as antibacterial activity. Natural antioxidants like selenium, vitamin E, myricetin, quercetin, and kaempferol act as anticancer agents *via* free radicals such as superoxide anion (O_2−), hydrogen peroxide (H_2O_2), hydroxyl radicals (OH) (Kumar and Adki, 2018). Antibiotics like azithromycin, doxycycline, tigecycline, pyrvinium pamoate, chloramphenicol, 17-allylaminogeldanamycin, methotrexate, and anthracycline are principally used in the treatment of bacterial infections and manifest anticancer activity by inhibiting the cell growth on cell lines like MCF7, T47D, etc. at the concentration range of 50–200 nM.

Anti-inflammatory agents also act as anticancer agents by inhibiting various inflammatory mediators like TNF-α, IL2 IL12, transforming growth factor beta (TGF-β), etc. Scientists have reported that COX2 and EGFR signaling is quite common to both cancer and inflammation, so COX2 inhibitors and the combination of both COX2 and EGFR inhibitors are potential anticancer agents at lower doses. COX2 enzyme has a crucial role

TABLE 3 | Multitarget-based anti-cancer natural compounds.

Nature molecule/Crude drug	Inhibitory effect on biological targets or cancer cell lines	References
Anthracycline	MCF-7 and T47D	Cragg and Pezzuto (2016)
Pyrano-quinolone	COX-2 and EGFR signalling	Kumar and Adki (2018)
Taxol and Vinblastin	PI3K, APC, and RB signalling	Taylor et al. (2019)
Deacetylnemorone	SKMEL5 (melanoma cancer cells), MG-63 (osteosarcoma), SK-OV-3 (ovarian adenocarcinoma), MDA-MB-231 (breast cancer), HCT 116 (colorectal carcinoma), HCT 116/200 (FdUrd resistant subclone of HCT 116 cells), A2780ADR (a doxorubicin-resistant subclone of the ovarian carcinoma A2780), and HUVEC (Normal human umbilical vein endothelial cells).	Liu and Quinn (2019)
Curcumin	NF-κB, miR-221, COX-2, and their effectors such as PTEN, p27, p57, and pro-inflammatory cytokines. STAT-1, STAT-3 phosphorylation, and Notch signaling pathway. Pancreatic cancer cell lines (MiaPaCa-2, Panc-1, AsPC-1, BxPC-3, and Pan02)	Sahebkar (2016)
Curcumin	COX-2, STAT-1 and STAT-3 signaling, NF-κB, VEFG, EGFR signaling, PI3/Akt, and m-TOR signaling, CDK, B-catenine, Tcf-4	Sahebkar (2016)
Piperine	Nuclear factor-κB (NF-κB), c-Fos, CREB, ATF-2, Melanoma cell line (B16F-10 piperine concentration = 2.5, 5, and 10 μg/ml)	Pradeep and Kuttan (2004)

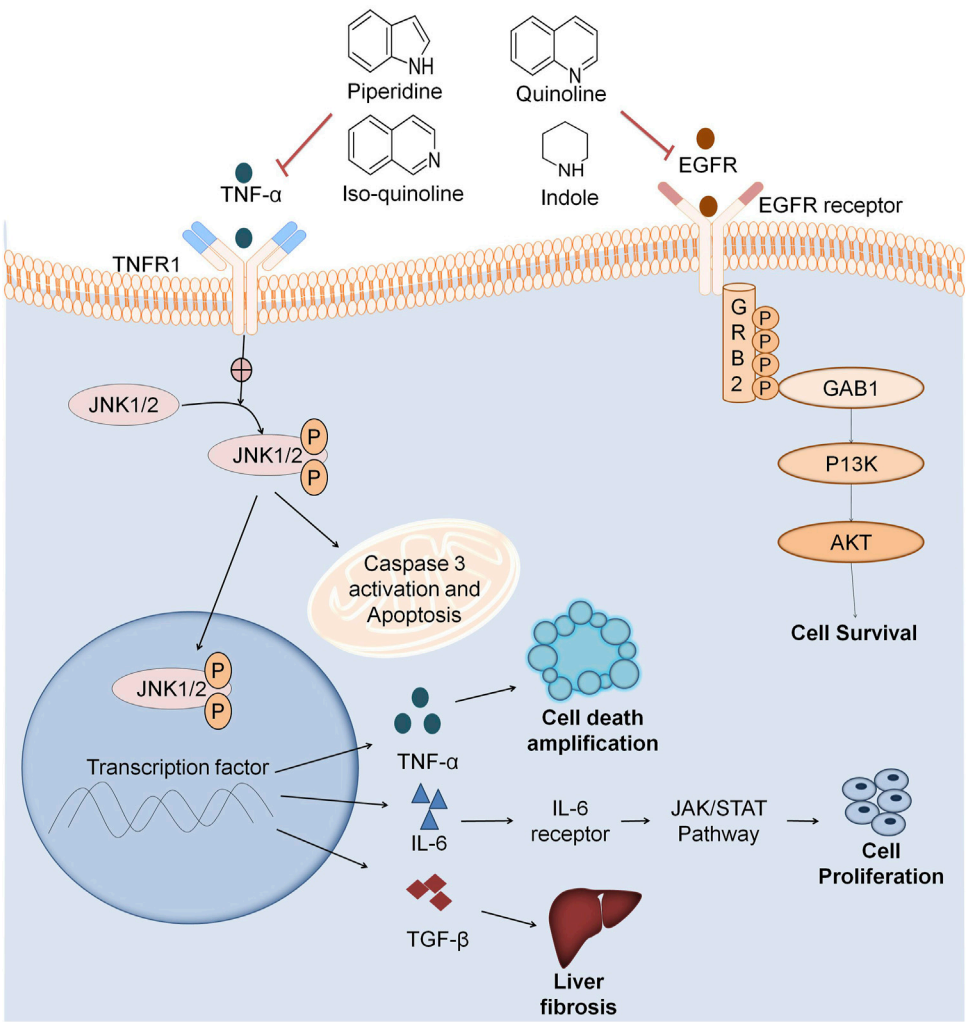

FIGURE 5 | Multitarget based screening of anticancer natural compounds. Pro-inflammatory mediators like TNFα, JL2, JL12, etc. binds to the receptor on the cell surface which undergoes a conformational change and activates JNK 1/2. JNK1/2 phosphorylation leads to apoptosis that releases inflammatory factors like NFKβ that also releases inflammatory factors like TNF-α which plays role in cell death amplification. IL6 activates JAK/STAT pathway that results in cancer cell proliferation. TGFFβ also activates various pathways leading to liver fibrosis. EGFR binds to the cell surface receptor that activates GRB2. Phosphorylation of GRB2 activates the downstream pathway as GABI further activates P13K that activates AKT leading to cell survival. Natural fragments like indole, quinoline, isoquinoline, and piperidine inhibit both the inflammation pathway and EGFR in cancer cell growth.

in tumor growth (Rayburn et al., 2009). Various natural alkaloids comprising indole, quinoline, isoquinoline, and piperidine manifests COX-2 inhibition (**Figure 5**). Pyrano-quinolone analogs also inhibit TNF-α and IL6 which are also pro-inflammatory mediators. Therefore, from the above discussion, it is clear that anti-inflammatory agents also act as anticancer agents (Dey et al., 2020).

Naturally occurring anti-mitotic agents like Nocodazole, Taxol, AZ138, BPR0L075, Vinblastine, Taxanes, and Epothilones, act by inhibition of PI3K and APC and RB pathways, and microtubule destabilizing agent which is related to the anticancer activity (Dall'Acqua, 2014). Dolastatin-10, Aplidine, Halichondrine-B, and Descodermolide inhibit the microtubule growth, ultimately, acting as anti-cancer agents. Therefore, from the above discussion, the naturally occurring compounds act by multi-targeting anticancer agents (Kumar and Adki, 2018).

Taylor et al. reported a rare natural product, Deacetylnemorone member of the diterpenoid family, as an anticancer agent which inhibits cell growth on different cancer cell lines (Taylor et al., 2019). Deacetylnemorone acts by resensitizing chemotherapy resistance of cancer. Activity reported for Deacetylnemorone is anti-angiogenic and cancer cell growth inhibitor. Curcumin was reported as a natural active constituent used in the treatment of pancreatic cancer by the multitarget approach. Curcumin inhibited various targets like NF-κB, miR-221, COX-2, and their effectors such as PTEN, p27, p57, and pro-inflammatory cytokines which ultimately causes cancer cell growth and progression (Sahebkar, 2016). Curcumin also inhibits phosphorylation STAT-1, STAT-3, and Notch signaling pathways which are responsible for pancreatic cancer cell growth. Reports also portray that curcumin is effective and selective towards different pancreatic cancer cell lines namely MiaPaCa-2, Panc-1, AsPC-1, BxPC-3, and Pan02.

Diederich et al. reported curcumin as a multitarget natural compound with its application in cancer interruption and therapy. Curcumin modulates numerous molecular targets and blocks signaling tracks such as COX-2, STAT, NF- κB, VEGFR, EGFR, P13/Akt, and mTOR. It also influences cell cycle regulators like CDK, B-catenin, Tcf-4 for cancer progression (Teiten et al., 2010; Teiten et al., 2014). Curcumin activates the cancer cell death proteins, namely PARP, Bcl-2, Bcl-xL, LC-3II, and cyclin-B1. Curcumin and its analogs also act against diverse cancers like multiple myeloma, rectal cancer, pancreatic cancer, osteosarcoma, colon neoplasm, and colorectal cancer. Hence, curcumin is a multitargeting agent in cancer mitigation (Teiten et al., 2010).

Another study reported piperine as an anticancer agent which acts on various targets such as NF-κB, c-Fos, cAMP response element-binding protein (CREB), activated transcription factor 2 (ATF-2), and proinflammatory cytokine gene expression in B16F-10 melanoma cells. Piperine inhibited collagen matrix at a concentration of 2.5, 5, and 10 μg/ml against B16F-10 melanoma cells at a dose-dependent analysis (Pradeep and Kuttan, 2004). It also inhibited matrix metalloproteases with the aid of the zymographic method. Piperine restrained nuclear translocation of p65, p50, c-Rel subunits of NF-κB and other transcription factors such as ATF-2, c-Fos, and CREB that resulted in cancer growth inhibition (Pradeep and Kuttan, 2004).

THERANOSTICS PERSPECTIVE OF NATURAL ANTICANCER COMPOUNDS

Theranostics is the combination of diagnosis and treatments. It is a therapy in which a combination of one radioactive drug will diagnose the tumor and other radioactive drugs will treat the main tumor and metastatic tumors (Silva et al., 2019). This combination will diagnose cancer at various locations effectively and monitor the progress of the disease and guide for another treatment of chemotherapy or surgery whichever may be needed depending on the disease condition (Garofalo et al., 2020).

For many years, natural products have been used for their diverse chemical structures and unique targeted activities. Natural products are easily compatible with the human body and display low toxicity. Many natural products including porphyrins, perylene quinone derivatives, curcumin are photosensitizers and sono-sensitizers, which have been widely applied in fluorescence imaging, diagnosis, photodynamic therapy (PDT), and sonodynamic therapy (SDT) (Cova et al., 2019). In PDT, excited photosensitizers oxidize cellular macromolecules like nucleic acids and proteins, resulting in tumour cell apoptosis by producing reactive oxygen species. In SDT, ultrasound wave interacts with the water molecules in the environment, causing ultrasonic cavitation during which tiny cavities nucleate, grow, and collapse (Ma et al., 2019). Theranostic agents like porphyrin and its derivatives are approved for therapeutic usage in cancer management as they have lower toxicity and appropriate biocompatibility. Hematoporphyrin derivatives are photosensitizers, approved for clinical PDT. Porphyrinoid biohybrid materials are approved for phototheranostics. The light sensitivity of curcumin and its derivatives is weaker in the therapeutic window of wavelength, that limits their role as theranostic agents (de Araújo et al., 2020).

The theranostic role of SDT is only to tumorstastic action as it only inhibits the tumor growth especially of solid tumors. On the other hand, PDT has "-cidal effect" on the tumors. It is interesting to note here that to date, there is no SDT approved for the medicinal use however several photosensitizers are used for cancer management as a part of photodymanic therapy. The exact mechanism behind the SDT needs to be revealed soon, and natural SDT with better safety and efficacy in cancer management must be produced (Sharma et al., 2017).

Some of the examples of natural products used as theranostic agents are as follows:

- Porphyrin
- Perylene quinine (Hypocrellin, Hypericin, Cercosporin, Elsinochrome)
- Cercosporin
- Elsinochrome
- Curcumin
- Pheophytin

- Psoralens
- Berberine chloride
- Graphene

Porphyrin, as a theranostic agent, has photodynamic, sonodynamic, and radiotherapeutic roles in the treatment of cancer. It is also used as a diagnostic agent for fluorescence imaging, magnetic resonance imaging, and photoacoustic imaging. The use of porphyrin is limited as a theranostic agent due to its poor selectivity for tumor cells. When nanoparticles are used as carriers of porphyrins, their anticancer effect improves. Perylene quinone has many pigments which show chemical and biological properties, making them diagnostic and therapeutic agents in PDT and SDT. Some pigments such as hypocrellins, elsinochrome, hypericin, cercosporin are included in perylenequinones. Hypocrellin, a pigment of perylenequinone category, is extracted and isolated from the *Hypocrella bambusae*, which is parasitic on Fargesia plant, has absorption between 400–800 nm, and has a high oxygen species yield, making it suitable for the treatment of tumors. It is less toxic and has a fast metabolism rate *in vivo*, and it is one of the best-known new generation phototheronostic agents that has potential for the development of drugs (Bisen, 2016; Peyvandipour et al., 2018).

Cercosporin is a photodynamic photosensitive pereylene quinoline derivative that is often used with a co-polymer to target carcinogenic cells. Polymer releases cercosporin in acidic conditions and offers cancer treatment for patients. Elsinochrome is a theranostic agent showing photodynamic property which is used for targeted drug delivery to cancerous cells (Wilken et al., 2011).

Pheophytin, a form of seagrass, is a natural anticancer pigment that is evaluated in the management of adenocarcinoma A549 cells. Photo-reduction of pheophytin has been observed in various mixtures containing PSII reaction centers. Similarly, Psoralens (furanocoumarins) are explored for the treatment of certain lymphomas as targeted therapeutics in conjunction with ultraviolet rays (Shailaja et al., 2019).

Berberine chloride is an orally bioavailable, hydrochloride salt form of berberine, a quaternary ammonium salt of an isoquinoline alkaloid and active component of various Chinese herbs (*Coptis chinensis* French, *Coptis deltoidea* C. Y. Cheng et Hsiao *and Coptis teetoides* C. Y. Cheng) (Neag et al., 2018), with good anticancer, photodynamic, anti-inflammatory, and anti-lipidemic activities (Belwal et al., 2020). Berberines are isoquinoline derivatives and belong to protoberberines alkaloids. Berberine has been shown to have a major hormetic dose-response, where a low dose actively promotes the development of cancer cells whereas a high dose serves as an anticancer agent. Furthermore, because of its widespread presence in numerous plant species and low toxicity, berberine hydrochloride has the potential to be a powerful anticancer agent in the future (Singh and Sharma, 2018).

Graphene is an inorganic material that is used for making nanocomposites for drug delivery due to its lower toxicity and additional anticancer action (Hoseini-Ghahfarokhi et al., 2020). Apart from being an anticancer agent, the graphene is also has photodynamic action (Yang et al., 2019). Graphene is generally used as a nanocarrier for drug delivery, especially anticancer drug delivery (Jampilek and Kralova, 2021). The graphene nanocomposites have better drug loading and protective action, targeted delivery, are suitable for theranostic role, and have effective photodynamic action. It is used as a theranostic agent due to its anticancer action (Rosli et al., 2019).

NATURAL ANTICANCER COMPOUNDS FOR PERSONALIZED MEDICINE

There is substantial increase in our understanding of health and disease related aspects of human life due to technological advancement and multiomics approaches. To achieve proper effectiveness, the use of personalized pairings of precision targeted drugs recognized by proteogenomics will necessitate specialized modelling based on the latest methodologies (Li and Bergan, 2020). Personalized medicine is a domain which aims to develop therapeutics for a single subject or group of subjects derived from current and past data capturing of physiological health and the environment exposure. Precision oncology has demonstrated some significant success in the last decade, despite the fact that it is expensive (Cutler, 2020). Consequently, the precision medicine approach, which was endorsed in 2015, has propelled the personalized medicine forward by necessitating the FDA to design new technologies for evaluating personalized medicine (Krzyszczyk et al., 2018).

Well over 700 natural compounds have now been confirmed to have pharmacological function, with many of them capable of targeting cellular processes or deregulated genes that inhibit tumorigenesis (Mazumder et al., 2018). For every cancer patient or group of patients, there is unique genetic makeup that serves as a cancer operator and can shift throughout therapy to stimulate response processes. When it is used in conjunction with certain drugs, several natural compounds with established molecular targets demonstrated good therapeutic benefits by restricting signalling proteins that facilitate tumor progression (Cerella et al., 2015). The continuously advancing domain of immunooncology has improved our understanding of tumor-specific immune responses as well as the ability of targeted chemotherapy drugs to stimulate the anti - tumor immunity toward carcinoma. It was recently noted that targeted therapies like oxaliplatin, that also kill cancer cells by triggering a host immune system, can make tumours more susceptible to checkpoint blockade treatment (Pfirschke et al., 2016). The distribution of key anti-apoptotic Bcl-2 proteins forecasted a complementary response (Mazumder et al., 2018). The brominated alkaloid isofistularin-3, derived from the marine sponge *Aplysina aerophoba*, is shown to suppress DNA methyltransferase (DNMT1) (Florean et al., 2016; Mazumder et al., 2018). In RAJI and U937 cells, isofistularin-3 combined with tumour necrosis factor related apoptosis inducing ligand (TRAIL) demonstrated strong synergy (Florean et al., 2016; Mazumder et al., 2018). Recently, it was observed that combining ursolic acid, curcumin, and resveratrol to locate STAT3, mTORC1, and AMPK action substantially lowered

prostate cell proliferation and attenuated glutamine metabolism, thereby attacking a critical true sign of cellular kinetics (Kuntz et al., 2017).

Taken together, the important development of identified targeted agents of natural origin, as well as the immunogenic capability of such agents when combined with existing drugs, will contribute to future pharmacotherapy opportunities for tumour targeting.

CONCLUSION AND FUTURE PROSPECTS

For a long time, natural phytochemicals have been proven to be effective against different types of cancer. The opportunities and prospects of natural products for drug discovery are being significantly extended with the exploration of plant endophytic fungi, which have been recognized as a decent source of certain bioactive metabolites having an anticancer activity (Chandra, 2012). Major natural anticancer compounds like camptothecin, taxol, vinca alkaloids, and podophyllotoxin have been obtained from an endophytic fungus. Marine-derived bioactive compounds also have a large potential to produce an anti-cancer effect (Abdelmohsen et al., 2014). Similarly, bioactive metabolites from insects have potential for drug discovery in the rapidly growing areas of research like microbial genomics through genome mining and metagenomics (Bachmann et al., 2014; Charlop-Powers et al., 2014).

Drug research and production would necessitate a close multidisciplinary partnership in the exploration of natural product leads using combinatorial and medicinal chemistry, complete synthesis, combinatorial biochemistry, and nanotechnology. Natural product analysis that combines nanotechnology and analytical methods is a dominant strategy for identifying biologically active substances having distinct structures as well as modes of activity. Given nature's immeasurable diversity, it is obvious that chemical leads capable of interacting with all therapeutic targets can be produced, indicating a greater potential for the production of highly effective therapeutic agents. Several technological advancements in the drug discovery fields will lead to speeding up the process of finding suitable drug candidates of natural origin that have potential anticancer activity. The multitarget approach of drug discovery has provided an attractive niche for medicinal scientists as it reduces the burden of the multidrug regime for cancer management and also reduces the side effects associated with them. Cutting edge analytical tools and bioinformatics especially machine learning will help in the process of drug discovery to find out the suitable hits in the early drug discovery phase of natural anticancer discovery. Natural phytochemicals continue to be a valuable substitute of scaffolds with high structural diversity and diverse antitumor activity that can be established directly or used as starting points for modeling into new therapeutics. The theranostic potential of such natural compounds is immense and we will witness much future research towards such theranostic agents of natural origin.

AUTHOR CONTRIBUTIONS

VPC conceived the plot; VPC researched the literature and wrote the manuscript along with other co-authors; VC made the figures and revised the manuscript with the help of YNE, KA and MC. YE and MC critically reviewed the manuscript. All authors reviewed the final manuscript and approved the same.

ACKNOWLEDGMENTS

We are very thankful to Dr. Chirag Patel (Assistant Professor, Department of Pharmacology, LMCP, Ahmadabad, India) for helping us in redesigning of **Figure 5**.

REFERENCES

Abdelmohsen, U. R., Bayer, K., and Hentschel, U. (2014). Diversity, Abundance and Natural Products of marine Sponge-Associated Actinomycetes. *Nat. Prod. Rep.* 31, 381–399. doi:10.1039/c3np70111e

Abdollahpour-Alitappeh, M., Lotfinia, M., Gharibi, T., Mardaneh, J., Farhadihosseinabadi, B., Larki, P., et al. (2019). Antibody-drug Conjugates (ADCs) for Cancer Therapy: Strategies, Challenges, and Successes. *J. Cel. Physiol.* 234, 5628–5642. doi:10.1002/jcp.27419

AlAjmi, M. F., Rehman, M. T., Hussain, A., and Rather, G. M. (2018). Pharmacoinformatics Approach for the Identification of Polo-like Kinase-1 Inhibitors from Natural Sources as Anti-cancer Agents. *Int. J. Biol. Macromolecules* 116, 173–181. doi:10.1016/j.ijbiomac.2018.05.023

Aljofan, M., and Riethmacher, D. (2019). Anticancer Activity of Metformin: a Systematic Review of the Literature. *Future Sci. OA* 5, FSO410. doi:10.2144/fsoa-2019-0053

Amaral, M. E. A., Nery, L. R., Leite, C. E., de Azevedo Junior, W. F., and Campos, M. M. (2018). Pre-clinical Effects of Metformin and Aspirin on the Cell Lines of Different Breast Cancer Subtypes. *Invest. New Drugs* 36, 782–796. doi:10.1007/s10637-018-0568-y

Arba, M., Yamin, Ihsan, S., and Tjahjono, D. H. (2018). Computational Approach toward Targeting the Interaction of Porphyrin Derivatives with Bcl-2. *J. App. Pharm. Sci.* 8 (12), 060–066.

Bachmann, B. O., Van Lanen, S. G., and Baltz, R. H. (2014). Microbial Genome Mining for Accelerated Natural Products Discovery: Is a Renaissance in the Making? *J. Ind. Microbiol. Biotechnol.* 41, 175–184. doi:10.1007/s10295-013-1389-9

Barbuti, A., and Chen, Z.-S. (2015). Paclitaxel through the Ages of Anticancer Therapy: Exploring its Role in Chemoresistance and Radiation Therapy. *Cancers* 7, 2360–2371. doi:10.3390/cancers7040897

Beck, A., Goetsch, L., Dumontet, C., and Corvaïa, N. (2017). Strategies and Challenges for the Next Generation of Antibody-Drug Conjugates. *Nat. Rev. Drug Discov.* 16, 315–337. doi:10.1038/nrd.2016.268

Belwal, T., Bisht, A., Devkota, H. P., Ullah, H., Khan, H., Pandey, A., et al. (2020). Phytopharmacology and Clinical Updates of Berberis Species against Diabetes and Other Metabolic Diseases. *Front. Pharmacol.* 11, 41. doi:10.3389/fphar.2020.00041

Bisen, P. S. (2016). Experimental and Computational Approaches in Leveraging Natural Compounds for Network Based Anti-cancer Medicine. *J. Can. Sci. Res.* 02, e103. doi:10.4172/2576-1447.1000e103

Boucher, I. W., McMillan, P. J., Gabrielsen, M., Akerman, S. E., Brannigan, J. A., Schnick, C., et al. (2006). Structural and Biochemical Characterization of a Mitochondrial Peroxiredoxin from Plasmodium Falciparum. *Mol. Microbiol.* 61, 948–959. doi:10.1111/j.1365-2958.2006.05303.x

Cerella, C., Muller, F., Gaigneaux, A., Radogna, F., Viry, E., Chateauvieux, S., et al. (2015). Early Downregulation of Mcl-1 Regulates Apoptosis Triggered by

Cardiac Glycoside UNBS1450. *Cell Death Dis.* 6, e1782. doi:10.1038/cddis.2015.134

Chakraborti, C. (2011). Vitamin D as a Promising Anticancer Agent. *Indian J. Pharmacol.* 43, 113–120. doi:10.4103/0253-7613.77335

Chandra, S. (2012). Endophytic Fungi: Novel Sources of Anticancer lead Molecules. *Appl. Microbiol. Biotechnol.* 95, 47–59. doi:10.1007/s00253-012-4128-7

Charlop-Powers, Z., Milshteyn, A., and Brady, S. F. (2014). Metagenomic Small Molecule Discovery Methods. *Curr. Opin. Microbiol.* 19, 70–75. doi:10.1016/j.mib.2014.05.021

Charmsaz, S., Prencipe, M., Kiely, M., Pidgeon, G., and Collins, D. (2018). Innovative Technologies Changing Cancer Treatment. *Cancers* 10, 208. doi:10.3390/cancers10060208

Chavda, V. P., Mohapatra, S. S., Ranjan, S., Dasgupta, N., Mishra, R. K., and Thomas, D. S. (2019). *"Chapter 4 - Nanobased Nano Drug Delivery: A Comprehensive Review," in* Micro And Nano Technologies. Elsevier, 69–92. doi:10.1016/B978-0-12-814029-1.00004-1

Chen, D., Dai, F., Chen, Z., Wang, S., Cheng, X., Sheng, Q., et al. (2016). Dimethoxy Curcumin Induces Apoptosis by Suppressing Survivin and Inhibits Invasion by Enhancing E-Cadherin in Colon Cancer Cells. *Med. Sci. Monit.* 22, 3215–3222. doi:10.12659/msm.900802

Chen, X., Chen, X., Zhang, X., Wang, L., Cao, P., Rajamanickam, V., et al. (2019). Curcuminoid B63 Induces ROS-Mediated Paraptosis-like Cell Death by Targeting TrxR1 in Gastric Cells. *Redox Biol.* 21, 101061. doi:10.1016/j.redox.2018.11.019

Cheung, J. Y., Ong, R. C., Suen, Y. K., Ooi, V., Wong, H. N., Mak, T. C., et al. (2005). Polyphyllin D Is a Potent Apoptosis Inducer in Drug-Resistant HepG2 Cells. *Cancer Lett.* 217, 203–211. doi:10.1016/j.canlet.2004.06.042

Cova, T. F. G. G., Bento, D. J., and Nunes, S. C. C. (2019). Computational Approaches in Theranostics: Mining and Predicting Cancer Data. *Pharmaceutics* 11, 119. doi:10.3390/pharmaceutics11030119

Cragg, G. M., and Pezzuto, J. M. (2016). Natural Products as a Vital Source for the Discovery of Cancer Chemotherapeutic and Chemopreventive Agents. *Med. Princ. Pract.* 25, 41–59. doi:10.1159/000443404

Cutler, D. M. (2020). Early Returns From the Era of Precision Medicine. *JAMA.* 323, 109–110. doi:10.1001/jama.2019.20659

Dall'Acqua, S. (2014). Natural Products as Antimitotic Agents. *Curr. Top. Med. Chem.* 14, 2272–2285. doi:10.2174/1568026614666141130095311

Das, A. (2015). Anticancer Effect of AntiMalarial Artemisinin Compounds. *Ann. Med. Health Sci. Res.* 5, 93–102. doi:10.4103/2141-9248.153609

David, B., Grondin, Antonio., Schambel, Philippe., and Vitorino, Marc. (2020). Plant Natural Fragments, an Innovative Approach for Drug Discovery. *Phytochem. Rev.* 19, 1141–1156.

de Araújo, R. S. A., da Silva-Junior, E. F., de Aquino, T. M., Scotti, M. T., Ishiki, H. M., Scotti, L., et al. (2020). Computer-Aided Drug Design Applied to Secondary Metabolites as Anticancer Agents. *Ctmc* 20, 1677–1703. doi:10.2174/1568026620666200607191838

Dey, P., Kundu, A., Kumar, A., Gupta, M., Lee, B. M., Bhakta, T., et al. (2020). Analysis of Alkaloids (Indole Alkaloids, Isoquinoline Alkaloids, Tropane Alkaloids). *Recent Adv. Nat. Prod. Anal.*, 505–567. doi:10.1016/B978-0-12-816455-6.00015-9

Elyashberg, M., and Argyropoulos, D. (2020). Computer Assisted Structure Elucidation (CASE): Current and Future Perspectives. *Magn. Reson. Chem.* 59, 669–690. doi:10.1002/mrc.5115

Elyashberg, M., Blinov, K., Molodtsov, S., Smurnyy, Y., Williams, A. J., and Churanova, T. (2009). Computer-assisted Methods for Molecular Structure Elucidation: Realizing a Spectroscopist's Dream. *J. Cheminform.* 1, 3. doi:10.1186/1758-2946-1-3

Florean, C., Schnekenburger, M., Lee, J. Y., Kim, K. R., Mazumder, A., Song, S., et al. (2016). Discovery and Characterization of Isofistularin-3, a Marine Brominated Alkaloid, as a New DNA Demethylating Agent Inducing Cell Cycle Arrest and Sensitization to TRAIL in Cancer Cells. *Oncotarget.* 7, 24027–24049. doi:10.18632/oncotarget.8210

Garofalo, M., Grazioso, G., Cavalli, A., and Sgrignani, J. (2020). How Computational Chemistry and Drug Delivery Techniques Can Support the Development of New Anticancer Drugs. *Molecules* 25, 1756. doi:10.3390/molecules25071756

Gupta, P., Wright, S. E., Kim, S.-H., and Srivastava, S. K. (2014). Phenethyl Isothiocyanate: a Comprehensive Review of Anti-cancer Mechanisms. *Biochim. Biophys. Acta (Bba) - Rev. Cancer* 1846, 405–424. doi:10.1016/j.bbcan.2014.08.003

Harn, Y.-C., Su, B.-H., Ku, Y.-L., Lin, O. A., Chou, C.-F., and Tseng, Y. J. (2017). NP-StructurePredictor: Prediction of Unknown Natural Products in Plant Mixtures. *J. Chem. Inf. Model.* 57, 3138–3148. doi:10.1021/acs.jcim.7b00565

Holohan, C., Van Schaeybroeck, S., Longley, D. B., and Johnston, P. G. (2013). Cancer Drug Resistance: An Evolving Paradigm. *Nat. Rev. Cancer* 13, 714–726. doi:10.1038/nrc3599

Hoseini-Ghahfarokhi, M., Mirkiani, S., Mozaffari, N., Abdolahi Sadatlu, M. A., Ghasemi, A., Abbaspour, S., et al. (2020). Applications of Graphene and Graphene Oxide in Smart Drug/Gene Delivery: Is the World Still Flat?. *Ijn* 15, 9469–9496. doi:10.2147/IJN.S265876

Jampilek, J., and Kralova, K. (2021). Advances in Drug Delivery Nanosystems Using Graphene-Based Materials and Carbon Nanotubes. *Materials* 14, 1059. doi:10.3390/ma14051059

Khalifa, S. A. M., Elias, N., Farag, M. A., Chen, L., Saeed, A., Hegazy, M.-E. F., et al. (2019). Marine Natural Products: A Source of Novel Anticancer Drugs. *Mar. Drugs* 17, 491. doi:10.3390/md17090491

Kind, T., and Fiehn, O. (2010). Advances in Structure Elucidation of Small Molecules Using Mass Spectrometry. *Bioanal. Rev.* 2, 23–60. doi:10.1007/s12566-010-0015-9

Kljun, J., and Turel, I. (2017). β-Diketones as Scaffolds for Anticancer Drug Design - from Organic Building Blocks to Natural Products and Metallodrug Components. *Eur. J. Inorg. Chem.* 2017, 1655–1666. doi:10.1002/ejic.2016013142017

Ko, J.-H., Sethi, G., Um, J.-Y., Shanmugam, M. K., Arfuso, F., Kumar, A. P., et al. (2017). The Role of Resveratrol in Cancer Therapy. *Ijms* 18, 2589. doi:10.3390/ijms18122589

Koos, M. R. M., Navarro-Vázquez, A., Anklin, C., and Gil, R. R. (2020). Computer-Assisted 3D Structure Elucidation (CASE-3D): The Structural Value of 2 J CH in Addition to 3 J CH Coupling Constants. *Angew. Chem. Int. Ed.* 59, 3938–3941. doi:10.1002/anie.201915103

Korga, A., Ostrowska, M., Jozefczyk, A., Iwan, M., Wojcik, R., Zgorka, G., et al. (2019). Apigenin and Hesperidin Augment the Toxic Effect of Doxorubicin against HepG2 Cells. *BMC Pharmacol. Toxicol.* 20, 22. doi:10.1186/s40360-019-0301-2

Krzyszczyk, P., Acevedo, A., Davidoff, E. F., Timmins, L. M., Marrero-Berrios, I., Patel, M., et al. (2018). The Growing Role of Precision and Personalized Medicine for Cancer Treatment. *Technol.* 6, 79–100. doi:10.1142/S2339547818300020

Kumar, M. S., and Adki, K. M. (2018). Marine Natural Products for Multi-Targeted Cancer Treatment: A Future Insight. *Biomed. Pharmacother.* 105, 233–245. doi:10.1016/j.biopha.2018.05.142

Kumar, P. (2018). Recent Advancement in Cancer Treatment. *Elsevier Inc*, 621–651. doi:10.1016/B978-0-12-813669-0.00016-6

Kuntz, E. M., Baquero, P., Michie, A. M., Dunn, K., Tardito, S., Holyoake, T. L., et al. (2017). Targeting Mitochondrial Oxidative Phosphorylation Eradicates Therapy-Resistant Chronic Myeloid Leukemia Stem Cells. *Nat. Med.* 23, 1234–1240. doi:10.1038/nm.4399

Kwak, T. W., Park, S.-B., Kim, H.-J., Jeong, Y.-I., and Kang, D. H. (2017). Anticancer Activities of Epigallocatechin-3-Gallate against Cholangiocarcinoma Cells. *Ott* 10, 137–144. doi:10.2147/OTT.S112364

Lee, I.-C., and Choi, B. (2016). Withaferin-A-A Natural Anticancer Agent with Pleitropic Mechanisms of Action. *Ijms* 17, 290. doi:10.3390/ijms17030290

Lee, J., Sul, J., Park, J., Lee, M., Cha, E., and Ko, Y. (2019). Honokiol Induces Apoptosis and Suppresses Migration and Invasion of Ovarian Carcinoma Cells *via* AMPK/mTOR Signaling Pathway. *Int. J. Mol. Med.* 43, 1969–1978. doi:10.3892/ijmm.2019.4122

Li, A., and Bergan, R. C. (2020). Clinical Trial Design: Past, Present, and Future in the Context of Big Data and Precision Medicine. *Cancer* 126, 4838–4846. doi:10.1002/cncr.33205

Li, Q. (2020). Application of Fragment-Based Drug Discovery to Versatile Targets. *Front. Mol. Biosci.* 7, 180. doi:10.3389/fmolb.2020.00180

Li, X., Chu, S., Lin, M., Gao, Y., Liu, Y., Yang, S., et al. (2020). Anticancer Property of Ginsenoside Rh2 from Ginseng. *Eur. J. Med. Chem.* 203, 112627. doi:10.1016/j.ejmech.2020.112627

Liang, J.-W., Wang, M.-Y., Wang, S., Li, X.-Y., and Meng, F.-H. (2019). Fragment-Based Structural Optimization of a Natural Product Itampolin A as a P38α Inhibitor for Lung Cancer. *Mar. Drugs* 17, 53. doi:10.3390/md17010053

Lin, L.-G., Xie, H., Li, H.-L., Tong, L.-J., Tang, C.-P., Ke, C.-Q., et al. (2008). Naturally Occurring Homoisoflavonoids Function as Potent Protein Tyrosine Kinase Inhibitors by C-Src-Based High-Throughput Screening. *J. Med. Chem.* 51, 4419–4429. doi:10.1021/jm701501x

Ling, H., Yang, H., Tan, S.-H., Chui, W.-K., and Chew, E.-H. (2010). 6-Shogaol, an Active Constituent of Ginger, Inhibits Breast Cancer Cell Invasion by Reducing Matrix Metalloproteinase-9 Expression *via* Blockade of Nuclear Factor-Kb Activation. *Br. J. Pharmacol.* 161, 1763–1777. doi:10.1111/j.1476-5381.2010.00991.x

Ling, M. T., Luk, S. U., Al-Ejeh, F., and Khanna, K. K. (2012). Tocotrienol as a Potential Anticancer Agent. *Carcinogenesis* 33, 233–239. doi:10.1093/carcin/bgr261

Liu, K. K.-C., Bagrodia, S., Bailey, S., Cheng, H., Chen, H., Gao, L., et al. (2010). 4-Methylpteridinones as Orally Active and Selective PI3K/mTOR Dual Inhibitors. *Bioorg. Med. Chem. Lett.* 20, 6096–6099. doi:10.1016/j.bmcl.2010.08.045

Liu, M., and Quinn, R. J. (2019). Fragment-based Screening with Natural Products for Novel Anti-parasitic Disease Drug Discovery. *Expert Opin. Drug Discov.* 14, 1283–1295. doi:10.1080/17460441.2019.1653849

Lu, M.-D., Li, L.-Y., Li, P.-H., You, T., Wang, F.-H., Sun, W.-J., et al. (2017). Gossypol Induces Cell Death by Activating Apoptosis and Autophagy in HT-29 Cells. *Mol. Med. Rep.* 16, 2128–2132. doi:10.3892/mmr.2017.6804

Ma, Z., Wan, H., Wang, W., Zhang, X., Uno, T., Yang, Q., et al. (2019). A Theranostic Agent for Cancer Therapy and Imaging in the Second Near-Infrared Window. *Nano Res.* 12, 273–279. doi:10.1007/s12274-018-2210-x

Majnooni, M. B., Fakhri, S., Smeriglio, A., Trombetta, D., Croley, C. R., Bhattacharyya, P., et al. (2019). Antiangiogenic Effects of Coumarins against Cancer: From Chemistry to Medicine. *Molecules* 24, 4278. doi:10.3390/molecules24234278

Maruca, A., Rocca, R., Catalano, R., Mesiti, F., Costa, G., Lanzillotta, D., et al. (2020). Natural Products Extracted from Fungal Species as New Potential Anti-cancer Drugs: A Structure-Based Drug Repurposing Approach Targeting HDAC7. *Molecules* 25, 5524. doi:10.3390/molecules25235524

Mazumder, A., Cerella, C., and Diederich, M. (2018). Natural Scaffolds in Anticancer Therapy and Precision Medicine. *Biotechnol. Adv.* 36, 1563–1585. doi:10.1016/j.biotechadv.2018.04.009

Mullard, A. (2014a). 2013 FDA Drug Approvals. *Nat. Rev. Drug Discov.* 13, 85–89. doi:10.1038/nrd4239

Mullard, A. (2014b). New Drugs Cost US$2.6 Billion to Develop. *Nat. Rev. Drug Discov.* 13, 877. doi:10.1038/nrd4507

Murray, C. W., and Rees, D. C. (2009). The Rise of Fragment-Based Drug Discovery. *Nat. Chem* 1, 187–192. doi:10.1038/nchem.217

Neag, M. A., Mocan, A., Echeverría, J., Pop, R. M., Bocsan, C. I., Crișan, G., et al. (2018). Berberine: Botanical Occurrence, Traditional Uses, Extraction Methods, and Relevance in Cardiovascular, Metabolic, Hepatic, and Renal Disorders. *Front. Pharmacol.* 9, 557. doi:10.3389/fphar.2018.00557

Newman, D. J., and Cragg, G. M. (2012). Natural Products as Sources of New Drugs over the 30 Years from 1981 to 2010. *J. Nat. Prod.* 75, 311–335. doi:10.1021/np200906s

NIH (2021). Cancer. Available at: https://www.cancer.gov/publications/dictionaries/cancer-terms/def/cancer (Accessed April 25, 2021).

Nugroho, A. E., and Morita, H. (2019). Computationally-assisted Discovery and Structure Elucidation of Natural Products. *J. Nat. Med.* 73, 687–695. doi:10.1007/s11418-019-01321-8

Ontikatze, T., Rudner, J., Handrick, R., Belka, C., and Jendrossek, V. (2014). Dihydroartemisinin Is a Hypoxia-Active Anti-cancer Drug in Colorectal Carcinoma Cells. *Front. Oncol.* 4, 116. doi:10.3389/fonc.2014.00116

Ortiz-Hidalgo, C., and Pina-Oviedo, S. (2019). Hematoxylin: Mesoamerica's Gift to Histopathology. Palo de Campeche (Logwood Tree), Pirates' Most Desired Treasure, and Irreplaceable Tissue Stain. *Int. J. Surg. Pathol.* 27, 4–14. doi:10.1177/1066896918787652

Parsai, S., Keck, R., Skrzypczak-Jankun, E., and Jankun, J. (2014). Analysis of the Anticancer Activity of Curcuminoids, Thiotryptophan and 4-phenoxyphenol Derivatives. *Oncol. Lett.* 7, 17–22. doi:10.3892/ol.2013.1679

Petrelli, A., and Valabrega, G. (2009). Multitarget Drugs: The Present and the Future of Cancer Therapy. *Expert Opin. Pharmacother.* 10, 589–600. doi:10.1517/14656560902781907

Peyvandipour, A., Saberian, N., Shafi, A., Donato, M., and Draghici, S. (2018). A Novel Computational Approach for Drug Repurposing Using Systems Biology. *Bioinformatics* 34, 2817–2825. doi:10.1093/bioinformatics/bty133

Pfirschke, C., Engblom, C., Rickelt, S., Cortez-Retamozo, V., Garris, C., Pucci, F., et al. (2016). Immunogenic Chemotherapy Sensitizes Tumors to Checkpoint Blockade Therapy. *Immun.* 44, 343–354. doi:10.1016/j.immuni.2015.11.024

Pradeep, C. R., and Kuttan, G. (2004). Piperine Is a Potent Inhibitor of Nuclear Factor-Kb (NF-Kb), C-Fos, CREB, ATF-2 and Proinflammatory Cytokine Gene Expression in B16F-10 Melanoma Cells. *Int. Immunopharmacology* 4, 1795–1803. doi:10.1016/j.intimp.2004.08.005

Ramsay, R. R., Popovic-Nikolic, M. R., Nikolic, K., Uliassi, E., and Bolognesi, M. L. (2018). A Perspective on Multi-target Drug Discovery and Design for Complex Diseases. *Clin. Translational Med.* 7, 3. doi:10.1186/s40169-017-0181-2

Rayburn, E., Ezell, S. J., and Zhang, R. (2009). Anti-Inflammatory Agents for Cancer Therapy. *Mol. Cel. Pharmacol.* 1, 29–43. doi:10.4255/mcpharmacol.09.05

Rinschen, M. M., Ivanisevic, J., Giera, M., and Siuzdak, G. (2019). Identification of Bioactive Metabolites Using Activity Metabolomics. *Nat. Rev. Mol. Cel Biol.* 20, 353–367. doi:10.1038/s41580-019-0108-4

Rosli, N. F., Fojtů, M., Fisher, A. C., and Pumera, M. (2019). Graphene Oxide Nanoplatelets Potentiate Anticancer Effect of Cisplatin in Human Lung Cancer Cells. *Langmuir* 35, 3176–3182. doi:10.1021/acs.langmuir.8b03086

Sahebkar, A. (2016). Curcumin. *Integr. Cancer Ther.* 15, 333–334. doi:10.1177/1534735415624139

Setlow, R. B. (2001). Human Cancer: Etiologic Agents/dose Responses/DNA Repair/cellular and Animal Models. *Mutat. Research/Fundamental Mol. Mech. Mutagenesis* 477, 1–6. doi:10.1016/s0027-5107(01)00090-2

Shahinozzaman, M., Ishii, T., Ahmed, S., Halim, M. A., and Tawata, S. (2020). A Computational Approach to Explore and Identify Potential Herbal Inhibitors for the P21-Activated Kinase 1 (PAK1). *J. Biomol. Struct. Dyn.* 38, 3514–3526. doi:10.1080/07391102.2019.1659855

Shailaja, V. L., Christina, V. S., Mohanapriya, C. D., Sneha, P., Lakshmi Sundaram, R., Magesh, R., et al. (2019). A Natural Anticancer pigment,Pheophytin A,from a Seagrass Acts as a High Affinity Human Mitochondrial Translocator Protein (TSPO) Ligand, In Silico, to Reduce Mitochondrial Membrane Potential ($\Delta\psi$) in Adenocarcinomic A549 Cells. *Phytomedicine* 61, 152858. doi:10.1016/j.phymed.2019.152858

Sharma, R., Mody, N., Agrawal, U., and Vyas, S. P. (2017). Theranostic Nanomedicine; A Next Generation Platform for Cancer Diagnosis and Therapy. *Mrmc* 17, 1746–1757. doi:10.2174/1389557516666160219122524

Shi, J., Kantoff, P. W., Wooster, R., and Farokhzad, O. C. (2017). Cancer Nanomedicine: Progress, Challenges and Opportunities. *Nat. Rev. Cancer* 17, 20–37. doi:10.1038/nrc.2016.108

Shi, J., Li, J., Xu, Z., Chen, L., Luo, R., Zhang, C., et al. (2020). Celastrol: A Review of Useful Strategies Overcoming its Limitation in Anticancer Application. *Front. Pharmacol.* 11, 558741. doi:10.3389/fphar.2020.558741

Silva, C. O., Pinho, J. O., Lopes, J. M., Almeida, A. J., Gaspar, M. M., and Reis, C. (2019). Current Trends in Cancer Nanotheranostics: Metallic, Polymeric, and Lipid-Based Systems. *Pharmaceutics* 11, 22. doi:10.3390/pharmaceutics11010022

Singh, N., and Sharma, B. (2018). Toxicological Effects of Berberine and Sanguinarine. *Front. Mol. Biosci.* 5, 21. doi:10.3389/fmolb.2018.00021

Sivasankarapillai, V. S., Madhu Kumar Nair, R., Rahdar, A., Bungau, S., Zaha, D. C., Aleya, L., et al. (2020). Overview of the Anticancer Activity of Withaferin A, an Active Constituent of the Indian Ginseng Withania Somnifera. *Environ. Sci. Pollut. Res.* 27, 26025–26035. doi:10.1007/s11356-020-09028-0

Soong, R., Pautler, B. G., Moser, A., Jenne, A., Lysak, D. H., Adamo, A., et al. (2020). CASE (Computer-Assisted Structure Elucidation) Study for an Undergraduate Organic Chemistry Class. *J. Chem. Educ.* 97, 855–860. doi:10.1021/acs.jchemed.9b00498

Su, B.-H., Shen, M.-Y., Harn, Y.-C., Wang, S.-Y., Schurz, A., Lin, C., et al. (2017). An Efficient Computer-Aided Structural Elucidation Strategy for Mixtures Using an Iterative Dynamic Programming Algorithm. *J. Cheminform.* 9, 57. doi:10.1186/s13321-017-0244-9

Tay, K.-C., Tan, L. T.-H., Chan, C. K., Hong, S. L., Chan, K.-G., Yap, W. H., et al. (2019). Formononetin: A Review of its Anticancer Potentials and Mechanisms. *Front. Pharmacol.* 10, 820. doi:10.3389/fphar.2019.00820

Taylor, W. F., Moghadam, S. E., Moridi Farimani, M., N. Ebrahimi, S., Tabefam, M., and Jabbarzadeh, E. (2019). A Multi-Targeting Natural Compound with Growth Inhibitory and Anti-angiogenic Properties Re-sensitizes Chemotherapy Resistant Cancer. *PLoS One* 14, e0218125–17. doi:10.1371/journal.pone.0218125

Teiten, M.-H., Dicato, M., and Diederich, M. (2014). Hybrid Curcumin Compounds: a New Strategy for Cancer Treatment. *Molecules* 19, 20839–20863. doi:10.3390/molecules191220839

Teiten, M.-H., Eifes, S., Dicato, M., and Diederich, M. (2010). Curcumin—The Paradigm of a Multi-Target Natural Compound with Applications in Cancer Prevention and Treatment. *Toxins* 2, 128–162. doi:10.3390/toxins2010128

Tomeh, M., Hadianamrei, R., and Zhao, X. (2019). A Review of Curcumin and its Derivatives as Anticancer Agents. *Ijms* 20, 1033. doi:10.3390/ijms20051033

Tripathi, S. K., and Biswal, B. K. (2020). Piperlongumine, a Potent Anticancer Phytotherapeutic: Perspectives on Contemporary Status and Future Possibilities as an Anticancer Agent. *Pharmacol. Res.* 156, 104772. doi:10.1016/j.phrs.2020.104772

Wang, L.-S., and Stoner, G. D. (2008). Anthocyanins and Their Role in Cancer Prevention. *Cancer Lett.* 269, 281–290. doi:10.1016/j.canlet.2008.05.020

Wang, Y., Liu, Y., Du, X., Ma, H., and Yao, J. (2020). The Anti-cancer Mechanisms of Berberine: A Review. *Cmar* 12, 695–702. doi:10.2147/CMAR.S242329

Ward, C. C., Kleinman, J. I., Brittain, S. M., Lee, P. S., Chung, C. Y. S., Kim, K., et al. (2019). Covalent Ligand Screening Uncovers a RNF4 E3 Ligase Recruiter for Targeted Protein Degradation Applications. *ACS Chem. Biol.* 14, 2430–2440. doi:10.1021/acschembio.8b01083

Weng, J.-R., Tsai, C.-H., Kulp, S. K., and Chen, C.-S. (2008). Indole-3-carbinol as a Chemopreventive and Anti-cancer Agent. *Cancer Lett.* 262, 153–163. doi:10.1016/j.canlet.2008.01.033

Who (2021a). Cancer Today. Available at: https://gco.iarc.fr/today/.

Who (2021b). WHO FactSheets: Cancer. 3 March 2021. Available at: https://www.who.int/news-room/fact-sheets/detail/cancer (Accessed April 25, 2021).

Wilken, R., Veena, M. S., Wang, M. B., and Srivatsan, E. S. (2011). Curcumin: A Review of Anti-cancer Properties and Therapeutic Activity in Head and Neck Squamous Cell Carcinoma. *Mol. Cancer* 10, 12. doi:10.1186/1476-4598-10-12

Wogan, G. N., Hecht, S. S., Felton, J. S., Conney, A. H., and Loeb, L. A. (2004). Environmental and Chemical Carcinogenesis. *Semin. Cancer Biol.* 14, 473–486. doi:10.1016/j.semcancer.2004.06.010

Xu, J.-Y., Meng, Q.-H., Chong, Y., Jiao, Y., Zhao, L., Rosen, E. M., et al. (2012). Sanguinarine Inhibits Growth of Human Cervical Cancer Cells through the Induction of Apoptosis. *Oncol. Rep.* 28, 2264–2270. doi:10.3892/or.2012.2024

Yang, W., Deng, X., Huang, W., Qing, X., and Shao, Z. (2019). The Physicochemical Properties of Graphene Nanocomposites Influence the Anticancer Effect. *J. Oncol.* 2019, 1–10. doi:10.1155/2019/7254534

Zhang, S., Gao, Q., Li, W., Zhu, L., Shang, Q., Feng, S., et al. (2019). Shikonin Inhibits Cancer Cell Cycling by Targeting Cdc25s. *BMC Cancer* 19, 20. doi:10.1186/s12885-018-5220-x

Conflict of Interest: The authors declare that the research was conducted in the absence of any commercial or financial relationships that could be construed as a potential conflict of interest.

Publisher's Note: All claims expressed in this article are solely those of the authors and do not necessarily represent those of their affiliated organizations, or those of the publisher, the editors and the reviewers. Any product that may be evaluated in this article, or claim that may be made by its manufacturer, is not guaranteed or endorsed by the publisher.

frontiers in Pharmacology

REVIEW
published: 27 August 2021
doi: 10.3389/fphar.2021.703761

Natural Small Molecules Targeting NF-κB Signaling in Glioblastoma

Md. Sahab Uddin[1,2†], Md. Tanvir Kabir[3], Abdullah Al Mamun[4], Md. Shahid Sarwar[5], Fatema Nasrin[6,7], Talha Bin Emran[8], Ibtesam S. Alanazi[9], Abdur Rauf[10], Ghadeer M. Albadrani[11], Amany A. Sayed[12], Shaker A. Mousa[13] and Mohamed M. Abdel-Daim[14,15]*

[1]Department of Pharmacy, Southeast University, Dhaka, Bangladesh, [2]Pharmakon Neuroscience Research Network, Dhaka, Bangladesh, [3]Department of Pharmacy, Brac University, Dhaka, Bangladesh, [4]Teaching and Research Division, School of Chinese Medicine, Hong Kong Baptist University, Kowloon, Hong Kong, [5]Department of Pharmacy, Noakhali Science and Technology University, Noakhali, Bangladesh, [6]Institute of Health and Biomedical Innovation, Translational Research Institute, Brisbane, QLD, Australia, [7]School of Clinical Sciences, Queensland University of Technology, Brisbane, QLD, Australia, [8]Department of Pharmacy, BGC Trust University Bangladesh, Chittagong, Bangladesh, [9]Department of Biology, Faculty of Sciences, University of Hafr Al Batin, Hafr Al Batin, Saudi Arabia, [10]Department of Chemistry, University of Swabi, Khyber Pakhtunkhwa, Pakistan, [11]Department of Biology, College of Science, Princess Nourah bint Abdulrahman University, Riyadh, Saudi Arabia, [12]Zoology Department, Faculty of Science, Cairo University, Giza, Egypt, [13]Pharmaceutical Research Institute, Albany College of Pharmacy and Health Sciences, Rensselaer, NY, United States, [14]Department of Pharmaceutical Sciences, Pharmacy Program, Batterjee Medical College, Jeddah, Saudi Arabia, [15]Pharmacology Department, Faculty of Veterinary Medicine, Suez Canal University, Ismailia, Egypt

OPEN ACCESS

Edited by:
Rajeev K. Singla, Sichuan University, China

Reviewed by:
Yang Liu, Peking University Third Hospital, China
Manoj Kumar Sabnani, University of Texas at Arlington, United States

***Correspondence:**
Md. Sahab Uddin
msu.neuropharma@gmail.com

†ORCID:
Md. Sahab Uddin
https://orcid.org/0000-0002-0805-7840

Specialty section:
This article was submitted to Ethnopharmacology, a section of the journal Frontiers in Pharmacology

Received: *30 April 2021*
Accepted: *09 August 2021*
Published: *27 August 2021*

Citation:
Uddin MS, Kabir MT, Mamun AA, Sarwar MS, Nasrin F, Emran TB, Alanazi IS, Rauf A, Albadrani GM, Sayed AA, Mousa SA and Abdel-Daim MM (2021) Natural Small Molecules Targeting NF-κB Signaling in Glioblastoma. Front. Pharmacol. 12:703761. doi: 10.3389/fphar.2021.703761

Nuclear factor-κB (NF-κB) is a transcription factor that regulates various genes that mediate various cellular activities, including propagation, differentiation, motility, and survival. Abnormal activation of NF-κB is a common incidence in several cancers. Glioblastoma multiforme (GBM) is the most aggressive brain cancer described by high cellular heterogeneity and almost unavoidable relapse following surgery and resistance to traditional therapy. In GBM, NF-κB is abnormally activated by various stimuli. Its function has been associated with different processes, including regulation of cancer cells with stem-like phenotypes, invasion of cancer cells, and radiotherapy resistance identification of mesenchymal cells. Even though multimodal therapeutic approaches such as surgery, radiation therapy, and chemotherapeutic drugs are used for treating GBM, however; the estimated mortality rate for GBM patients is around 1 year. Therefore, it is necessary to find out new therapeutic approaches for treating GBM. Many studies are focusing on therapeutics having less adverse effects owing to the failure of conventional chemotherapy and targeted agents. Several studies of compounds suggested the involvement of NF-κB signaling pathways in the growth and development of a tumor and GBM cell apoptosis. In this review, we highlight the involvement of NF-κB signaling in the molecular understanding of GBM and natural compounds targeting NF-κB signaling.

Keywords: NF-κB, glioblastoma, brain cancer, malignant, natural products, small molecules

INTRODUCTION

In the United States, around 17,000 malignant glioma incidents are identified yearly, and more than 80% of these are glioblastoma multiforme (GBM) (Dolecek et al., 2012). GBM is characterized by a remarkably heterogeneous and invasive kind of malignant brain cancer (Uddin et al., 2020a). It is considered the deadliest cancer, with a projected survival of about 14 months after confirming the

diagnosis (Furnari et al., 2007). Resistance to conventional therapies and tumor relapse after surgery are mainly responsible for this poor prognosis. GBM is highly heterogeneous and shows various distinctive properties with the unique origin of cell types and different genetic lesions lead to various clinical behaviors (Stiles and Rowitch, 2008; Huse and Holland, 2010). Current developments in molecular technology, primarily next-generation sequencing and high-density microarrays, have made it possible to classify GBM into subtypes according to the histological level and signatures of gene expression. Although many studies have tried to describe the various molecular subtypes of GBM (Phillips et al., 2006; Cooper et al., 2010; Verhaak et al., 2010; Huse et al., 2011), among them two subtypes, called proneural and mesenchymal (MES), tend to be stable and normally consistent amid the various proposed classifications. Furthermore, tumors identified as subtype MES demonstrate poor prognosis and have been associated with poor response to radiation, overexpression of CD44, and activation of nuclear factor-κB (NF-κB) (Bhat et al., 2013). There is still an inadequate comprehending of the fundamental processes of development and the reappearance of gliomagenesis, despite the advancement in genetic analysis and GBM classification.

NF-κB belongs to a family of transcription factors that leads to the formation of various heterodimers or homodimers and attach to consensus DNA sequences at the promoter regions of target gene (Friedmann-Morvinski et al., 2016). NF-κB plays a pivotal role in the control of immunity, inflammation, and cell survival, as well as involves in various functions associated with cellular activities (Tilstra et al., 2011; Uddin et al., 2021). Activation of NF-κB pathways could be triggered by different stimuli, such as DNA damage, cytokines, oncogenic stress, ultraviolet and ionizing radiation, pathogen-related molecular patterns, reactive oxygen species, and growth factors (Xia et al., 2014). Even though NF-κB has been revealed to develop cancer by triggering and maintaining a pro-inflammatory microenvironment, however; constitutive activation of NF-κB seems to induce tumor initiation and progression through several mechanisms, including apoptosis, proliferation of cells, metastasis of tumor, angiogenesis, and metabolism reprogramming (Xia et al., 2014). GBM has revealed that the constitutive NF-κB activation induces development and survival. Moreover, sulfasalazine (an anti-inflammatory drug) has shown inhibitory action of NF-κB that triggers the apoptosis in glioma cells (Robe et al., 2004), and a decoy oligonucleotide strategy to prevent NF-κB that played a crucial role in the decline in the number of cells (Gill et al., 2002). Recently, the activation of NF-κB has been found to connect with the transformation of MES differentiation from proneural glioma stem cells, with related radioresistant properties.

The natural compounds-based treatment has paid attention in scientists in the last 2 decades as an efficient and possibly less toxic therapy for cancer (Kumar et al., 2020; Lin et al., 2020; Aziz et al., 2021; Huang et al., 2021). Long years ago, American Indians had used *Podophyllum peltatum* L. roots for the treatment of various skin cancers (Mann, 2002). Furthermore, the key anticancer ingredient podophyllotoxin and its semi-synthetic derivatives, such as etoposide, etopophos, and teniposide are used to treat many cancers (Schacter, 1996). From 1960 to 1985, two mega-scale anti-cancer drug-screening projects were launched by the National Cancer Institute (NCI) (Cragg et al., 1996). After screening, they have found a significant compound paclitaxel (Taxol), separated from the *Taxus brevifolia* Nutt. bark, which has subsequently been applied in the treatment of several solid tumors (Cragg et al., 1996). Furthermore, almost one-third of the therapeutic agents accepted for cancer by the Food and Drug Administration (FDA) were from natural compounds or their derivatives (Mann, 2002; Altmann and Gertsch, 2007). Plant flavonol quercetin inhibits NF-κB transactivation in the U87 human glioma cell line at 20 μM and demonstrates antiproliferative effects, necrosis/apoptosis activation, and cell cycle arrest in the U138MG human glioma cell line with lower cytotoxicity to normal cells (Braganhol et al., 2006; Braganhol et al., 2007; Park and Min, 2011). Another study has suggested that by regulating NF-κB nuclear translocation and caspase-3 activation, a quercetin derivative causes cell death in glioma cells (Kiekow et al., 2016a). In this review, we focus on the role of NF-κB as a potential biomarker of GBM and highlight various natural compounds that affect the signaling pathway of NF-κB for treating GBM.

STRUCTURAL AND FUNCTIONAL PROPERTIES OF NF-κB

NF-κB is a protein complex that regulates DNA synthesis, survival, and cytokine production (Taniguchi and Karin, 2018). Indeed, all the proteins that belong to the NF-κB family possess the Rel homology domain in their N-terminal part. In terms of its structure, NF-κB contains homodimers and heterodimers of the five members Rel family that are categorized into two groups. Furthermore, the first group of the protein complex is composed of c-Rel, RelA (p65), and RelB; on the other hand, the next group comprises NF-κB1 (p105/p50) and NFκB2 (p100/p52) (Sun, 2011; Puliyappadamba et al., 2014) as shown in **Figure 1**. It has been reported that the first group (c-Rel, RelA, and RelB) proteins contain a transactivation domain in their C-terminus region. Alternatively, second group specifically NF-κB1 and NF-κB2 proteins are generated as large precursors comprising p105 and p100 that play crucial roles in producing mature NF-κB subunits such as p50 and p52, successively. These NF-κB subunits have no inherent capacity to mediate transcription, and when they interact as homodimers κB components, they act as transcriptional repressors (Park and Hong, 2016).

It is known that kappa B (IκBs) inhibitors are a group of related enzymes with an N-terminal structural area, along with six or more ankyrin chains as well as a PEST domain adjacent to their C terminal domain. Even though the IκB family is composed of various proteins including Bcl-3, IκBα, IκBβ, and IκBε, among them IκBα has been extensively studied (Zhou et al., 2005). NF-κB is inactive in unstimulated cells due to its interaction with IκBα inhibitor, and the structure is usually found in the cytoplasm. IκB kinases (IKKβ or IKKα) are induced and

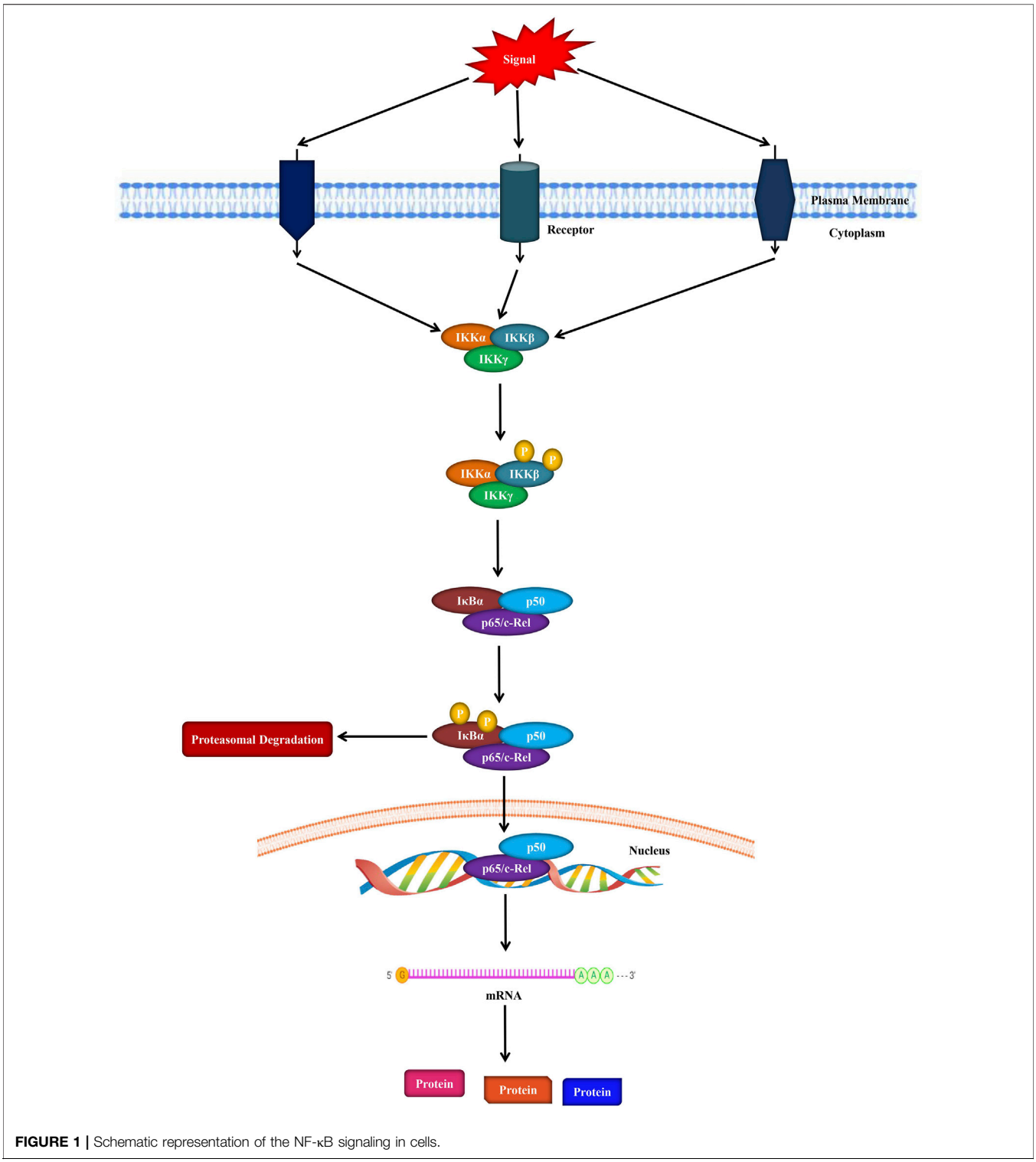

FIGURE 1 | Schematic representation of the NF-κB signaling in cells.

phosphorylate IκBα in response to various inducers including DNA damage, vascular endothelial growth factor (VEGF), epidermal growth factor (EGF), and cytokines [i.e., tumor necrosis factor (TNF)-α and TRAIL] that can further result in its degradation via a K48 ubiquitin-induced proteasomal mechanism (Park and Hong, 2016).

Several stimuli may induce the mammalian NF-κB signaling pathways, such as growth factors, reactive oxygen species (ROS), oncogenic stress, DNA damage, pathogen-associated molecular patterns, ionizing and ultraviolet irradiation, various cytokines (TNF–α and IL-1β), and stress (Gilmore, 2006; Sun, 2011). It has been revealed that NF-κB is associated with many processes

including inflammation, chemoresistance, cell survival, angiogenesis, metastasis, tumor progression, invasion, cell cycle progression, immunity, metabolic reprogramming, and apoptosis (Dolcet et al., 2005; Grivennikov and Karin, 2010). Increased levels of inflammatory cytokines (for example, IL-1, IL-15, IL-11, IL-6, and IL-8), C–C motif chemokine ligand (CCL)-2, and genes associated with pathological processes such as cyclooxygenase (COX)-2, cell adhesion (CD44), cell cycle modulators (Cyclin D1), and proteolysis (TFPI2, PLAU) are all known targets of the NF-κB signaling pathway (Richmond and Yang, 2016). Along with the nuclear translocation, several regulatory mechanisms, such as nuclear export processes, protein-protein interactions located in certain gene regulatory regions, and post-translatory changes of specific subunits of NF-κB, are controlled by the NF-κB signaling pathway. As a result, various cellular responses to NF-κB are frequently caused by specific and complex pathways that vary in their upstream stimuli and/or downstream targets (Gilmore, 2006).

NF-κB IN GLIOBLASTOMA

In case of GBM and other cancers, the NF-κB signaling pathway is found to be activated and is associated with a higher grade of astrocytic tumors. Characteristics of the mesenchymal subtype of GBM include increased concentrations of NF-κB signaling pathway constituents such as TNF receptor superfamily member 1A [(TNFRSF1A), v-rel reticuloendotheliosis viral oncogene homolog B (RELB), and TNFR1-associated death domain protein (TRADD)], elevated resistance towards chemotherapy and a lesser prognosis as compared to individuals with other GBM types (Verhaak et al., 2010). It has been established that an NF-κB/TNF- (tumor necrosis factor)-mediated mechanism can differentiate proneural individual-derived neurospheres to a mesenchymal phenotype, which has been linked to poor prognosis and radioresistance (Bhat et al., 2013). These findings collectively suggest the significance of the NF-κB signaling during the development and advancement of glioma. Applying gliomas as an experimental model for network analyses, it was observed that NF-κB signaling pathway dysregulation was 1 of 4 signaling mechanisms whose perturbation was slightly satisfactory to maintain the phenotype of malignant glioma (Karlebach and Shamir, 2010).

Nonetheless, the specific mechanism(s) of *in vivo* NF-κB activation in case of GBM is still unidentified. However, various proteins and signaling mechanisms are dysregulated in the case of GBM which might result in NF-κB activation. TNF-α is a very strong NF-κB activator (Grivennikov and Karin, 2011). TNF-α is a pro-inflammatory chemical that is released by astrocytes, microglia, and certain neurons in the CNS. Indeed, TNF-α exhibits its effect *via* two receptors including TNF receptor 1 (TNFR1) and TNF receptor 2 (TNFR2) (Grivennikov and Karin, 2011). Usually, TNFR1 is expressed in most type of the cells, whereas TNFR2 is expressed in oligodendrocytes and immune cells, including microglia. Furthermore, TNFR1 expression was found to be higher in GBM and GBM-linked endothelial cells than in normal brain tissues or low-grade gliomas (Hayashi et al., 2001; Kargiotis et al., 2006; Huang et al., 2012a).

Many signaling pathways or growth factors that are dysregulated in case of gliomas may result in the activation of NF-κB (Nogueira et al., 2011a). Particularly, NF-κB is activated *via* epidermal growth factor (EGF), and/or its receptor, (EGFR). It has been observed that EGFR is often mutated and constitutively activated (Bonavia et al., 2012; Yang et al., 2012; Puliyappadamba et al., 2013). Furthermore, oncogenic EGFR is associated with NF-κB activation by means of mechanistic target of rapamycin complex 2, and this signaling pathway mediates chemoresistance (Tanaka et al., 2011). Phosphatase and tensin homolog (PTEN) is a suppressor of tumor and a negative regulator of the Akt signaling pathway (Atkinson et al., 2010). It has been found that numerous gliomas exhibited loss of PTEN function (Atkinson et al., 2010). Akt is constitutively activated in case of PTEN absence, which can further result in NF-κB activation. Increased insulin-like growth factor binding protein-2 (IGFBP-2) concentrations and the signaling mechanism were found to be connected with an increased level of NF-κB signaling pathway (Holmes et al., 2012). In case of GBM, IGFBP2 binds specifically with β1 integrin in order to activate an integrin-linked kinase (ILK)/NF-κB cascade that further mediates the growth of glioma.

Various findings have suggested that abnormal expression of regulators can lead to increased activation of NF-κB. In GBM, the inhibitor of growth family member 4 (ING4, a negative NF- κB regulator) is expressed at very low concentrations or is mutated. In addition, deficiency of the ING4 effect activates NF-κB to remain active (Nozell et al., 2008). In contrast, peptidyl-prolyl isomerase (Pin1, a positive NF-κB regulator) was found to be overexpressed in case of GBM and plays role in constitutive activation of NF-κB (Atkinson et al., 2009). Plant homeodomain finger protein 20 (PHF20, an effector protein that binds with methylated p65) is a newly identified NF-κB regulator in GBM, which averts phosphatase PP2A recruitment, therefore it prolongs the presence of an active species of NF-κB in case of GBM (Zhang et al., 2013). It has been reported that the NFKBIA gene (that encodes IκBα) shows mono-allelic deletions in some GBM types, which is often lost in a subtype-specific manner in GBM, and this associates with increased levels of NF-κB as well as inferior prognosis of patients (Bredel et al., 2011). In a study, Pantane et al. (2013) confirmed that deletions of NFKBIA were elevated when tumors were spread as neurospheres in comparison with the deletions of parent tumor, which is further indicating that NFKBIA loss can mediate tumor-propagating activities and the formation of neurosphere. Collectively, these findings suggest the significance of the NF-κB signaling pathway in the stem cells of glioblastoma (Hjelmeland et al., 2010; Nogueira et al., 2011b).

Although many microRNAs (miRs) were found to be dysregulated and associated with the clinical-pathological characteristics of gliomas, but few of these were related to the NF-κB signaling pathway (Hummel et al., 2011). Oncogenic miRs (including miR-30e, miR-182, and miR-21) were linked with the NF-κB signaling pathway in GBM. Furthermore, miR-21 levels

were much higher than in non-cancerous brain tissue in GBM, and were inversely related to patient prognosis. miR-21 levels were markedly increased as compared to non-cancerous brain tissue in GBM and inversely associated with the prognosis of patients (Chan et al., 2005; Ciafrè et al., 2005; Chen et al., 2008; Papagiannakopoulos et al., 2008; Lakomy et al., 2011). In GBM, overexpressed miR-21 induces NF-κB signaling pathway via targeting the leucine-rich repeat flightless-1-interacting protein 1 (LRRFIP1, a DNA-binding protein that inhibits the NF-κB signaling pathway) (Li et al., 2009). In terms of miR-182, around 98% of gliomas showed increased levels of miR-182. Moreover, the number of miR-182 copy was increased by 2–3 folds in approximately 35.6% glioma cases (Song et al., 2012). TGF-β increases miR-182 levels in GBM, which further mediates NF-κB signaling pathway *via* targeting various negative regulators of NF-κB, such as TNF-α-induced protein 3-interacting protein 1 (TNIP1), optineurin (OPTN), ubiquitin specific peptidase 15 (USP15), and cylindromatosis (CYLD). As compared to normal brain, the miR-30e level was increased in GBM and sustained NF-κB signaling pathway through the targeting of IκBα (Jiang et al., 2012).

Only a few tumor suppressive miRs have been related to the NF-κB signaling pathway in GBM until now. Some studies have been reported that miR-31 is mainly absent or downregulated in GBM (Hua et al., 2012; Wang et al., 2014) and its existence is found in both the classical and mesenchymal subtypes of GBM. Decreased levels of miR-31 are also a part of 10 miR expression feature that predicts patient survival independently (Srinivasan et al., 2011). It was revealed that miR-31 inhibits the NF-κB signaling pathway by targeting TRADD (a protein that plays a role as an upstream activator). In addition, both increased TRADD levels and miR-31 loss have been identified in case of mesenchymal subtype of GBM. Indeed, the aforesaid miRs offer an interesting miRs sampling which play role in NF-κB regulation, however the list of such miRs is quite lengthy and increasing (Song et al., 2013; Xia et al., 2013; Yang et al., 2014).

PRECLINICAL STUDIES OF NF-κB SIGNALING IN GLIOBLASTOMA

Still, it is challenging to target NF-κB for GBM. Furthermore, there is also a deficiency of specific and effective compounds. Nonetheless, bortezomib is a promising proteasome inhibitor that hinders the breakdown of IκBα as well as other proteins (Yin et al., 2005; Phuphanich et al., 2010). In addition, phase I clinical trials were also started for evaluating the maximum tolerated dose and side effects of bortezomib (Phuphanich et al., 2010). Even though that study did not provide extensive data regarding the efficacy of bortezomib in GBM, but there were some findings to suggest its clinical efficacy (Phuphanich et al., 2010). However, bortezomib is not yet considered a single-agent therapy for GBM treatment. In recent times, BAY-11 (an inhibitor of IKK) has been identified as the eminent NF-κB signaling pathway inhibitor. This inhibitor also mediated *in vivo* and *in vitro* senescence of GBM cells, ameliorated sensitivity towards photodynamic (5-ALA) therapy, and reversed chemoresistance (Coupienne et al., 2011; Nogueira et al., 2011b; Shukla et al., 2013). Interestingly, dehydroxymethylepoxyquinomicin (DHMEQ) has been identified as a unique small molecule NF-κB inhibitor (Fukushima et al., 2012). It has been confirmed by preclinical studies that DHMEQ inhibited activation of NF-κB and its nuclear translocation, resulting in decreased tumor growth *in vivo* as well as reduced proliferation in GBM cells *in vitro*. Furthermore, treatment with DHMEQ was found to be synergized with radiation and temozolomide, which is suggesting its significant therapeutic potential (Brassesco et al., 2013). It has also been confirmed that withaferin A (an inhibitor of IKKβ) significantly inhibits NF-κB signaling and GBM growth *in vivo* (McFarland et al., 2013). Even though withaferin A is presently being studied in a schizophrenia clinical trial (ClinicalTrials.gov Withan, 1793) and its extract for endurance exercise performance (ClinicalTrials.gov The Ef, 2021) but it is not under consideration for GBM treatment.

NATURAL PRODUCTS TARGETING NF-κB SIGNALING IN GLIOBLASTOMA

Resveratrol

Resveratrol (a stilbenoid, naturally occurring polyphenolic compound, **Figure 2**) exhibited anti-invasion, immunomodulation, anti-inflammatory, and antitumor properties in several cancer cells (El-Readi et al., 2019; Jeandet et al., 2021). Numerous experiments have confirmed that resveratrol significantly supresses the NF-κB signaling *via* suppressing the activities of IκB kinase and NF-κB, which has provided a novel approach for cancer treatment (Ren et al., 2013; Vervandier-Fasseur and Latruffe, 2019). In a study, Jiao et al. (2015) confirmed that resveratrol suppressed PI3K/Akt/NF-κB signaling cascade that led to the inhibition of matrix metalloproteinase (MMP)-2 expression, which further resulted in suppression of attack in GBM-initiating cells. Furthermore, it was confirmed that there is a connection between the NF-κB effect and invasiveness of GBM (which takes place because of the processing of fibronectin *via* MMPs), which allows the direct integration of MMPs into the surrounding tumor cells (Westhoff et al., 2013). In addition, in GBM cells (T98G), resveratrol reversed the temozolomide resistance *via* O-6-methylguanine-DNA methyltransferase (MGMT) downregulation *via* the NF-κB-dependent pathway (Huang et al., 2012b). Many studies suggested that the NF-κB activation in multiple tumor cells (primarily associated with drug resistance), which was found to be facilitated *via* numerous chemotherapy medicines and radiation because of its action in MGMT transcription (Li and Sethi, 2010). Interestingly, NF-κB-p65 (an NF-κB subunit) resulted in increased MGMT expression, whereas an inhibitor of NF-κB abolished the increased expression of MGMT. (Hegi et al., 2005; Arepalli et al., 2015). Therefore, targeting MGMT, IκB kinase, and NF-κB may be beneficial in the resveratrol's anti-GBM potential.

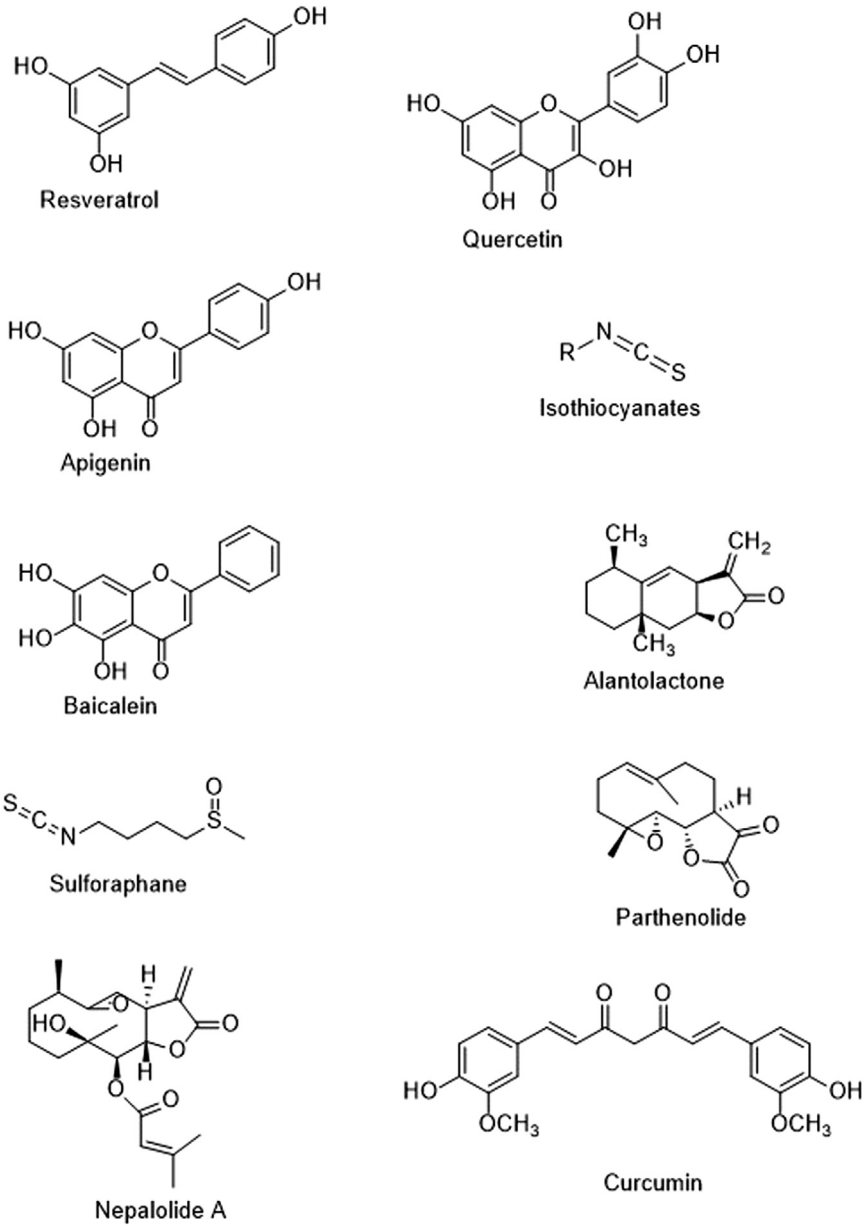

FIGURE 2 | Chemical structures of the discussed molecules.

Quercetin

Quercetin (a plant flavonoid, **Figure 2**) can induce cell death of brain, liver, and breast cancer cells (Anand David et al., 2016). Furthermore, this phenolic compound shows antioxidant, neuroprotective, anti-inflammatory, anticarcinogenic, and antihypertensive properties (Reyes-Farias and Carrasco-Pozo, 2019; Zaplatic et al., 2019). It has been revealed that quercetin has the capacity to regulate several protein kinases, particularly the PI3K pathway (Liu et al., 2017a). In a study, Liu et al. (2017b) studied the activity of quercetin (10 μg/ml) on cell invasion and migration. These researchers observed that a low dose of quercetin suppressed *in vitro* angiogenesis and glioblastoma cell invasion. In addition to this, they reported that quercetin (10 μg/ml) suppressed cell migration and human umbilical vein endothelial cell tube formation mediated via the U251 cell culture-derived conditioned medium. This suppressive action of quercetin on angiogenesis and migration might be induced by the downregulation of protein concentrations of MMP-2, MMP-9, and vascular endothelial growth factor (Liu et al., 2017b). In a study, Kiekow et al. (2016b) revealed that quercetin stimulates apoptosis in GBM cells *via* regulating activation of caspase-3 and nuclear translocation of NF-κB, which is further indicating the potential of quercetin as a novel anti-GBM therapy. Phospholipase D (PLD)

overexpression induced MMP-2 expression. Therefore, GBM cell invasion by protein kinase A (PKA)/NF-κB and protein kinase C-induced signaling mechanisms (Park et al., 2009; Tang et al., 2017). Furthermore, it was shown that quercetin suppressed the NF-κB-mediated expression of PLD-1 by the mitigation of NF-κB transactivation (Park and Min, 2011).

Apigenin

Apigenin is a natural flavone, (**Figure 2**) which is mostly found in tea leaves and fruits exhibits several biological properties including anticancer (prostate, liver, breast, and lung cancers), anti-inflammatory, antiviral, cytotoxic, antioxidant, and immunoregulatory properties (Erdogan et al., 2016; Yan et al., 2017). Apigenin's immunoregulatory property is induced *via* the suppression of PI3K/Akt/NF-κB signaling cascade (control of IKK and IκBα) signaling pathways in various cancers (Chang et al., 2015; Erdogan et al., 2016; Qin et al., 2016), which can further result in a decreased level of metastasis and invasion. Chen et al. (2016) confirmed that apigenin in a dose-dependent manner markedly reduced cell viability and triggered apoptotic cell death of U87 cells. In U87 cells, it was confirmed that apigenin markedly elevated the levels of microRNAs (miR)-16, inhibited the NF-κB/MMP-9 pathway, and also inhibited the expression of BCL2 protein. Interestingly, anti-miR-16 plasmid-mediated miR-16 downregulation was found to reverse the activity of apigenin on NF-κB/MMP-9 signaling pathway, expression of BCL2 protein, and cell viability. Collectively, findings of the study indicated that apigenin suppresses glioma cell growth *via* inducing miR-16 and inhibiting NF-κB/MMP-9 and BCL2 (Chen et al., 2016).

Isothiocyanates

Isothiocyanates (**Figure 2**) are natural compounds derived from the glucosinolate precursors of cruciferous vegetables, which exert anticancer, anti-invasion, and anti-inflammatory actions *via* inhibiting breast cancer, pancreatic cancer, and myeloma (Prawan et al., 2009; Brunelli et al., 2010). Many studies have reported that the anti-inflammatory effects of isothiocyanates in multiple cancer cells (Subedi et al., 2017; Mitsiogianni et al., 2019). The consequences have indicated that the anti-inflammatory properties of isothiocyanates may be mediated by the inhibition of c-Jun N-terminal kinase (JNK)/NF-κB/TNF-α signaling pathways (Subedi et al., 2017). In a study, Guo et al. (2019) assessed the possible synergistic action of phenethyl isothiocyanate in combination with temozolomide and theorized that phenethyl isothiocyanate might facilitate the anticancer role of temozolomide partly *via* NF-κB-dependent signaling pathway reducing MGMT expression. Furthermore, treatment with phenethyl isothiocyanate elevated the sensitivity of temozolomide resistant U373, U87, and T98 cells *via* suppressing the MGMT expression through the NF-κB signaling cascade (Guo et al., 2019). In order to examine the inhibitory effects of isothiocyanates on cancer invasion and migration, Lee et al. (2015) looked at isothiocyanate-regulated MMP-9 activation in C6 glioma cells. MMP-9 is a crucial enzyme in cancer metastasis that destroys the extracellular matrix. They revealed that isothiocyanates suppressed MMP-9 transcription levels *via* inhibiting NF-κB and activator protein-1 (AP-1), which further preventing C6 GBM cell motility and invasion (Lee et al., 2015).

Sulforaphane

Sulforaphane (a natural isothiocyanate group of organosulfur compounds, **Figure 2**) is derived from broccoli sprouts (Uddin et al., 2020b). Sulforaphane shows cancer-protective effects *via* detoxifying and ameliorating antioxidant capacity (Clarke et al., 2008; Cheung and Kong, 2010). In human cancer cells, sulforaphane-mediated inhibition of NF-κB and NF-κB-regulated gene expression takes place *via* IκBα and IKK signaling pathways (Xu et al., 2005). Sulforaphane altered caspase-9/-12 cleavage, cytochrome C release, calpain effect, DNA fragmentation, intracellular Ca^{2+} level, morphological characteristics, Bcl-2-associated X-protein (Bax)/B-cell lymphoma 2 (Bcl-2) ratio, and levels of IκBa protein in U-87 MG and T98G GBM cells (Lenzi et al., 2014). In GBM cells, sulforaphane suppressed the inhibitor of apoptosis proteins and IκBα up-regulation, resulting in downregulation of NF-κB expression (Huang et al., 2012c). Lan et al. (2016) showed that sulforaphane might markedly inhibit proliferation of temozolomide-resistant GBM cells. Sulforaphane also suppressed the function of NF-κB pathway and then decreased the expression of MGMT in order to reverse the chemo-resistance to temozolomide in U373-R, U87-R, and T98G cell lines. Moreover, sequential combination with temozolomide synergistically elevated apoptosis induction and suppressed survival capability in temozolomide-resistant GBM cells. It was also suggested that sulforaphane might significantly increase cell death and inhibit cell growth in a chemo-resistant xenograft nude-mouse model (Lan et al., 2016). In a different study, Li et al. (2014) observed that sulforaphane suppresses invasion *via* inducing activation of ERK1/2 signaling pathway in human glioblastoma U373MG and U87MG cells. Bijangi-Vishehsaraeiv et al. (2017) confirmed that sulforaphane markedly suppresses GBM cell survivals and triggers apoptosis in GBM cells linked with the elevated activity of caspase-3 and -7. In addition, sulforaphane did not influence normal human mesenchymal stromal cells and exerted modest action on the nontumor brain cells.

Alantolactone

Alantolactone, a sesquiterpene lactone extracted from *Inula helenium* L. (**Figure 2**), has many pharmacological properties, including anticancer, antibacterial, antifungal, and anti-inflammatory properties (Chun et al., 2012). Alantolactone's antitumor activities were observed in chronic myelogenous leukemia, brain tumors, colorectal cancer, lung cancer, and liver cancer (Khan et al., 2012; Rasul et al., 2013; Wei et al., 2013). In GBM cells, alantolactone caused cell death through glutathione depletion, mitochondrial dysfunction, and ROS production (Khan et al., 2012). Furthermore, alantolactone-induced other mechanisms triggered involve suppression of inducible nitric oxide synthase (iNOS) and COX-2 expression and downregulation of NF-κB and AP-1 through myeloid differentiation primary response 88 (MyD88) signaling (Chun

et al., 2012). In a study, Wang et al. (2017) revealed that alantolactone's antitumor activity against GBM. This study found that the alantolactone dramatically inhibited the growth of GBM. Alantolactone inhibited the kinase activity of IKKβ by targeting the ATP-binding site and then attenuated the binding of NF-κB to the COX-2 promoter area, resulting in a considerable reduction in COX-2 expression. Alantolactone also triggered apoptosis by activating the caspase/cytochrome c signaling pathway. Furthermore, alantolactone can penetrate the blood-brain barrier (BBB). Thus anti-tumor effects of alantolactone is facilitated by blocking the activity of IKKβ kinase as well as affecting NF-κB/COX-2-induced signaling mechanisms in GBM (Wang et al., 2017). Therefore, due to its dual inhibitory effects on NF-κB and IKKβ expression, alantolactone may be considered a promising natural compound against GBM.

Baicalein

Baicalein (a bioactive flavone, **Figure 2**) is derived initially from *Scutellaria baicalensis* Georgi and *Scutellaria lateriflora* L. (Varsha et al., 2017). This flavone has traditionally been utilized because of its anticancer activities (Liu et al., 2016; Zhao et al., 2016). In multiple cancer cell lines, aicalein inhibited the nuclear translocation of NF-κB and exerted anti-inflammatory activities (Seo et al., 2011; Yu et al., 2018a). Moreover, baicalein inhibited the C33A growth and accelerated cellular apoptosis by blocking NF-κB spathway (Yu et al., 2018a). After treatment with baicalein, NF-κB-p65 activity and expression were markedly suppressed in U251 GBM cells (Jiang et al., 2016). The use of an NF-kB-p65 inhibitor (EVP4593) combined with baicalein resulted in a synergistic reduction of Bcl-2 expression, followed by an increase in Bax and cleaved-caspase-3 expression, as well as the inhibition of U251 cell survival (Jiang et al., 2016). All of these finding indicating that baicalein might be therapeutically used as a natural compound against GBM.

Parthenolide

Parthenolide (a naturally occurring sesquiterpene lactone, **Figure 2**) is extracted from Tanac*etum parthenium* L. (Chaturvedi, 2019). This naturally occurring compound inhibits NF-κB *via* suppressing the activity of IκB kinase as well as altering the p65 subunit (Kwok et al., 2001). Furthermore, parthenolide has traditionally been used to treat rheumatoid arthritis and migraine because of its anti-inflammatory properties and low toxicity (Heptinstall, 1988). In numerous studies, the effects of parthenolide on animal malignancies have been widely explored (Gilmore, 2006; Haffner et al., 2006). It was revealed that parthenolide inhibited proliferation, angiogenesis, and invasion of GBM cells (U87MG and U373). In a study, Yu et al. (2018b) revealed that the suppression of NF-κB resulted in anti-GBM effect and suppressed temozolomide-mediated chemoresistance *via* downregulation of *MGMT* gene expression. Furthermore, it has been confirmed by Nakabayashi and Shimizu (2012) that parthenolide inhibits angiogenesis and decreases phosphorylation of Akt and activated mitochondrial signaling pathway, which is suggesting that the antitumor effect of parthenolide might be induced *via* stimulation of apoptosis, suppression of Akt signaling pathway, and NF-κB suppression. In glioblastoma xenografts, parthenolide reduced neovascularity and tumor development (Nakabayashi and Shimizu, 2012). However, it has been observed that treatment with parthenolide causes rapid cell death *via* caspase-3/-7 without influencing the regulation of NF-κB in GBM cells (Anderson and Bejcek, 2008).

Nepalolide A

Nepalolide A (a naturally occurring germacranolide sesquiterpene lactone, **Figure 2**) is derived from *Carpesium nepalense* Less. (Wang et al., 1999). In C6 glioma cells and primary astrocytes, the effects of nepalolide A on the production of iNOS generated by LPS/IFN-γ or TNF-α/IL-1β/IFN-γ were studied by Wang et al. (1999). This study reported that nepalolide A inhibited signaling pathways induced *via* cytokine and lipopolysaccharide and also suppressed the phosphorylation of IκB protein (Wang et al., 1999). Thus, suppression of NF-κB activation *via* nepalolide A was facilitated *via* blocking IκB degradation, which can further result in suppression of iNOS expression (Wang et al., 1999).

Curcumin

Curcumin (a polyphenol, **Figure 2**) is the major bioactive compound of *Curcuma longa* L. that exerts anti-inflammatory and antioxidant properties by decreasing the activity of AP-1 and NF-κB (Saberi-Karimian et al., 2019). Its potential to treat various high-risk cancers has also been assessed in phase I clinical trials (Cheng et al., 2001). Furthermore, curcumin might exert numerous beneficial effects in GBM cells, such as suppression of angiogenesis, cell development, and invasion (Ambegaokar et al., 2003; Gao et al., 2005; Kim et al., 2005). Its activities on GBM development were also studied in the rat (C6) and human (T98G, T67, and U87MG) GBM cell lines. Furthermore, curcumin decreased the survival of cells in a p53-and caspase-independent manner, an activity which is linked with the suppression of NF-κB and AP-1 signaling pathways by the deterrence of constitutive Akt and JNK activation (Dhandapani et al., 2007). Curcumin also induced the antitumor effect of nimustine (a nitrosourea with antineoplastic activity) against GBM *via* inhibiting the NF-κB/COX-2 and PI3K/Akt signaling cascades (Zhao et al., 2017a). In a study, Fratantonio et al. (2019) reported that curcumin triggered the anti-GBM effect of paclitaxel by suppressing NF-κB activation in rat C6 cells. In U87 cells, demethoxycurcumin (a curcuminoid) exerted anti-proliferative effects *via* inhibition of the Akt/NF-κB signaling cascade (Kumar et al., 2018).

In a study, Wu et al. (2015) determined whether the cytotoxic effects of curcumin in glioblastoma cells is facilitated *via* miR-146a upregulation. Roles of curcumin and temozolomide (alone or in combination) on apoptosis and cell proliferation were assessed in human U-87 MG glioblastoma cells. Curcumin treatment resulted in miR-146a upregulation in U-87 MG cells. As compared to single treatment, combined treatment curcumin and temozolomide markedly ($p < 0.05$) stimulated apoptotic death and suppressed proliferation of U-87 MG cells. Depletion of miR-146a blocked the curcumin-induced

enhancement of temozolomide-mediated apoptosis (Wu et al., 2015). Overexpression of miR-146a inhibited activation of NF-κB and increased apoptosis in temozolomide-treated cells. Furthermore, pharmacological suppression of NF-κB signaling pathway markedly elevated temozolomide-mediated apoptosis (Wu et al., 2015).

NATURAL MOLECULES AND BLOOD-BRAIN BARRIER PERMEABILITY

The brain is incredibly equipped with a significant protective element known as the BBB. BBB plays a role in preventing harmful substances from entering the brain. Because of this property of BBB, most of the new drugs cannot enter into and treat the brain tumor. Furthermore, BBB is one of the major challenges that researchers need to overcome to develop novel and effective treatments for individuals with malignant brain tumors (Noch et al., 2018). Indeed, BBB regulates the entry of various molecules into the brain *via* transcellular or paracellular signaling pathways. It has been reported that BBB also contains many tight junctions between endothelial cells, ATP-dependent multidrug resistance pathway proteins called P-glycoprotein (P-gp), enzymes, and receptors (Chow and Gu, 2015). Components of the BBB microenvironment include extracellular matrix, basement membrane, fibroblasts, neurons, pericytes, microglia, and astrocytes (Obermeier et al., 2013), which also affect BBB activities (Lécuyer et al., 2016; Zhao et al., 2017b). It has been identified that blood-brain tumor-barrier (BBTB) arises from tumor capillaries providing oxygen and nutrients to the tumor (Tellingen et al., 2015). On the other hand, the glioma BBTB microenvironment contains infiltrating macrophages, tumor-linked microglia, extracellular matrix, tumor cells, and various other types of cells. In rat GBM models, tumor growth was suppressed by targeting the glioma microenvironment (Jacobs et al., 2012). Targeted therapy has gained a lot of attention over time, but this therapy did not raise the overall survival of individuals with GBM, partly owing to the poor drug penetration across the BBB. Thus, there is a growing interest regarding the molecules that can modulate BBB permeability to ameliorate the bioavailability of therapeutic agents into tumors. Furthermore, nanotechnology is essential to mask the physicochemical properties of therapeutic agents to prolong half-life across the BBB (Gerstner and Fine, 2007).

In the case of brain cancer treatment, targeted delivery of resveratrol into the brain tumor tissue might overcome various issues, including chemical instability, poor water solubility, and low bioavailability of resveratrol. Multiple types of polymeric nanoparticles and liposomes have already been developed to enhance GBM treatment. In a study, Vijayakumar et al. (2016) showed that the antiglioma cytotoxicity, passive brain targeting, and biological half-life of resveratrol were markedly improved *via* utilizing D-α-tocopheryl polyethylene glycol-1000 succinate-coated liposomes. In another study, Guo et al. (2013) altered the surface of resveratrol-loaded polyethylene glycol-polylactic acid nanoparticles with transferrin moieties (Tf-NP), which further resulted in increased cytotoxicity, elevated level of intracellular uptake, and apoptosis of human U-87 MG GBM cell lines and C6 rat glioma cells *in vitro*, as compared to nanoparticles without transferrin and free resveratrol. As transferrin receptors are only expressed in brain capillaries (Johnsen et al., 2017), the buildup of Tf-NP-resveratrol in tumor tissues prolonged survival and reduced tumor volume in rat models containing C6 orthotopic glioma. In a study, Wei et al. (2015) observed that treatment with resveratrol protected BBB integrity *via* regulating activities and expressions of TIMP-1 and MMP-9 in brains of rat models that were reperfused after ischemic injury.

Quercetin was found to cross the BBB and decrease the advancement of degenerative diseases (Li et al., 2015). It has been suggested that α-tocopherol can mediate the transport of quercetin through the BBB. In the brain, the combination of quercetin and rutin mediated the buildup of quercetin and/or its conjugated derivatives (Ferri et al., 2015). Quercetin was found to improve BBB dysfunction, reduce BBB leakage, and decrease brain edema (Aziz et al., 2021). Quercetin may decrease the expressions of axin, GSK-3β, and MMP-9, and elevate the expression of β-catenin, claudin-5, and ZO-1. Interestingly, all these protective activities of quercetin might be reversed *via* DKK-1 (Aziz et al., 2021). Adhesion molecules, membrane proteins, or invasion-linked proteins may play roles in tumor invasion and migration. In human glioblastoma cells, sulforaphane-cysteine suppressed the invasion and migration by increasing the fusion of mitophagosome to the lysosome (Zhou et al., 2020). Collectively, these findings might help in developing low-toxicity and high-efficiency anticancer drugs to suppress invasion and migration in GBM. Wang et al. (2013) confirmed that curcumin has the ability to maintain the integrity of BBB *via* regulating the expressions of occludin and ZO-1 during glucose deprivation and hypoxia. Curcumin and curcumin-loaded PLGA nanoparticles penetrated the BBB to enter brain tissues, where it was accumulated primarily in the hippocampus. Nanotechnology markedly increased the retention time of curcumin in the hippocampus (elevated by 83%) and cerebral cortex (elevated by 96%) (Tsai et al., 2011). In brain microvascular endothelial cells, curcumin improved the permeability of BBB during hypoxia *via* upregulating the expression of heme oxygenase-1 (Phillips et al., 2006). All of the evidence warrant more preclinical and clinical studies for better understand the potential therapeutic benefits.

CONCLUSION

Considerable efforts are being invested to develop antineoplastic agents, but these agents have various limitations, including severe side effects and high cost. Since there are several adverse effects of currently available inhibitors of NF-κB, thus investigating the currently available naturopathic formulations can provide a perfect platform for identifying novel inhibitors of NF-κB considering the specific and non-specific multi-target activities of phytochemicals on several constituents of the NF-κB signaling pathway. The activation of NF-κB ensures a pro-proliferative activity in GBM. Inhibiting this pathway *via* suppressing the

NF-κB effect or specially NF-κB–inducible genes might be a promising therapeutic method to treat GBM. Numerous attempts have been made to include inhibition of NF-κB into GBM treatment, but no precise outcome has been attained so far. Even though some naturally occurring compounds that inhibit NF-κB signaling pathways (particularly IKK inhibitors) are available, but more specific inhibitors of IKK and other upstream kinases need to be further studied clinically to confirm their potential in patients with GBM. Various natural compounds contain auspicious NF-κB modulatory activities in the treatment of GBM. As NF-κB modulators exhibited low toxic effects against normal astrocytes (which indicate their selectivity towards cancer cells), hence phytochemicals might play a role as potential agents in clinical trials, facilitating the finding of better therapy to treat GBM. In GBM patients, most of the chemotherapy trials failed partially because of the poor drug penetration across the BBB. It has been observed that natural products might alter the permeability of BBB *via* modifying the action of its constituents. Most of these mentioned phytochemicals are yet to be studied in human clinical trials and/or cancer models for their anticancer properties, bioavailability, and biocompatibility. As compared to available synthetic inhibitors of NF-κB, these natural products possess several advantages, including efficacy and safety. Along with conventional cancer therapy, the use of these natural products as adjunctive chemotherapy might establish a better therapeutic approach. However, structural alterations of these phytochemicals ought to be evaluated to conceivably improve the antineoplastic property of these natural compounds. Enormous data are available to support more studies in utilizing natural compounds in GBM. Indeed, this poor prognosis requires the exploration of alternative therapeutic agents to ameliorate outcomes for the affected individuals. Prospective randomized trials are required to find the use of adjunctive natural therapies for the better targeting of resistance, to study safety profiles, and synergistically ameliorating existing therapies.

AUTHOR CONTRIBUTIONS

MU conceived of the original idea and designed the outlines of the study. MU, MK, and AM wrote the draft of the manuscript. MU and MK prepared the figures for the manuscript. MS, FN, TE, IA, AR, GA, AS, SM, and MA-D performed the literature review and aided in revising the manuscript. All authors have read and agreed to the published version of the manuscript.

ACKNOWLEDGMENTS

This work was funded by the Deanship of Scientific Research at Princess Nourah bint Abdulrahman University through the Fast-Track Research Funding Program.

REFERENCES

Altmann, K. H., and Gertsch, J. (2007). Anticancer Drugs from Nature-Nnatural Products as a Unique Source of New Microtubule-Stabilizing Agents. *Nat. Prod. Rep.* 24, 327–357. doi:10.1039/b515619j

Ambegaokar, S. S., Wu, L., Alamshahi, K., Lau, J., Jazayeri, L., Chan, S., et al. (2003). Curcumin Inhibits Dose-Dependently and Time-Dependently Neuroglial Cell Proliferation and Growth. *Neuro. Endocrinol. Lett.* 24, 469–473.

Anand David, A. V., Arulmoli, R., and Parasuraman, S. (2016). Overviews of Biological Importance of Quercetin: A Bioactive Flavonoid. *Pharmacogn. Rev.* 10, 84–89. doi:10.4103/0973-7847.194044

Anderson, K. N., and Bejcek, B. E. (2008). Parthenolide Induces Apoptosis in Glioblastomas without Affecting NF-kappaB. *J. Pharmacol. Sci.* 106, 318–320. doi:10.1254/jphs.SC0060164

Arepalli, S. K., Choi, M., Jung, J. K., and Lee, H. (2015). Novel NF-Kb Inhibitors: a Patent Review (2011 - 2014). *Expert Opin. Ther. Pat.* 25, 319–334. doi:10.1517/13543776.2014.998199

Atkinson, G. P., Nozell, S. E., and Benveniste, E. T. (2010). NF-kappaB and STAT3 Signaling in Glioma: Targets for Future Therapies. *Expert Rev. Neurother.* 10, 575–586. doi:10.1586/ern.10.21

Atkinson, G. P., Nozell, S. E., Harrison, D. K., Stonecypher, M. S., Chen, D., and Benveniste, E. N. (2009). The Prolyl Isomerase Pin1 Regulates the NF-kappaB Signaling Pathway and Interleukin-8 Expression in Glioblastoma. *Oncogene* 28, 3735–3745. doi:10.1038/onc.2009.232

Aziz, M. A., Sarwar, M. S., Akter, T., Uddin, M. S., Xun, S., Zhu, Y., et al. (2021). Polyphenolic Molecules Targeting STAT3 Pathway for the Treatment of Cancer. *Life Sci.* 268, 118999. doi:10.1016/j.lfs.2020.118999

Bhat, K. P. L., Balasubramaniyan, V., Vaillant, B., Ezhilarasan, R., Hummelink, K., Hollingsworth, F., et al. (2013). Mesenchymal Differentiation Mediated by NF-Kb Promotes Radiation Resistance in Glioblastoma. *Cancer Cell* 24, 331–346. doi:10.1016/j.ccr.2013.08.001

Bijangi-Vishehsaraei, K., Reza Saadatzadeh, M., Wang, H., Nguyen, A., Kamocka, M. M., Cai, W., et al. (2017). Sulforaphane Suppresses the Growth of Glioblastoma Cells, Glioblastoma Stem Cell-like Spheroids, and Tumor Xenografts through Multiple Cell Signaling Pathways. *J. Neurosurg.* 127, 1219–1230. doi:10.3171/2016.8.JNS161197

Bonavia, R., Inda, M. M., Vandenberg, S., Cheng, S. Y., Nagane, M., Hadwiger, P., et al. (2012). EGFRvIII Promotes Glioma Angiogenesis and Growth through the NF-Kb, Interleukin-8 Pathway. *Oncogene* 31, 4054–4066. doi:10.1038/onc.2011.563

Braganhol, E., Tamajusuku, A. S., Bernardi, A., Wink, M. R., and Battastini, A. M. (2007). Ecto-5'-nucleotidase/CD73 Inhibition by Quercetin in the Human U138MG Glioma Cell Line. *Biochim. Biophys. Acta* 1770, 1352–1359. doi:10.1016/J.BBAGEN.2007.06.003

Braganhol, E., Zamin, L. L., Canedo, A. D., Horn, F., Tamajusuku, A. S., Wink, M. R., et al. (2006). Antiproliferative Effect of Quercetin in the Human U138MG Glioma Cell Line. *Anticancer. Drugs* 17, 663–671. doi:10.1097/01.CAD.0000215063.23932.02

Brassesco, M. S., Roberto, G. M., Morales, A. G., Oliveira, J. C., Delsin, L. E., Pezuk, J. A., et al. (2013). Inhibition of NF- κ B by Dehydroxymethylepoxyquinomicin Suppresses Invasion and Synergistically Potentiates Temozolomide and γ-Radiation Cytotoxicity in Glioblastoma Cells. *Chemother. Res. Pract.* 2013, 593020. doi:10.1155/2013/593020

Bredel, M., Scholtens, D. M., Yadav, A. K., Alvarez, A. A., Renfrow, J. J., Chandler, J. P., et al. (2011). NFKBIA Deletion in Glioblastomas. *N. Engl. J. Med.* 364, 627–637. doi:10.1056/nejmoa1006312

Brunelli, D., Tavecchio, M., Falcioni, C., Frapolli, R., Erba, E., Iori, R., et al. (2010). The Isothiocyanate Produced from Glucomoringin Inhibits NF-kB and Reduces Myeloma Growth in Nude Mice *In Vivo*. *Biochem. Pharmacol.* 79, 1141–1148. doi:10.1016/j.bcp.2009.12.008

Chan, J. A., Krichevsky, A. M., and Kosik, K. S. (2005). MicroRNA-21 Is an Antiapoptotic Factor in Human Glioblastoma Cells. *Cancer Res.* 65, 6029–6033. doi:10.1158/0008-5472.CAN-05-0137

Chang, X., He, H., Zhu, L., Gao, J., Wei, T., Ma, Z., et al. (2015). Protective Effect of Apigenin on Freund's Complete Adjuvant-Induced Arthritis in Rats via Inhibiting P2X7/NF-Kb Pathway. *Chem. Biol. Interact.* 236, 41–46. doi:10.1016/j.cbi.2015.04.021

Chaturvedi, D. (2019). "Recent Developments in the Anti-inflammatory Potential of Sesquiterpene Lactones and Their Semisynthetic Analogs", in *Natural Product Drug Discovery, Discovery and Development of Anti-Inflammatory Agents from Natural Products*. Editor G. Brahmachari (Amsterdam: Elsevier), 185–205.

Chen, X. J., Wu, M. Y., Li, D. H., and You, J. (2016). Apigenin Inhibits Glioma Cell Growth through Promoting microRNA-16 and Suppression of BCL-2 and Nuclear Factor-Kb/mmp-9. *Mol. Med. Rep.* 14, 2352–2358. doi:10.3892/mmr.2016.5460

Chen, Y., Liu, W., Chao, T., Zhang, Y., Yan, X., Gong, Y., et al. (2008). MicroRNA-21 Down-Regulates the Expression of Tumor Suppressor PDCD4 in Human Glioblastoma Cell T98G. *Cancer Lett.* 272, 197–205. doi:10.1016/j.canlet.2008.06.034

Cheng, A. L., Hsu, C. H., Lin, J. K., Hsu, M. M., Ho, Y. F., Shen, T. S., et al. (2001). Phase I Clinical Trial of Curcumin, a Chemopreventive Agent, in Patients with High-Risk or Pre-malignant Lesions. *Anticancer Res.* 21, 2895–2900.

Cheung, K. L., and Kong, A. N. (2010). Molecular Targets of Dietary Phenethyl Isothiocyanate and Sulforaphane for Cancer Chemoprevention. *AAPS J.* 12, 87–97. doi:10.1208/s12248-009-9162-8

Chow, B. W., and Gu, C. (2015). The Molecular Constituents of the Blood-Brain Barrier. *Trends Neurosciences* 38, 598–608. doi:10.1016/J.TINS.2015.08.003

Chun, J., Choi, R. J., Khan, S., Lee, D. S., Kim, Y. C., Nam, Y. J., et al. (2012). Alantolactone Suppresses Inducible Nitric Oxide Synthase and Cyclooxygenase-2 Expression by Down-Regulating NF-Kb, MAPK and AP-1 via the MyD88 Signaling Pathway in LPS-Activated RAW 264.7 Cells. *Int. Immunopharmacol.* 14, 375–383. doi:10.1016/j.intimp.2012.08.011

Ciafrè, S. A., Galardi, S., Mangiola, A., Ferracin, M., Liu, C. G., Sabatino, G., et al. (2005). Extensive Modulation of a Set of microRNAs in Primary Glioblastoma. *Biochem. Biophys. Res. Commun.* 334, 1351–1358. doi:10.1016/j.bbrc.2005.07.030

Clarke, J. D., Dashwood, R. H., and Ho, E. (2008). Multi-targeted Prevention of Cancer by Sulforaphane. *Cancer Lett.* 269, 291–304. doi:10.1016/j.canlet.2008.04.018

ClinicalTrials.gov The Effects of Ashwagandha in Endurance Exercise Performance. Available online: https://clinicaltrials.gov/ct2/show/NCT03596307 (Accessed on Feb 15, 2021).

ClinicalTrials.gov Withania Somnifera An Immunomodulator and Anti-inflammatory Agent for Schizophrenia. Available online: https://clinicaltrials.gov/ct2/show/NCT01793935 (Accessed on Feb 15, 2021).

Cooper, L. A., Kong, J., Gutman, D. A., Wang, F., Cholleti, S. R., Pan, T. C., et al. (2010). An Integrative Approach for In Silico Glioma Research. *IEEE Trans. Biomed. Eng.* 57, 2617–2621. doi:10.1109/TBME.2010.2060338

Coupienne, I., Bontems, S., Dewaele, M., Rubio, N., Habraken, Y., Fulda, S., et al. (2011). NF-kappaB Inhibition Improves the Sensitivity of Human Glioblastoma Cells to 5-aminolevulinic Acid-Based Photodynamic Therapy. *Biochem. Pharmacol.* 81, 606–616. doi:10.1016/j.bcp.2010.12.015

Cragg, G. M., Simon, J. E., Jato, J. G., and Snader, K. M. (1996). "Drug Discovery and Development at the National Cancer Institute: Potential for New Pharmaceutical Crops," in *Proceedings of the Drug Discovery and Development at the National Cancer Institute: Potential for New Pharmaceutical Crops*. Editor J. Janick (Arlington, VA: ASHS), 554–560.

Dhandapani, K. M., Mahesh, V. B., and Brann, D. W. (2007). Curcumin Suppresses Growth and Chemoresistance of Human Glioblastoma Cells via AP-1 and NFkappaB Transcription Factors. *J. Neurochem.* 102, 522–538. doi:10.1111/j.1471-4159.2007.04633.x

Dolcet, X., Llobet, D., Pallares, J., and Matias-Guiu, X. (2005). NF-kB in Development and Progression of Human Cancer. *Virchows Arch.* 446, 475–482. doi:10.1007/s00428-005-1264-9

Dolecek, T. A., Propp, J. M., Stroup, N. E., and Kruchko, C. (2012). CBTRUS Statistical Report: Primary Brain and central Nervous System Tumors Diagnosed in the United States in 2005-2009. *Neuro. Oncol.* 14 Suppl 5, v1–49. doi:10.1093/neuonc/nos218

El-Readi, M. Z., Eid, S., Abdelghany, A. A., Al-Amoudi, H. S., Efferth, T., and Wink, M. (2019). Resveratrol Mediated Cancer Cell Apoptosis, and Modulation of Multidrug Resistance Proteins and Metabolic Enzymes. *Phytomedicine* 55, 269–281. doi:10.1016/j.phymed.2018.06.046

Erdogan, S., Doganlar, O., Doganlar, Z. B., Serttas, R., Turkekul, K., Dibirdik, I., et al. (2016). The Flavonoid Apigenin Reduces Prostate Cancer CD44(+) Stem Cell Survival and Migration through PI3K/Akt/NF-Kb Signaling. *Life Sci.* 162, 77–86. doi:10.1016/j.lfs.2016.08.019

Ferri, P., Angelino, D., Gennari, L., Benedetti, S., Ambrogini, P., Grande, P. D., et al. (2015). Enhancement of Flavonoid Ability to Cross the Blood-Brain Barrier of Rats by Co-administration with α-tocopherol. *Food Funct.* 6, 394–400. doi:10.1039/C4FO00817K

Fratantonio, D., Molonia, M. S., Bashllari, R., Muscarà, C., Ferlazzo, G., Costa, G., et al. (2019). Curcumin Potentiates the Antitumor Activity of Paclitaxel in Rat Glioma C6 Cells. *Phytomedicine* 55, 23–30. doi:10.1016/j.phymed.2018.08.009

Friedmann-Morvinski, D., Narasimamurthy, R., Xia, Y., Myskiw, C., Soda, Y., and Verma, I. M. (2016). Targeting NF-Kb in Glioblastoma: A Therapeutic Approach. *Sci. Adv.* 2, e1501292. doi:10.1126/sciadv.1501292

Fukushima, T., Kawaguchi, M., Yorita, K., Tanaka, H., Takeshima, H., Umezawa, K., et al. (2012). Antitumor Effect of Dehydroxymethylepoxyquinomicin, a Small Molecule Inhibitor of Nuclear Factor-Kb, on Glioblastoma. *Neuro. Oncol.* 14, 19–28. doi:10.1093/neuonc/nor168

Furnari, F. B., Fenton, T., Bachoo, R. M., Mukasa, A., Stommel, J. M., Stegh, A., et al. (2007). Malignant Astrocytic Glioma: Genetics, Biology, and Paths to Treatment. *Genes Dev.* 21, 2683–2710. doi:10.1101/gad.1596707

Gao, X., Deeb, D., Jiang, H., Liu, Y. B., Dulchavsky, S. A., and Gautam, S. C. (2005). Curcumin Differentially Sensitizes Malignant Glioma Cells to TRAIL/Apo2L-mediated Apoptosis through Activation of Procaspases and Release of Cytochrome C from Mitochondria. *J. Exp. Ther. Oncol.* 5, 39–48.

Gerstner, E. R., and Fine, R. L. (2007). Increased Permeability of the Blood-Brain Barrier to Chemotherapy in Metastatic Brain Tumors: Establishing a Treatment Paradigm. *J. Clin. Oncol.* 25, 2306–2312. doi:10.1200/JCO.2006.10.0677

Gill, J. S., Zhu, X., Moore, M. J., Lu, L., Yaszemski, M. J., and Windebank, A. J. (2002). Effects of NFkappaB Decoy Oligonucleotides Released from Biodegradable Polymer Microparticles on a Glioblastoma Cell Line. *Biomaterials* 23, 2773–2781. doi:10.1016/S0142-9612(02)00013-3

Gilmore, T. D. (2006). Introduction to NF-kappaB: Players, Pathways, Perspectives. *Oncogene* 25, 6680–6684. doi:10.1038/sj.onc.1209954

Grivennikov, S. I., and Karin, M. (2010). Dangerous Liaisons: STAT3 and NF-kappaB Collaboration and Crosstalk in Cancer. *Cytokine Growth Factor. Rev.* 21, 11–19. doi:10.1016/j.cytogfr.2009.11.005

Grivennikov, S. I., and Karin, M. (2011). Inflammatory Cytokines in Cancer: Tumour Necrosis Factor and Interleukin 6 Take the Stage. *Ann. Rheum. Dis.* 70 Suppl 1, i104–8. doi:10.1136/ard.2010.140145

Guo, W., Li, A., Jia, Z., Yuan, Y., Dai, H., and Li, H. (2013). Transferrin Modified PEG-PLA-Resveratrol Conjugates: *In Vitro* and *In Vivo* Studies for Glioma. *Eur. J. Pharmacol.* 718, 41–47. doi:10.1016/J.EJPHAR.2013.09.034

Guo, Z., Wang, H., Wei, J., Han, L., and Li, Z. (2019). Sequential Treatment of Phenethyl Isothiocyanate Increases Sensitivity of Temozolomide Resistant Glioblastoma Cells by Decreasing Expression of MGMT via NF-Kb Pathway. *Am. J. Transl. Res.* 11, 696–708.

Haffner, M. C., Berlato, C., and Doppler, W. (2006). Exploiting Our Knowledge of NF-kappaB Signaling for the Treatment of Mammary Cancer. *J. Mammary Gland Biol. Neoplasia* 11, 63–73. doi:10.1007/s10911-006-9013-5

Hayashi, S., Yamamoto, M., Ueno, Y., Ikeda, K., Ohshima, K., Soma, G., et al. (2001). Expression of Nuclear Factor-Kappa B, Tumor Necrosis Factor Receptor Type 1, and C-Myc in Human Astrocytomas. *Neurol. Med. Chir (Tokyo)* 41, 187–195. doi:10.2176/nmc.41.187

Hegi, M. E., Diserens, A. C., Gorlia, T., Hamou, M. F., de Tribolet, N., Weller, M., et al. (2005). MGMT Gene Silencing and Benefit from Temozolomide in Glioblastoma. *N. Engl. J. Med.* 352, 997–1003. doi:10.1056/nejmoa043331

Heptinstall, S. (1988). Feverfew--an Ancient Remedy for Modern Times?. *J. R. Soc. Med.* 81, 373–374. doi:10.1177/014107688808100701

Hjelmeland, A. B., Wu, Q., Wickman, S., Eyler, C., Heddleston, J., Shi, Q., et al. (2010). Targeting A20 Decreases Glioma Stem Cell Survival and Tumor Growth. *Plos Biol.* 8, e1000319. doi:10.1371/journal.pbio.1000319

Holmes, K. M., Annala, M., Chua, C. Y., Dunlap, S. M., Liu, Y., Hugen, N., et al. (2012). Insulin-like Growth Factor-Binding Protein 2-driven Glioma Progression Is Prevented by Blocking a Clinically Significant Integrin, Integrin-Linked Kinase, and NF-Kb Network. *Proc. Natl. Acad. Sci. U. S. A.* 109, 3475–3480. doi:10.1073/pnas.1120375109

Hua, D., Ding, D., Han, X., Zhang, W., Zhao, N., Foltz, G., et al. (2012). Human miR-31 Targets Radixin and Inhibits Migration and Invasion of Glioma Cells. *Oncol. Rep.* 27, 700–706. doi:10.3892/or.2011.1555

Huang, H., Lin, H., Zhang, X., and Li, J. (2012). Resveratrol Reverses Temozolomide Resistance by Downregulation of MGMT in T98G Glioblastoma Cells by the NF-κb-dependent Pathway. *Oncol. Rep.* 27, 2050–2056. doi:10.3892/or.2012.1715

Huang, M., Lu, J. J., and Ding, J. (2021). Natural Products in Cancer Therapy: Past, Present and Future. *Nat. Prod. Bioprospect* 11, 5–13. doi:10.1007/s13659-020-00293-7

Huang, P., Rani, M. R., Ahluwalia, M. S., Bae, E., Prayson, R. A., Weil, R. J., et al. (2012). Endothelial Expression of TNF Receptor-1 Generates a Proapoptotic Signal Inhibited by Integrin α6β1 in Glioblastoma. *Cancer Res.* 72, 1428–1437. doi:10.1158/0008-5472.CAN-11-2621

Huang, T. Y., Chang, W. C., Wang, M. Y., Yang, Y. R., and Hsu, Y. C. (2012). Effect of Sulforaphane on Growth Inhibition in Human Brain Malignant Glioma GBM 8401 Cells by Means of Mitochondrial- and MEK/ERK-Mediated Apoptosis Pathway. *Cell Biochem. Biophys.* 63, 247–259. doi:10.1007/s12013-012-9360-3

Hummel, R., Maurer, J., and Haier, J. (2011). MicroRNAs in Brain Tumors : a New Diagnostic and Therapeutic Perspective?. *Mol. Neurobiol.* 44, 223–234. doi:10.1007/s12035-011-8197-x

Huse, J. T., and Holland, E. C. (2010). Targeting Brain Cancer: Advances in the Molecular Pathology of Malignant Glioma and Medulloblastoma. *Nat. Rev. Cancer* 10, 319–331. doi:10.1038/nrc2818

Huse, J. T., Phillips, H. S., and Brennan, C. W. (2011). Molecular Subclassification of Diffuse Gliomas: Seeing Order in the Chaos. *Glia* 59, 1190–1199. doi:10.1002/glia.21165

Jacobs, V. L., Landry, R. P., Liu, Y., Romero-Sandoval, E. A., and De Leo, J. A. (2012). Propentofylline Decreases Tumor Growth in a Rodent Model of Glioblastoma Multiforme by a Direct Mechanism on Microglia. *Neuro. Oncol.* 14, 119–131. doi:10.1093/NEUONC/NOR194

Jeandet, P., Vannozzi, A., Sobarzo-Sánchez, E., Uddin, M. S., Bru, R., Martínez-Márquez, A., et al. (2021). Phytostilbenes as Agrochemicals: Biosynthesis, Bioactivity, Metabolic Engineering and Biotechnology. *Nat. Prod. Rep.* 38, 1282–1329. doi:10.1039/d0np00030b

Jiang, G., Zhang, L., Wang, J., and Zhou, H. (2016). Baicalein Induces the Apoptosis of U251 Glioblastoma Cell Lines via the NF-kB-P65-Mediated Mechanism. *Anim. Cell Syst.* 20, 296–302. doi:10.1080/19768354.2016.1229216

Jiang, L., Lin, C., Song, L., Wu, J., Chen, B., Ying, Z., et al. (2012). MicroRNA-30e* promotes human glioma cell invasiveness in an orthotopic xenotransplantation model by disrupting the NF-κB/IκBα negative feedback loop. *J. Clin. Invest.* 122, 33–47. doi:10.1172/JCI58849

Jiao, Y., Li, H., Liu, Y., Guo, A., Xu, X., Qu, X., et al. (2015). Resveratrol Inhibits the Invasion of Glioblastoma-Initiating Cells via Down-Regulation of the PI3K/Akt/NF-Kb Signaling Pathway. *Nutrients* 7, 4383–4402. doi:10.3390/nu7064383

Johnsen, K. B., Burkhart, B., Melander, F., Kempen, P. J., Vejlebo, J. B., Siupka, P., et al. (2017). Targeting Transferrin Receptors at the Blood-Brain Barrier Improves the Uptake of Immunoliposomes and Subsequent Cargo Transport into the Brain Parenchyma. *Sci. Rep.* 7. doi:10.1038/S41598-017-11220-1

Kargiotis, O., Rao, J. S., and Kyritsis, A. P. (2006). Mechanisms of Angiogenesis in Gliomas. *J. Neurooncol.* 78, 281–293. doi:10.1007/s11060-005-9097-6

Karlebach, G., and Shamir, R. (2010). Minimally Perturbing a Gene Regulatory Network to Avoid a Disease Phenotype: The Glioma Network as a Test Case. *BMC Syst. Biol.* 4, 15. doi:10.1186/1752-0509-4-15

Khan, M., Yi, F., Rasul, A., Li, T., Wang, N., Gao, H., et al. (2012). Alantolactone Induces Apoptosis in Glioblastoma Cells via GSH Depletion, ROS Generation, and Mitochondrial Dysfunction. *IUBMB Life* 64, 783–794. doi:10.1002/iub.1068

Kiekow, C. J., Figueiró, F., Dietrich, F., Vechia, L. D., Pires, E. N., Jandrey, E. H., et al. (2016). Quercetin Derivative Induces Cell Death in Glioma Cells by Modulating NF-Kb Nuclear Translocation and Caspase-3 Activation. *Eur. J. Pharm. Sci.* 84, 116–122. doi:10.1016/J.EJPS.2016.01.019

Kiekow, C. J., Figueiró, F., Dietrich, F., Vechia, L. D., Pires, E. N., Jandrey, E. H., et al. (2016). Quercetin Derivative Induces Cell Death in Glioma Cells by Modulating NF-Kb Nuclear Translocation and Caspase-3 Activation. *Eur. J. Pharm. Sci.* 84, 116–122. doi:10.1016/j.ejps.2016.01.019

Kim, S. Y., Jung, S. H., and Kim, H. S. (2005). Curcumin Is a Potent Broad Spectrum Inhibitor of Matrix Metalloproteinase Gene Expression in Human Astroglioma Cells. *Biochem. Biophys. Res. Commun.* 337, 510–516. doi:10.1016/j.bbrc.2005.09.079

Kumar, R., Harilal, S., Parambi, D. G. T., Narayanan, S. E., Uddin, M. S., Marathakam, A., et al. (2020). Fascinating Chemo Preventive story of Wogonin: A Chance to Hit on the Head in Cancer Treatment. *Curr. Pharm. Des.* 26. doi:10.2174/1385272824999200427083040

Kumar, R., Lal, N., Nemaysh, V., and Luthra, P. M. (2018). Demethoxycurcumin Mediated Targeting of MnSOD Leading to Activation of Apoptotic Pathway and Inhibition of Akt/NF-Kb Survival Signalling in Human Glioma U87 MG Cells. *Toxicol. Appl. Pharmacol.* 345, 75–93. doi:10.1016/j.taap.2018.02.020

Kwok, B. H., Koh, B., Ndubuisi, M. I., Elofsson, M., and Crews, C. M. (2001). The Anti-inflammatory Natural Product Parthenolide from the Medicinal Herb Feverfew Directly Binds to and Inhibits IkappaB Kinase. *Chem. Biol.* 8, 759–766. doi:10.1016/S1074-5521(01)00049-7

Lakomy, R., Sana, J., Hankeova, S., Fadrus, P., Kren, L., Lzicarova, E., et al. (2011). MiR-195, miR-196b, miR-181c, miR-21 Expression Levels and O-6-Methylguanine-DNA Methyltransferase Methylation Status Are Associated with Clinical Outcome in Glioblastoma Patients. *Cancer Sci.* 102, 2186–2190. doi:10.1111/j.1349-7006.2011.02092.x

Lan, F., Yang, Y., Han, J., Wu, Q., Yu, H., and Yue, X. (2016). Sulforaphane Reverses Chemo-Resistance to Temozolomide in Glioblastoma Cells by NF-κb-dependent Pathway Downregulating MGMT Expression. *Int. J. Oncol.* 48, 559–568. doi:10.3892/IJO.2015.3271

Lécuyer, M.-A., Kebir, H., and Prat, A. (2016), Glial Influences on BBB Functions and Molecular Players in Immune Cell Trafficking. *Biochim. Biophys. Acta* 1862, 472–482. doi:10.1016/J.BBADIS.2015.10.004

Lee, C. S., Cho, H. J., Jeong, Y. J., Shin, J. M., Park, K. K., Park, Y. Y., et al. (2015). Isothiocyanates Inhibit the Invasion and Migration of C6 Glioma Cells by Blocking FAK/JNK-mediated MMP-9 Expression. *Oncol. Rep.* 34, 2901–2908. doi:10.3892/or.2015.4292

Lenzi, M., Fimognari, C., and Hrelia, P. (2014). Sulforaphane as a Promising Molecule for Fighting Cancer. *Cancer Treat. Res.* 159, 207–223. doi:10.1007/978-3-642-38007-5_12

Li, C., Zhou, Y., Peng, X., Du, L., Tian, H., Yang, G., et al. (2014). Sulforaphane Inhibits Invasion via Activating ERK1/2 Signaling in Human Glioblastoma U87MG and U373MG Cells. *PLoS One* 9, e90520. doi:10.1371/JOURNAL.PONE.0090520

Li, F., and Sethi, G. (2010). Targeting Transcription Factor NF-kappaB to Overcome Chemoresistance and Radioresistance in Cancer Therapy. *Biochim. Biophys. Acta* 1805, 167–180. doi:10.1016/j.bbcan.2010.01.002

Li, Y., Li, W., Yang, Y., Lu, Y., He, C., Hu, G., et al. (2009). MicroRNA-21 Targets LRRFIP1 and Contributes to VM-26 Resistance in Glioblastoma Multiforme. *Brain Res.* 1286, 13–18. doi:10.1016/j.brainres.2009.06.053

Li, Y., Zhou, S., Li, J., Sun, Y., Hasimu, H., Liu, R., et al. (2015). Quercetin Protects Human Brain Microvascular Endothelial Cells from Fibrillar β-amyloid1–40-induced Toxicity. *Acta Pharm. Sin. B* 5, 47–54. doi:10.1016/J.APSB.2014.12.003

Lin, S. R., Chang, C. H., Hsu, C. F., Tsai, M. J., Cheng, H., Leong, M. K., et al. (2020). Natural Compounds as Potential Adjuvants to Cancer Therapy: Preclinical Evidence. *Br. J. Pharmacol.* 177, 1409–1423. doi:10.1111/bph.14816

Liu, H., Dong, Y., Gao, Y., Du, Z., Wang, Y., Cheng, P., et al. (2016). The Fascinating Effects of Baicalein on Cancer: A Review. *Int. J. Mol. Sci.* 17. doi:10.3390/ijms17101681

Liu, Y., Tang, Z. G., Lin, Y., Qu, X. G., Lv, W., Wang, G. B., et al. (2017). Effects of Quercetin on Proliferation and Migration of Human Glioblastoma U251 Cells. *Biomed. Pharmacother.* 92, 33–38. doi:10.1016/j.biopha.2017.05.044

Liu, Y., Tang, Z. G., Yang, J. Q., Zhou, Y., Meng, L. H., Wang, H., et al. (2017). Low Concentration of Quercetin Antagonizes the Invasion and Angiogenesis of Human Glioblastoma U251 Cells. *Onco. Targets Ther.* 10, 4023–4028. doi:10.2147/OTT.S136821

Mann, J. (2002). Natural Products in Cancer Chemotherapy: Past, Present and Future. *Nat. Rev. Cancer* 2, 143–148. doi:10.1038/nrc723

McFarland, B. C., Hong, S. W., Rajbhandari, R., Twitty, G. B., Gray, G. K., Yu, H., et al. (2013). NF-κB-induced IL-6 Ensures STAT3 Activation and Tumor Aggressiveness in Glioblastoma. *PLoS One* 8, e78728. doi:10.1371/journal.pone.0078728

Mitsiogianni, M., Koutsidis, G., Mavroudis, N., Trafalis, D. T., Botaitis, S., Franco, R., et al. (2019). The Role of Isothiocyanates as Cancer Chemo-Preventive,

Chemo-Therapeutic and Anti-melanoma Agents. *Antioxidants (Basel)* 8. doi:10.3390/antiox8040106

Nakabayashi, H., and Shimizu, K. (2012). Involvement of Akt/NF-Kb Pathway in Antitumor Effects of Parthenolide on Glioblastoma Cells *In Vitro* and *In Vivo*. *BMC Cancer* 12, 453. doi:10.1186/1471-2407-12-453

Noch, E. K., Ramakrishna, R., and Magge, R. (2018). Challenges in the Treatment of Glioblastoma: Multisystem Mechanisms of Therapeutic Resistance. *World Neurosurg.* 116, 505–517. doi:10.1016/J.WNEU.2018.04.022

Nogueira, L., Ruiz-Ontañon, P., Vazquez-Barquero, A., Lafarga, M., Berciano, M. T., Aldaz, B., et al. (2011). Blockade of the NFκB Pathway Drives Differentiating Glioblastoma-Initiating Cells into Senescence Both *In Vitro* and *In Vivo*. *Oncogene* 30, 3537–3548. doi:10.1038/onc.2011.74

Nogueira, L., Ruiz-Ontañon, P., Vazquez-Barquero, A., Moris, F., and Fernandez-Luna, J. L. (2011). The NFκB Pathway: a Therapeutic Target in Glioblastoma. *Oncotarget* 2, 646–653. doi:10.18632/oncotarget.322

Nozell, S., Laver, T., Moseley, D., Nowoslawski, L., De Vos, M., Atkinson, G. P., et al. (2008). The ING4 Tumor Suppressor Attenuates NF-kappaB Activity at the Promoters of Target Genes. *Mol. Cel. Biol.* 28, 6632–6645. doi:10.1128/mcb.00697-08

Obermeier, B., Daneman, R., and Ransohoff, R. M. (2013). Development, Maintenance and Disruption of the Blood-Brain Barrier. *Nat. Med.* 19, 1584–1596. doi:10.1038/NM.3407

Papagiannakopoulos, T., Shapiro, A., and Kosik, K. S. (2008). MicroRNA-21 Targets a Network of Key Tumor-Suppressive Pathways in Glioblastoma Cells. *Cancer Res.* 68, 8164–8172. doi:10.1158/0008-5472.CAN-08-1305

Park, M. H., Ahn, B. H., Hong, Y. K., and Min, do. S. (2009). Overexpression of Phospholipase D Enhances Matrix Metalloproteinase-2 Expression and Glioma Cell Invasion via Protein Kinase C and Protein Kinase A/NF-kappaB/Sp1-mediated Signaling Pathways. *Carcinogenesis* 30, 356–365. doi:10.1093/carcin/bgn287

Park, M. H., and Hong, J. T. (2016). Roles of NF-Kb in Cancer and Inflammatory Diseases and Their Therapeutic Approaches. *Cells* 5, 15. doi:10.3390/cells5020015

Park, M. H., and Min, do. S. (2011). Quercetin-induced Downregulation of Phospholipase D1 Inhibits Proliferation and Invasion in U87 Glioma Cells. *Biochem. Biophys. Res. Commun.* 412, 710–715. doi:10.1016/j.bbrc.2011.08.037

Patanè, M., Porrati, P., Bottega, E., Morosini, S., Cantini, G., Girgenti, V., et al. (2013). Frequency of NFKBIA Deletions Is Low in Glioblastomas and Skewed in Glioblastoma Neurospheres. *Mol. Cancer* 12, 160. doi:10.1186/1476-4598-12-160

Phillips, H. S., Kharbanda, S., Chen, R., Forrest, W. F., Soriano, R. H., Wu, T. D., et al. (2006). Molecular Subclasses of High-Grade Glioma Predict Prognosis, Delineate a Pattern of Disease Progression, and Resemble Stages in Neurogenesis. *Cancer Cell* 9, 157–173. doi:10.1016/j.ccr.2006.02.019

Phuphanich, S., Supko, J. G., Carson, K. A., Grossman, S. A., Burt Nabors, L., Mikkelsen, T., et al. (2010). Phase 1 Clinical Trial of Bortezomib in Adults with Recurrent Malignant Glioma. *J. Neurooncol.* 100, 95–103. doi:10.1007/s11060-010-0143-7

Prawan, A., Saw, C. L., Khor, T. O., Keum, Y. S., Yu, S., Hu, L., et al. (2009). Anti-NF-kappaB and Anti-inflammatory Activities of Synthetic Isothiocyanates: Effect of Chemical Structures and Cellular Signaling. *Chem. Biol. Interact.* 179, 202–211. doi:10.1016/j.cbi.2008.12.014

Puliyappadamba, V. T., Chakraborty, S., Chauncey, S. S., Li, L., Hatanpaa, K. J., Mickey, B., et al. (2013). Opposing Effect of EGFRWT on EGFRvIII-Mediated NF-Kb Activation with RIP1 as a Cell Death Switch. *Cell Rep* 4, 764–775. doi:10.1016/j.celrep.2013.07.025

Puliyappadamba, V. T., Hatanpaa, K. J., Chakraborty, S., and Habib, A. A. (2014). The Role of NF-Kb in the Pathogenesis of Glioma. *Mol. Cel. Oncol.* 1, e963478. doi:10.4161/23723548.2014.963478

Qin, Y., Zhao, D., Zhou, H. G., Wang, X. H., Zhong, W. L., Chen, S., et al. (2016). Apigenin Inhibits NF-Kb and Snail Signaling, EMT and Metastasis in Human Hepatocellular Carcinoma. *Oncotarget* 7, 41421–41431. doi:10.18632/oncotarget.9404

Rasul, A., Khan, M., Ali, M., Li, J., and Li, X. (2013). Targeting Apoptosis Pathways in Cancer with Alantolactone and Isoalantolactone. *ScientificWorldJournal* 2013, 248532. doi:10.1155/2013/248532

Ren, Z., Wang, L., Cui, J., Huoc, Z., Xue, J., Cui, H., et al. (2013). Resveratrol Inhibits NF-kB Signaling through Suppression of P65 and IkappaB Kinase Activities. *Pharmazie* 68, 689–694.

Reyes-Farias, M., and Carrasco-Pozo, C. (2019). The Anti-cancer Effect of Quercetin: Molecular Implications in Cancer Metabolism. *Int. J. Mol. Sci.* 20, 3177. doi:10.3390/ijms20133177

Richmond, A., and Yang, J. (2016). The Role of NF-kB in Modulating Antitumor Immunity. *Oncoimmunology* 5, e1005522. doi:10.1080/2162402X.2015.1005522

Robe, P. A., Bentires-Alj, M., Bonif, M., Rogister, B., Deprez, M., Haddada, H., et al. (2004). *In Vitro* and *In Vivo* Activity of the Nuclear Factor-kappaB Inhibitor Sulfasalazine in Human Glioblastomas. *Clin. Cancer Res.* 10, 5595–5603. doi:10.1158/1078-0432.CCR-03-0392

Saberi-Karimian, M., Katsiki, N., Caraglia, M., Boccellino, M., Majeed, M., and Sahebkar, A. (2019). Vascular Endothelial Growth Factor: An Important Molecular Target of Curcumin. *Crit. Rev. Food Sci. Nutr.* 59, 299–312. doi:10.1080/10408398.2017.1366892

Schacter, L. (1996). Etoposide Phosphate: what, Why, where, and How? *Semin. Oncol.* 23, 1–7.

Seo, M. B., Lee, S. K., Jeon, Y. J., and Im, J. S. (2011). Inhibition of P65 Nuclear Translocation by Baicalein. *Toxicol. Res.* 27, 71–76. doi:10.5487/TR.2011.27.2.071

Shukla, S., Pia Patric, I. R., Thinagararjan, S., Srinivasan, S., Mondal, B., Hegde, A. S., et al. (2013). A DNA Methylation Prognostic Signature of Glioblastoma: Identification of NPTX2-PTEN-NF-Kb Nexus. *Cancer Res.* 73, 6563–6573. doi:10.1158/0008-5472.CAN-13-0298

Song, L., Lin, C., Gong, H., Wang, C., Liu, L., Wu, J., et al. (2013). miR-486 Sustains NF-Kb Activity by Disrupting Multiple NF-Kb-Negative Feedback Loops. *Cell Res.* 23, 274–289. doi:10.1038/cr.2012.174

Song, L., Liu, L., Wu, Z., Li, Y., Ying, Z., Lin, C., et al. (2012). TGF-β Induces miR-182 to Sustain NF-Kb Activation in Glioma Subsets. *J. Clin. Invest.* 122, 3563–3578. doi:10.1172/JCI62339

Srinivasan, S., Patric, I. R., and Somasundaram, K. (2011). A Ten-microRNA Expression Signature Predicts Survival in Glioblastoma. *PLoS One* 6, e17438. doi:10.1371/journal.pone.0017438

Stiles, C. D., and Rowitch, D. H. (2008). Glioma Stem Cells: A Midterm Exam. *Neuron.* 58, 832–846. doi:10.1016/j.neuron.2008.05.031

Subedi, L., Venkatesan, R., and Kim, S. Y. (2017). Neuroprotective and Anti-inflammatory Activities of Allyl Isothiocyanate through Attenuation of JNK/NF-κB/TNF-α Signaling. *Int. J. Mol. Sci.* 18. doi:10.3390/ijms18071423

Sun, S. C. (2011). Non-canonical NF-Kb Signaling Pathway. *Cel. Res.* 21, 71–85. doi:10.1038/cr.2010.177

Tanaka, K., Babic, I., Nathanson, D., Akhavan, D., Guo, D., Gini, B., et al. (2011). Oncogenic EGFR Signaling Activates an mTORC2-NF-Kb Pathway that Promotes Chemotherapy Resistance. *Cancer Discov.* 1, 524–538. doi:10.1158/2159-8290.CD-11-0124

Tang, W., Liang, R., Duan, Y., Shi, Q., Liu, X., and Liao, Y. (2017). PLD1 Overexpression Promotes Invasion and Migration and Function as a Risk Factor for Chinese Glioma Patients. *Oncotarget* 8, 57039–57046. doi:10.18632/oncotarget.18961

Taniguchi, K., and Karin, M. (2018). NF-κB, Inflammation, Immunity and Cancer: Coming of Age. *Nat. Rev. Immunol.* 18, 309–324. doi:10.1038/nri.2017.142

Tellingen, v. T., Yetkin-Arik, B., Gooijer, M. C., Wesseling, P., Wurdinger, T., and Vries, H. E. (2015). Overcoming the Blood-Brain Tumor Barrier for Effective Glioblastoma Treatment. *Drug Resist. Updat.* 19, 1–12. doi:10.1016/J.DRUP.2015.02.002

Tilstra, J. S., Clauson, C. L., Niedernhofer, L. J., and Robbins, P. D. (2011). NF-κB in Aging and Disease. *Aging Dis.* 2, 449–465.

Tsai, Y. M., Chien, C-F., Lin, L-C., and Tsai, T-H. (2011). Curcumin and its Nano-Formulation: the Kinetics of Tissue Distribution and Blood-Brain Barrier Penetration. *Int. J. Pharm.* 416, 331–338. doi:10.1016/J.IJPHARM.2011.06.030

Uddin, M. S., Hasana, S., Ahmad, J., Hossain, M. F., Rahman, M. M., Behl, T., et al. (2021). Anti-Neuroinflammatory Potential of Polyphenols by Inhibiting NF-Kb to Halt Alzheimer's Disease. *Curr. Pharm. Des.* 27, 402–414. doi:10.2174/1381612826666201118092422

Uddin, M. S., Mamun, A. A., Jakaria, M., Thangapandiyan, S., Ahmad, J., Rahman, M. A., et al. (2020). Emerging Promise of Sulforaphane-Mediated Nrf2

Signaling cascade against Neurological Disorders. *Sci. Total Environ.* 707, 135624. doi:10.1016/j.scitotenv.2019.135624

Uddin, M. S., Mamun, A. A., Alghamdi, B. S., Tewari, D., Jeandet, P., Sarwar, M. S., et al. (2020). Epigenetics of Glioblastoma Multiforme: From Molecular Mechanisms to Therapeutic Approaches. *Semin. Cancer Biol.* doi:10.1016/j.semcancer.2020.12.015

Varsha, K., Sharma, A., Kaur, A., Madan, J., Pandey, R. S., Jain, U. K., et al. (2017). "Natural Plant-Derived Anticancer Drugs Nanotherapeutics: A Review on Preclinical to Clinical Success," in *Natural Product Drug Discovery, Discovery and Development of Anti-Inflammatory Agents from Natural Products*. Editor A. Ficai and A. M. Grumezescu (Amsterdam: Elsevier), 775–809.

Verhaak, R. G., Hoadley, K. A., Purdom, E., Wang, V., Qi, Y., Wilkerson, M. D., et al. (2010). Integrated Genomic Analysis Identifies Clinically Relevant Subtypes of Glioblastoma Characterized by Abnormalities in PDGFRA, IDH1, EGFR, and NF1. *Cancer Cell* 17, 98–110. doi:10.1016/j.ccr.2009.12.020

Vervandier-Fasseur, D., and Latruffe, N. (2019). The Potential Use of Resveratrol for Cancer Prevention. *Molecules* 24. doi:10.3390/molecules24244506

Vijayakumar, M. R., Vajanthri, K. Y., Balavigneswaran, C. K., Mahto, S. K., Mishra, N., Muthu, M. S., et al. (2016). Pharmacokinetics, Biodistribution, *In Vitro* Cytotoxicity and Biocompatibility of Vitamin E TPGS Coated Trans Resveratrol Liposomes. *Colloids Surf. B. Biointerfaces* 145, 479–491. doi:10.1016/J.COLSURFB.2016.05.037

Wang, C.-N., Shiao, Y.-J., Lin, Y.-L., and Chen, C.-F. (1999). Nepalolide A Inhibits the Expression of Inducible Nitric Oxide Synthase by Modulating the Degradation of IκB-α and IκB-β in C6 Glioma Cells and Rat Primary Astrocytes. *Br. J. Pharmacol.* 128, 345–356. doi:10.1038/sj.bjp.0702785

Wang, S., Jiao, B., Geng, S., Song, J., Liang, Z., and Lu, S. (2014). Concomitant microRNA-31 Downregulation and Radixin Upregulation Predicts Advanced Tumor Progression and Unfavorable Prognosis in Patients with Gliomas. *J. Neurol. Sci.* 338, 71–76. doi:10.1016/j.jns.2013.12.019

Wang, X., Yu, Z., Wang, C., Cheng, W., Tian, X., Huo, X., et al. (2017). Alantolactone, a Natural Sesquiterpene Lactone, Has Potent Antitumor Activity against Glioblastoma by Targeting IKKβ Kinase Activity and Interrupting NF-Kb/cox-2-Mediated Signaling Cascades. *J. Exp. Clin. Cancer Res.* 36, 93. doi:10.1186/s13046-017-0563-8

Wang, Y-F., Gu, Y-T., Qin, G-H., Zhong, L., and Meng, Y-N. (2013). Curcumin Ameliorates the Permeability of the Blood-Brain Barrier during Hypoxia by Upregulating Heme Oxygenase-1 Expression in Brain Microvascular Endothelial Cells. *J. Mol. Neurosci.* 51, 344–351. doi:10.1007/S12031-013-9989-4

Wei, W., Huang, H., Zhao, S., Liu, W., Liu, C. X., Chen, L., et al. (2013). Alantolactone Induces Apoptosis in Chronic Myelogenous Leukemia Sensitive or Resistant to Imatinib through NF-Kb Inhibition and Bcr/Abl Protein Deletion. *Apoptosis* 18, 1060–1070. doi:10.1007/s10495-013-0854-2

Wei, H., Wang, S., Zhen, L., Yang, Q., Wu, Z., Lei, X., et al. (2015). Resveratrol attenuates the blood-brain barrier dysfunction by regulation of the MMP-9/TIMP-1 balance after cerebral ischemia reperfusion in rats. *J. Mol. Neurosci*. 55 (4), 872–879. doi:10.1007/s12031-014-0441-12

Westhoff, M. A., Zhou, S., Nonnenmacher, L., Karpel-Massler, G., Jennewein, C., Schneider, M., et al. (2013). Inhibition of NF-Kb Signaling Ablates the Invasive Phenotype of Glioblastoma. *Mol. Cancer Res.* 11, 1611–1623. doi:10.1158/1541-7786.MCR-13-0435-T

Wu, H., Liu, Q., Cai, T., Chen, Y.-D., and Wang, Z.-F. (2015). Induction of microRNA-146a Is Involved in Curcumin-Mediated Enhancement of Temozolomide Cytotoxicity against Human Glioblastoma. *Mol. Med. Rep.* 12, 5461–5466. doi:10.3892/MMR.2015.4087

Xia, H., Yan, Y., Hu, M., Wang, Y., Wang, Y., Dai, Y., et al. (2013). MiR-218 Sensitizes Glioma Cells to Apoptosis and Inhibits Tumorigenicity by Regulating ECOP-Mediated Suppression of NF-Kb Activity. *Neuro. Oncol.* 15, 413–422. doi:10.1093/neuonc/nos296

Xia, Y., Shen, S., and Verma, I. M. (2014). NF-κB, an Active Player in Human Cancers. *Cancer Immunol. Res.* 2, 823–830. doi:10.1158/2326-6066.CIR-14-0112

Xu, C., Shen, G., Chen, C., Gélinas, C., and Kong, A.-N. T. (2005). Suppression of NF-Kb and NF-Kb-Regulated Gene Expression by Sulforaphane and PEITC through IκBα, IKK Pathway in Human Prostate Cancer PC-3 Cells. *Oncogene* 24, 4486–4495. doi:10.1038/sj.onc.1208656

Yan, X., Qi, M., Li, P., Zhan, Y., and Shao, H. (2017). Apigenin in Cancer Therapy: Anti-cancer Effects and Mechanisms of Action. *Cell Biosci.* 7, 50. doi:10.1186/s13578-017-0179-x

Yang, G., Han, D., Chen, X., Zhang, D., Wang, L., Shi, C., et al. (2014). MiR-196a Exerts its Oncogenic Effect in Glioblastoma Multiforme by Inhibition of IκBα Both *In Vitro* and *In Vivo*. *Neuro. Oncol.* 16, 652–661. doi:10.1093/neuonc/not307

Yang, W., Xia, Y., Cao, Y., Zheng, Y., Bu, W., Zhang, L., et al. (2012). EGFR-induced and PKCε Monoubiquitylation-dependent NF-Kb Activation Upregulates PKM2 Expression and Promotes Tumorigenesis. *Mol. Cel.* 48, 771–784. doi:10.1016/j.molcel.2012.09.028

Yin, D., Zhou, H., Kumagai, T., Liu, G., Ong, J. M., Black, K. L., et al. (2005). Proteasome Inhibitor PS-341 Causes Cell Growth Arrest and Apoptosis in Human Glioblastoma Multiforme (GBM). *Oncogene* 24, 344–354. doi:10.1038/sj.onc.1208225

Yu, X., Liu, Y., Wang, Y., Mao, X., Zhang, Y., and Xia, J. (2018). Baicalein Induces Cervical Cancer Apoptosis through the NF-Kb Signaling Pathway. *Mol. Med. Rep.* 17, 5088–5094. doi:10.3892/mmr.2018.8493

Yu, Z., Chen, Y., Wang, S., Li, P., Zhou, G., and Yuan, Y. (2018). Inhibition of NF-Kb Results in Anti-glioma Activity and Reduces Temozolomide-Induced Chemoresistance by Down-Regulating MGMT Gene Expression. *Cancer Lett.* 428, 77–89. doi:10.1016/j.canlet.2018.04.033

Zaplatic, E., Bule, M., Shah, S. Z. A., Uddin, M. S., and Niaz, K. (2019). Molecular Mechanisms Underlying Protective Role of Quercetin in Attenuating Alzheimer's Disease. *Life Sci.* 224, 109–119. doi:10.1016/j.lfs.2019.03.055

Zhang, T., Park, K. A., Li, Y., Byun, H. S., Jeon, J., Lee, Y., et al. (2013). PHF20 Regulates NF-Kb Signalling by Disrupting Recruitment of PP2A to P65. *Nat. Commun.* 4, 2062. doi:10.1038/ncomms3062

Zhao, J., Zhu, J., Lv, X., Xing, J., Liu, S., Chen, C., et al. (2017). Curcumin Potentiates the Potent Antitumor Activity of ACNU against Glioblastoma by Suppressing the PI3K/AKT and NF-Kb/cox-2 Signaling Pathways. *Onco. Targets Ther.* 10, 5471–5482. doi:10.2147/OTT.S149708

Zhao, Q., Chen, X. Y., and Martin, C. (2016). Scutellaria Baicalensis, the golden Herb from the Garden of Chinese Medicinal Plants. *Sci. Bull. (Beijing)* 61, 1391–1398. doi:10.1007/s11434-016-1136-5

Zhao, X., Chen, C., Liu, M., Feng, J., Chen, J., and Hu, K. (2017). Remodeling the Blood-Brain Barrier Microenvironment by Natural Products for Brain Tumor Therapy. *Acta Pharm. Sin. B* 7, 541–553. doi:10.1016/J.APSB.2017.07.002

Zhou, Y., Eppenberger-Castori, S., Eppenberger, U., and Benz, C. C. (2005). The NFkappaB Pathway and Endocrine-Resistant Breast Cancer. *Endocr. Relat. Cancer* 12 Suppl 1, S37–S46. doi:10.1677/erc.1.00977

Zhou, Y., Wang, Y., Wu, S., Yan, Y., Hu, Y., Zheng, Z., et al. (2020). Sulforaphane-cysteine Inhibited Migration and Invasion via Enhancing Mitophagosome Fusion to Lysosome in Human Glioblastoma Cells. *Cell Death Dis.* 11, 1–16. doi:10.1038/s41419-020-03024-5

Conflict of Interest: The authors declare that the research was conducted in the absence of any commercial or financial relationships that could be construed as a potential conflict of interest.

Publisher's Note: All claims expressed in this article are solely those of the authors and do not necessarily represent those of their affiliated organizations, or those of the publisher, the editors and the reviewers. Any product that may be evaluated in this article, or claim that may be made by its manufacturer, is not guaranteed or endorsed by the publisher.

frontiers in Pharmacology

ORIGINAL RESEARCH
published: 10 September 2021
doi: 10.3389/fphar.2021.701568

Evaluation of the IKKβ Binding of Indicaxanthin by Induced-Fit Docking, Binding Pose Metadynamics, and Molecular Dynamics

Mario Allegra, Marco Tutone, Luisa Tesoriere, Alessandro Attanzio, Giulia Culletta and Anna Maria Almerico*

Dipartimento di Scienze e Tecnologie Biologiche Chimiche e Farmaceutiche (STEBICEF), Università degli Studi di Palermo, Palermo, Italy

Background: Indicaxanthin, a betaxanthin belonging to the betalain class of compounds, has been recently demonstrated to exert significant antiproliferative effects inducing apoptosis of human melanoma cells through the inhibition of NF-κB as the predominant pathway. Specifically, Indicaxanthin inhibited IκBα degradation in A375 cells. In resting cells, NF-κB is arrested in the cytoplasm by binding to its inhibitor protein IκBα. Upon stimulation, IκBα is phosphorylated by the IKK complex, and degraded by the proteasome, liberating free NF-κB into the nucleus to initiate target gene transcription. Inhibition of the IKK complex leads to the arrest of the NF-κB pathway.

Methods: To acquire details at the molecular level of Indicaxanthin's inhibitory activity against hIKKβ, molecular modeling and simulation techniques including induced-fit docking (IFD), binding pose metadynamics (BPMD), molecular dynamics simulations, and MM-GBSA (molecular mechanics-generalized Born surface area continuum solvation) have been performed.

Results: The computational calculations performed on the active and inactive form, and the allosteric binding site of hIKKβ, revealed that Indicaxanthin inhibits prevalently the active form of the hIKKβ. MM-GBSA computations provide further evidence of Indicaxanthin's stability inside the active binding pocket with a binding free energy of –22.2 ± 4.3 kcal/mol with respect to the inactive binding pocket with a binding free energy of –20.7 ± 4.7 kcal/mol. BPMD and MD simulation revealed that Indicaxanthin is likely not an allosteric inhibitor of hIKKβ.

Conclusion: As a whole, these in silico pieces of evidence show that Indicaxanthin can inhibit the active form of the hIKKβ adding novel mechanistic insights on its recently discovered ability to impair NF-κB signaling in melanoma A375 cells. Moreover, our results suggest the phytochemical as a new lead compound for novel, more potent IKKβ inhibitors to be employed in the treatment of cancer and inflammation-related conditions.

Keywords: indicaxanthin, IKKβ, induced fit docking, molecular dynamics, anticancer activity, binding pose metadynamics

OPEN ACCESS

Edited by:
Carlos Alberto Manssour Fraga, Federal University of Rio de Janeiro, Brazil

Reviewed by:
Roberta Tesch, Lead Discovery Center GmbH, Germany
Isabella Alvim Guedes, National Laboratory for Scientific Computing (LNCC), Brazil

****Correspondence:***
Marco Tutone
marco.tutone@unipa.it

Specialty section:
This article was submitted to Pharmacology of Anti-Cancer Drugs, a section of the journal Frontiers in Pharmacology

Received: *30 April 2021*
Accepted: *24 August 2021*
Published: *10 September 2021*

Citation:
Allegra M, Tutone M, Tesoriere L, Attanzio A, Culletta G and Almerico AM (2021) Evaluation of the IKKβ Binding of Indicaxanthin by Induced-Fit Docking, Binding Pose Metadynamics, and Molecular Dynamics. Front. Pharmacol. 12:701568. doi: 10.3389/fphar.2021.701568

INTRODUCTION

Indicaxanthin, ((2S)-2,3-dihydro-4-[2-[(2S)-2-carboxypyrrolidin-1-yl]ethenyl]pyridine-2,6 dicarboxylic acid), is a betalain pigment belonging to the betalain class compounds (**Figure 1**). This includes vacuole pigments restricted to fruits and flowers of 10 families of Cariophyllalae plants and a few superior fungi of the genus Amanita of the Basidiomycetes (Slimen et al., 2017). Indicaxanthin has been investigated over the last 20 years by the author's research group for its chemical and nutraceutical properties. Interestingly the phytochemical has been demonstrated to be highly bioavailable in humans and even permeable to the rat brain-blood-barrier (Tesoriere et al., 2004; Allegra et al., 2015). Moreover, because of its reducing and amphipathic properties, it has been shown to interfere with cellular, redox-dependent signal transduction pathways in several experimental models of inflammatory-related, oxidative stress-dependent pathological conditions. Along these lines, Indicaxanthin has been demonstrated to exert significant reducing, anti-oxidative, anti-inflammatory, spasmolytic, and neuromodulatory effects both *in vitro* and *in vivo* (Allegra et al., 2019).

In addition to its redox-modulating and anti-inflammatory properties, Indicaxanthin has also been shown to exert antiproliferative effects against melanoma cells being also able to significantly impair tumor progression in a mouse model of cutaneous melanoma (Allegra et al., 2018). Mechanistic evaluations have individuated in the inhibition of the nuclear factor-κB (NF-κB) signaling, a key event underlying the antitumoral effects exerted by the pigment.

The NF-κB transcription factor family consists of five different DNA-binding proteins that form a variety of homodimers and heterodimers regulating both the innate and adaptive immune responses (Taniguchi and Karin, 2018). More interestingly, besides its modulating effects on the entire inflammatory response, NF-κB is responsible for accelerating cancer progression, metastasis, angiogenesis, and drug resistance (Zhang et al., 2017). Indeed, in several types of cancer, both in malignant cells and in the tumor microenvironment, NF-κB is constitutively activated, and only rarely is such activation due to NF-κB-related genetic alterations (Staudt, 2010; Ben-Neriah and Karin, 2011).

Melanoma is an aggressive skin cancer, notoriously resistant to current cancer therapies (Van Herck et al., 2021). To effectively prevent chemoresistance development and reduce the risk of unwanted side effects, current pharmacological strategies employ a multi-targeted approach. Given that constitutive or drug-induced upregulation of NF-κB activity is associated with chemoresistance, NF-κB is considered one of the most relevant targets to discover new active compounds (Taniguchi and Karin, 2018). Permanent activation of NF-κB signaling in melanoma has been reported to proceed through the activation of the so-called canonical pathway (Yang and Richmond, 2001; Dhawan and Richmond, 2002; Amiri and Richmond, 2005; Amschler et al., 2010). Through this process, activation of NF-κB depends on the degradation of its specific inhibitors (IκB) consisting of IκBα, IκBβ, and IκBε. Typically, IκBs bind to NF-κB complexes,

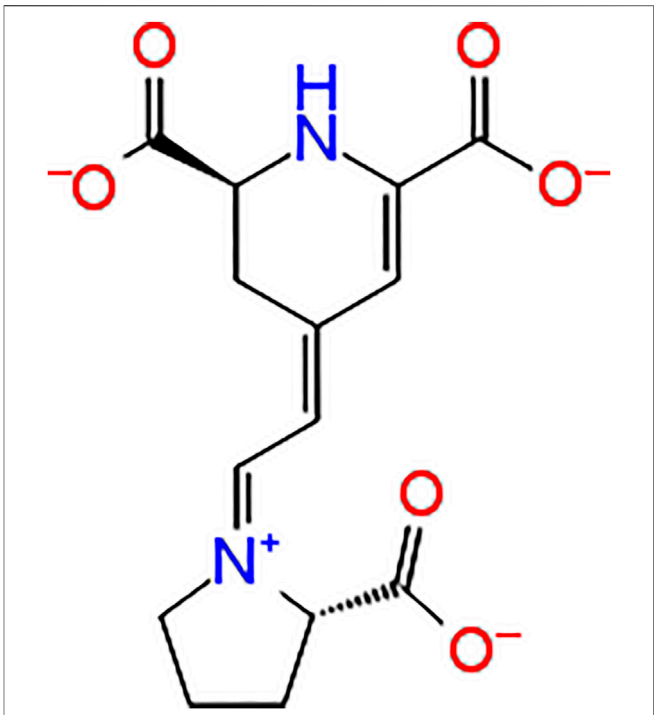

FIGURE 1 | Indicaxanthin structure.

inhibiting their DNA binding and keeping them in a predominantly, inactive cytoplasmic form. Tumour microenvironmental stimuli can lead to the activation of a large cytoplasmic protein complex: the IκB kinase (IKK). The precise nature of this molecular mechanism remains to be elucidated but it contains IKKα, IKKβ, and IKKγ as the three seminal components. The phosphorylated and thus activated IKK complex is responsible for the phosphorylation of IκB, marking it for degradation through the proteasomal degradation machinery. The free NF-κB dimers (p50-p65) can, then, translocate from the cytoplasm to the nucleus, bind to DNA, and regulate gene transcription. Typical targets within the classical NF-κB signaling include genes encoding pro-inflammatory cytokines, growth factors, chemokines, matrix metalloproteinases, pro-proliferative proteins, anti-apoptotic proteins, pro-inflammatory enzymes, angiogenic factors, and adhesion molecules (Staudt, 2010). As a primary druggable mediator of canonical NF-κB signaling, the IKKβ enzyme inhibition has been the historical focus of drug development pipelines. Thousands of compounds with activity against IKKβ have been characterized, with much demonstrating promising efficacy in pre-clinical models of cancer. However, severe on-target toxicities and other safety concerns associated with systemic IKKβ inhibition have so far prevented the clinal approval of any IKKβ inhibitors (Prescott and Cook, 2018).

Indicaxanthin has been demonstrated to inhibit IκBα degradation in melanoma A375 cells at 100 μM, a concentration at which it impairs NF-κB signaling and inhibits 50% cell proliferation (IC_{50}) (Allegra et al., 2018). In the light of this evidence, we employed an *in silico* approach to evaluate

Indicaxanthin's inhibitory activity against IKK. To this end, molecular modeling and simulation techniques including induced-fit docking (IFD), binding pose metadynamics (BPMD), molecular dynamics simulations, and MM-GBSA (molecular mechanics-generalized Born surface area continuum solvation) free energy calculation have been performed.

MATERIALS AND METHODS

Protein and Ligand Preparation

For the purpose study, the 2.83 Å resolution crystal structure of human IKKβ (hIKKβ), which is partially phosphorylated and bound to the staurosporine analog K252a (PDB ID: 4KIK) (Liu et al., 2013) was used. The structure was optimized using the Protein Preparation Wizard in Maestro (Schrödinger, 2017) adding bond orders and hydrogen atoms to the crystal structure using the OPLS3 force field. Prime was used to fix missing residues or atoms in the protein and to remove co-crystallized water molecules. PROPKA was used to check for the protonation state of ionizable protein groups (pH = 7.0). The hydrogen bonds were optimized through the reorientation of hydroxyl bonds, thiol groups, and amide groups. In the end, the system was minimized with the value of convergence of the RMSD of 0.3 Å. Indicaxanthin and staurosporine analog K252a were prepared using LigPrep The force field adopted was OPLS3 (Jorgensen et al., 1996) and Epik 3.9 (Schrödinger, 2017-1) was selected as an ionization tool at pH 7.2 ± 0.2. Tautomers generation was unflagged and the maximum number of conformers generated was set at 32.

Induced-Fit Docking

The induced-fit docking (IFD) is a method for modeling the conformational changes induced by ligand binding developed by Schrödinger (Sherman et al., 2006). This protocol models induced-fit docking of one or more ligands using the steps as also reported in (Tutone et al., 2019). Initial docking of each ligand is performed using a softened potential (van der Waals radii scaling). Then, a side-chain prediction within a given distance of any ligand pose is performed. Subsequently, a minimization of the same set of residues and the ligand for each protein/ligand complex pose is performed. After this stage, any receptor structure in each pose reflects an induced fit to the ligand structure and conformation. Finally, the ligand is rigorously docked, using Glide XP, into the induced-fit receptor structure. The grid boxes for the binding sites of Chain A (inactive form) and B (active form) were built considering the co-crystallized ligand staurosporine analog K252a as a centroid. For the allosteric sites of Chain A, the amino acid residues previously identified by Liu et al. (2018) were considered crucial for centering the docking grid. During the initial docking procedure, the van der Waals scaling factor was set at 0.5 for both receptor and ligand. The Prime refinement step was set on side chains of residues within 5 Å of the ligand. For each ligand docked, a maximum of 20 poses was retained to be then redocked at XP mode.

Binding Pose Metadynamics

Binding pose Metadynamics (BPMD) is an automated, enhanced sampling, metadynamics-based protocol. During the simulations, the ligands are forced to stir in their binding pose. This method showed the ability to reliably discriminate between the correct ligand binding pose and plausible alternative generate with docking or induced-fit docking studies (Clark et al., 2016).

Ten independent metadynamics simulations of 10 ns each were performed using as a collective variable (CV) the measure of the root-mean-square deviation (RMSD) of the ligand heavy atoms concerning their starting position. The alignment before the RMSD calculation was done by selecting protein residues within 3 Å of the ligand. The alpha carbons of these binding site residues were then aligned to those of the first frame of the metadynamics trajectory before calculating the heavy atom RMSD to the ligand conformation in the first frame. The hill height and width were set to 0.05 kcal/mol (about 1/10 of the characteristic thermal energy of the system, kBT) and 0.02 Å, respectively (Clark et al., 2016). Before the metadynamics run, the system was solvated in a box of SPC water molecules followed by several minimizations and restrained MD steps that allow the system to reach slowly the desired temperature of 300 K as well as releasing any bad contacts and/or strain in the initial starting structure. The final snapshot of the short unbiased MD simulation of 0.5 ns is then used as the reference for the following metadynamics production phase. The pivotal idea of BPMD is that ligands that are not stably bound to the target binding pocket will move forward higher RMSD as compared to the stably bound ones if they are exposed to the same biasing force. After the simulation, the stability of the ligand during the course is represented by three scores: PoseScore, PersistenceScore (PersScore), and CompositeScore (CompScore). PoseScore is indicative of the average RMSD from the starting pose. The steepest increase of this value is a symptom that the ligand is not in a well-defined energy minimum and probably it might not have been accurately modeled. PersScore is a measure of the hydrogen bond persistence calculated in the last 2ns of the simulation that have the same number of hydrogen bonds as the input structure, averaged over all the 10 repeated simulations. PersScore covers a range between 0 and 1, where 0 indicates that either the starting ligand pose did not have any interaction with the target or that the interactions have been lost during the simulations, while 1 indicates that the interactions between the staring ligand pose and the last 2 ns of the simulations have been retained. CompositeScore is the linear combination of PoseScore and PersScore, lower values equate to more stable complexes. Each complex, previously obtained, was run on Desmond on a single node with 1 GPU card, taking for a typical system (1 complex = 1 × 10 metadynamics run) 72 h.

MD Simulations

The plain MD simulations were carried out using Desmond 4.9 (Bowers et al., 2007) using the OPLS3 force field (Jorgensen et al., 1996). The complexes were solvated in orthorhombic boxes using

the TIP3P water model. Ions were added to neutralize charges. The systems were minimized and equilibrated at a temperature of 303.15 K and a pressure of 1.013 bar. The system was simulated as an NPT ensemble; a Nose–Hover thermostat and Martyna–Tobia–Klein barostat were used. The integration time step was chosen to be 2 fs. To keep the hydrogen–heavy atom bonds rigid, the SHAKE algorithm was used. A 9 Å cutoff radius was set for the short-range Coulomb interactions, and smooth particle mesh Ewald was used for the long-range interactions. For each system, we carried out 100 ns MD, with 1.2 ps detection ranges for energy, and 4.8 ps for the trajectory frames. Visualization and analysis of the MD trajectories were performed using Desmond simulation analysis tools in Maestro.

MM-GBSA Binding Free Energy Calculation

The MM-GBSA approach employs molecular mechanics, the generalized Born model, and the solvent accessibility method to determine free energies from structural information circumventing the computational complexity of free energy simulations wherein the net free energy is treated as a sum of a comprehensive set of individual energy components, each with a physical basis (Genheden and Ryde, 2015). We applied this method to the snapshots extracted from the 100 ns production MD trajectories. Protein-ligand binding free energy using MM-GBSA was calculated as the difference between the energy of the bound complex and the energy of the unbound protein and ligand. In this work MM-GBSA calculations were also achieved in Prime software (Jacobson et al., 2004); the entropy term −TΔS was not calculated to reduce computational time. The VSGB solvation model was chosen using OPLS3 Force Field with minimized sampling method.

RESULTS AND DISCUSSION

The hIKKβ protomer adopts a trimodular structure that closely resembles that of *Xenopus laevis* (xIKKβ): an N-terminal kinase domain (KD), a central ubiquitin-like domain (ULD), and a C-terminal scaffold/dimerization domain (SDD). In particular, the selected crystal structure has one protomer in the active conformation with phosphorylated Ser177 and Ser181 (Chain B), and the other protomer is in the inactive conformation with the same residues of serine unphosphorylated in the activation loop (Chain A). Recently, Liu and co. identified a druggable allosteric site between KD and ULD.

To evaluate the binding capability of Indicaxanthin into the hIKKβ, we performed a series of computational studies with increasing accuracy, induced-fit docking (IFD), binding pose metadynamics (BPMD), unbiased molecular dynamics (MD) followed by MM-GBSA (molecular mechanics-generalized Born surface area continuum solvation) free energy calculation. We began the computational studies by selecting the crystal structure of the human IKKβ (PDB ID: 4KIK) (Liu et al., 2013) bound to the staurosporine analog K252a in the KD (**Figures 2A,B**). Firstly, we optimized the crystal structure by completing and refining the missing loops and residues and optimizing amide groups of asparagine (Asn) and glutamine (Gln), and the imidazole ring in histidine (His); and predicting protonation states of histidine, His, aspartic acid (Asp) and glutamic acid (Glu) and tautomeric states of histidine. Then, the docking studies have been performed centering the docking boxes on the 3D coordinates of K252a, both in the inactive Chain A and in the active Chain B. The RMSD of K252a in Chain B and A was calculated showing values 0.8–0.18 Å respectively (The superimposition of re-docked structures are reported in **Supplementary Material**). Moreover, another docking box for the allosteric binding pocket was centered on the previously identified residues by Liu and Co. (Liu et al., 2018).

Induced Fit Docking

Induced-Fit docking (IFD) experiments were first carried out. IFD confers flexibility to the protein side chains, allowing the ligand to adjust and optimize binding interactions within the active site. We performed the IFD of K252a and Indicaxanthin in the two sites previously identified, and the IFD of Indicaxanthin in the allosteric binding site.

In most kinases, the ATP binding site is a narrow hydrophobic pocket located between the N-lobe and C-lobe of the kinase domain (KD) which are linked by a flexible hinge region. This binding site is partly covered by an activation loop comprised of Serine, Threonine, and Tyrosine residues in the unphosphorylated state. The N-terminal side of the activation loop consisting of a highly conserved triplet DLG (Asp166, Leu167, and Gly168) which is involved in the catalytic transfer of the γ-phosphate group (Xu et al., 2011). In IKKβ the residues Glu97, Tyr98, and Cys99 are part of the hinge region. The backbone groups of Glu97 and Cys99 can provide hydrogen bonding interactions with an inhibitor. (Leung et al., 2013).

Docking of K252a in Chain A showed a single H-bond interaction with Cys99 (hinge region), with the carbonyl of lactam ring. Other H-bonds were found between the amine of the K252a lactam group and Glu97 and the hydroxyl group and Glu149. Moreover, an aromatic H-bond was found with Asp166 (DLG triad). In chain B, K252a, as in Chain A, established the same interactions with Glu97, Cys99 (hinge region), and Glu149, with the only difference in another H-bond interaction between the carbonyl group of ether group and Thr23, and an aromatic H-bond with Tyr98. (**Figures 3A,B**).

We performed the IFD of Indicaxanthin in the three sites identified previously. In the best IFD result, in particular, considering the Chain A (Docking score = −6.166, **Table 1**), the carboxyl group of the pyrrolidinium ring interacts with Thr23 and Gly24 forming two H-bonds, while the Cys99 simultaneously interacts with the carboxyl groups and the nitrogen of pyridine moiety. The carboxyl group of pyridine in position 11 interacts with Tyr98 (hinge region) with another H-bond and with Lys106 (solvent accessible region) through one salt bridge. The carboxyl groups in the pyridine moiety establish two aromatic H-bonds with Tyr98. Finally, another salt bridge involves the pyrrolidinium nitrogen and the Asp103. In Chain B (Docking score = −7.293), Indicaxanthin showed similar interactions as in Chain A. Two H-bond interactions involve the carboxyl group of the pyrrolidinium ring and Thr23, and Asn28; one of the carboxyl

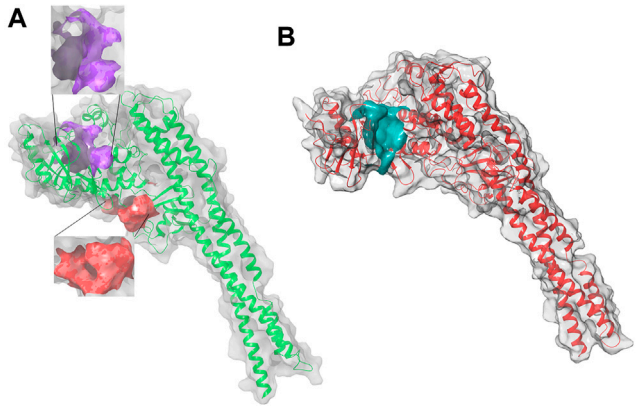

FIGURE 2 | 3D structure of hIKK forms: **(A)** the inactive form, Chain A, in purple the KD binding pocket, in red the allosteric binding site; **(B)** the active form, Chain B, in cyan the KD binding pocket of the inactive Chain A with a volume of 551 Å. This pocket is surrounded by three α helixes (Arg118-Ser127, Leu265-Leu273, and Leu303-His313) of KD and a loop (Thr368-Leu386) between two β sheets of ULD. They suggested that small molecules binding in the pocket between KD and ULD probably interfere with the kinase function by disrupting the interaction between these two domains (Liu et al., 2018).

TABLE 1 | BPMD and docking scores for the Indicaxanthin and K252a complexes.

	Docking score	Pose Score	Pers Score	Comp Score
Indi/Chain A	−6.166	3.133	0.12	2.53
Indi/Chain B	−7.293	4.631	0.04	4.44
K252a/Chain A	−13.700	1.206	0.81	−2.85
K252a/Chain B	−14.121	0.909	0.64	−2.28
Indi/Chain A allosteric	−6.117	>6	0.0	>6

groups of pyridine interacts through H-bond with Tyr98, Lys106. The last interactions were a salt bridge between two carboxyl groups of the pyridine and Lys106 (**Figures 3C,D**). The IFD study of Indicaxanthin in the allosteric site (Docking score = −6.117) showed a single H-bond interaction was found between one of the carboxyl group of pyridine and His380; another interaction was a salt bridge, between the nitrogen of pyrrolidinium moiety and Asp373 (**Figure 4**).

Moreover, we performed docking simulations with different hIKKβ inhibitors to be considered as reference compounds for the analyses of the binding interactions with key residues from the binding sites and to compare with the predicted binding affinity for Indicaxanthin. We selected three known orthosteric inhibitors: MLN120B (IC_{50} = 60 nM) (Prescott and Cook, 2018); the imidazo [1,2-a]quinaxoline derivative 6a (IC_{50} = 324 nM) (Moarbess et al., 2016); LASSBio-1524 (IC_{50} = 20 μM) (Guedes et al., 2016); and one allosteric inhibitor: BMS345521 (IC_{50} = 300 nM) (Prescott and Cook, 2018). The docking scores of these known inhibitors are consistent with the experimental IC_{50}, considering that Indicaxanthin showed an IC_{50} = 100 μM. Additionally, the key residues identified for these known inhibitors are similar to those identified for Indicaxanthin (Cys99, Asp103, Lys106). The allosteric inhibitor BMS345521 showed key interactions with His380, already identified for indicaxanthin, Asn308, Ser127. The 2D and 3D figures of the docked reference inhibitors together with key interactions and docking scores are reported in **Supplementary Material**.

Binding Pose Metadynamics

Binding pose metadynamics (BPMD) is an automated, enhanced sampling, metadynamics-based protocol, in which the ligand is forced to move around its binding pose. This method showed the ability to reliably discriminate between the correct ligand binding pose and plausible alternative generate with docking studies. In particular, Clark and colleagues introduced this metadynamics plus IFD strategy for accurate and reliable prediction of the structures of protein–ligand complexes at a useful computational cost. Their strategy allows treating the problem in full atomistic details, significantly enhancing the predictive power of IFD methods (Clark et al., 2016).

Firstly, we decided to use BPMD to evaluate the stability of the K252a best poses (in terms of docking scores) obtained from IFD studies into the binding site in Chain A and Chain B to evaluate the reliability of the IFD poses obtained as validation of the docking scoring functions. The results were defined in terms of pose stability based on the PoseScore that is the RMSD of the ligand related to the starting coordinates of the heavy atoms of the ligand. A PoseScore <2 Å is considered stable for the co-crystallized ligand. Moreover, another metric is used to evaluate the results such as the PersScore that is a clue of H-bonding formed between the ligand and the target during the simulations. In general, maintaining 60% of the total H-bonds (PersScore>0.6) is considered a good sign of stable interaction. The linear combination of these two scores provides a third score, the CompScore which is calculated as follows:

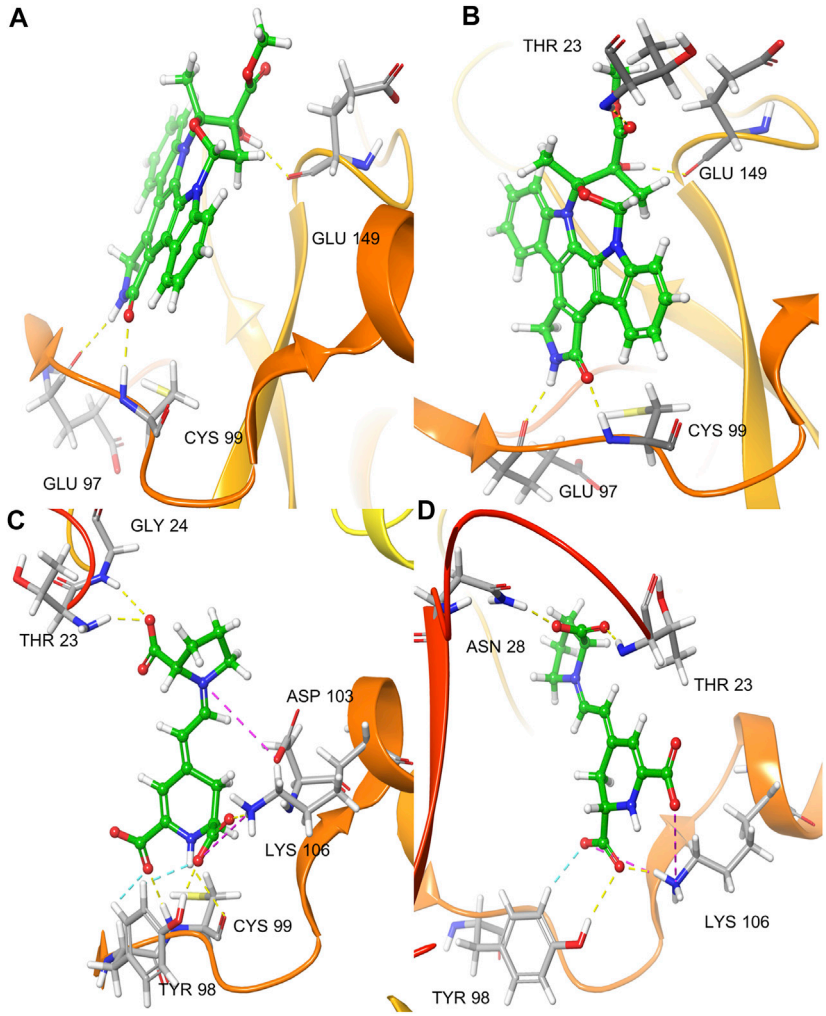

FIGURE 3 | IFD pose of K252a in the inactive Chain A **(A)**; IFD pose of K252a in the active Chain B **(B)**; IFD pose of Indicaxanthin in the inactive Chain A **(C)**; IFD pose of Indicaxanthin in the active Chain B **(D)**. H-bonds interactions are represented in yellow dashes, aromatic H-bonds are represented in light blue dashes, the salt bridges in purple dashes.

CompScore = PoseScore—5 × PersScore.

Lower values of this equate indicate more stable complexes.

The simulation performed on K252a pose in Chain A showed a PoseScore of 1.206. The PersScore showed that the hydrogen bonds were kept for 81% of the simulation time. The interactions by the lactam ring were confirmed to stabilize the molecule, in particular, we observed for 98.2% of the simulation time, interactions between the amine group and Glu97, for 97.3% of the simulation time interactions between the carbonyl oxygen and Cys99. The H-bond interaction between the hydroxyl group and Glu149 was kept for 48.2% of the simulation time. The CompScore of −2.852 confirmed that the starting molecule pose is stable into the active site.

The results of the K252a pose in Chain B showed a PoseScore of 0.909, the PersScore proves that for 63.9% of the simulation time, the H-bonds were maintained. As in Chain A, the interactions by the lactam ring were confirmed, in particular, 100% of the simulation time, the interaction between the carbonyl oxygen and Cys99, and 98.2% of the simulation time interaction between the amine group and Glu97. The same for H-bond interaction between the hydroxyl group and Glu149 was kept for 57.3% of the time. The linear combination of PoseScore and PersScore, CompScore, was −2.284. The result obtained confirmed the accuracy of the identified IFD poses. (**Table 1**).

Successively the BPDM simulations have been performed at the binding site in Chain A, the best pose of Indicaxanthin reached a steady PoseScore of 3.133, considered stable, while PersScore showed that the hydrogen bonds identified at the start of the metadynamics run were kept for 12% of the averaged time. In particular, the H-bond between carboxyl oxygen and Cys99. The CompScore value was 2.533.

At the binding site in chain B, the averaged RMSD of Indicaxanthin reached a steady PoseScore of 4.631, PersScore of 0.04. In particular, three H-bond were recorded during the ten replicas. H-bond interaction between the carboxyl group of

pyrrolidinium moiety and Thr23 was kept for 11.8% of the simulation time, the same group showed an ulterior H-bond with Asn28 for 7.3% of the simulation time. The last interaction was between one of the carboxyl groups of pyrimidine and Lys106 for 2.7% of the simulation time. This interaction was supported by salt bridges between the two inferior carboxyl groups and Lys106. The last score, CompScore was 4.441. The BPMD analysis confirmed that the poses obtained from the IFD are valuable for Indicaxanthin and they can be used to perform a time-dependent study which could give more insights about the binding of Indicaxanthin. The BPDM results of Indicaxanthin into the allosteric binding site give unstable values suggesting that Indicaxanthin is not a stable binder of the allosteric site. However, to gain more insights, we decided to perform also the time-dependent simulation of this latter complex. (**Table 1**).

Molecular Dynamics Simulations

The running of dynamics simulations of protein-ligand complexes over time could be considered the major accuracy step in computer-assisted drug design. In this study, unbiased molecular dynamics simulations have been performed to explain the stability of Indicaxanthin as an inhibitor against the two forms of hIKKβ, active and inactive, and allosteric inhibitor of the inactive form. Additionally, we tried to understand if the protein target undergoes conformational alteration after interacting with Indicaxanthin. Therefore, starting from the previous IFD poses which BPMD analysis showed to be accurate and reliable except for Indicaxanthin in the allosteric site, five systems have been generated and submitted each for 100 ns in MD simulations (Chain A-Indicaxanthin, Chain B-Indicaxanthin, Chain A allosteric site-Indicaxanthin, Chain A-K252a, Chain B-K252a). The various analysis such as the root mean square deviation (RMSD), the root mean square fluctuation (RMSF), number, and types of protein-ligand contacts have been carried to have a more detailed analysis of Indicaxanthin-target complexes compared to the co-crystallized ligand.

Stability Analysis

The RMSD has been selected as a criterion to evaluate the dynamic stability of ligand-bound systems. The first systems took into consideration are Chain A and Chain B bound to the co-crystallized inhibitor K252a. We decided to perform these analyses to compare the behavior of Indicaxanthin with respect to an inhibitor with experimental evidence in terms of binding interactions. All protein frames are first aligned on the reference frame backbone, and then the RMSD is calculated based on the atom selection, in these cases on the Cα. For these complexes, the RMSD values of protein's Cα atoms and ligand are reported in **Figure 5**. The Ligand RMSD indicates how stable the ligand is with respect to the protein and its binding pocket. This plot shows the RMSD of a ligand when the protein-ligand complex is first aligned on the protein backbone of the reference and then the RMSD of the ligand heavy atoms is measured. If the values observed are significantly larger than the RMSD of the protein, then it is likely that the ligand has diffused away from its initial binding site. The Chain A-K252a system reached equilibrium quickly and fluctuated around the average value of 3 Å, the low average value of ligand RMSD = 1.8 Å indicated strong stability of K252a in the binding pocket as expected due to the low number of rotatable bonds and the eight fused rings. The Chain B-K252a behavior is slightly different. The system reached equilibrium after ~10 ns and the fluctuation of the protein is higher than the previous system analyzed (~4.3 Å). The same evidence is reported for the average ligand RMSD that is higher (3.72 Å). This first analysis showed that the phosphorylation of the serine residues in the active form (Chain B) could confer more flexibility to the binding pocket in the KD, as confirmed by the higher fluctuations of K252a despite the rigid structure.

For the Chain A-Indicaxanthin and Chain B-Indicaxanthin systems, the RMSD values of protein's Cα atoms and ligand are reported in **Figure 6** showing the behavior of these along the 100 ns of simulations. The Chain A-Indicaxanthin complex, after fluctuating in the first 10 ns, between RMSD values of 2-6Å, reached the equilibrium maintaining the fluctuation around the average value of 3.46Å. But it is worthy to note that ligand RMSD undergoes a biphasic behavior. In fact, in the first 38ns of simulation, the average ligand RMSD value is 6.0 Å, while in the rest of the simulation this value grows about 12 Å, stabilizing around ~17.5 Å but the ligand continues to occupy the binding pocket acting as a lid. The behavior of the Chain B-Indicaxanthin complex is quite stable if compared to the previously discussed. The system reached rapidly the equilibrium around 7 ns and maintained stable fluctuations along the rest of the simulation with an average RMSD = 5.1 Å. The ligand RMSD, unless a quick cliff around 36–37.5 ns, maintains an average value = 3.2 Å that is similar to the behavior of the co-crystallized K252a. This value is interesting considering the less rigid structure of Indicaxanthin and explaining the good stability of this compound in the KD binding pocket.

For the complex of the Indicaxanthin docked into the allosteric site of Chain A, the protein maintains a stable behavior for the whole duration of simulation with an average RMSD value = 3.5 Å. In contrast, the ligand maintains its stability around the allosteric pocket for about 23 ns, but this stability is not maintained over time, and around 40 ns, Indicaxanthin flies out from the allosteric pocket until the end of the simulation. We repeated the simulations two times: in the second simulation the ligand flies out in the first nanoseconds, and in the third, it remains in the allosteric pocket for about 15 ns to fly out in the next nanoseconds (**Supplementary Material**). These last findings confirmed the BPDM results in which the unstable binding of Indicaxanthin in the allosteric pocket was retrieved.

Residues Mobility Analysis

To examine the structural flexibility effect of K252a and Indicaxanthin upon the Chain A, Chain B and the effect of Indicaxanthin when bound to the allosteric site per residue, the main chain average RMSF of the complexes have been calculated for the entire 100ns of simulation. The residue-wise fluctuation of the complexes was plotted and presented in **Figure 7**. The plot has been coupled according to the chain bound to K252a and Indicaxanthin, respectively, to compare the differences due to different ligands. As reported, the RMSF plot of Chain A is quite

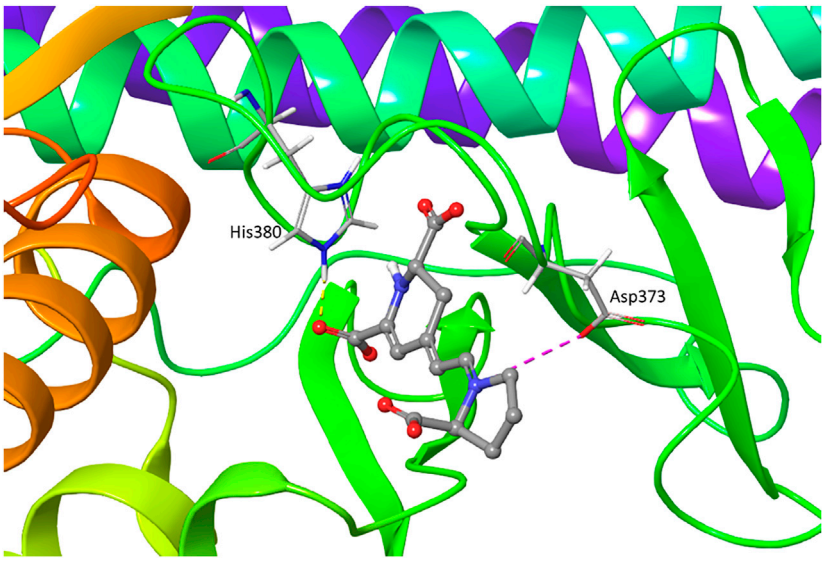

FIGURE 4 | IFD pose of Indicaxanthin in the inactive Chain A allosteric binding site. H-bonds interactions are represented in yellow dashes, the salt bridges in purple dashes.

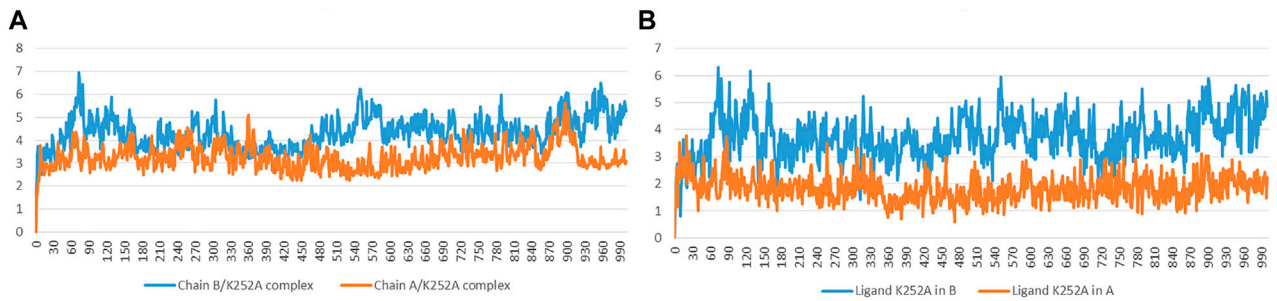

FIGURE 5 | Time evolution of the RMSD (Å) values of backbone atoms **(A)** and ligand K252a **(B)** in the active form (Chain B) and the inactive form (Chain A).

comparable for the residues of the active site with ΔRMSF <1 Å. The same could be observed for Chain B in which the ΔRMSF <0.5 Å. The major fluctuations happen in the allosteric pocket where the presence of Indicaxanthin determines an ΔRMSF>5 Å, in particular in the loop Thr368-Lys386. From this RMSF analysis, it can be concluded that the binding of Indicaxanthin determines similar fluctuations of the Chain A and Chain B backbone atoms with respect to K252a, in particular in the residues involved in the binding pocket. Contrariwise, the RMSF of the allosteric pocket is highly influenced by the presence of the Indicaxanthin.

Protein-Ligands Contact Analysis

Estimation of protein interactions provides a measure of interaction power between the ligands and the target protein. Protein interactions with the ligand can be monitored throughout the simulations. These interactions can be categorized by type and summarized, as shown in the plot represented in **Figure 8**. Protein-ligand interactions (or "contacts"") are categorized into four types: Hydrogen Bonds, Hydrophobic, Ionic, and Water Bridges. The stacked bar charts are normalized throughout the trajectory: a value of 1.0 suggests that 100% of the simulation time the specific interaction is maintained. A timeline representation of the interactions and contacts (H-bonds, Hydrophobic, Ionic, Water bridges) summarize the total number of specific contacts the protein makes with the ligand throughout the simulation. The bottom panel of **Figure 8** shows which residues interact with the ligand in each trajectory frame. Some residues make more than one specific contact with the ligand, which is represented by a darker shade of orange, according to the scale to the right of the plot.

Analyzing the trajectories of Chain A and Chain B with the co-crystallized ligand K252a, it is interesting to note that the residues involved in the interactions are variable both in terms of the type of contacts and in the time of interactions. As reported in **Figure 8**, K252a has four key residues involved: Met96, Glu97, Cys99, and Ile165 in both active and inactive forms. The H-bonds with Glu97 and Cys99 stable all 100ns simulations long.

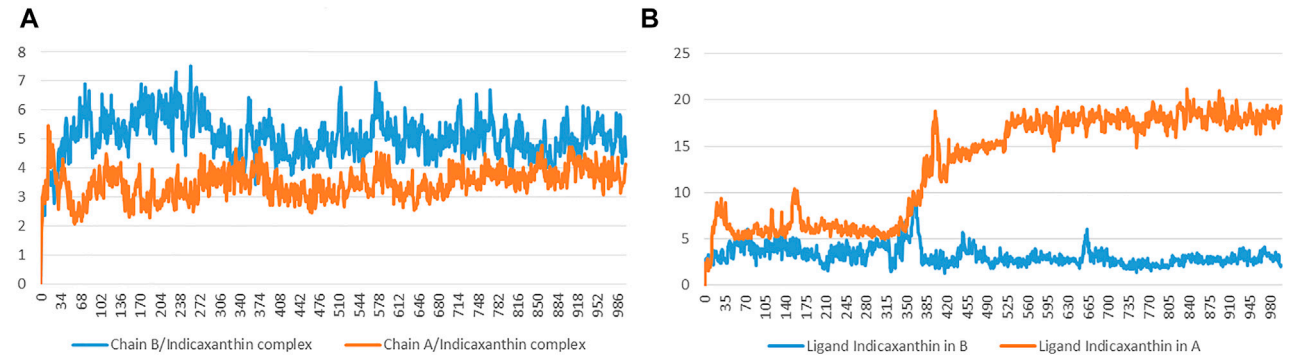

FIGURE 6 | Time evolution of the RMSD (Å) values of backbone atoms **(A)** and ligand Indicaxanthin **(B)** in the active form (Chain B) and the inactive form (Chain A).

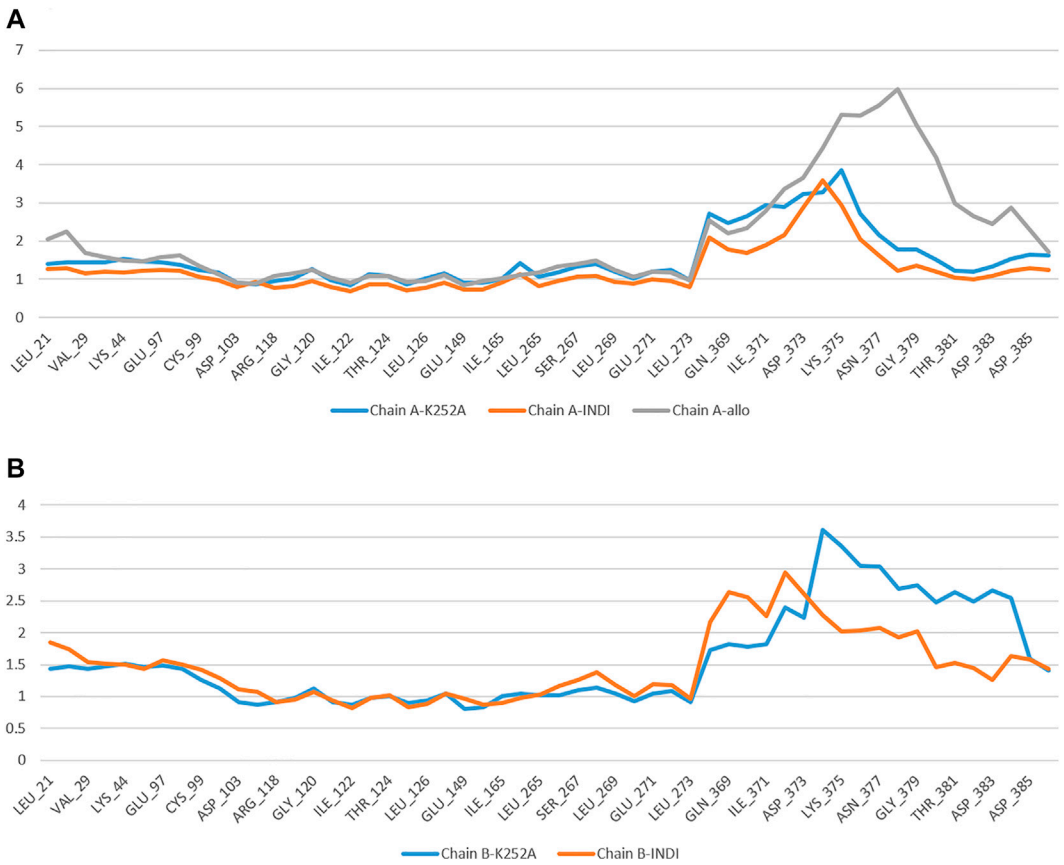

FIGURE 7 | The comparative RMSF values for the complexes of backbone atoms of Chain A **(A)** and Chain B **(B)** bound to K252a, Indicaxanthin, and of the allosteric pocket.

Hydrophobic contacts of Ile165 are maintained for the major part of the simulations, while hydrophobic contacts with Met96 are involved in both simulations but just for a little fraction of time. The differences in the two complexes regard the less interaction time of the H-bond with Glu149 in Chain B. In Chain A, an H-Bond with Gln175 is observed during the simulation in a discontinuous fashion, while in Chain B, Hydrophobic contacts are observed with Phe26 for about 50% of the simulation time. Other interactions are involved in both complexes such as with Leu21, Thr23, Val29, Ala42, Tyr98, Val152.

The behavior of Indicaxanthin, when bound to the two forms of IKK, is rather different in terms of interactions, but above in terms of residence in the binding pocket. As previously commented, in Chain A after ~38 ns

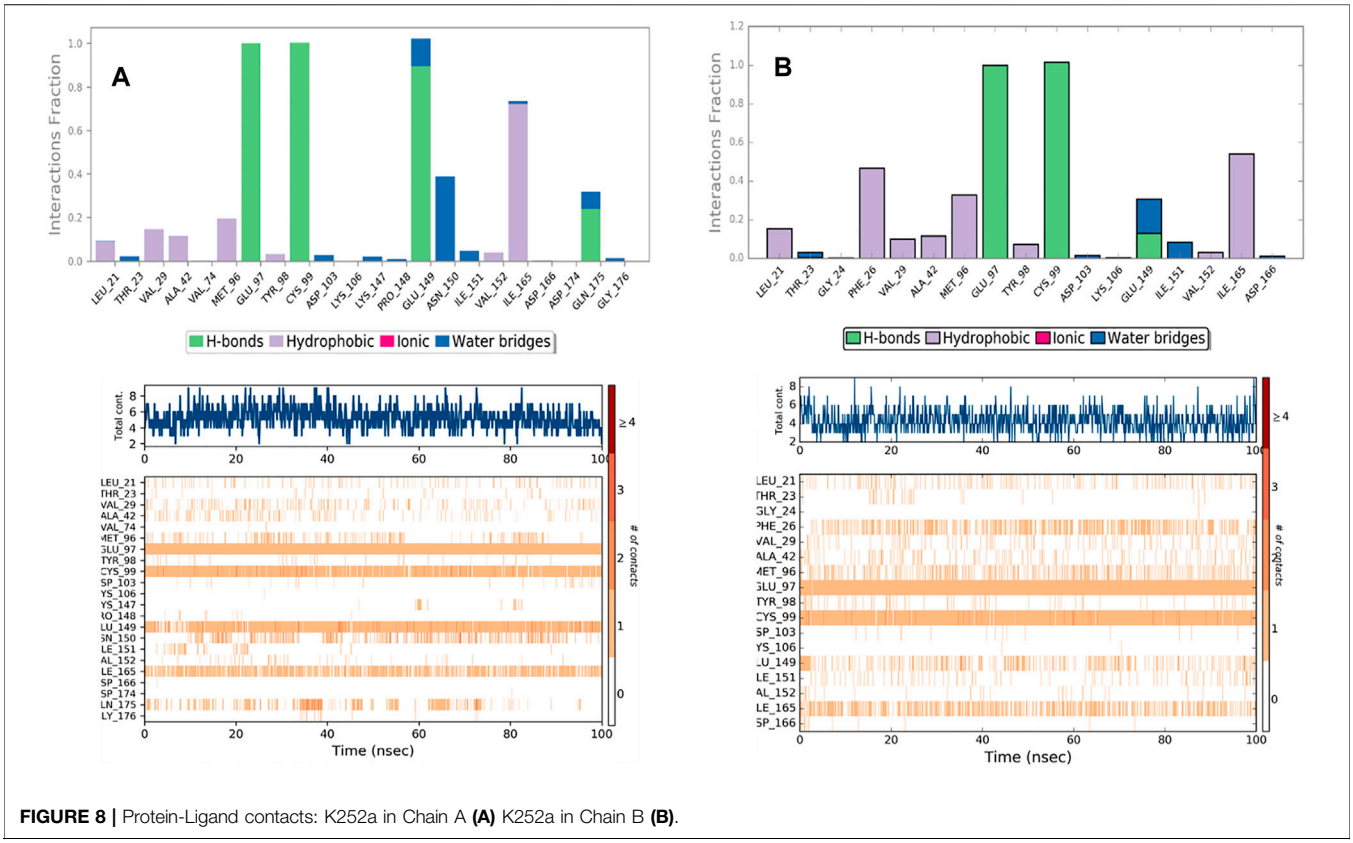

FIGURE 8 | Protein-Ligand contacts: K252a in Chain A **(A)** K252a in Chain B **(B)**.

Indicaxanthin moves from the deep pocket but remains over it by interacting with H-bonds and ionic interaction with Arg427, Arg575, Arg579, Arg582 acting as a lid. In the first 40ns, the interactions of Indicaxanthin are both ionic and H-bond interactions involving the residues of the pocket such as residues 20–24 and 103–106. Indicaxanthin remains confined into the binding pocket for all the simulation time when Chain B is considered. Even though the residues involved in the protein-ligand interactions are different from those involved in the interaction with K252a. Indicaxanthin interacts for the major of time with Thr23, Asn28, Arg47, and Lys106 through H-bonds, but a key role for the binding stability is due to the ionic interaction with Asp103 and Lys 106 (**Figure 9**).

The stability of the Indicaxanthin's binding is also mediated by several water bridges that are hydrogen-bonded protein-ligand interactions mediated by a water molecule. The hydrogen-bond geometry is slightly relaxed from the standard H-bond definition. The current geometric criteria for a protein-water or water-ligand H-bond are a distance of 2.8 Å between the donor and acceptor atoms (D—H···A); a donor angle of 110° between the donor-hydrogen-acceptor atoms (D—H···A); and an acceptor angle of 90° between the hydrogen-acceptor-bonded atoms (H···A—X).

Due to the evidence that during the simulation of Indicaxanthin into the allosteric pocket of Chain A, the ligand flies out after about 40 ns of simulation time, we do not comment on the evolution of the interaction in this analysis. Likely, Indicaxanthin does not act as an allosteric inhibitor of IKK.

MM-GBSA and Binding Free Energy Analysis

To understand the biophysical basis of molecular recognition of Indicaxanthin with targets (the inactive form of IKK, and active form of IKK), a molecular mechanics-generalized Born surface area MM-GBSA approach was used. As a comparative analysis, we performed the binding free energy analysis for the K252a complexes. It provides different individual components such as ΔG_{vdW}, ΔG_{Coul}, ΔG_{Hbond}, ΔG_{Lipo}. The conformational entropy change $-T\Delta S$ can be computed by normal-mode analysis on a set of conformational snapshots taken from MD simulations, but many authors have reported that the lack of the evaluation of the entropy is not critical for calculating the MM-GBSA (or MM-PBSA) free energies for similar systems (Hou and Yu, 2007; Massova and Kollman, 2000; Wang and Kollman, 2001). For these reasons, we did not carry out $-T\Delta S$ calculation in our study. For binding free calculation of Indicaxanthin and K252a/protein systems, 101 frames from 100 ns (each 1 ns) were retrieved to calculate ΔGbind and individual contributions. A summary of binding components in the binding free energy is reported in **Table 2**. Furthermore, in **Figure 10** it is reported the free energy landscape of Indicaxanthin in Chains A and B. To get a better view of which energy terms have more impact on the inhibitory potency, these individual energy components were compared. As expected from previous analysis of the MD trajectories, Indicaxanthin showed a higher binding affinity for the Chain B concerning Chain A (ΔG_{bind} =

TABLE 2 | Predicted MM-GBSA free energies (kcal/mol) and individual energy terms of the Indicaxanthin-target complexes and K252a-target complexes.

	ΔG_{bind}	ΔG_{Coul}	ΔG_{Hbond}	ΔG_{Lipo}	ΔG_{Solv}	ΔG_{vdW}
Indi/Chain B	−22.2 ± 4.3	67.5 ± 11.5	−3.9 ± 1.0	−4.5 ± 0.8	−59.2 ± 11.2	−24.6 ± 4.3
Indi/Chain A	−20.7 ± 4.7	10.6 ± 30.3	−4.3 ± 1.5	−3.4 ± 1.3	−3.2 ± 0.28	−22.3 ± 5.4
K252a/Chain B	−72.02 ± 4.1	−16.78 ± 3.0	−1.33 ± 0.2	−20.62 ± 1.3	24.2 ± 2.1	−57.6 ± 2.5
K252a/Chain A	−74.45 ± 4.0	−22.42 ± 3.3	−1.68 ± 0.3	−18.67 ± 0.3	26.6 ± 1.9	−57.96 ± 2.9

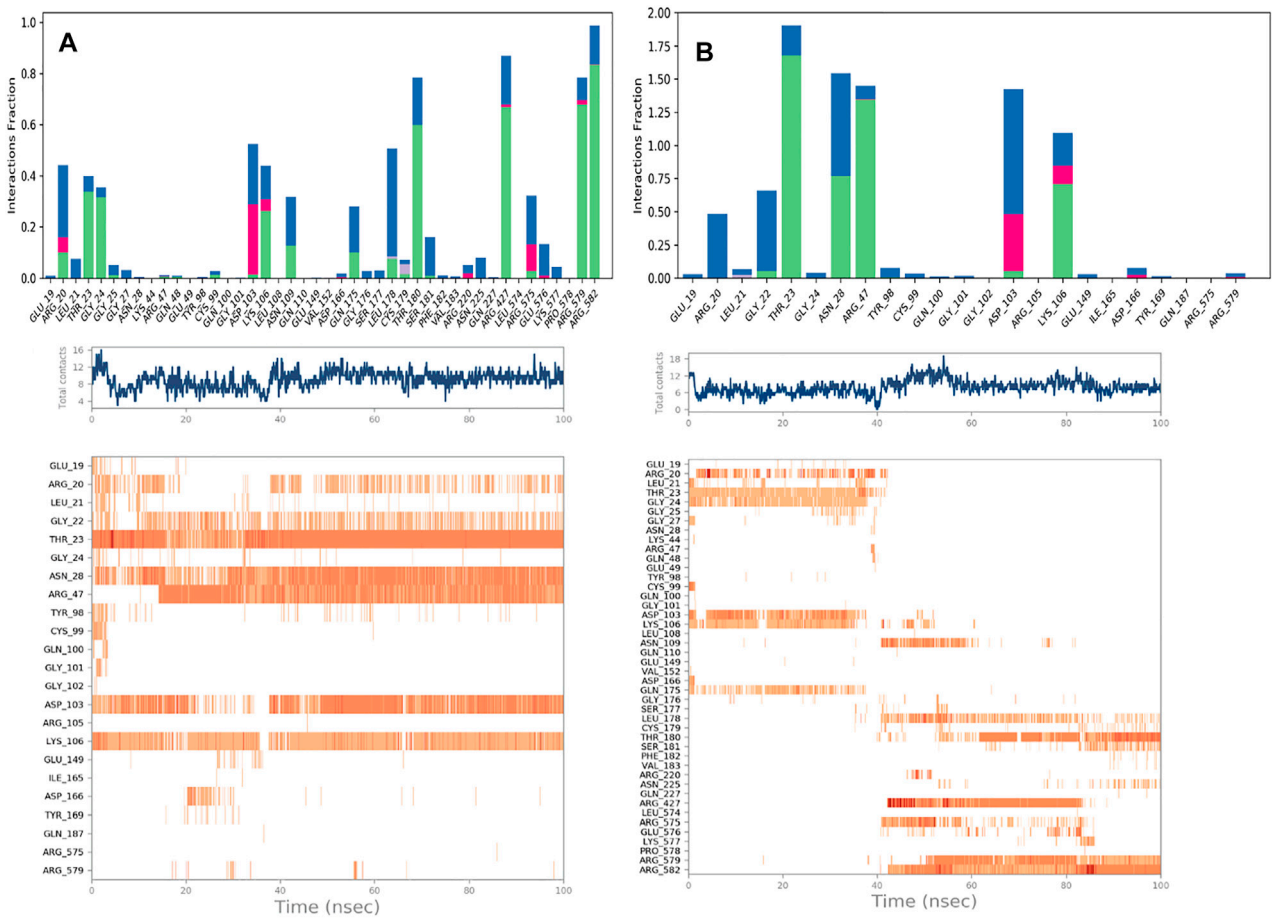

FIGURE 9 | Protein-Ligand contacts: Indicaxantin in Chain A **(A)** Indicaxanthin in Chain B **(B)**. Legenda is the same as **Figure 8**.

−22.2 ± 4.3 kcal/mol, ΔG_{bind} = −20.7 ± 4.7 kcal/mol, respectively) that it could be justified by the shifting of Indicaxanthin towards the mouth of the binding pocket. It can be seen that ΔG_{vdW} has the major favorable contribution to the total free energy in both complexes. The same consideration could be stated for ΔG_{Hbond} and ΔG_{Lipo}, but there is no great difference among these values for different complexes even though it has minor weight on the total free energy. ΔG_{Hbond} has a major impact in Chain A, while ΔG_{Lipo} has a major impact in Chain B. The ΔG_{Coul} has the same effect in the complexes with a negative contribution to the global free energy which is partially balanced by the ΔG_{Solv}. As previously stated, Indicaxanthin has been demonstrated to inhibit 50% cell proliferation at 100 μM (Allegra et al., 2018), while K252a showed to be an efficient inhibitor of IKK at IC_{50} = 0.09–018 μM (Sadler et al., 2004). Comparing the binding free energy values of Indicaxanthin and K252a, they are consistent with the experimental evidence (K252a ΔG_{bind} = −72.02 ± 4.1 kcal/mol for Chain B, and ΔG_{bind} = −74.45 ± 4.0 for Chain A) (**Table 2**).

CONCLUSION

The stability of Indicaxanthin-hIKKβ complexes compared to K252a, a co-crystallized inhibitor, was assessed by using Induced fit docking, binding pose metadynamics, and molecular

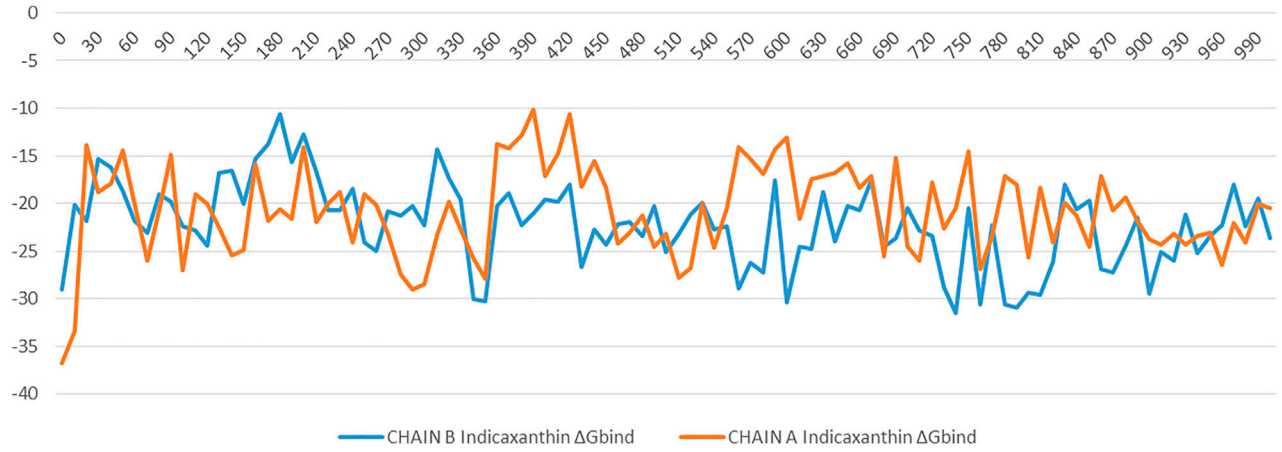

FIGURE 10 | The binding energy (ΔG expressed in kcal/mol) landscape of Indicacaxanthin bound to Chain A and Chain B.

dynamics. Finally, MM-GBSA free energy calculations have been performed to establish what form of IKK Indicaxanthin prefers. Induced fit docking results showed that the binding of Indicaxanthin with the active form, the inactive form, and the allosteric site of hIKKβ showed has the strongest stability with the active form. MD trajectories analysis (RMSD, RMSF, and protein-ligand contacts number and along the time) also showed that Indicaxanthin enhanced the stability of the active form at the same level of the known inhibitor K252a. The stability of the inactive form complex with Indicaxanthin is quite similar but it did not reach the quality of the active form. Contrariwise, even though for 40 ns over 100 nsIndicaxanthin can bind the allosteric pocket, it should not be considered as an allosteric inhibitor of hIKKβ.

As a whole, this work shows that Indicaxanthin is able, *in silico*, to inhibit the active form of the hIKKβ and adds novel mechanistic insights on its recently discovered ability to impair NF-κB signaling in melanoma A375 cells. Along these lines, present results further suggest the molecule as a useful nutraceutical tool in combo-therapy i.e., with other therapeutical agents targeting different checkpoints of melanoma development.

The currently demonstrated ability of Indicaxanthin to inhibit the active form of hIKKβ may, then, suggest the phytochemical as a new lead compound to synthesize novel and more potent IKKβ inhibitors for the treatment of cancer and inflammation-related conditions.

DATA AVAILABILITY STATEMENT

The raw data supporting the conclusions of this article will be made available by the authors, without undue reservation.

AUTHOR CONTRIBUTIONS

MA and MT designed experiments. MT and GC carried out the experiments. MT and GC analyzed experimental results. MT and GC analyzed and interpreted the data. MA, AMA, LT, AA, and MT drafted and revised the manuscript. All authors contributed to the article and approved the submitted version.

SUPPLEMENTARY MATERIAL

The Supplementary Material for this article can be found online at: https://www.frontiersin.org/articles/10.3389/fphar.2021.701568/full#supplementary-material

REFERENCES

Allegra, M., Carletti, F., Gambino, G., Tutone, M., Attanzio, A., Tesoriere, L., et al. (2015). Indicaxanthin from Opuntia Ficus-Indica Crosses the Blood-Brain Barrier and Modulates Neuronal Bioelectric Activity in Rat hippocampus at Dietary-Consistent Amounts. *J. Agric. Food Chem.* 63, 7353–7360. doi:10.1021/acs.jafc.5b02612

Allegra, M., De Cicco, P., Ercolano, G., Attanzio, A., Busà, R., Cirino, G., et al. (2018). Indicaxanthin from Opuntia Ficus Indica (L. Mill) Impairs Melanoma Cell Proliferation, Invasiveness, and Tumor Progression. *Phytomedicine* 50, 19–24. doi:10.1016/j.phymed.2018.09.171

Allegra, M., Tutone, M., Tesoriere, L., Almerico, A. M., Culletta, G., Livrea, M. A., et al. (2019). Indicaxanthin, a Multi-Target Natural Compound from Opuntia Ficus-Indica Fruit: From its Poly-Pharmacological Effects to Biochemical Mechanisms and Molecular Modelling Studies. *Eur. J. Med. Chem.* 179, 753–764. doi:10.1016/j.ejmech.2019.07.006

Amiri, K. I., and Richmond, A. (2005). Role of Nuclear Factor-Kappa B in Melanoma. *Cancer Metastasis Rev.* 24, 301–313. doi:10.1007/s10555-005-1579-7

Amschler, K., Schön, M. P., Pletz, N., Wallbrecht, K., Erpenbeck, L., and Schön, M. (2010). NF-kappaB Inhibition through Proteasome Inhibition or IKKbeta Blockade Increases the Susceptibility of Melanoma Cells to Cytostatic Treatment through Distinct Pathways. *J. Invest. Dermatol.* 130, 1073–1086. doi:10.1038/jid.2009.365

Belhadj Slimen, I., Najar, T., and Abderrabba, M. (2017). Chemical and Antioxidant Properties of Betalains. *J. Agric. Food Chem.* 65, 675–689. doi:10.1021/acs.jafc.6b04208

Ben-Neriah, Y., and Karin, M. (2011). Inflammation Meets Cancer, with NF-κB as the Matchmaker. *Nat. Immunol.* 12, 715–723. doi:10.1038/ni.2060

Bowers, K. J., Chow, D. E., Xu, H., Dror, R. O., Eastwood, M. P., Gregersen, B. A., et al. (2006). "Scalable Algorithms for Molecular Dynamics Simulations on Commodity Clusters," in SC '06: Proceedings of the 2006 ACM/IEEE Conference on Supercomputing (Institute of Electrical and Electronics Engineers (IEEE)), 43. doi:10.1109/sc.2006.54

Clark, A. J., Tiwary, P., Borrelli, K., Feng, S., Miller, E. B., Abel, R., et al. (2016). Prediction of Protein-Ligand Binding Poses via a Combination of Induced Fit Docking and Metadynamics Simulations. *J. Chem. Theor. Comput.* 12, 2990–2998. doi:10.1021/acs.jctc.6b00201

Dhawan, P., and Richmond, A. (2002). A Novel NF-Kappa B-Inducing Kinase-MAPK Signaling Pathway Up-Regulates NF-Kappa B Activity in Melanoma Cells. *J. Biol. Chem.* 277, 7920–7928. doi:10.1074/jbc.M112210200

Genheden, S., and Ryde, U. (2015). The MM/PBSA and MM/GBSA Methods to Estimate Ligand-Binding Affinities. *Expert Opin. Drug Discov.* 10, 449–461. doi:10.1517/17460441.2015.1032936

Guedes, I. A., Freitas, R. H., Cordeiro, N. M., do Nascimento, T. S., Valerio, T. S., Fernandes, P. D., et al. (2016). LASSBio-1829 Hydrochloride: Development of a New Orally Active N-Acylhydrazone IKK2 Inhibitor with Anti-inflammatory Properties. *Chem. Med. Chem.* 11, 234–244. doi:10.1002/cmdc.201500266

Jacobson, M. P., Pincus, D. L., Rapp, C. S., Day, T. J., Honig, B., Shaw, D. E., et al. (2004). A Hierarchical Approach to All-Atom Protein Loop Prediction. *Proteins* 55, 351–367. doi:10.1002/prot.10613

Jorgensen, W. L., Maxwell, D. S., and Tirado-Rives, J. (1996). Development and Testing of the OPLS All-Atom Force Field on Conformational Energetics and Properties of Organic Liquids. *J. Am. Chem. Soc.* 118, 11225–11236. doi:10.1021/ja9621760

Leung, C. H., Chan, D. S., Li, Y. W., Fong, W. F., and Ma, D. L. (2013). Hit Identification of IKKβNatural Product Inhibitor. *BMC Pharmacol. Toxicol.* 14, 3. doi:10.1186/2050-6511-14-3

Liu, H., Liang, H., Meng, H., Deng, X., Zhang, X., and Lai, L. (2018). A Novel Allosteric Inhibitor that Prevents IKKβActivation. *Medchemcomm* 9, 239–243. doi:10.1039/c7md00599g

Liu, S., Misquitta, Y. R., Olland, A., Johnson, M. A., Kelleher, K. S., Kriz, R., et al. (2013). Crystal Structure of a Human IκB KinaseβAsymmetric Dimer. *J. Biol. Chem.* 288, 22758–22767. doi:10.1074/jbc.M113.482596

Moarbess, G., Guichou, J. F., Paniagua-Gayraud, S., Chouchou, A., Marcadet, O., Leroy, F., et al. (2016). New IKK Inhibitors: Synthesis of New Imidazo[1,2-A] quinoxaline Derivatives Using Microwave Assistance and Biological Evaluation as IKK Inhibitors. *Eur. J. Med. Chem.* 115, 268–274. doi:10.1016/j.ejmech.2016.03.006

Prescott, J., and Cook, S. (2018). Targeting IKKβin Cancer: Challenges and Opportunities for the Therapeutic Utilisation of IKKβInhibitors. *Cells* 7, 115. doi:10.3390/cells7090115

Sadler, T. M., Achilleos, M., Ragunathan, S., Pitkin, A., LaRocque, J., Morin, J., et al. (2004). Development and Comparison of Two Nonradioactive Kinase Assays for I Kappa B Kinase. *Anal. Biochem.* 326, 106–113. doi:10.1016/j.ab.2003.11.021

Schrödinger (2017). *Schrödinger*. New York: Schrödinger Release, 2017–2021.

Sherman, W., Day, T., Jacobson, M. P., Friesner, R. A., and Farid, R. (2006). Novel Procedure for Modeling Ligand/receptor Induced Fit Effects. *J. Med. Chem.* 49, 534–553. doi:10.1021/jm050540c

Staudt, L. M. (2010). Oncogenic Activation of NF-kappaB. *Cold Spring Harb. Perspect. Biol.* 2, a000109. doi:10.1101/cshperspect.a000109

Taniguchi, K., and Karin, M. (2018). NF-κB, Inflammation, Immunity and Cancer: Coming of Age. *Nat. Rev. Immunol.* 18, 309–324. doi:10.1038/nri.2017.142

Tesoriere, L., Allegra, M., Butera, D., and Livrea, M. A. (2004). Absorption, Excretion, and Distribution of Dietary Antioxidant Betalains in LDLs: Potential Health Effects of Betalains in Humans. *Am. J. Clin. Nutr.* 80, 941–945. doi:10.1093/ajcn/80.4.941

Tutone, M., Pibiri, I., Lentini, L., Pace, A., and Almerico, A. M. (2019). Deciphering the Nonsense Readthrough Mechanism of Action of Ataluren: An In Silico Compared Study. *ACS Med. Chem. Lett.* 10, 522–527. doi:10.1021/acsmedchemlett.8b00558

Van Herck, Y., Antoranz, A., Andhari, M. D., Milli, G., Bechter, O., De Smet, F., et al. (2021). Multiplexed Immunohistochemistry and Digital Pathology as the Foundation for Next-Generation Pathology in Melanoma: Methodological Comparison and Future Clinical Applications. *Front. Oncol.* 11, 636681. doi:10.3389/fonc.2021.636681

Xu, G., Lo, Y. C., Li, Q., Napolitano, G., Wu, X., Jiang, X., et al. (2011). Crystal Structure of Inhibitor ofκB Kinaseβ. *Nature* 472, 325–330. doi:10.1038/nature09853

Yang, J., and Richmond, A. (2001). Constitutive IkappaB Kinase Activity Correlates with Nuclear Factor-kappaB Activation in Human Melanoma Cells. *Cancer Res.* 61, 4901–4909.

Zhang, Q., Lenardo, D., and Baltimore, D. (2017). 30 Years of NF-κB: A Blossoming of Relevance to Human Pathobiologyy. *Cell* 168, 37–57. doi:10.1016/j.cell.2016.12.012

Conflict of Interest: The authors declare that the research was conducted in the absence of any commercial or financial relationships that could be construed as a potential conflict of interest.

Publisher's Note: All claims expressed in this article are solely those of the authors and do not necessarily represent those of their affiliated organizations, or those of the publisher, the editors and the reviewers. Any product that may be evaluated in this article, or claim that may be made by its manufacturer, is not guaranteed or endorsed by the publisher.

frontiers in Pharmacology

ORIGINAL RESEARCH
published: 20 September 2021
doi: 10.3389/fphar.2021.698375

Evaluation of the Anticancer Properties of Geranyl Isovalerate, an Active Ingredient of *Argyreia nervosa* Extract in Colorectal Cancer Cells

Fayyaz Rasool[1], *Deepu Sharma*[1], *P. Shanmukha Anand*[2], *SKJ Magani*[1*†] and *Srinivasan Tantravahi*[3*†]

[1]Department of Life Sciences, School of Natural Sciences, Shiv Nadar University, Greater Noida, India, [2]Department of Biotechnology, GITAM Institute of Science, Gandhi Institute of Technology and Management (GITAM) Deemed to be University, Visakhapatnam, India, [3]Department of Botany, Indira Gandhi National Tribal University, Amarkantak, India

Chemotherapy is a general treatment procedure for cancer. The diversity in cancer incidence and the failure of therapy due to chemoresistance lead to increased cancer-related deaths. Therefore, new drugs with fewer secondary complications targeting diverse pathways are the need of the hour. Geranyl isovalerate (GIV), one of the active ingredients of ethyl acetate fraction of *Argyreia nervosa* is routinely used as a food flavoring agent. In this study, we found that GIV also exhibits anticancer activity when tested against the HCT116 cell line. It influenced the viability of the cells in a dose- and time-dependent manner. We examined whether GIV could induce oxidative stress and affect the mitochondrial membrane potential, thereby leading to apoptosis induction. Moreover, GIV could suppress the expression of antiapoptotic genes, such as BCl2 and PARP, and induce the expression of proapoptotic genes, such as Caspase 3 and 9. This is the first study demonstrating the anticancer activity of GIV and providing evidence for its mechanism of action. In conclusion, this study proposes GIV as a potential lead or supplementary molecule in treating and preventing colorectal cancer (CRC). Based on our findings, we conclude that GIV may be a viable lead or supplementary molecule for treating and preventing CRC.

Keywords: geranyl isovalerate, anticancer activity, HCT116 cell line, apoptosis, membrane potential

OPEN ACCESS

Edited by:
Rajeev K. Singla,
Sichuan University, China

Reviewed by:
Manoj Kumar Sabnani,
Alloy Therapeutics, Inc., United States
Shikha Joon,
Sichuan University, China

***Correspondence:**
SKJ Magani
jayadevmsk@snu.edu.in
Srinivasan Tantravahi
srinivasan@igntu.ac.in

[†]*These authors have contributed equally to this work*

Specialty section:
This article was submitted to Ethnopharmacology, a section of the journal Frontiers in Pharmacology

Received: *21 April 2021*
Accepted: *24 August 2021*
Published: *20 September 2021*

Citation:
Rasool F, Sharma D, Anand PS, Magani SKJ and Tantravahi S (2021) Evaluation of the Anticancer Properties of Geranyl Isovalerate, an Active Ingredient of Argyreia nervosa *Extract in Colorectal Cancer Cells. Front. Pharmacol. 12:698375. doi: 10.3389/fphar.2021.698375*

INTRODUCTION

Cancer is the second major cause of death worldwide after cardiovascular disease. The number of deaths due to cancer has been estimated to increase to 14.6 million by 2035. Colorectal cancer (CRC) ranks as the second most diagnosed cancer in women and the third most diagnosed cancer in men. However, deaths due to CRC in women are approximately 25% lower than in men (Dekker et al., 2019). CRC is the fourth most fatal malignancy worldwide, accounting for almost 0.9 Million deaths per year. Risk factors that can increase the incidence of CRC include inflammatory bowel disease, obesity, large intake of processed foods with high calories, and a lack of exercise leading to type II diabetes (Center et al., 2009). Chemotherapy is a general treatment procedure for any cancer, including CRC. The molecular diversity in cancer incidence and progression along with increased chemoresistance demands novel therapeutics for cancer. Phytochemicals have been a prominent source of anticancer agents that are used in clinics today. Traditional medicinal herbs are regarded as

one of the major source of pharmacologically active compounds (Fridlender et al., 2015). Some of the plant-derived therapeutic molecules used in present-day clinics include vinblastine, vincristine, topotecan, irinotecan, etoposide, and paclitaxel (Cragg and Newman, 2005). The importance of biologically active phytochemicals and natural compounds drew the attention of scientists, and it has been reported that in 2014 alone 3,26,000 new natural compounds had been discovered (Banerjee et al., 2015). Out of these 3,26,000 compounds, only around 5% have been found to be effective. Therefore, investigation for new drugs targeting diverse pathways plays an important role in the success of cancer chemotherapy.

Argyreia nervosa (Burm.f.) Bojer, a popular herbal high (Paulke et al., 2014), is known to exhibit multiple medicinal properties, such as antimicrobial, immunomodulatory, anti-inflammatory (Bansal and Bharati, 2014), antihyperglycemic (Hema Latha et al., 2008), antidiarrheal, antitumor (Sharma et al., 2015), analgesic, and others (Lalan et al., 2015). Organic fractions exhibit most of the above activities. Ethyl acetate fraction in an earlier study by the authors showed immunostimulatory activity in Balb/c mice (data not shown). On evaluation of the ethyl acetate fraction by gas chromatography–mass spectrometry (GC-MS) studies, geranyl isovalerate (GIV) was identified as one of its major components (**Supplementary Data**). GIV was the least investigated ethnopharmacological compound of the extract, with only one commercial application as a food additive. In all the scientific reports till date, GIV has been mostly mentioned as a constituent of essential oil without any specific activity assigned to it (Rajeswara Rao et al., 2000; Couladis et al., 2001; Giannoulis et al., 2020). This is the first study reporting a bioactive effect of the compound. GIV is used as a food flavoring agent (WHO report, 1997). This chemical, when consumed, might come in direct contact with the cells of the gastrointestinal epithelium. With this basic idea, we chose HCT116, a colon cancer cell line, for the evaluation of the anticancer properties of GIV in this study. Monoterpenes, geraniol, and geranyl acetate, which are structurally similar to GIV, have been reported to exhibit anticancer activity against Colo-205, a colon cancer cell line (Zhang et al., 2018). This study is designed to evaluate the anticancer properties of GIV in colon cancer cell lines.

MATERIALS AND METHODS

Isolation of Geranyl Isovalerate

Shade dried *A. nervosa* leaf powder was extracted using water, ethyl acetate, and ethanol. The extracts were studied for immunomodulatory activity. The promising ethyl acetate extract was further analyzed by GC-MS for its components, where GIV was reported to be one of its major constituents. GIV used for this study was procured from Sigma-Aldrich (109-20-6), and various concentrations ranging from 500 µm to 5 mM were used to understand its antiproliferative activity and mechanism of action.

Cell Culture

HCT116 and HT29 epithelial adherent colon cancer cell lines were used in this study. These were grown in Dulbecco's Modified Eagle's Medium (Gibco, Thermo Fisher Scientific, REF 11995-065) and 10% fetal bovine serum, 2 mM L-glutamine (Gibco, REF 10270-106), and 1% penicillin/streptomycin (HIMEDIA, REF A001-100ML) was used as a supplement. Cells were incubated at 37°C and 5% CO_2 in a humidified incubator.

Cytotoxicity Evaluation Using MTT Assay

Cytotoxicity of GIV was checked against the HCT116 and HT29 cells using the MTT (3-(4,5-dimethylthiazol-2-yl)-2,5-diphenyltetrazolium bromide) assay. Cells were harvested and seeded in a 96-well culture plate with a density of 1×10^4 cells per well and incubated for 24 h. The cells were treated with different concentrations of GIV ranging from 0.5 to 8 mM for 48 h. After 48 h of treatment, cells were incubated with 50 µg of MTT (5 mg/ml, HIMEDIA, REF-TC191-1G) for 2 h. The formazan crystals formed were solubilized with 100 µl of dimethyl sufoxide (Fisher Scientific Prod. No. 12435), and the absorbance was recorded at 595 nm (Senthilraja and Kathiresan, 2015). The percent viability of the cells was calculated with respect to the untreated control cells. The standard procedure was used to calculate the IC_{50} of the cells.

Live/Dead Detection by Propidium Iodide Exclusion Assay

Additionally, to corroborate the MTT experiment results, 6×10^4 cells/well of the HCT116 and HT29 cell lines were harvested and seeded in a six-well cell culture plate for 24 h. The cells were then treated with different concentrations of GIV from 0.5 to 5 mM. After the treatment of cells for the respective incubation period, the cells were stained using propidium iodide (PI, HIMEDIA, REF ML067) at a concentration of 10 µg/µl and incubated for 15–20 min. The cells were washed with phosphate-buffered saline (PBS) and then imaged at ×20 magnification using a Leica fluorescence microscope (Vyas et al., 2021).

JC-1 Staining for Mitochondrial Membrane Potential Loss

To understand the mechanism of cell death, changes in mitochondrial membrane potential (MMP) were studied using JC-1 staining (Invitrogen, REF M34152) of GIV-treated cells. Cells treated with GIV for 24 and 48 h were stained with JC1 at a final concentration of 2 µM and incubated for 15–20 min. Cells were washed with PBS, and the image was taken by using a Leica fluorescence microscope at ×20 magnification. The stained cells were also used for flow cytometric analysis. Carbonyl cyanide m-chlorophenyl hydrazine (CCCP, Invitrogen, REF M34152) was used as a positive control to check the MMP loss during apoptosis (Sivandzade et al., 2019).

Reactive Oxygen Species Generation and Geranyl Isovalerate

Cellular reactive oxygen species (ROS) generation was evaluated by dichlorofluorescein (DCFH-DA) dye (G-Biosciences Cat. #RC1066). Cells treated with GIV for 48 h were stained with

dichlorofluorescein dye to a final concentration of 1 µM and incubated for 20 min. The cells were then washed with PBS and imaged at ×20 magnification using Leica fluorescence microscope (Wu and Yotnda, 2011).

Gene Expression Profiling of Apoptotic Genes by qRT-PCR Analyses

The HCT116 cells were seeded in a T25 flask and treated with GIV. RNA was isolated from the cells using total RNA isolation kit (Promega, REF Z6111). RNA was quantified using Nanodrop, and 1 µg of the total RNA was used to synthesize cDNA using the cDNA synthesis kit (Promega, REF A3800). The cDNA obtained was used as a template to check the expression of apoptosis-associated genes, such as Caspase3, Caspase9, Bcl2, and Parp (primers were purchased from Imperialls, ILS) using SYBR Green Master Mix (Promega, REF A6001). 18s rRNA was used as an internal control. The Ct values attained through q-PCR were used to analyze the expression of the genes (Jozefczuk and Adjaye, 2011).

Western Blot Analysis of Apoptosis-Associated Proteins

Western Blot Analysis

To check the expression of apoptosis-associated proteins, HCT116 cells were seeded in a T25 flask and treated with IC_{50} concentration and a concentration lower than IC_{50} of GIV for 24 h. After incubation, cells were harvested, and total protein was isolated using mammalian protein lysis buffer. The concentration of the protein was quantified using the Bradford assay. About 20 µg of the total protein was loaded on SDS gel. The resolved proteins were transferred on to a PVDF membrane, and the membrane was blocked using 5% non-fat skimmed milk and then probed with the following antibodies: beta-actin antibody (1: 5,000) (ImmunoTag, Cat No. ITT07018, S. Rabbit), cleaved Caspase-3 (1:1,000) (ImmunoTag, Cat No. ITC0004, S. Rabbit), cleaved Caspase-9 (1:1,000) (ImmunoTag, Cat No. ITC0013, S. Rabbit), anti-Bcl2 (1:1,000) (ImmunoTag, Cat No. ITM3041, S. Mouse), cleaved PARP (1:1,000) (ImmunoTag, Cat No. ITT07023, S. Rabbit), secondary Goat anti-Rabbit IgG/HRP (1:5,000) (ImmunoTag), Goat anti-Mouse (1:5,000) (Thermo Fisher, Product No. 31431) (Gwozdz and Dorey, 2017; Taylor et al., 2013).

Statistical Analyses

All the data are the representations of mean ± SD of at least three different experiments. Student' *t*-test was performed to derive *p* values, and $p < 0.05$ was considered as statistically significant.

RESULTS AND DISCUSSION

Cytotoxicity Study of Geranyl Isovalerate

Cytotoxicity of GIV was evaluated against two different CRC cell lines (HCT116 and HT29) using the MTT assay (**Figure 1** and **Supplementary Figure S2**), which is a calorimetric assay to calculate the metabolic activity of the cell (Stockert et al., 2018). NADPH-dependent oxidoreductase enzyme in a healthy cell has the capability to reduce the tetrazolium dye—MTT (3-(4,5-dimethylthiazol-2-yl)-2,5-diphenyltetrazolium bromide)—to the insoluble purple dye called formazan (Senthilraja and Kathiresan, 2015). The higher the amount of formazan formed, the more viable the cells become. The IC_{50} value of GIV was found to be around 1.8 mM for HCT116 cells and approximately 4 mM for HT29 cells.

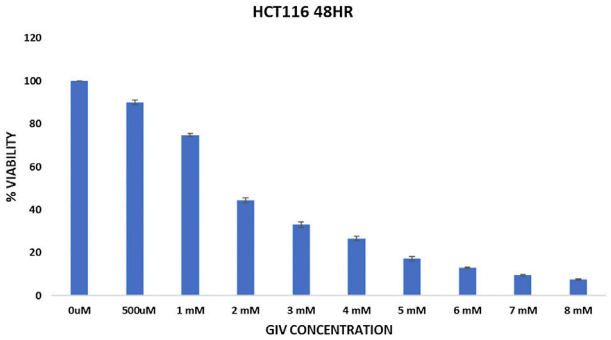

FIGURE 1 | Cytotoxicity of GIV evaluated using MTT assay. GIV shows IC_{50} around 1.6–1.8 mM concentration. The x-axis denotes GIV concentration and y-axis represents percentage viability. Data are represented as mean ± SD values of three independent experiments for 48 h of incubation, and *p* value < 0.05 is considered significant.

Live and Dead Cell Detection

Further to confirm the cytotoxicity observed by the MTT assay, PI staining was performed for which images were captured under fluorescence microscope. PI is a membrane impermeant red fluorescent DNA intercalating dye. This dye can cross the membranes only when the membranes are compromised (Lukowiak et al., 2001). It is used to differentiate live/dead cells on the basis of membrane integrity. The loss of membrane integrity is one of the hallmark features of cell death. PI when bound to DNA excites at 493 nm and emits a fluorescent red light of 636 nm (Cummings and Schnellmann, 2004; Lukowiak et al., 2001). Cells treated with GIV exhibited an increase in red fluorescence in comparison to the untreated control cells. As shown in **Figure 2** and **Supplementary Figure S3**, this increase in red fluorescence was observed to be concentration dependent. All these results of PI microscopy supported the results of cytotoxicity observed by using the MTT assay.

JC-1 Staining

To further confirm the process of cell death and contribution of the mitochondria in cell death, JC-1 staining was performed. The loss of MMP is one of the hallmark features of apoptosis. To evaluate the loss of MMP, JC-1—a lipophilic cationic dye—was used. In healthy cells, this dye gets accumulated in the negatively charged mitochondria, thus forming J-aggregates that emit red fluorescence. However, in unhealthy apoptotic cells, there is less negative charge inside the mitochondria due to membrane

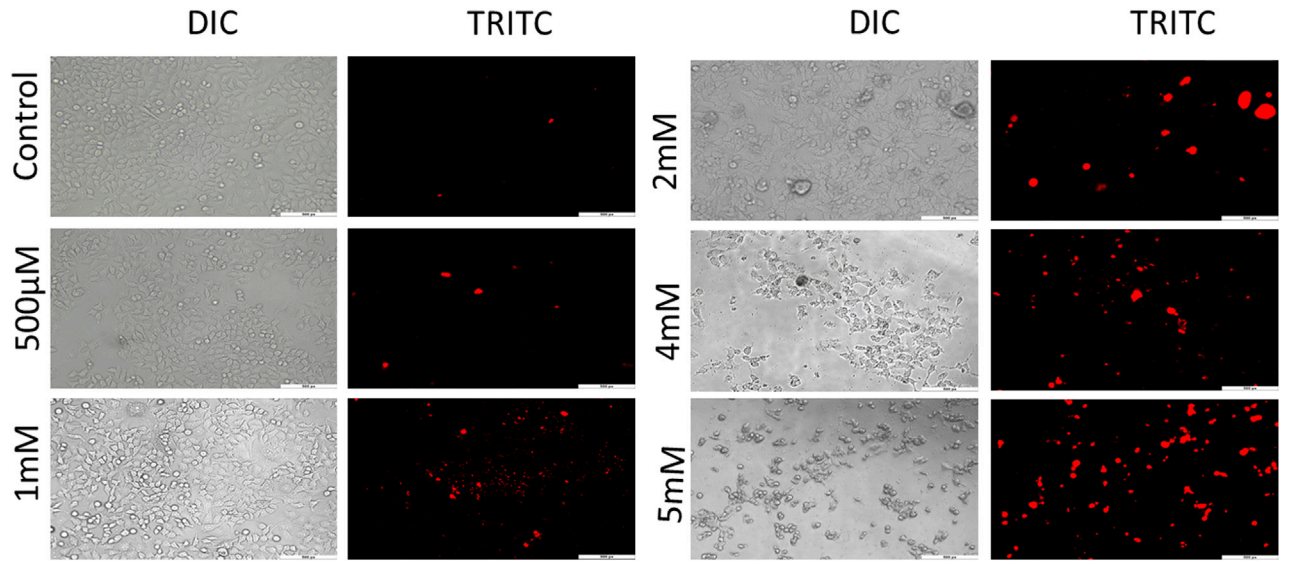

FIGURE 2 | PI staining for live/dead exclusion. HCT116 cells treated with GIV show higher PI positivity, an indication of compromised cell membranes. The cells were imaged at ×20 magnification.

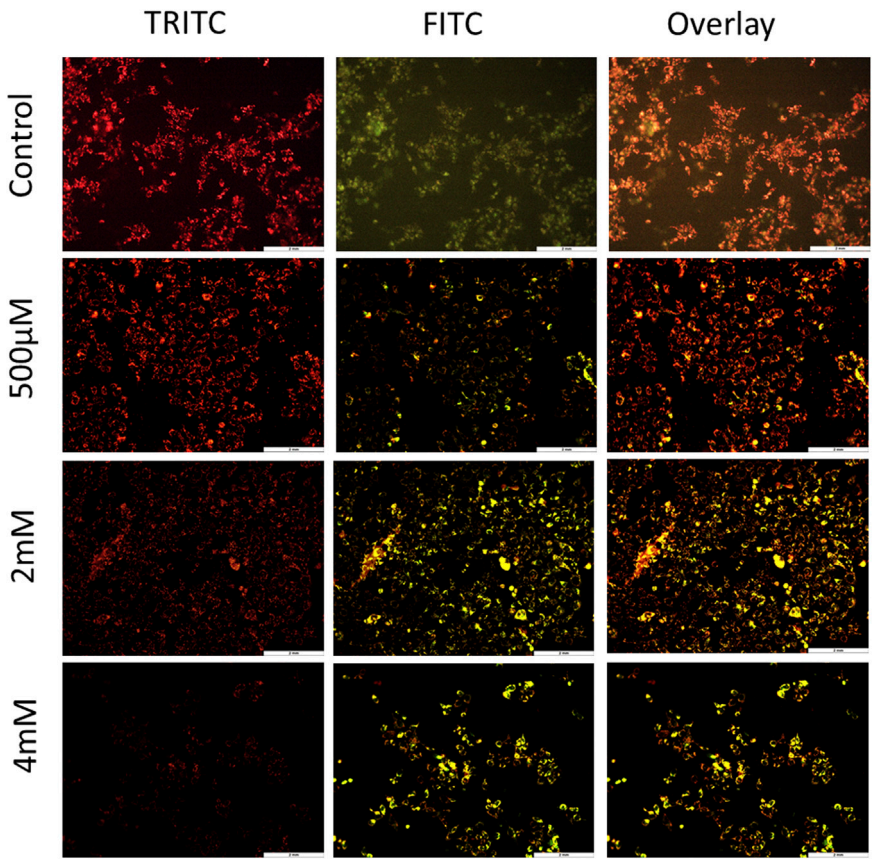

FIGURE 3 | HCT116 cells treated with GIV and analyzed for MMP loss using JC-1 staining. Cells exhibit more green fluorescence with increasing GIV concentrations, indicating membrane potential loss. The cells were imaged at ×20 magnification.

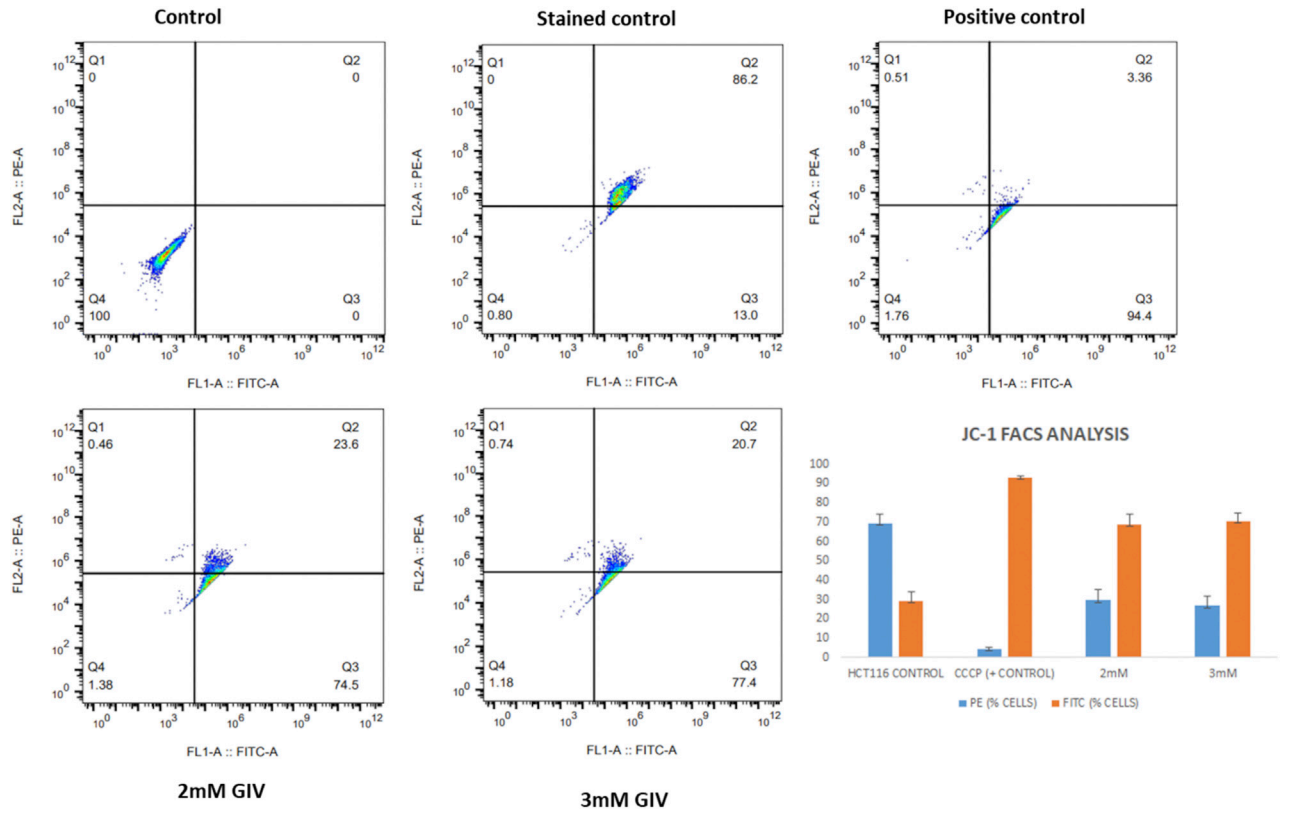

FIGURE 4 | HCT116 cells treated with GIV and analyzed for loss of MMP by flow cytometry using JC-1 staining. PE and FITC-positive cells under different experimental conditions are represented in the bar diagram.

potential loss and therefore JC-1 dye enters the mitochondria but is unable to form stable J-aggregates. It exists in a monomeric form which emits green fluorescence (Sivandzade et al., 2019). For JC-1 stain imaging by fluorescence microscopy, TRITC and FITC channels were used, and both the images were overlayed to examine the concentration of J-aggregates verses J-monomers. As shown in **Figure 3** and **Supplementary Figure S4**, cells treated with GIV clearly showed an increase in J-monomers, with increasing GIV concentration showing MMP loss. This indicates that GIV induces apoptosis through the mitochondria-mediated pathway. It has been reported that chemotherapeutic drugs are shown to induce MMP loss, thereby inducing apoptosis (Vyas et al., 2021).

This depolarization of the mitochondria and the induction of apoptosis were also quantified by the flow cytometry experiment. As shown in **Figure 4**, there is an increase in cells in the FITC channel upon treatment with GIV, representing the loss of MMP. CCCP is used as a positive control that depolarizes the mitochondria in almost all the cells. The bar diagram in **Figure 4** shows the extent of depolarization with different concentrations of GIV.

Generation of Reactive Oxygen Species by Geranyl Isovalerate

ROS generally have a short life span and are highly reactive. At a moderate level, ROS are good for regulating normal physiological functions, and for maintenance of the redox balance and immune system. However, an excess of ROS damages nucleic acids, proteins, lipids, membranes, and organelles, leading to apoptosis-related cell death. ROS have an essential role in cell signaling and also regulate key pathways related to apoptosis, which are mediated by death receptors, the mitochondria, and the endoplasmic reticulum (Redza-Dutordoir and Averill-Bates, 2016). ROS generation has been reported to be a part of the activity of many chemotherapeutic drugs. There are various methods to measure free radical production in mammalian cells, but the use of 2′-7′-dichlorodihydrofluorescein diacetate (DCFH-DA) is the most common for this purpose. DCFH-DA is basically a cell-permeable, intracellular nonfluorescent precursor of DCF that is used as a probe to measure oxidative stress of cells. DCFH-DA gets hydrolyzed to DCFH that is impermeable and therefore remains inside the cell, which is finally oxidized to dichlorofluorescein that emits green fluorescence (Eruslanov and Kusmartsev, 2010). This DCF accumulation is measured by the increase in fluorescence at 530 nm by the FL-1 green channel of fluorescence microscopy. In the experiment of this study, HCT116 and HT29 cells treated with GIV showed an increase in green fluorescence in a concentration-dependent manner. As shown in **Figure 5** and **Supplementary Figure S5**, the number of cells exhibiting green fluorescence increased with higher concentrations of

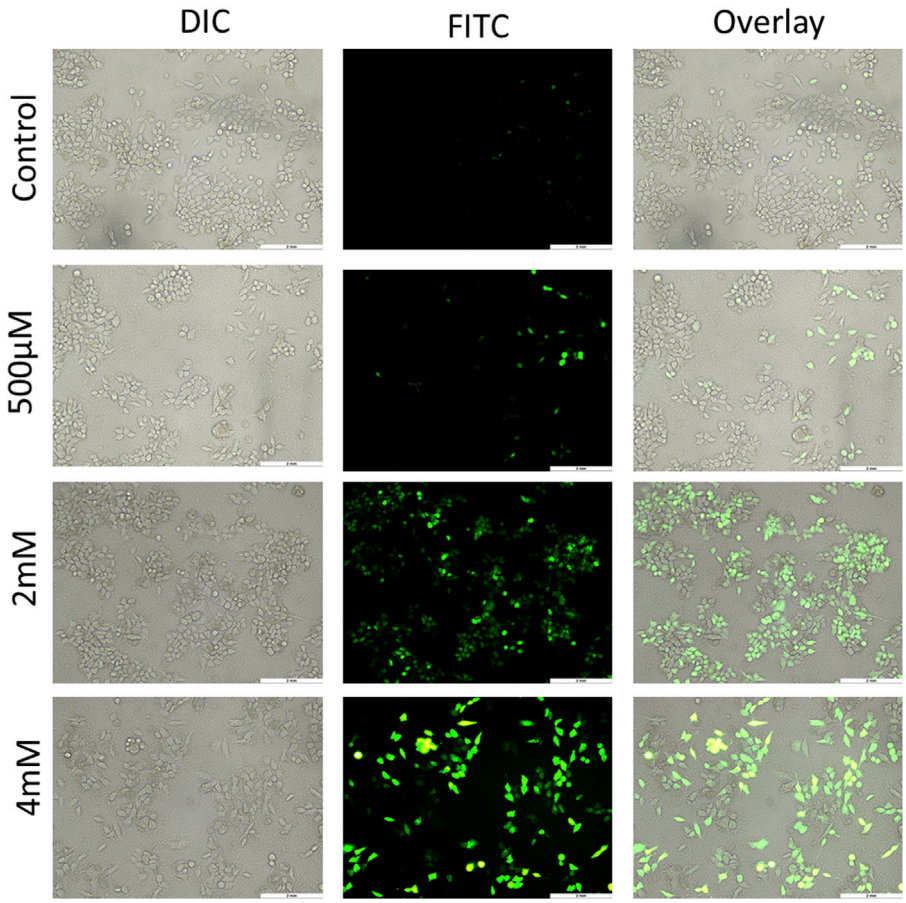

FIGURE 5 | HCT116 cells treated with GIV, analyzed for ROS generation using DCFH-DA dye, and imaged at ×20 magnification. The cells show increased green fluorescence with increasing concentrations of GIV in comparison with the control cells, indicating ROS generation with GIV treatment.

GIV than did control cells. This indicates an increase in ROS generation upon treatment with GIV.

Change in Expression of Apoptosis-Related Genes Induced by Geranyl Isovalerate

To check the apoptosis-related genes at the transcriptome level, gene expression profiling was performed in control HCT116 cells and 48-h drug-treated cells at concentrations of 1, 2, and 3 mM. BCl2, Caspase 3, Caspase 9, and PARP were used for expression profiling, and 18S RNA was used as a housekeeping gene. we continued our experiments with HCT116 cells alone as HT29 had an IC50 value at higher concentration IC_{50} value at higher concentration, so we continued our experiments with HCT116 cells alone.

Bcl2 protein family is a well characterized protein family which has an important role in regulating the intrinsic pathway of apoptosis. This family of proteins contain both proapoptotic and antiapoptotic members. Bcl2 is an antiapoptotic member of this protein family (Tsujimoto, 1998). Bcl2 protein has been shown to promote an increase in cancer cell population by preventing cell death and promote resistance to chemotherapy in cancer cells (Reed et al., 1996). It conserves the integrity of the mitochondrial membrane to inhibit apoptosis, as it contains a hydrophobic carboxyl-terminal domain that is linked to the outer mitochondrial membrane. Bcl2

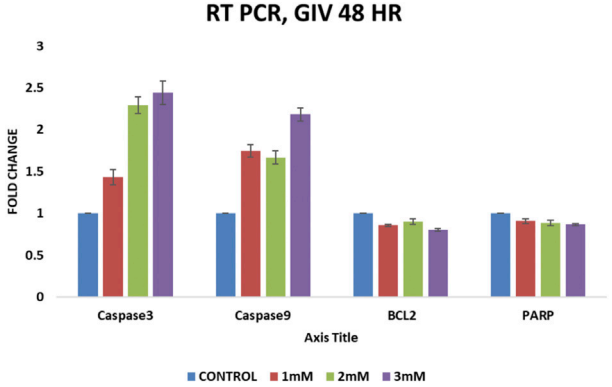

FIGURE 6 | QPCR analysis of apoptosis-regulating genes Bcl2, Caspase-3, Caspase-9, and PARP. HCT116 cells treated with different concentrations of GIV show an increase in expression of proapoptotic caspase-3 and -9 and a decrease in expression of antiapoptotic Bcl-2 and PARP genes.

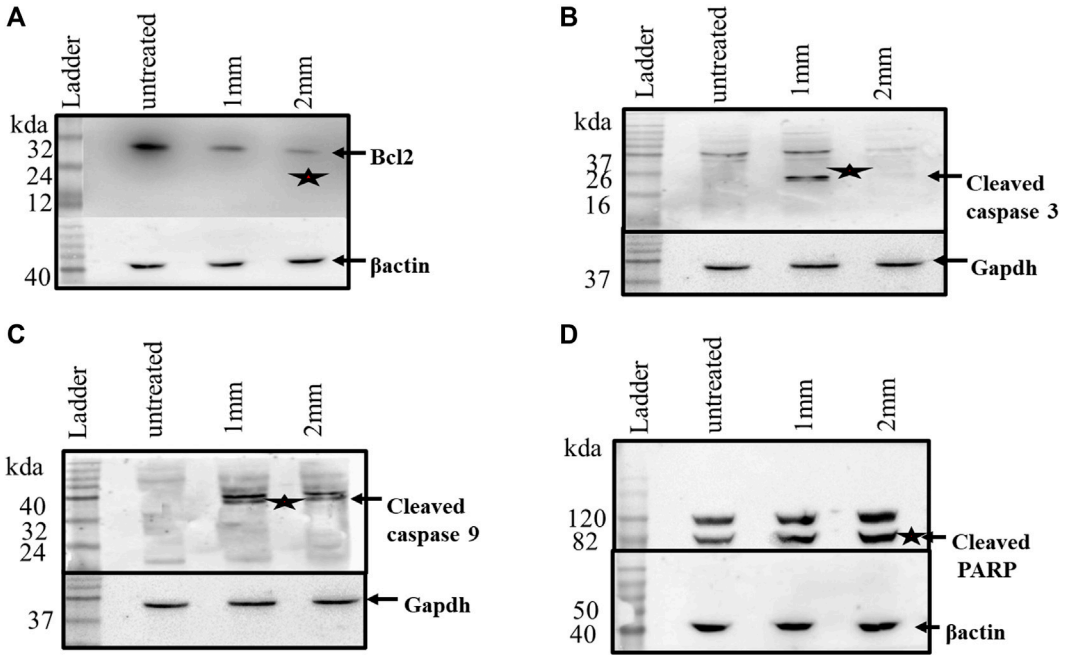

FIGURE 7 | HCT116 cells treated with GIV and analyzed for expression of apoptosis-associated proteins. **(A)** Expression of Bcl2 in the control and GIV-treated cells. **(B)** Cleaved caspase-3 protein levels in the control and GIV-treated cells. **(C)** Cleaved caspase-9 protein levels in the control and GIV-treated cells. **(D)** Cleaved PARP levels in the control and GIV-treated cells. β-actin and GAPDH proteins have been used as the internal controls.

interacts with proapoptotic BAX, thereby preventing oligomerization of BAX and BAK and their translocation to the mitochondrial membrane. The translocation of BAX–BAK oligomer to the mitochondrial membrane punches pores in the membrane, releasing various proapoptotic factors such as cytochrome C from the mitochondria. Thus increased Bcl-2 expression prevents the apoptosome complex formation, preventing the activation of downstream caspase cascade. Bcl-2 has been also shown to control the initiation of some initiator caspases such as caspse2, thereby preventing apoptosis (Guo et al., 2002).

Caspases are endopeptidases, which are widely divided into three groups, namely, initiator (caspase 2, 8, 9, and 10), executioner (caspase 3, 6, and 7), and inflammatory (caspase 1, 4, 5, 11, and 12). The initiator caspases activate the apoptotic signaling cascade; however, the executioner does the proteolysis of important proteins that is important for apoptosis (Role of caspases in apoptosis, 2021). Caspase 9 is an initiator caspase that activates downstream executioner caspases, thus initiating apoptosis. By forming an apoptosome, the seven APAF-1 subunits activate one caspase-9; the activated caspase-9 then cleaves-3,-6 and -7, Which in turn cleaves various cellular targets, resulting in (Kuida, 2000). Caspase-3 is an executioner caspase, which upon activation performs an effective function of/in apoptosis by degrading intracellular protein (Porter et al., 2021). Tetrandrine citrate shows antitumor activity in glioma cells by increasing the expression of caspase-3 and ROS generation, while decreasing Bcl2 expression (Sun et al., 2019). The data from earlier JC-1 staining and ROS generation point toward the involvement of the intrinsic pathway of apoptosis. As a result, the levels of caspase-9, the intrinsic pathway intiator caspase, and executionary caspase-3 were measured.

PARPs (poly ADP–ribose polymerases) are the enzymes that catalyse the transfer of ADP–ribose to target proteins. PARPs also have an important role in various biological processes inside a cell, such as chromatin structure modulation, replication, transcription, recombination, and DNA repair (Morales et al., 2014). PARP helps damaged cells to repair themselves, thereby playing an important role in cancer. Therefore, PARP inhibitors stop PARP from performing repair work, thereby making cancer cells die (Cancer Research UK, 2021). PARP cleavage is found to be associated with cell death. Therefore, the cleavage product enhances apoptosis and prevents cell survival (D'Amours et al., 2001).

RT-QPCR experiments after GIV treatment show a significant increase in caspase-3 and caspase-9 levels in a concentration-dependent manner. However, a slight change in expression of Bcl-2 (antiapoptotic gene) and PARP (damaged cells repair gene) has been also observed, as shown in **Figure 6**. The increased expression of proapoptotic caspases and decreased expressions of antiapoptotic Bcl-2 and DNA repair–associated PARP further confirm apoptosis induction by GIV treatment.

Change in Expression of Apoptosis-Related Proteins

After investigating the expression of apoptosis-related genes at the transcriptional level, their expressions at the protein level

were checked by western blot analyses. Caspases have been reported to exist in an inactive zymogen state in healthy cells, but upon induction of apoptosis, these inactive zymogens cleaved to form an active caspase. As shown in **Figure 7**, caspases3 and 9 show cleaved products, which is a feature of apoptosis. The western blot analyses further confirmed the decrease in Bcl-2 expression as observed in the Rt-PCR experiments. Cleavage of PARP is another important event during apoptosis, which was also reported after GIV treatment. The western blots further confirmed that GIV induces apoptosis by activation of caspases, decreasing the expression of Bcl-2. These results confirmed the involvement of an intrinsic pathway of apoptosis in cell death of GIV-treated cells. Furthermore, the morphological features of dying cells along with the expression changes of the Bcl-2, Parp, and Caspase genes support apoptosis rather than any other form of cell death.

CONCLUSION

This study was performed to evaluate the anticancer properties of GIV, an active ingredient of *A. nervosa* extracts. To establish the anticancer properties of GIV, cytotoxicity studies, ROS generation, loss of MMP, and expression profiling of apoptosis-associated genes at the transcriptional and translational levels were evaluated. Based on the results, it can be concluded that GIV induces apoptosis through oxidative stress–mediated pathways in both the cell lines studied. The increased ROS generation, loss of MMP, decreased expression of antiapoptotic genes, and increased expression of proapoptotic genes supported oxidative stress–mediated cell death. GIV is already a WHO-approved food additive. Furthermore, *in vivo* experimental data are required to determine if this compound can be used as a food supplement along with other chemotherapeutic agents in order to see if this molecule can increase the efficacy of therapy. A detailed study is also required to understand if structural modifications of GIV could increase the efficacy of the compound and can be individually used as a therapeutic agent.

DATA AVAILABILITY STATEMENT

The original contributions presented in the study are included in the article/**Supplementary Material**; further inquiries can be directed to the corresponding authors.

AUTHOR CONTRIBUTIONS

FR and DS: experimentation and data analysis. PSA, SKJM, and TS: conceptualized, data analyses, and manuscript preparation.

FUNDING

The authors thank SNU for the opportunity to carry out this research study. They acknowledge the DST-FIST support to the Department of Botany, Indira Gandhi National Tribal University, Amarkantak, Madhya Pradesh, India. DST-FIST grant number: SR/FST/LS-I/2018/132.

SUPPLEMENTARY MATERIAL

The Supplementary Material for this article can be found online at: https://www.frontiersin.org/articles/10.3389/fphar.2021.698375/full#supplementary-material

REFERENCES

Banerjee, P., Erehman, J., Gohlke, B. O., Wilhelm, T., Preissner, R., and Dunkel, M. (2015). Super Natural II-Aa Database of Natural Products. *Nucleic Acids Res.* 43, D935–D939. doi:10.1093/nar/gku886

Bharati, A. J., and Bansal, Y. K. (2014). Phytochemical Investigation of Natural and *In Vitro* Raised Vṛddhadāruka Plants. *Anc. Sci. Life* 34, 80–84. doi:10.4103/0257-7941.153463

Cancer Research UK (2021). PARP Inhibitors | Targeted Cancer Drugs. Available at: https://www.cancerresearchuk.org/about-cancer/cancer-in-general/treatment/targeted-cancer-drugs/types/PARP-inhibitors (Accessed March 21, 2021).

Center, M. M., Jemal, A., and Ward, E. (2009). International Trends in Colorectal Cancer Incidence Rates. *Cancer Epidemiol. Biomarkers Prev.* 18, 1688–1694. doi:10.1158/1055-9965.EPI-09-0090

Couladis, M., Tsortanidou, V., Francisco-Ortega, J., Santos-Guerra, A., and Harvala, C. (2001). Composition of the Essential Oils of Argyranthemum Species Growing in the Canary Islands. *Flavour Fragr. J.* 16, 103–106. doi:10.1002/ffj.954

Cragg, G. M., and Newman, D. J. (2005). Plants as a Source of Anti-cancer Agents. *J. Ethnopharmacol.* 100, 72–79. doi:10.1016/j.jep.2005.05.011

Cummings, B. S., and Schnellmann, R. G. (2004). Measurement of Cell Death in Mammalian Cells. *Curr. Protoc. Pharmacol.* 12, 1–8. doi:10.1002/0471141755.ph1208s25

D'Amours, D., Sallmann, F. R., Dixit, V. M., and Poirier, G. G. (2001). Gain-of-function of poly(ADP-Ribose) Polymerase-1 upon Cleavage by Apoptotic Proteases: Implications for Apoptosis. *J. Cell Sci.* 114, 3771–3778. doi:10.1242/jcs.114.20.3771

Dekker, E., Tanis, P. J., Vleugels, J. L. A., Kasi, P. M., and Wallace, M. B. (2019). Colorectal Cancer. *Lancet* 394, 1467–1480. doi:10.1016/S0140-6736(19)32319-0

Eruslanov, E., and Kusmartsev, S. (2010). Identification of ROS Using Oxidized DCFDA and Flow-Cytometry. *Methods Mol. Biol.* 594, 57–72. doi:10.1007/978-1-60761-411-1_4

Fridlender, M., Kapulnik, Y., and Koltai, H. (2015). Plant Derived Substances with Anti-cancer Activity: From Folklore to Practice. *Front. Plant Sci.* 6, 799. doi:10.3389/fpls.2015.00799

Giannoulis, K. D., Kamvoukou, C.-A., Eleni Wogiatzi, N. G., and Wogiatzi, E. (2020). Matricaria Chamomilla L. (German Chamomile) Flower Yield and Essential Oil Affected by Irrigation and Nitrogen Fertilization. *Emir J. Food Agric.* 32, 328–335. doi:10.9755/ejfa.2020.v32.i5.2099

Guo, Y., Srinivasula, S. M., Druilhe, A., Fernandes-Alnemri, T., and Alnemri, E. S. (2002). Caspase-2 Induces Apoptosis by Releasing Proapoptotic Proteins from Mitochondria. *J. Biol. Chem.* 277, 13430–13437. doi:10.1074/JBC.M108029200

Gwozdz, T., and Dorey, K. (2017). Western Blot. *Basic Sci. Methods Clin. Res.* 1, 99–117. doi:10.1016/B978-0-12-803077-6.00006-0

Hema Latha, E., Satyanarayana, T., Ramesh, A., Durga Prasad, Y., Routhu, K. V., and Srinivas, R. L. A. (2008). Hypoglycemic and Antihyperglycemic Effect of

Argyreia Speciosa Sweet. In normal and in Alloxan Induced Diabetic Rats. *J. Nat. Remedies* 8, 203–208. doi:10.18311/jnr/2008/334

Jozefczuk, J., and Adjaye, J. (2011). Quantitative Real-Time PCR-Based Analysis of Gene Expression. *Methods Enzymol.* 500, 99–109. doi:10.1016/B978-0-12-385118-5.00006-2

Kuida, K. (2000). Caspase-9. *Int. J. Biochem. Cell Biol.* 32, 121–124. doi:10.1016/S1357-2725(99)00024-2

Lalan, B. K., Hiray, R. S., and Ghongane, B. B. (2015). Evaluation of Analgesic and Anti-inflammatory Activity of Extract of Holoptelea Integrifolia and Argyreia Speciosa in Animal Models. *J. Clin. Diagn. Res.* 9, FF01–4. doi:10.7860/JCDR/2015/12059.6200

Morales, J., Li, L., Fattah, F. J., Dong, Y., Bey, E. A., and Patel, M. (2014). Review of Poly (ADP-Ribose) Polymerase (PARP) Mechanisms of Action and Rationale for Targeting in Cancer and Other Diseases. *Crit. Rev. Eukaryot. Gene Expr.* 24, 15–28. doi:10.1615/CritRevEukaryotGeneExpr.2013006875

Paulke, A., Kremer, C., Wunder, C., Wurglics, M., Schubert-Zsilavecz, M., and Toennes, S. W. (2014). Identification of Legal Highs - Ergot Alkaloid Patterns in Two Argyreia Nervosa Products. *Forensic Sci. Int.* 242, 62–71. doi:10.1016/j.forsciint.2014.06.025

Porter, A. G., Ja, R. U., and Nicke, È. (2021). Emerging Roles of Caspase-3 in Apoptosis. Available at: http://www.stockton-press.co.uk/cdd (Accessed March 21, 2021).

Lukowiak, B., Vandewalle, B., Riachy, R., Kerr-Conte, J., Gmyr, V., and Belaich, S. (2001). Identification and Purification of Functional Human Beta-Cells by a New Specific Zinc-Fluorescent Probe. *J. Histochem. Cytochem.* 49 (4), 519–528. doi:10.1177/002215540104900412

Rajeswara Rao, B. R., Sastry, K. P., Saleem, S. M., Prakasa Rao, E. V. S., Syamasundar, K. V., and Ramesh, S. (2000). Volatile Flower Oils of Three Genotypes of Rose-Scented geranium (Pelargonium sp.). *Flavour Fragr. J.* 15, 105–107. doi:10.1002/(sici)1099-1026(200003/04)15:2<105::aid-ffj875>3.0.co;2-g

Redza-Dutordoir, M., and Averill-Bates, D. A. (2016). Activation of Apoptosis Signalling Pathways by Reactive Oxygen Species. *Biochim. Biophys. Acta - Mol. Cell Res.* 1863, 2977–2992. doi:10.1016/j.bbamcr.2016.09.012

Reed, J. C., Miyashita, T., Takayama, S., Wang, H. G., Sato, T., Krajewski, S., et al. (1996). BCL-2 Family Proteins: Regulators of Cell Death Involved in the Pathogenesis of Cancer and Resistance to Therapy. *J. Cell Biochem.* 60 (1), 23–32. doi:10.1002/(SICI)1097-4644(19960101)60:1%3C23::AID-JCB5%3E3.0.CO;2-5

Role of caspases in apoptosis (2021). Abcam. Available at: https://www.abcam.com/kits/role-of-caspases-in-apoptosis (Accessed March 21, 2021).

Senthilraja, P., and Kathiresan, K. (2015). *In Vitro* cytotoxicity MTT Assay in Vero, HepG2 and MCF-7 Cell Lines Study of Marine Yeast ARTICLE INFO ABSTRACT. *J. Appl. Pharm. Sci.* 5, 80–084. doi:10.7324/JAPS.2015.50313

Sharma, B., Dhamija, I., Kumar, S., and Chaudhary, H. (2015). *In Vitro* and *In Vivo* Evaluation of Antitumor Activity of Methanolic Extract of Argyreia Nervosa Leaves on Ehrlich Ascites Carcinoma. *Bangladesh J. Pharmacol.* 10, 399–408. doi:10.3329/bjp.v10i2.22334

Sivandzade, F., Bhalerao, A., and Cucullo, L. (2019). Analysis of the Mitochondrial Membrane Potential Using the Cationic JC-1 Dye as a Sensitive Fluorescent Probe. *Bio Protoc.* 9, e3128. doi:10.21769/BioProtoc.3128

Stockert, J. C., Horobin, R. W., Colombo, L. L., and Blázquez-Castro, A. (2018). Tetrazolium Salts and Formazan Products in Cell Biology: Viability Assessment, Fluorescence Imaging, and Labeling Perspectives. Available at: http://eprints.gla.ac.uk/158899/http://eprints.gla.ac.uk (Accessed March 3, 2021). doi:10.1016/j.acthis.2018.02.005

Sun, J., Zhang, Y., Zhen, Y., Cui, J., Hu, G., and Lin, Y. (2019). Antitumor Activity of Tetrandrine Citrate in Human Glioma U87 Cells *In Vitro* and *In Vivo*. *Oncol. Rep.* 42, 2345–2354. doi:10.3892/or.2019.7372

Taylor, S. C., Berkelman, T., Yadav, G., and Hammond, M. (2013). A Defined Methodology for Reliable Quantification of Western Blot Data. *Mol. Biotechnol.* 553 (55), 217–226. doi:10.1007/S12033-013-9672-6

Tsujimoto, Y. (1998). Role of Bcl-2 Family Proteins in Apoptosis: Apoptosomes or Mitochondria?. *Genes to Cells* 3, 697–707. doi:10.1046/j.1365-2443.1998.00223.x

Vyas, K. M., Sharma, D., Magani, S. R. K., Mobin, S. M., and Mukhopadhyay, S. (2021). In-Vitro Evaluation of Cytotoxicity and Antimetastatic Properties of Novel Arene Ruthenium(II)-Tetrazolato Compounds on Human Cancer Cell Lines. *Appl. Organomet Chem.* doi:10.1002/aoc.6187

Wu, D., and Yotnda, P. (2011). Production and Detection of Reactive Oxygen Species (ROS) in Cancers. *J. Vis. Exp.* 57, 3357. doi:10.3791/3357

Zhang, G., Qi, F., Yan, Q., Liu, J., Chen, Y., and Zhang, Z. (2008). Geraniol and Geranyl Acetate Induce Potent Anticancer Effects in Colon Cancer Colo-205 Cells by Inducing Apoptosis, DNA Damage and Cell Cycle Arrest. *J. BUON* 23, 346–352.

Conflict of Interest: The authors declare that the research was conducted in the absence of any commercial or financial relationships that could be construed as a potential conflict of interest.

Publisher's Note: All claims expressed in this article are solely those of the authors and do not necessarily represent those of their affiliated organizations, or those of the publisher, the editors, and the reviewers. Any product that may be evaluated in this article, or claim that may be made by its manufacturer, is not guaranteed or endorsed by the publisher.

frontiers in Pharmacology

ORIGINAL RESEARCH
published: 07 October 2021
doi: 10.3389/fphar.2021.720368

Downregulation of ATP1A1 Expression by *Panax notoginseng* (Burk.) F.H. Chen Saponins: A Potential Mechanism of Antitumor Effects in HepG2 Cells and *In Vivo*

Xiao-Yi Feng†, Wei Zhao†, Zheng Yao, Ning-Yi Wei, An-Hua Shi and Wen-Hui Chen**

Faculty of Basic Medicine, Yunnan University of Chinese Medicine, Kunming, China

The Na^+/K^+-ATPase α1 subunit (ATP1A1) is a potential target for hepatic carcinoma (HCC) treatment, which plays a key role in Na^+/K^+ exchange, metabolism, signal transduction, etc. *In vivo*, we found that *Panax notoginseng* saponins (PNS) could inhibit tumor growth and significantly downregulate the expression and phosphorylation of ATP1A1/AKT/ERK in tumor-bearing mice. Our study aims to explore the potential effects of PNS on the regulation of ATP1A1 and the possible mechanisms of antitumor activity. The effects of PNS on HepG2 cell viability, migration, and apoptosis were examined *in vitro*. Fluorescence, Western blot, and RT-PCR analyses were used to examine the protein and gene expression. Further analysis was assessed with a Na^+/K^+-ATPase inhibitor (digitonin) and sorafenib *in vitro*. We found that the ATP1A1 expression was markedly higher in HepG2 cells than in L02 cells and PNS exhibited a dose-dependent effect on the expression of ATP1A and the regulation of AKT/ERK signaling pathways. Digitonin did not affect the expression of ATP1A1 but attenuated the effects of PNS on the regulation of ATP1A1/AKT/ERK signaling pathways and enhanced the antitumor effect of PNS by promoting nuclear fragmentation. Taken together, PNS inhibited the proliferation of HepG2 cells *via* downregulation of ATP1A1 and signal transduction. Our findings will aid a data basis for the clinical use of PNS.

Keywords: Na+/K+-ATPase α1 subunit, *Panax notoginseng* saponins, digitonin, antitumor, AKT/ERK signaling pathways

OPEN ACCESS

Edited by:
Marcus Scotti,
Federal University of Paraíba, Brazil

Reviewed by:
Lei Chen,
Guangdong Ocean University, China
Xiaoyin Chen,
Jinan University, China

****Correspondence:***
An-Hua Shi
ynshianhua@126.com
Wen-Hui Chen
cwh6581908@126.com

†These authors have contributed equally to this work

Specialty section:
This article was submitted to Ethnopharmacology, a section of the journal Frontiers in Pharmacology

Received: *04 June 2021*
Accepted: *24 August 2021*
Published: *07 October 2021*

Citation:
Feng X-Y, Zhao W, Yao Z, Wei N-Y, Shi A-H and Chen W-H (2021) Downregulation of ATP1A1 Expression by Panax notoginseng *(Burk.) F.H. Chen Saponins: A Potential Mechanism of Antitumor Effects in HepG2 Cells and* In Vivo. *Front. Pharmacol. 12:720368. doi: 10.3389/fphar.2021.720368*

INTRODUCTION

The Na^+/K^+-ATPase sodium pump (NKA) is widely distributed in mammalian cell membranes and participates in Na^+/K^+ exchange, maintaining ion balance and cellular osmotic pressure (Lan et al., 2018). The NKA consists of α1, α2, α3, α4, β1, β2, β3, and γ subtypes (Chen et al., 2006). The α subunit includes the binding sites of ATP, cardiac glycosides (CTS), Na^+, K^+, and ouabain (Lingrel et al., 2007). A recent study reported that any mutations in the NKA gene may cause serious

Abbreviations: AKT, protein kinase B; CTS, cardiac glycosides; ERK, extracellular signal–regulated kinase 1/2; EGFR, epidermal growth factor receptor; HCC, hepatocellular carcinoma; HepG2 cells, human hepatoblastoma HepG2 cells; H22, murine hepatoma-22; IC_{50}, half-maximal inhibitory concentration; L02 cells, HL-7702 (L-02) normal human liver cells; MAPK, mitogen-activated protein kinase; mTOR, mechanistic target of rapamycin; NF-κB, nuclear transcription factor-κB; NKA, Na^+/K^+-ATPase sodium pump; PI3K, phosphatidylinositol 3-kinase; and Src, Src-family protein kinases.

physiological disturbances compared to the inactivation of ion pump function. Such physiological disturbances may be caused by leakage of ion channels, protein instability, or misfolding (Sweadner et al., 2019). The α1 subunit (ATP1A1) is overexpressed in liver cancer (Zhuang et al., 2015), glioma (Xu et al., 2010), etc. Downregulating the expression of ATP1A1 can significantly reduce the proliferation and migration of hepatic carcinoma (HCC) cells and promote cell apoptosis, reducing their tumorigenicity *in vivo*. The change in the α subunit will disrupt the homeostasis of the Src family of protein kinases (Src). Activated Src can bind to the epidermal growth factor receptor (EGFR) to induce subsequent activation of phosphoinositide 3-kinase (PI3K), Ras/Raf/ERK, and PLC/PKC. Meanwhile, Src can induce the mitochondria to produce a large amount of ROS and upregulate intracellular Ca^{2+} concentration to activate the second messenger (Yu et al., 2019).

Panax notoginseng (Burk.) F.H. Chen is widely used in traditional Chinese medicine (TCM). *Panax notoginseng* saponins (PNS) are the major active ingredient of *P. notoginseng* and also the main ingredient of Xuesaitong, Xueshuantong, and other Chinese patent medicines to treat cardio–cerebrovascular diseases. Nowadays, the pharmacological effects of PNS are not limited to the treatment of cardiovascular diseases but also include anti-inflammatory, (Hu et al., 2018; Zhao et al., 2018; Lu et al., 2020), antitumor (Wang et al., 2014; Yang et al., 2016; Li Q. et al., 2020), antithrombotic, and anti-arterial injury properties (Hui et al., 2020). The saponins in *P. notoginseng* are mainly dammarane-type and ocotillol-type. PNS mainly contain five active ingredients: notoginsenoside R_1, ginsenoside Rg_1, ginsenoside Re, ginsenoside Rb_1, and ginsenoside Rd. The five main compounds are dammarane-type saponins. The latest systematic research on the composition of PNS showed that 28 compounds were isolated from PNS, including several rare saponins, and they exhibited antitumor activities (Li Q. et al., 2020). The antitumor mechanisms mainly included promoting cell apoptosis, inhibiting the mTOR/PI3K/AKT signaling pathway (Wei Li et al., 2019), reducing the ERK signaling pathway (Meng et al., 2019), downregulating miR-21 (Li Y. et al., 2020), promoting DNA damage (Cai et al., 2021), etc.

However, these previous reports did not investigate the mechanism of action that led to the downregulation of signaling pathways. In addition, *in vitro* study of PNS on the regulation of cell membrane proteins was very limited. In the present study, we hypothesized that PNS can inhibit AKT/ERK signaling pathways *via* downregulating the ATP1A1 expression. Therefore, we designed the experiment to illustrate the effect of PNS on ATP1A1 in HepG2 cells and explore the possible mechanisms.

MATERIALS AND METHODS

Regents and Chemicals

PNS were purchased from Xi'an TianBao Guangyuan Biotech. Ltd. (Shanxi Province, China, purity > 95%), and they include notoginsenoside R_1>5.0%, ginsenoside Rg_1>25.0%, ginsenoside Re >2.5%, ginsenoside Rb_1>30.0%, and ginsenoside Rd >5.0% (Pharmacopoeia of the People's Republic of China (2020)). A Dulbecco's Modified Eagle Medium (DMEM) with high glucose was brought from Gibco (United States, 1980922). The ATP1A1 inhibitor (digitonin, ST1272) was brought from Biotech (Beijing, China). Sorafenib (SC0236) was purchased from Beyotime, China. The Servicebio® RT First Strand cDNA Synthesis Kit (G3330) and 2×SYBR Green qPCR Master Mix (High ROX) (G3322) were obtained from Servicebio. TRIzol and RAPA were used in this study. ATP1A1, ERK, and p-ERK antibodies were purchased from Cell Signaling Technology (United States; batch numbers are 23565S-1, 4695S-14, 9101S-28); mTOR, p-mTOR, AKT, and p-AKT were purchased from Abcam (Abcam, United Kingdom; batch numbers are GR3181969-14, GR112975-29, GR43522-33, and GR297104-1). β-Actin antibody (Wuhan Servicebio Company; lot number: 180926), FITC rabbit antibody (Beijing Zhongshan Jinqiao Biotechnology Co., Ltd.; lot number: 133027), and DAPI (Beijing Beyotime Biotechnology Co., Ltd.; lot number: C1005) were also used.

Cell Culture and Animals

HepG2 cells, HL-7702 (L-02) normal human liver (L02) cells, and H22 cells were incubated in a DMEM (Gibco) supplemented with 10% fetal bovine serum (Gibco), 10,000 U/mL penicillin, and 1% streptomycin. HepG2 cells (5×10^5 cells/well) were incubated in 12-well plates for 24 h. Then, cells were treated with different doses of PNS (600 mg/L and 300 mg/L, resp.) and incubated for 48 h. C57bl/6 mice (male, body weight 16 ± 2 g) were purchased from Hunan STA Laboratory Animal Co., Ltd. (Changsha, China, SCXK (Xiang) 2016-0002). The procedures of animal studies were designed according to the national and international guidelines and approved by the Committee of the Yunnan University of Chinese Medicine (SYXK (Dian) K2017-0005).

Antitumor Evaluation *In Vivo*

A total of 2×10^6 H22 cells/200 μl were injected into mice by subcutaneous injections to establish a tumor growth model. Mice were weighed, and the tumor volumes were measured once every 2 days according to the formula $(A \times B^2)/2$ (A: the tumor length and B: the tumor width). After the tumor volumes reached 50–100 mm^3, they were randomly divided into four groups and treated with normal saline, sorafeinb (60 mg/kg), and different dosages of PNS by intragastric administration once per day, for 14 days, with 6 mice/each group. The doses of PH (high dosage of PNS) and PL (low dosage of PNS) groups were 100 mg/kg/day and 50 mg/kg/day, respectively. The control groups were given the same volume of normal saline.

Cell Viability Assay

HepG2 cells (1×10^4 cells/well) were incubated in 96-well plates in a complete DMEM. Cells were treated with different concentrations of PNS (0, 18.75, 37.5 75, 150, 300, and 600 mg/L) for 48 h. Cell viability was determined by the MTT assay. 20 μl MTT was added to each well and incubated for 3 h. The formazan was dissolved in 150 μl of dimethyl sulfoxide. The optical density was measured at 490 nm, and cell viability was normalized as the percentage of control. Cell viability $(\%)=(OD_{control}-OD_{sample})/(OD_{control}-OD_{blank}) \times 100\%$. IC_{50}

TABLE 1 | Primer sequences of target genes.

Target gene	Primer sequences (5'→3')
ATP1A1 (forward)	GGCAGTGTTTCAGGCTAACCAG
ATP1A1 (reverse)	TCTCCTTCACGGAACCACAGCA
AKT (forward)	CCGCCTGATCAAGTTCTCCT
AKT (reverse)	TTCAGATGATCCATGCGGGG
ERK (forward)	GCTCTGCTTATGATAATCTC
ERK (reverse)	GATGCCAATGATGTTCTC
β-Actin (forward)	TGAGCTGCGTTTTACACCCT
β-Actin (reverse)	GCCTTCACCGTTCCAGTTTT

(half-maximal inhibitory concentration) was calculated by SPSS software.

Cell Migration Assay

HepG2 cells (8×10^4 cells/well) were incubated in 24-well plates in a complete DMEM. Using a sterile 200 μl pipette tip, a scratch of 1 mm width was made in triplicate. Floating cells were removed by washing with phosphate buffer solution (PBS), and then, fresh media or PNS were added. Cells were treated with 300 mg/L or 600 mg/L of PNS for 48 h. Images were recorded using an inverted microscope (Olympus, CK40, Japan). The images from 0 to 48 h were compared, and the migration distance was calculated by ImageJ software.

Annexin V-FITC/PI Staining

HepG2 cells (5×10^5 cells/well) were incubated in 6-well plates. Cells were treated with 300 mg/L or 600 mg/L of PNS for 24 h. Then, the cells were stained with Annexin V/PI for 30 min at 4°C in the dark, and the apoptosis analysis was carried out by flow cytometry (Accuri C6, BD, CA, United States). The apoptotic rate was calculated by FlowJo software version 10 (Ashland, OR, United States).

RNA Isolation and Real-Time Quantitative PCR Analysis

Total mRNA was obtained from HepG2 cells using the TRIzol reagent, and cDNA was obtained using a cDNA synthesis kit. The primer sequences are listed in **Table 1**. According to the manufacturer's protocol, Q-PCR was performed in a real-time PCR system. The $2^{-\Delta\Delta}$CT method was used for quantitative analysis, and results were normalized with β-actin.

Inhibitor Treatment

To clarify the effects of PNS on ATP1A1 and signaling pathways in HepG2, the Na^+/K^+-ATPase inhibitor (digitonin) was used in the experiment. The treatment was divided into five groups, including 10 nmoL/L digitonin group, 10 nmoL/L digitonin combined with 600 mg/L PNS group, 10 nmoL/L digitonin combined with 300 mg/L PNS group, 600 mg/L PNS group, and 300 mg/L PNS group. After 48 h of drug treatment, the proteins of HepG2 cells were detected by Western blot.

Colony Formation Assay

HepG2 cells (600 cells/well) were incubated in 6-well plates and were treated with 600 and 300 mg/L PNS. One week later, visible colonies were formed. Then, the colonies were fixed with 4% polymethanol and stained with crystal violet (0.005%). The number of colonies was calculated using a microscope.

Hoechst Staining Assay

HepG2 cells were incubated in 6-well plates and treated with PNS (600 mg/L and 300 mg/L) for 48 h. The cells were then incubated with 500 μl/well of Hoechst stain (Beyotime, Nanjing, China) for 15 min at room temperature. The cells were observed under a fluorescence microscope (Nikon, Japan).

Fluorescence

Cells (4×10^5/well) were incubated in a 12-well plate containing cell slides for 24 h and continued to be incubated for 48 h after administration. The cells were washed 3 times with PBS, at room temperature, then 1 ml of 4% paraformaldehyde was added to each well for 30 min, and finally the cells were washed thrice with PBS. After blocking

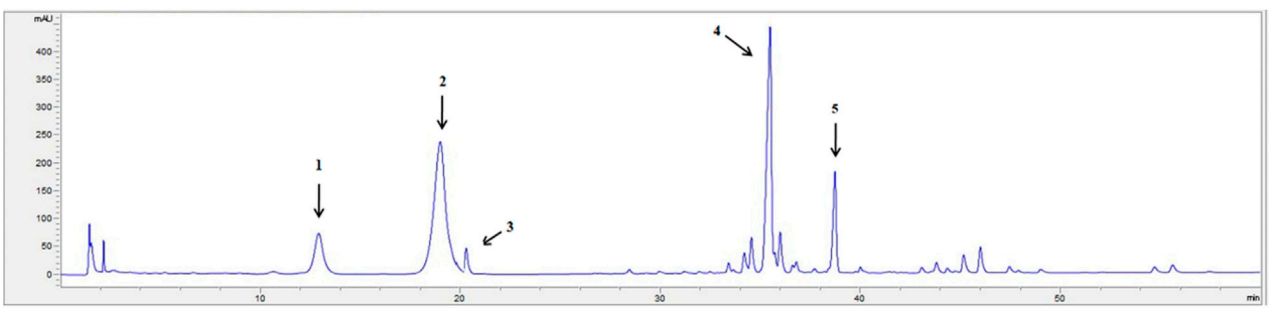

FIGURE 1 | The HPLC fingerprint profile of PNS. 1: notoginsenoside R_1; 2: ginsenoside Rg_1; 3: ginsenoside Re; 4: ginsenoside Rb_1; 5: ginsenoside Rd. The chromatography was performed on an Agilent SB-C18 column (250 × 4.6 mm, 5 μm), at 30°C, with a UV detection rate of λ = 203 nm and flow rate = 1.5 ml/min. Gradient elution: acetonitrile (A) and Water (B): 0 min 20% A, 20 min 20% A, 45 min 46% A, 55 min 55% A, 60 min 55% A. The HPLC chromatogram of PNS was authenticated according to the Pharmacopoeia of the People's Republic of China identification key (2015, Volume 1).

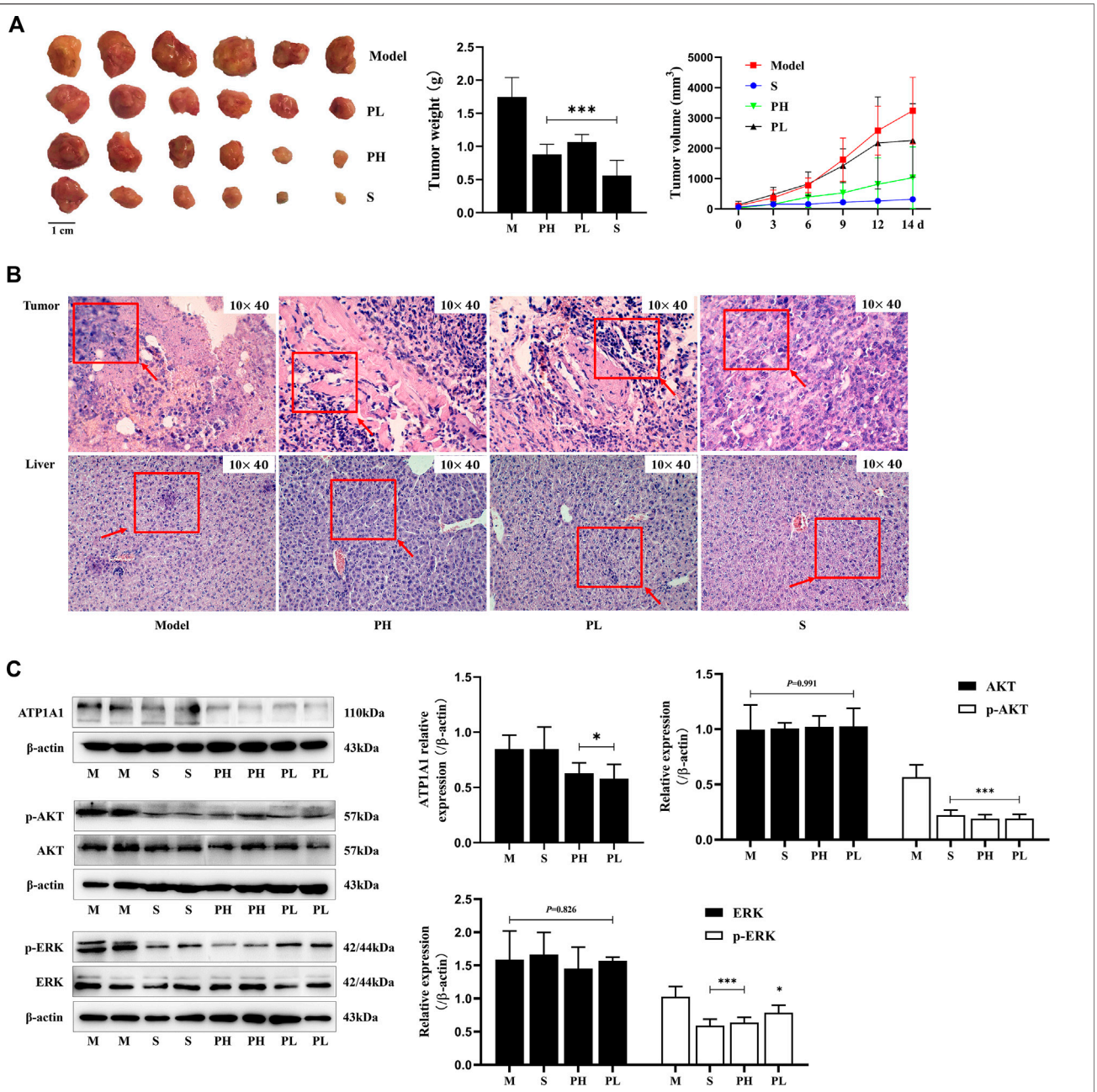

FIGURE 2 | PNS inhibited tumor growth and downregulated the ATP1A1/AKT/ERK signaling pathway. Twenty-four tumor-bearing mice were treated with saline, sorafenib (60 mg/kg), or PNS (50 and 100 mg/kg) by intragastric administration every day for 14 days. **(A)** The morphologies of tumors were photographed, and tumor weights and volumes were measured. **(B)** The HE-stained images of tumors were photographed. **(C)** The Western blot images of ATP1A1, AKT, p-AKT, ERK, and p-ERK and their quantitative analysis are shown. M: saline group; S: sorafenib group; PH: 100 mg/kg PNS group; PL: 50 mg/kg PNS group. Data are expressed as mean ± SD. *$p < 0.05$, **$p < 0.01$, and ***$p < 0.001$ vs. the model group.

with an antibody-blocking solution (FDB) for 30 min, the cells were incubated with the primary antibody (1:100 dilution) overnight at 4°C and washed 3 times with PBS, and the secondary antibody (FITC-goat anti-rabbit IgG antibody, 1: 200-fold dilution) of 200 μl/well was added. The cells were washed 5 times with PBS, incubated with DPAI (100 μl/well) for 10 min at room tenmperature in the dark, and then washed 3 times with PBS. The cells were detected with a laser confocal microscope.

Western Blot Analysis

Tumor tissues and HepG2 cells were lysed in an RIPA buffer solution containing PMSF and protein inhibitors (Roche, Germany). A nucleic acid and protein microanalyzer

TABLE 2 | Effects of PNS on cell viability of HepG2 cells ($\bar{x} \pm s$, n = 3).

Group	Concentration (mg•L^{-1})	Cell viability (%)
Control PNS	—	100 ± 0.32
	18.75	79.71 ± 5.23
	37.5	85.43 ± 4.27
	75	64.48 ± 3.21
	150	54.07 ± 2.12
	300	29.25 ± 4.08
	600	8.03 ± 0.94
IC_{50} (mg•L^{-1})		124.83 ± 11.24

(Molecular Devices, United States) was used to determine the protein concentration. The proteins were separated using 10% SDS-PAGE gel and transferred onto PVDF membranes. The membranes were blocked with 5% nonfat milk for 2 h and incubated with primary antibodies at 4°C overnight. The membranes were washed with PBST, and the protein bands were detected by the ECL and were exposed to the TANON gel imager (Shanghai, China). The results were analyzed by ImageJ software. Because the molecular weights of the target proteins were the same, the primary and secondary antibodies were removed using a stripping buffer (P0025N, Beyotime Biotechnology, China) and then the membranes were washed with PBST and finally blocked and incubated with the antibodies for subsequent experiments.

Molecular Docking

The structure of ATP1A1 (PDB code 3KDP) was utilized as a receptor. The three-dimensional chemical structure of ginsenoside Rg_1 and ginsenoside Rb_1 was obtained from ChemDraw 3D software, and they were prepared for ligand binding. All of them were preserved in the PDB format for the following procedures. By optimizing Autodock Vina software, ginsenoside Rg_1 and ginsenoside Rb_1 interacted with ATP1A1 at a molecular simulative level. The docking center was set as center_x = −21.896, center_y = −12.893, and center_z = 82.863, respectively, and the number of points was set as 60 individually.

Statistical Analysis

Data were presented as the mean ± standard deviation (SD). Independent two-sample t-tests were used to compare differences between two groups, and one-way ANOVA with the least significant difference (LSD) test for post hoc comparisons was used to compare differences between groups. $P < 0.05$ was indicated as statistical significance. Statistical analysis was performed using SPSS 21.0 software (SPSS Inc., Chicago, IL, United States). Figures were constructed using GraphPad Prism 8 software.

RESULTS

The Quality Control Results of PNS

The HPLC chromatogram of PNS is displayed in **Figure 1**. The contents of each ingredient in the PNS extract included notoginsenoside R_1 (10.16 ± 0.31%), ginsenoside Rg_1 (36.47 ± 1.78%), ginsenoside Re (3.51 ± 0.37%), ginsenoside Rb_1 (30.79 ± 2.00%), and ginsenoside Rd (9.07 ± 0.25%) and met the Chinese Pharmacopoeia (2015 edition) criterion (**Supplementary Figure S1**).

PNS Inhibited Tumor Growth and Suppressed ATP1A1/AKT/ERK Signaling Pathways at the Tumor Sites

PNS inhibited tumor growth in H22 tumor-bearing mice (**Figure 2A**). 0–7 days after administration, the mice had a better diet and mental state. After 7 days, with the rapid increase in the tumor volume (**Figure 2A**), the mice's diet gradually decreased, they were too lazy to exercise, and the amount of feces and urine decreased. The pathological morphology results showed that there was no clear boundary between the tumor and the muscle tissue in the model group and they were completely fused together. The nest-like structure of the tumor tissue in the PH group had obvious boundaries, and the area surrounding the muscle was less. The tumor cells were deeply stained, and the arrangement of cells was crowded and disorderly in the PL group (**Figure 2B**). As displayed in **Figure 2C**, ATP1A1 expression and phosphorylation of ERK and AKT were significantly reduced in the PNS and sorafenib groups ($P < 0.05$), but not the expression of ERK and AKT.

PNS Inhibited the Viability, Migration, and Proliferation of HepG2 Cells

The MTT assay was used to better evaluate the antitumor viability of PNS (**Table 2**). The IC_{50} was 124.83 ± 11.24 mg/L. Based on the result, we used two and four times the IC_{50} for experiments as follows (300 mg/L and 600 mg/L). As shown in **Figure 3A**, the cell viability of HepG2 cells decreased in a dose-dependent manner after PNS treatment. The results of cell migration and colony experiments showed that 300 mg/L of PNS could significantly inhibit the migration of HepG2 cells and the formation of cell clones (**Figures 3B,C**) and the effect of 600 mg/L was more significant. Flow cytometry and Hoechst staining were used to detect changes in the rate of apoptosis and nuclear condensation and lysis in HepG2 cells (**Figures 3D,E**). The results showed that compared with the control group, the apoptosis rate of nuclear fragmentation of HepG2 cells increased after PNS treatment for 48 h. PNS inhibited the survival rate and migration rate and increased the apoptosis rate of HepG2 cells.

PNS Regulated ATP1A1–Activated AKT, ERK, and PKC Signaling

ATP1A1 expression levels were higher in HepG2 cells than in L02 cells (**Figure 4A**). PNS could inhibit the expression and phosphorylation of ATP1A1 in both cell lines. We detected the effect of PNS on ATP1A1–relative signaling pathways. Compared with L02 cells, the AKT and ERK signaling pathways were activated in HepG2 cells, especially the expression and phosphorylation of AKT. PNS inhibited

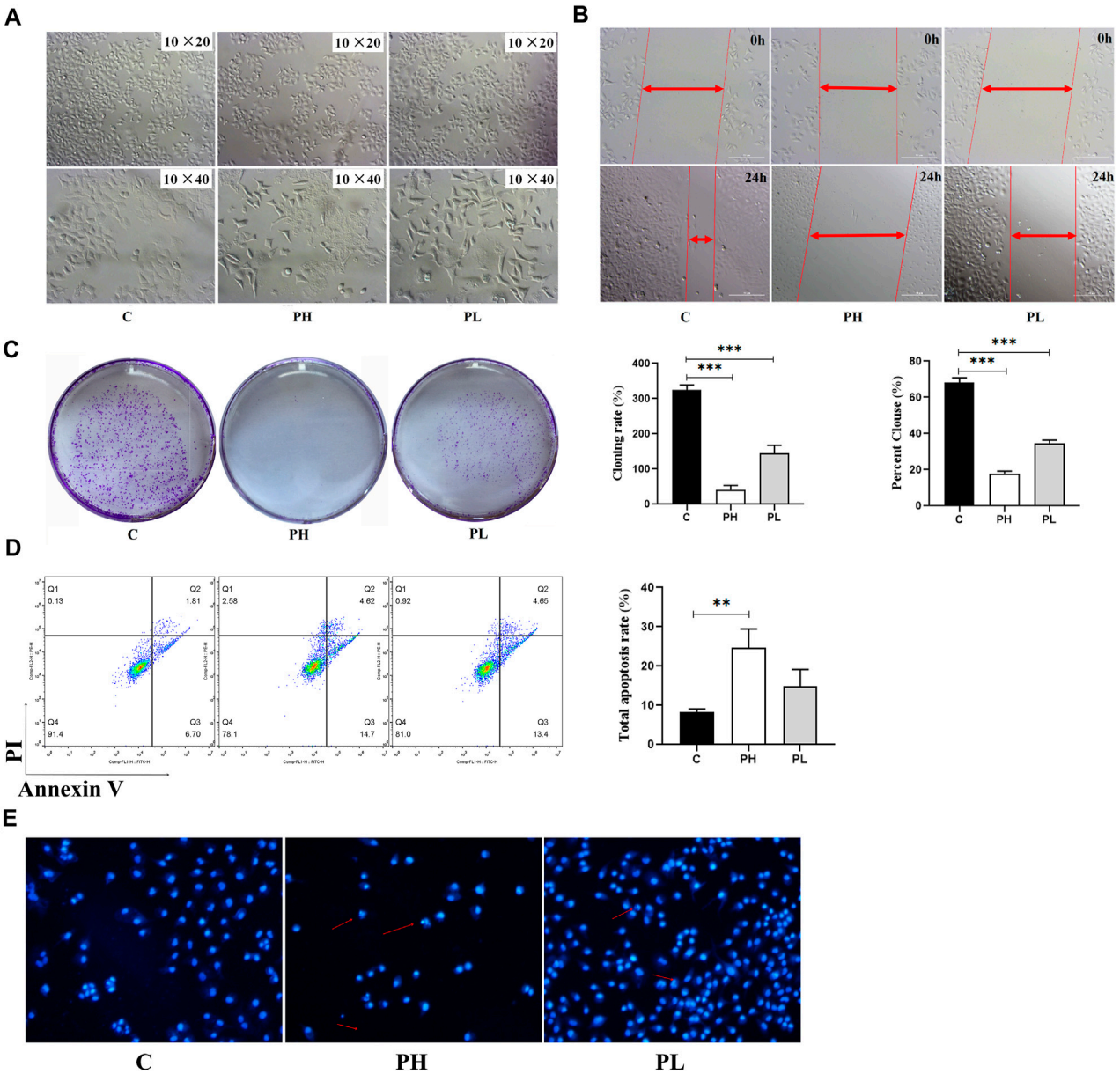

FIGURE 3 | PNS inhibited the proliferation and migration of HepG2 cells. C: control group; PH: high-dose PNS group (600 mg/L); PL: PNS low-dose PNS group (300 mg/L). **(A)** The morphology images of HepG2 cells treated with saline and PNS for 48 h. **(B)** The effect of PNS on the migration of HepG2 cells. **(C)** Giemsa-stained colonies were observed under an inverted microscope. **(D)** FACS analysis of apoptosis in HepG2 cells. The cells were double-stained with Annexin V and PI. Early apoptotic cells were in the lower right quadrant, and late apoptotic cells were in the upper right quadrant. The histogram in the right panel showed average percentages of apoptotic cells which contained the early apoptotic cells and late apoptotic cells. **(E)** Fluorescence images were detected by Hoechst staining. Data are presented as the means ± SD of triplicate experiments. $^{*}p < 0.05$, $^{**}p < 0.01$, and $^{***}p < 0.001$, vs. the control group.

the phosphorylation of AKT and ERK and promoted the expression of Bax but inhibited Bcl 2. Compared with the control, both sorafenib and PNS downregulated the phosphorylation of AKT, ERK, and mTOR but sorafenib did not regulate the expression and phosphorylation of ATP1A1. Compared with the PNS groups, sorafenib had a more significant effect on AKT/ERK signaling pathways (**Figure 4B**). As shown in **Figure 4C**, PNS decreased the expression and phosphorylation of ATP1A1 in a dose-dependent manner, inhibiting the activation of AKT, ERK, and p38. PNS reduced the expression of PKC α but promoted the activation of PKC δ. The results of Q-PCR showed the same changes in the expression of AKT, ERK, and ATP1A1. The fluorescence intensity of ATP1A1 in HepG2 cells was decreased after PNS treatment and showed a dose-dependent manner (**Figure 4D**).

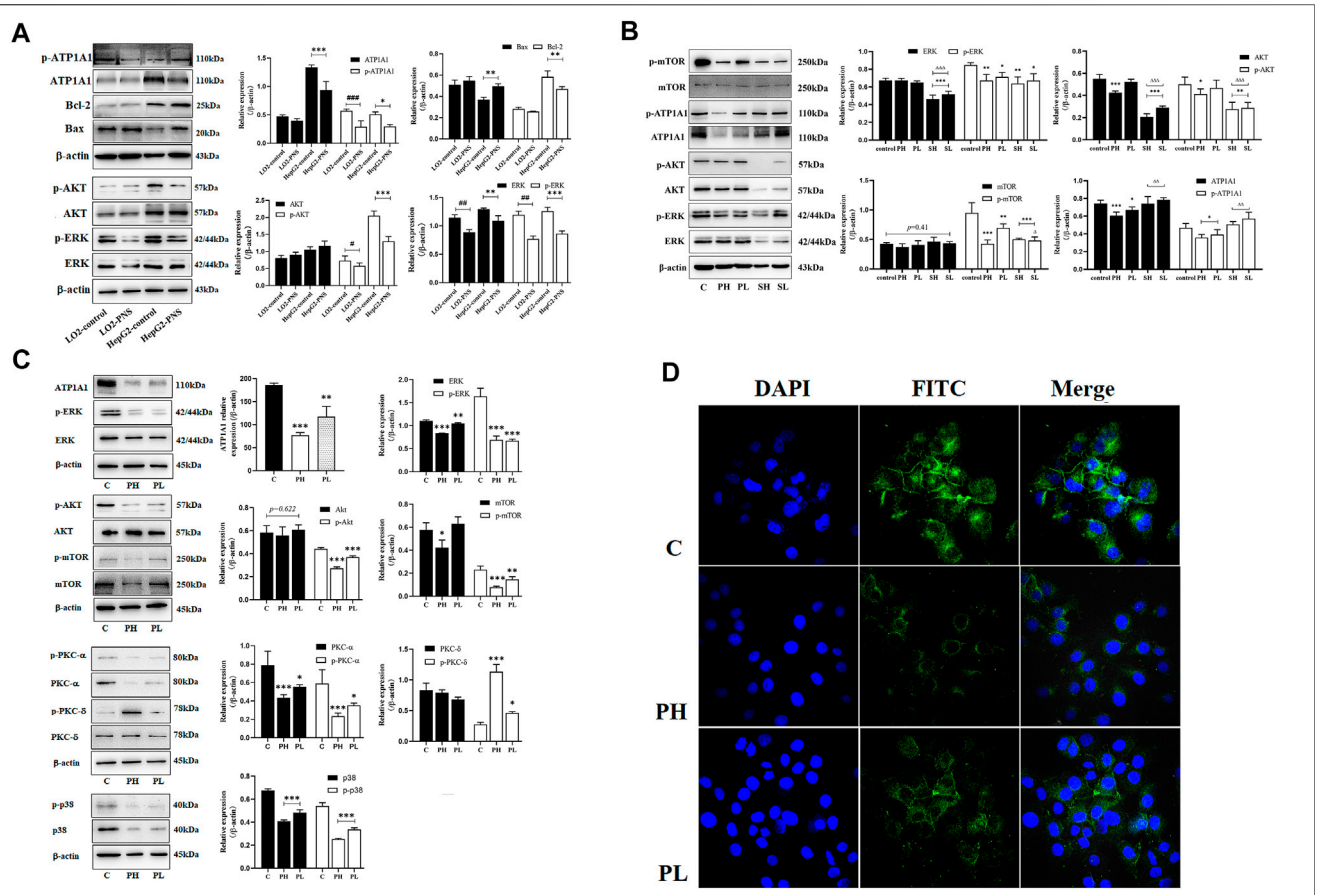

FIGURE 4 | PNS reduced the expression of ATP1A1 and downregulated AKT/ERK signaling pathways. SH: 20 μmoL●L^{-1}; SL: 10 μmoL●L^{-1}. **(A)** The effects of PNS on regulating the expression of ATP1A1 and AKT/ERK signaling pathways in L02 cells and HepG2 cells. **(B)** The effects of PNS and sorafenib on regulating the expression and phosphorylation of ATP1A1/AKT/ERK signaling pathways. **(C)** The image of proteins after PNS treatment in HepG2 cells. **(D)** The fluorescence image of laser confocal detection of ATP1A1 expression in the HepG2 cell membrane (10 × 60). Scale bar = 50 μm. Data are expressed as mean ± standard deviation. $^{*}p < 0.05$, $^{**}p < 0.01$, and $^{***}p < 0.001$ vs. the control group; $^{\#}p < 0.05$, $^{\#\#}p < 0.01$, and $^{\#\#\#}p < 0.001$ vs. the L02 control group. $^{\Delta}p < 0.05$, $^{\Delta\Delta}p < 0.01$, and $^{\Delta\Delta\Delta}p < 0.001$ vs. the PNS group.

Digitonin Decreased the Role of PNS on the Regulation of PI3K/AKT/mTOR and ERK Signaling Pathways, but Not the PKC Signaling Pathway

Low concentrations of digitonin block tumor cell growth without affecting the Na^+/K^+-ATPase activity (Fujii et al., 2018). The results showed that the expression of ATP1A1 in the PNS group was significantly reduced, but not in the digitonin group and in the cotreatment group (**Figure 5A**). The Western blot analysis showed that the expression and phosphorylation of AKT, mTOR, and ERK in HepG2 cells were inhibited after PNS treatment for 48 h. Digitonin attenuated the effect of PNS on AKT and ERK signaling pathways. The expression and phosphorylation of PKC δ were dramatically upregulated in all groups. qRT-PCR results showed similar results (**Figure 5B**). Fluorescence results showed that there was no complete nuclear morphology in the digitonin group and the relative fluorescence intensity of ATP1A1 did not decrease but increased (**Figure 5C**). The result of ATP1A1 expression in PNS co-treatment group was same in digitonin group. ATP1A1 was significantly reduced in PNS groups, and compared with the digitonin group, the amount of cell death was reduced.

PNS Combined With Na^+/K^+-ATPase α1 Subunit

As shown in **Figure 6**, the α1 subunit was essentially involved in modulating the binding with cardiotonic steroids. The high affinity of Na^+/K^+-ATPase phosphoenzyme (E2P) was because of the transmembrane helices αM1–6 of the α subunit, forming an active pocket exposed to the outside of the cell. Rg_1 and Rb_1 mainly communicated with residues of αM1–4, such as VAL132, ASP121, and VAL798. The forces that they interacted with were predominantly the conjugation effect and H-bond force. The computational results suggested that the conjugated energy of Rb_1 is less than that of Rg_1 and more stable than that of Rg_1.

DISCUSSION

Panax notoginseng, as a classic traditional Chinese medicine, has been widely used in clinical treatment, including trauma,

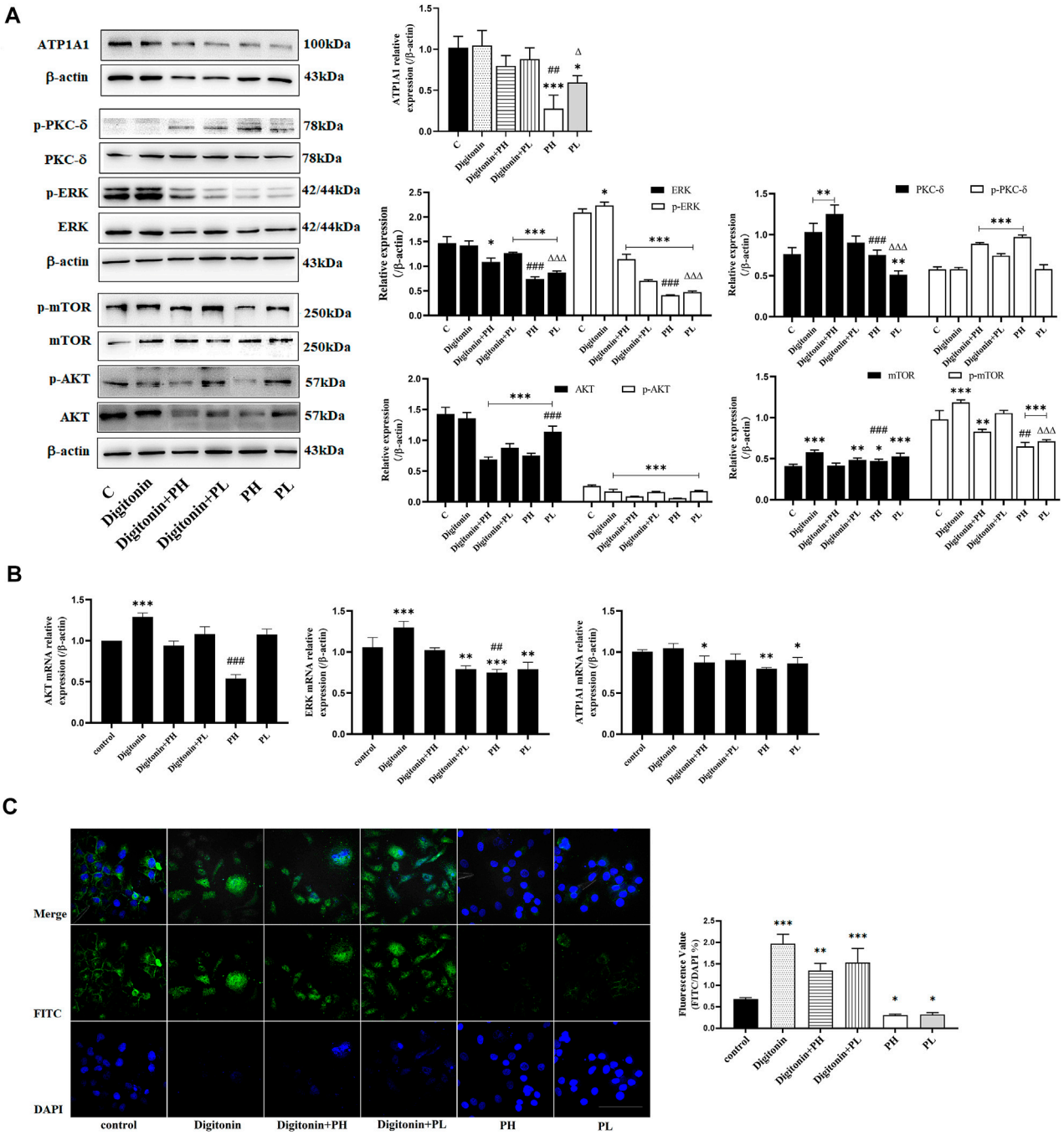

FIGURE 5 | PNS and digitonin regulated the expression of proteins and mRNA of ATP1A1/AKT/ERK signaling pathways. Digitonin: 10 nmol/L; PH: 600 mg/L PNS; and PL: 300 mg/L PNS. **(A)** The representative image of Western blot after treatment with PNS and digitonin and their quantitative analysis are shown. **(B)** The relative expression of AKT, ERK1/2, and ATP1A1 by Q-PCR and their quantitative analysis are shown. **(C)** The fluorescence image of laser confocal detection of the expression of ATP1A1 on the HepG2 cell membrane (10 × 60). Scale bar = 50 μm. Data are expressed as mean ± standard deviation. $^{*}p < 0.05$, $^{**}p<0.01$, and $^{***}p < 0.001$ vs. the control group; $^{\Delta}p < 0.05$, $^{\Delta\Delta}p < 0.01$, and $^{\Delta\Delta\Delta}p < 0.001$ vs. the digitonin + PH group; $^{\#}p < 0.05$, $^{\#\#}p < 0.01$, and $^{\#\#\#}p < 0.001$ vs. the digitonin + PL group.

cardiovascular disease, and cerebral ischemic stroke. As the main active components of *Panax notoginseng* (Burk.) F.H. Chen, PNS have multiple biological activities, including anti-inflammatory, antioxidative, and antitumor properties. Although the antitumor effect of PNS has been widely studied, the exact mechanism has not been fully elucidated. PNS could inhibit the tumor growth *in vivo* and inhibit proliferation and migration of tumor cells *in vitro*. The mechanisms are related to the regulation of PI3K/AKT/mTOR and NF-κB signaling pathways. However, how PNS regulate the signaling pathways has not yet been explained. Our present

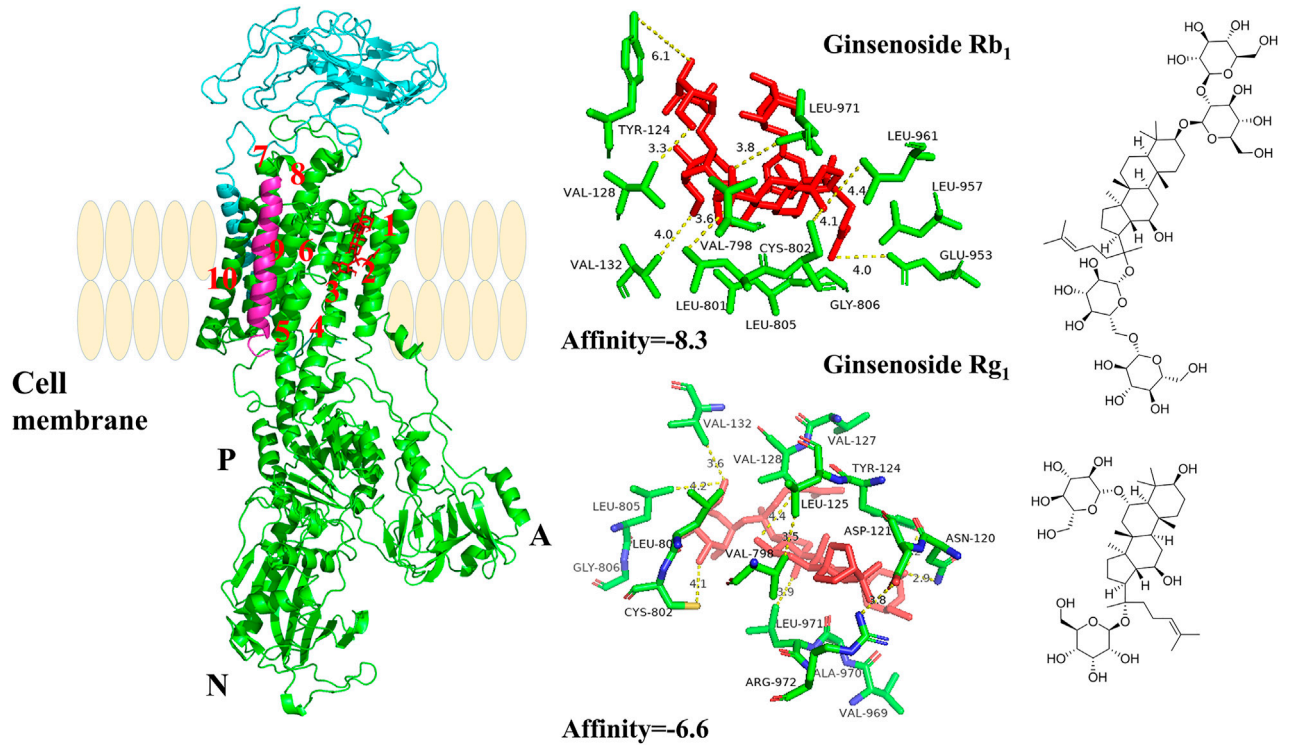

FIGURE 6 | The crystal structure of the high-affinity Na^+/K^+-ATPase α1 subunit–ginsenoside Rb1 or –ginsenoside Rg1 complex. Ginsenoside Rb1 or ginsenoside Rg1 are depicted in red, and the chains of Na+/K+-ATPase α/β/γ subunits are represented by green, cyan blue, and magenta, respectively. Data deposition: the crystallography, atomic coordinates, and structure factors have been deposited in the Protein Data Bank (www.pdb.org (PDB ID code 3KDP)).

study focused on the effect of PNS on the ATP1A1 activity of HepG2 cells and the possible mechanism. ATP1A1 is a widely expressed membrane protein. Research studies had showed that ATP1A1 could be a novel therapeutic target for hepatocellular carcinoma. Based on the antitumor activity of PNS *in vivo* and *in vitro* and its regulatory effect on ATP1A1, we hypothesized that PNS could inhibit the proliferation and migration of HepG2 cells *via* the regulation of ATP1A1 transduction signaling and promote HepG2 cell apoptosis *in vitro*.

The expression of ATP1A1 in tumor tissues is higher than in surrounding tissues, and only about 30% of ATP1A1 participates in the function of NKAs. Most NKAs are involved in tyrosine kinase–dependent cell signal transduction, such as Src, of which ATP1A1 is the main participant in Src-mediated signal transduction (Liang et al., 2007; Zhuang et al., 2015). When knocking out a copy of the ATP1A1 gene, the expression of the α1 subunit will be reduced by 20–30%, resulting in at least a one-fold decrease in the activity of Src and MAPK (Chen et al., 2009; Lan et al., 2018). Src can regulate downstream proteins and cell functions (Wu et al., 2013), including PI3K/AKT, PLC/PKC, and JAK/STAT signaling pathways. In this study, we first observed that PNS could reduce the expression of ATP1A1 in tumor tissues of tumor-bearing mice. At the same time, we found that PNS downregulated the phosphorylation of AKT and ERK. *In vitro,* the results showed that the ATP1A1 expression was higher in HepG2 cells than in L02 cells. PNS could downregulate the expression of ATP1A1 and phosphate-ATP1A1 in L02 and HepG2 cells; meanwhile, PNS promoted the apoptosis of HepG2 cells and inhibited AKT/mTOR and ERK/MAPK activation. Sorafenib is a well-known drug used to treat HCC in clinics, as a Raf inhibitor, which significantly inhibits the phosphorylation of MEK and ERK, but not the expression of MEK and ERK, and inhibits the AKT signaling pathway. Compared with the control group, both sorafenib and PNS downregulated the phosphorylation of AKT, ERK, and mTOR. It was worth noting that sorafenib significantly reduced the expression of ERK and AKT, but not the expression and phosphorylation of ATP1A1. However, compared with the PNS groups, sorafenib had a more significant effect on the AKT/ERK signaling pathways. Combined with the antitumor effects of PNS, we suggested that one possible mechanism of PNS exerted the antitumor effect *via* inhibiting ATP1A1/AKT/MAPK signaling pathways *in vitro*.

The crosstalk between AKT and ERK signaling regulates each other and coregulates downstream signaling in certain cells (Lan et al., 2018). This study showed that PNS could inhibit the expression and phosphorylation of AKT and ERK and showed a dose-dependent effect. To better know the effect of PNS on the regulation of NKA, we used digitonin to inhibit the activation of NKA. We found that digitonin could significantly induce HepG2 cell lysis without affecting the expression of ATP1A1. When PNS were used in combination with digitonin, the expression of ATP1A1 was significantly downregulated compared with the digitonin group. The

reasons were that digitonin reduced Na^+/K^+ exchange to cause cytomembrane depolarization by increasing intracellular Na^+ concentration and reduced the dephosphorylation level of ATP to increase the permeability of the cytomembrane, promote nuclear fragmentation, and cause cell death (Robinson, 1980). The combined effect of the two drugs reduced the expression of ATP1A1 and promoted the death of HepG2 cells. Besides, digitonin attenuated the effects of PNS on the AKT/ERK signaling pathways. These observations implied that ATP1A1 played an important role in the regulation of AKT/ERK signaling pathways. Additional studies are also needed to determine the mutual regulation of ATP1A1 and the AKT/ERK signaling pathway and whether PNS can affect ATP1A1 in patients with HCC. The mechanism of PNS on tumors with a low expression of ATP1A1 needs to be further illustrated.

CONCLUSION

Taken together, the study demonstrated for the first time that PNS could inhibit proliferation and migration of HepG2 cells by the regulation of ATP1A1 to affect AKT and ERK signaling pathways. The antitumor mechanism of PNS was related to suppressing the AKT and ERK signaling pathways to trigger apoptosis. Our findings will be helpful for further research and could provide a data basis for the clinical use of PNS.

DATA AVAILABILITY STATEMENT

The original contributions presented in the study are included in the article/**Supplementary Material**; further inquiries can be directed to the corresponding authors.

ETHICS STATEMENT

The animal study was reviewed and approved by the Animal Ethics Committee of Yunnan University of Chinese Medicine (No. R062019061).

AUTHOR CONTRIBUTIONS

The original draft was prepared by X-YF. Data curation was performed by ZY and N-YW. Formal analysis was carried out by WZ. Conceptualization of the work was explored by W-HC. Reviewing and editing were performed by A-HS. All authors have read and agreed to the published version of the manuscript.

FUNDING

This research was supported financially by the National Natural Science Foundation of China (No. 82060737), the Science and Technology Planning Project of Yunnan Province (No. 202001AT070122), and Xu Hongxi Expert Workstation of the Yunnan University of Traditional Chinese Medicine (No. 2019IC020).

SUPPLEMENTARY MATERIAL

The Supplementary Material for this article can be found online at https://www.frontiersin.org/articles/10.3389/fphar.2021.720368/full#supplementary-material

REFERENCES

Cai, T., Wu, W., Guo, L., Xia, Y., Jiang, X., Zhang, L., et al. (2021). Notoginsenoside R1 Induces DNA Damage via PHF6 Protein to Inhibit Cervical Carcinoma Cell Proliferation. *Mol. Med. Rep.* 23 (4), 242. doi:10.3892/mmr.2021.11881

Chen, J. Q., Contreras, R. G., Wang, R., Fernandez, S. V., Shoshani, L., Russo, I. H., et al. (2006). Sodium/potassium ATPase (Na+,K+-ATPase) Andouabain/related Cardiac Glycosides: a New Paradigm for Development of Anti-breast Cancer Drugs. *Breast Cancer Res. Treat.* 96, 1–15. doi:10.1007/s10549-005-9053-3

Chen, Y., Cai, T., Wang, H., Li, Z., Loreaux, E., Lingrel, J. B., et al. (2009). Regulation of Intracellular Cholesterol Distribution by Na/K-ATPase. *J. Biol. Chem.* 284 (22), 14881–14890. doi:10.1074/jbc.M109.003574

Fujii, T., Shimizu, T., Yamamoto, S., Funayama, K., Fujita, K., Tabuchi, Y., et al. (2018). Crosstalk between Na+,K+-ATPase and a Volume-Regulated Anion Channel in Membrane Microdomains of Human Cancer Cells. *Biochim. Biophys. Acta Mol. Basis Dis.* 1864 (11), 3792–3804. doi:10.1016/j.bbadis.2018.09.014

Hu, S., Wu, Y., Zhao, B., Hu, H., Zhu, B., Sun, Z., et al. (2018). Panax Notoginseng Saponins Protect Cerebral Microvascular Endothelial Cells against Oxygen-Glucose Deprivation/Reperfusion-Induced Barrier Dysfunction via Activation of PI3K/Akt/Nrf2 Antioxidant Signaling Pathway. *Molecules* 23 (11), 2781. doi:10.3390/molecules23112781

Hui, D., Rui-Zhi, T., Jian-Chun, L., Xia, Z., Dan, W., Jun-Ming, F., et al. (2020). *Astragalus propinquus* Schischkin and Panax Notoginseng (A&P) Compound Relieved Cisplatin-Induced Acute Kidney Injury through Inhibiting the Mincle Maintained Macrophage Inflammation. *J. Ethnopharmacol.* 252, 112637. doi:10.1016/j.jep.2020.112637

Lan, Y. L., Wang, X., Lou, J. C., Xing, J. S., Zou, S., Yu, Z. L., et al. (2018). Marinobufagenin Inhibits Glioma Growth through Sodium Pump α1 Subunit and ERK Signaling-Mediated Mitochondrial Apoptotic Pathway. *Cancer Med.* 7 (5), 2034–2047. doi:10.1002/cam4.1469

Lan, Y. L., Yu, Z. L., Lou, J. C., Ma, X. C., and Zhang, B. (2018). Update on the Effects of the Sodium Pump α1 Subunit on Human Glioblastoma: from the Laboratory to the Clinic. *Expert Opin. Investig. Drugs.* 27, 753–763. doi:10.1080/13543784.2018.1512582

Li, Q., Yuan, M., Li, X., Li, J., Xu, M., Wei, D., et al. (2020a). New Dammarane-type Triterpenoid Saponins from Panax Notoginseng Saponins. *J. Ginseng Res.* 44 (5), 673–679. doi:10.1016/j.jgr.2018.12.001

Li, W., She, W., Hu, X., and Wu, X. (2019). Targeted Antitumor Activity of Ginsenoside (Rg1) in Paclitaxel-Resistant Human Nasopharyngeal Cancer Cells Are Mediated through Activation of Autophagic Cell Death, Cell Apoptosis, Endogenous ROS Production, S Phase Cell Cycle Arrest and Inhibition of M-Tor/pi3k/AKT Signalling Pathway. *J. BUON* 24 (5), 2056–2061.

Li, Y., Li, Z., Jia, Y., Ding, B., and Yu, J. (2020b). *In Vitro* Anti-hepatoma Activities of Notoginsenoside R1 through Downregulation of Tumor Promoter miR-21. *Dig. Dis. Sci.* 65 (5), 1364–1375. doi:10.1007/s10620-019-05856-4

Liang, M., Tian, J., Liu, L., Pierre, S., Liu, J., Shapiro, J., et al. (2007). Identification of a Pool of Non-pumping Na/K-ATPase. *J. Biol. Chem.* 282 (14), 10585–10593. doi:10.1074/jbc.M609181200

Lingrel, J. B., Williams, M. T., Vorhees, C. V., and Moseley, A. E. (2007). Na,K-ATPase and the Role of Alpha Isoforms in Behavior. *J. Bioenerg. Biomembr.* 39 (5-6), 385–389. doi:10.1007/s10863-007-9107-9

Lu, Q. G., Zeng, L., Li, X. H., Liu, Y., Du, X. F., Bai, G. M., et al. (2020). Protective Effects of Panax Notoginseng Saponin on Dextran Sulfate Sodium-Induced Colitis in Rats through Phosphoinositide-3-Kinase Protein Kinase B Signaling Pathway Inhibition. *World J. Gastroenterol.* 26 (11), 1156–1171. doi:10.3748/wjg.v26.i11.1156

Meng, L., Ji, R., Dong, X., Xu, X., Xin, Y., and Jiang, X. (2019). Antitumor Activity of Ginsenoside Rg3 in Melanoma through Downregulation of the ERK and Akt Pathways. *Int. J. Oncol.* 54 (6), 2069–2079. doi:10.3892/ijo.2019.4787

Robinson, J. D. (1980). Sensitivity of the (Na+ + K+)-Atpase to State-dependent Inhibitors. Effects of Digitonin and Triton X-100. *Biochim. Biophys. Acta.* 598 (3), 543–553. doi:10.1016/0005-2736(80)90034-6

Sweadner, K. J., Arystarkhova, E., Penniston, J. T., Swoboda, K. J., Brashear, A., and Ozelius, L. J. (2019). Genotype-structure-phenotype Relationships Diverge in Paralogs ATP1A1, ATP1A2, and ATP1A3. *Neurol. Genet.* 5 (1), e303. doi:10.1212/NXG.0000000000000303

Wang, P., Cui, J., Du, X., Yang, Q., Jia, C., Xiong, M., et al. (2014). Panax Notoginseng Saponins (PNS) Inhibits Breast Cancer Metastasis. *J. Ethnopharmacol.* 154 (3), 663–671. doi:10.1016/j.jep.2014.04.037

Wu, J., Akkuratov, E. E., Bai, Y., Gaskill, C. M., Askari, A., and Liu, L. (2013). Cell Signaling Associated with Na(+)/K(+)-ATPase: Activation of Phosphatidylinositide 3-kinase IA/Akt by Ouabain Is Independent of Src. *Biochemistry* 52 (50), 9059–9067. doi:10.1021/bi4011804

Xu, Z. W., Wang, F. M., Gao, M. J., Chen, X. Y., Hu, W. L., and Xu, R. C. (2010). Targeting the Na(+)/K(+)-ATPase Alpha1 Subunit of Hepatoma HepG2 Cell Line to Induce Apoptosis and Cell Cycle Arresting. *Biol. Pharm. Bull.* 33 (5), 743–751. doi:10.1248/bpb.33.743

Yang, Q., Wang, P., Cui, J., Wang, W., Chen, Y., and Zhang, T. (2016). Panax Notoginseng Saponins Attenuate Lung Cancer Growth in Part through Modulating the Level of Met/miR-222 axis. *J. Ethnopharmacol.* 193, 255–265. doi:10.1016/j.jep.2016.08.040

Yu, Y., Chen, C., Huo, G., Deng, J., Zhao, H., Xu, R., et al. (2019). ATP1A1 Integrates AKT and ERK Signaling via Potential Interaction with Src to Promote Growth and Survival in Glioma Stem Cells. *Front. Oncol.* 9, 320. doi:10.3389/fonc.2019.00320

Zhao, Y., Zheng, J., Yu, Y., and Wang, L. (2018). Panax Notoginseng Saponins Regulate Macrophage Polarization under Hyperglycemic Condition via NF-Kb Signaling Pathway. *Biomed. Res. Int.* 2018, 9239354. doi:10.1155/2018/9239354

Zhuang, L., Xu, L., Wang, P., Jiang, Y., Yong, P., Zhang, C., et al. (2015). Na+/K+-ATPase α1 Subunit, a Novel Therapeutic Target for Hepatocellular Carcinoma. *Oncotarget* 6 (29), 28183–28193. doi:10.18632/oncotarget.4726

Conflict of Interest: The authors declare that the research was conducted in the absence of any commercial or financial relationships that could be construed as a potential conflict of interest.

Publisher's Note: All claims expressed in this article are solely those of the authors and do not necessarily represent those of their affiliated organizations, or those of the publisher, the editors, and the reviewers. Any product that may be evaluated in this article, or claim that may be made by its manufacturer, is not guaranteed or endorsed by the publisher.

frontiers in Pharmacology

REVIEW
published: 19 October 2021
doi: 10.3389/fphar.2021.732266

Natural Product-Based Studies for the Management of Castration-Resistant Prostate Cancer: Computational to Clinical Studies

Rajeev K. Singla[1,2†], Pooja Sharma[3,4†], Ankit Kumar Dubey[5], Rohit Gundamaraju[6], Dinesh Kumar[7], Suresh Kumar[3], Reecha Madaan[8], Richa Shri[3], Christos Tsagkaris[9], Salvatore Parisi[10], Shikha Joon[1,2], Shailja Singla[2], Mohammad Amjad Kamal[11,12,13] and Bairong Shen[1]**

[1]Institutes for Systems Genetics, Frontiers Science Center for Disease-Related Molecular Network, West China Hospital, Sichuan University, Chengdu, China, [2]iGlobal Research and Publishing Foundation, New Delhi, India, [3]Department of Pharmaceutical Sciences and Drug Research, Punjabi University, Patiala, India, [4]Khalsa College of Pharmacy, Amritsar, India, [5]Institute of Scholars, Chikmagalur, India, [6]ER Stress and Mucosal Immunology Lab, School of Health Sciences, College of Health and Medicine, University of Tasmania, Launceston, TAS, Australia, [7]Department of Pharmaceutical Sciences, Sri Sai College of Pharmacy, Amritsar, India, [8]Chitkara College of Pharmacy, Chitkara University, Punjab, India, [9]Faculty of Medicine, University of Crete, Heraklion, Greece, [10]Lourdes Matha Institute of Hotel Management and Catering Technology, Thiruvananthapuram, India, [11]West China School of Nursing/Institutes for Systems Genetics, Frontiers Science Center for Disease-Related Molecular Network, West China Hospital, Sichuan University, Chengdu, China, [12]King Fahd Medical Research Center, King Abdulaziz University, Jeddah, Saudi Arabia, [13]Enzymoics; Novel Global Community Educational Foundation, Hebersham, NSW, Australia

OPEN ACCESS

Edited by:
Bey Hing Goh,
Monash University Malaysia, Malaysia

Reviewed by:
Channing Judith Paller,
The Johns Hopkins Hospital, United States
Ali H. Eid,
Qatar University, Qatar

***Correspondence:**
Bairong Shen
bairong.shen@scu.edu.cn
Suresh Kumar
thakur_pu@yahoo.com

[†]These authors have contributed equally to this work and share first authorship

Specialty section:
This article was submitted to Ethnopharmacology, a section of the journal Frontiers in Pharmacology

Received: *28 June 2021*
Accepted: *06 September 2021*
Published: *19 October 2021*

Citation:
Singla RK, Sharma P, Dubey AK, Gundamaraju R, Kumar D, Kumar S, Madaan R, Shri R, Tsagkaris C, Parisi S, Joon S, Singla S, Kamal MA and Shen B (2021) Natural Product-Based Studies for the Management of Castration-Resistant Prostate Cancer: Computational to Clinical Studies. Front. Pharmacol. 12:732266. doi: 10.3389/fphar.2021.732266

Background: With prostate cancer being the fifth-greatest cause of cancer mortality in 2020, there is a dire need to expand the available treatment options. Castration-resistant prostate cancer (CRPC) progresses despite androgen depletion therapy. The mechanisms of resistance are yet to be fully discovered. However, it is hypothesized that androgens depletion enables androgen-independent cells to proliferate and recolonize the tumor.

Objectives: Natural bioactive compounds from edible plants and herbal remedies might potentially address this need. This review compiles the available cheminformatics-based studies and the translational studies regarding the use of natural products to manage CRPC.

Methods: PubMed and Google Scholar searches for preclinical studies were performed, while ClinicalTrials.gov and PubMed were searched for clinical updates. Studies that were not in English and not available as full text were excluded. The period of literature covered was from 1985 to the present.

Results and Conclusion: Our analysis suggested that natural compounds exert beneficial effects due to their broad-spectrum molecular disease-associated targets. *In vitro* and *in vivo* studies revealed several bioactive compounds, including rutaecarpine, berberine, curcumin, other flavonoids, pentacyclic triterpenoids, and steroid-based phytochemicals. Molecular modeling tools, including machine and deep learning, have made the analysis more comprehensive. Preclinical and clinical studies on resveratrol, soy

isoflavone, lycopene, quercetin, and gossypol have further validated the translational potential of the natural products in the management of prostate cancer.

Keywords: castration-resistant prostate cancer (CRPC), hormone-sensitive cancer, advance staged cancer, natural products (NP), natural anticancer agents, tumor microenvironment, cheminformatics

INTRODUCTION

With the global burden of cancer increasing at an alarming rate, health systems struggle to find any cost-effective strategies, particularly in poor and developing countries (Suryanarayana et al., 2015). Despite advancements in screening and early diagnosis strategies, about 20% of men have prostate cancer (PCa). PCa is predominantly controlled by androgen-binding and transcription signals from the androgen receptor (AR) (Studer et al., 2004; Singer et al., 2008; Padmanabha and Hariharan, 2016). Men with PCa usually respond to androgen deprivation therapy (ADT). However, in most individuals, the illness progresses remarkably within 2 years, which has been termed castration-resistant prostate cancer (CRPC). CRPC is a kind of advanced PCa that progresses with the circulating testosterone levels (<50 ng/dl) after being castrated surgically or pharmaceutically (Hotte and Saad, 2010; Kirby et al., 2011). Most individuals with advanced disease acquire resistance to ADT and develop CRPC (Sarkar et al., 2010). Although it has not been fully understood how the prostate cells become castrate-resistant, one of the accepted reasons is the deprivation of androgen that eventually gives androgen-independent cells a selection advantage, thus allowing them to flourish and eventually recolonize the tumor (Hoimes and Kelly, 2009). However, studies have reported that PCa cells could overcome castration-induced growth inhibition by upregulating enzymes that promote androgen production in tumor tissue (Grossmann et al., 2001). The realization that CRPC still plays a significant function in the androgen axis has prompted more research and development of therapy methods (Kirby et al., 2011; Chandrasekar et al., 2015). Even though new therapy options for individuals with advanced-stage PCa have recently been authenticated, the fact remains that CRPC is catastrophic (Lian et al., 2015).

Recent research developments have resulted in significant progress in strategies for managing PCa in terms of diagnosis and treatment. Complementary and alternative medicines (CAMs), including those from plant, animal, and microbial sources, are eliciting strong potential for the treatment management of various diseases and disorders, including cancer (Al-Menhali et al., 2015; El Hasasna et al., 2015; Athamneh et al., 2017; Fardoun et al., 2017; Elmas et al., 2018; Song et al., 2019; Nishimura et al., 2021). Pieces of evidence have supported the utility potential of CAMs; therefore, clinical studies were carried out so that CAMs would reach the patient's bedside. With advances in organic chemistry and chemical analysis, the analytical investigation has opened the door to the isolation/purification and characterization of numerous active compounds of plants (Newman et al., 2000; Singla et al., 2020a; Shen and Singla, 2020). One significant advantage of medicinal plant-based drug development is the availability of ethnopharmacological data, which can be used to narrow down the vast number of probable leads and choose the most promising ones (Choudhari et al., 2020; Singla, 2020). However, the integrated drug discovery approach supported by multidisciplinary fields, including medicinal chemistry, pharmacology, natural product chemistry, biochemistry, and molecular and cellular biology, is expected to lead to a better understanding of the potential of phytochemicals (Newman and Cragg, 2016; Singla et al., 2020b; Choudhari et al., 2020; Singla and Shen, 2020). A large number of phytochemicals, such as quercetin (Rauf et al., 2018), fisetin (Lall et al., 2016), curcumin (Ide et al., 2018), genistein (Basak et al., 2008), resveratrol (Lee et al., 2014), have been found to modulate AR activity and expression. Bioactive metabolites produced from edible plants (nutraceuticals) and traditional folk sources are potentially multitarget and are thus preferred over the primarily single-target anticancer agents, such as kinase inhibitors (Kallifatidis et al., 2016).

CASTRATION-RESISTANT PROSTATE CANCER

Epidemiology

PCa is the second most common cancer in males and the fifth-greatest cause of cancer mortality in 2020, with an anticipated 1.4

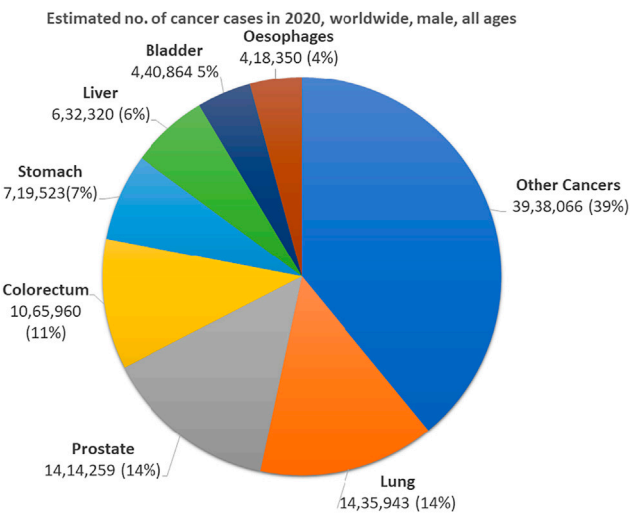

FIGURE 1 | Pie chart depicting the distribution of global prevalence of the seven most frequent cancers in 2020 for all ages. Adapted from the data published by Wild et al. (2020).

million new cases and 375,000 deaths globally (**Figure 1**) (Lin et al., 2018; Sung et al., 2021). It is considered the second leading cause of cancer-related male fatalities and the most common noncutaneous malignancy in males, with more than 160,000 new cases reported in 2017 in the United States (Zhu et al., 2015; Howlader et al., 2017; Teo et al., 2019). According to the GLOBOCAN database, in 2018, an estimated 1.2 million new cases of PCa were recorded worldwide, with developed nations having a greater prevalence. Moreover, the global burden is expected to increase to over 2.3 million and 7,40,000 deaths by 2040 (Ferlay et al., 2018; Rawla, 2019; Culp et al., 2020). PCa is prevalent in almost all major countries and is the leading cancer-related cause of death in males in over 100 nations after lung cancer (112 of 185). The incidence rate ranges from 6.3 to 110.4 per 100,000 males across countries. The higher rates were observed in Northern and Western Europe, the Caribbean, Australia/New Zealand, Northern America, and Southern Africa, whereas the lowest rates were found in Asia and Northern Africa. Previous research studies have suggested that African-American males have the highest prevalence of PCa worldwide and are more prone than other racial and ethnic groups to get the disease at a younger age (Kheirandish and Chinegwundoh, 2011). The higher rates may indicate a greater disease incidence and higher rates of PCa than other places across the globe (Wild et al., 2020; Sung et al., 2021). For a prevalent illness like PCa, little is known about its genesis, and only a few risk factors have been discovered (Lin et al., 2021). Several factors are responsible for changes in its prevalence at the regional level due to changes in the susceptibility of different population groups to environmental risk factors, including racial/ethnic backgrounds, geographical heterogeneity, advancing age and an intact hypothalamic-pituitary-gonadal axis, family history, genetic mutations (e.g., BRCA1 and BRCA2), and diagnosis and access to good quality treatment (Hoimes and Kelly, 2009; Rebbeck et al., 2013; Shackleton et al., 2021). PCa incidence and death rates differ significantly between ethnic groups, implying ethnic and genetic susceptibility (Shackleton et al., 2021). However, since the 1990s, mortality rates in PCa have declined in most high-income countries, including Northern America, Oceania, and Northern and Western Europe, due to advances in therapeutics and earlier diagnostics using enhanced screening methods (Tsodikov et al., 2017). This diversity in PCa mortality rates throughout the world is partly due to underlying biological disparities in risk and treatment availability. For example, places with higher diagnosis rates of low-grade malignancies and improved treatment choices (such as Northern America and Asia) have lower death rates than those with poor screening rates, concomitant diagnoses of aggressive tumors, and limited treatment choices (such as Sub-Saharan Africa).

Tumor Microenvironment in Castration-Resistant Prostate Cancer

Immune cells are key components of the tumor microenvironment associated with tumor progression. T regulatory cells (Tregs), tumor-associated macrophages (TAMs), tumor-infiltrating B lymphocytes (TILs), neutrophils, and myeloid-derived suppressor cells (MDSCs) are part of the infiltrated immune cell of the prostate tumor microenvironment. However, various studies have reported that the progression of PCa is influenced by the tumor-associated immune cells and inflammatory cytokines, such as IL-23 (Ammirante et al., 2010; Si et al., 2013; Calcinotto et al., 2018; Wang et al., 2019; Zhang Z. et al., 2020). TAMs are a major component in the development of PCa, though the specific pathway for the release of cytokines, matrix metalloproteinases, and growth factors is still unknown (Shimura et al., 2000; Arora et al., 2018). Castration resistance is characterized by both hyper- and/or constitutively active androgen receptor expression (AR) in PCa cells toward cellular interactions between stem cells and bone microenvironmental systems (Karamanolakis et al., 2016). The cancer cell dependency on the tumor microenvironment indicates that the noncancer cell component of the tumor can regulate the spread of PCa. However, the immune response from the tumor microenvironment contributing to the development of CRPC is unknown (Calcinotto et al., 2018). The typical prostate gland comprises prostatic ducts surrounded by epithelium and a stroma made up of smooth muscle cells with a few fibroblasts, endothelial cells, and nerve cells. ARs are widely expressed in several normal prostate stromal cell types, including smooth muscle cells, endothelial cells, and epithelial cells (Cunha et al., 1996). Multiple nonmalignant cells, such as fibroblasts, myofibroblasts, endothelial cells, and immune cells, chemokines, cytokines, growth factors, extracellular matrices (ECMs), and matrix-degrading enzymes make up the stromal compartment (Corn, 2012). The connection between the epithelial and stromal sections facilitates the progression of tumors through processes such as ECM reintegration, increasing penetration and releasing soluble growth factors for castrate-resistant growth, and angiogenesis stimulation (Rowley, 1998; Karlou et al., 2010). Immune cells are typical inhabitants and have a protective function against infections that infiltrate healthy prostatic tissue. However, histological investigations have revealed that high-grade PCa is associated with enhanced stromal immune cell infiltration with differences between tumor-stage cell types (Gurel et al., 2014).

Signaling Pathways Orchestrating Castration-Resistant Prostate Cancer

One of the factors contributing to PCa progression is androgen binding to androgen receptors. Herein, androgens play a pivotal role in the growth and survival of PCas. Moreover, increased expression of androgen receptors is often observed in CRPC (Gelmann, 2002). Androgen receptor translocates into the nucleus with the aid of ligand binding, where it orchestrates transcription, modulates growth signaling pathways, and dictates programmed cell death, cellular proliferation, and androgen-associated genes (Andersen et al., 2010). PI3K-Akt-mTOR pathway stands at the forefront of the initiation of CRPC, which is essentially triggered by G protein-coupled receptors (GPCR). Accumulating evidence has suggested that perturbations in the PI3K-Akt-mTOR pathway occur in the vast majority of

metastatic cancers; hence, PI3K-Akt-mTOR can be a potential therapeutic target (Huang et al., 2018). Phosphatase and tensin homolog (PTEN) has been associated with PI3K-Akt-mTOR triggering in advanced stages of the disease, especially the downregulation of this gene (McMenamin et al., 1999). A previous study has proven that AR is interlinked with PI3K-Akt-mTOR, where combination therapy of AR and PI3K-Akt-mTOR inhibition by EPI-002 and BEZ235 *in vitro* and *in vivo* successfully reduced LNCaP95 cell growth and was noted as a potential therapeutic avenue in CRPC (Kato et al., 2016).

Similarly, the JAK/STAT pathway is also a membrane-to-nucleus signaling pathway, which is vital for the development, proliferation, migration, and apoptosis of cells, often triggered by agents, such as cytokines and growth factors (Ramalingam et al., 2017). When triggered, JAKs induce phosphorylation of STAT proteins. Therefore, STATs are dimerized and thereby translocated to the nucleus *via* importin α-5 and the Ran nuclear import pathway. STATs display a specific stimulation or suppression of transcription of target genes by binding to specific sequences inside the nucleus (Ramalingam et al., 2017). JAK/STAT3 pathway is a well-established prosurvival inducing mechanism, where repression of this pathway reduced the PCa cell growth and induced programmed cell death (Liu et al., 2012). Oncogenes like BRAC induce proliferation and migration *via* the JAK/STAT3 pathway (Gao et al., 2001). Furthermore, STAT3 activation triggers other genes linked to the cell cycle, angiogenesis, and tumor progression (Dhir et al., 2002; Zhu and Kyprianou, 2008). In various conditions, JAK/STAT3 is a predictor of poor disease prognosis (Liu et al., 2012).

Src signaling has been implicated in promoting growth factors and inflammatory cytokines, such as IL-8, and inducing angiogenesis (Park et al., 2007). Additionally, Src signaling triggers nuclear factor-KB (Nf-KB) and tumor necrosis factors involved in evading apoptosis and promoting bone metastasis of PCa (Park et al., 2007). Targeting Src has immensely slowed down tumor growth and hindered invasion, which can be achieved using the two clinical drugs, dasatinib and saracatinib (Yang et al., 2010; Araujo et al., 2013). Moreover, growth factors, such as IGF-1, IL-6, and EGFR, can individually promote CRPC (Bettedi and Foukas, 2017). Activation of Her-2/neu, a receptor tyrosine kinase, has been observed to increase the growth of CRPC in clinical samples and xenograft models (Wen et al., 2000; Neto et al., 2010). A clinical study on targeting growth factor signaling pathways with the help of cabozantinib and tyrosine kinase inhibitor has achieved a therapeutic advantage in various stages, such as survival devoid of disease progression and marked decrease of metastatic lesions (Smith et al., 2013).

Recent evidence has revealed a regulatory mechanism, that is, crosstalk between AR and Wnt pathway, where suppression of Wnt pathway facilitates reducing AIPC cell growth by inhibiting cell cycle progression and promoting apoptosis *in vitro*. Further, a correlation between Wnt genes, like WNT5A and LEF1, and metastatic PCa has been observed (Luo et al., 2020). Wnt catenin pathway plays a principal role in homeostasis, proliferation, migration, and cell transitions (Kuhl and Kuhl, 2013). Increased catenin in PCas leads to phosphorylation and inactivation of GSK3 (Chesire and Isaacs, 2003; He et al., 2004). Inclined expression of Wnt is correlated with disease progression and metastasis. Furthermore, FZD4 overexpression favors EMT in CRPC (Polakis, 2007; Gupta et al., 2010).

Long noncoding RNAs (lncRNAs) are a group of transcripts widely employed as diagnostic tools and have received great attention because they are expressed in a more tissue-specific manner. Recent emerging evidence has shown that lncRNAs play vital roles in cancer initiation and progression, including PC progression and AR-related pathways (Ren et al., 2013; Fang et al., 2016). In a very recent study by Yao et al., LINC00675 has been abundantly found in both androgen-insensitive cells and CRPC patients. In the same study, it has been confirmed that LINC00675 binds to GATA2 mRNA and makes GATA2 an activator in the AR signaling mechanism in the nucleus, contributing to both castration resistance and disease progression (Yao et al., 2020). Signaling pathways associated with castration-resistant prostate cancer are illustrated in **Figure 2**.

An androgen receptor-dependent mechanism of resistance in hormone-naïve PCa leads to castration resistance. Apart from the AR, survival can be achieved and enhanced via cell-intrinsic pathways or progrowth signals from the microenvironment.

Genomic Targets of Phytomolecules Against Castration-Resistant Prostate Cancer

Expansion of malignant prostatic cells and normal cells and proliferation of CRPC are extremely dependent on androgens. Consequently, it has been hypothesized that androgens play a fundamental role in prostate tumor genesis. As a result, the main remedial target for PCa is reducing the levels of androgens (Zhou et al., 2015), which is accomplished through ADT. Despite this, severe complications are the resurrection of androgens and elevation of PSA. This condition is called CRPC and is characterized by a loss in the ability to respond to ADT, leading to reappearance of PCa and metastasis (Perlmutter and Lepor, 2007; Hotte and Saad, 2010). The translation of hormone-dependent PCa cells to CRPC is chiefly driven by the upregulation of AR activity. Urbanucci et al. have reported the overexpression of AR receptors in 22–30% of patients with CRPC (Urbanucci et al., 2011; Petrylak, 2013; Coutinho et al., 2016). In another study, Hay et al. have declared that the AR gene mutation was found in 22–30% of CRPC cases (Lobaccaro et al., 2012; Eisermann et al., 2013). Sharifi has shown the metabolic transformation of DHT (dihydrotestosterone). The USFDA has approved docetaxel for the management of CRPC. Similarly, cabazitaxel, another taxol derivative, has been tested in phase III clinical trial against CRPC. Numerous research groups have reported differentially expressed genes and phytochemicals established as inhibitors of identified targets for CRPC (Sharifi, 2013).

Rotimi et al. have conducted differential gene expression analysis of phytoconstituents target for CRPC. Plant-based phytomolecules were subjected to virtual screening toward GUCY1A2 variants. The results have revealed that SYT4, GUCY1A2, and GRIN3A were the most pharmacologically

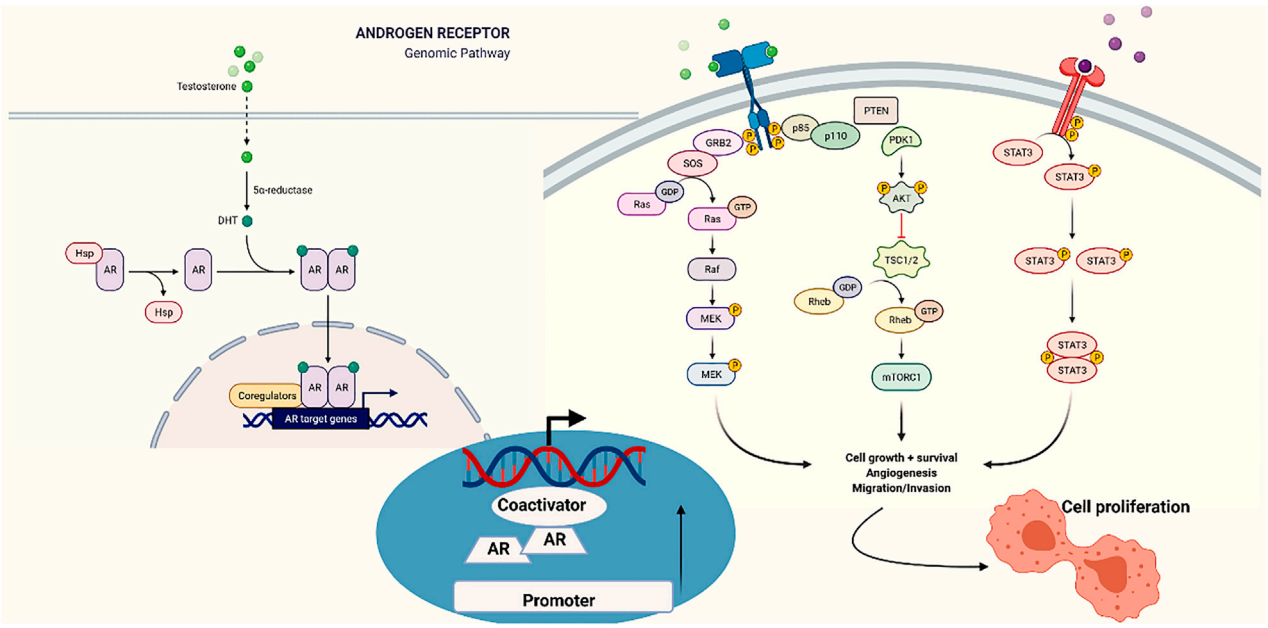

FIGURE 2 | Signaling pathways in castration-resistant prostate cancer.

significant genes implicated in the pathogenesis of CRPC in the xenograft model (Rotimi et al., 2019). The docking scores of (8′S)-neochrome and (8′R)-neochrome were −152.102 and −160.75, respectively, when targeting G723S and Q217H. In another report, Cai et al. have observed an elevated expression of the α-subunit of soluble guanylyl cyclases (α-sGC) in hormone-refractory PCa at both the mRNA and protein levels (Krumenacker et al., 2004; Cai et al., 2006). It has been found that α-sGC leads to suppression of apoptosis via accumulation of p53 in the cytoplasm; hence, it is proposed as a target for CRPC. In another approach, Liao et al. have reported the screening of natural products, including terpenes, alkaloids, flavonoids, and polyphenols. Among them, rutaecarpine, obtained from *Tetradium ruticarpum* (A.Juss.) T.G.Hartley, has been found to exhibit potential effects against CRPC using *in vitro* and *in vivo* studies in LNCap and 22 RV1 cell lines and in xenograft models, respectively. The outcomes of western blotting analysis have revealed that AR-V7 and AR-FL were expressed in LNCaP and 22Rv1. Moreover, rutaecarpine has been found to exhibit a dose-dependent downregulated AR-V7 protein expression (Liao et al., 2020). Mendiratta et al. have established the genomic stratagem to manage CRPC using a transcription-based androgen receptor activity signature toward LNCaP cell lines (Mendiratta et al., 2009). AR signature has been employed to determine whether AR activity varies with hormone therapy; progression and oncogenic pathway assays were used to recognize biologic pathways associated with AR activity. The probability of AR activity was 0.13, 0.11, 0.96, and 087 against PC-3, DU-145, LNCaP, and 22Rv PCa cell lines, respectively (Amler et al., 2000; Febbo et al., 2005; Hieronymus et al., 2006). Moreover, these genomic targets served as diagnostic and prognostic biomarkers, and their discovery has been expedited multifold due to NGS technologies (Chen et al., 2013a; Chen et al., 2013b; Shen et al., 2021). Thus, discovering these biomarkers is fundamental for developing diagnostic biosensors (Jiang et al., 2014).

NATURAL PRODUCTS FOR THE TREATMENT MANAGEMENT OF CASTRATION-RESISTANT PROSTATE CANCER

Cheminformatics and Bioinformatics-Based Studies for Anti-Castration-Resistant Prostate Cancer Natural Products

Molecular Docking-Based Studies

Molecular modeling analyses are effective tools for studying structure–activity relationships (SARs). Several plant-based molecules have been screened to detect and identify various biological activities (Willett, 1994; Kumar and Jain, 2016; Sharma et al., 2016; Kumar et al., 2017; Kaur et al., 2019; Kumar et al., 2021). In the literature, numerous phytomolecules have been obtained from plants, such as alkaloids, tannins, glycosides, coumarins, flavonoids, and polyphenolic constituents, which have been evaluated against various cancer cell lines (Kumar D. et al., 2015; Kumar et al., 2016a; Kumar et al., 2016b; Kumar et al., 2018a; Kumar et al., 2018b; Kaur et al., 2020; Sharma et al., 2021). A wide range of natural products with high biocompatibility, low toxicity, good sustainability, and a good safety profile is extensively used to manage CRPC.

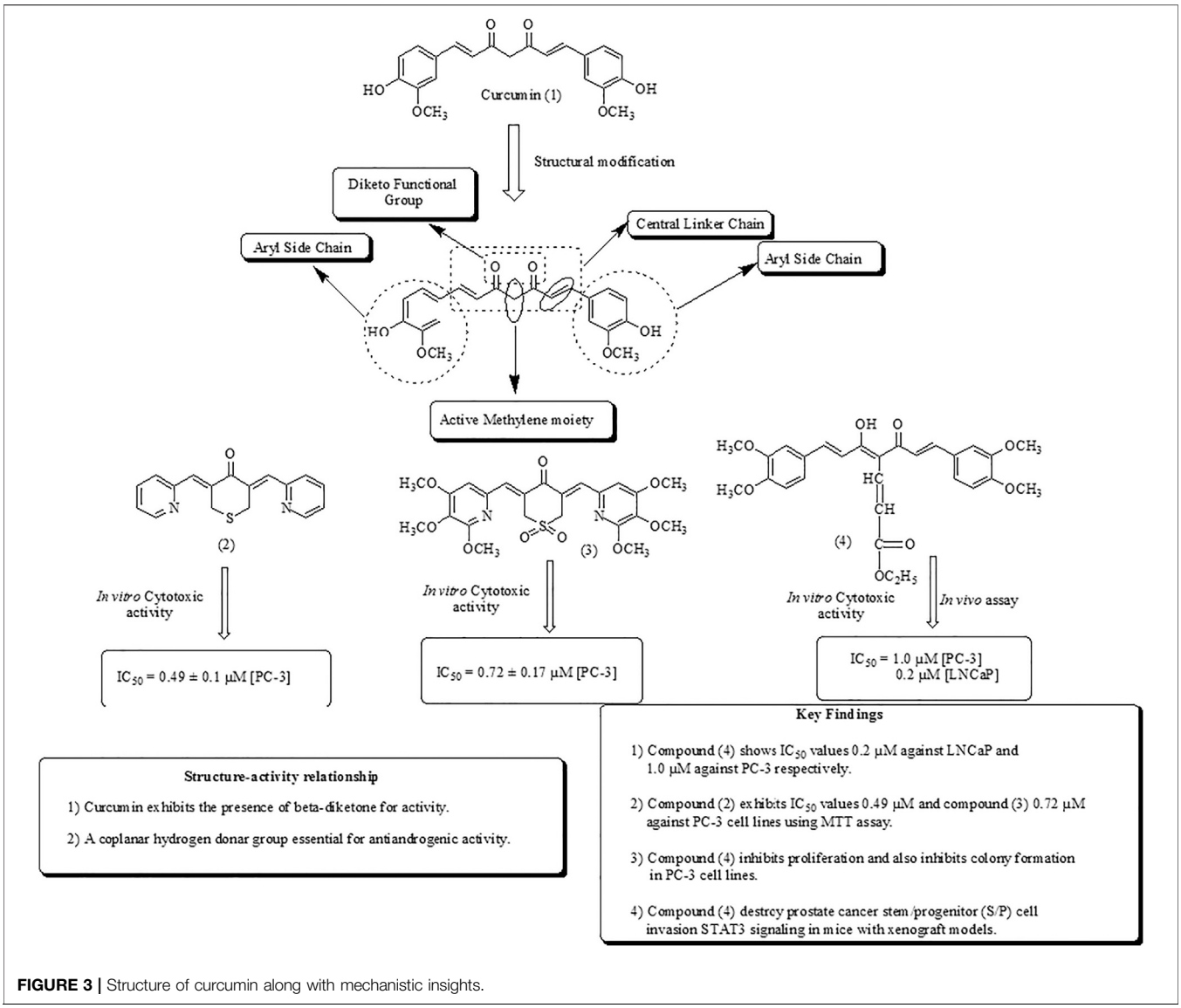

FIGURE 3 | Structure of curcumin along with mechanistic insights.

Structure–Activity Relationship and Mechanistic Insights

Several phytoconstituents have been isolated from various plants and screened for *in vitro, in vivo, in silico,* and mechanistic insights into mitigating CRPC. Mbese et al. have reported the therapeutic role of curcumin and its derivatives in treating PCa (Mbese et al., 2019). Curcumin is one of the main constituents of *Curcuma longa* L. (Zingiberaceae). It is a polyphenolic compound widely used as a pigment and spice, available in the market as turmeric and commonly known as Haldi. Curcumin structure and its most potent analogs (1–4) are shown in **Figure 3** (Mukhopadhyay et al., 2001; Yang et al., 2006; Choi et al., 2010; Yallapu et al., 2014; Schmidt and Figg, 2016).

Xu et al. have reported the docking studies and three-dimensional quantitative SARs of curcumin analogs as androgen receptor antagonists. The bioactive conformation was explored using molecular docking in SYBYL with binding interaction of AR. The oxygen atom of the methoxy group forms binding interactions as a hydrogen bond acceptor by creating hydrogen bonds with HIS920 and GLU893, respectively, as depicted in **Figure 4** (Cramer et al., 1988; Lill, 2007; Xu et al., 2012).

Zhou et al. have established the role of curcumin and its analogs in androgen receptor activation and inhibiting the growth of human PCa, such as LNCaP and CWR-22Rv1 cell lines. SAR and the apoptotic effect of curcumin and its analogs (5–7) are presented in **Figure 5** (Zhou et al., 2014).

Numerous research groups have established molecular targets of curcumin (1) associated with cell proliferation, cell death, and inflammation. Androgen receptor signaling, activation of protein-1, PI3K/Akt/mTOR, Bcl-2 family, NF-$_K$B, and wingless β-catenin signaling are shown in

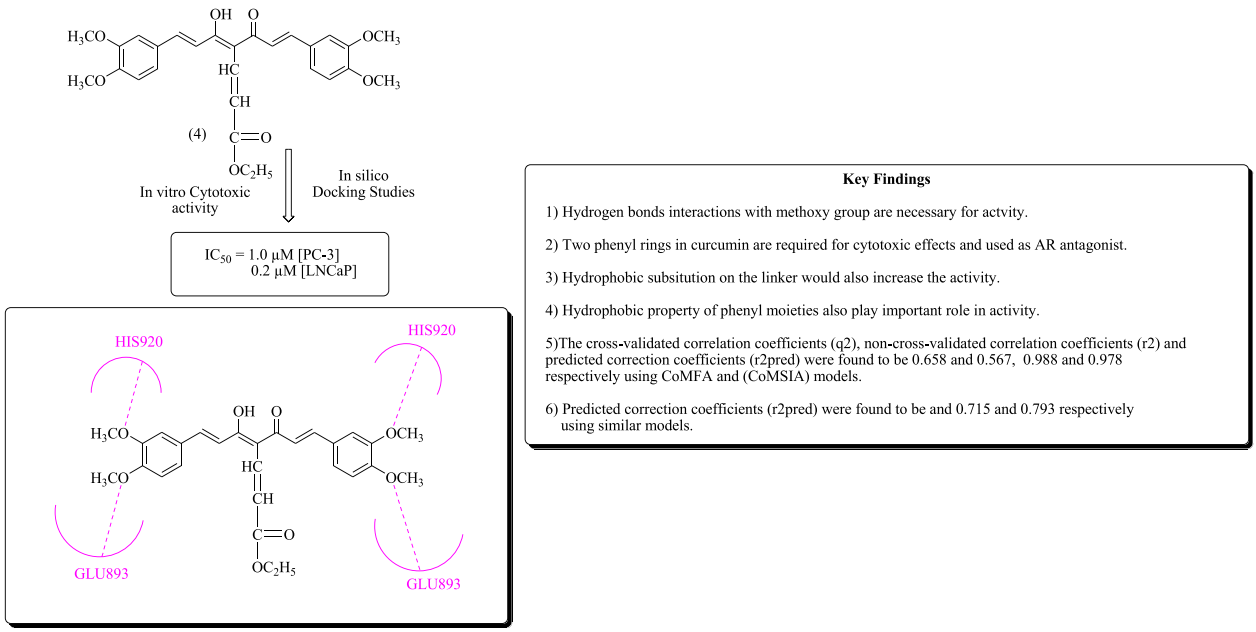

FIGURE 4 | Binding interactions of compound (4) with amino acid residues along with important key findings.

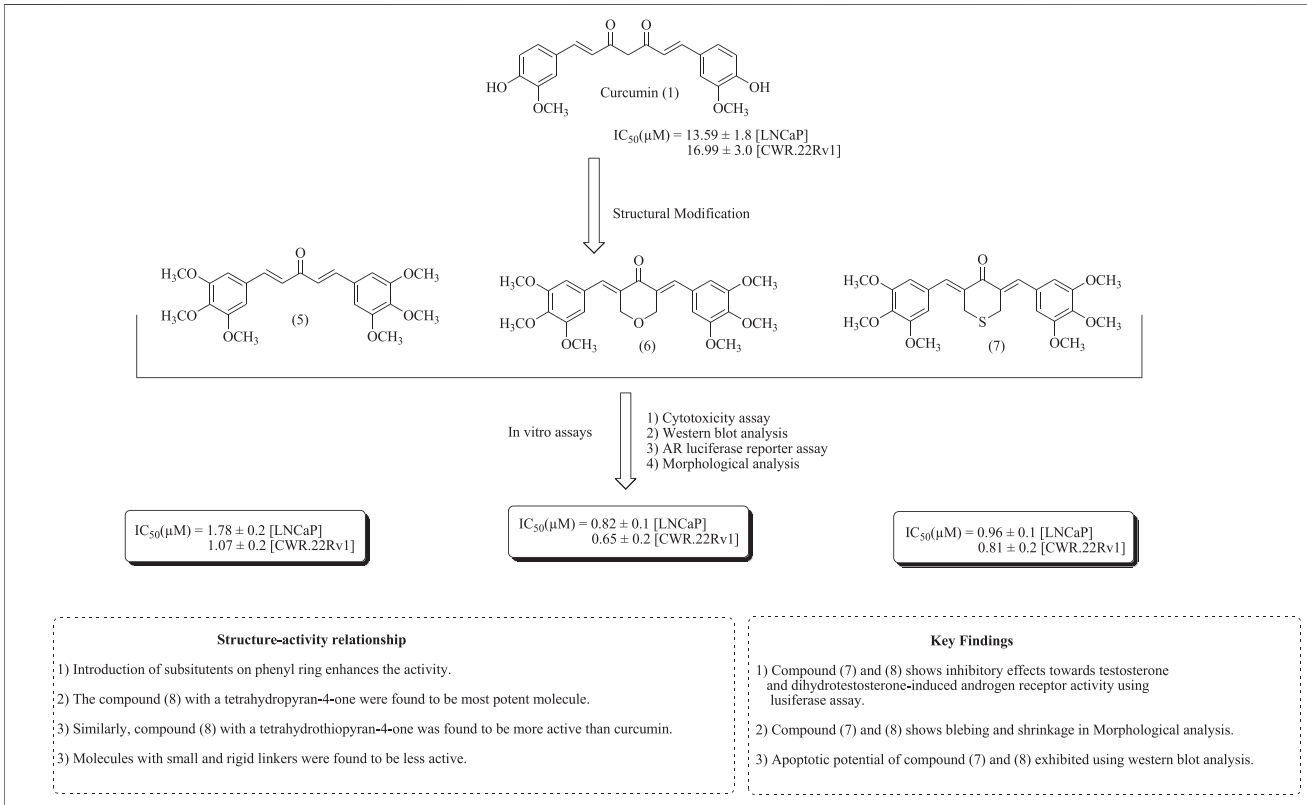

FIGURE 5 | Structure of curcumin and its analogs (5–7) along with structure–activity relationships and mechanistic insights.

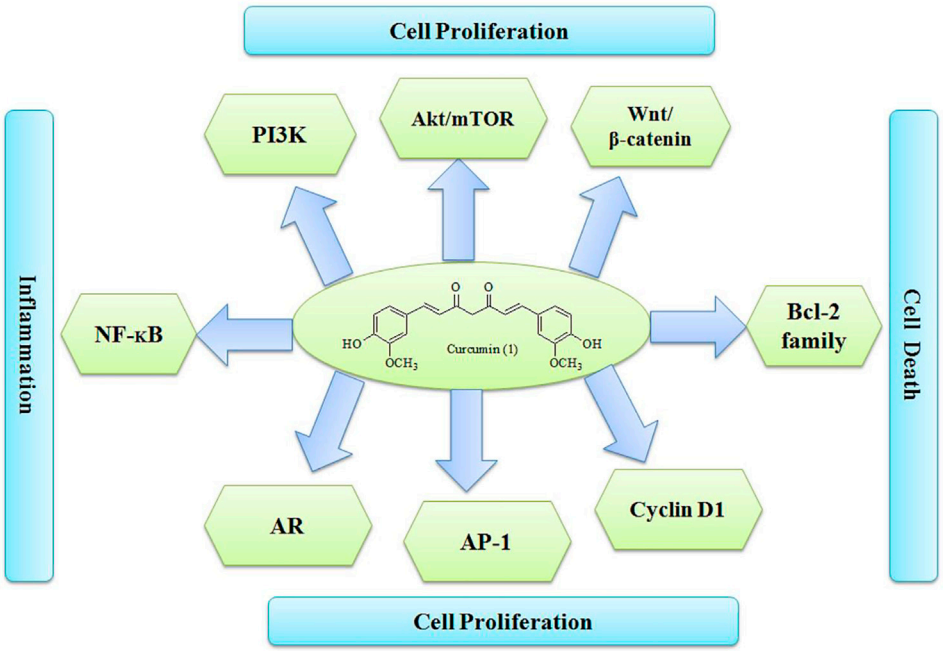

FIGURE 6 | Molecular targets of curcumin.

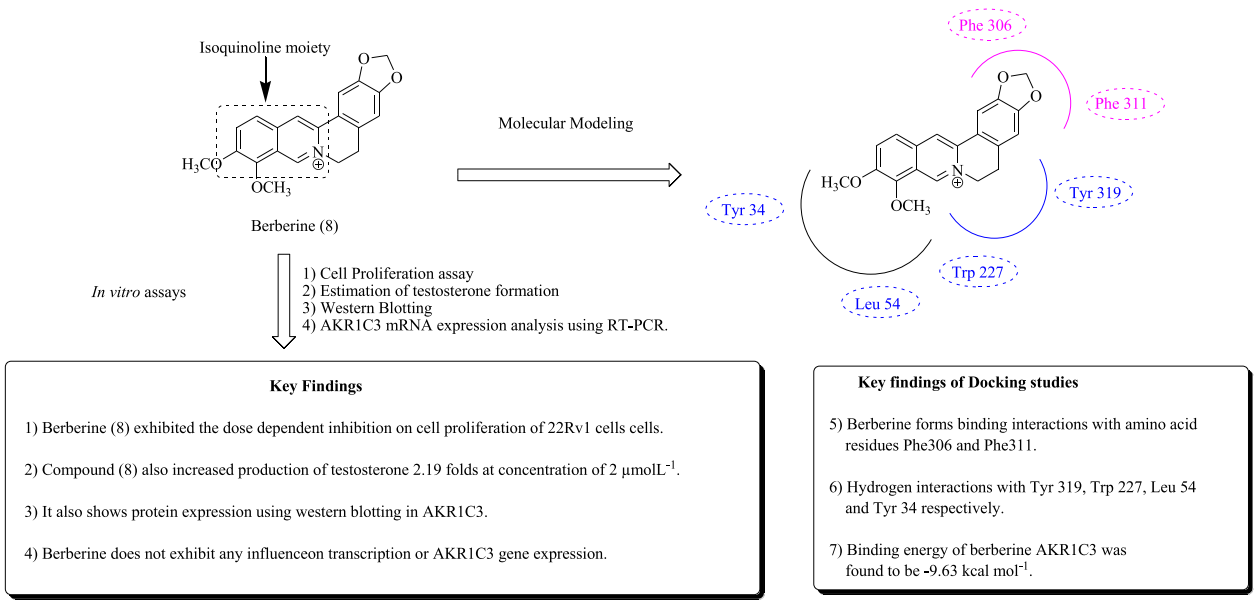

FIGURE 7 | Structure of berberine along with important key findings.

Figure 6, along with important mechanistic insights (Abd. Wahab et al., 2020). Curcumin can also be recommended along with prednisone and docetaxel in individuals with CRPC. It can also be given in combination with isoflavones in patients who had prostate biopsy due to elevated PSA levels (Ide et al., 2010; Mahammedi et al., 2016).

Berberine (8) is an isoquinoline derivative and has been evaluated for anticancer activities against PCa (Li et al., 2011; Wang et al., 2012). Tian et al. have reported the effect of berberine in inhibiting synthesis, which employs the interaction with aldo-keto reductase 1C3 as a potential target against 22Rv1 prostate cancerous cell lines. Berberine delayed the progression of CRPC

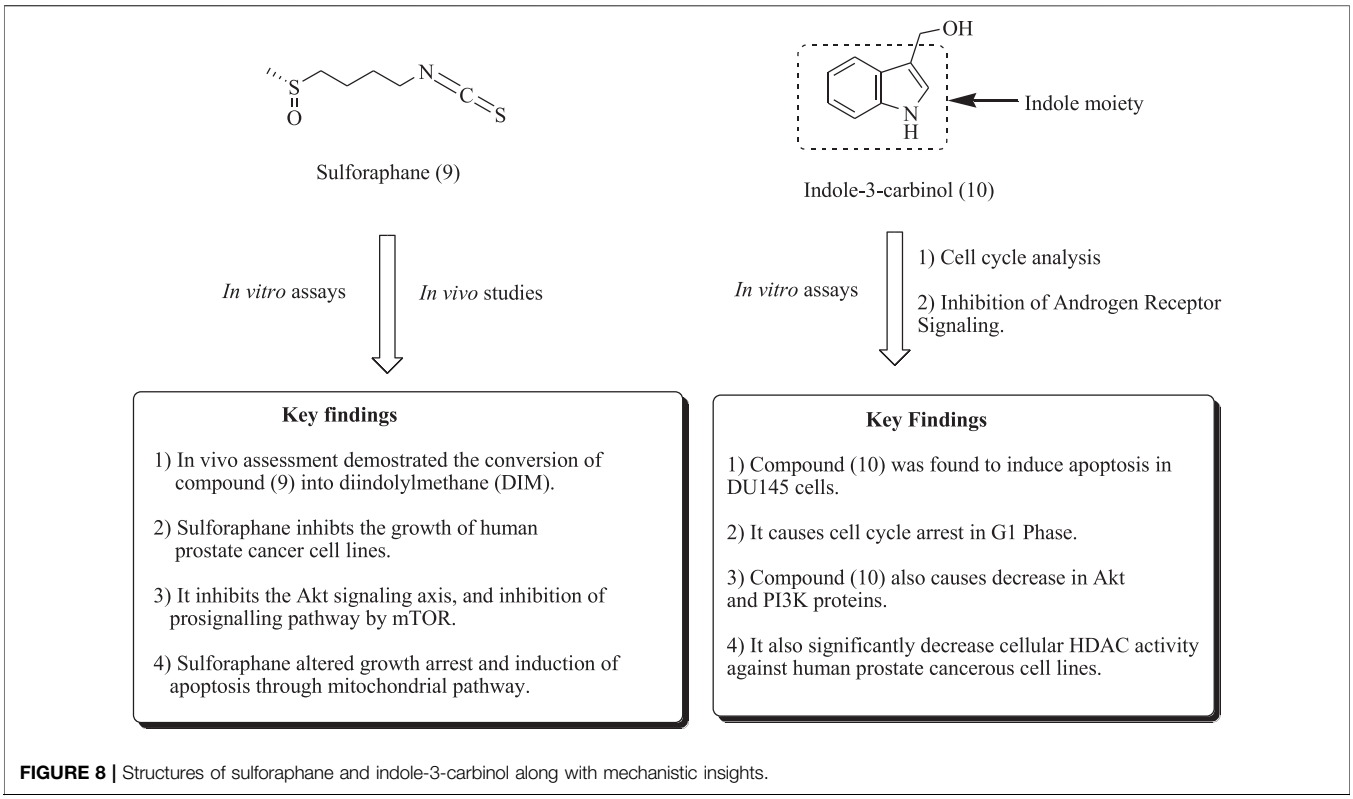

FIGURE 8 | Structures of sulforaphane and indole-3-carbinol along with mechanistic insights.

by reducing androgen synthesis. Moreover, protein levels were determined using western blotting and RT-PCR, respectively (Li et al., 2016). Molecular docking studies of berberine are shown in **Figure 7**. In another study, Mantena et al. have reported the apoptotic potential of berberine; that is, berberine induces cell cycle arrest in the G1 phase and caspase-3 inhibition in human PCa cell lines (Mantena et al., 2006).

In another report, Watson et al. have identified the secondary metabolites produced from cruciferous vegetables, such as broccoli, cauliflower, and brussels sprouts. These metabolic products, such as sulforaphane (9) and indole-3-carbinol (10), were potential candidates for inhibiting PCa as an epigenetic modulator. Structures of sulforaphane and indole-3-carbinol are depicted in **Figure 8** along with mechanistic insights (Chinni et al., 2001; Li, 2005; Garikapaty et al., 2006; Beaver et al., 2012; W.; Watson et al., 2013).

Docetaxel (11) is a semisynthetic taxane derivative and is widely used to mitigate numerous cancers, such as prostate, breast, ovarian, lung, and pancreatic cancers (Oudard et al., 2017). Similarly, cabazitaxel (12) is a second-generation docetaxel derivative with activity against docetaxel-resistant tumors. Compound (12) exerts its action by inhibiting microtubule functions in PCa cell lines (Kotsakis et al., 2016). Bono et al. have reported the use of cabazitaxel in combination with prednisone in metastatic CRPC (de Bono et al., 2010). The structure of taxanes derivatives is depicted in **Figure 9**.

Flavonoid-based phytochemicals are characterized by a 15-carbon frame as a common phenyl benzopyrone association (C_6–C_3–C_6) in their scaffolds (Sharma et al., 2021). Flavonoids are a potential bioactive class of natural products and are subdivided into flavones, flavanones, flavan-3-ols, flavonols, flavanones, and isoflavones. Among these, phytomolecules, quercetin, kaempferol, luteolin, apigenin, genistein, fisetin, epigallocatechin-3-gallate, and a mixture of flavo-lignans, such as silibinin-A and silibinin-B, have been screened against CRPC using *in vitro*, *in vivo,* and preclinical studies (Kallifatidis et al., 2016; Taylor and Jabbarzadeh, 2017; Salehi et al., 2019; Fontana et al., 2020). Lin et al. have isolated wedelolactone from *Sphagneticola calendulacea* (L.) Pruski and evaluated its effect on the growth of PCa cell lines, such as 22Rv1 and LNCaP, with IC_{50} values of 0.4 μg/ml and 0.8 μg/ml, respectively (Lin et al., 2007). Structures of flavonoid-based phytochemicals (13–29) are shown in **Figure 10**.

Various pentacyclic triterpenoids and steroid-based phytochemicals were found to be potential candidates for the treatment of CRPC (Fulda, 2008; Reiner et al., 2013). Among these, betulinic acid (30), ursolic acid (31), ginsenoside Rh2 (32), and ginsenoside Rh3 (33), as depicted in **Figure 11**, exhibited remarkable effects against PCa (Kallifatidis et al., 2016).

Mokbel et al. have reported the phytomolecules obtained from dietary components, which exhibited remarkable effects against PCa. The effects of these compounds have been revealed using *in vitro* assays, cell proliferation assay, and cell cycle arrest studies in PCa cell lines (Fontana et al., 2019a; Fontana et al., 2019b; Luo et al., 2019; Mokbel et al., 2019; Montagnani Marelli et al., 2019). Structures of the compounds (34–41) are shown in **Figure 12**.

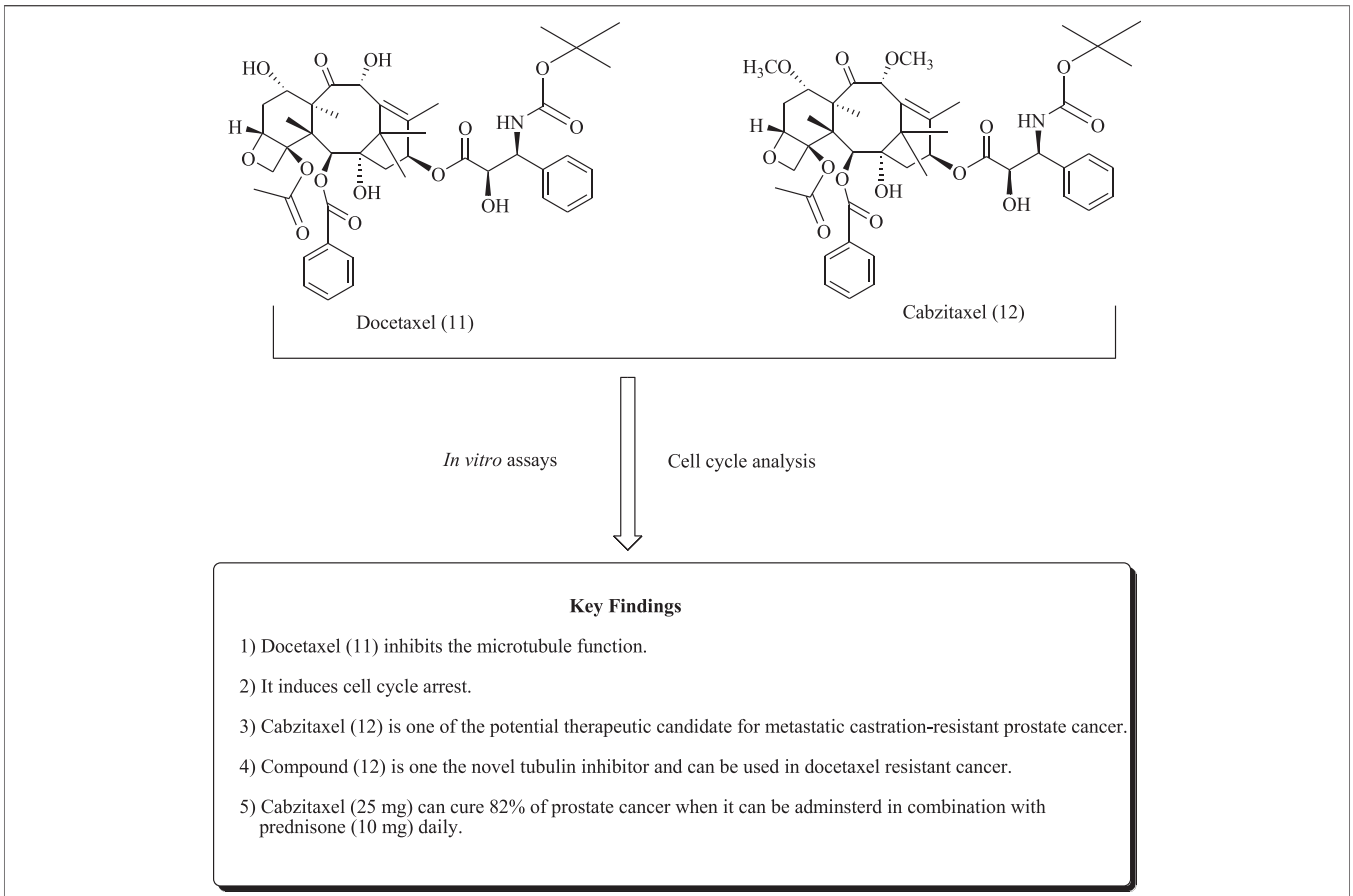

FIGURE 9 | Structure of docetaxel and cabazitaxel.

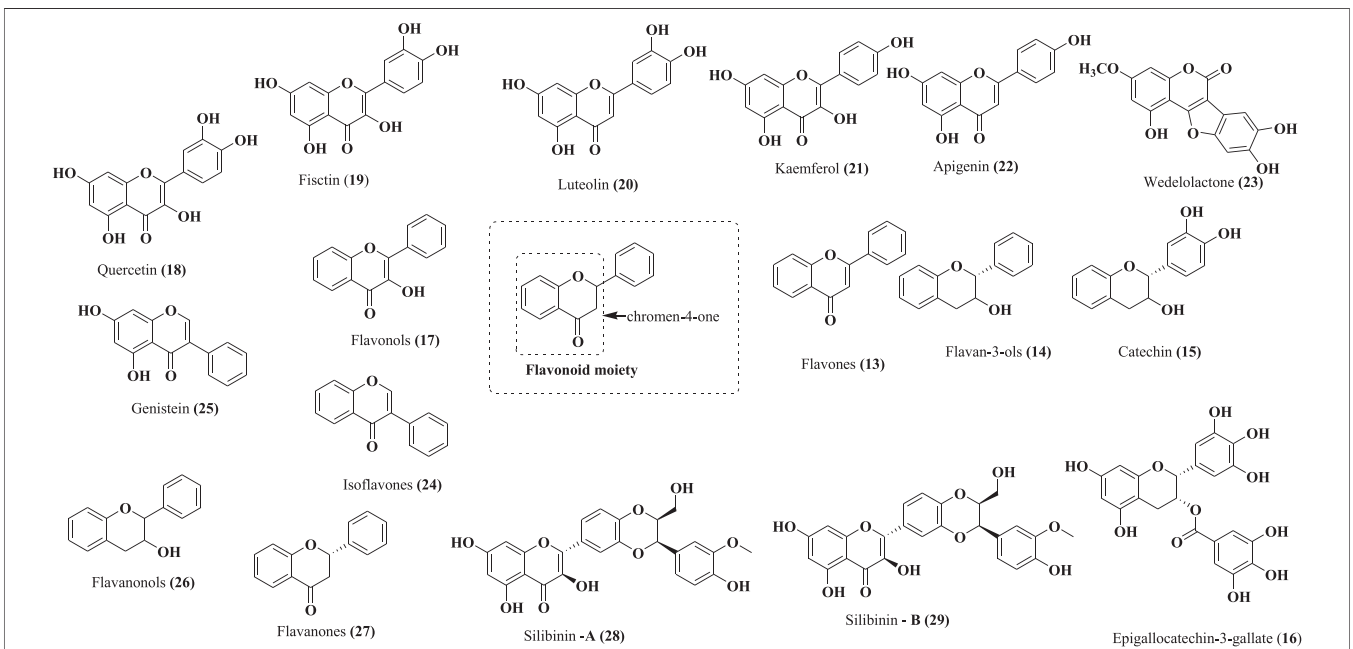

FIGURE 10 | Structures of flavonoid-based phytochemicals (13–29).

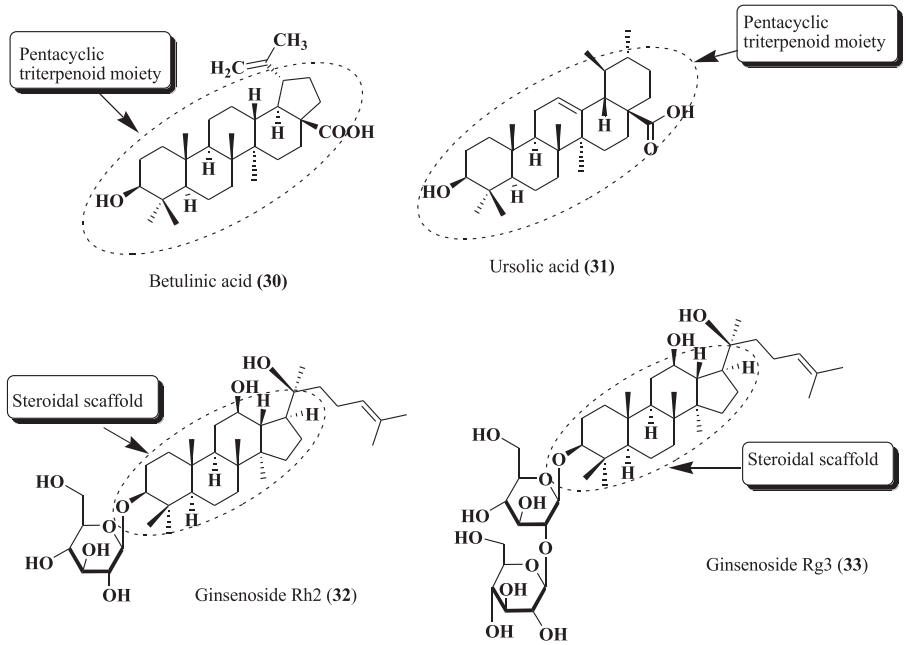

FIGURE 11 | Structure of compounds (30–33).

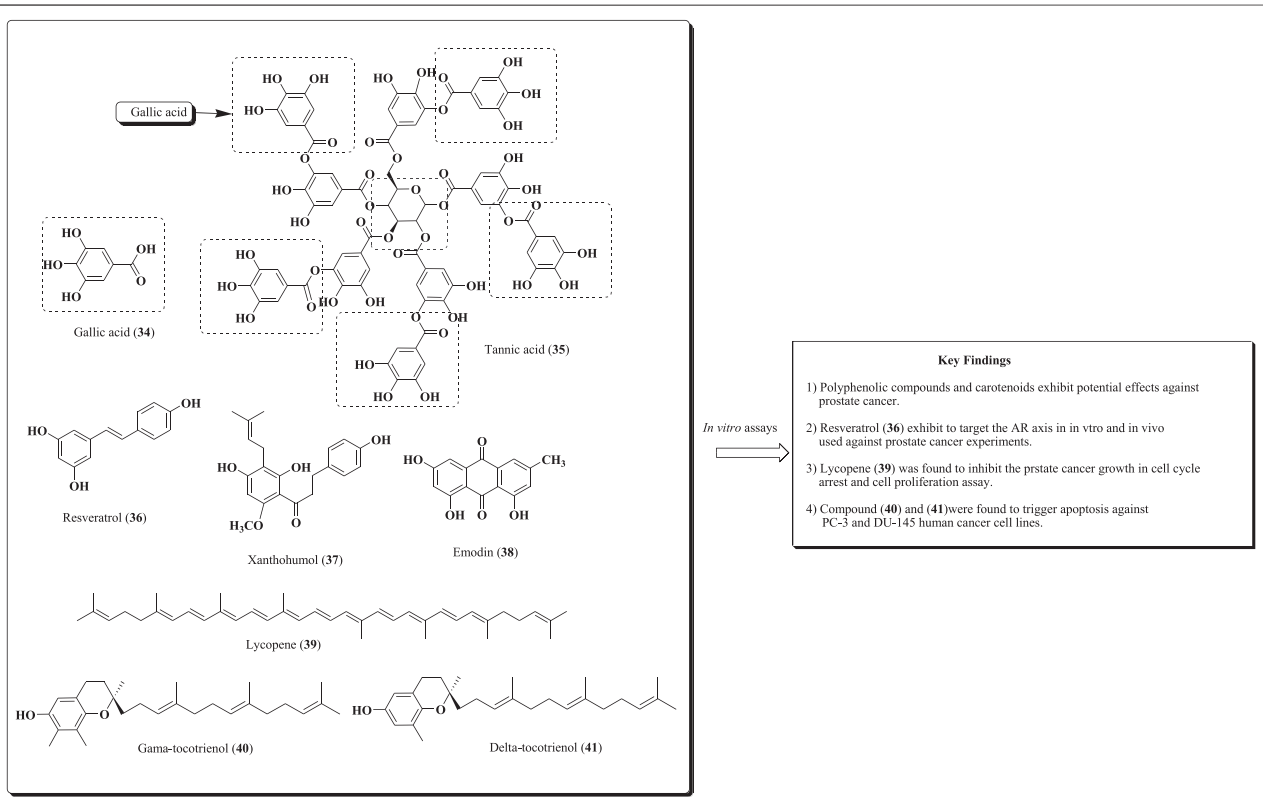

FIGURE 12 | Structure of compounds (34–41) along with important key findings.

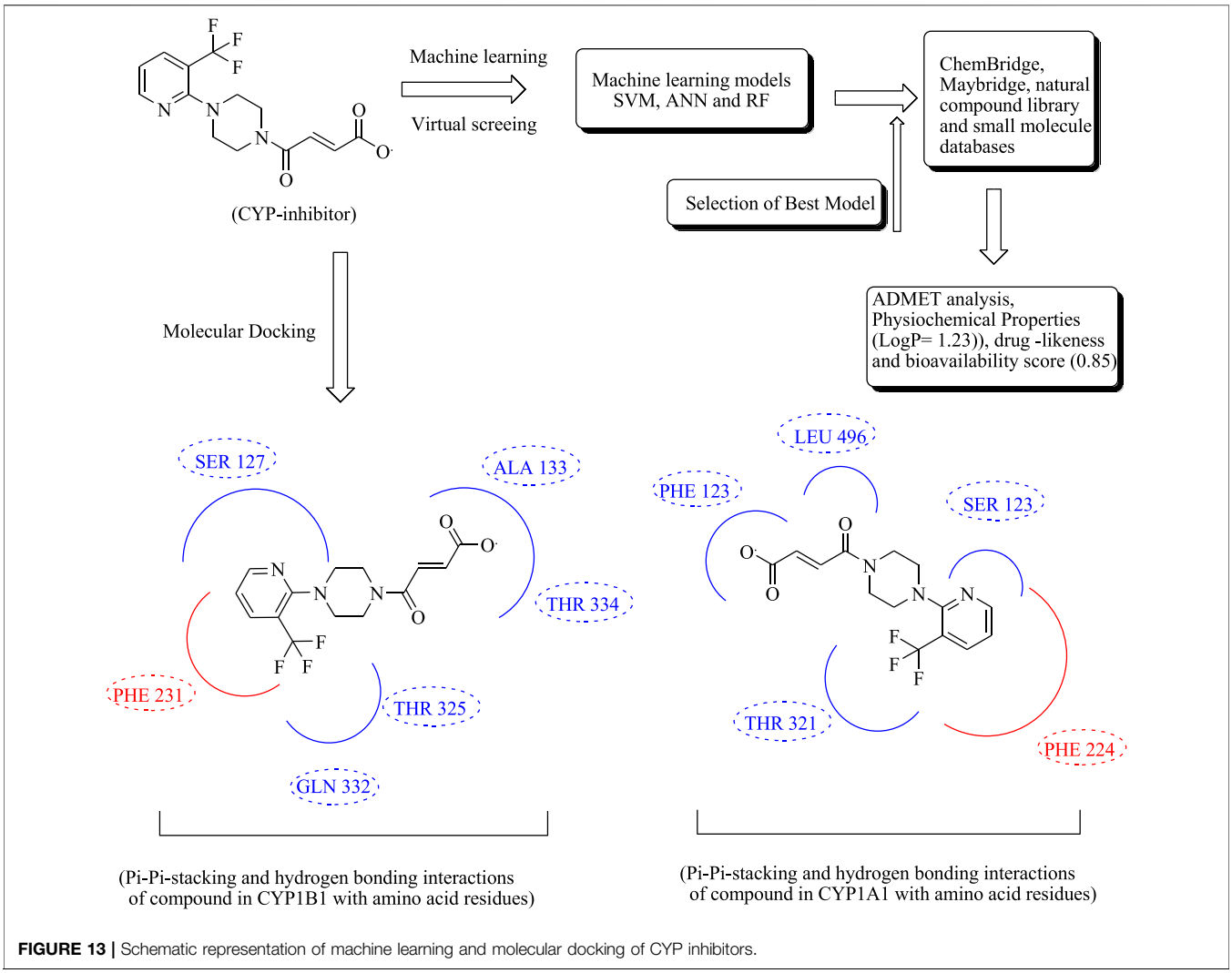

FIGURE 13 | Schematic representation of machine learning and molecular docking of CYP inhibitors.

Machine Learning-Based Studies

Deep learning and machine learning have been implemented in various drug discovery processes such as physiochemical activity, pharmacophore modeling, QSAR, toxicity prediction, and structure based-virtual screening (Mishra et al., 2017; Joon et al., 2021). With the recent advancement in modern technologies, integrated artificial intelligence algorithms and computer-aided drug design can help overcome the hurdles and challenges of conventional drug design (Duch et al., 2007; Lipinski et al., 2019). Badillo et al. have reported the advancements in predicting biomarkers using machine learning to provide physicians with new insights into diagnosis. Using deep machine learning, the application of biomarkers such as prostate-specific antigen (PSA) and its clinical relevance in the prediction of metastasis of PCa are examined. One of the primary challenges in PCa management is deciding which patients have clinically significant tumors. This concern includes not only new patients but also relapsed patients after primary treatment (Majumdar, 1985; Zhang et al., 2017; Badillo et al., 2020; Gupta et al., 2021).

In another study, Pantuck et al. have developed CURATE.AI to determine adequate drug doses. In this study, a combination of enzalutamide and experimental drug ZEN-3694 was administered to a patient with metastatic CRPC. Using CURATE.AI, it was found that a dose 50% lower than the starting dose of ZEN-3694 can achieve the desired results and arrest PCa growth (Pantuck et al., 2018; Su et al., 2019). Similarly, Kaiwen Deng et al. have reported treating patients with mCRPC by machine learning using a computational model. Through this model, patients were accurately allocated to docetaxel-intolerable and docetaxel-tolerable groups. This algorithm predicts the adverse effects of docetaxel treatment in patients. In this experiment, the data were collected from 1600 patients in phase III clinical trials for PCa treatment. These data generated the gold standards framework, including treatment status, discontinuation, and the number of deaths. The discontinuation status can be envisaged using models with clinical parameters. Moreover, death and treatment status were associated with discontinuation (Deng et al., 2020).

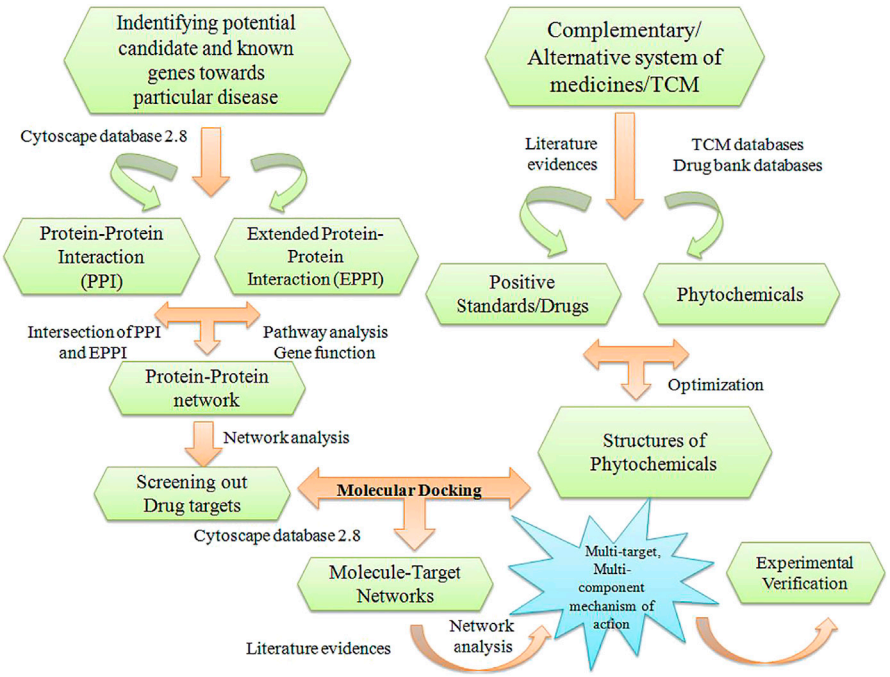

FIGURE 14 | Schematic representation of network pharmacology framework.

Lee et al. have developed the novel machine learning model for investigating non-mCRPC. In this model (Survival Quilts), an algorithm automatically tunes and selects ensembles of survival models based on clinical-pathological parameters using the Surveillance, Epidemiology, and End Results (SEER) datasheet. Data have been collected from (approximately) 30% of the US population, especially from men aged 35–95 years (Adamo et al., 2016; Lee et al., 2021). Survival Quilts is open-source software designed to mechanize the operation of machine learning in estimating survival rates. Demographic characteristics of patients were age, T-stage, PSA, primary and secondary Gleason grades score or grade groups, PCa-specific mortality, and all-cause mortalities. This machine learning model is competent in predicting ten-year PCa-specific mortality (Lee C. et al., 2019).

In another study, Raju et al. have conducted multiple machine learning, ADMET screening, and molecular docking studies to identify selective inhibitors of CYP1B1. Different machine learning models have been developed along with molecular databases, including Maybridge, ChemBridge, and a natural compound library, from which the selected models of CYP1B1 and CYP1A1 were evaluated. These inhibitors were highly expressed in wide varieties of cancer such as prostate, colon, and breast. The most widely used anticancer compounds, including paclitaxel, tamoxifen, docetaxel, and imatinib, are rapidly inactivated by CYP1B1, eventually leading to drug resistance (Androutsopoulos et al., 2009; Afarinkia et al., 2013; Raju et al., 2021). These inhibitors were subjected to molecular docking and pharmacokinetic analysis, as shown in **Figure 13**.

Role of Network Pharmacology Approach in Castration-Resistant Prostate Cancer

Traditional Chinese systems of medicine and complementary and alternative systems of medicine are the three main systems used to manage many types of cancer such as colon, gastric, breast, ovarian, and prostate cancer. The mechanisms of phytomolecules against CRPC have not been fully explored in the literature (Chen et al., 1996; Liu et al., 2018). Various research groups have reported the network pharmacology-based approach to explore natural products such as curcumin, quercetin, and ursolic acid as potential candidates for the treatment of CRPC (Barton et al., 2008; Hopkins, 2008; Li et al., 2014; Ru et al., 2014; Lee D. et al., 2019). Li et al. have demonstrated the network pharmacology of TCM based on the binding interactions of natural herbs, isolated phytochemicals, targets, genes, and diseases (Li et al., 2010; Li and Zhang, 2013). The main goal of network pharmacology is to investigate a potential candidate against disease with high efficiency, minimal side effects, and less toxicity. Song et al. have developed a network pharmacology-based technique to explore the mechanism of *Scleromitrion diffusum* (Willd.) R.J.Wang as a therapeutic candidate against CRPC. Prospective target genes of PCa were screened using databases such as OMIM, DisGeNET, and GeneCards. A network was constructed by evaluating the possible interactions among diverse target nodes. Protein–protein interaction, Kyoto Encyclopedia of Genes and Genomes (KEGG), and Gene Oncology enrichment analyses have been performed to explore and discover the mechanistic insights and pathways for therapy against PCa (Zhu et al., 2014; Yu et al., 2020). The PPI network revealed the multiple imperative targets and PCa-related targets, such as

PI3K, AkT1, mTOR, BCL2, Cyclin D1, PARP1, MAPK1, MMP3, MMP9, caspase-3, caspase-9, STAT-3, and RAF-1 (Song et al., 2019). A general schematic representation of the network pharmacology framework is depicted in **Figure 14** (de Carvalho et al., 2014).

Bi et al. have established the mechanism of curcumin against tumors based on pharmacology networking using DAVID 6.8 and GeneMANIA server database for analysis. This study identified multiple drug targets, target pathways, and signaling pathways (Bi et al., 2018). Thus, phytomolecules can also be used in the future to manage other diseases, as stated in complementary and traditional systems of medicine (Choi et al., 2010).

Translational Studies of Phytomolecules for Castration-Resistant Prostate Cancer: Assessment of Translation Potential for Bench to Bedside

Over the last 40 years, most chemotherapy drugs used to treat cancer originated from natural products. Moreover, phytomolecules may provide various lead structures used as templates to synthesize new, pharmacologically more effective agents (Mann, 2002). Since concomitant side effects, if any, are reported to be mild, plants and their metabolites are considered to be potentially acceptable choices for chemoprevention. It has been shown that several phytocompounds, such as genistein, green tea polyphenols, curcumin, lycopene, and vitamin D, prevent or postpone the onset of PCa or its development to CRPC (Kallifatidis et al., 2016). Basic and applied research are two types of study that are usually separated. Basic research is important for better understanding normal and pathological states, but it does not directly translate this information into therapeutically relevant applications. Based on our understanding of illness formation and progression, applied research aids in the development of novel diagnostic tools or treatments for patients. The major objective of "translational" research is to combine molecular biology advances with clinical trials, bringing research from the bench to the patients' bedside (Gibbs, 2000; Saijo et al., 2003; Goldblatt and Lee, 2010). Most cancers likely develop due to multiple genetic abnormalities, implying the need for a cocktail of agents against multiple targets in cancer cells or the use of agents with a broad range of targets, which is one of the most critical factors limiting the effectiveness of targeted therapy. The treatment of CRPC patients is still a serious clinical issue. Researchers now have a better knowledge of the mechanisms of CRPC owing to molecular, basic, and translational studies (Amaral et al., 2012). Many clinical trials to assess the efficacy of phytochemicals in human subjects have been undertaken, and they have partially corroborated the encouraging results found *in vitro* and preclinical models. We will only discuss those clinical studies where the pure phytocompounds or the characterized phytofractions were considered. We have excluded studies on extracts and juices, as they would have deviated content from the theme. Plant-derived constituents showing remarkable anticancer effects against CRPC in clinical trials are discussed as follows.

Resveratrol. Resveratrol is a polyphenol found in nature that has been shown to inhibit PCa growth and development. In several preclinical investigations, resveratrol has been shown to decrease prostate cancer development *in vitro* and in animal models. Moreover, resveratrol has been found to reduce androgen receptor expression, decrease proliferation, induce apoptosis in PCa cell lines, and improve their ionizing radiation sensitivity (Jasinski et al., 2013). Dietary resveratrol suppresses β-catenin-mediated AR signaling and represses nuclear localization of β-catenin by reducing HIF-1 production, perhaps in a proteasome-independent way, contributing to the reduction of CRPC tumor progression (Mitani et al., 2014). Kjaer et al. have conducted a randomized controlled trial (RCT) using two doses of resveratrol (150 mg or 1,000 mg resveratrol daily) for 4 months in 66 middle-aged men suffering from metabolic syndrome. High-dose resveratrol (1,000 mg daily) treatment for 4 months dramatically reduced blood levels of the androgen precursors androstenedione, dehydroepiandrosterone, and dehydroepiandrosterone sulfate. However, the prostate size and circulating levels of PSA, testosterone, free testosterone, and dihydrotestosterone were unchanged (Kjaer et al., 2015). Patients with nonmetastatic biochemically recurrent PCa were allocated to escalating doses of MPX (pulverized muscadine grape skin rich in ellagic acid, quercetin, and resveratrol) in cohorts of two patients, with six patients at the maximum dose in the phase I section of this phase I/II trial, which used a modified continuous reassessment technique. The phase I section revealed that the largest dose tested, 4,000 mg/d, was safe, with only grade 1 adverse event being recorded. Even though the phase I population was small and there was no sustained decrease in serum PSA from baseline, the findings show that 4,000 mg/d of muscadine grape skin extract is safe (Paller et al., 2015).

Furthermore, Paller et al. have conducted a randomized, multicenter, placebo-controlled, dose-evaluating phase II trial. The results on 112 biochemically recurrent (BCR) patients were evaluated, revealing that MPX did not significantly improve the prostate-specific antigen doubling time (PSADT) compared with the placebo. Nevertheless, other benefits have been observed in the exploratory analysis (Paller et al., 2018). Further, testing resveratrol's chemopreventive effects in conjunction with other antioxidants occurring naturally together, such as in grapes, might be beneficial (Singh et al., 2016).

Soy Isoflavone. Incidence rates of PCa are lowest in Asian nations, where soy foods are frequently part of a normal diet (Jian, 2009). In some animal models, physiologically active isoflavones found in soy products, such as genistein, daidzein, equol, and glycitin, prevented PCa (Mahmoud et al., 2014). Antioxidant defense, DNA repair, suppression of angiogenesis and metastasis, potentiation of radio- and chemotherapeutic drugs, and antagonism of estrogen- and androgen-mediated signaling pathways are all involved in soy isoflavone-induced growth arrest and death of PCa cells (Mahmoud et al., 2014). In numerous clinical trials (**Table 1**), soy isoflavones have been found to reduce PSA levels.

Lycopene. Lycopene, a natural pigment found mostly in the ripe tomato fruits, is gaining popularity in preventing and

TABLE 1 | Clinical studies evaluating the potential of soy isoflavones in reducing PSA levels.

Clinical study protocol	Outcome	PMIDs	References
Healthy men (*N* = 112 aged 50–80 years) were randomly allocated to groups drinking either a soy protein drink with 83 mg of isoflavones (+ISO) or a comparable drink with isoflavones removed in a double-blind, parallel-arm, randomized experiment for 12 months			
In the isoflavone therapy group, there was no significant change in blood PSA level, velocity, or PCa incidence	15066931	Adams et al. (2004)	
For 3 months, 24 males were put on a high or low soy diet in a randomized, double-blind, crossover clinical trial	14% decrease in circulating blood PSA levels was observed but with no change in testosterone levels	16775579	Maskarinec et al. (2006)
In a randomized study, 58 men at high risk of PCa were allocated to groups taking one of three protein isolates containing 40 g/d protein at random (107 mg/d isoflavones, <6 mg/d isoflavones, or 0 mg/d isoflavones) for 6 months	Soy protein isolate intake reduces AR expression in the prostate but did not affect ER β expression	17585029	Hamilton-Reeves et al. (2007)
Twenty patients with increasing PSA following previous local treatment were treated with soy milk with 47 mg of isoflavonoid per 8 oz serving three times per day for 12 months in an open-labeled phase II study			
In six patients, the slope of PSA after study enrollment was substantially lower than that before entering the study, while in two individuals, the slope of PSA after study admission was significantly greater	18471323	Pendleton et al. (2008)	
In a randomized, double-blind experiment, 25 PCa patients were given placebo or soy isoflavone supplements for 2 weeks before prostatectomy	In PCa patients, soy isoflavones decreased prostate COX-2 mRNA while increasing p21 mRNA	19127598	Swami et al. (2009)
In the phase II trial, 29 patients with increasing PSA levels following intense radiotherapy for prostate cancer were told to drink 500 ml of soy beverage every day for 6 months	In 41% of PCa patients, soy caused a substantial delay in PSA doubling time	20099194	Kwan et al. (2010)
53 men with PCa took a daily supplement comprising 450 mg genistein, 300 mg daidzein, and other isoflavones for 6 months in a double-blind, placebo-controlled, randomized study	In men with low-volume PCa, there was no significant reduction in PSA levels	21058191	deVere White et al. (2010)
33 males undergoing androgen deprivation therapy for PC were given either 20 g of soy protein with 160 mg of total isoflavones or a taste-matched placebo (20 g whole milk protein) for a 12-weeks	In androgen-deficient males, high-dose isoflavones do not enhance metabolic or inflammatory markers	20798386	Napora et al. (2011)
Phase II, randomized, double-blind, placebo-controlled trial, or oral isoflavone (60 mg/day) for 12 months, *N* = 158	PSA levels did not significantly change, following treatment with isoflavones. The isoflavone group had a substantially reduced PCa incidence in 53 individuals aged 65 years	21988617	Miyanaga et al. (2012)
47 Norwegian patients were given 30 mg genistein or placebo capsules daily for 3–6 weeks before prostatectomy in a phase 2 placebo-controlled, randomized, double-blind clinical study	mRNA level of KLK4 in tumor cells was considerably decreased, while androgen and cell cycle-related biomarkers were not significantly lowered	22397815	Lazarevic et al. (2012)
A double-blinded, randomized, placebo-controlled trial included 86 men given soy isoflavone capsules (80 mg/d of total isoflavones and 51 mg/d aglucon units) for 6 weeks	After consuming soy isoflavones for a short time, no significant changes in blood hormone levels, total cholesterol, or PSA were observed	23874588	Hamilton-Reeves et al. (2013)
In 177 men at high risk of recurrence following radical prostatectomy for PCa, a randomized, double-blind trial comparing daily use of beverage powder containing 20 g of protein in the form of either soy protein isolate (*n* = 87) or as placebo calcium caseinate (*n* = 90). Within 4 months of surgery, supplementation was started and was followed up for 2 years	Following radical prostatectomy, daily intake of a beverage powder supplement containing soy protein isolate for 2 years did not prevent biochemical recurrence of PCa in men at high risk of PSA failure	23839751	Bosland et al. (2013)

treating heart disease and cancer (Heber and Lu, 2002). Lycopene's anticancer actions on PCa cells are mediated via decreasing cell proliferation, inducing apoptosis, stopping the cell cycle, and lowering DNA damage in various investigations (Ivanov et al., 2007; Holzapfel et al., 2013). *In vitro* studies have shown that a normal physiological concentration of lycopene in culture conditions inhibits the growth of PCa cell lines, which are either androgen-dependent or androgen-independent (Kim et al.,

2002; Mirahmadi et al., 2020). A human intervention study has demonstrated that consumption of carotenoid-containing plant products significantly decreased oxidative base damage (Pool-Zobel et al., 1997). In phase II randomized clinical trial, 26 men with newly diagnosed, clinically localized PCa randomly allocated to groups taking 15 mg of lycopene twice daily (n = 15) or no supplementation (n = 11) for 3 weeks before radical prostatectomy exhibited reduced PSA, connexin 43, and insulin-like growth factor-1 levels (Kucuk et al., 2001). In an unblinded randomized phase I clinical study, 32 patients with localized prostate adenocarcinoma consumed tomato sauce-based pasta dishes for 3 weeks (30 mg lycopene/day), which resulted in higher lycopene levels in prostate tissues and serum, reduction in PSA serum levels, and DNA damage in both prostate and leukocyte cells in prostatectomy (Bowen et al., 2002). In a prospective trial, 20 metastatic HRPC patients were given 10 mg lycopene daily for 3 months and in almost all men, disease progression inversely changed to a lower grade. Moreover, PSA levels were reduced and ECOG function and bone pain improved (Ansari and Gupta, 2004). In phase II clinical trial, 10 mg lycopene per day for 1 year resulted in a reduced PSA velocity in 40 individuals (Barber et al., 2006). Bunker et al. have conducted a randomized, unblinded phase I clinical trial in 81 high-risk Afro-Caribbean patients with neoplasia and found that 30 mg/day of lycopene for 4 months lowers PSA serum concentrations (Bunker et al., 2007). In a phase II research, 46 androgen-independent PC patients were given lycopene (15 mg twice daily), which resulted in a 50% drop in PSA levels; however, the trial showed no clinical benefit for the advanced stage of cancer (Jatoi et al., 2007). In another trial, 32 patients with high-grade prostatic intraepithelial neoplasia were given a lycopene-enriched diet (20–25 mg/day) for 6 months; however, no meaningful effect was observed in terms of lycopene's effects on cancer development or PSA levels in these individuals (Mariani et al., 2014). In phase II research, Zhuang et al. have studied the clinical efficacy and safety profile of docetaxel with lycopene in CRPC patients and revealed that the combination of docetaxel and lycopene resulted in enhanced PSA response rate and tolerability (Zhuang et al., 2021).

Quercetin. Quercetin, a flavonoid found in fruits and vegetables, has been shown to have anti-inflammatory, antioxidant, and cancer-fighting properties. The activity of promoters of two major genes implicated in PCa pathogenesis, i.e., AR and PSA, is inhibited by quercetin (Ghafouri-Fard et al., 2021). By suppressing the main survival protein Akt, quercetin has also been shown to promote the apoptosis of PCa dose-dependently (Ghafouri-Fard et al., 2021). On PC-3 cells (model cells of CRPC), quercetin and paclitaxel coadministration significantly reduced cell proliferation, increased apoptosis, triggered cell cycle arrest at the G2/M stage, activated endoplasmic reticulum stress, and enhanced reactive oxygen species production (Zhang X. et al., 2020). Henning et al. have conducted a prospective randomized, parallel design, placebo-controlled trial in which 31 men with PCa were given either 1 g of green tea extract containing 830 mg of green tea polyphenols with 800 mg of quercetin or placebo for 4 weeks before prostatectomy (Henning et al., 2020). Following the coadministration of green tea extract and quercetin, they have found a significant rise in quercetin concentrations in plasma, urine, and prostate tissue. Furthermore, this regimen decreased epicatechin gallate levels in the urine. In prostate tissue or RBCs, no significant change in the concentration of green tea polyphenols or methylation activity across the groups was observed and there was no evidence of liver injury (Henning et al., 2020).

Gossypol. (-)-Gossypol, a polyphenolic chemical found in cottonseed, improves radiation therapy response and shrinks human PCa tumors (Xu et al., 2005). (-)-Gossypol induced apoptosis in DU-145 cells by downregulating Bcl-2 and Bcl-xL and increasing Bax at the mRNA and protein levels. It also enhances PARP cleavage and activates caspase-3, -8, and -9 (Huang et al., 2006). In PCa cells and prostate tumor-initiating cells, gossypol activates p53 and induces apoptosis (Volate et al., 2010). AT-101 (R-(-)-gossypol acetic acid; Ascenta Therapeutics, Inc.), a derivative of gossypol, exhibited anticancer activity in various tumor models. Liu et al. have conducted a phase I/II study of AT-101 in 23 patients with CRPC and investigated that AT-101 was well tolerated when given at a dose of 20 mg/day for 28 days (Liu et al., 2009).

(-)-Epigallocatechin-3-gallate (EGCG). (-)-Epigallocatechin-3-gallate (EGCG), biologically active catechin of green tea, has been evaluated for its chemopreventive activity against CRPC using *in vitro* and *in vivo* animal studies (Ju et al., 2005; Thangapazham et al., 2007; Rahmani et al., 2015). Bettuzzi et al. have explored cancer-preventive effects of green tea catechins (GTCs) in volunteers with high-grade prostatic intraepithelial neoplasia (HGPIN). The volunteers were given 200 mg of GTC three times daily for a total of 600 mg/d and followed up after 1 year. Only one instance of PCa in the treatment group (incidence 3%) and nine cases of PCa (incidence 30%) in the placebo group were observed (Bettuzzi et al., 2006). A decrease in PSA levels, although not significant, and a significant decrease in International Prostate Symptom Score were observed in the GTC group. Furthermore, during a 2-year follow-up, two of the nine placebo males and one of the 13 GTC patients were diagnosed with PCa, demonstrating an 80% reduction in PCa diagnosis in patients with HGPIN (Brausi et al., 2008). Polyphenon E (PolyE), a mix of GTCs, containing 400 mg of EGCG, was given daily for 1 year to men with HGPIN in a placebo-controlled, randomized clinical trial (Kumar NB. et al., 2015). A decrease in serum PSA levels and ASAP in the PolyE group was observed. In another study, males with PCa were given 1.3 g of PolyE containing 800 mg of EGCG daily (McLarty et al., 2009). A significant reduction in PSA, HGF, and VEGF serum levels was observed at the time of prostatectomy (after 3–6 weeks). Moreover, supplementation with PolyE containing 800 mg of EGCG for 3–6 weeks resulted in a beneficial but nonsignificant reduction in serum PSA in a similar clinical study (Nguyen et al., 2012). Contrary to the above observations, minimal antineoplastic action was identified after daily dosages of EGCG were given to 42 patients with androgen-independent PCa in phase II clinical study (Jatoi et al., 2003).

Curcumin. Curcumin, diferuloylmethane, inhibits PCa proliferation and metastatic development by downregulating

androgen receptor and epidermal growth factor receptors and causing cell cycle arrest (Teiten et al., 2010). Twenty-six patients with advanced CRPC and elevated PSA were given docetaxel/prednisone in usual settings for six cycles, along with curcumin (6,000 mg per os each day; day −4 to day +2 of docetaxel) (Mahammedi et al., 2016). This study demonstrates that curcumin has a high response rate, good tolerability, and patient acceptability, justifying the need for a randomized trial. An RCT was conducted on 64 eligible patients with PCa to assess the beneficial role of nanocurcumin in preventing and/or mitigating radiation-induced proctitis in PCa patients undergoing RT (Saadipoor et al., 2019). 33 patients received nanocurcumin (120 mg/day) 3 days before and during the RT course. Radiation-induced proctitis occurred in 18/31 (58.1%) of placebo-treated patients compared to 15/33 (45.5%) of nanocurcumin-treated patients (Saadipoor et al., 2019). The role of anticancer effects of curcumin in patients with PCa that undergo intermittent androgen deprivation (IAD) treatment has been studied. A randomized, double-blind, placebo-controlled trial was performed on 97 patients with PCa (49 patients took oral curcumin (1440 mg/day) and 48 received placebo for 6 months) who received IAD treatment (Choi et al., 2019). The results have demonstrated that oral administration of curcumin for 6 months can lower PSA levels significantly in patients compared to those in the placebo group. Curcumin (total 3 g/day), a radiosensitizing and radioprotective agent, showed significant improvement of antioxidant status in patients with PCa who received radiotherapy (Hejazi et al., 2016). Another clinical study has been conducted to examine the effect of curcumin supplements and isoflavones on serum PSA levels (Ide et al., 2010). The isoflavones and curcumin were administered orally to patients who had prostate biopsy due to elevated PSA levels for 6 months, and a significant decrease of serum PSA level was observed. Two clinical studies on the effect of adjuvant use of curcumin after prostatectomy on improving recurrence-free survival in PCa patients (clinicaltrials.gov; NCT02064673) and reducing the risk of PCa progression in low-risk men (clinicaltrials.gov; NCT03769766) are undergoing.

CONCLUSION AND FUTURE PERSPECTIVES

PCa is a leading cause of cancer-related morbidity and mortality. CRPC poses a pathophysiological and therapeutic challenge that imposes a significant burden on individuals and the healthcare system (Tang et al., 2013). A growing number of studies have focused on deciphering its mechanistic underpinnings and targeting the key elements of its pathogenesis. Therefore, it might be more effective to address several pathogenetic mechanisms contributing simultaneously to castration resistance and cancer progression. These mechanisms can also complement conventional and novel anticancer treatments. The main findings of our review can be summarized as follows:

- The tumor microenvironment, with its immune cells, cytokines, chemokines, androgen receptors and their molecular interactions, plays an important role in castration resistance. Simulating this environment can be a key to the success of cheminformatics modeling studies.
- Multiple signaling pathways and transcription factors are associated with CRPC. Natural compounds may be used to target their elements and disrupt them. However, this may be ground for potential side effects stemming from other body systems.
- Oncogenes and mutations (SYT4, GUCY1A2, GRIN3A, and BRAC) that are implicated in PCa resistance constitute therapeutic targets. Exploring the effect of natural products alongside the genetic traits of CRPC can lead to more precise and, therefore, effective treatment approaches.
- Molecular docking studies and structure–activity models can play an important role in identifying potent molecules for further exploration in *in vitro*, *in vivo*, and clinical studies.
- The use of disruptive technologies, including machine and deep learning and artificial intelligence, can accelerate drug discovery using comprehensive risk and efficacy analysis.
- Network pharmacology can reveal the evidence behind the potential efficacy of complementary medicine in CRPC.

The present study attempts to provide an overview of a rapidly expanding topic. It provides insights and guidance for future studies that will examine specific elements mentioned in this analysis, such as molecular docking or structure–activity modeling. Relevant future studies may benefit from a systematic review and a metanalysis methodology assessing both the available quantitative and qualitative evidence. Disruptive technology is expected to play an important role in future research. Artificial intelligence models based on deep machine learning can broadly analyze several natural compounds and their interactions. Quantum computing can act as an accelerator in such studies enabling the screening of big databases.

The adoption of a translational approach is a critical step toward clinical practice and application. Computational analysis of the effect of natural compounds on CRPC in combination with specific biomarkers extracted from the patients' histopathological specimens can lead to the identification of compounds that may be beneficial. The clinical outcomes of the patients receiving these compounds and their regular treatment can be compared with those of the control groups. Nonetheless, such an approach would be possible only using natural compounds that have been approved for clinical use by the respective health authorities. The use of a broader number of natural compounds might be possible in end-stage CRPC under compassionate authorization. However, such studies might reduce the efficacy of natural products due to the poor prognosis of the patients. In other words, it should be understood that the results of these studies do not necessarily reflect the efficacy of natural compounds administered at earlier stages of the disease.

Finally, yet importantly, it is important to integrate social and health economics factors in this research. Cultural factors have been shown to affect patients' attitudes toward several anticancer drugs; moreover, the attitudes toward natural compounds need to be assessed. People of different nationalities may be more open to

receiving phytochemicals that they are already familiar with because of their cultural background. On top of this, the integration of phytochemicals as supplements in anticancer treatment may be evaluated in terms of cost-effectiveness. This will determine whether insurance systems and policymakers are willing to make such treatments widely available to the public. In the long run, patients, physicians, and regulatory authorities will accept the use of natural compounds for managing CRPC, which will result in conducting more large-scale studies and collecting better evidence and data.

As advanced-stage PCas are prone to the extensive point mutations that lead to drug resistance, single-targeted and specific drugs are no longer beneficial and cannot go further in clinical trials. In contrast, many natural products, such as resveratrol, soy isoflavone, lycopene, quercetin, gossypol, EGCG, and curcumin, progressed to clinical studies because of their multitarget anticancer potential.

Moreover, formulation advancements and the discovery of potent natural products play a crucial role in overcoming the limitations concerning the poor pharmacokinetics and bioavailability of natural products. Nanocurcumin-based clinical studies are a small step toward addressing the solubility and bioavailability related issues.

Utilizing all means available to integrate the use of natural compounds sources into clinical practices can be extremely beneficial in the management of CRPC in the future.

AUTHOR CONTRIBUTIONS

RS, PS, AD, RG, DK, RM, CT, SP, SJ, and SS wrote different manuscript sections. SK, RS, MK, and BS laid down the idea and manuscript outline and compiled and finalized the manuscript. BS arranged the funding source. All the authors have reviewed the final version of the manuscript.

FUNDING

This work was supported by the National Natural Science Foundation of China (32070671), the COVID-19 Research Projects of West China Hospital Sichuan University (Grant no. HX-2019-nCoV-057), and the Regional Innovation Cooperation between Sichuan and Guangxi Provinces (2020YFQ0019).

ACKNOWLEDGMENTS

The authors acknowledge the financial support received from the National Natural Science Foundation of China, the West China Hospital Sichuan University, and the Regional Innovation Cooperation between Sichuan and Guangxi Provinces. Authors are thankful to the Vice-Chancellor of Punjabi University Patiala, Punjab, India for his encouragement.

REFERENCES

Abd Wahab, N. A., Abas, F., Naidu, R., Othman, I., et al. (2020). Mechanism of Anti-cancer Activity of Curcumin on Androgen-dependent and Androgen-independent Prostate Cancer. *Nutrients* 12 (3). doi:10.3390/nu12030679

Adamo, M., Adamo, M. P., Boten, J. A., Coyle, L. M., Cronin, K. A., Lam, C. J., et al. (2016). Validation of Prostate-specific Antigen Laboratory Values Recorded in Surveillance, Epidemiology, and End Results Registries. *Cancer* 123 (4), 697–703. doi:10.1002/cncr.30401

Adams, K. F., Chen, C., Newton, K. M., Potter, J. D., and Lampe, J. W. (2004). Soy Isoflavones Do Not Modulate Prostate-specific Antigen Concentrations in Older Men in a Randomized Controlled Trial. *Cancer Epidemiol. Biomarkers Prev.* 13 (4), 644–648. doi:10.1111/bju.12435

Al-Menhali, A., Al-Rumaihi, A., Al-Mohammed, H., Al-Mazrooey, H., Al-Shamlan, M., AlJassim, M., et al. (2015). Thymus Vulgaris (Thyme) Inhibits Proliferation, Adhesion, Migration, and Invasion of Human Colorectal Cancer Cells. *J. Med. Food* 18 (1), 54–59. doi:10.1089/jmf.2013.3121

Amaral, T. M., Macedo, D., Fernandes, I., and Costa, L. (2012). Castration-Resistant Prostate Cancer: Mechanisms, Targets, and Treatment. *Prostate Cancer* 2012, 327253–327311. doi:10.1155/2012/327253

Amler, L. C., Agus, D. B., LeDuc, C., Sapinoso, M. L., Fox, W. D., Kern, S., et al. (2000). Dysregulated Expression of Androgen-Responsive and Nonresponsive Genes in the Androgen-independent Prostate Cancer Xenograft Model CWR22-R1. *Cancer Res.* 60 (21), 6134–6141.

Ammirante, M., Luo, J. L., Grivennikov, S., Nedospasov, S., and Karin, M. (2010). B-cell-derived Lymphotoxin Promotes Castration-Resistant Prostate Cancer. *Nature* 464 (7286), 302–305. doi:10.1038/nature08782

Andersen, R. J., Mawji, N. R., Wang, J., Wang, G., Haile, S., Myung, J. K., et al. (2010). Regression of Castrate-Recurrent Prostate Cancer by a Small-Molecule Inhibitor of the Amino-Terminus Domain of the Androgen Receptor. *Cancer Cell* 17 (6), 535–546. doi:10.1016/j.ccr.2010.04.027

Androutsopoulos, V. P., Spyrou, I., Ploumidis, A., Papalampros, A. E., Kyriakakis, M., Delakas, D., et al. (2013). Expression Profile of CYP1A1 and CYP1B1 Enzymes in Colon and Bladder Tumors. *PLoS ONE* 8 (12), e82487. doi:10.1371/journal.pone.0082487

Androutsopoulos, V. P., Tsatsakis, A. M., and Spandidos, D. A. (2009). Cytochrome P450 CYP1A1: Wider Roles in Cancer Progression and Prevention. *BMC Cancer* 9 (1), 187. doi:10.1186/1471-2407-9-187

Ansari, M. S., and Gupta, N. P. (2004). Lycopene: a Novel Drug Therapy in Hormone Refractory Metastatic Prostate Cancer. *Urol. Oncol.* 22 (5), 415–420. doi:10.1016/j.urolonc.2004.05.009

Araujo, J. C., Trudel, G. C., Saad, F., Armstrong, A. J., Yu, E. Y., Bellmunt, J., et al. (2013). Docetaxel and Dasatinib or Placebo in Men with Metastatic Castration-Resistant Prostate Cancer (READY): a Randomised, Double-Blind Phase 3 Trial. *Lancet Oncol.* 14 (13), 1307–1316. doi:10.1016/s1470-2045(13)70479-0

Arora, H., Panara, K., Kuchakulla, M., Kulandavelu, S., Burnstein, K. L., Schally, A. V., et al. (2018). Alterations of Tumor Microenvironment by Nitric Oxide Impedes Castration-Resistant Prostate Cancer Growth. *Proc. Natl. Acad. Sci. U S A.* 115 (44), 11298–11303. doi:10.1073/pnas.1812704115

Athamneh, K., Hasasna, H. E., Samri, H. A., Attoub, S., Arafat, K., Benhalilou, N., et al. (2017). Rhus Coriaria Increases Protein Ubiquitination, Proteasomal Degradation and Triggers Non-canonical Beclin-1-independent Autophagy and Apoptotic Cell Death in colon Cancer Cells. *Sci. Rep.* 7 (1), 11633. doi:10.1038/s41598-017-11202-3

Badillo, S., Banfai, B., Birzele, F., Davydov, I. I., Hutchinson, L., Kam-Thong, T., et al. (2020). An Introduction to Machine Learning. *Clin. Pharmacol. Ther.* 107 (4), 871–885. doi:10.1002/cpt.1796

Barber, N. J., Zhang, X., Zhu, G., Pramanik, R., Barber, J. A., Martin, F. L., et al. (2006). Lycopene Inhibits DNA Synthesis in Primary Prostate Epithelial Cells *In Vitro* and its Administration Is Associated with a Reduced Prostate-specific Antigen Velocity in a Phase II Clinical Study. *Prostate Cancer Prostatic Dis.* 9 (4), 407–413. doi:10.1038/sj.pcan.4500895

Barton, H. A., Pastoor, T. P., Baetcke, K., Chambers, J. E., Diliberto, J., Doerrer, N. G., et al. (2008). The Acquisition and Application of Absorption, Distribution, Metabolism, and Excretion (ADME) Data in Agricultural Chemical Safety Assessments. *Crit. Rev. Toxicol.* 36 (1), 9–35. doi:10.1080/10408440500534362

Basak, S., Pookot, D., Noonan, E. J., and Dahiya, R. (2008). Genistein Down-Regulates Androgen Receptor by Modulating HDAC6-Hsp90 Chaperone Function. *Mol. Cancer Ther.* 7 (10), 3195–3202. doi:10.1158/1535-7163.Mct-08-0617

Beaver, L. M., Yu, T. W., Sokolowski, E. I., Williams, D. E., Dashwood, R. H., and Ho, E. (2012). 3,3'-Diindolylmethane, but Not Indole-3-Carbinol, Inhibits Histone Deacetylase Activity in Prostate Cancer Cells. *Toxicol. Appl. Pharmacol.* 263 (3), 345–351. doi:10.1016/j.taap.2012.07.007

Bettedi, L., and Foukas, L. C. (2017). Growth Factor, Energy and Nutrient Sensing Signalling Pathways in Metabolic Ageing. *Biogerontology* 18 (6), 913–929. doi:10.1007/s10522-017-9724-6

Bettuzzi, S., Brausi, M., Rizzi, F., Castagnetti, G., Peracchia, G., and Corti, A. (2006). Chemoprevention of Human Prostate Cancer by Oral Administration of green tea Catechins in Volunteers with High-Grade Prostate Intraepithelial Neoplasia: a Preliminary Report from a One-Year Proof-Of-Principle Study. *Cancer Res.* 66 (2), 1234–1240. doi:10.1158/0008-5472.CAN-05-1145

Bi, Y. H., Zhang, L. H., Chen, S. J., and Ling, Q. Z. (2018). Antitumor Mechanisms of Curcumae Rhizoma Based on Network Pharmacology. *Evid. Based Complement. Alternat Med.* 2018, 4509892–4509899. doi:10.1155/2018/4509892

Bosland, M. C., Kato, I., Zeleniuch-Jacquotte, A., Schmoll, J., Enk Rueter, E., Melamed, J., et al. (2013). Effect of Soy Protein Isolate Supplementation on Biochemical Recurrence of Prostate Cancer after Radical Prostatectomy: a Randomized Trial. *JAMA* 310 (2), 170–178. doi:10.1001/jama.2013.7842

Bowen, P., Chen, L., Stacewicz-Sapuntzakis, M., Duncan, C., Sharifi, R., Ghosh, L., et al. (2002). Tomato Sauce Supplementation and Prostate Cancer: Lycopene Accumulation and Modulation of Biomarkers of Carcinogenesis. *Exp. Biol. Med. (Maywood)* 227 (10), 886–893. doi:10.1177/153537020222701008

Brausi, M., Rizzi, F., and Bettuzzi, S. (2008). Chemoprevention of Human Prostate Cancer by green tea Catechins: Two Years Later. A Follow-Up Update. *Eur. Urol.* 54 (2), 472–473. doi:10.1016/j.eururo.2008.03.100

Bunker, C. H., McDonald, A. C., Evans, R. W., de la Rosa, N., Boumosleh, J. M., and Patrick, A. L. (2007). A Randomized Trial of Lycopene Supplementation in Tobago Men with High Prostate Cancer Risk. *Nutr. Cancer* 57 (2), 130–137. doi:10.1080/01635580701274046

Cai, C., Chen, S. Y., Zheng, Z., Omwancha, J., Lin, M. F., Balk, S. P., et al. (2006). Androgen Regulation of Soluble Guanylyl Cyclasealpha1 Mediates Prostate Cancer Cell Proliferation. *Oncogene* 26 (11), 1606–1615. doi:10.1038/sj.onc.1209956

Calcinotto, A., Spataro, C., Zagato, E., Di Mitri, D., Gil, V., Crespo, M., et al. (2018). IL-23 Secreted by Myeloid Cells Drives Castration-Resistant Prostate Cancer. *Nature* 559 (7714), 363–369. doi:10.1038/s41586-018-0266-0

Chandrasekar, T., Yang, J. C., Gao, A. C., and Evans, C. P. (2015). Targeting Molecular Resistance in Castration-Resistant Prostate Cancer. *BMC Med.* 13 (1), 206. doi:10.1186/s12916-015-0457-6

Chen, J., Wang, Y., Shen, B., and Zhang, D. (2013a). Molecular Signature of Cancer at Gene Level or Pathway Level? Case Studies of Colorectal Cancer and Prostate Cancer Microarray Data. *Comput. Math. Methods Med.* 2013, 909525. doi:10.1155/2013/909525

Chen, J., Zhang, D., Yan, W., Yang, D., and Shen, B. (2013b). Translational Bioinformatics for Diagnostic and Prognostic Prediction of Prostate Cancer in the Next-Generation Sequencing Era. *Biomed. Res. Int.* 2013, 901578. doi:10.1155/2013/901578

Chen, Y., Robles, A. I., Martinez, L. A., Liu, F., Gimenez-Conti, I. B., and Conti, C. J. (1996). Expression of G1 Cyclins, Cyclin-dependent Kinases, and Cyclin-dependent Kinase Inhibitors in Androgen-Induced Prostate Proliferation in Castrated Rats. *Cell Growth Differ* 7 (11), 1571–1578.

Chesire, D. R., and Isaacs, W. B. (2003). Beta-catenin Signaling in Prostate Cancer: an Early Perspective. *Endocr. Relat. Cancer* 10 (4), 537–560. doi:10.1677/erc.0.0100537

Chinni, S. R., Li, Y., Upadhyay, S., Koppolu, P. K., and Sarkar, F. H. (2001). Indole-3-carbinol (I3C) Induced Cell Growth Inhibition, G1 Cell Cycle Arrest and Apoptosis in Prostate Cancer Cells. *Oncogene* 20 (23), 2927–2936. doi:10.1038/sj.onc.1204365

Choi, H. Y., Lim, J. E., and Hong, J. H. (2010). Curcumin Interrupts the Interaction between the Androgen Receptor and Wnt/β-Catenin Signaling Pathway in LNCaP Prostate Cancer Cells. *Prostate Cancer Prostatic Dis.* 13 (4), 343–349. doi:10.1038/pcan.2010.26

Choi, Y. H., Han, D. H., Kim, S. W., Kim, M. J., Sung, H. H., Jeon, H. G., et al. (2019). A Randomized, Double-Blind, Placebo-Controlled Trial to Evaluate the Role of Curcumin in Prostate Cancer Patients with Intermittent Androgen Deprivation. *Prostate* 79 (6), 614–621. doi:10.1002/pros.23766

Choudhari, A. S., Mandave, P. C., Deshpande, M., Ranjekar, P., and Prakash, O. (2020). Phytochemicals in Cancer Treatment: From Preclinical Studies to Clinical Practice. *Front. Pharmacol.* 10, 1614. doi:10.3389/fphar.2019.01614

Corn, P. G. (2012). The Tumor Microenvironment in Prostate Cancer: Elucidating Molecular Pathways for Therapy Development. *Cmar*, 183. doi:10.2147/cmar.S32839

Coutinho, I., Day, T. K., Tilley, W. D., and Selth, L. A. (2016). Androgen Receptor Signaling in Castration-Resistant Prostate Cancer: a Lesson in Persistence. *Endocr. Relat. Cancer* 23 (12), T179–T197. doi:10.1530/erc-16-0422

Cramer, R. D., Patterson, D. E., and Bunce, J. D. (1988). Comparative Molecular Field Analysis (CoMFA). 1. Effect of Shape on Binding of Steroids to Carrier Proteins. *J. Am. Chem. Soc.* 110 (18), 5959–5967. doi:10.1021/ja00226a005

Culp, M. B., Soerjomataram, I., Efstathiou, J. A., Bray, F., and Jemal, A. (2020). Recent Global Patterns in Prostate Cancer Incidence and Mortality Rates. *Eur. Urol.* 77 (1), 38–52. doi:10.1016/j.eururo.2019.08.005

Cunha, G. R., Hayward, S. W., Dahiya, R., and Foster, B. A. (1996). Smooth Muscle-Epithelial Interactions in Normal and Neoplastic Prostatic Development. *Acta Anat. (Basel)* 155 (1), 63–72. doi:10.1159/000147791

de Bono, J. S., Oudard, S., Ozguroglu, M., Hansen, S., Machiels, J. P., Kocak, I., et al. (2010). Prednisone Plus Cabazitaxel or Mitoxantrone for Metastatic Castration-Resistant Prostate Cancer Progressing after Docetaxel Treatment: a Randomised Open-Label Trial. *Lancet* 376 (9747), 1147–1154. doi:10.1016/s0140-6736(10)61389-x

Deng, K., Li, H., and Guan, Y. (2020). Treatment Stratification of Patients with Metastatic Castration-Resistant Prostate Cancer by Machine Learning. *iScience* 23 (2), 100804. doi:10.1016/j.isci.2019.100804

deVere White, R. W., Tsodikov, A., Stapp, E. C., Soares, S. E., Fujii, H., and Hackman, R. M. (2010). Effects of a High Dose, Aglycone-Rich Soy Extract on Prostate-specific Antigen and Serum Isoflavone Concentrations in Men with Localized Prostate Cancer. *Nutr. Cancer* 62 (8), 1036–1043. doi:10.1080/01635581.2010.492085

Dhir, R., Ni, Z., Lou, W., DeMiguel, F., Grandis, J. R., and Gao, A. C. (2002). Stat3 Activation in Prostatic Carcinomas. *Prostate* 51 (4), 241–246. doi:10.1002/pros.10079

Duch, W., Swaminathan, K., and Meller, J. (2007). Artificial Intelligence Approaches for Rational Drug Design and Discovery. *Curr. Pharm. Des.* 13 (14), 1497–1508. doi:10.2174/138161207780765954

Eisermann, K., Wang, D., Jing, Y., Pascal, L. E., and Wang, Z. (2013). Androgen Receptor Gene Mutation, Rearrangement, Polymorphism. *Transl Androl. Urol.* 2 (3), 137–147. doi:10.3978/j.issn.2223-4683.2013.09.15

El Hasasna, H., Athamneh, K., Al Samri, H., Karuvantevida, N., Al Dhaheri, Y., Hisaindee, S., et al. (2015). Rhus Coriaria Induces Senescence and Autophagic Cell Death in Breast Cancer Cells through a Mechanism Involving P38 and ERK1/2 Activation. *Sci. Rep.* 5 (1), 13013. doi:10.1038/srep13013

Elmas, L., Secme, M., Mammadov, R., Fahrioglu, U., and Dodurga, Y. (2018). The Determination of the Potential Anticancer Effects ofCoriandrum Sativum in PC-3 and LNCaP Prostate Cancer Cell Lines. *J. Cell Biochem.* 120 (3), 3506–3513. doi:10.1002/jcb.27625

Fang, Z., Xu, C., Li, Y., Cai, X., Ren, S., Liu, H., et al. (2016). A Feed-Forward Regulatory Loop between Androgen Receptor and PlncRNA-1 Promotes Prostate Cancer Progression. *Cancer Lett.* 374 (1), 62–74. doi:10.1016/j.canlet.2016.01.033

Fardoun, M., Al-Shehabi, T., El-Yazbi, A., Issa, K., Zouein, F., Maaliki, D., et al. (2017). Ziziphus Nummularia Inhibits Inflammation-Induced Atherogenic Phenotype of Human Aortic Smooth Muscle Cells. *Oxid Med. Cel Longev* 2017, 4134093–4134110. doi:10.1155/2017/4134093

Febbo, P. G., Lowenberg, M., Thorner, A. R., Brown, M., Loda, M., and Golub, T. R. (2005). Androgen Mediated Regulation and Functional Implications of Fkbp51 Expression in Prostate Cancer. *J. Urol.* 173 (5), 1772–1777. doi:10.1097/01.ju.0000155845.44729.ba

Ferlay, J., Lam, F., Colombet, M., Mery, L., Pineros, M., Znaor, A., et al. (2018). *Global Cancer Observatory: Cancer Today* [Online]. Lyon, France: International Agency for Research on Cancer. Available at: https://gco.iarc.fr/today [Accessed 07.06.2021].

Fontana, F., Moretti, R. M., Raimondi, M., Marzagalli, M., Beretta, G., Procacci, P., et al. (2019a). δ-Tocotrienol Induces Apoptosis, Involving Endoplasmic Reticulum Stress and Autophagy, and Paraptosis in Prostate Cancer Cells. *Cell Prolif* 52 (3), e12576. doi:10.1111/cpr.12576

Fontana, F., Raimondi, M., Marzagalli, M., Di Domizio, A., and Limonta, P. (2020). Natural Compounds in Prostate Cancer Prevention and Treatment: Mechanisms of Action and Molecular Targets. *Cells* 9 (2). doi:10.3390/cells9020460

Fontana, F., Raimondi, M., Marzagalli, M., Moretti, R. M., Marelli, M. M., and Limonta, P. (2019b). Tocotrienols and Cancer: From the State of the Art to Promising Novel Patents. *Recent Pat Anticancer Drug Discov.* 14 (1), 5–18. doi:10.2174/1574892814666190116111827

Fulda, S. (2008). Betulinic Acid for Cancer Treatment and Prevention. *Int. J. Mol. Sci.* 9 (6), 1096–1107. doi:10.3390/ijms9061096

Gao, B., Shen, X., Kunos, G., Meng, Q., Goldberg, I. D., Rosen, E. M., et al. (2001). Constitutive Activation of JAK-STAT3 Signaling by BRCA1 in Human Prostate Cancer Cells. *FEBS Lett.* 488 (3), 179–184. doi:10.1016/s0014-5793(00)02430-3

Garikapaty, V. P., Ashok, B. T., Tadi, K., Mittelman, A., and Tiwari, R. K. (2006). 3,3'-Diindolylmethane Downregulates Pro-survival Pathway in Hormone Independent Prostate Cancer. *Biochem. Biophys. Res. Commun.* 340 (2), 718–725. doi:10.1016/j.bbrc.2005.12.059

Gelmann, E. P. (2002). Molecular Biology of the Androgen Receptor. *J. Clin. Oncol.* 20 (13), 3001–3015. doi:10.1200/JCO.2002.10.018

Ghafouri-Fard, S., Shabestari, F. A., Vaezi, S., Abak, A., Shoorei, H., Karimi, A., et al. (2021). Emerging Impact of Quercetin in the Treatment of Prostate Cancer. *Biomed. Pharmacother.* 138, 111548. doi:10.1016/j.biopha.2021.111548

Gibbs, J. B. (2000). Mechanism-based Target Identification and Drug Discovery in Cancer Research. *Science* 287 (5460), 1969–1973. doi:10.1126/science.287.5460.1969

Goldblatt, E. M., and Lee, W. H. (2010). From Bench to Bedside: the Growing Use of Translational Research in Cancer Medicine. *Am. J. Transl Res.* 2 (1), 1–18.

Grossmann, M. E., Huang, H., and Tindall, D. J. (2001). Androgen Receptor Signaling in Androgen-Refractory Prostate Cancer. *J. Natl. Cancer Inst.* 93 (22), 1687–1697. doi:10.1093/jnci/93.22.1687

Gupta, R., Srivastava, D., Sahu, M., Tiwari, S., Ambasta, R. K., and Kumar, P. (2021). Artificial Intelligence to Deep Learning: Machine Intelligence Approach for Drug Discovery. *Mol. Divers.* 25, 1315–1360. doi:10.1007/s11030-021-10217-3

Gupta, S., Iljin, K., Sara, H., Mpindi, J. P., Mirtti, T., Vainio, P., et al. (2010). FZD4 as a Mediator of ERG Oncogene-Induced WNT Signaling and Epithelial-To-Mesenchymal Transition in Human Prostate Cancer Cells. *Cancer Res.* 70 (17), 6735–6745. doi:10.1158/0008-5472.CAN-10-0244

Gurel, B., Lucia, M. S., Thompson, I. M., Goodman, P. J., Tangen, C. M., Kristal, A. R., et al. (2014). Chronic Inflammation in Benign Prostate Tissue Is Associated with High-Grade Prostate Cancer in the Placebo Arm of the Prostate Cancer Prevention Trial. *Cancer Epidemiol. Biomarkers Prev.* 23 (5), 847–856. doi:10.1158/1055-9965.Epi-13-1126

Hamilton-Reeves, J. M., Banerjee, S., Banerjee, S. K., Holzbeierlein, J. M., Thrasher, J. B., Kambhampati, S., et al. (2013). Short-term Soy Isoflavone Intervention in Patients with Localized Prostate Cancer: a Randomized, Double-Blind, Placebo-Controlled Trial. *PLoS One* 8 (7), e68331. doi:10.1371/journal.pone.0068331

Hamilton-Reeves, J. M., Rebello, S. A., Thomas, W., Slaton, J. W., and Kurzer, M. S. (2007). Isoflavone-rich Soy Protein Isolate Suppresses Androgen Receptor Expression without Altering Estrogen Receptor-Beta Expression or Serum Hormonal Profiles in Men at High Risk of Prostate Cancer. *J. Nutr.* 137 (7), 1769–1775. doi:10.1093/jn/137.7.1769

Hariharan, K., and Padmanabha, V. (2016). Demography and Disease Characteristics of Prostate Cancer in India. *Indian J. Urol.* 32 (2), 103–108. doi:10.4103/0970-1591.174774

Hay, C. W., McEwan, I. J., and McEwan, I. J. (2012). The Impact of Point Mutations in the Human Androgen Receptor: Classification of Mutations on the Basis of Transcriptional Activity. *PLoS ONE* 7 (3), e32514. doi:10.1371/journal.pone.0032514

He, B., You, L., Uematsu, K., Xu, Z., Lee, A. Y., Matsangou, M., et al. (2004). A Monoclonal Antibody against Wnt-1 Induces Apoptosis in Human Cancer Cells. *Neoplasia* 6 (1), 7–14. doi:10.1016/s1476-5586(04)80048-4

Heber, D., and Lu, Q. Y. (2002). Overview of Mechanisms of Action of Lycopene. *Exp. Biol. Med. (Maywood)* 227 (10), 920–923. doi:10.1177/153537020222701013

Hejazi, J., Rastmanesh, R., Taleban, F. A., Molana, S. H., Hejazi, E., Ehtejab, G., et al. (2016). Effect of Curcumin Supplementation during Radiotherapy on Oxidative Status of Patients with Prostate Cancer: A Double Blinded, Randomized, Placebo-Controlled Study. *Nutr. Cancer* 68 (1), 77–85. doi:10.1080/01635581.2016.1115527

Henning, S. M., Wang, P., Lee, R. P., Trang, A., Husari, G., Yang, J., et al. (2020). Prospective Randomized Trial Evaluating Blood and Prostate Tissue Concentrations of green tea Polyphenols and Quercetin in Men with Prostate Cancer. *Food Funct.* 11 (5), 4114–4122. doi:10.1039/d0fo00565g

Hieronymus, H., Lamb, J., Ross, K. N., Peng, X. P., Clement, C., Rodina, A., et al. (2006). Gene Expression Signature-Based Chemical Genomic Prediction Identifies a Novel Class of HSP90 Pathway Modulators. *Cancer Cell* 10 (4), 321–330. doi:10.1016/j.ccr.2006.09.005

Hoimes, C. J., and Kelly, W. K. (2009). Redefining Hormone Resistance in Prostate Cancer. *Ther. Adv. Med. Oncol.* 2 (2), 107–123. doi:10.1177/1758834009356433

Holzapfel, N. P., Holzapfel, B. M., Champ, S., Feldthusen, J., Clements, J., and Hutmacher, D. W. (2013). The Potential Role of Lycopene for the Prevention and Therapy of Prostate Cancer: From Molecular Mechanisms to Clinical Evidence. *Int. J. Mol. Sci.* 14 (7), 14620–14646. doi:10.3390/ijms140714620

Hopkins, A. L. (2008). Network Pharmacology: the Next Paradigm in Drug Discovery. *Nat. Chem. Biol.* 4 (11), 682–690. doi:10.1038/nchembio.118

Hotte, S. J., and Saad, F. (2010). Current Management of Castrate-Resistant Prostate Cancer. *Curr. Oncol.* 17 Suppl 2 (12), S72–S79. doi:10.3747/co.v17i0.718

Howlader, N., Noone, A., Krapcho, M., Miller, D., Bishop, K., Kosary, C., et al. (2017). SEER Cancer Statistics Review. Online. Bethesda, MD: National Cancer Institute, 1975–2014. Available: https://seer.cancer.gov/csr/1975_2014/ (Accessed 06 20, 2021).

Huang, Y., Jiang, X., Liang, X., and Jiang, G. (2018). Molecular and Cellular Mechanisms of Castration Resistant Prostate Cancer. *Oncol. Lett.* 15 (5), 6063–6076. doi:10.3892/ol.2018.8123

Huang, Y. W., Wang, L. S., Chang, H. L., Ye, W., Dowd, M. K., Wan, P. J., et al. (2006). Molecular Mechanisms of (-)-Gossypol-Induced Apoptosis in Human Prostate Cancer Cells. *Anticancer Res.* 26 (3A), 1925–1933.

Ide, H., Lu, Y., Noguchi, T., Muto, S., Okada, H., Kawato, S., et al. (2018). Modulation of AKR1C2 by Curcumin Decreases Testosterone Production in Prostate Cancer. *Cancer Sci.* 109 (4), 1230–1238. doi:10.1111/cas.13517

Ide, H., Tokiwa, S., Sakamaki, K., Nishio, K., Isotani, S., Muto, S., et al. (2010). Combined Inhibitory Effects of Soy Isoflavones and Curcumin on the Production of Prostate-specific Antigen. *Prostate* 70 (10), 1127–1133. doi:10.1002/pros.21147

Ivanov, N. I., Cowell, S. P., Brown, P., Rennie, P. S., Guns, E. S., and Cox, M. E. (2007). Lycopene Differentially Induces Quiescence and Apoptosis in Androgen-Responsive and -independent Prostate Cancer Cell Lines. *Clin. Nutr.* 26 (2), 252–263. doi:10.1016/j.clnu.2007.01.002

Jasinski, M., Jasinska, L., and Ogrodowczyk, M. (2013). Resveratrol in Prostate Diseases - a Short Review. *Ceju* 66 (2), 144–149. doi:10.5173/ceju.2013.02.art8

Jatoi, A., Burch, P., Hillman, D., Vanyo, J. M., Dakhil, S., Nikcevich, D., et al. (2007). A Tomato-Based, Lycopene-Containing Intervention for Androgen-independent Prostate Cancer: Results of a Phase II Study from the North Central Cancer Treatment Group. *Urology* 69 (2), 289–294. doi:10.1016/j.urology.2006.10.019

Jatoi, A., Ellison, N., Burch, P. A., Sloan, J. A., Dakhil, S. R., Novotny, P., et al. (2003). A Phase II Trial of green tea in the Treatment of Patients with Androgen Independent Metastatic Prostate Carcinoma. *Cancer* 97 (6), 1442–1446. doi:10.1002/cncr.11200

Jian, L. (2009). Soy, Isoflavones, and Prostate Cancer. *Mol. Nutr. Food Res.* 53 (2), 217–226. doi:10.1002/mnfr.200800167

Jiang, J., Jia, P., Zhao, Z., and Shen, B. (2014). Key Regulators in Prostate Cancer Identified by Co-expression Module Analysis. *BMC Genomics* 15 (1), 1015. doi:10.1186/1471-2164-15-1015

Joon, S., Singla, R. K., Shen, B., and Kamal, M. A. (2021). QSCR Analysis of Cytotoxicity of 6-Fluoro-3-(4h-1,2,4-Triazol-3-Yl)quinolin-4(1h)-Ones on

Chinese Hamster Ovary Cell Line: Design of REPUBLIC1986. *Curr. Med. Chem.* 28. doi:10.2174/0929867328666210623150552

Ju, J., Hong, J., Zhou, J. N., Pan, Z., Bose, M., Liao, J., et al. (2005). Inhibition of Intestinal Tumorigenesis in Apcmin/+ Mice by (-)-Epigallocatechin-3-Gallate, the Major Catechin in green tea. *Cancer Res.* 65 (22), 10623–10631. doi:10.1158/0008-5472.CAN-05-1949

Kallifatidis, G., Hoy, J. J., and Lokeshwar, B. L. (2016). Bioactive Natural Products for Chemoprevention and Treatment of Castration-Resistant Prostate Cancer. *Semin. Cancer Biol.* 40-41, 160–169. doi:10.1016/j.semcancer.2016.06.003

Karamanolakis, D., Armakolas, A., and Koutsilieris, M. (2016). Castration-resistant Prostate Cancer: The Targeting of Bone Microenvironment-Related Survival Factors for Prostate Cancer Cells. *Ccand* 3 (1), 16–22. doi:10.2174/2212697x03666151203202934

Karlou, M., Tzelepi, V., and Efstathiou, E. (2010). Therapeutic Targeting of the Prostate Cancer Microenvironment. *Nat. Rev. Urol.* 7 (9), 494–509. doi:10.1038/nrurol.2010.134

Kato, M., Banuelos, C. A., Imamura, Y., Leung, J. K., Caley, D. P., Wang, J., et al. (2016). Cotargeting Androgen Receptor Splice Variants and mTOR Signaling Pathway for the Treatment of Castration-Resistant Prostate Cancer. *Clin. Cancer Res.* 22 (11), 2744–2754. doi:10.1158/1078-0432.Ccr-15-2119

Kaur, R., Sharma, P., Gupta, G. K., Ntie-Kang, F., and Kumar, D. (2020). Structure-Activity-Relationship and Mechanistic Insights for Anti-HIV Natural Products. *Molecules* 25 (9). doi:10.3390/molecules25092070

Kaur, T., Sharma, P., Gupta, G. K., Ntie-Kang, F., and Kumar, D. (2019). Treatment of Tuberculosis by Natural Drugs: A Review. *Plant Arch.* 19 (2), 2168–2176.

Kheirandish, P., and Chinegwundoh, F. (2011). Ethnic Differences in Prostate Cancer. *Br. J. Cancer* 105 (4), 481–485. doi:10.1038/bjc.2011.273

Kim, L., Rao, A. V., and Rao, L. G. (2002). Effect of Lycopene on Prostate LNCaP Cancer Cells in Culture. *J. Med. Food* 5 (4), 181–187. doi:10.1089/109662002763003320

Kirby, M., Hirst, C., and Crawford, E. D. (2011). Characterising the Castration-Resistant Prostate Cancer Population: a Systematic Review. *Int. J. Clin. Pract.* 65 (11), 1180–1192. doi:10.1111/j.1742-1241.2011.02799.x

Kjaer, T. N., Ornstrup, M. J., Poulsen, M. M., Jørgensen, J. O., Hougaard, D. M., Cohen, A. S., et al. (2015). Resveratrol Reduces the Levels of Circulating Androgen Precursors but Has No Effect on, Testosterone, Dihydrotestosterone, PSA Levels or Prostate Volume. A 4-month Randomised Trial in Middle-Aged Men. *Prostate* 75 (12), 1255–1263. doi:10.1002/pros.23006

Kotsakis, A., Matikas, A., Koinis, F., Kentepozidis, N., Varthalitis, I. I., Karavassilis, V., et al. (2016). A Multicentre Phase II Trial of Cabazitaxel in Patients with Advanced Non-small-cell Lung Cancer Progressing after Docetaxel-Based Chemotherapy. *Br. J. Cancer* 115 (7), 784–788. doi:10.1038/bjc.2016.281

Krumenacker, J. S., Hanafy, K. A., and Murad, F. (2004). Regulation of Nitric Oxide and Soluble Guanylyl Cyclase. *Brain Res. Bull.* 62 (6), 505–515. doi:10.1016/s0361-9230(03)00102-3

Kucuk, O., Sarkar, F. H., Sakr, W., Djuric, Z., Pollak, M. N., Khachik, F., et al. (2001). Phase II Randomized Clinical Trial of Lycopene Supplementation before Radical Prostatectomy. *Cancer Epidemiol. Biomarkers Prev.* 10 (8), 861–868.

Kühl, S. J., and Kühl, M. (2013). On the Role of Wnt/β-Catenin Signaling in Stem Cells. *Biochim. Biophys. Acta* 1830 (2), 2297–2306. doi:10.1016/j.bbagen.2012.08.010

Kumar, D., and Jain, S. K. (2016). A Comprehensive Review of N-Heterocycles as Cytotoxic Agents. *Curr. Med. Chem.* 23 (38), 4338–4394. doi:10.2174/0929867323666160809093930

Kumar, D., Malik, F., Bedi, P. M., and Jain, S. (2016a). 2,4-Diarylpyrano[3,2-c] chromen-5(4H)-ones as Antiproliferative Agents. *Chem. Pharm. Bull. (Tokyo)* 64 (5), 399–409. doi:10.1248/cpb.c15-00958

Kumar, D., Nepali, K., Bedi, P. M., Kumar, S., Malik, F., and Jain, S. (2015a). 4,6-diaryl Pyrimidones as Constrained Chalcone Analogues: Design, Synthesis and Evaluation as Antiproliferative Agents. *Anticancer Agents Med. Chem.* 15 (6), 793–803. doi:10.2174/1871520615666150318101436

Kumar, D., Sharma, P., Nepali, K., Mahajan, G., Mintoo, M. J., Singh, A., et al. (2018a). Antitumour, Acute Toxicity and Molecular Modeling Studies of 4-(pyridin-4-Yl)-6-(thiophen-2-Yl) Pyrimidin-2(1h)-One against Ehrlich Ascites Carcinoma and Sarcoma-180. *Heliyon* 4 (6), e00661. doi:10.1016/j.heliyon.2018.e00661

Kumar, D., Singh, G., Sharma, P., Qayum, A., Mahajan, G., Mintoo, M. J., et al. (2018b). 4-aryl/heteroaryl-4H-fused Pyrans as Anti-proliferative Agents: Design, Synthesis and Biological Evaluation. *Anticancer Agents Med. Chem.* 18 (1), 57–73. doi:10.2174/1871520617666170918143911

Kumar, D., Singh, O., Nepali, K., Bedi, P., Qayum, A., Singh, S., et al. (2016b). Naphthoflavones as Antiproliferative Agents: Design, Synthesis and Biological Evaluation. *Anticancer Agents Med. Chem.* 16 (7), 881–890. doi:10.2174/1871520616666160204113536

Kumar, D., Sharma, P., Kaur, R., Lobe, M. M., Gupta, G. K., and Ntie-Kang, F. (2021). In Search of Therapeutic Candidates for HIV/AIDS: Rational Approaches, Design Strategies, Structure–Activity Relationship and Mechanistic Insights. *RSC Adv.* 11 (29), 17936–17964. doi:10.1039/d0ra10655k

Kumar, D., Sharma, P., Singh, H., Nepali, K., Gupta, G. K., Jain, S. K., et al. (2017). The Value of Pyrans as Anticancer Scaffolds in Medicinal Chemistry. *RSC Adv.* 7 (59), 36977–36999. doi:10.1039/c7ra05441f

Kumar, N. B., Pow-Sang, J., Egan, K. M., Spiess, P. E., Dickinson, S., Salup, R., et al. (2015b). Randomized, Placebo-Controlled Trial of Green Tea Catechins for Prostate Cancer Prevention. *Cancer Prev. Res. (Phila)* 8 (10), 879–887. doi:10.1158/1940-6207.CAPR-14-0324

Kwan, W., Duncan, G., Van Patten, C., Liu, M., and Lim, J. (2010). A Phase II Trial of a Soy Beverage for Subjects without Clinical Disease with Rising Prostate-specific Antigen after Radical Radiation for Prostate Cancer. *Nutr. Cancer* 62 (2), 198–207. doi:10.1080/01635580903305318

Lall, R. K., Adhami, V. M., and Mukhtar, H. (2016). Dietary Flavonoid Fisetin for Cancer Prevention and Treatment. *Mol. Nutr. Food Res.* 60 (6), 1396–1405. doi:10.1002/mnfr.201600025

Lazarevic, B., Hammarström, C., Yang, J., Ramberg, H., Diep, L. M., Karlsen, S. J., et al. (2012). The Effects of Short-Term Genistein Intervention on Prostate Biomarker Expression in Patients with Localised Prostate Cancer before Radical Prostatectomy. *Br. J. Nutr.* 108 (12), 2138–2147. doi:10.1017/S0007114512000384

Lee, C., Light, A., Alaa, A., Thurtle, D., van der Schaar, M., and Gnanapragasam, V. J. (2021). Application of a Novel Machine Learning Framework for Predicting Non-metastatic Prostate Cancer-specific Mortality in Men Using the Surveillance, Epidemiology, and End Results (SEER) Database. *Lancet Digit Health* 3 (3), e158–e165. doi:10.1016/s2589-7500(20)30314-9

Lee, C., Zame, W., Alaa, A., and Schaar, M. (2019a). "Temporal Quilting for Survival Analysis," in Proceedings of the Twenty-Second International Conference on Artificial Intelligence and Statistics, Naha, Okinawa, Japan. Editors C. Kamalika and S. Masashi (Proceedings of Machine Learning Research: PMLR)

Lee, D., Lee, W. Y., Jung, K., Kwon, Y. S., Kim, D., Hwang, G. S., et al. (2019b). The Inhibitory Effect of Cordycepin on the Proliferation of MCF-7 Breast Cancer Cells, and its Mechanism: An Investigation Using Network Pharmacology-Based Analysis. *Biomolecules* 9 (9). doi:10.3390/biom9090414

Lee, M. H., Kundu, J. K., Keum, Y. S., Cho, Y. Y., Surh, Y. J., and Choi, B. Y. (2014). Resveratrol Inhibits IL-6-Induced Transcriptional Activity of AR and STAT3 in Human Prostate Cancer LNCaP-FGC Cells. *Biomol. Ther. (Seoul)* 22 (5), 426–430. doi:10.4062/biomolther.2014.061

Li, J., Cao, B., Liu, X., Fu, X., Xiong, Z., Chen, L., et al. (2011). Berberine Suppresses Androgen Receptor Signaling in Prostate Cancer. *Mol. Cancer Ther.* 10 (8), 1346–1356. doi:10.1158/1535-7163.MCT-10-0985

Li, S., Fan, T. P., Jia, W., Lu, A., and Zhang, W. (2014). Network Pharmacology in Traditional Chinese Medicine. *Evid. Based Complement. Alternat Med.* 2014, 138460–138462. doi:10.1155/2014/138460

Li, S., Zhang, B., Jiang, D., Wei, Y., and Zhang, N. (2010). Herb Network Construction and Co-module Analysis for Uncovering the Combination Rule of Traditional Chinese Herbal Formulae. *BMC Bioinformatics* 11 (S11), S6. doi:10.1186/1471-2105-11-s11-s6

Li, S., and Zhang, B. (2013). Traditional Chinese Medicine Network Pharmacology: Theory, Methodology and Application. *Chin. J. Nat. Med.* 11 (2), 110–120. doi:10.1016/s1875-5364(13)60037-0

Li, Y., Chinni, S. R., and Sarkar, F. H. (2005). Selective Growth Regulatory and Pro-apoptotic Effects of DIM Is Mediated BY AKT and NF-kappaB Pathways in Prostate Cancer Cells. *Front. Biosci.* 10 (1–3), 236–243. doi:10.2741/1523

Lian, F., Sharma, N. V., Moran, J. D., and Moreno, C. S. (2015). The Biology of Castration-Resistant Prostate Cancer. *Curr. Probl. Cancer* 39 (1), 17–28. doi:10.1016/j.currproblcancer.2014.11.004

Liao, Y., Liu, Y., Xia, X., Shao, Z., Huang, C., He, J., et al. (2020). Targeting GRP78-dependent AR-V7 Protein Degradation Overcomes Castration-Resistance in

Prostate Cancer Therapy. *Theranostics* 10 (8), 3366–3381. doi:10.7150/thno.41849

Lill, M. A. (2007). Multi-dimensional QSAR in Drug Discovery. *Drug Discov. Today* 12 (23–24), 1013–1017. doi:10.1016/j.drudis.2007.08.004

Lin, F. M., Chen, L. R., Lin, E. H., Ke, F. C., Chen, H. Y., Tsai, M. J., et al. (2007). Compounds from Wedelia Chinensis Synergistically Suppress Androgen Activity and Growth in Prostate Cancer Cells. *Carcinogenesis* 28 (12), 2521–2529. doi:10.1093/carcin/bgm137

Lin, Y., Chen, F., Shen, L., Tang, X., Du, C., Sun, Z., et al. (2018). Biomarker microRNAs for Prostate Cancer Metastasis: Screened with a Network Vulnerability Analysis Model. *J. Transl Med.* 16 (1), 134. doi:10.1186/s12967-018-1506-7

Lin, Y., Miao, Z., Zhang, X., Wei, X., Hou, J., Huang, Y., et al. (2021). Identification of Key MicroRNAs and Mechanisms in Prostate Cancer Evolution Based on Biomarker Prioritization Model and Carcinogenic Survey. *Front. Genet.* 11. doi:10.3389/fgene.2020.596826

Lipinski, C. F., Maltarollo, V. G., Oliveira, P. R., da Silva, A. B. F., and Honorio, K. M. (2019). Advances and Perspectives in Applying Deep Learning for Drug Design and Discovery. *Front. Robot AI* 6, 108. doi:10.3389/frobt.2019.00108

Liu, G., Kelly, W. K., Wilding, G., Leopold, L., Brill, K., and Somer, B. (2009). An Open-Label, Multicenter, Phase I/II Study of Single-Agent AT-101 in Men with Castrate-Resistant Prostate Cancer. *Clin. Cancer Res.* 15 (9), 3172–3176. doi:10.1158/1078-0432.Ccr-08-2985

Liu, X., He, Z., Li, C. H., Huang, G., Ding, C., and Liu, H. (2012). Correlation Analysis of JAK-STAT Pathway Components on Prognosis of Patients with Prostate Cancer. *Pathol. Oncol. Res.* 18 (1), 17–23. doi:10.1007/s12253-011-9410-y

Liu, X., Wu, J., Zhang, D., Wang, K., Duan, X., Meng, Z., et al. (2018). Network Pharmacology-Based Approach to Investigate the Mechanisms ofHedyotis diffusaWilld. In the Treatment of Gastric Cancer. *Evidence-Based Complement. Altern. Med.* 2018, 1–17. doi:10.1155/2018/7802639

Luo, H., Vong, C. T., Chen, H., Gao, Y., Lyu, P., Qiu, L., et al. (2019). Naturally Occurring Anti-cancer Compounds: Shining from Chinese Herbal Medicine. *Chin. Med.* 14 (1), 48. doi:10.1186/s13020-019-0270-9

Luo, J., Wang, D., Wan, X., Xu, Y., Lu, Y., Kong, Z., et al. (2020). Crosstalk between AR and Wnt Signaling Promotes Castration-Resistant Prostate Cancer Growth. *Onco Targets Ther.* 13, 9257–9267. doi:10.2147/OTT.S245861

Mahammedi, H., Planchat, E., Pouget, M., Durando, X., Curé, H., Guy, L., et al. (2016). The New Combination Docetaxel, Prednisone and Curcumin in Patients with Castration-Resistant Prostate Cancer: A Pilot Phase II Study. *Oncology* 90 (2), 69–78. doi:10.1159/000441148

Mahmoud, A. M., Yang, W., and Bosland, M. C. (2014). Soy Isoflavones and Prostate Cancer: a Review of Molecular Mechanisms. *J. Steroid Biochem. Mol. Biol.* 140, 116–132. doi:10.1016/j.jsbmb.2013.12.010

Majumdar, D. D. (1985). Trends in Pattern Recognition and Machine Learning. *Dsj* 35 (3), 327–351. doi:10.14429/dsj.35.6027

Mann, J. (2002). Natural Products in Cancer Chemotherapy: Past, Present and Future. *Nat. Rev. Cancer* 2 (2), 143–148. doi:10.1038/nrc723

Mantena, S. K., Sharma, S. D., and Katiyar, S. K. (2006). Berberine, a Natural Product, Induces G1-phase Cell Cycle Arrest and Caspase-3-dependent Apoptosis in Human Prostate Carcinoma Cells. *Mol. Cancer Ther.* 5 (2), 296–308. doi:10.1158/1535-7163.MCT-05-0448

Mariani, S., Lionetto, L., Cavallari, M., Tubaro, A., Rasio, D., De Nunzio, C., et al. (2014). Low Prostate Concentration of Lycopene Is Associated with Development of Prostate Cancer in Patients with High-Grade Prostatic Intraepithelial Neoplasia. *Int. J. Mol. Sci.* 15 (1), 1433–1440. doi:10.3390/ijms15011433

Maskarinec, G., Morimoto, Y., Hebshi, S., Sharma, S., Franke, A. A., and Stanczyk, F. Z. (2006). Serum Prostate-specific Antigen but Not Testosterone Levels Decrease in a Randomized Soy Intervention Among Men. *Eur. J. Clin. Nutr.* 60 (12), 1423–1429. doi:10.1038/sj.ejcn.1602473

Mbese, Z., Khwaza, V., and Aderibigbe, B. A. (2019). Curcumin and its Derivatives as Potential Therapeutic Agents in Prostate, Colon and Breast Cancers. *Molecules* 24 (23). doi:10.3390/molecules24234386

McLarty, J., Bigelow, R. L., Smith, M., Elmajian, D., Ankem, M., and Cardelli, J. A. (2009). Tea Polyphenols Decrease Serum Levels of Prostate-specific Antigen, Hepatocyte Growth Factor, and Vascular Endothelial Growth Factor in Prostate Cancer Patients and Inhibit Production of Hepatocyte Growth Factor and Vascular Endothelial Growth Factor *In Vitro*. *Cancer Prev. Res. (Phila)* 2 (7), 673–682. doi:10.1158/1940-6207.CAPR-08-0167

McMenamin, M. E., Soung, P., Perera, S., Kaplan, I., Loda, M., and Sellers, W. R. (1999). Loss of PTEN Expression in Paraffin-Embedded Primary Prostate Cancer Correlates with High Gleason Score and Advanced Stage. *Cancer Res.* 59 (17), 4291–4296.

Mendiratta, P., Mostaghel, E., Guinney, J., Tewari, A. K., Porrello, A., Barry, W. T., et al. (2009). Genomic Strategy for Targeting Therapy in Castration-Resistant Prostate Cancer. *J. Clin. Oncol.* 27 (12), 2022–2029. doi:10.1200/jco.2008.17.2882

Mirahmadi, M., Azimi-Hashemi, S., Saburi, E., Kamali, H., Pishbin, M., and Hadizadeh, F. (2020). Potential Inhibitory Effect of Lycopene on Prostate Cancer. *Biomed. Pharmacother.* 129, 110459. doi:10.1016/j.biopha.2020.110459

Mishra, R., Sareen, S., Sharma, B., Goyal, S., Kaur, G., Bhardwaj, S., et al. (2017). Phenothiazines and Related Drugs as Multi Drug Resistance Reversal Agents in Cancer Chemotherapy Mediated by P-Glycoprotein. *Cctr* 13 (1). doi:10.2174/1573394713666170524122904

Mitani, T., Harada, N., Tanimori, S., Nakano, Y., Inui, H., and Yamaji, R. (2014). Resveratrol Inhibits Hypoxia-Inducible Factor-1α-Mediated Androgen Receptor Signaling and Represses Tumor Progression in Castration-Resistant Prostate Cancer. *J. Nutr. Sci. Vitaminol (Tokyo)* 60 (4), 276–282. doi:10.3177/jnsv.60.276

Miyanaga, N., Akaza, H., Hinotsu, S., Fujioka, T., Naito, S., Namiki, M., et al. (2012). Prostate Cancer Chemoprevention Study: an Investigative Randomized Control Study Using Purified Isoflavones in Men with Rising Prostate-specific Antigen. *Cancer Sci.* 103 (1), 125–130. doi:10.1111/j.1349-7006.2011.02120.x

Mokbel, K., Wazir, U., and Mokbel, K. (2019). Chemoprevention of Prostate Cancer by Natural Agents: Evidence from Molecular and Epidemiological Studies. *Anticancer Res.* 39 (10), 5231–5259. doi:10.21873/anticanres.13720

Montagnani Marelli, M., Marzagalli, M., Fontana, F., Raimondi, M., Moretti, R. M., and Limonta, P. (2019). Anticancer Properties of Tocotrienols: A Review of Cellular Mechanisms and Molecular Targets. *J. Cel Physiol* 234 (2), 1147–1164. doi:10.1002/jcp.27075

Mukhopadhyay, A., Bueso-Ramos, C., Chatterjee, D., Pantazis, P., and Aggarwal, B. B. (2001). Curcumin Downregulates Cell Survival Mechanisms in Human Prostate Cancer Cell Lines. *Oncogene* 20 (52), 7597–7609. doi:10.1038/sj.onc.1204997

Napora, J. K., Short, R. G., Muller, D. C., Carlson, O. D., Odetunde, J. O., Xu, X., et al. (2011). High-dose Isoflavones Do Not Improve Metabolic and Inflammatory Parameters in Androgen-Deprived Men with Prostate Cancer. *J. Androl.* 32 (1), 40–48. doi:10.2164/jandrol.110.010983

Neto, A. S., Tobias-Machado, M., Wroclawski, M. L., Fonseca, F. L., Pompeo, A. C., and Del Giglio, A. (2010). Molecular Oncogenesis of Prostate Adenocarcinoma: Role of the Human Epidermal Growth Factor Receptor 2 (HER-2/neu). *Tumori* 96 (5), 645–649. doi:10.1177/030089161009600501

Newman, D. J., and Cragg, G. M. (2016). Natural Products as Sources of New Drugs from 1981 to 2014. *J. Nat. Prod.* 79 (3), 629–661. doi:10.1021/acs.jnatprod.5b01055

Newman, D. J., Cragg, G. M., and Snader, K. M. (2000). The Influence of Natural Products upon Drug Discovery. *Nat. Prod. Rep.* 17 (3), 215–234. doi:10.1039/a902202c

Nguyen, M. M., Ahmann, F. R., Nagle, R. B., Hsu, C. H., Tangrea, J. A., Parnes, H. L., et al. (2012). Randomized, Double-Blind, Placebo-Controlled Trial of Polyphenon E in Prostate Cancer Patients before Prostatectomy: Evaluation of Potential Chemopreventive Activities. *Cancer Prev. Res. (Phila)* 5 (2), 290–298. doi:10.1158/1940-6207.CAPR-11-0306

Nishimura, M., Fuchino, H., Takayanagi, K., Kawakami, H., Nakayama, H., Kawahara, N., et al. (2021). Toxicity of Jegosaponins A and B from Styrax japonica Siebold Zuccarini in Prostate Cancer Cells and Zebrafish Embryos Resulting from Increased Membrane Permeability. *Ijms* 22 (12), 6354. doi:10.3390/ijms22126354

Oudard, S., Fizazi, K., Sengeløv, L., Daugaard, G., Saad, F., Hansen, S., et al. (2017). Cabazitaxel versus Docetaxel as First-Line Therapy for Patients with Metastatic Castration-Resistant Prostate Cancer: A Randomized Phase III Trial-FIRSTANA. *J. Clin. Oncol.* 35 (28), 3189–3197. doi:10.1200/jco.2016.72.1068

Paller, C. J., Rudek, M. A., Zhou, X. C., Wagner, W. D., Hudson, T. S., Anders, N., et al. (2015). A Phase I Study of Muscadine Grape Skin Extract in Men with Biochemically Recurrent Prostate Cancer: Safety, Tolerability,

and Dose Determination. *Prostate* 75 (14), 1518–1525. doi:10.1002/pros.23024

Paller, C. J., Zhou, X. C., Heath, E. I., Taplin, M. E., Mayer, T., Stein, M. N., et al. (2018). Muscadine Grape Skin Extract (MPX) in Men with Biochemically Recurrent Prostate Cancer: A Randomized, Multicenter, Placebo-Controlled Clinical Trial. *Clin. Cancer Res.* 24 (2), 306–315. doi:10.1158/1078-0432.CCR-17-1100

Pantuck, A. J., Lee, D.-K., Kee, T., Wang, P., Lakhotia, S., Silverman, M. H., et al. (2018). Modulating BET Bromodomain Inhibitor ZEN-3694 and Enzalutamide Combination Dosing in a Metastatic Prostate Cancer Patient Using CURATE.AI, an Artificial Intelligence Platform. *Adv. Therap.* 1 (6), 1800104. doi:10.1002/adtp.201800104

Park, S. I., Shah, A. N., Zhang, J., and Gallick, G. E. (2007). Regulation of Angiogenesis and Vascular Permeability by Src Family Kinases: Opportunities for Therapeutic Treatment of Solid Tumors. *Expert Opin. Ther. Targets* 11 (9), 1207–1217. doi:10.1517/14728222.11.9.1207

Pendleton, J. M., Tan, W. W., Anai, S., Chang, M., Hou, W., Shiverick, K. T., et al. (2008). Phase II Trial of Isoflavone in Prostate-specific Antigen Recurrent Prostate Cancer after Previous Local Therapy. *BMC Cancer* 8, 132. doi:10.1186/1471-2407-8-132

Perlmutter, M. A., and Lepor, H. (2007). Androgen Deprivation Therapy in the Treatment of Advanced Prostate Cancer. *Rev. Urol.* 9 (Suppl. 1), S3–S8.

Petrylak, D. P. (2013). Current State of Castration-Resistant Prostate Cancer. *Am. J. Manag. Care* 19 (18 Suppl. l), s358–65.

Polakis, P. (2007). The many Ways of Wnt in Cancer. *Curr. Opin. Genet. Dev.* 17 (1), 45–51. doi:10.1016/j.gde.2006.12.007

Pool-Zobel, B. L., Bub, A., Müller, H., Wollowski, I., and Rechkemmer, G. (1997). Consumption of Vegetables Reduces Genetic Damage in Humans: First Results of a Human Intervention Trial with Carotenoid-Rich Foods. *Carcinogenesis* 18 (9), 1847–1850. doi:10.1093/carcin/18.9.1847

Rahmani, A. H., Al Shabrmi, F. M., Allemailem, K. S., Aly, S. M., and Khan, M. A. (2015). Implications of Green Tea and its Constituents in the Prevention of Cancer via the Modulation of Cell Signalling Pathway. *Biomed. Res. Int.* 2015, 925640. doi:10.1155/2015/925640

Raju, B., Verma, H., Narendra, G., Sapra, B., and Silakari, O. (2021). Multiple Machine Learning, Molecular Docking, and ADMET Screening Approach for Identification of Selective Inhibitors of CYP1B1. *J. Biomol. Struct. Dyn.*, 1–16. doi:10.1080/07391102.2021.1905552

Ramalingam, S., Ramamurthy, V. P., and Njar, V. C. O. (2017). Dissecting Major Signaling Pathways in Prostate Cancer Development and Progression: Mechanisms and Novel Therapeutic Targets. *J. Steroid Biochem. Mol. Biol.* 166, 16–27. doi:10.1016/j.jsbmb.2016.07.006

Rauf, A., Imran, M., Khan, I. A., ur-Rehman, M., Gilani, S. A., Mehmood, Z., et al. (2018). Anticancer Potential of Quercetin: A Comprehensive Review. *Phytother Res.* 32 (11), 2109–2130. doi:10.1002/ptr.6155

Rawla, P. (2019). Epidemiology of Prostate Cancer. *World J. Oncol.* 10 (2), 63–89. doi:10.14740/wjon1191

Rebbeck, T. R., Devesa, S. S., Chang, B. L., Bunker, C. H., Cheng, I., Cooney, K., et al. (2013). Global Patterns of Prostate Cancer Incidence, Aggressiveness, and Mortality in Men of African Descent. *Prostate Cancer* 2013, 560857–560912. doi:10.1155/2013/560857

Reiner, T., Parrondo, R., de Las Pozas, A., Palenzuela, D., and Perez-Stable, C. (2013). Betulinic Acid Selectively Increases Protein Degradation and Enhances Prostate Cancer-specific Apoptosis: Possible Role for Inhibition of Deubiquitinase Activity. *PLoS One* 8 (2), e56234. doi:10.1371/journal.pone.0056234

Ren, S., Liu, Y., Xu, W., Sun, Y., Lu, J., Wang, F., et al. (2013). Long Noncoding RNA MALAT-1 Is a New Potential Therapeutic Target for Castration Resistant Prostate Cancer. *J. Urol.* 190 (6), 2278–2287. doi:10.1016/j.juro.2013.07.001

Rotimi, S. O., Rotimi, O. A., Salako, A. A., Jibrin, P., Oyelade, J., and Iweala, E. E. J. (2019). Gene Expression Profiling Analysis Reveals Putative Phytochemotherapeutic Target for Castration-Resistant Prostate Cancer. *Front. Oncol.* 9, 714. doi:10.3389/fonc.2019.00714

Rowley, D. R. (1998). What Might a Stromal Response Mean to Prostate Cancer Progression? *Cancer Metastasis Rev.* 17 (4), 411–419. doi:10.1023/a:1006129420005

Ru, J., Li, P., Wang, J., Zhou, W., Li, B., Huang, C., et al. (2014). TCMSP: a Database of Systems Pharmacology for Drug Discovery from Herbal Medicines. *J. Cheminform* 6 (1), 13. doi:10.1186/1758-2946-6-13

Saadipoor, A., Razzaghdoust, A., Simforoosh, N., Mahdavi, A., Bakhshandeh, M., Moghadam, M., et al. (2019). Randomized, Double-Blind, Placebo-Controlled Phase II Trial of Nanocurcumin in Prostate Cancer Patients Undergoing Radiotherapy. *Phytother Res.* 33 (2), 370–378. doi:10.1002/ptr.6230

Saijo, N., Nishio, K., and Tamura, T. (2003). Translational and Clinical Studies of Target-Based Cancer Therapy. *Int. J. Clin. Oncol.* 8 (4), 187–192. doi:10.1007/s10147-003-0324-x

Salehi, B., Fokou, P. V. T., Yamthe, L. R. T., Tali, B. T., Adetunji, C. O., Rahavian, A., et al. (2019). Phytochemicals in Prostate Cancer: From Bioactive Molecules to Upcoming Therapeutic Agents. *Nutrients* 11 (7). doi:10.3390/nu11071483

Sarkar, F. H., Li, Y., Wang, Z., and Kong, D. (2010). Novel Targets for Prostate Cancer Chemoprevention. *Endocr. Relat. Cancer* 17 (3), R195–R212. doi:10.1677/erc-10-0074

Schmidt, K. T., and Figg, W. D. (2016). The Potential Role of Curcumin in Prostate Cancer: the Importance of Optimizing Pharmacokinetics in Clinical Studies. *Transl Cancer Res.* 5 (Suppl. 6), S1107–S1110. doi:10.21037/tcr.2016.11.04

Shackleton, E. G., Ali, H. Y., Khan, M., Pockley, G. A., and McArdle, S. E. (2021). Novel Combinatorial Approaches to Tackle the Immunosuppressive Microenvironment of Prostate Cancer. *Cancers (Basel)* 13 (5). doi:10.3390/cancers13051145

Sharifi, N. (2013). Mechanisms of Androgen Receptor Activation in Castration-Resistant Prostate Cancer. *Endocrinology* 154 (11), 4010–4017. doi:10.1210/en.2013-1466

Sharma, P., Sharma, R., Rao, H., and Kumar, D. (2016). Phytochemistry and Medicinal Attributes of A. Scholaris: A Review. *Int. J. Pharm. Sci. Res.* 7 (2), 1000–1010. doi:10.13040/ijpsr.0975-8232.6(12).505-13doi:10.13040/ijpsr.0975-8232.7(10).4164-69

Sharma, P., Shri, R., Ntie-Kang, F., and Kumar, S. (2021). Phytochemical and Ethnopharmacological Perspectives of Ehretia Laevis. *Molecules* 26 (12), 3489. doi:10.3390/molecules26123489

Shen, L., Bai, J., Wang, J., and Shen, B. (2021). The Fourth Scientific Discovery Paradigm for Precision Medicine and Healthcare: Challenges Ahead. *Precision Clin. Med.* 4 (2), 80–84. doi:10.1093/pcmedi/pbab007

Shi, S. H., Cai, Y. P., Cai, X. J., Zheng, X. Y., Cao, D. S., Ye, F. Q., et al. (2014). A Network Pharmacology Approach to Understanding the Mechanisms of Action of Traditional Medicine: Bushenhuoxue Formula for Treatment of Chronic Kidney Disease. *PLoS ONE* 9 (3), e89123. doi:10.1371/journal.pone.0089123

Shimura, S., Yang, G., Ebara, S., Wheeler, T. M., Frolov, A., and Thompson, T. C. (2000). Reduced Infiltration of Tumor-Associated Macrophages in Human Prostate Cancer: Association with Cancer Progression. *Cancer Res.* 60 (20), 5857–5861.

Si, T. G., Wang, J. P., and Guo, Z. (2013). Analysis of Circulating Regulatory T Cells (CD4+CD25+CD127-) after Cryosurgery in Prostate Cancer. *Asian J. Androl.* 15 (4), 461–465. doi:10.1038/aja.2013.22

Singer, E. A., Golijanin, D. J., Miyamoto, H., and Messing, E. M. (2008). Androgen Deprivation Therapy for Prostate Cancer. *Expert Opin. Pharmacother.* 9 (2), 211–228. doi:10.1517/14656566.9.2.211

Singh, C. K., Siddiqui, I. A., El-Abd, S., Mukhtar, H., and Ahmad, N. (2016). Combination Chemoprevention with Grape Antioxidants. *Mol. Nutr. Food Res.* 60 (6), 1406–1415. doi:10.1002/mnfr.201500945

Singla, R. K., Guimarães, A. G., and Zengin, G. (2020a). Editorial: Application of Plant Secondary Metabolites to Pain Neuromodulation. *Front. Pharmacol.* 11, 623399. doi:10.3389/fphar.2020.623399

Singla, R. K. (2020). Secondary Metabolites as Treatment of Choice for Metabolic Disorders and Infectious Diseases and Their Metabolic Profiling: Part 1. *Curr. Drug Metab.* 21 (7), 480–481. doi:10.2174/1389200221072009251016 31

Singla, R. K., and Shen, B. (2020). In Silico ADME-T Evaluation of Natural DPP-IV Inhibitors for Rational Drug Design against Diabetes. *Curr. Drug Metab.* 21 (10), 768–777. doi:10.2174/1389200221999200901202945

Singla, R. K., and Singla, R. K. (2020). Secondary Metabolites as Treatment of Choice for Metabolic Disorders and Infectious Diseases and Their Metabolic Profiling: Part 1. *Curr. Drug Metab.* 21 (14), 480–481. doi:10.2174/1389200221142012301422041 0.2174/1389200221072009251016 31

Singla, R. K., Sultana, A., Alam, M. S., and Shen, B. (2020b). Regulation of Pain Genes-Capsaicin vs Resiniferatoxin: Reassessment of Transcriptomic Data. *Front. Pharmacol.* 11, 551786. doi:10.3389/fphar.2020.551786

Smith, D. C., Smith, M. R., Sweeney, C., Elfiky, A. A., Logothetis, C., Corn, P. G., et al. (2013). Cabozantinib in Patients with Advanced Prostate Cancer: Results of a Phase II Randomized Discontinuation Trial. *J. Clin. Oncol.* 31 (4), 412–419. doi:10.1200/jco.2012.45.0494

Song, Y., Wang, H., Pan, Y., and Liu, T. (2019). Investigating the Multi-Target Pharmacological Mechanism of Hedyotis Diffusa Willd Acting on Prostate Cancer: A Network Pharmacology Approach. *Biomolecules* 9 (10). doi:10.3390/biom9100591

Studer, U. E., Hauri, D., Hanselmann, S., Chollet, D., Leisinger, H. J., Gasser, T., et al. (2004). Immediate versus Deferred Hormonal Treatment for Patients with Prostate Cancer Who Are Not Suitable for Curative Local Treatment: Results of the Randomized Trial SAKK 08/88. *J. Clin. Oncol.* 22 (20), 4109–4118. doi:10.1200/jco.2004.11.514

Su, P.-J., Fang, Y.-A., Chang, Y.-C., Kuo, Y.-C., and Lin, Y.-C. (2019). Establish a Predictive Model for High-Risk De Novo Metastatic Prostate Cancer Patients by Machine Learning. *Jgo* 5 (Suppl. l), 13. doi:10.1200/JGO.2019.5.suppl.13

Sung, H., Ferlay, J., Siegel, R. L., Laversanne, M., Soerjomataram, I., Jemal, A., et al. (2021). Global Cancer Statistics 2020: GLOBOCAN Estimates of Incidence and Mortality Worldwide for 36 Cancers in 185 Countries. *CA A. Cancer J. Clin.* 71 (3), 209–249. doi:10.3322/caac.21660

Suryanarayana, R., Kumar, T. N. V. G., Mathew, J., Kandale, A., and Singla, R. K. (2015). Synthesis & Biological Evaluation of 1, 3, 4- Oxadiazoles as Anticancer Agents. *Igjps* 05 (1), 01–05. doi:10.35652/igjps.2015.17

Swami, S., Krishnan, A. V., Moreno, J., Bhattacharyya, R. S., Gardner, C., Brooks, J. D., et al. (2009). Inhibition of Prostaglandin Synthesis and Actions by Genistein in Human Prostate Cancer Cells and by Soy Isoflavones in Prostate Cancer Patients. *Int. J. Cancer* 124 (9), 2050–2059. doi:10.1002/ijc.24161

Tang, Y., Yan, W., Chen, J., Luo, C., Kaipia, A., and Shen, B. (2013). Identification of Novel microRNA Regulatory Pathways Associated with Heterogeneous Prostate Cancer. *BMC Syst. Biol.* 7 (Suppl. 3), S6. doi:10.1186/1752-0509-7-s3-s6

Taylor, W. F., and Jabbarzadeh, E. (2017). The Use of Natural Products to Target Cancer Stem Cells. *Am. J. Cancer Res.* 7 (7), 1588–1605.

Teiten, M. H., Gaascht, F., Eifes, S., Dicato, M., and Diederich, M. (2010). Chemopreventive Potential of Curcumin in Prostate Cancer. *Genes Nutr.* 5 (1), 61–74. doi:10.1007/s12263-009-0152-3

Teo, M. Y., Rathkopf, D. E., and Kantoff, P. (2019). Treatment of Advanced Prostate Cancer. *Annu. Rev. Med.* 70 (1), 479–499. doi:10.1146/annurev-med-051517-011947

Thangapazham, R. L., Singh, A. K., Sharma, A., Warren, J., Gaddipati, J. P., and Maheshwari, R. K. (2007). Green tea Polyphenols and its Constituent Epigallocatechin Gallate Inhibits Proliferation of Human Breast Cancer Cells *In Vitro* and *In Vivo*. *Cancer Lett.* 245 (1-2), 232–241. doi:10.1016/j.canlet.2006.01.027

Tian, Y., Zhao, L., Wang, Y., Zhang, H., Xu, D., Zhao, X., et al. (2016). Berberine Inhibits Androgen Synthesis by Interaction with Aldo-Keto Reductase 1C3 in 22Rv1 Prostate Cancer Cells. *Asian J. Androl.* 18 (4), 607–612. doi:10.4103/1008-682x.169997

Tsodikov, A., Gulati, R., Heijnsdijk, E. A. M., Pinsky, P. F., Moss, S. M., Qiu, S., et al. (2017). Reconciling the Effects of Screening on Prostate Cancer Mortality in the ERSPC and PLCO Trials. *Ann. Intern. Med.* 167 (7), 449–455. doi:10.7326/m16-2586

Urbanucci, A., Sahu, B., Seppälä, J., Larjo, A., Latonen, L. M., Waltering, K. K., et al. (2011). Overexpression of Androgen Receptor Enhances the Binding of the Receptor to the Chromatin in Prostate Cancer. *Oncogene* 31 (17), 2153–2163. doi:10.1038/onc.2011.401

Volate, S. R., Kawasaki, B. T., Hurt, E. M., Milner, J. A., Kim, Y. S., White, J., et al. (2010). Gossypol Induces Apoptosis by Activating P53 in Prostate Cancer Cells and Prostate Tumor-Initiating Cells. *Mol. Cancer Ther.* 9 (2), 461–470. doi:10.1158/1535-7163.MCT-09-0507

W Watson, G., M Beaver, L., E Williams, D., H Dashwood, R. R., and Ho, E. (2013). Phytochemicals from Cruciferous Vegetables, Epigenetics, and Prostate Cancer Prevention. *AAPS J.* 15 (4), 951–961. doi:10.1208/s12248-013-9504-4

Wang, Y., Liu, Q., Liu, Z., Li, B., Sun, Z., Zhou, H., et al. (2012). Berberine, a Genotoxic Alkaloid, Induces ATM-Chk1 Mediated G2 Arrest in Prostate Cancer Cells. *Mutat. Res.* 734 (1-2), 20–29. doi:10.1016/j.mrfmmm.2012.04.005

Wen, Y., Hu, M. C., Makino, K., Spohn, B., Bartholomeusz, G., Yan, D. H., et al. (2000). HER-2/neu Promotes Androgen-independent Survival and Growth of Prostate Cancer Cells through the Akt Pathway. *Cancer Res.* 60 (24), 6841–6845.

Wild, C., Weiderpass, E., and Stewart, B. (2020). *World Cancer Report: Cancer Research For Cancer Prevention* [Online]. Lyon, France: International Agency for Research on Cancer. Available: http://publications.iarc.fr/586 [Accessed 19.06.2021].

Willett, W. C. (1994). Diet and Health: what Should We Eat? *Science* 264 (5158), 532–537. doi:10.1126/science.8160011

Wu, S. Q., Su, H., Wang, Y. H., and Zhao, X. K. (2019). Role of Tumor-Associated Immune Cells in Prostate Cancer: Angel or Devil? *Asian J. Androl.* 21 (5), 433–437. doi:10.4103/aja.aja_47_19

Xu, G., Chu, Y., Jiang, N., Yang, J., and Li, F. (2012). The Three Dimensional Quantitative Structure Activity Relationships (3D-QSAR) and Docking Studies of Curcumin Derivatives as Androgen Receptor Antagonists. *Int. J. Mol. Sci.* 13 (5), 6138–6155. doi:10.3390/ijms13056138

Xu, L., Yang, D., Wang, S., Tang, W., Liu, M., Davis, M., et al. (2005). (-)-Gossypol Enhances Response to Radiation Therapy and Results in Tumor Regression of Human Prostate Cancer. *Mol. Cancer Ther.* 4 (2), 197–205.

Yallapu, M. M., Khan, S., Maher, D. M., Ebeling, M. C., Sundram, V., Chauhan, N., et al. (2014). Anti-cancer Activity of Curcumin Loaded Nanoparticles in Prostate Cancer. *Biomaterials* 35 (30), 8635–8648. doi:10.1016/j.biomaterials.2014.06.040

Yang, J. C., Bai, L., Yap, S., Gao, A. C., Kung, H. J., and Evans, C. P. (2010). Effect of the Specific Src Family Kinase Inhibitor Saracatinib on Osteolytic Lesions Using the PC-3 Bone Model. *Mol. Cancer Ther.* 9 (6), 1629–1637. doi:10.1158/1535-7163.Mct-09-1058

Yang, L., Chen, L., Meng, B., Suo, J., Wang, H., Xie, H., et al. (2006). The Effect of Curcumin on Proliferation and Apoptosis in LNCaP Prostate Cancer Cells. *Chin. J. Clin. Oncol.* 3 (1), 55–60. doi:10.1007/s11805-006-0072-6

Yao, M., Shi, X., Li, Y., Xiao, Y., Butler, W., Huang, Y., et al. (2020). LINC00675 Activates Androgen Receptor axis Signaling Pathway to Promote Castration-Resistant Prostate Cancer Progression. *Cell Death Dis* 11 (8), 638. doi:10.1038/s41419-020-02856-5

Yu, C., Qi, X., Lin, Y., Li, Y., and Shen, B. (2020). iODA: An Integrated Tool for Analysis of Cancer Pathway Consistency from Heterogeneous Multi-Omics Data. *J. Biomed. Inform.* 112, 103605. doi:10.1016/j.jbi.2020.103605

Zhang, L., Tan, J., Han, D., and Zhu, H. (2017). From Machine Learning to Deep Learning: Progress in Machine Intelligence for Rational Drug Discovery. *Drug Discov. Today* 22 (11), 1680–1685. doi:10.1016/j.drudis.2017.08.010

Zhang, X., Huang, J., Yu, C., Xiang, L., Li, L., Shi, D., et al. (2020a). Quercetin Enhanced Paclitaxel Therapeutic Effects towards PC-3 Prostate Cancer through ER Stress Induction and ROS Production. *Onco Targets Ther.* 13, 513–523. doi:10.2147/ott.S228453

Zhang, Z., Karthaus, W. R., Lee, Y. S., Gao, V. R., Wu, C., Russo, J. W., et al. (2020b). Tumor Microenvironment-Derived NRG1 Promotes Antiandrogen Resistance in Prostate Cancer. *Cancer Cell* 38 (2), 279–e9. e279. doi:10.1016/j.ccell.2020.06.005

Zhou, D. Y., Ding, N., Du, Z. Y., Cui, X. X., Wang, H., Wei, X. C., et al. (2014). Curcumin Analogues with High Activity for Inhibiting Human Prostate Cancer Cell Growth and Androgen Receptor Activation. *Mol. Med. Rep.* 10 (3), 1315–1322. doi:10.3892/mmr.2014.2380

Zhou, Y., Bolton, E. C., and Jones, J. O. (2015). Androgens and Androgen Receptor Signaling in Prostate Tumorigenesis. *J. Mol. Endocrinol.* 54 (1), R15–R29. doi:10.1530/jme-14-0203

Zhu, F., Liu, Q., Zhang, X., and Shen, B. (2014). "Protein-protein Interaction Network Constructing Based on Text Mining and Reinforcement Learning

with Application to Prostate Cancer," in 2014 IEEE International Conference on Bioinformatics and Biomedicine (Belfast, UK: BIBM). doi:10.1109/bibm.2014.6999302

Zhu, J., Wang, S., Zhang, W., Qiu, J., Shan, Y., Yang, D., et al. (2015). Screening Key microRNAs for Castration-Resistant Prostate Cancer Based on miRNA/mRNA Functional Synergistic Network. *Oncotarget* 6 (41), 43819–43830. doi:10.18632/oncotarget.6102

Zhu, M. L., and Kyprianou, N. (2008). Androgen Receptor and Growth Factor Signaling Cross-Talk in Prostate Cancer Cells. *Endocr. Relat. Cancer* 15 (4), 841–849. doi:10.1677/ERC-08-0084

Zhuang, E., Uchio, E. M., Lilly, M. B., and Fruehauf, J. P. (2021). A Phase II Study to Evaluate the Effects of Docetaxel Plus Lycopene in Advanced Castrate-Resistant Prostate Cancer. *Jco* 39 (6_Suppl. l), 77. doi:10.1200/JCO.2021.39.6_suppl.77

Conflict of Interest: RS, SJ and SS are having honorary-based association with iGlobal Research and Publishing Foundation, New Delhi, India. All the authors declare that the research was conducted in the absence of any commercial or financial relationships that could be construed as a potential conflict of interest.

Publisher's Note: All claims expressed in this article are solely those of the authors and do not necessarily represent those of their affiliated organizations, or those of the publisher, the editors and the reviewers. Any product that may be evaluated in this article, or claim that may be made by its manufacturer, is not guaranteed or endorsed by the publisher.

Advantages of publishing in Frontiers

OPEN ACCESS
Articles are free to read for greatest visibility and readership

FAST PUBLICATION
Around 90 days from submission to decision

HIGH QUALITY PEER-REVIEW
Rigorous, collaborative, and constructive peer-review

TRANSPARENT PEER-REVIEW
Editors and reviewers acknowledged by name on published articles

Frontiers
Avenue du Tribunal-Fédéral 34
1005 Lausanne | Switzerland

Visit us: www.frontiersin.org
Contact us: frontiersin.org/about/contact

REPRODUCIBILITY OF RESEARCH
Support open data and methods to enhance research reproducibility

DIGITAL PUBLISHING
Articles designed for optimal readership across devices

FOLLOW US
@frontiersin

IMPACT METRICS
Advanced article metrics track visibility across digital media

EXTENSIVE PROMOTION
Marketing and promotion of impactful research

LOOP RESEARCH NETWORK
Our network increases your article's readership